

EFFECTS OF SOME FLAVONOIDS ON OBESITY-LINKED TYPE 2 DIABETES: ROLE OF AUTOPHAGY

Ph.D. THESIS

by

RITU VARSHNEY



**DEPARTMENT OF BIOTECHNOLOGY
INDIAN INSTITUTE OF TECHNOLOGY ROORKEE
ROORKEE- 247 667 (INDIA)
JULY, 2018**

EFFECTS OF SOME FLAVONOIDS ON OBESITY-LINKED TYPE 2 DIABETES: ROLE OF AUTOPHAGY

A THESIS

*Submitted in partial fulfilment of the
requirements for the award of the degree*

of

DOCTOR OF PHILOSOPHY

in

BIOTECHNOLOGY

by

RITU VARSHNEY



**DEPARTMENT OF BIOTECHNOLOGY
INDIAN INSTITUTE OF TECHNOLOGY ROORKEE
ROORKEE- 247 667 (INDIA)
JULY, 2018**



**©INDIAN INSTITUTE OF TECHNOLOGY ROORKEE, ROORKEE-2018
ALL RIGHTS RESERVED**



INDIAN INSTITUTE OF TECHNOLOGY ROORKEE ROORKEE

CANDIDATE'S DECLARATION

I hereby certify that the work which is being presented in the thesis entitled “**EFFECTS OF SOME FLAVONOIDS ON OBESITY-LINKED TYPE 2 DIABETES: ROLE OF AUTOPHAGY**” in partial fulfilment of the requirements for the award of the Degree of Doctor of Philosophy and submitted in the Department of Biotechnology of the Indian Institute of Technology Roorkee, Roorkee is an authentic record of my own work carried out during a period from July, 2012 to July, 2018 under the supervision of Dr. Partha Roy, Professor, Department of Biotechnology, Indian Institute of Technology Roorkee, Roorkee, India.

The matter presented in this thesis has not been submitted by me for the award of any other degree of this or any other institute.

(RITU VARSHNEY)

This is to certify that the above statement made by the candidate is correct to the best of my knowledge.

(Partha Roy)
Supervisor

Dated:

Abstract

Diabetes Mellitus (DM) is a group of metabolic disorders characterized by an increased level of blood glucose due to defects in insulin secretion or action or both. Among all diabetic conditions, type 2 diabetes is most prevalent and accounts for nearly 90-95% of patients diagnosed with diabetes worldwide. Type 2 diabetes mellitus (T2DM) is a metabolic disease characterized by elevated blood glucose level and insulin resistance. The world health organization (WHO) reported that the worldwide number of people with diabetes has risen to 422 million in 2014 from 108 million in 1980 with an estimated 1.5 million deaths in 2012 (World Health Organization, 2016). As the knowledge of heterogeneity of this disorder increases, there is a need to search for more efficacious agents with lesser side effects. Although the modern medicines and therapies can mitigate diabetes to some extent, there are several unprecedented complications that need to be addressed through a holistic approach of therapy. Towards this end, a validation of our traditional knowledge of Ayurveda and then combining it with the modern scientific approach may provide the best possible solution to it. The traditional plant-based medicines are safe, effective, economical, non-toxic with no or lesser side effects as compared to other synthetic drugs. Hence these herbal plants or active phytoconstituents are considered to be the best possible alternative candidates in diabetes management.

The present thesis entitled “**Effects of some flavonoids on obesity-linked type 2 diabetes: role of autophagy**” deals with evaluating the anti-obesity and antidiabetic effects of some flavonoids using *in vitro* and *in vivo* approaches followed by evaluating the autophagy stimulatory activity of these flavonoids. Out of four flavonoids selected for this study, kaempferol was found to be most potent in stimulating autophagy and restoring β -cell mass and function. Thus, kaempferol was chosen for further detailed and mechanistic studies using *in vitro*, *ex vivo* and *in vivo* models to establish the exact cross-talks among various pathways in causing autophagy and its related antidiabetic effects.

In the beginning, the **Chapter 1** introduces briefly the present scenario of diabetes and therapeutic drugs available for the management of this metabolic disorder. It also deals with the key mechanisms and major signaling pathways involved in the pathophysiology of this disease that needs to be targeted for its prevention and cure. These mechanisms can serve as a

major target to select a natural molecule for its respective efficacy. Finally, the detailed objective to be attained in this study is specified in this chapter.

Followed by this, **Chapter 2** presents: (i) a detailed review on diabetes and its link to obesity; (ii) detailed mechanisms involved in pathophysiology of diabetes with special emphasis on insulin resistance and β -cell failure; (iii) conventional and current therapies for diabetes management and their limitations; (iv) understanding the molecular mechanism of autophagy and its role in obesity-linked diabetes, insulin resistance and β -cell failure with major focus on molecular pathways and their therapeutic targets; (v) recent research detailing benefits of phytochemicals and their characteristic to target multiple pathway on various target tissues and (vi) the hypothetic idea behind the present thesis to elucidate the efficacy of flavonoids for their potential to stimulate autophagy and their antidiabetic role. Each of these hypotheses was further explored in subsequent chapters of the thesis.

The main objective of the present work is to decipher anti-obesity, antidiabetic and autophagy stimulatory effects of flavonoids followed by understanding their mode of action. There are various *in vitro* and *in vivo* assays which are already established to confirm a compound to be anti-obese and antidiabetic. All these parameters are elaborated in **Chapter 3** of this thesis. In this regards, this chapter contains the details about various cell lines, *ex vivo* and *in vivo* models used in the study and the overall principles and methodology of all the experimental assays that were performed to identify the autophagy stimulatory and antidiabetic effects of flavonoids. Hence, various biochemical methods such as cell proliferation assays, adipocyte differentiation assays, Oil Red O staining, glucose uptake assay, specific assays to detect apoptosis and autophagy, which were used initially to screen the selected flavonoids' potential as antidiabetic or anti-obese potentiality are described in detail. Further, the principles of the biological mechanisms were studied at the transcriptional and translational levels of various genes to evaluate their mode of actions intracellularly.

T2DM is a metabolic disorder with an elevated blood glucose level and insulin resistance, are mostly associated with obesity thus indicating a direct correlation between these two pathological conditions. Recent studies showed that dysfunctional autophagy is involved in the loss of β -cell mass and function, hence, demonstrating pathophysiology of obesity-linked diabetes. Therefore, identifying agents that could restore autophagy in degenerated β -cells are of great importance under the current therapeutic regime. Currently, an active area of diabetes research focuses on identifying naturally occurring phytochemicals that can be

modulated or developed into therapeutic for diabetes due to their intriguing role in treating various diseases. One such group of phytochemicals found extensively in various plants is flavonoid. In **Chapter 4**, few of these flavonoids were screened using *in vitro* and *in vivo* models for their anti-obesity and antidiabetic effects. These flavonoids were further analyzed for their potential to stimulate autophagy under lipid overload conditions. Our results showed that among all-selected flavonoids, kaempferol had potent antidiabetic and autophagy stimulating activities as obtained from initial screening tests and thus selected for further detailed and mechanistic studies.

Lipotoxicity of pancreatic β -cells is the pathological manifestation of obesity-linked type II diabetes. Autophagy is a lysosomal degradation pathway of dysfunctional macromolecules and organelles which protects cells from stressed conditions and acts as an adaptive pro-survival response. In **Chapter 5**, we intended to determine the cytoprotective effect of kaempferol on pancreatic β -cells undergoing apoptosis in palmitic acid (PA)-stressed condition. The data showed that kaempferol treatment increased cell viability and anti-apoptotic activity in PA-stressed clonal pancreatic β -cells (RIN-5F cell line) and isolated primary cultures of rat islets. Further, it was found that kaempferol exerts its cytoprotective actions by inducing autophagy via AMPK/mTOR signaling pathway in PA-stressed pancreatic β -cells.

Chapter 6, depicts the molecular mechanism involved in cross-talk between kaempferol-mediated autophagy and its anti-apoptotic effect in PA-stressed β -cells. Endoplasmic reticulum (ER) stress generated due to the accumulation of lipid in β -cells is one of the major features of pathological conditions involved in cell death under lipid overload conditions. Interestingly, autophagy is involved in the alleviation of lipid-induced ER stress thus protecting β -cell from apoptosis. On the other hand, autophagy is also reported to degrade lipid droplets in hepatocytes, however, its role in lipid metabolism of β -cell is rarely reported. Based on this information in this study, the inhibitory effects of kaempferol-induced autophagy on PA-induced lipid deposition and ER stress were evaluated. Our studies showed that kaempferol-induced AMPK/mTOR-mediated autophagy abolished the PA-induced ER stress and lipid accumulation which seems to be one of the possible mechanisms involved in the kaempferol-mediated restoration of β -cell mass. Additionally, this study revealed that kaempferol-induced autophagy also restored the β -cell function.

In **Chapter 7**, we intended to validate our findings in a more promising diabetic model, the high fat diet (HFD) and streptozotocin (STZ)-induced type 2 diabetic mice, an alternative animal model of type 2 diabetes, simulating human syndrome which has been extensively used to test antidiabetic effects of various drugs/compounds. Our results exhibited that kaempferol treatment resulted in significant improvement in glycemic control and metabolic profile in HFD-STZ-induced diabetic mice. The improved glucose homeostasis was found to be associated with increased insulin sensitivity. Further, it was evident that kaempferol-induced autophagy is involved in the protection of β -cell mass and function which in part ameliorates diabetes in HFD-STZ induced diabetic mice.

The two pathophysiologic abnormalities which link obesity to T2DM, are β -cell failure and insulin resistance. Hence, in **Chapter 8**, the effects of kaempferol on hepatic insulin resistance and insulin signal transduction were evaluated *in vitro* and *in vivo* in PA-challenged HepG2 cells and livers of HFD-STZ-induced diabetic mice respectively. Dysfunctional autophagy and ER stress due to increased ectopic lipid accumulation in hepatocytes are the pathological manifestation involved in the lipid-induced impairment of insulin signaling and thus insulin resistance. In this study, lipid inhibitory effects of kaempferol were determined in *in vitro* and *in vivo* models. Further, to explore the possible underlying mechanism, the role of autophagy and β -oxidation were investigated. Our results showed that kaempferol exerted its lipid inhibitory effects in hepatocytes through autophagy and β -oxidation mechanism under lipid overload conditions. Further, kaempferol treatment significantly abolished the HFD-mediated increase in ER-stress induced JNK (Thr183/Tyr185) and IRS-1 phosphorylation (Ser307) which finally helped in the restoration of insulin-stimulated phosphorylation of Akt (Ser473). Together, this study revealed that kaempferol-induced AMPK-mTOR-mediated autophagy is involved in the alleviation of hepatic lipid accumulation and impaired insulin signal transduction in PA-induced HepG2 cells and livers of HFD-STZ-induced diabetic mice which, in part, ameliorates insulin resistance and hyperglycemia.

Finally, **Chapter 9** summarizes the major findings of the current thesis and provides suggestions for future work in this area. The scientific findings dealt with in this thesis may be of use to the future researchers working in this area. Last but not least, **Chapter 10** of this thesis listed the bibliography which was consulted in course of the present work.

Acknowledgements

The success and final outcome of this project required a lot of guidance, support and assistance from many people and I am extremely privileged to have them all along the completion of my thesis.

*I consider this my esteemed privilege to thank and express my profound gratitude to my supervisor, **Professor Partha Roy** for giving me the opportunity to work along with him. I would like to express my special appreciation and thanks to him for his patience, tremendous attention, enthusiasm, healthy scientific discussions, and constructive criticism. This would not have been possible at all without his immense knowledge, unaltered guidance, constant feedback and support throughout the course of research and writing of this thesis. His precious guidance and constructive criticism during the tenure keep the research alive inside me. Professional expertise, open discussions, endless advice and constant unflinching support rendered by Professor Partha Roy have shaped this thesis to its present form. To him, I remain, professionally and emotionally indebted. I could not have imagined having a better advisor and mentor for my Ph.D. study.*

*I would like to extend my thanks to the Students Research Committee members **Professor R.P Singh, Dr. A.K Sharma** from the Department of Biotechnology and **Professor M.R Maurya** from Department of Chemistry for sparing their valuable time in monitoring the work progress and providing useful tips, critical comments and suggestions from time to time. Head, Department of Biotechnology, is gratefully acknowledged for providing me the necessary central research facilities of the department to complete this work. I also extend my gratitude to all the faculties of the department who had been warm to me.*

*I would like to acknowledge the **University Grant Commission (UGC)**, India and **Indian Institute of Technology, Roorkee**, for providing me financial assistance throughout the course of my study which facilitated me to perform my work.*

*Most importantly I am thankful to **Professor Ronald M. Evans** (The Salk Institute for Biological Studies, California, USA) and **Professor Michael R. Stallcup** (University of Southern California, Los Angeles, CA, USA) for providing me with important research materials which were very essential to complete the study. Without their help this thesis would have been impossible.*

*I would like to extend my thanks to the members of **Molecular Endocrinology Lab** who have contributed immensely to my personal and professional time all this while during the*

research. I thank the former members of my lab; **Dr. Bhavna, Dr. Swati, Dr. Nikhil, Dr. Narender and Dr. Shruti** for being a source of inspiration for me in my early years as a research scholar which kept me going at the beginning. I also wish to thank my current lab members **Dr. Lokesh, Dr. Swati, Ritusmita, Somesh, Rahul, Neeladri, Sandip, Parul, Viney and Souvik** for all the scientific as well as non-scientific discussions and all the off-work enjoyment in the lab and outside that we have had. I also thank all of them for providing me a peaceful and friendly academic environment to work in the lab. I would like to express my special thanks to **Ritusmita**, for all the fun-filled moments we shared. Thank you for tolerating, accepting, loving and supporting me throughout this period. The time that we spent in both lab and hostel was entertaining and respite from the stress.

I further acknowledge all the M.Sc. and B.Tech. students who did their thesis under my supervision. I would like to particularly thank **Aashish, Shreya, Rutuja and Shreesh** for helping me with experiments and giving me an opportunity to improve my academic and research skills through my mentorship.

I would like to extend my warm regards to all the research scholars, the non-teaching staffs from Department of Biotechnology, the administrative staffs and staffs from B.Tech. and M.Sc. labs who were always helpful to me and provided their assistance whenever needed.

Without my friends and family, this emotional journey would have been a tiring one. I would like to express my love to each and every one of them. For the numerous discussions, endless chit chats, from cooking late night snacks to full-fledged dinners, the birthday celebrations and much more. Thank you for all the lovely times and for being the moral support during this roller coaster ride called Ph.D. Supporting each other through this journey; I would especially like to thank **Ritusmita, Rimpi, Swati, Richa, Gunjan, Neethu, Sugu, Niru, Archna and Noopur**. All your love and support kept me going when things felt difficult.

My work would not have been so easy without the specific help of all my friends and colleagues from **IVRI, AIIMS, KGMC, NBRI, IGIB, JNU, ILS, NISER, CDRI, I.I.T and IISER** who have contributed directly or indirectly towards the successful completion of my work.

I wish to extend my sincere thanks to some of my close friends **Dr. Sam, Dr. Uday, Dr. Rajat, Babita, Deepak, Debasish, Supriya, Sachin, Nisha, Vinay, Manni, Poornima, and Abhishek**. Although they were physically far from me, but electronically were really close to

me all the times and all their encouraging words and messages boosted me through thick and thin.

I also extend my sincere thanks to another very important person **Mrs. Roopa Roy**, for her support, care and culinary dishes that helped me to find a “home away from home”.

Besides this, I would like to thank everyone who has knowingly or unknowingly helped me in this successful completion of this thesis.

Lastly, I am indebted to **my parents, brothers and sister** for all their love, support, sacrifices and abundant patience shown throughout the years. Thank you for believing in me and being the invisible shield of my life. Thanks will be too small a word. So, lots of love to all my family members for being there for me always and supporting and encouraging me unconditionally.

Above all, my heartfelt gratitude to **Lord Ganesha** for bestowing his endless blessings on me, to provide wisdom to complete this Ph.D. thesis and to help me overcoming all the hardships and obstacles during this entire tenure. Without his divine presence in my life, I would have never been successful.

I also pray for the soul of animals who sacrificed their lives to complete this study, without which this thesis would not have been possible.

At last, I would like to dedicate this thesis to **Lord Ganesha, my family and my supervisor**.

Ritu Varshney

List of Publications

1. **Varshney, R.**, Gupta, S. and Roy, P., 2017. Cytoprotective effect of kaempferol against palmitic acid-induced pancreatic β -cell death through modulation of autophagy via AMPK/mTOR signaling pathway. *Molecular and cellular endocrinology*, 448, pp.1-20.
2. **Varshney, R.**, Varshney, R., Mishra, R., Gupta, S., Sircar, D. and Roy, P., 2018. Kaempferol alleviates palmitic acid-induced lipid stores, endoplasmic reticulum stress and pancreatic β -cell dysfunction through AMPK/mTOR-mediated lipophagy. *The Journal of nutritional biochemistry*, 57, pp.212-227.
3. **Varshney, R.**, Das, N., Mishra, R., Varshney, R., Sircar, D. and Roy, P., Kaempferol restores functional pancreatic β -cell mass through enhancing autophagy in a murine model of type 2 diabetes *The Journal of nutritional biochemistry (Under review)*.
4. **Varshney, R.**, Mishra, R., Das, N., Varshney, R., Sircar, D. and Roy, P., Kaempferol ameliorates hepatic lipid accumulation and insulin resistance by restoring autophagy via AMPK/mTOR mediated pathway: an *in vitro* and *in vivo* study (*In communication*).
5. **Varshney, R.** and Roy, P., A comparative analysis of various flavonoids in the regulation of obesity and diabetes: *in vitro* and *in vivo* study (*In communication*).
6. **Varshney, R.** and Roy, P., Hepatoprotective effect of kaempferol-mediated autophagy: an *in vitro* and *in vivo* study (*Under preparation*).
7. **Varshney, R.** and Roy, P., Role of lipophagy in preservation of functional β -cell mass in a murine model of type 2 diabetes (*Under preparation*).

Book chapters

8. **Varshney, R.**, Mishra, R., Das, N., Banerjee, S. and Roy, P. Phytochemicals: Their use in the cure and management of various diseases as part of traditional healthcare system. *CSIR-NISCAIR, New Delhi. (under revision)*.
9. **Varshney, R.**, Das, N., Mishra, R. and Roy, P. Structure-function elucidation of flavonoids by modern technologies. *CRC press (under review)*.

List of other Publications

10. Gupta, S., **Varshney, R.**, Jha, R.K., Pruthi, P.A., Roy, P. and Pruthi, V., 2017. In Vitro Apoptosis Induction in a Human Prostate Cancer Cell Line by Thermotolerant Glycolipid from *Bacillus licheniformis* SV1. *Journal of Surfactants and Detergents*, 20(5), pp.1141-1151.
11. Verma, P., Kar, B., **Varshney, R.**, Roy, P. and Sharma, A.K., 2017. Characterization of AICAR transformylase/IMP cyclohydrolase (ATIC) from *Staphylococcus lugdunensis*. *The FEBS journal*, 284(24), pp.4233-4261.
12. Singh, U.P., Singh, N., **Varshney, R.**, Roy, P. and Butcher, R.J., 2018. Synthesis of Fluorescent Nanoscale Salts/Metal–Organic Frameworks for Live-Cell Imaging. *Crystal Growth & Design*, 18(5), pp.2804-2813.
13. Saini, M., Masirkar, Y., **Varshney, R.**, Roy, P. and Sadhu, K.K., 2017. Fluorogen-free aggregation induced NIR emission from gold nanoparticles. *Chemical Communications*, 53(46), pp.6199-6202.
14. Bhardwaj, S., Maurya, N., Singh, A.K., **Varshney, R.** and Roy, P., 2016. Promising ESIPT-based fluorescence sensor for Cu²⁺ and CN⁻ ions: investigation towards logic gate behaviour, anticancer activities and bioimaging application. *RSC Advances*, 6(104), pp.102096-102101.
15. Gupta, S., Raghuvanshi, N., **Varshney, R.**, Banat, I.M., Srivastava, A.K., Pruthi, P.A. and Pruthi, V., 2017. Accelerated in vivo wound healing evaluation of microbial glycolipid containing ointment as a transdermal substitute. *Biomedicine & Pharmacotherapy*, 94, pp.1186-1196.
16. Raghuvanshi, N., Arora, N., **Varshney, R.**, Roy, P. and Pruthi, V., 2017. Antineoplastic and antioxidant potential of phycofabricated silver nanoparticles using microalgae *Chlorella minutissima*. *IET Nanobiotechnology*, 11(7), pp.827-834.
17. Raghuvanshi, N., Patel, A., Arora, N., **Varshney, R.**, Srivastava, A.K. and Pruthi, V., 2017. Antineoplastic and Antimicrobial Potential of Novel Phytofabricated Silver Nanoparticles from *Pterospermum acerifolium* Leaf Extract, 7, pp.220-232.

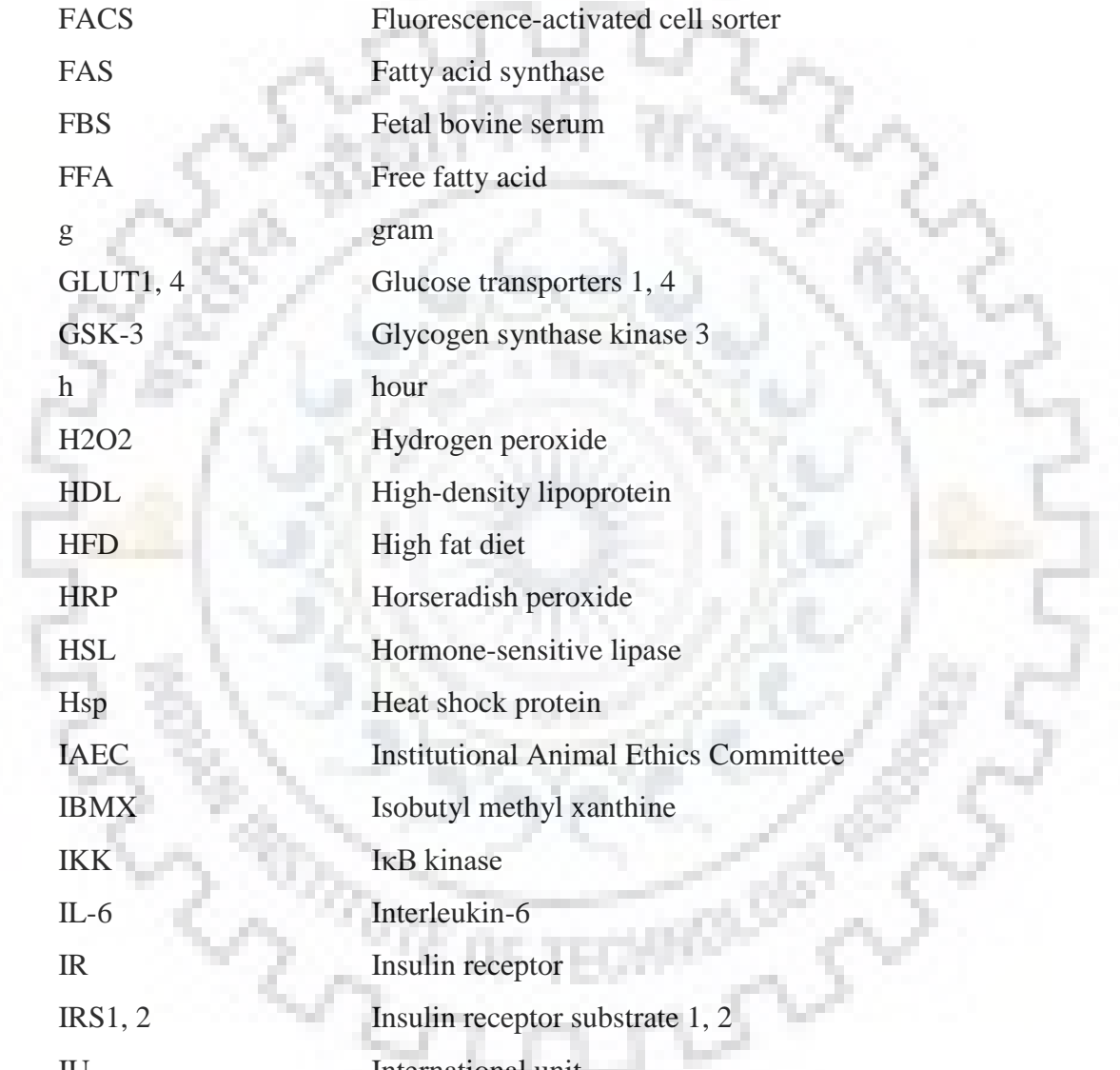
Conference Publications/Presentations

18. **Varshney, R.** and Roy, P., 2017. The role of lipophagy in kaempferol-facilitated regulation of lipid metabolism in pancreatic β -cells. *Autophagy: Cellular mechanism(s) and significance in health and disease. EMBO Symposia*, Bhubaneswar India.
19. **Varshney, R.** and Roy, P., 2014. A comparative analysis of various flavonoids in the regulation of Diabetes and Obesity: an in vitro study. *International conference on molecular signaling: recent trends in biomedical and translational research*, I.I.T Roorkee, India.
20. Kumar, N., **Varshney, R.** and Roy, P., 2017. From traditional ayurvedic medicine to modern medicine: polyphenolic compounds for suppression of cancer and other allied diseases, *NMPB-Sponsored National Conference on "Recent Advances in Ayurvedic Herbal Medicine - From Source to Manufacturing"* Organised by Faculty of Biomedical Sciences, Uttarakhand Ayurved University, Dehradun, India.
21. Gupta, P., Agrawal, A., **Varshney, R.**, Beniwal, S., Manhas, S., Roy, P. and Lahiri, D., 2015. Comparison of Neural Cell Adhesion and Neurite Outgrowth on Carbon Nanofiller Reinforced Biomimetic Polymeric Substrates, *International Conference on Nanostructured Polymeric Materials and Polymer Nanocomposites*, Kottayam, India.
22. Gupta, S., Raghuwanshi, N., **Varshney, R.**, Banat, I.M., Srivastava, A.K., Pruthi, P.A. and Pruthi, V., 2018. Bioprocessed surface-active glycolipid from *Bacillus licheniformis* SV1 for impaired skin wound interactions, *ECO-BIO 2018*, Dublin, Ireland.

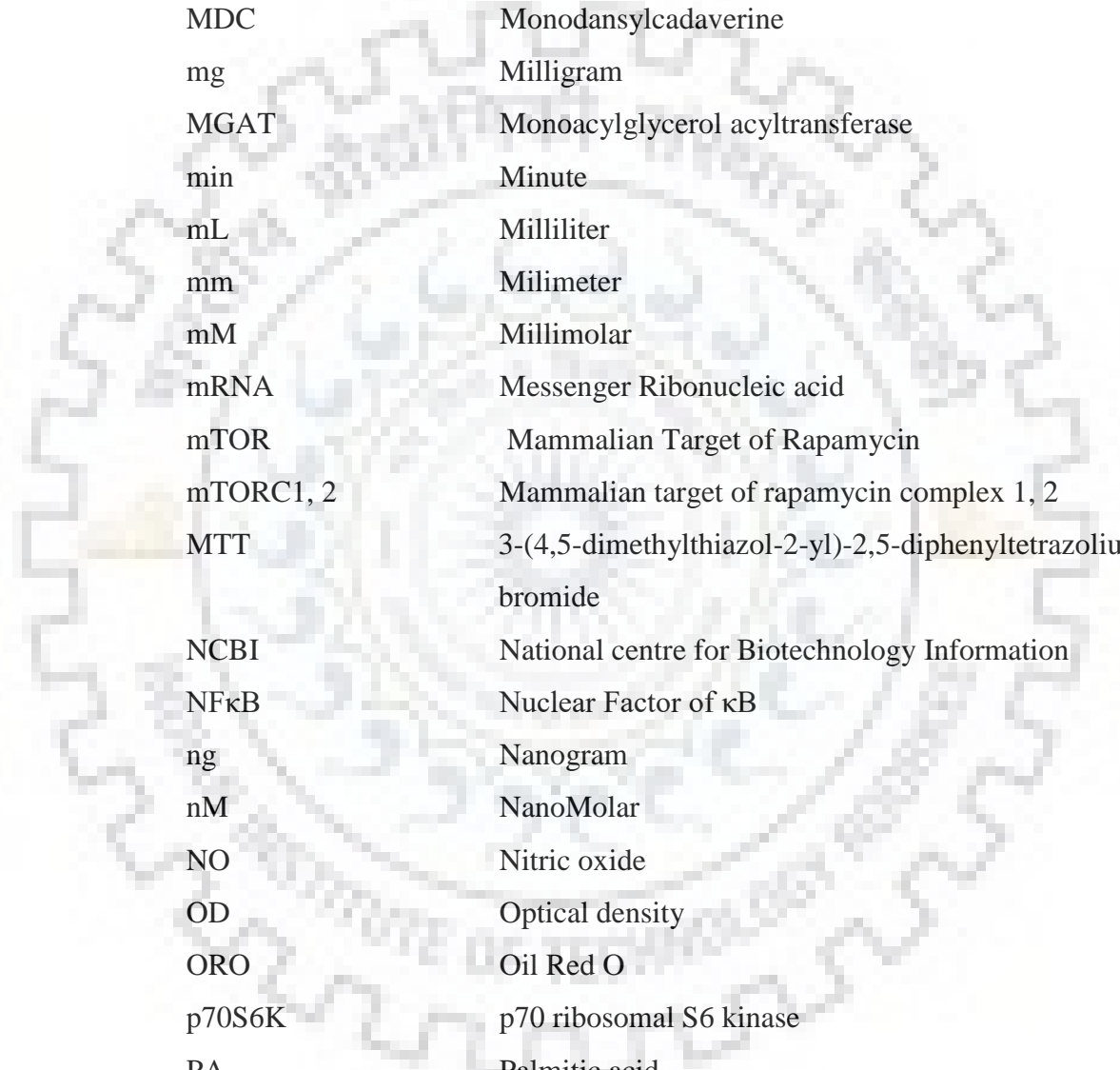


List of Abbreviations

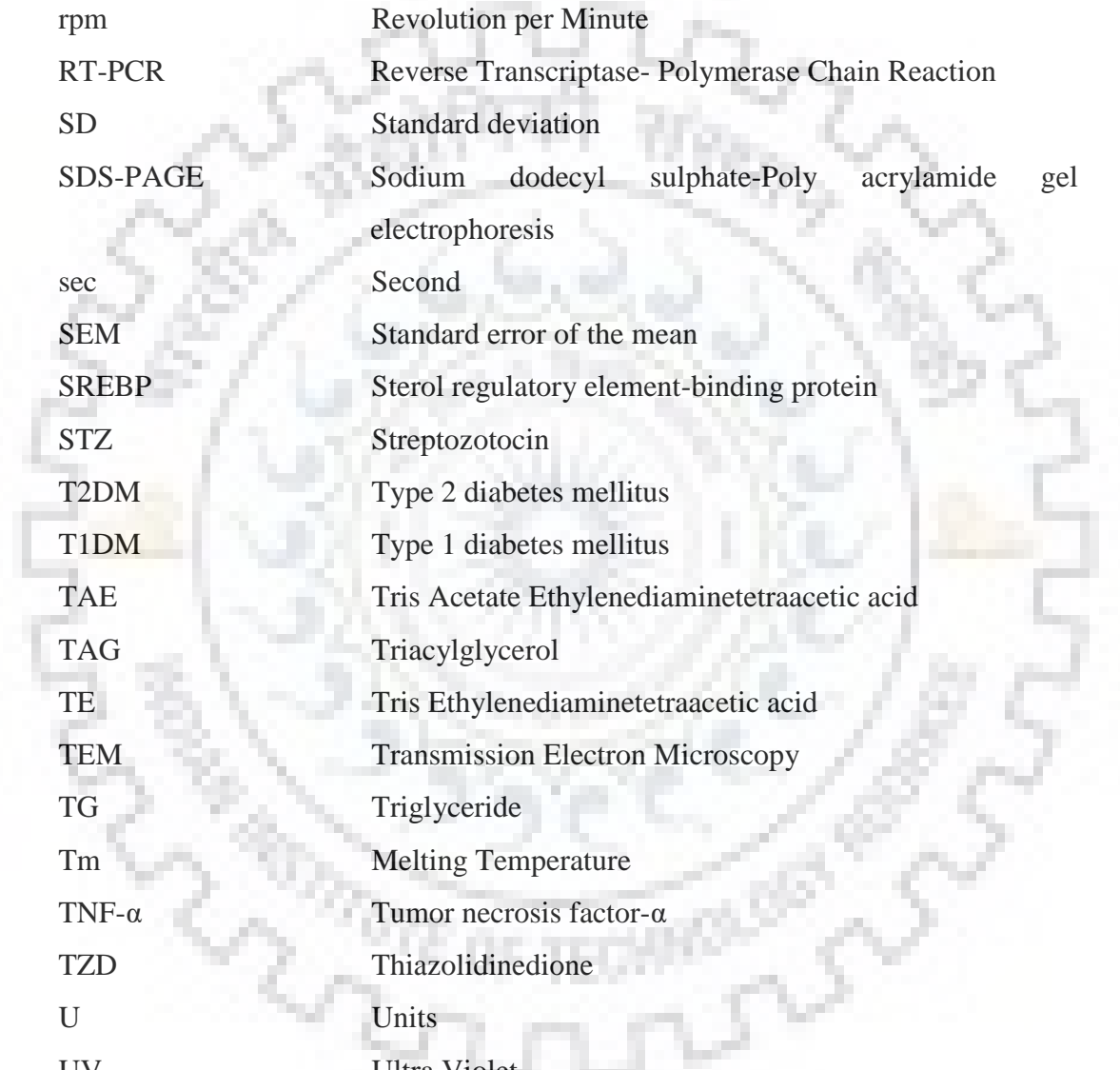
%	Percentage
°C	Degree centigrade
µg	Microgram
µl	Microliter
µm	Micrometer
µM	Micromolar
AMPK	5' adenosine monophosphate-activated protein kinase
ANOVA	Analysis of Variance
Atg	Autophagy-related protein
ATGL	Adipose triacylglyceride lipase
ATP	Adenosine triphosphate
Bax	BCL2-Associated X Protein
BCA	Bicinchoninic acid
BCL2	B-Cell Lymphoma 2
BMI	Body mass index
bp	Base pair
BSA	Bovine Serum Albumin
C	Control
C.C.	Compound C
cAMP	Cyclic Adenosine Monophosphate
cDNA	Complementary DNA
CHOP	C/EBP-protein homologous
CQ	Chloroquine
DAPI	4',6-diamidino-2-phenylindole
DGAT	Diacylglycerol acyltransferase
dH ₂ O	deionised water
dl	Deciliter
DMSO	Dimethyl sulfoxide
DNA	deoxyribonucleic acid
dNTP	deoxynucleotide Triphosphate
DTT	Dithiothreitol



EB	Ethidium Bromide
ECL	Enhanced chemiluminescence
EDTA	Ethylene diamine tetra acetic acid
ER	Endoplasmic Reticulum
ERK	Extracellular-signal regulated kinases
FABP4/aP2	Fatty acid binding protein 4
FACS	Fluorescence-activated cell sorter
FAS	Fatty acid synthase
FBS	Fetal bovine serum
FFA	Free fatty acid
g	gram
GLUT1, 4	Glucose transporters 1, 4
GSK-3	Glycogen synthase kinase 3
h	hour
H2O2	Hydrogen peroxide
HDL	High-density lipoprotein
HFD	High fat diet
HRP	Horseradish peroxidase
HSL	Hormone-sensitive lipase
Hsp	Heat shock protein
IAEC	Institutional Animal Ethics Committee
IBMX	Isobutyl methyl xanthine
IKK	I κ B kinase
IL-6	Interleukin-6
IR	Insulin receptor
IRS1, 2	Insulin receptor substrate 1, 2
IU	International unit
I κ B	Inhibitor of kappa B
JNK	c-Jun N-terminal kinase
K	Kaempferol
kD	Kilo Dalton
kg	Kilogram
L	Liter



LC3	Light chain 3
LD	Lipid droplet
LDL	Low-density lipoprotein
LPL	Lipoprotein lipase
M	Molar
MAPK	Mitogen associated protein kinase
MDC	Monodansylcadaverine
mg	Milligram
MGAT	Monoacylglycerol acyltransferase
min	Minute
mL	Milliliter
mm	Millimeter
mM	Millimolar
mRNA	Messenger Ribonucleic acid
mTOR	Mammalian Target of Rapamycin
mTORC1, 2	Mammalian target of rapamycin complex 1, 2
MTT	3-(4,5-dimethylthiazol-2-yl)-2,5-diphenyltetrazolium bromide
NCBI	National centre for Biotechnology Information
NF κ B	Nuclear Factor of κ B
ng	Nanogram
nM	NanoMolar
NO	Nitric oxide
OD	Optical density
ORO	Oil Red O
p70S6K	p70 ribosomal S6 kinase
PA	Palmitic acid
PBS	Phosphate buffer saline
PCR	Polymerase Chain Reaction
PI3K	Phosphoinositide 3-kinase
PKA, B, C	Protein kinase A, B, C
PLIN	Perilipin
PMSF	Phenylmethylsulphonyl fluoride



PPAR	Peroxisome proliferator-activated receptors
ppm	Parts Per Million
PPRE	Peroxisome proliferating response element
PVDF	Polyvinylidene fluoride
RNA	Ribo Nucleic Acid
ROS	Reactive oxygen species
rpm	Revolution per Minute
RT-PCR	Reverse Transcriptase- Polymerase Chain Reaction
SD	Standard deviation
SDS-PAGE	Sodium dodecyl sulphate-Poly acrylamide gel electrophoresis
sec	Second
SEM	Standard error of the mean
SREBP	Sterol regulatory element-binding protein
STZ	Streptozotocin
T2DM	Type 2 diabetes mellitus
T1DM	Type 1 diabetes mellitus
TAE	Tris Acetate Ethylenediaminetetraacetic acid
TAG	Triacylglycerol
TE	Tris Ethylenediaminetetraacetic acid
TEM	Transmission Electron Microscopy
TG	Triglyceride
T _m	Melting Temperature
TNF- α	Tumor necrosis factor- α
TZD	Thiazolidinedione
U	Units
UV	Ultra Violet
VLDL	Very-low density lipoprotein
WHO	World health organization
WT	Wortmannin

List of Contents

Abstract	i
Acknowledgement	v
List of Publications	ix
List of abbreviations	xiii
List of Contents	xvii
List of Figures	xxviii
List of Tables	xxxvii
1. Introduction	1
2. Literature Review	5
2.1. Introduction	5
2.1.1. Type 1 diabetes /insulin dependent diabetes	5
2.1.2. Type 2 diabetes /non-insulin dependent diabetes	6
2.1.3. Gestational diabetes mellitus (GDM)	6
2.1.4. Specific types of diabetes due to other causes	7
2.2. Diagnostic criteria for diabetes	7
2.3. Global burden of diabetes	8
2.4. Complications associated with diabetes	8
2.4.1. Microvascular complications	9
2.4.1.1. Diabetic retinopathy	9
2.4.1.2. Diabetic neuropathy	9
2.4.1.3. Diabetic nephropathy	9
2.4.2. Macrovascular complications	9
2.4.2.1. Cardiovascular complications	9
2.4.3. Other related complications	10
2.4.3.1. Cataract	10
2.4.3.2. Glaucoma	10
2.4.3.3. Osteoarthritis and osteoporosis	10
2.5. Type 2 diabetes mellitus (T2DM)	10
2.5.1. Risk factors associated with type 2 diabetes mellitus progression	10
2.5.1.1. Body mass index (BMI)	11
2.5.1.2. Genetic factors	11
2.5.1.3. Hypertension	11

2.5.1.4. Physical inactivity	12
2.5.1.5. Dietary pattern	12
2.5.1.6. Obesity	12
2.5.2. Obesity and Diabetes – the connecting link	13
2.5.3. Pathophysiology of type 2 diabetes mellitus	14
2.5.3.1. β -cell dysfunction	15
2.5.3.1.1. Pancreas	16
2.5.3.1.2. Insulin	17
2.5.3.1.3. Insulin release	18
2.5.3.1.4. Cellular action of insulin	19
2.5.3.1.4.1. Glucose metabolism	19
2.5.3.1.4.2. Lipid metabolism	19
2.5.3.1.4.3. Protein metabolism	20
2.5.3.1.5. Insulin signaling pathway	20
2.5.3.2. Insulin resistance	21
2.5.3.2.1. Adipocytes and insulin resistance	23
2.5.3.2.1.1. Lipotoxicity	23
2.5.3.2.1.2. Inflammation	23
2.5.3.2.1.3. Mitochondrial dysfunction	24
2.5.3.2.1.4. ER stress	24
2.5.3.2.2. Skeletal muscle and insulin resistance	24
2.5.3.2.3. Hepatocytes and insulin resistance	24
2.6. Treatment	26
2.6.1. Conventional therapy	26
2.6.1.1. Insulin secretagogues	27
2.6.1.1.1. Sulfonylureas	27
2.6.1.1.2. Meglitinides	27
2.6.1.2. Insulin sensitizers	27
2.6.1.2.1. Metformin	27
2.6.1.2.2. Thiazolidinediones	28
2.6.1.3. Insulin	28
2.6.1.4. α -glucosidase inhibitors	28
2.6.2. Novel anti-diabetic drugs	28

2.6.2.1. Incretin system	29
2.6.2.2. GLP-1 receptor agonists	29
2.6.2.3. Dipeptidyl peptidase 4 inhibitors	29
2.6.2.4. Pramlintide	29
2.6.3. Bariatric surgery	30
2.6.4. Current therapies	30
2.6.4.1. β -cell regeneration therapy	30
2.6.4.2. Transdifferentiation/ reprogramming of various non- β -cells	31
2.6.4.3. Induction of replication of existing β -cell and islet neogenesis	32
2.6.4.4. Cytoprotection of apoptotic β -cells	33
2.7. Autophagy	33
2.7.1. Types of autophagy	34
2.7.1.1. Microautophagy	34
2.7.1.2. Chaperone-mediated autophagy (CMA)	35
2.7.1.3. Macroautophagy	35
2.7.1.3.1. Molecular mechanism of macroautophagy	35
2.7.2. Autophagy in diabetes	40
2.7.3. Liver complications and autophagy	40
2.7.4. Hepatic steatosis and lipophagy	41
2.7.5. ER stress-induced hepatic insulin resistance	43
2.7.6. Autophagy: a potential link between ER stress and insulin resistance	45
2.7.7. Autophagy and β -cell	47
2.7.7.1. Autophagy in the resolution of β -cell ER stress	49
2.7.7.2. Extracellular signals that regulate β -cell autophagy	51
2.7.8. Novel therapeutic approaches to target autophagy in endocrine and metabolic disorders	53
2.7.8.1. mTORC1 inhibitors and rapalogs	53
2.7.8.2. AMPK/SIRT1 activators	53
2.7.8.3. Other strategies to modulate autophagy in metabolic disorders	54
2.8. Conventional versus herbal medicines	55
2.8.1. Phytochemicals	56
2.8.1.1. Phenolics	57
2.8.1.1.1. Flavonoids	58

2.8.1.1.1.1. Flavonols	58
2.8.1.1.1.1.1. Quercetin	59
2.8.1.1.1.1.2. Rutin	60
2.8.1.1.1.1.3. Myricetin	61
2.8.1.1.1.1.4. Kaempferol	62
2.9. The problems addressed in the present thesis	63
3. Materials and Methods	
3.1. Introduction	65
3.2. Materials	
3.3. <i>In vitro</i> experimental models	66
3.3.1. Cell lines and cell culture	66
3.4. Isolation and culture of rat pancreatic islets for <i>ex vivo</i> studies	67
3.4.1. Identification of pancreatic islets	67
3.5. <i>In vivo</i> experimental models	67
3.5.1. Experimental design	68
3.5.2. Model development	68
3.5.3. Experimental treatment	69
3.5.4. Autophagy flux determination	69
3.6. Preparation of palmitic acid-containing media	69
3.7. MTT assay for cell viability	69
3.8. Adipocyte differentiation	70
3.9. Oil Red O staining for lipids	70
3.10. Measurement of intracellular triglyceride content	71
3.11. Labeling of lipid droplets with BODIPY stain	71
3.12. L6 cell differentiation	72
3.13. Glucose uptake assay	72
3.14. Bromo-2'-deoxyuridine (BrdU) incorporation assay	72
3.15. Hoechst 33342 staining for monitoring nuclear morphology of apoptotic cells	73
3.16. DNA ladder assay	73
3.17. Labeling of autophagic vacuoles and lysosomes with MDC and LysoTracker	74

3.18. Cell transfection and stable cell line establishment	74
3.19. LC3 puncta assays	75
3.20. Flow cytometer analysis for autophagy quantification	75
3.21. Transmission electron microscopy analysis	75
3.22. Insulin secretion and content analysis	76
3.23. Bacterial transformation and plasmid preparation	76
3.24. Plasmid isolation	77
3.25. Transfection of DNA into mammalian cell lines	77
3.26. Luciferase assay	78
3.27. siRNA transfections	78
3.28. RNA isolation	78
3.29. Semi-quantitative reverse transcription polymerase chain reaction (RT PCR)	79
3.29.1. First strand cDNA synthesis (reverse transcription)	79
3.29.2. PCR amplification	79
3.29.3. Agarose gel electrophoresis	82
3.30. Western blot analysis	82
3.31. Immunofluorescence study	83
3.32. Double immunofluorescence and co-localization studies	84
3.33. Measurement of lipid profile	85
3.34. Estimation of fasting blood glucose (FBG) and glucose tolerance test (GTT)	85
3.35. Insulin tolerance test	85
3.36. Fasting and glucose-stimulated insulin secretion	85
3.37. Pancreatic insulin content analysis	85
3.38. Histopathological studies	86
3.39. Immunohistochemistry	86
3.40. Statistical analysis	87

4. Screening of various flavonoids for their anti-obesity and antidiabetic activities: an *in vitro* and *in vivo* study

4.1. Introduction	89
4.2. Brief methodology	91
4.2.1. Cell culture and treatment	91

4.2.2. MTT assay for determination of cell viability	91
4.2.3. Adipocyte differentiation assay	91
4.2.4. Estimation of intracellular lipid contents	91
4.2.5. Preparation of palmitic acid (PA)-containing media	92
4.2.6. L6 cell culture and differentiation	92
4.2.7. Glucose uptake assay	92
4.2.8. Experimental animals	93
4.2.9. Experimental design	93
4.2.10. Model development	93
4.2.11. Experimental treatment	94
4.2.12. Estimation of blood parameters	94
4.2.13. Glucose tolerance test (GTT) and insulin tolerance test (ITT)	94
4.2.14. Statistical analysis	95
4.3. Results	95
4.3.1. Anti-adipogenic activity of flavonoids on 3T3-L1 cells	95
4.3.2. Flavonoids alter genes involved in pre-adipocyte differentiation	97
4.3.3. Flavonoids instigate glucose uptake in PA-induced L6 muscle cells	99
4.3.4. Flavonoids stimulate GLUT4 expression and related insulin signaling pathway in PA-induced L6 muscle cells	101
4.3.5. Flavonoids improve body weight and lipid profile in HFD-STZ-induced diabetic mice	103
4.3.6. Flavonoids improve fasting blood glucose level, glucose tolerance and insulin sensitivity in HFD-STZ-induced diabetic mice	105
4.3.7. Effects of flavonoids in autophagy induction in RIN-5F clonal pancreatic β -cells	107
4.4. Discussion	109

5. Understanding the autophagy stimulatory and anti-apoptotic effects of kaempferol

5.1. Establishment of RIN-5F EGFP-LC3 expressing stable cell line

5.1.1. Introduction	113
5.1.2. Methodology	115
5.1.2.1. Cell line and culture	115
5.1.2.2. Bacterial transformation and plasmid preparation	115

5.1.2.3. Plasmid isolation	115
5.1.2.4. Cell transfection and stable cell line establishment	115
5.1.3. Results	116
5.1.4. Discussion	118

5.2. Role of kaempferol in the modulation of autophagy and its effect on protection of pancreatic β -cells under lipid overload condition

5.2.1. Introduction	121
5.2.2. Brief methodology	124
5.2.2.1. Cell culture and treatment	124
5.2.2.2. siRNA transfections	124
5.2.2.3. Animals	124
5.2.2.4. Islets isolation and treatment	125
5.2.2.5. Preparation of PA-containing media	125
5.2.2.6. 5-Bromo-2'-deoxyuridine (BrdU) incorporation assay	126
5.2.2.7. Hoechst 33342 staining for monitoring nuclear morphology of apoptotic cells	126
5.2.2.8. DNA ladder assay	126
5.2.2.9. Labeling of autophagic vacuoles and lysosomes with MDC and LysoTracker	126
5.2.2.10. Cell transfection and stable cell line establishment	126
5.2.2.11. LC3 puncta assays	127
5.2.2.12. Flow cytometer analysis for autophagy quantification	127
5.2.2.13. Transmission electron microscopy analysis of autophagic vacuoles	128
5.2.2.14. Immunofluorescence study	128
5.2.2.15. Statistical analysis	128
5.2.3. Results	129
5.2.3.1. Effect of kaempferol on cell viability and proliferation	129
5.2.3.2. Kaempferol attenuates PA-induced lipotoxicity in RIN-5F cells	130
5.2.3.3. Kaempferol induces autophagy in PA-stressed RIN-5F cells	132
5.2.3.4. Autophagy inhibitors impair kaempferol-induced autophagic activity	136
5.2.3.5. Kaempferol instigates autophagy through AMPK/mTOR pathway	142
5.2.3.6. Inhibition of autophagy impairs the cytoprotective role of kaempferol	146

5.2.3.7. Effects of kaempferol on isolated rat pancreatic islets under PA-induced condition	150
5.2.4. Discussion	152
6. Role of kaempferol-mediated autophagy in alleviation of palmitic acid-induced lipid stores, endoplasmic reticulum stress and pancreatic β-cell dysfunction	
6.1. Introduction	157
6.2. Brief methodology	160
6.2.2. Cell culture and treatment	160
6.2.3. siRNA transfections	160
6.2.4. Animals	161
6.2.5. Islets isolation and treatment	161
6.2.6. Preparation of palmitic acid-containing media	161
6.2.7. Labeling of lipid droplets with BODIPY stain	161
6.2.8. Double immunofluorescence and co-localization studies	162
6.2.9. Insulin secretion and content analysis	162
6.2.10. Statistical analysis	163
6.3. Results	163
6.3.1. Kaempferol inhibits intracellular lipid accumulation in RIN-5F cells	163
6.3.2. Kaempferol-induced autophagy facilitates a decrease in PA-induced lipid stores	166
6.3.3. AMPK/mTOR pathway signaling mediates kaempferol-mediated lipophagy	172
6.3.4. Kaempferol-induced autophagy abolishes PA-induced ER stress in RIN-F cells	175
6.3.5. Kaempferol-induced autophagy restores the PA-induced β -cells dysfunction	177
6.3.6. Kaempferol-induced autophagy abolishes PA-induced increased lipid stores, ER stress and β -cell dysfunction in primary islets	179
6.4. Discussion	183
7. Role of kaempferol in restoration of autophagy and functional pancreatic β-cell mass in a murine model of type 2 diabetes	
7.1. Introduction	187

7.2. Brief methodology	189
7.2.1. Experimental animals	189
7.2.2. Experimental design	190
7.2.3. Model development	190
7.2.4. Experimental treatment	191
7.2.5. Autophagy flux determination	191
7.2.6. Estimation of blood parameters	191
7.2.7. Glucose tolerance test (GTT) and insulin tolerance test (ITT)	192
7.2.8. Fasting and glucose-stimulated insulin secretion	192
7.2.9. Pancreatic insulin content analysis	192
7.2.10. Immunoblot analysis	192
7.2.11. Histopathological studies	193
7.2.12. Immunohistochemistry	193
7.2.13. Statistical analysis	193
7.3. Results	194
7.3.1. Kaempferol improves body weight and lipid profile in HFD-STZ-induced diabetic mice	194
7.3.2. Kaempferol improves fasting glucose level, glucose tolerance and insulin sensitivity	195
7.3.3. Kaempferol improves pancreatic insulin content and insulin secretion	196
7.3.4. Kaempferol induces autophagy in HFD-STZ-induced diabetic mice	198
7.3.5. Chloroquine treatment impairs kaempferol-induced autophagic flux	201
7.3.6. Kaempferol-induced autophagy alleviates ER stress and apoptosis of β -cells and preserves β -cell mass	204
7.3.7. Kaempferol-induced autophagy improved insulin content and secretion	207
7.4. Discussion	209

8. Role of kaempferol-induced autophagy in amelioration of hepatic lipid accumulation and insulin resistance: an in vitro and in vivo study

8.1 Introduction	215
8.2. Materials and methods	217
8.2.1. Cell culture and treatment	217
8.2.2. siRNA transfections	217
8.2.3. Luciferase reporter assay	218

8.2.4. Preparation of PA-containing media	218
8.2.5. Oil Red O staining for lipids	218
8.2.6. Labeling of autophagic vacuoles and lysosomes with mono dansylcadaverine (MDC) and LysoTracker stains	219
8.2.7. Experimental animals	219
8.2.8. Experimental design	219
8.2.9. Model development	220
8.2.10. Experimental treatment	220
8.2.11. Autophagy flux determination	221
8.2.12. Transmission electron microscopy (TEM) analysis	221
8.2.13. Measurement of lipid profile	221
8.2.14. Statistical analysis	221
8.3. Results	222
8.3.1. Kaempferol inhibits lipid accumulation in PA-induced HepG2 cells	222
8.3.2. Kaempferol up-regulates PPAR- α expression and increases cytosolic lipolysis in PA-induced HepG2 cells	224
8.3.3. Kaempferol enhances autophagy in PA-induced HepG2 cells	225
8.3.4. AMPK signaling is involved in kaempferol-mediated autophagy induction	230
8.3.5. Inhibition of autophagy blocks kaempferol-induced reduction of lipid accumulation	232
8.3.6. Kaempferol improves lipid profile and insulin resistance in HFD-STZ induced diabetic mice	234
8.3.7. Kaempferol induces autophagy in the liver of HFD-STZ mice	235
8.3.8. Kaempferol-induced autophagy is involved in inhibition of lipid accumulation in the liver of HFD-STZ mice	237
8.3.9. Kaempferol-induced autophagy rescues HFD induced ER-stress and insulin signaling	241
8.4. Discussion	243
9. Summary	247
10. Bibliography	259

List of Figures

Figure 2.1.	Diagnostic criteria for diabetes mellitus (as standardized by ADA)	7
Figure 2.2.	Major complications associated with diabetes mellitus	8
Figure 2.3.	Risk factors associated with development and progression of type 2 diabetes mellitus.	11
Figure 2.4.	General scheme of insulin production and function in type 2 diabetes mellitus	15
Figure 2.5.	Diagrammatic representation of structure of human insulin	17
Figure 2.6.	Mechanism showing glucose stimulated insulin release in pancreatic β -cells	18
Figure 2.7.	Schematic representation of insulin signaling pathway	21
Figure 2.8.	Negative regulation of Ser/Thr activation on insulin signalling molecules	22
Figure 2.9.	General scheme showing obesity linked hepatic insulin resistance	25
Figure 2.10.	General scheme showing activation of the UPR and ER stress signalling pathways in the liver under normal and diabetic conditions	26
Figure 2.11.	Schematic representation of microautophagy and macroautophagy in yeast	34
Figure 2.12.	General scheme showing mechanism of macroautophagy	37
Figure 2.13.	General scheme showing effect of autophagy in liver	41
Figure 2.14.	Schematic representation showing crosstalk between obesity, hyper-insulinemia and autophagy	43
Figure 2.15.	Autophagy in the context of β -cell dysfunction	48
Figure 2.16.	Shematic representation showing regulation of β -cell autophagy	52
Figure 2.17.	Structure of 2-phenylbenzopyrone	58
Figure 2.18.	Hydroxyflavone as a basic flavone structure	59

Figure 2.19.	Structure of Quercetin	59
Figure 2.20.	Structure of Rutin	60
Figure 2.21.	Structure of myricetin	61
Figure 2.22.	Structure of Kaempferol	62
Figure 4.1.	Effects of flavonoids on cell viability and 3T3-L1 pre-adipocyte differentiation. (a) MTT assay after 48 h; (b) Representative images showing Oil Red O staining after 8 days of differentiation. Histogram representing (c) lipid content and (d) intracellular triglyceride content of treated cells.	96
Figure 4.2.	Effects of flavonoids on adipocyte-specific genes in differentiated 3T3-L1 adipocytes. Representative (a) RT-PCR analysis of genes involved in adipogenesis; (b) Immunoblot of PPAR- γ protein in response to 10 μ M concentration of quercetin/ rutin/ myricetin or kaempferol.	98
Figure 4.3.	Role of flavonoids on cell viability and insulin-stimulated glucose uptake in differentiated L6 muscle cells. Representative histogram showing MTT assay in (a) absence and (b) presence of PA (0.5 mM) along with respective flavonoids for 24 h; (c) Glucose uptake in insulin-stimulated differentiated L6 cells in presence of PA treatment.	100
Figure 4.4.	Effects of flavonoids on insulin signaling pathway in PA-induced insulin resistant L6 myotubes. Representative (a) RT-PCR analysis of <i>Glut4</i> gene; (b) Immunoblots of proteins involved in insulin signaling pathway and glucose uptake.	102
Figure 4.5.	Effects of flavonoids on metabolic profile in diabetic mice. Histogram showing (a) Body weight; (b) Total cholesterol; (c) Triglycerides; (d) LDL and (e) NEFA level in serum of treated mice. Blood glucose concentrations measured (f) during fasting condition; after administration of (g) glucose for glucose tolerance test (GTT) and (h) insulin for insulin tolerance test (ITT) after 16 weeks of the experiment.	104
Figure 4.6.	Effects of flavonoids in the improvement of glucose and insulin tolerance in diabetic mice. (a) Histogram showing fasting glucose levels of mice from different treatment groups. Blood glucose concentrations measured after administration of (b) glucose for glucose tolerance test and	106

(c) insulin for insulin tolerance test after 16 weeks of the experiment.

- Figure 4.7.** Role of flavonoids in instigating autophagy in PA-induced RIN-5F clonal β -cells. (a) MTT assay (b) Representative confocal images of MDC-LysoTracker stained cells to selectively stain autophagosomes and lysosomes in response to 10 μ M concentration of quercetin/ rutin/ myricetin/ kaempferol or 200 nM temsirolimus (positive control) in presence of 0.5 mM PA for 24 h. 108
- Figure. 5.1.1.** Schematic representation showing EGFP-LC3 puncta formation in response to autophagy induction in EGFP-LC3 transfected cells. 114
- Figure. 5.1.2.** Phase contrast and fluorescent microscopic images of EGFP-LC3 transfected RIN-5F cells at different time intervals. 117
- Figure. 5.1.3.** Phase contrast and fluorescent microscopic images of RIN-5F-EGFP-LC3 cells stably expressing EGFP-LC3 at different passage numbers in culture. 118
- Figure. 5.2.1.** Effect of kaempferol on the viability and proliferation of RIN-5F cells. (a) MTT assay and (b) BrdU incorporation assay. 129
- Figure. 5.2.2.** Kaempferol attenuates PA-induced lipotoxicity of RIN-5F cells. (a) Cell viability as determined by MTT assay; (b) Nuclear morphological changes as monitored by Hoechst 33342 staining; (c) Apoptotic nucleic acid as detected by DNA ladder formation analysis; (d) Representative RT-PCR for pro-apoptotic and anti-apoptotic marker genes. (e) Immunoblot analysis for cleaved caspase-3. 131
- Figure. 5.2.3.** Kaempferol induces autophagy in PA-stressed clonal pancreatic β -cells. (a) Representative confocal images to show autophagosomes, lysosomes and autophagolysosomes stained cells using MDC-LysoTracker stain. Images are representative of three independent experiments. (b) Representative RT-PCR analysis showing autophagy-related genes in response to increasing doses of kaempferol. 134
- Figure. 5.2.4.** Kaempferol induces autophagy by altering the expression of genes involved in autophagic process in RIN-5F cells. (a) Representative confocal images depicting EGFP-LC3 puncta formation in response to various treatments. Representative immunoblot analysis for the expression of LC3 and p62 with (b) increasing doses and (c) time duration of kaempferol treatment. 136

- Figure. 5.2.5.** Autophagy inhibitors impair kaempferol-induced autophagy. Representative confocal images of three independent experiments showing autophagosomes, lysosomes and autophagolysosomes stained by MDC-LysoTracker stain. 137
- Figure. 5.2.6.** Autophagy inhibitors alter cellular architectures in kaempferol-induced autophagy. Representative TEM images showing ultrastructure of RIN-5F cells incubated with kaempferol (10 μ M) with or without chloroquine (10 μ M) in presence of PA (0.5 mM). 138
- Figure. 5.2.7.** Autophagy inhibitors impair kaempferol-induced autophagy by altering autophagy-linked gene expressions. (a) Representative confocal images of EGFP-LC3 puncta formation in response to various treatments. (b) Representative histogram showing normalized frequency percentage versus EGFP-LC3 fluorescence intensity as depicted by flow cytometry analysis of RIN-5F cells stably expressing EGFP-LC3. Representative data is of three independent experiments. (c) and (d) Representative immunoblot analysis of autophagy marker proteins in response to various treatments. 141
- Figure. 5.2.8.** Effects of autophagy inhibitors on the expression LC3 protein. Representative immunofluorescence analysis for the expression of LC3 in RIN-5F cells in presence of various treatments and imaged under a confocal microscope. 142
- Figure. 5.2.9.** Kaempferol-induced regulation of autophagy through AMPK/mTOR pathway. Representative immunoblot analysis of the phosphorylation of AMPK and mTOR in RIN-5F cells in response to kaempferol treatment for varying (a) time period; (b) dosages; (c) dosages in presence of AMPK inhibitor i.e. compound C (10 μ M); and (d) at 10 μ M dose in presence of AMPK siRNA. 143
- Figure. 5.2.10.** Effect of AMPK inhibitor on autophagolysosomes formation in RIN-5F cells. Representative confocal images depicting (a) Autophagosomes, lysosomes and autophagolysosomes stained by MDC-LysoTracker stain; (b) EGFP-LC3 puncta formation and (c) Immunofluorescence analysis for the expression of LC3 in RIN-5F cells treated with kaempferol (10 μ M) with or without compound C (10 μ M) in presence of PA. 145
- Figure. 5.2.11.** Inhibition of autophagy impairs the cytoprotective role of kaempferol. The histograms in (a), (b) and (c) represent percentage cell viability in response to various treatments and expressed as percent of cell viability over control (BSA) as depicted by MTT assay. (d) The histogram shows 147

quantification of incorporated BrdU represented as fold change in fluorescent intensity of control in response to various treatments. (e) Representative confocal images of nuclear staining of treated cells showing condensed and fragmented nucleus (arrows).

- Figure. 5.2.12.** AMPK/mTOR mediated autophagy is involved in kaempferol-mediated cytoprotective role on PA-stressed RIN-5F cells. (a) Representative gel image showing the DNA ladder formation in response to various treatments. Representative immunoblot showing the expression of cleaved caspase-3 in response to (b) wortmannin and chloroquine, (c) compound C, (d) Atg7 siRNA and (e) AMPK siRNA. 149
- Figure. 5.2.13.** Kaempferol exerts cytoprotective role on rat pancreatic islets through AMPK/mTOR-mediated autophagy induction. (a) Representative confocal images to show autophagosomes, lysosomes and autophagolysosomes stained islet cells using MDC-LysoTracker stain. Representative immunoblot analysis of various proteins in response to inhibitors of (b) autophagy and (c) AMPK. 151
- Figure 6.1.** Kaempferol alleviates PA-induced clonal pancreatic β -cells lipid stores. RIN-5F cells were treated with kaempferol (10 μ M) in presence or absence of PA (0.5 mM) for 48 h. (a) Microscopic images of Oil Red O stained cells; Histogram representing (b) lipid content; (c) triglyceride content within treated cells. Results are the mean \pm S.D. of three independent experiments; (d) Representative confocal images showing BODIPY- and DAPI-stained cells. 164
- Figure 6.2.** Kaempferol alters expression of genes involved in lipid metabolism. Representative (a) RT-PCR analysis of lipid droplets marker genes and (b) immunoblot of PLIN2 with increasing dose and (c) time durations. 165
- Figure 6.3.** Kaempferol-induced autophagy facilitates decrease in PA-induced lipid stores. (a) Microscopic images of Oil Red O stained cells; Histogram representing (b) lipid content; (c) triglyceride content of treated cells. 167
- Figure 6.4.** Autophagy inhibition abolishes kaempferol-reduced lipid droplets accumulation. Representative confocal images showing lipid droplets as stained by BODIPY stain and counterstaining with DAPI after RIN-5F cells were incubated with (a) kaempferol (10 μ M) with or without wortmannin (100 nM) or chloroquine (10 μ M) in presence of PA (0.5 mM) for 48 h; (b) kaempferol in two different 168

conditions i.e., co-treatment with PA and kaempferol for 48 h or pre-incubated with PA for 12 h followed by kaempferol treatment for next 36 h.

- Figure 6.5.** Kaempferol treatment exhibits co-localization of lipid droplets to autophagolysosomes. Representative confocal images showing co-localization of BODIPY stained lipid droplets to autophagosomes as well as lysosomes stained by MDC and LysoTracker respectively. 169
- Figure 6.6.** Autophagy inhibitors impair kaempferol-induced reduction of lipid deposition by altering autophagy-linked gene expressions. Representative immunoblots of various proteins in response to (a) wortmannin and chloroquine and (b) Atg7 siRNA. 170
- Figure 6.7.** Autophagy inhibitors attenuate kaempferol-induced sequestration of lipid droplets into autophagosomes. Representative confocal images showing co-localization of immunostained LC3 protein with BODIPY-stained lipid droplets after RIN-5F cells were treated with kaempferol (10 μ M) with or without various inhibitors in presence of PA (0.5 mM) for 48 h. 171
- Figure 6.8.** Inhibition of autophagy impairs interaction of LC3 protein with PLIN2 protein. Representative confocal images showing co-localization of LC3 protein with PLIN2 protein as visualized by double immunofluorescence labeling. 172
- Figure 6.9.** AMPK/mTOR signaling is involved in kaempferol-induced reduction of lipid stores. (a) Representative microscopic images of Oil Red O stained cells. Histograms represent quantification of (b) lipid and (c) triglyceride content within cells. (d) Representative confocal images showing BODIPY- and DAPI-stained cells. 173
- Figure 6.10.** AMPK inhibitors abolish kaempferol-mediated lipophagy. Representative immunoblots of various proteins in presence of (a) compound C (10 μ M) and (b) AMPK siRNA. 174
- Figure 6.11.** Inhibition of AMPK prevents sequestration of lipid droplets into autophagosomes. Representative confocal images showing immunostained co-localization of (a) LC3 protein with BODIPY-stained lipid droplets and (b) LC3 and PLIN2, as detected by double immunofluorescence staining. 175
- Figure 6.12.** Kaempferol-induced autophagy abolishes PA-induced ER stress in RIN-5F cells. Representative immunoblot showing expression of CHOP protein in response to kaempferol treatment with (a) increasing doses; (b) varying time; (c) 176

chemical inhibitors of autophagy; (d) Atg7 siRNA; (e) chemical inhibitor of AMPK and (f) AMPK siRNA.

- Figure 6.13.** Kaempferol-induced autophagy restores the insulin-secreting function of PA-stressed RIN 5F cells. The histograms in (a) and (b) represents the level of secreted insulin in response to various treatments in presence of 2.8 or 16.7 mM glucose; while (c) and (d) represents intracellular insulin contents in presence of 16.7 mM glucose. 178
- Figure 6.14.** AMPK/mTOR-mediated lipophagy is involved in kaempferol-facilitated decrease in lipid stores in rat primary islets cells. (a) Representative confocal images showing co-localization of BODIPY stained lipid droplets to autophagosomes as well as lysosomes stained by MDC and LysoTracker respectively. Representative immunoblots of various proteins in presence of (b) wortmannin and chloroquine; (c) compound C. 180
- Figure 6.15.** Autophagy and AMPK inhibitors abolish the kaempferol-mediated restoration of insulin content in isolated rat pancreatic β -cells. (a) Representative confocal images showing immunostained co-localization of insulin and LC3 as detected by double immunofluorescence staining. The histograms at (b) and (c) represent the level of secreted insulin for various treatments in presence of 2.8 or 16.7 mM glucose; while (d) and (e) represents intracellular insulin contents for various treatments in presence of 16.7 mM glucose. 182
- Figure 7.1.** Kaempferol decreases the body weight of HFD-STZ induced diabetic mice. (a) Representative images of mice fed with normal chow diet (control) or with high-fat diet for 10 weeks followed by injection with streptozotocin (35 mg/kg bw) and successive treatments for 4 weeks; (b) Body weight measurements of mice of respective groups. 194
- Figure 7.2.** Kaempferol improves glucose and insulin tolerance in diabetic mice. (a) Histogram showing fasting glucose levels of mice from different treatment groups. Blood glucose concentrations measured after administration of (b) glucose for glucose tolerance test (GTT) and (c) insulin for insulin tolerance test (ITT) after 16 weeks of the experiment. 196
- Figure 7.3.** Kaempferol enhances insulin secretion and content in pancreatic islet cells. Histogram showing (a) plasma insulin; (b) pancreatic insulin content; (c) plasma insulin measured during intraperitoneal glucose tolerance test of mice treated with various chemicals as mentioned. 198

- Figure 7.4.** Kaempferol induces autophagy and inhibits apoptosis in pancreatic islet cells. Representative immunoblot analysis of (a) autophagy-, lipid droplets, ER stress- and apoptosis-related proteins and (b) p-AMPK and p-mTOR, in isolated islets from respective mice groups. 200
- Figure 7.5.** Chloroquine treatment inhibited kaempferol-induced autophagic flux. (a) Representative immunoblot analysis of autophagy marker proteins in the respective groups. (b) Representative transmission electron microscopy images of pancreatic β -cells after various treatments. 203
- Figure 7.6.** Inhibition of autophagy abolished the kaempferol-mediated protection of pancreatic β -cells. Representative immunoblot analysis for lipid droplets, ER stress and apoptosis marker proteins in (a) absence and (b) presence of chloroquine, over and above the respective treatments as mentioned in materials and methods.(c) Representative histological images of hematoxylin and eosin stained pancreases of respective groups (original magnification, $\times 400$); (d) Representative immunofluorescence images of pancreatic islets from mice of various treatment groups for presence of insulin. 206
- Figure 7.7.** Inhibition of autophagy by chloroquine abolished kaempferol-mediated insulin functions. Histogram showing the level of insulin in the (a) plasma of fasting mice; (b) pancreatic tissues of treated mice; (c) plasma of glucose administered mice measured during intraperitoneal glucose tolerance test after treated with various chemicals as mentioned. 208
- Figure 7.8.** Inhibition of autophagy abrogated kaempferol-mediated enhanced glucose and insulin tolerance. Histogram showing (a) body weights and (b) fasting blood glucose levels of mice treated with respective treatments; Blood glucose concentrations measured during (c) intraperitoneal glucose tolerance test and (d) intraperitoneal insulin tolerance test from mice of various groups. 209
- Figure 8.1.** Kaempferol treatment inhibits PA-induced lipid accumulation in HepG2 cells. HepG2 cells were treated with various concentrations of kaempferol in presence of 0.5 mM PA for 24 h. (a) Microscopic images of Oil Red O stained-HepG2 cells; Histograms showing (b) lipid content; (c) triglycerides content of treated cells; Representative (d) RT PCR analysis of PLIN2 gene; (e) immunoblot analysis of PLIN2 with increasing dose and (f) time durations. 223
- Figure 8.2.** Kaempferol alters expression of genes involved in cytosolic 225

lipolysis and β -oxidation. Representative (a) histogram showing relative PPAR- α luciferase activity expressed as fold of vehicle-treated control; (b) RT-PCR analysis of genes involved in cytosolic lipolysis and β -oxidation and (c) immunoblot analysis of PPAR- α protein.

- Figure 8.3.** Kaempferol induces autophagy in PA-challenged HepG2 cells. (a) Representative confocal images of MDC-LysoTracker stained cells to selectively stain autophagosomes and lysosomes. Representative immunoblot analysis for the expression of LC3 and p62 with (b) increasing doses and (c) time duration of kaempferol treatment. 227
- Figure 8.4.** Chloroquine treatment impairs kaempferol-mediated autophagic flux. Representative (a) confocal images of EGFP-LC3 puncta formation in response to various treatments and (b) immunoblot analysis of autophagy marker proteins in response to various treatments. 229
- Figure 8.5.** Kaempferol instigates autophagy through AMPK/mTOR pathway. Representative immunoblot analysis of the phosphorylation of AMPK and mTOR in HepG2 cells in response to kaempferol treatment for varying (a) dosages; (b) time period and (c) at 10 μ M dose in presence of AMPK siRNA. 231
- Figure 8.6.** Kaempferol-induced autophagy facilitates a decrease in PA-induced lipid stores. (a) Representative immunoblots of various proteins in response to Atg7 siRNA. (b) Microscopic images of Oil Red O stained cells with or without various inhibitors; Histogram representing (c) and (d) lipid content; (e) and (f) triglyceride content of treated cells. 233
- Figure 8.7.** Kaempferol improves metabolic profile in diabetic mice. Histogram showing (a) Total cholesterol (b) Triglycerides (c) LDL (d) NEFA level in serum of treated mice. 235
- Figure 8.8.** Kaempferol induces autophagy in livers of HFD-STZ diabetic mice. Representative immunoblots of (a) autophagy-related proteins and (b) p-AMPK and p-mTOR, in livers of respective mice groups. 237
- Figure 8.9.** Kaempferol-mediated autophagy induces inhibition of lipid stores in livers of HFD-STZ diabetic mice. Histogram showing (a) liver weight; (b) liver triglycerides; (c) serum ALT and (d) serum AST level of mice treated with various chemicals as mentioned. (e) Representative histological images of hematoxylin and eosin stained livers of respective 239

- groups (original magnification, $\times 400$); (f) Representative immunoblots of PLIN2 in the respective groups. (g) Representative transmission electron microscopy images of pancreatic β -cells after various treatments
- Figure 8.10.** Kaempferol-mediated autophagy improves insulin sensitivity and insulin signal transduction in livers of HFD-STZ diabetic mice. Representative immunoblots of (a) proteins involved in HFD-mediated insulin resistance and insulin signal transduction and (b) insulin-stimulated Akt and p-Akt proteins. 242
- Figure 9.1.** Schematic representation showing the anti-obesity and antidiabetic activities of various flavonoids. 250
- Figure 9.2.** Schematic representation showing mechanism underlying the kaempferol-mediated protection of β -cell mass involving autophagy. 253
- Figure 9.3.** Proposed mechanism of kaempferol-mediated autophagy in PA-challenged pancreatic β -cells and in islets of HFD-STZ diabetic mice. 255
- Figure 9.4.** The proposed mechanism of kaempferol-mediated effects in hepatic cells. 257

List of Tables

Table 3.1. List of primers used in semi-quantitative RT-PCR	80
Table 3.2. List of primary antibodies used in western blotting	83





CHAPTER 1

INTRODUCTION

Chapter 1. Introduction

Diabetes Mellitus (DM) is a group of metabolic disorders characterized by increased level of blood glucose due to defects in insulin secretion or action or both which is further associated with other long-term complications such as diabetic retinopathy, cardiovascular disorders, liver, kidney and neurovascular dysfunctions (American diabetes association, 2009). It is one of the most prevalent diseases worldwide and its incidence is progressively increasing each passing days.

The world health organization (WHO 2016) validated that the worldwide number of people with diabetes has risen to 422 million in 2014 from 108 million in 1980 with an estimated death of 1.5 million people in 2012. WHO projects that by 2030, diabetes will be the seventh leading cause of death globally (World Health Organization, 2016).

DM is classified into two main categories: (1) Insulin-dependent diabetes mellitus (IDDM)/Type 1 diabetes and (2) Noninsulin-dependent diabetes mellitus (NIDDM)/ Type 2 diabetes. Among all diabetic conditions, type 2 diabetes is most prevalent and accounts for nearly 90-95% of patients diagnosed with diabetes worldwide.

Type 2 diabetes mellitus (T2DM) is a metabolic disease characterized by elevated blood glucose level and insulin resistance. A common health condition which often accompanies T2DM is obesity and thus draws a clear–correlation between these adverse situations (American Diabetes Association, 2011). It is already known that obese conditions render the individual even more susceptible to develop T2DM. The saturated fats derived from fat depots of obese individual increases free fatty acids in circulation which consequently impairs skeletal muscle responsiveness to insulin. The hyperglycemic conditions that subsequently prevails, induces the compensatory increase in insulin synthesis and secretion which break down at later time points due to pancreatic β -cell failure (Donath and Halban, 2004; Boden, 2011; Al-Goblan et al., 2014). Progressive β -cell failure and dysfunction are major pathogenic features of the development and continued progression of T2DM. Therefore, the protection and recovery of β -cell mass and function should be the prime target for treatment and prevention of T2DM (Chen et al., 2017).

Recently, it has been established that autophagy dysfunction due to lipid overload can lead to endoplasmic reticulum (ER) and mitochondrial dysfunction in β -cells that in turn may lead to loss of β -cell mass and function (Chen et al., 2017). Autophagy is an intracellular

lysosomal degradative process of defective proteins, macromolecules, damaged organelles and toxic aggregates, which plays a pivotal role in maintaining cell homeostasis (Mizushima, 2007; Jana, 2010; Ahn et al., 2016). Apart from this, autophagy can also be instigated in response to stress conditions like nutrient deprivation, infection and diseased state, wherein it plays a cytoprotective role. The role of autophagy in sustaining pancreatic β -cell mass and function is well established and its failure has been linked to the pathophysiology of type 2 diabetes (Codogno and Meijer, 2010). Recent studies have elucidated that in the presence of saturated fatty acids and hyperglycemic conditions, β -cells undergo apoptosis due to impairment of autophagic turnover. Exposure of human pancreatic islets and β -cell lines to fatty acids and glucose blocks autophagic flux which in turn leads to apoptotic β -cell death (Mir et al., 2015). Both type 2 diabetic patients and high-fat diet mice model often exhibit a dysregulated autophagic activity which further ascertains the implication of impaired autophagy in the pathophysiology of T2DM (Masini et al., 2009; Codogno and Meijer, 2010).

On the basis of this pre-notion, rapamycin (a mTOR inhibitor and known activator of autophagy) has been validated to exert the cytoprotective effect on palmitic acid (PA)-induced β -cells by reducing the blockage of autophagic turnover (Mir et al., 2015). Similarly, other regularly prescribed antidiabetic drugs like rosiglitazone and metformin were also found to rescue β -cells from PA-induced apoptosis through modulation of autophagy (Wu et al., 2013; Jiang et al., 2014). Thus, induction of autophagy could be a potential target to combat saturated fatty acid-mediated apoptotic cell death (Stienstra et al., 2014). Hence, identifying agents that could modulate autophagy in pancreatic β -cells in lipid-excess stressful conditions could be a better target in developing therapies for obesity-linked T2DM.

As the knowledge of heterogeneity of this disorder increases, there is a need to search for more efficacious agents with lesser side effects. Although the current medicines and therapies can mitigate diabetes to some extent, there are several unprecedented complications. The major one of them is that these therapies do not significantly improve β -cell mass and function simultaneously, thus become less effective over time as a result of progressive loss of β -cell number and function, with the consequence a majority of type 2 diabetic patients do not attain current glycemic goals (Sena et al., 2013; Chen et al., 2017). Thus, targeting β -cell failure early in disease progression has emerged as a new therapeutic approach to treat T2DM. Currently, no antidiabetic drug has been proven clinically effective for the prevention of β -cell atrophy although thiazolidinediones (TZDs) and glucagon-like peptide-1 (GLP-1) analogues have testified being effective in animals (Gastaldelli et al., 2007; Tourrel et al., 2002).

Recent research focuses mainly on improving glucose homeostasis by protection or regeneration of β -cell. These cellular-based therapeutic approaches are focused on the stimulation of β -cell proliferation, transplantation of the islet cells or β -cells, protection of β -cells from apoptosis and *in vivo* β -cell regeneration. However, none of these approaches are in clinical use due to several reasons like shortage of donors, inadequate techniques of β -cells generation and β -cells in adult humans do not grow sufficiently (Vetere et al., 2014; Kim et al., 2016).

Currently, an active area of diabetes research focuses on identifying naturally occurring flavonoids, a group of phytochemicals that can be modulated or developed into diabetes therapeutics due to their intriguing role in treating various diseases (Chang et al., 2013). Also, these phytochemicals because of their lesser side effects, more reliable in pharmacological actions and cost-effectiveness, are considered to be excellent alternative candidates in diabetes management. Keeping in mind all the above mentioned recent strategies and targets, the major focus of this work was to find out novel autophagy modulators which can protect β -cell mass and function as a principal approach in the prevention of obesity-linked type 2 diabetes with an additional impact on liver functions and further understanding their mechanism of action in detail. Overall, the present study attempted to achieve the following **objectives**:

1. Screening of various flavonoids for their anti-obesity and antidiabetic activities: *in vitro* and *in vivo* studies.
2. Understanding the role of kaempferol in the modulation of autophagy and its effect on cytoprotection of pancreatic β -cells under lipid overload condition in *in vitro* and *ex vivo* models.
3. To determine the role of kaempferol-mediated autophagy in the alleviation of lipid deposition, ER stress and β -cell dysfunction and its mechanism of action *in vitro* and *ex vivo*.
4. Validation of the role of kaempferol in the modulation of autophagy and restoration of β -cell mass and function in high-fat diet (HFD)-streptozotocin (STZ) mice.
5. Role of kaempferol-mediated autophagy in amelioration of lipid deposition and insulin resistance in lipid-induced hepatocytes (in HepG2 cells) and liver of HFD-STZ mice.





CHAPTER 2

LITERATURE REVIEW

Chapter 2. Literature Review

2.1. Introduction

Diabetes Mellitus (DM) is a group of metabolic disorders characterized by increased level of blood glucose due to defects in insulin secretion/insulin action or both which is further associated with other long-term complications such as diabetic retinopathy, cardiovascular disorders, liver dysfunction, kidney dysfunction and neurovascular dysfunction (American diabetes association, 2014; Asmat et al., 2016; McCracken et al., 2018). These complications are attributed to the imbalance in metabolic storage and mobilization of the energy sources such as carbohydrates, proteins and lipids. It is one of the most prevalent diseases worldwide and its incidence is progressively increasing each passing day. The current trend of classification of diabetes follows the categorization pattern according to the etiology and clinical manifestations. According to the recent classification pattern ascribed by American Diabetes Association (ADA), diabetes can be categorized into the following types (Baynes, 2015; American diabetes association, 2018):

- (i) Type 1 diabetes mellitus /insulin dependent diabetes
- (ii) Type 2 diabetes mellitus /non-insulin dependent diabetes
- (iii) Gestational diabetes mellitus (GDM)
- (iv) Specific types of diabetes due to other causes

2.1.1. Type 1 diabetes mellitus /insulin dependent diabetes

In Type 1 diabetes mellitus (T1DM), the body does not produce enough insulin due to the gradual destruction of insulin-secreting pancreatic β -cells by its autoimmune system which results in increased blood glucose level (Liston et al., 2017). It is predominantly found in children (childhood onset/juvenile diabetes) and adults (in their later stage of life). It is often called as autoimmune diabetes, the onset of which is characterized by progressive loss of pancreatic β -cells due to the autoimmune destruction of β -cells, mediated by T-cells (Katsarou et al., 2017; Knip, 2017). T1DM accounts for approximately 5-10% of the total diabetic population globally (Brownlee et al., 2017). Individuals having autoantibodies against insulin (IAA) and glutamic acid decarboxylase (GADA) in their childhood or antibodies against zinc transporter 8 (ZnT8) and islet antigen-2 (IA2) at their later stage of

life, pose a greater risk of developing T1DM (Grulich-Henn and Klose, 2017). Often type 1 diabetes represented at the late stage (generally termed LADA) provides ambiguity for the current classification system (Schwartz et al., 2016). Several microvascular complications associated with T1DM are diabetic kidney disease, retinopathy, neuropathy and albuminuria (Bjerg et al., 2018). T1DM management includes regular lifelong insulin therapy whereas recent therapeutic innovations like insulin analogues are also being explored that deal with significant reductions in hemoglobin A_{1c} (HbA_{1c}) (Brownlee et al., 2017).

2.1.2. Type 2 diabetes mellitus /non-insulin dependent diabetes

Type 2 diabetes mellitus (T2DM) is the most prevalent form that is found in 90% of the diabetes cases globally. It was formerly known as non-insulin dependent or adult-onset diabetes. Usually, adults suffer from this condition most frequently whereas increasing prevalence in adolescents is being observed as well. T2DM is caused by the progressive loss of β -cell mass and function with an impairment of insulin secretion and subsequent development of insulin resistance (World Health Organization, 2016; Chatterjee et al., 2017). As a result of which there is a decreased uptake of glucose by the major insulin-responsive tissues such as liver, skeletal muscle and adipocyte. There are several predisposing factors driving the onset of type 2 diabetes. However, obesity plays a crucial role in the pathogenesis of type 2 diabetes. Circulating free fatty acid cause the impaired insulin action and decreased glucose uptake by the organs along. The increased inflammatory cytokines like leptin, resistin, adiponectin, TNF- α also implicate insulin resistance and possibly β -cell dysfunction. Lots of micro and macrovascular complications are associated with the severity of the disease. However, reports suggest that these microvascular complications are more prominent among type 2 diabetes patients compared with type 1 diabetes patients diagnosed in a group of teenagers and young adults (Dabelea et al., 2017). The detail pathophysiology and associated complications are discussed in the next section.

2.1.3. Gestational diabetes mellitus (GDM)

Gestational diabetes mellitus (GDM) is usually defined as a condition with a hyperglycemia and glucose intolerance with onset or first recognition during pregnancy. Gestational diabetes mellitus happens during the second or third trimester of pregnancy which was not evident earlier to gestation. The complication is prevalent around 7% among all pregnancies. The underlying mechanisms involve pancreatic β -cell dysfunction because of

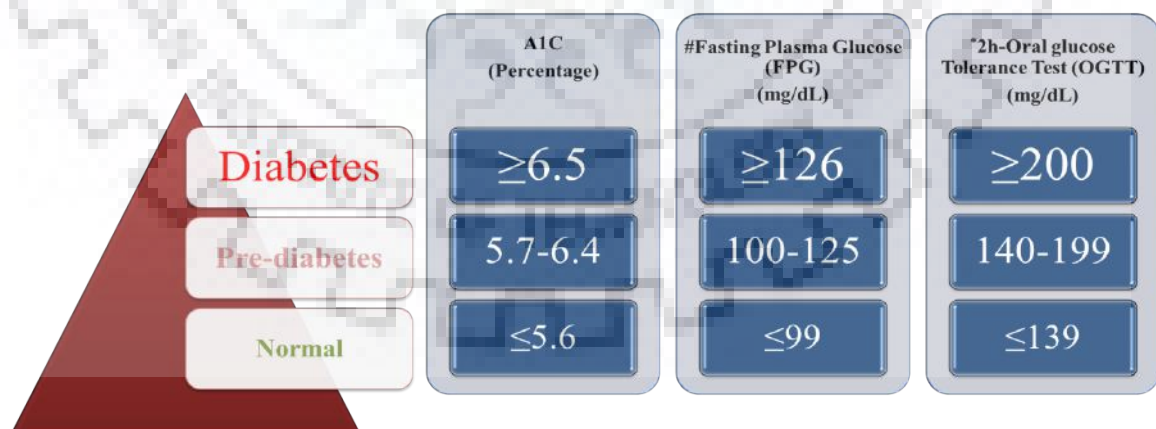
obesity and chronic insulin resistance. Another reason may be the occurrence of circulating immune markers (for example, anti-islet cell antibodies or antibodies to glutamate decarboxylase 65) that are usually diagnosed with type 1 diabetes mellitus (T1DM).

2.1.4. Specific types of diabetes due to other causes

Several other specific types of diabetes results from the occurrence of monogenic diabetes syndromes (such as neonatal diabetes and maturity-onset diabetes of the young [MODY]), diabetes of the exocrine pancreas (as an universal nomenclature) due to surgical resection, pancreatitis or inflammation which was mostly referred earlier as type 3c-diabetes (Woodmansey et al., 2017) and chemical or drug-induced diabetes (such as after organ transplantation or with glucocorticoid use during HIV/AIDS treatment).

2.2. Diagnostic criteria for diabetes

According to the standardized guidelines of American Diabetes Association (ADA), diabetes may be diagnosed on the criteria of glycated hemoglobin (HbA1c) or plasma glucose. The fasting plasma glucose (FPG) or the 2-h plasma glucose (2-h PG) value after a 75-g oral glucose tolerance test (OGTT) is used as a gold standard estimation criterion for diabetes diagnosis and care. The following criteria are recommended for diabetes diagnosis (American diabetes association, 2015) (Fig. 2.1).



#Fasting is defined as no caloric intake for at least 8 h
 *2-h plasma glucose (2-h PG) value after a 75-g oral glucose tolerance test (OGTT) -The test should be performed as described by the WHO, using a glucose load containing the equivalent of 75 g anhydrous glucose dissolved in water.
 mg/dL-milligram/deciliter

Fig. 2.1. Diagnostic criteria for diabetes mellitus (as standardized by ADA)

2.3. Global burden of diabetes

According to a report published in WHO fact sheet, around 422 million adults were living globally with diabetes in 2014 which had almost quadrupled to 108 million as reported in 1980 (World Health Organization, 2016; NCD Risk Factor Collaboration, 2016). According to a report, this number has been estimated to reach 642 million (uncertainty interval: 521–829 million) of age group 20–79 by the year 2040 (Ogurtsova et al., 2017). However, T2DM is the most prevalent form and about 90% of the diabetic population is diagnosed with T2DM (Zheng et al., 2018). Recently it has been reported that 1 among 11 individuals suffers from diabetes mellitus and currently Asia is predicted to be the epicenter of this global epidemic of T2DM (Ogurtsova, 2017; Zheng et al., 2018). The global occurrence and prevalence of diabetes differ a lot according to diverse geographical regions, a great part (about 80%) of diabetic patients are from low-to-middle-income countries (Ogurtsova et al., 2017). However, the overall increasing trend of the global burden of diabetes is attributed to the increased prevalence in almost every country since 1980 (NCD Risk Factor Collaboration, 2016).

2.4. Complications associated with diabetes

Diabetes mellitus is not a single endocrine dysfunction, rather a multifaceted cluster of heterogeneous metabolic afflictions (Piero et al., 2015; Deepthi et al., 2017). Complications associated with diabetes are majorly grouped under microvascular (caused by damage in small blood vessels) and macrovascular (caused by damage in larger blood vessels) (Lotfy et al., 2017; Schwartz et al., 2017) (Fig. 2.2).

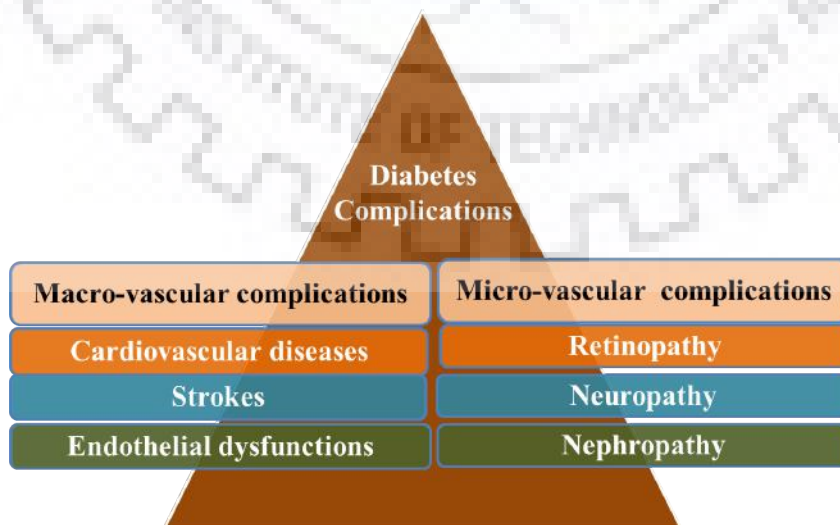


Fig 2.2. Major complications associated with diabetes mellitus.

2.4.1. Microvascular complications

Microvascular complications associated ailments are retinopathy, nephropathy and neuropathy (Menezes Zanolivi et al., 2016; Trikkalinou et al., 2017; Emanuel et al., 2017; Khan et al., 2017).

2.4.1.1. Diabetic retinopathy

Long-term diabetes and severe hyperglycaemia often cause blurred vision due to the damage in the retina which is known as diabetic retinopathy. Both type 1 and type 2 patients suffer from this condition, the latter case being more prominent (Khan et al., 2017).

2.4.1.2. Diabetic neuropathy

The high blood glucose level often leads to damage in the peripheral and central nervous system resulting into the impaired motor and cognitive functions. Diabetic neuropathy leads to depression which also affects the quality of life (Menezes Zanolivi et al., 2016; Trikkalinou et al., 2017; Emanuel et al., 2017).

2.4.1.3. Diabetic nephropathy

Damage to the small blood vessels in the kidneys due to hyperglycemia and hypertension leads to nephropathy and ultimately kidney failure and death (Karthi et al., 2008).

2.4.2. Macrovascular complications

Macrovascular complications include the risk of cardiovascular diseases such as heart attacks, strokes and insufficiency of blood supply to legs (Chandel et al., 2017).

2.4.2.1. Cardiovascular complications

There is a great risk of cardiovascular diseases (CVD) and other related complications like peripheral vascular disease and stroke in the patients suffering from diabetes due to hypertension, dyslipidemia, hypercholesterolemia and obesity. Moreover, T2DM patients are more prone to CVD than those not having T2DM (Shah et al., 2015; Retnakaran and Shah, 2017).

2.4.3. Other related complications

2.4.3.1. Cataract

Cataract is one of the earliest complications associated with diabetes which results into visual impairment due to the lens opacification caused by hyperglycaemia (Sayin et al., 2015).

2.4.3.2. Glaucoma

Diabetic patients develop a condition of glaucoma in which the optic nerve gets damaged due to the increased fluid pressure inside the eyes (Sayin et al., 2015)..

2.4.3.3. Osteoarthritis and osteoporosis

Diabetic patients suffer from loss of joint cartilage and deteriorated bone microarchitecture. T1DM patients are exposed more to osteoporosis whereas T2DM patients suffer from joint pain, inflammation and osteoarthritis (Lin and Dass, 2018; Hameed et al., 2015; Kabadi, 2017; Jin et al., 2017).

2.5. Type 2 diabetes mellitus (T2DM)

Type 2 diabetes mellitus (adult-onset diabetes), previously known to be non-insulin-dependent diabetes, emanates from the insufficient insulin secretion and utilization in the body due to the loss of mass and function of pancreatic β -cells with the ultimate occurrence of insulin resistance in several organs (WHO, 2016; Chatterjee et al., 2017). Usually, an individual is speculated to have type 2 diabetes if he/she does not show any general symptoms of type 1 diabetes (insulin-dependence, characteristic rapid childhood onset and ketoacidosis when neglected), monogenetic diabetes or specific other types of diabetes (Internal Clinical Guidelines Team, 2015).

2.5.1. Risk factors associated with type 2 diabetes mellitus progression

Several factors that contribute to the pathogenesis of T2DM are body mass index (BMI), genetics, hypertension, physical inactivity, dietary patterns and obesity (Wu et al., 2014) (Fig. 2.3).

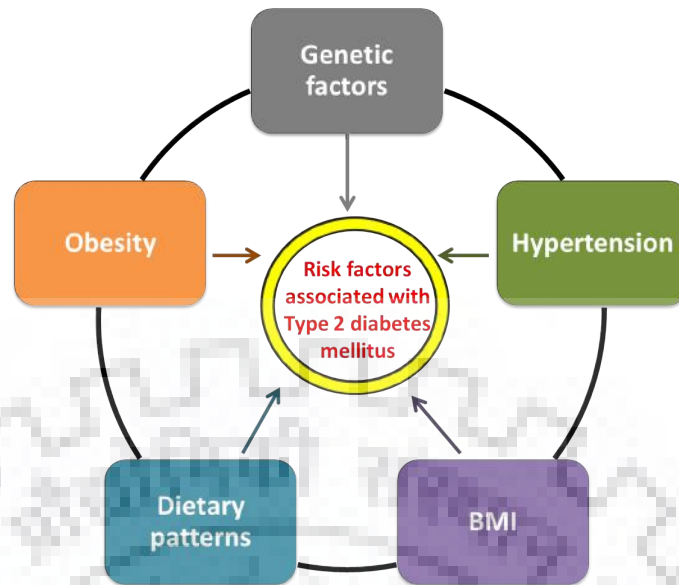


Fig 2.3. Risk factors associated with development and progression of type 2 diabetes mellitus.

2.5.1.1. Body mass index (BMI)

Increased body mass index in terms of increased obesity has a positive correlation with type 2 diabetes in men and women (Siegel et al., 2009). Also increased sedentary lifestyle and physical inactivity indirectly further promotes the disease.

2.5.1.2. Genetic factors

Several genes which are expressed in pancreatic cells controlling its function and insulin secretion play role in the development of T2DM. Researchers have identified several genes like FTO, KCNJ11, WFS1, TCF7L2, IGF2BP2, CDKAL1, SLC30A8, JAZF1, HHEX and NOTCH2 to be greatly involved in mediating risk of type 2 diabetes (Murea et al., 2012). The transcription factors 7-like 2 (TCF7L2) is one of the major genes expressed in pancreatic cells and also controls insulin gene expression and insulin secretion (Zhou et al., 2014).

2.5.1.3. Hypertension

Endothelial dysfunction, elevated blood pressure, and inflammatory markers such as C-reactive proteins are consistently involved in the development of type 2 diabetes (Sen and Tyagi, 2010; Lastra et al., 2014).

2.5.1.4. Physical inactivity

Sedentary lifestyle including physical inactivity potentiates the risk of type 2 diabetes. Studies suggest that maintaining a healthy lifestyle by doing exercise may help in preventing the development and progression of type 2 diabetes and thus may improve insulin sensitivity and BMI (Aune et al., 2015).

2.5.1.5. Dietary patterns

Dietary sources having high glycaemic index are the one of the major reason for the increased risk of type 2 diabetes (Imamura et al., 2016). Recently, studies have shown that excessive intake of saturated and trans fat are detrimental to health and negatively regulates glucose metabolism and cause insulin resistance whereas higher intake of polyunsaturated fat and long-chain n-3 fatty acids are beneficial to health (Coelho et al., 2017; Hu et al., 2001; Imamura et al., 2016). Similarly, a lot of evidences suggest the indispensable role of vitamin D in controlling type 2 diabetes (Mitri et al., 2012; Pittas et al., 2010). Low intake of vitamin D increases the risk of this disease (Pittas et al., 2010).

2.5.1.6. Obesity

Obesity is defined as the abnormal excessive accumulation of fat that ultimately impairs physical wellbeing of individuals. Body mass index (BMI) is considered to define obesity in terms of weight-for-height estimation in adults (Nuttall, 2015). BMI is calculated by considering a person's weight in kilograms divided by square of height in meters (kg/m^2) (Marín-Peñalver et al., 2016).

The BMI and obesity status for adults are defined as follows (National Institute for Clinical Excellence, 2014; Abarca-Gómez et al., 2017),

- Individuals having BMI <25 are considered to be normal
- Individuals having BMI ≥ 25 are considered to be overweight
- Individuals having BMI ≥ 30 are considered to be obese.

As per WHO obesity and overweight factsheet 2017, the global prevalence of obesity has tripled since 1975. In 2016, more than 1.9 billion adults, 18 years and older, were overweight. Of these, over 650 million were obese.

Obesity is one of the major causes of several metabolic disorders and is linked to increased mortality worldwide (Al-Goblan et al., 2014). The imbalance in energy intake and expenditure is the fundamental cause of obesity. Dietary sources rich in carbohydrate and fat, physical inactivity, sedentary lifestyle pattern positively correlate with obesity development and thus increase the risk of other associated metabolic disorders (Velásquez-Rodríguez et al., 2014). Obesity is the major predisposing factor for the prevalence of T2DM (DeFronzo et al., 2015; Boles et al., 2017; Saad et al., 2017). Adipose tissue is the major organ that store large amounts of energy in the form of triglycerides (TG) as well as hydrolyze and release triglycerides in the form of free fatty acids (Coelho et al., 2013). Adipocytes and the stromal vascular fraction in the adipose tissue execute an endocrine function by secreting several hormones that regulate glucose and lipid metabolism and overall maintains energy homeostasis (Coelho et al., 2013). However, increased metabolic load during obesity, leads to adipose tissue dysfunction characterized by enlarged adipocytes and secretion of pro-inflammatory cytokines (Goossens, 2008; Zhao and Liu, 2013). These conditions ultimately lead to ectopic fat accumulation where triglycerides are stored in tissues other than adipose tissue, such as the liver, skeletal muscle, pancreas and heart (Snel et al., 2012).

2.5.2. Obesity and Diabetes – the connecting link

The prevalence of T2DM is increasing worldwide with development of obesity (Giacca et al., 2010; Leitner et al., 2017). Most of the people diagnosed with obesity or diabetes are often found to be suffering from both (Mokdad et al., 2003). This is evident from the fact that the epidemiology of an obese person and that of type 2 diabetic person is almost same (Dietz, 2004). This interdependent relationship has even lead to the coining of a new term “diabesity” (Darlene, 2013).

In obese condition, the elevated level of circulating free fatty acids (FFAs) is one of the predisposing factors in the development of insulin resistance and hyperglycemia in the early phase of diabetes (Giacca et al., 2010). Although the complex relationship between obesity and diabetes is not fully understood, there are several proposed mechanism explaining this link. The initial concept was that circulating free fatty acids decrease the rate of glucose metabolism in muscles by affecting the Krebs cycle. To carry out the cells functioning, in these muscle cells free fatty acids become the preferential substrate (Shah et al., 2003). Besides reducing glucose oxidation, a rise in free fatty acids also decreases glucose storage in the cells by inhibiting glycogen synthase. These effects are seen in early obese conditions and now are seen

as the transition from obesity to diabetes. Premature insulin resistance and insulin secretion defect are also observed during the early phase of weight gain and slowly increases as the patient develops diabetes (Giacca et al., 2010). The initial response to increased insulin resistance in peripheral tissues is the compensatory increase in β -cell mass and insulin secretion by pancreatic β -cells. However, with the progression of diabetes, dysfunction and loss of β -cells occur in response to increased metabolic load which further leads to complications associated with T2DM (Assimacopoulos-Jeannet, 2004; Boden, 2011). Accumulating evidence suggests that the loss of β -cells in T2DM is closely related to increased apoptosis of β -cells, secondary to increased glucotoxicity and lipotoxicity (Maedler et al., 2001; Lupi et al., 2002; Yuan et al., 2010). Chronic lipid accumulation, endoplasmic reticulum (ER) stress and impaired autophagy could be the key pathways involved in the loss of β -cell mass and function (Assimacopoulos-Jeannet, 2004; Biden et al., 2014; Masini et al., 2009).

2.5.3. Pathophysiology of type 2 diabetes mellitus

The pathophysiological conditions of T2DM include increased hyperglycemia and concomitant insulin resistance due to pancreatic β -cell failure that majorly reported up to 50% loss in young patients (of age group-10-17) at diagnosis. The reason behind aberrant blood glucose level is the impaired utilization of glucose produced in the liver and decreased uptake in muscles and adipose tissue. Hence there is a subsequent overload on pancreatic β -cells to produce sufficient insulin which results into the development of insulin resistance. Disrupted feedback loops between insulin secretion and insulin action affect major organs (Fig. 2.4) such as the pancreas (β -cells and α cells), liver, adipose tissue, skeletal muscle, kidneys, small intestine and brain manifesting the development of type 2 diabetes (Zheng et al., 2018). The rising trend of obesity, energy-rich diet and physical inactivity additionally potentiate this unpredicted global surge of type 2 diabetes (Verma and Hussain, 2017; Eaton and Eaton, 2017).

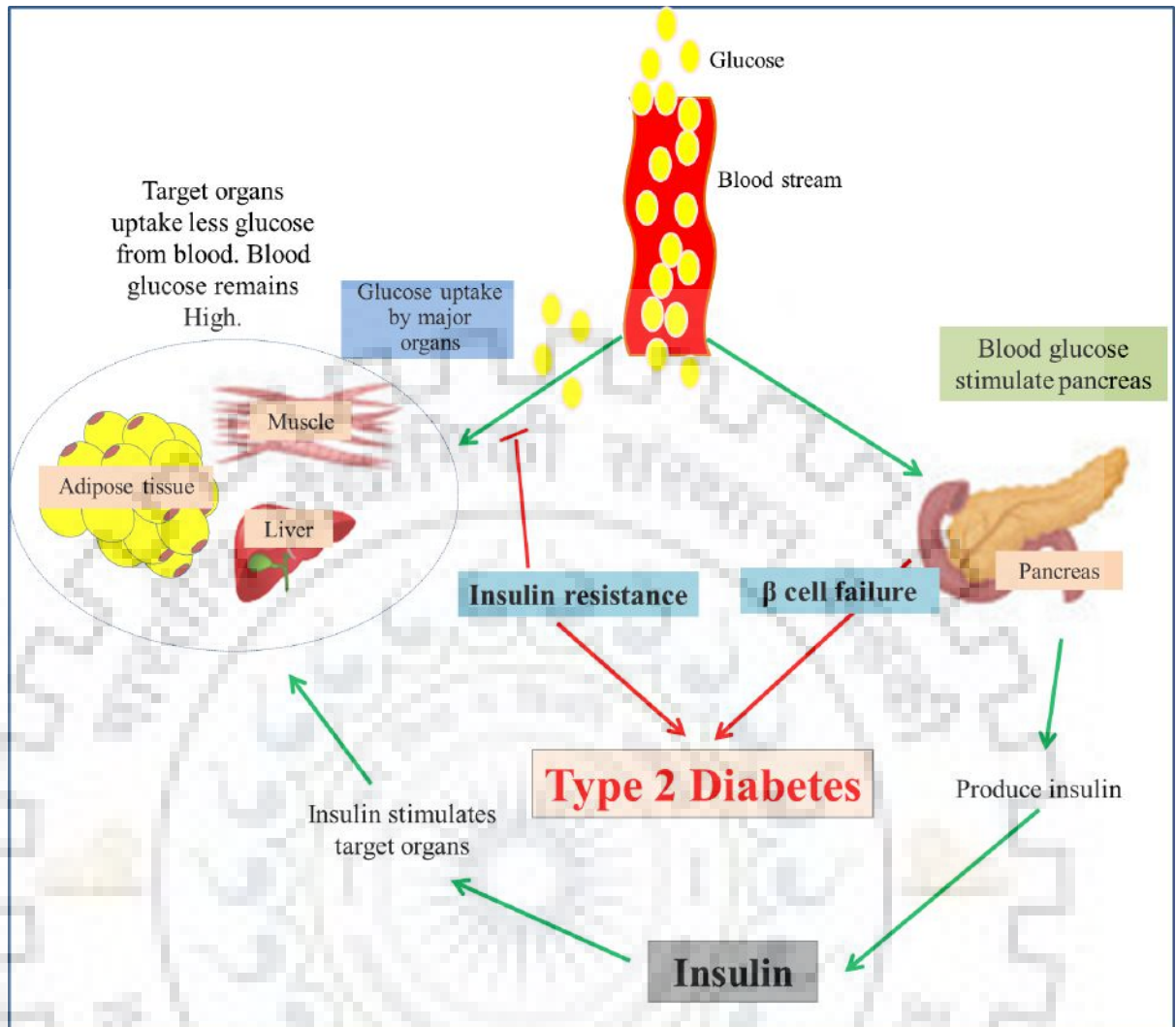


Fig. 2.4. The general scheme of insulin production and function in type 2 diabetes mellitus.

2.5.3.1. β -cell dysfunction

Recent research in diabetes has revealed that a profound reduction in pancreatic β -cell mass and function is the foremost cause of the insulin deficit in T2DM (Marrif and Al-Sunousi, 2016; Maria Elizabeth et al., 2017). When the β -cells fail to adapt the insulin resistance while compensating the increased insulin demand, the physiological dysfunction leads to hyperglycemia and development of T2DM (Cantley and Ashcroft, 2015; Modi et al., 2015; adipoChen et al., 2017). The first study on significant loss of pancreatic β -cell mass was reported when the autopsies samples from diabetic and non-diabetic patients were compared (Butler et al., 2003). In recent years, most of the studies have shown that there is a significant reduction in β -cell mass and function ranging from 24% to 65% in T2DM patients as compared

to nondiabetic controls (Sakuraba et al., 2002; Inaishi et al., 2016). However, some non-significant differences among these two groups were also reported simultaneously (Guiot et al., 2001). Additionally, there are evidence showing reduced yield and size of pancreatic islets isolated from type 2 diabetic donors as compared to the non-diabetic controls (Deng et al., 2004). The underlying mechanisms for the loss of β -cell mass and function mostly attribute to β -cell apoptosis (Marchetti et al., 2007; Marchetti et al., 2004) and not to the reduced neogenesis or the differences in the β -cell replication frequency (Butler et al., 2003).

Recently, the increased β -cell apoptosis has been correlated with a highly orchestrated process known as autophagy, the impairment of which, majorly contributes to the progressive loss of β -cell mass and function (Fujimoto et al., 2009; Jung et al., 2008; Ebato et al., 2008). It has been shown that autophagy-deficient mice undergo increased β -cell apoptosis (Sheng et al., 2017; Quan et al., 2012). Also, mice deficient in *Atg7* (autophagy deficient mice) have been reported to show extreme glucose intolerance and low level of serum insulin because of the increased β -cell apoptosis and decreased proliferation (Jung et al., 2008). In another study, the mean loss of β -cell mass was 24% in patients suffering from diabetes manifested over a period of 5 years and the deficit increased up to 54% in the population with diabetes persistent over a period of 15 years (Rahier et al., 2008). Apart from the reduced β -cell mass, a significant loss in β -cell function is observed majorly in type 2 diabetes patients. The insulin secretion capacity is also reported to diminish from 50% to 90% in T2DM patients (Gastaldelli et al., 2004; Ferrannini, et al., 2005; Jensen et al., 2002). All the above scientific assessments corroborate the fact that, in T2DM, the contribution of β -cell mass and function is principal to the pathogenesis of the disease and protection and recovery of which should be the major therapeutic approach for prevention and cure.

2.5.3.1.1. Pancreas

The pancreas plays an imperative role in the fine tune of micronutrient digestion and metabolic homeostasis *via* releasing various digestive enzymes and pancreatic hormones. Acinar or exocrine cells, the major cells of pancreas secrete the pancreatic juice containing digestive enzymes such as amylase, pancreatic lipase and trypsinogen into main pancreatic and accessory pancreatic duct while endocrine cells known as islet of Langerhans clustered within exocrine cells account for only 1–2% of the entire organ and secrete pancreatic hormone in endocrine fashion directly into the bloodstream. The α -cells that account for 15-20% of the total islet cells sense low blood glucose level and secrete glucagon which in turn escalate the

blood glucose level *via* hepatic and renal gluconeogenesis and hepatic glycogenolysis, hence, deems the catalytic activity (Roder et al., 2016). On the other hand, β -cells that account for 65–80% of the total islet cells secrete insulin in sense with high blood glucose level (Roder et al., 2016). Insulin facilitates the glucose entry to cells which in turn leads to drop off blood glucose level. The counter sensation stratagem of alpha and β -cells *vis a vis* blood glucose level that upholds glucose homeostasis. Insulin promotes glycogenesis, lipogenesis and the incorporation of amino acids into proteins and thus considered as an anabolic hormone. The β -cells also secrete amylin and peptide C. The δ -cells secrete somatostatin which inhibits glucagon and insulin. The γ -cells secrete pancreatic polypeptide (PP) and ϵ -cells secrete ghrelin. Auto-immune reaction toward β -cells resulted into type 1 diabetes (Yoom and Jun, 2005). Although, destruction of β -cells is less pronounced in type 2 diabetes, however, insensitivity of receptor toward insulin resulted into type 2 diabetes (Chen et al., 2017).

2.5.3.1.2. Insulin

Insulin is an anabolic hormone produced by β -cells of the pancreatic islets. This is a peptide hormone that regulates metabolism ensuring the absorption of glucose from blood to muscle, adipocyte and liver. The human insulin protein has a molecular weight of 5808 Da and consists of 51 amino acids. It is a dimer consisting of A-chain and B-chain interlinked by sulphide bonds (Mayer et al., 2007) (Fig. 2.5).

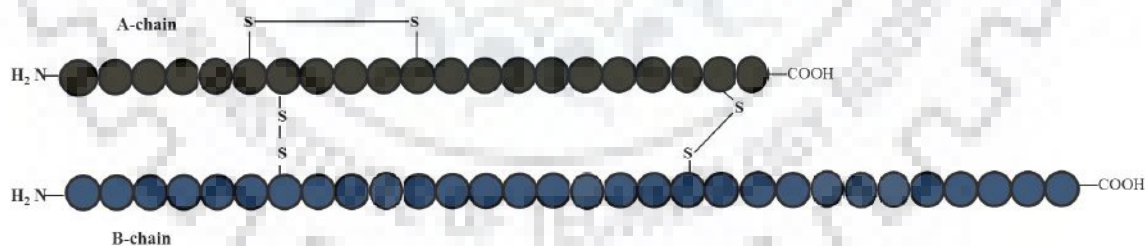


Fig. 2.5. Diagrammatic representation of the structure of human insulin

Some of the major actions of insulin involve;

- (a) It regulates blood sugar level by inducing muscle, fat and liver to take up excessive glucose and store it. For example, it promotes liver to store excessive energy (glucose) in the form of glycogen.
- (b) Circulating insulin catalyzes protein synthesis in several tissues

The autoimmune destruction of β -cells give rise to type 1 diabetes, where the pancreas is unable to produce insulin. Whereas, in type 2 diabetes, the pancreas produces insulin but the major organs become insulin insensitive which results into gradual loss of β -cell mass and function, one of the major cause of decreased insulin production in T2DM.

2.5.3.1.3. Insulin release

Insulin is primarily released by the β -cells stimulated by the elevated blood glucose after food intake. Glucose is transported into cells via facilitated diffusion through GLUT 2 transporter located on the surface of β -cells. Inside the β -cells, glucose undergoes a process of glycolysis resulting into adenosine triphosphate (ATP) generation and closure of ATP-sensitive K^+ -channels (K_{ATP} -channels) that in turn triggers membrane depolarization allowing the influx of Ca^{2+} ions from the voltage-gated calcium channels. The increased calcium triggers the fusion of insulin-containing granules with the membrane subsequently release insulin into the extracellular bloodstream (Fu et al., 2013) (Fig. 2.6).

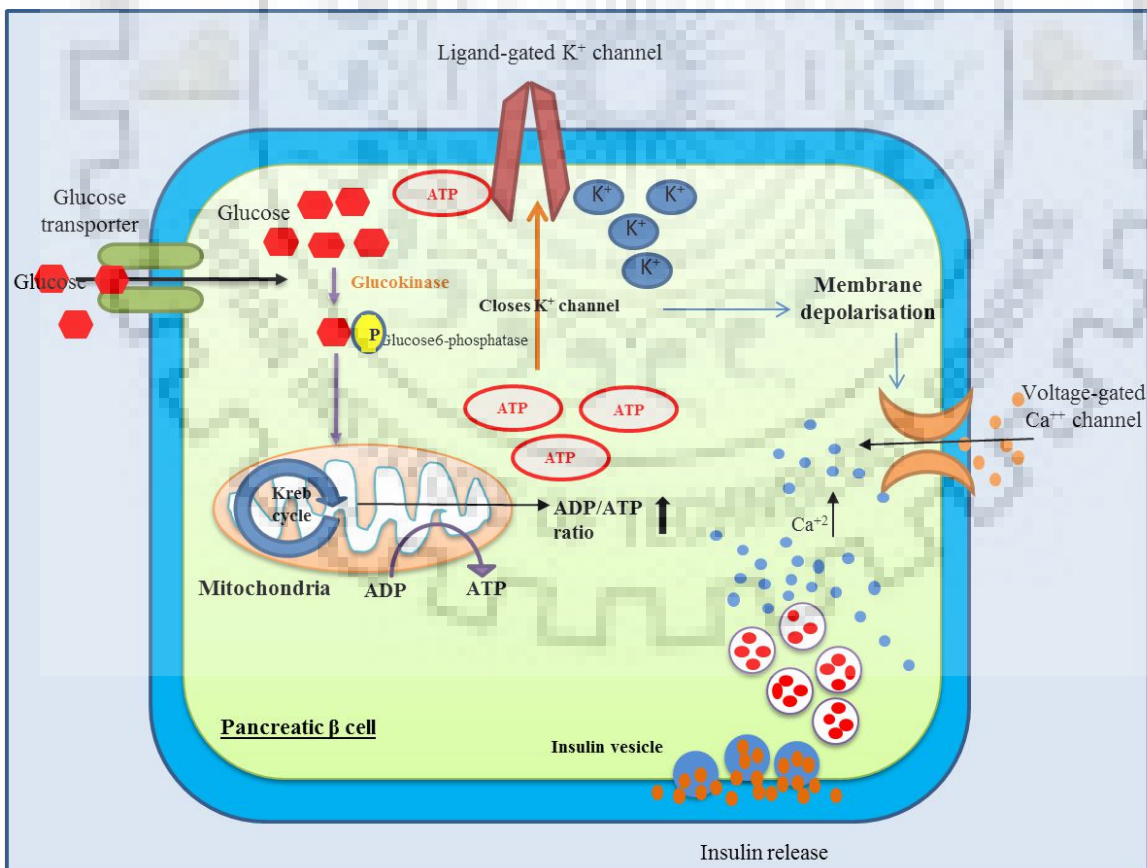


Fig. 2.6. Mechanism showing glucose-stimulated insulin release in pancreatic β -cells.

2.5.3.1.4. Cellular action of insulin

At the cellular level, insulin regulates key metabolic events such as carbohydrate, lipid and amino acid metabolism and mRNA transcription and translation (Wilcox, 2005).

2.5.3.1.4.1. Glucose metabolism

Insulin plays a major role in regulating glucose metabolism. Glucose liberated from dietary carbohydrate sources by their hydrolysis within the small intestine gets absorbed into the blood. Increased influx of glucose in the bloodstream stimulates the secretion of insulin which stimulates the uptake and utilization of glucose by adipose tissue, muscle and liver. Glucose is transported inside the cells by facilitated diffusion primed by hexose transporters. For example in muscles, GLUT4 is the major transporter that carries out glucose transport across the plasma membrane. Glucose absorbed from the small intestine is readily taken up by the hepatocytes in the liver and stored in the form of lipid and glycogen. Insulin activates hexokinase that in turn phosphorylates glucose and traps it within the cells. Insulin inhibits the activity of glucose-6-phosphatase. Also, simultaneously insulin inhibits gluconeogenesis and release of glucose from the liver. Insulin activates series of transcription factors and co-factors involved in glycolytic and fatty acid synthesis mechanism including PPAR γ co-activator 1 (PGC1), sterol regulatory element-binding protein (SREBP)-1, hepatic nuclear factor (HNF)-4, and the forkhead protein family (Fox) (Mounier and Posner, 2006). Moreover, enzymes like phosphofructokinase and glycogen synthase that are involved in the glycogen synthesis also get activated by insulin. The absence of insulin often results into the failure of glucose uptake by major organs.

2.5.3.1.4.2. Lipid metabolism

Insulin plays a key role in the synthesis of lipids and its storage in several major sites adipose tissue, liver and muscles. After dietary energy intake, insulin elicits the lipolysis of intravascular lipids via the action of lipoprotein lipase (LPL), VLDL and chylomicrons. The released fatty acids are taken up by adipose tissues and muscles where they get oxidized or esterified into the major form i.e. triglycerides. However, insulin signaling prevents the breakdown of these triglycerides inside the adipocytes.

When there is an increased glucose uptake, these get stored as lipid in the adipocytes because of the activation of enzymes that synthesize lipids such as pyruvate dehydrogenase, acetyl-CoA carboxylase and fatty acid synthase and (Saltiel and Kahn, 2001). Insulin also

inhibits lipolysis in the adipocytes, by inhibiting the enzyme, hormone-sensitive lipase (HSL). This enzyme is activated by PKA-dependent phosphorylation and inhibited owing to a combination of negative regulation of the kinases and activation of phosphatases. Lipase inhibitory regulation of insulin is driven by the reduction of cAMP levels due to cAMP-specific phosphodiesterase activation in the adipocytes.

2.5.3.1.4.3. Protein metabolism

Insulin facilitates protein synthesis in several tissues. Insulin indirectly regulates the transcription specific of mRNA encoding specific genes and translation of their respective proteins in the ribosomes. For examples, insulin enhances mRNA transcription for protein kinase, glucokinase, fatty acid synthase, and albumin in the liver and regulates the expression and expression of pyruvate carboxylase in the adipose tissue, amylase in the pancreas and casein in the mammary gland. Additionally, insulin decreases the transcription of mRNA encoding carbamoyl phosphate synthetase in the liver that is primarily involved in the urea cycle.

2.5.3.1.5. Insulin signaling pathway

The binding of insulin to the extracellular binding domain of its tyrosine kinase receptor (IR) results in its autophosphorylation at several tyrosine residues present inside the cell. These cascades of events result in the recruitment and phosphorylation of receptor substrates such as IRS and Shc proteins. Shc, in turn, activates the Ras-MAPK pathway while phosphorylated IRS proteins lead to activation of the PI3K-Akt pathway by recruiting a lipid kinase termed as phosphatidylinositol 3 kinases (PI3K) to the plasma membrane of the cell leading to the generation of second messenger Phosphatidylinositol (3,4,5)-trisphosphate (PIP₃). Activation of PI3K is essential for the regulation of protein, lipid and glycogen metabolism. Activated membrane-bound PIP₃ recruits PKB (protein kinase B) which further activates PDK-1, that in turn phosphorylates Akt and atypical PKCs (Fig. 2.7). Akt is crucial for glucose transport, gluconeogenesis, mediating insulin's metabolic effect, amino acid transport, glycogen and lipid synthesis. Akt also has a control on cell cycle and survival. Insulin receptor substrate-1 (IRS-1) associated PI3K pathway mediates insulin-induced inhibition of lipolysis in adipocytes via inhibiting hormone-sensitive lipase (HSL). The Shc-Grb2-Sos-Ras-Raf-MAPK pathway is another insulin signaling pathway that controls the cell proliferation, gene expression, differentiation and apoptosis (Siddle,

2011; Boucher et al., 2014). Insulin resistance the characteristic feature of T2DM occurs primarily at the level of insulin-sensitive tissues like liver, skeletal muscle, fat and can be triggered by several cellular perturbations like lipotoxicity, glucotoxicity, inflammation, mitochondrial dysfunction, and ER stress that results in to deregulation of genes and inhibitory protein modifications, resulting in impaired insulin and IGF-1 action (Saltiel and Kahn, 2001; Boucher et al., 2014).

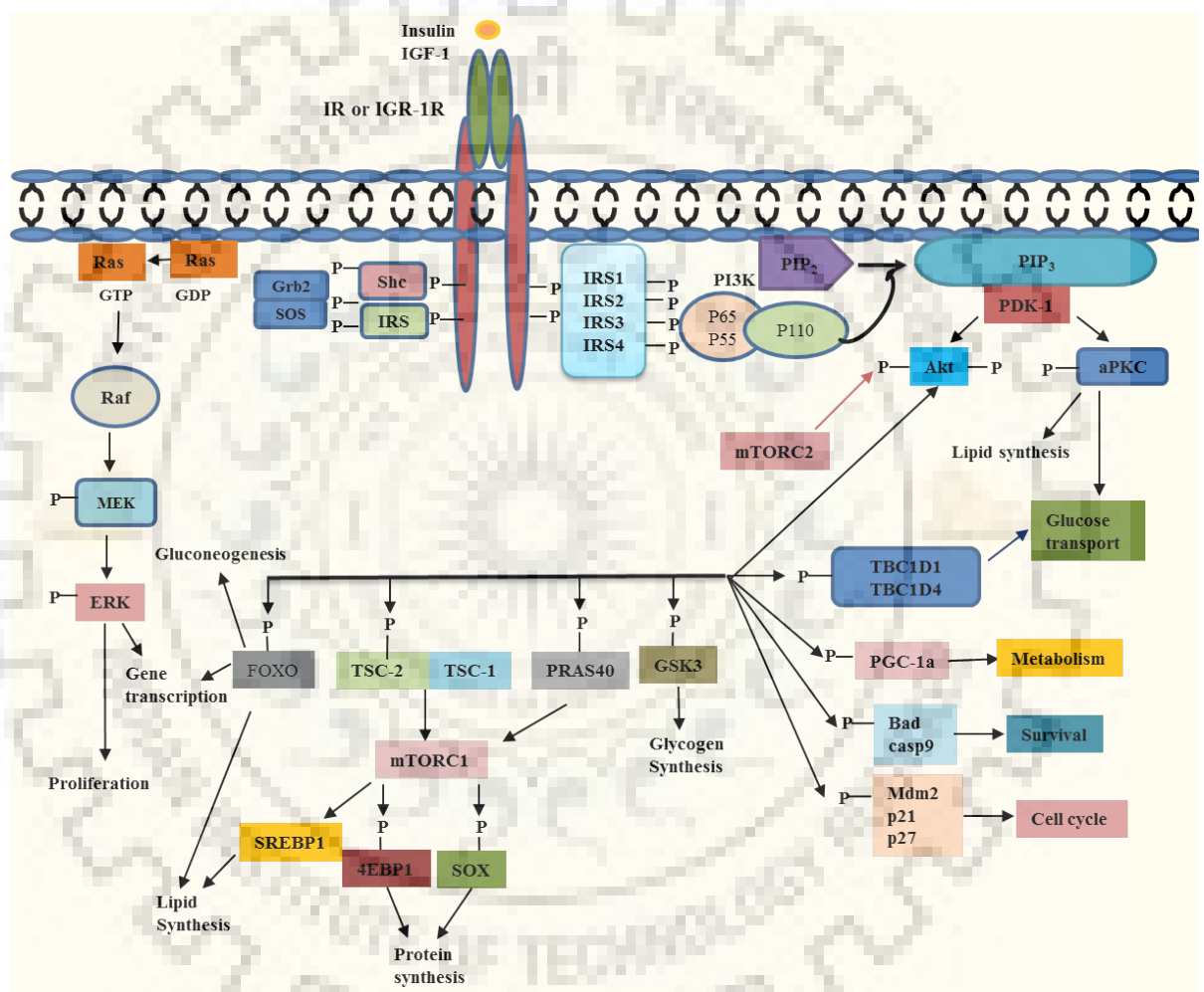


Fig. 2.7. Schematic representation of insulin signaling pathway.

2.5.3.2. Insulin resistance

Insulin resistance is a characteristic feature of type 2 diabetes and plays a major role in the pathogenesis of the disease (Jain et al., 2013). Insulin primarily lowers blood glucose by stimulating glucose uptake by the major insulin-sensitive tissues like skeletal muscle, liver, adipocytes and heart. However, when these insulin-sensitive tissues fail to respond to the

action of insulin, the abnormal physiological response is known as insulin resistance. The characteristic features of insulin resistance are hyperglycemia in fasting condition, increased glycosylated haemoglobin (HbA1c), hyperinsulinemia, postprandial hyperglycemia, hyperlipidemia, impaired glucose tolerance, decreased glucose infusion rate, increased hepatic glucose production, hypoadiponectinemia, loss of first phase secretion of insulin, impaired insulin tolerance and increased inflammatory markers in plasma.

Impaired insulin signaling pathway is the major reason of insulin resistance in type 2 diabetes. Tyrosine phosphorylation is quite essential for IR/IGF-1R and IRS activation whereas serine and threonine phosphorylation of the insulin receptor or IRS proteins is negatively associated with insulin signal cascade activation. The reduction in tyrosine phosphorylation of IRS-1 and -2 with increased Ser/Thr phosphorylation is elicited in response to hyperglycemia, fatty acids, cytokines, mitochondrial dysfunction and ER stress via activation of major kinases including c-Jun amino-terminal kinase (JNK), IKK, conventional and novel PKCs, mTORC1/S6K and MAPK (Fig. 2.8). In response to IRS serine/threonine phosphorylation, the PI3K levels are reduced mediating decreased activity of Akt and atypical PKC and results into decreased glucose uptake, due to reduced GLUT4 translocation (Agarwal et al., 2013; Boucher et al., 2014).

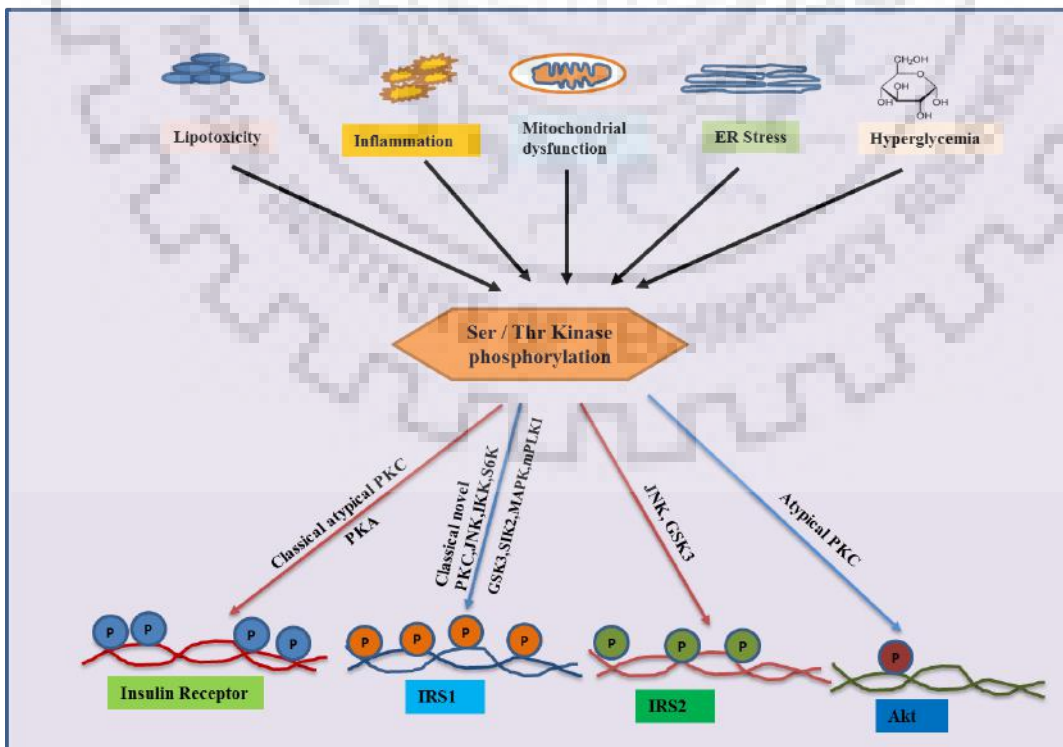


Fig. 2.8. Negative regulation of Ser/Thr activation on insulin signaling molecules.

Reduced responses of peripheral target tissues including adipose tissue, muscles and liver to a physiological concentration of insulin are profoundly observed in T2DM.

2.5.3.2.1. Adipocytes and insulin resistance

Adipocytes are the one of the major organ involved in insulin resistance in T2DM condition. Several major predisposing factors that confer insulin resistance in obesity-linked type 2 diabetes include, (a) Lipotoxicity (b) Inflammation (c) Mitochondrial dysfunction and (d) ER stress (Ye, 2013; Czech, 2017).

2.5.3.2.1.1. Lipotoxicity

Obesity is characterized by increased release of non-esterified fatty acids (NEFA), adiponectin, leptin and proinflammatory cytokines (Gastaldelli et al., 2017). Excessive caloric intake leads into metabolic overload and increased triglyceride input resulting into adipocytes enlargement (Smith and Kahn, 2016). Adipocytes from obese type 2 diabetic donors often shows reduced IRS-1 expression, resulting into decrease in IRS-1-associated PI3K activity. Also, FFA through its two intermediate metabolites DAG and ceramide, induce insulin resistance through an inflammatory response. DAG endogenously activates PKC (protein kinase C), which further activates IKKs and JNKs mediated inflammatory pathway to inhibit insulin sensitivity.

2.5.3.2.1.2. Inflammation

Hypertrophy of adipocytes due to metabolic overload increase the secretion of macrophage chemoattractants including secretion of monocyte chemoattractant protein-1 (MCP-1) that recruits macrophages eliciting a pro-inflammatory response in adipocytes (Ohlsson et al., 2017). Macrophages secrete a large amount of tumor-necrosis factor- α through IKK β -NF- κ B (inhibitor of nuclear factor (NF)- κ B (I κ B) kinase- β - NF- κ B) and the JNK-AP1 (Jun N-terminal kinase-4) that results into impaired TG deposition and increased lipolysis (Saltiel and Olefsky, 2017). Excessive circulating TGs and FFAs result in increased lipid accumulation in muscles. Thus ectopic lipid accumulation attenuate mitochondrial enzyme PPAR- γ coactivator-1 (PGC-1) expression, enhance the biosynthesis of ceramides and inhibit insulin-stimulated glucose transport through activation of protein kinase C (PKC), IKK β and JNK. Also, TNF- α inhibits insulin-stimulated GLUT4 glucose transport in muscle through MAP4K4 and JNK activation (Guilherme et al., 2008).

2.5.3.2.1.3. Mitochondrial dysfunction

Mitochondria are the major site for fatty acid oxidation and glucose metabolism. Reduction of mitochondrial function due to reduced number and size may contribute to FFA accumulation and lipid deposition favoring insulin resistance. In obese condition, lipid-induced mitochondrial over activation is needed due to increased demand of β -oxidation to disperse the excessive energy in muscle, liver and brown fat. Thus a large amount of ATP gets generated from fatty acid catabolism and when the ATP level surpasses the threshold limit, a negative feedback regulation is triggered for attenuation of the mitochondrial function (Szpigiel et al., 2018). Insulin-sensitizing substances can rescue the insulin resistance by inhibiting mitochondrial β -oxidation

2.5.3.2.1.4. ER stress

In obesity, chronic inflammation induced by activated JNK results in endoplasmic reticulum stress (ER stress) (Flamment et al., 2012). The aberrant accumulation of unfolded or misfolded proteins leads to ER stress that perpetuates the process of insulin resistance (Rieusset, 2017).

2.5.3.2.2. Skeletal muscle and insulin resistance

In the early stages of T2DM development, the impaired glycogen synthesis in muscle accounts for reduced insulin-stimulated glucose disposal and development of insulin resistance in skeletal muscle (Brøns and Grunnet, 2017). Also, chronic exposure of plasma FFA and mitochondrial dysfunction results into decreased fat oxidation in skeletal muscle which contributes to insulin resistance.

2.5.3.2.3. Hepatocytes and insulin resistance

In mammalian system, the liver plays a central role in modulation of fatty acid metabolism (Titchenell et al., 2017). The export of lipid in the form of triglycerides (TGs) deposited in the lipid droplets (LDs) within the hepatocyte depends on the synthesis as well as the availability of TGs (Zechner et al., 2012; Calo et al., 2016; Perry et al., 2014; Alves-Bezerra and Cohen, 2011). Decreased turnover of hepatic lipid droplets leads to the development of NAFLD (Greenberg et al., 2011). Excessive accumulation of these TGs leads to oxidative and ER stress which in turn triggers hepatic insulin resistance (Farese Jr et al., 2012) (Fig. 2.9).

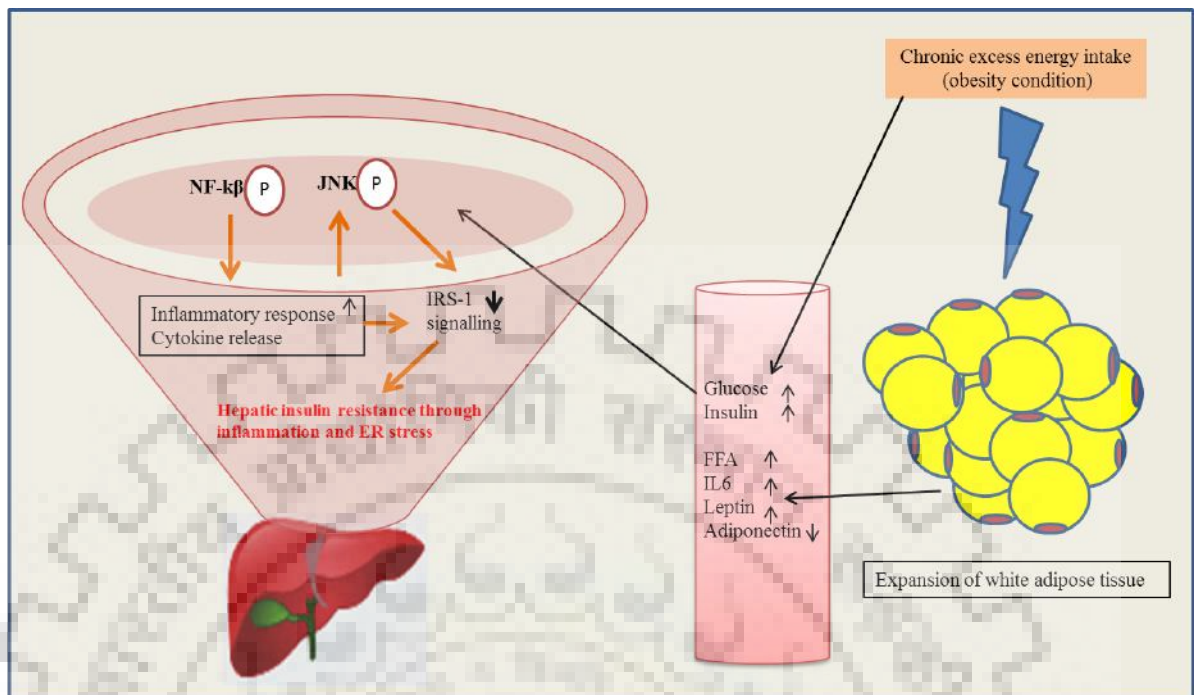


Fig. 2.9. General scheme showing obesity-linked hepatic insulin resistance

Several studies revealed the positive correlation between high-fat-diet-induced insulin resistance and its lipogenic effect, which leads to the fact that ectopic lipid accumulation can interrupt insulin signaling transduction (Samuel and Shulman, 2012). Importantly, ER stress recently emerges as another mechanism underlying insulin resistance (Samuel et al., 2004; Fu et al., 2012) (Fig. 2.10). Major regulators of unfolded protein response (UPR) pathways like protein kinase RNA-like endoplasmic reticulum kinase (PERK) and inositol-requiring enzyme 1 (IRE1) can activate c-Jun N-terminal kinase (JNK)/inhibitory-B kinase (IKK), that are involved in the inhibition of insulin signal transduction by phosphorylation of insulin receptor substrate 1 (IRS1) at serine sites (Urano et al., 2000; Aguirre et al., 2002; Liang et al., 2006).

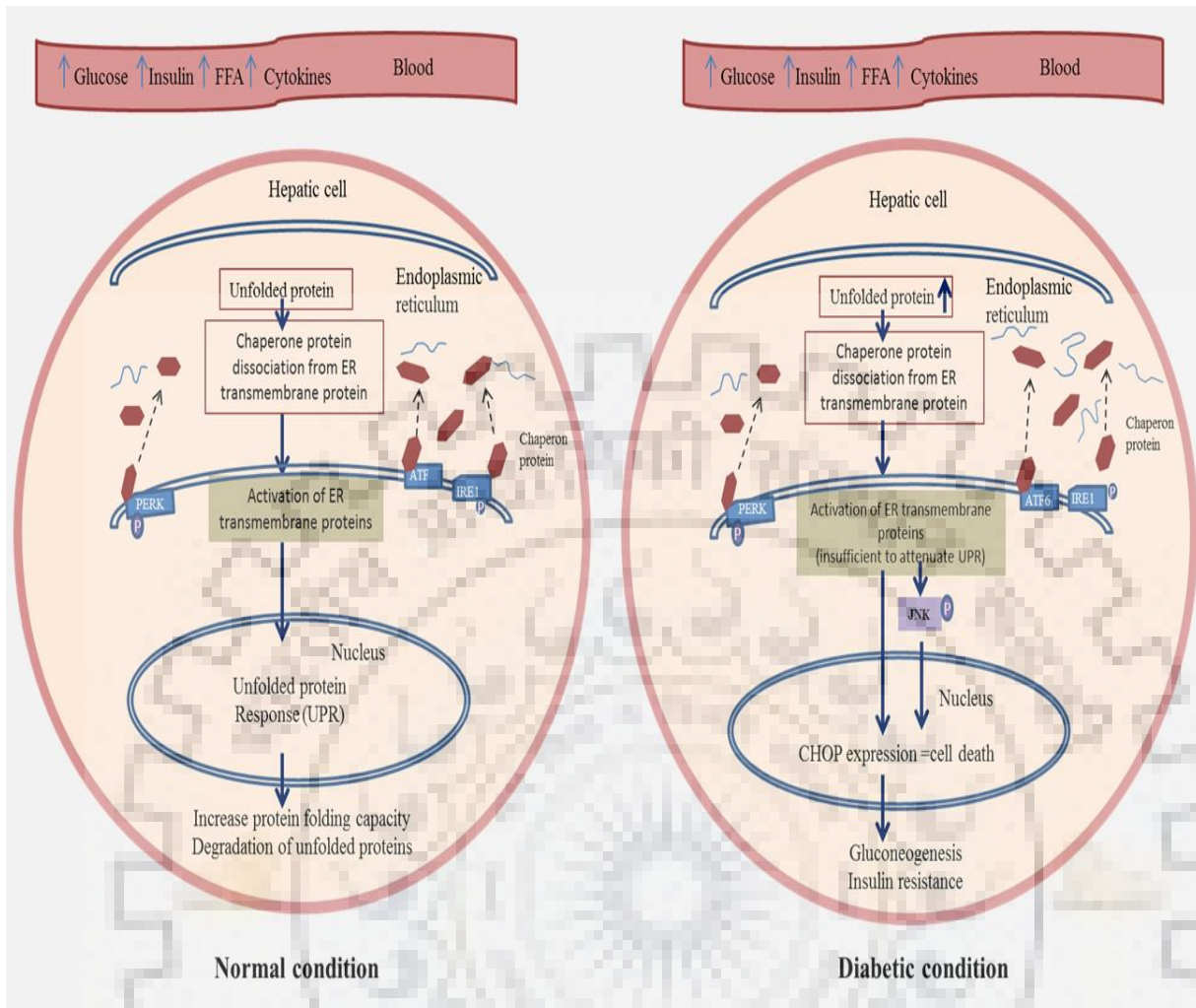


Fig. 2.10. General scheme showing activation of the UPR and ER stress signaling pathways in the liver under normal and diabetic conditions.

2.6. Treatment

2.6.1. Conventional therapy

The foremost step for prevention of T2DM is the control of diet and exercise (American Diabetes Association, 2018). If the blood sugar level deregulation still persists, the use of anti-hyperglycemic agents is advisable. The conventional drug treatment includes four major classes of anti-hyperglycemic agents, either as monotherapy or in combination with one another. These therapies include the use of following agents that are (Sena et al., 2013; Chaudhury et al., 2017; American Diabetes Association, 2018);

- Insulin secretagogues
- Insulin sensitizers
- Insulin
- α -glucosidase inhibitors

2.6.1.1. Insulin secretagogues

These compounds alleviate the hyperglycemia condition by stimulating insulin secretion. However, it is effective only if enough functional β -cells still exist. Their mode of action includes the closure of ATP-sensitive potassium channels in the β -cells which in turn increases insulin production. However, major side effects of these drugs are hypoglycemia and weight gain (Scheen, 2016).

2.6.1.1.1. Sulfonylureas

Sulfonylureas enhance insulin secretion by binding to a unique receptor on pancreatic β -cells and majorly affects fasting hyperglycemia (Kalra et al., 2015).

2.6.1.1.2. Meglitinides

It includes nateglinide, that binds to the same site of sulphonylurea receptor 1 and repaglinide, which binds to a nearby site of the receptor. However, both leads to rapid, short-lived, insulin secretion and insulin release (Black et al., 2007).

2.6.1.2. Insulin sensitizers

Insulin sensitizers are a class of compounds that increase the sensitivity of target organs to insulin.

2.6.1.2.1. Metformin

Metformin lowers blood glucose concentration and thereby improves insulin sensitivity. The major action includes reduction of hepatic gluconeogenesis and improvement

of insulin-stimulated glucose uptake ((Marín-Peñalver et al., 2016). However major complications of this therapy are renal dysfunction, vitamin B12 deficiency and cardiac failure.

2.6.1.2.2. Thiazolidinediones

Thiazolidinediones reduce hyperglycemia and increase insulin sensitivity by ameliorating dyslipidemia and inflammatory responses in T2DM (Marín-Peñalver et al., 2016; Marathe et al., 2017). It majorly includes rosiglitazone and pioglitazone. It activates peroxisome proliferators-activated receptor γ (PPAR- γ) expression and improves insulin sensitivity in muscle, adipose tissue and liver (Shrama and Singh, 2015). Major complications associated are weight gain, fluid retention causing edema and hepatotoxicity.

2.6.1.3. Insulin

Insulin is the most effective agent for restoring glycemic control and can effectively reduce the HbA1C level to the targeted range (American Diabetes Association, 2015; Raccah, 2017). Insulin is usually administered through injections and is of two types; (a) intermediate-acting or long-acting and given at bedtime (b) rapid-acting insulin administered before meals. However, insulin is typically administered subcutaneously and requires multiple injections per day. It results in weight gain and cardiovascular complications.

2.6.1.4. α -glucosidase inhibitors

The major α -glucosidase inhibitors include miglitol, acarbose, and voglibose that reduce the rate of oligosaccharide digestion and thereby reduce postprandial glucose levels and hyperinsulinemia. However, it is taken as multiple dosages per day, it gives rise to frequent gastrointestinal side effects and also is less potent than other oral anti-diabetic drugs.

2.6.2. Novel anti-diabetic drugs

As the conventional therapies do not address the issue of impaired β -cell function and reduction of β -cell mass in addition to no significant effect on insulin resistance, there has been a great research in the diabetes prevention and management field for developing novel anti-diabetic drugs. Some of them are listed below;

2.6.2.1. Incretin system

Increased postprandial insulin secretion in response to the gastrointestinal polypeptide (GIP) hormones after digestion of foods is generally regarded as the incretin effect. Two of the most important incretin hormones are GIP and GLP-1 (American Diabetes Association, 2018). The reduced insulintropic action of GIP and reduced postprandial GLP-1 secretion majorly account for the deficiency of incretin effect in T2DM patients (Holst et al., 2009). In recent years investigators have shown that GIP or GLP-1 infusion in type 2 diabetic patients could improve the first phase insulin response indicating improvement in β -cell function. Also in animal models, GLP-1 has shown stimulated neogenesis of β -cells and inhibition of apoptosis.

2.6.2.2. GLP-1 receptor agonists

Exenatide is the only GLP-1 receptor agonist that is currently available in the market (Lovshin, 2017; Tran et al., 2017). These agents are administered subcutaneously and have proven to be successful in lowering the HbA1C concentration by 0.5–1.0% resulting into significant weight loss (Abdul-Ghani and DeFronzo, 2017). The patients having reduced glycemic control even after treatment with sulfonylureas, metformin and/or TZDs are treated with this class of compounds. However, complications like nausea and vomiting are common with this treatment.

2.6.2.3. Dipeptidyl peptidase 4 inhibitors

Inhibitors of DPP-4 enzymes are orally active agents mediating acute surge of postprandial plasma insulin levels and also have shown to decrease the HbA1C by 0.5-0.9% upon clinical administration.

2.6.2.4. Pramlintide

Pramlintide is an analogue of human amylin analogue and is currently approved in the USA for its use as an adjuvant to insulin therapy. Subcutaneous injections are administered

before meals and it lowers the postprandial meal glucose excursions by reducing glucagon secretion.

2.6.3. Bariatric surgery

Bariatric surgery is done to maintain weight loss and is the most effective way to get rid of the physiological complications due to obesity-linked T2DM. It is achieved through malabsorptive surgery and gastric bypass. It can reduce the blood sugar up to 55-95% in diabetic people. However, it is expensive and often leads to several other complications like nutritional deficiency, osteoporosis and even pose death risks (American Diabetes Association, 2017).

2.6.4. Current therapies

In spite of the wide varieties of drug available for the treatment of diabetes mellitus, the severity of the disease yet persists with several concomitant physical aberrations like kidney failure, nerve damage, blindness and cardiovascular complications. Therefore to overcome the shortcomings of the conventional antidiabetic therapies, current research in the diabetes management and cure focuses on restoring the mass and functionality of β -cells either by differentiated stem cell therapy (Couri and Voltarelli, 2011; Hyo-Sup and Moon-Kyu, 2016) or by islet transplantation (Wang et al., 2015; Aly et al., 2013; Domínguez-Bendala et al., 2012). Several advanced therapeutics now focus on important aspects like (i) β -cell regeneration therapy (ii) non-pancreatic cell reprogramming (iii) proliferation of existing β -cell population and neogenesis (Domínguez-Bendala et al., 2012; Gianani, 2011).

2.6.4.1. β -cell regeneration therapy

Many researchers have designed several techniques to achieve β -cell regeneration (Chala and Ali, 2016) such as;

Induced pluripotent stem cells (iPSCs)

Induced pluripotent stem cell preparation by retroviral transduction of reprogramming factors to human fibroblast cells is an effective way of achieving β -cell regeneration (Maehr et al., 2009; Zhu et al., 2011). The iPSCs have greater success rates as it can be used as an

autologous cell therapy avoiding the chance of immune rejections and ethical issues. Reports suggest that islet-like clusters responding to glucose and producing insulin have been developed from iPSCs (Shaer et al., 2015).

Embryonic stem cells (ESCs) differentiation

Recently embryonic stem cells are being investigated for their potential to differentiate into functional β -cells. The first ever β -like cells were generated from a mouse ESC earlier in 2001 (Lumelsky et al., 2001). However, an insufficient number of differentiation of ESCs to insulin-producing cells and low insulin content of the cells limit the clinical advancement of this technique.

Adult mesenchymal stem cells (MSCs)

Adult mesenchymal stem cells have better ability to differentiate into β -cells and also have low immunogenicity as well as have a low chance of tumor growth, these may be used for β -cell generation. For example, dental pulp-derived MSCs, amnion derived MSCs, umbilical cord blood MSCs, placenta-derived MSCs, Wharton's jelly MSCs have been differentiated into glucose-responsive insulin-producing cells (Bhonde et al., 2014; Hashemian et al., 2015; Dang et al., 2017).

2.6.4.2. Transdifferentiation/ reprogramming of various non- β -cells

It has been recently reported that acinar cells can be transdifferentiated into β -cells *in vitro* and *in vivo*. Another study suggests that acinar cells were successfully reprogrammed to β -cells via viral expression of transcription factors like Ngn3, Pdx1 and MafA, and on transplantation, to streptozotocin-induced diabetic animals, it could rescue hyperglycemia. (Akinci et al., 2012; Quaranta et al., 2014).

α -cells to β -cells reprogramming

As the α - and β -cells emerge from similar lineage and express similar transcription factors, there is an opportunity for transdifferentiation among these cell types. As a result, α

cell reprogramming could be another attractive option for β -cell regeneration (Osipovich and Magnuson, 2018). Fomina and co-workers have explored a potential small molecule that can induce insulin expression by human α -like cells (Fomina-Yadlin et al., 2010).

Transdifferentiation of other cells to β -cells

Recently, cellular transdifferentiation of hepatocytes, gastrointestinal cells, biliary cells, keratinocytes neural cells and pancreatic ductal cells has been explored for developing functional β -cells suitable for cell replacement therapy (Wei and Hong, 2016).

2.6.4.3. Induction of replication of existing β -cell and islet neogenesis

Although the stem cell transplantation and cell reprogramming based therapies seem feasible, they pose many challenges and risk factors involving autoimmune rejections, repetitive usage of toxic immunosuppressive drugs and an insufficient number of β -cells for transplantation therapy.

However, as β -cell deficit underlies the pathogenesis of T2DM, the concept of replicating β -cells and inducing the pancreatic islets to undergo neogenesis may be amended for successful therapeutic interventions. It is known that β -cell turnover is very slow during adult life that maintains β -cell mass and there is a remarkable plasticity of the endocrine pancreas in rodents and humans to increase proliferation under secretory demand. It has been demonstrated that β -cell replication approximately increases five- to tenfold after partial pancreatectomy, during chronic glucose infusion, pregnancy and after treatment with GLP-1 analogues (Meier, 2008). Likewise, in rodents β -cell mass increases by ~ 2.5 -fold towards the end of pregnancy but at the post-partum stage, there is a rapid decline in β -cell mass through increased apoptosis. The β -cell replication decreases from 20% per day in pups to over 10% at weaning stage and up to 2-5% in young adults and finally reaches 0.07% in one-year-old mice (Márquez-Aguirre et al., 2015). The replication of pre-existing pancreatic β -cells has been demonstrated in adult mice, rats and humans. Several reports have been published showing the proliferation in primary β -cells through a variety of pharmacologic and genetic interventions. Recently it has been demonstrated that aminopyrazine compounds have successfully stimulated β -cell proliferation in adult primary islets. Also, human islets treated with aminopyrazine retained their functionality *in vitro* and even after transplantation into diabetic mice (Nathalie et al., 2010; Shen et al., 2015).

2.6.4.4. Cytoprotection of apoptotic β -cells

The major cause of onset and progression of T2DM is the loss of β -cell mass and function due to elevated levels of free fatty acids (lipotoxicity) and glucose (glucotoxicity) (Butler et al., 2003). *In vitro*, chronic exposure to free fatty acids (FFA) leads to pancreatic β -cell's apoptosis and impaired insulin secretion (Maedler et al., 2001; Lupi et al., 2002; Yuan et al., 2010). Therefore, protection of β -cells against lipid overload can be an effective strategy for counteracting obesity linked T2DM (DeFronzo and Abdul-Ghani, 2011; Song et al., 2015). As the conventional and antidiabetic drugs are expensive and have more side effects, it will be a better therapeutic stratagem to secure the existing pancreatic β -cell mass and restore its function.

Recent studies have elucidated that in the presence of saturated fatty acids and hyperglycemic conditions, β -cells undergo apoptosis due to impairment of autophagic turnover. Exposure of human pancreatic islets and β -cell lines to fatty acids and glucose blocks autophagic flux which leads to apoptotic cell death (Mir et al., 2015). Type 2 diabetic patients and high-fat diet mice model often exhibit a dysregulated autophagic activity which further ascertains the implication of impaired autophagy in the pathophysiology of T2DM (Masini et al., 2009; Codogno and Meijer, 2010). Therefore, restoring autophagy in β -cells in the diabetic condition has emerged as an effective therapeutic strategy to protect functional β -cell mass.

2.7. Autophagy

'Autophagy' was 1st termed by de Duve in 1963 from the Greek words *αὐτό* (self) and *φαγία* (eating). This is a lysosomal pathway for cell survival used mostly by eukaryotes to degrade and reuse cellular proteins and other organelles. Cells do this in order to compensate ATP and other elemental building blocks during nutrient/oxygen deprivation (Kundu et al., 2008). For a long period, autophagy was merely considered as a stress-induced cellular recycling mechanism. However, research during the past 10 years has disclosed the iscellaneous role of autophagy; this process occurs virtually in all mammalian cells, from oocytes to neurons in order to maintain homeostasis and quality control. Autophagy may target entire cytoplasm or selective cargo, clearing damaged mitochondria (mitophagy) or peroxisomes (pexophagy) (Tyagi et al., 2010). Additionally, autophagy participates in various

cellular processes such as aging, inflammation, innate and acquired immunity as well as cell differentiation (Rosenfeldt and Ryan, 2011). Loss of autophagy comes with the introduction of numbers of diseases including cancer, neurodegeneration, obesity and diabetes (Ahn et al., 2016; Rai et al., 2018). This is a highly conserved mechanism present in every eukaryotic cell from yeast to mammals having the same core autophagy machinery both morphologically as well as in protein constituents.

2.7.1. Types of autophagy

Autophagy is a well-conserved process from yeasts to mammals. There are three major types of autophagy i.e. macroautophagy, microautophagy and chaperone-mediated autophagy (CMA). Out of these three, macroautophagy is the most common form of autophagy and also referred to as “autophagy” in most of the cases. This process helps in delivering the cytoplasmic constituents to lysosomes for further degradation. All the three types of the autophagic process vary in the route of delivery of the cytoplasmic materials to the lysosomal lumen Fig. 2.11 shows the mechanism behind two major form of autophagy in yeasts.

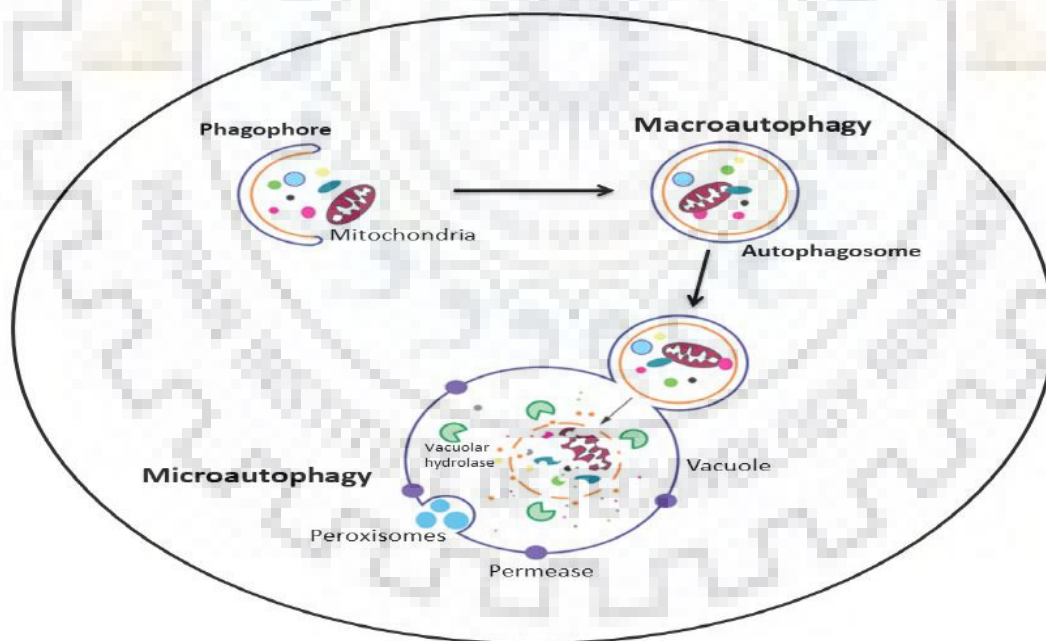


Fig. 2.11. Schematic representation of microautophagy and macroautophagy in yeast.

2.7.1.1. Microautophagy

Unlike macroautophagy and chaperone-mediated autophagy, microautophagy is mediated by direct lysosomal or vacuolar engulfment. In this process, the waste cytoplasmic

materials get trapped by the lysosome or vacuoles by membrane invagination. Along with macroautophagy, it is one of the necessary processes to encounter the nutrition recycling under starvation. Hence this pathway is vital for the cell survival in starvation as well as nitrogen deprivation condition.

2.7.1.2. Chaperone-mediated autophagy (CMA)

Chaperone-mediated autophagy is a secondary response to the nutrient starvation. In this mechanism, specific types of cytosolic proteins are targeted to lysosomes and eventually get degraded (Kaushik and Cuervo, 2012). In CMA, Chaperone Hsc70 binds to a consensus pentapeptide motif in the target protein. Hsc70 helps in targeting these proteins to the LAMP-2A (lysosome-associated membrane protein type 2A) receptor in lysosome membrane (Reynolds and Macian, 2018). The receptor, in turn, translocates the protein into lysosome for degradation.

2.7.1.3. Macroautophagy

This is the best characterized and most prevalent form of autophagy in which the autophagic cargos are delivered to lysosomes through *de novo* synthesized double-membrane vesicles known as autophagosomes (Huang and Klionsky, 2007). This type of autophagy is mainly triggered by the induction of a stress signal. This mechanism is vital to recycle cytoplasm and to generate energy as well as macromolecular building blocks in stress condition. This process also helps in removing damaged and superfluous organelles which in turn helps in the adaptation of cells during changing nutrient condition. The whole process of macroautophagy involves a battery of molecular players which helps in nucleation, elongation, maturation and degradation of the autophagosomes.

2.7.1.3.1. Molecular mechanism of macroautophagy

Low level of basal autophagy is observed constantly in the majority of mammalian cells. However, autophagy is induced due to starvation or certain stress like-ER stress, oxidative stress or hypoxia (He and Klionsky, 2009). The whole process can be divided into five different steps: initiation, autophagosome formation, fusion and degradation (Fig. 2.12).

Initiation

The relation between ULK1, AMPK and mTORC1 was described by Kim et al., 2011. During energy sufficient conditions, mTORC1 is active in an RHEB-dependent manner and phosphorylates ULK1 on Ser757 due to which its interaction with AMPK is prohibited. However, in glucose-starved condition, AMPK phosphorylates tuberous sclerosis protein 2 (TSC2) and RAPTOR which in turn inhibits mTORC1 and mTORC1-mediated ULK1 phosphorylation. As a result of this ULK1 is free to interact with AMPK, which phosphorylates ULK1 at Ser317 and Ser777 and activates it. However, it should be noted that autophagy induction by RAPA treatment or amino acid starvation usually occurs in an AMPK independent manner. Irrespective of the nutrient conditions, the ULKs form a complex with the mammalian ATG13 (Atg13 homolog) and the focal adhesion kinase family-interacting protein 200 i.e. FIP200 and Atg17 (Hara et al., 2008; Jung et al., 2009). Upon activation, ULKs phosphorylate and activate FIP200 and ATG13, and the activated ULK-ATG13-FIP200 complex is recruited to the phagophores (Hosokawa et al., 2009). It has also been observed that mTOR directly phosphorylate and inactivate ATG13 in normal condition (Jung et al., 2009).

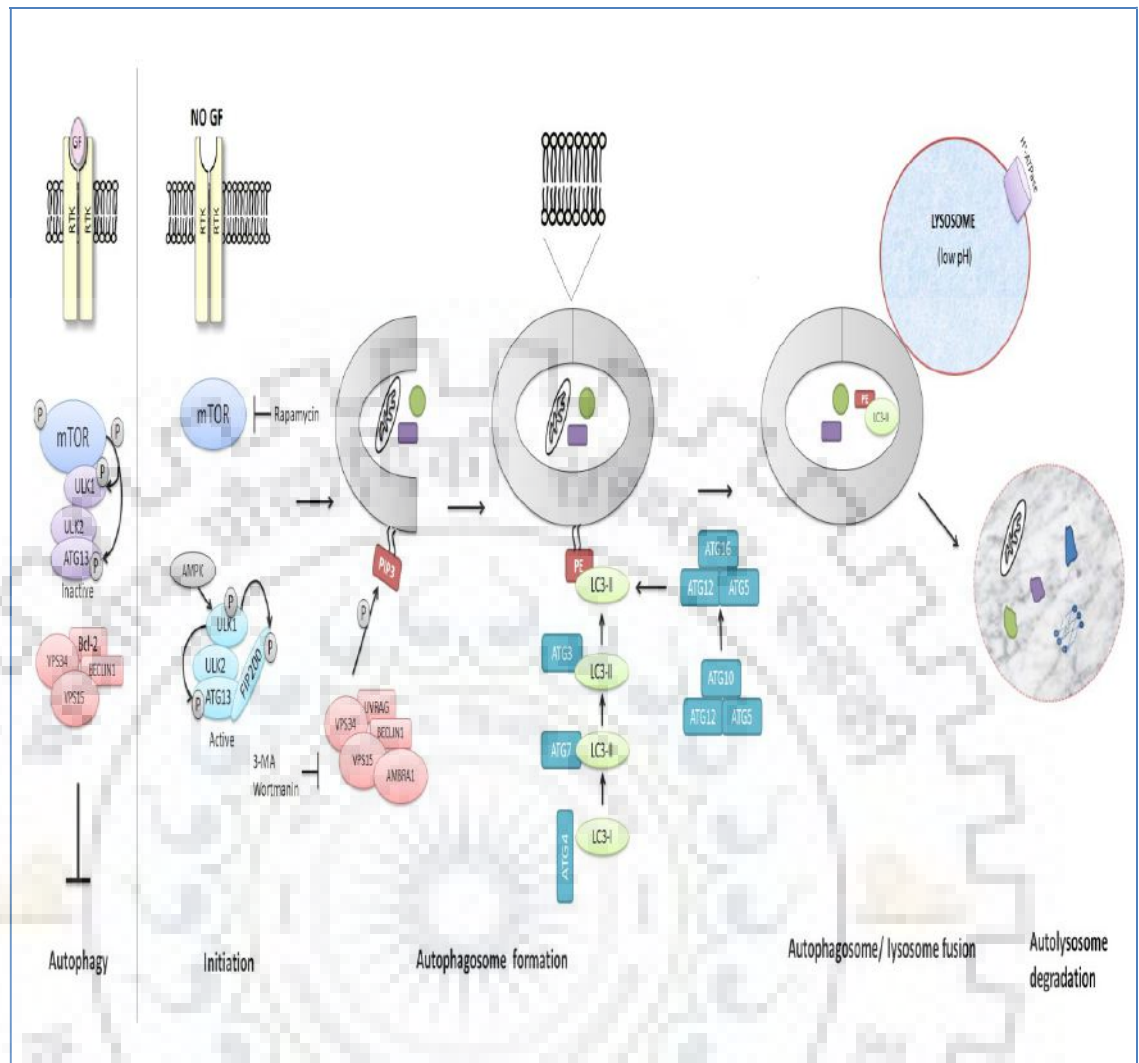


Fig. 2.12. General scheme showing mechanism of macroautophagy

Autophagosome formation

Autophagosome formation begins with the nucleation of the phagophore. Nucleation process is triggered by the complex formation of class III PI3K Vacuolar protein sorting 34 i.e. VPS34, VPS15 (Vanhaesebroeck et al., 2001; Lindmo and Stenmark, 2006) and BECLIN1 (Atg6 yeast homolog) (Kihara et al., 2001; Liang et al., 1999). Recently, BECLIN1-associated autophagy-related key regulator (BARKOR) is found to have an interaction with the aforesaid complex and this regulator has 32% similar sequence with Atg14. Hence BARKOR is also renamed as ATG14-Like protein (ATG14L) in mammals. As far as PI3K complexes are concerned, there are two PI3K complexes in yeast. First one is [Vps34-Vps15-Atg6]-Atg14, which participates in autophagy, and the later one [Vps34-Vps15-Atg6]-Vps38, is involved in the vacuolar protein-sorting pathway (Itakura et al., 2008). It is believed that the Atg14 and

Vps38 actually give a "tag" to complexes and hence determine to check their function and localization. Notably, in mammals, the core of the PI3K complex comprises of the VPS34-VPS15-BECLIN1 and depending on the attachment of specific interactors, like ATG14L or the UV irradiation resistance-associated gene (UVRAG; Vps38 yeast homolog) protein, the complex gains certain functions related to membrane trafficking. In the mammalian autophagy machinery, ATG14L targets the PI3K complexes to an ER subdomain which is essential for autophagy (Itakura and Mizushima, 2010; Matsunaga et al., 2010). Accordingly, in both yeast and mammals, ATG14L is mediating the localization of the PI3K complexes to the locale where the autophagosome is formed. Furthermore, the function of the PI3K complex can be monitored via interaction of BECLIN1 with its interactor. The apoptosis regulator protein BCL2 can arrest autophagy with the help of BH3-like domain in BECLIN1 (Maiuri et al., 2007). This interaction is, however, reversed during starvation which in turn allows BECLIN1 to cause autophagy (Pattingre et al., 2005). It has also been seen that the BECLIN1 interacts with UVRAG in order to activate autophagy (Liang et al., 2006). Another BECLIN1 binding molecule is 'activating molecule in BECLIN1-regulated autophagy protein 1' (AMBRA1). The PI3K core complex is docked to the cytoskeleton via dyneins through a BECLIN1/AMBRA1 interaction. Di Bartolomeo and colleagues proved that when autophagy is induced, AMBRA1 gets phosphorylated by ULK1, disrupting the interaction with BECLIN1 (Di Bartolomeo et al., 2010). This allows the PI3K complex to dissociate from dyneins and reach the ER which initiates the nucleation of the autophagosome. The origin of the autophagosomal membrane still needs to be solved. It has been suggested that either the ER or the Golgi is the source. However, others proposed that both ER and mitochondria or a de novo membrane generation are the sources of the autophagosomal membrane (Tooze and Yoshimori, 2010). The expansion of the phagophore which leads to the formation of the autophagosome relies on two ubiquitin-like (UBL) conjugation systems; the ATG12-ATG5 and the ATG8-PE (phosphatidylethanolamine) [ATG8 is also known as microtubule-associated protein 1 light chain 3 (LC3); Atg8 yeast homolog]. The proteins with UBL activity, ATG12 and ATG8, go through a series of coupling with different ATG binding partners ATG12-ATG5 system: ATG7, a homodimeric E1-like enzyme, activates ATG12. Additionally, ATG7 covalently conjugates ATG12 to ATG10 (E2-like enzyme) followed by ATG5. Then, the ATG12-ATG5 complex associates to ATG16-like complex (ATG16L; Atg16 yeast homolog), which mediates the binding of the complex to the phagophore (Mizushima et al., 2003). Afterward, the ATG12-ATG5-ATG16L promotes the loading of the ATG8-PE on the nascent

autophagosomal membrane (Nakatogawa et al., 2009). LC3-PE system: There are three LC3 isoforms (LC3A, -B, and -C) and four additional Atg8 yeast homologs (GABARAP, GEC1/GABARAPL1, GATE16/GABARAPL2, and GABARAPL3) identified in humans (He et al., 2003; Xin et al., 2001). Post-translational modification of LC3 is done by a cysteine protease called ATG4. This removes 22 amino acids from the C terminal of LC3, which exposes a glycine residue in order to generate the cytosolic form (LC3-I) (Kirisako et al., 2000; Kabeya et al., 2000). Once autophagy is induced, LC3 gets activated by ATG7 and transfers it to ATG3 (E2-like enzyme). At last, ATG12-ATG5 covalently binds PE to LC3-I (Fujita et al., 2008; Hanada et al., 2007), which generates the lipidated form, LC3-II (Kabeya et al., 2000). Autophagosomes contain double membrane having a different composition on both sides. LC3-II and ATG12 etc. seem to be the most indispensable building block for both inner and outer autophagic membranes. Some also suggest that the expanding autophagosomes engulf bulk cytoplasmic contents in a non-specific manner. Still, this process can be selective too; cargo receptors deliver ubiquitinated substrates for autophagic degradation. For example, mammalian protein p62/sequestosome 1 (SQSTM1), contains a C-terminal ubiquitin-associated (UBA) domain which binds to ubiquitin along with a conserved peptide motif of 22 acidic amino acids LC3-interacting region (LIR) that permits direct binding to human LC3 family members (Pankiv et al., 2007; Jana, 2010). The selective identification and degradation of p62 through autophagy were shown by its accumulation in autophagy-deficient cells (Wang et al., 2006; Nakai et al., 2007). NBR1 (neighbor of BRCA1 gene 1) is another autophagy receptor which contains a UBA domain along with a LIR region (Kirkin et al., 2009). NBR1 and p62 can work independently, or it can also interact and build oligomers.

Fusion and degradation

After complete autophagosome formation, ATG4 releases LC3 from the PE by disrupting the amide bonds (Geng and Klionsky, 2008). Though the complete mechanism of autophagosome fusion with lysosome is not fully understood, however, in mammals, the process requires LAMP-2, UVRAG and the small GTPase RAB7 (Jager et al., 2004; Tanaka et al., 2000). The complete lysis of cargo is done by cathepsins (Tanida et al., 2005). After lysis rest of the components are recycled to the cytosol for reuse. However, the process of autophagic recycling has yet to be identified.

2.7.2. Autophagy in diabetes

Recent research reveals the positive correlation between the increased incidence of type 2 diabetes and autophagy malfunction (Ebato et al., 2008; He et al., 2013; Jung et al., 2008; Rocchi and He, 2015). Sedentary lifestyle and intake of highly nutrient-rich food are the major factors contributing to the imbalance between energy intake and expenditure ratio which in result induce obesity and diabetes. As per some reports, physical exercises and fasting can induce autophagy (Grumati et al., 2011; He et al., 2012a; He et al., 2012b; Liu et al., 2009; Mizushima et al., 2004). Thus it is noteworthy to investigate the mechanism by which the autophagy can reduce the T2D and obesity. Recent evidence prove the link between autophagy and potential metabolic benefits but a lot of things are yet to be deciphered in terms of its therapeutic effect and the cell-specific requirement of autophagy. In addition, a proper coordination of insulin-producing β -cells and some organs like- liver, muscle and adipose tissues helps in the maintenance of glucose metabolism. However, very little is known about the role of autophagy in the coordination of these organs as well as glucose metabolism. Dysfunction of pancreatic β -cells can result in various forms of diabetes like type 1 diabetes, T2DM and maturity-onset diabetes in young. It has been observed that autophagy helps in the maintenance of the β -cells. In some recent evidence, a knockout of Atg7 gene in mice not only leads to impaired glucose tolerance and glucose-stimulated insulin secretion but also induced morphological abnormalities of islets and decreased β -cells (Ebato et al., 2008; Jung et al., 2008; Quan et al., 2012). Ubiquitinated protein accumulation and induction of apoptosis may result in the reduced number of β -cells.

2.7.3. Liver complications and autophagy

It is observed that the level of autophagy is reduced in hepatocytes in case of obesity. There are several mechanisms for the decline of the autophagy. As per a study, the calcium-dependent protease calpain 2 level is increased during obesity which results in down-regulation of Atg7 and a defective autophagy (Yang et al., 2010). Other important studies on the same theme also reveal that in obese mice, mTOR is up-regulated in liver and the over-activation of this autophagy inhibitor can result in muscle and insulin resistance probably due to phosphorylation of and inhibition of IRs1 by S6K (Tremblay and Marette, 2001; Um et al., 2004; Tremblay et al., 2005). Although controversial but down-regulation of autophagy in obese mice may also be induced by hyperinsulinemia. However, overexpression of Akt/PKB, a

key regulator of insulin pathway decreases autophagy in the hepatic cells of the obese mice (Liu et al., 2009). Few studies also suggest that destruction of pancreatic β -cells by streptozotocin does not increase autophagy in obese mice in comparison to lean mice (Liu et al., 2009). Although the reasons for this kind of disparity is very unclear, however, in obesity, an obstruction in hepatic autophagy can cause severe complications like a decrease in the rate of lysosomal degradation and increase in ER stress due to nutrient assimilation. Hence, in this context, it is noteworthy to mention that insulin resistance may be triggered by the effect of the decline in autophagy and increased ER stress.

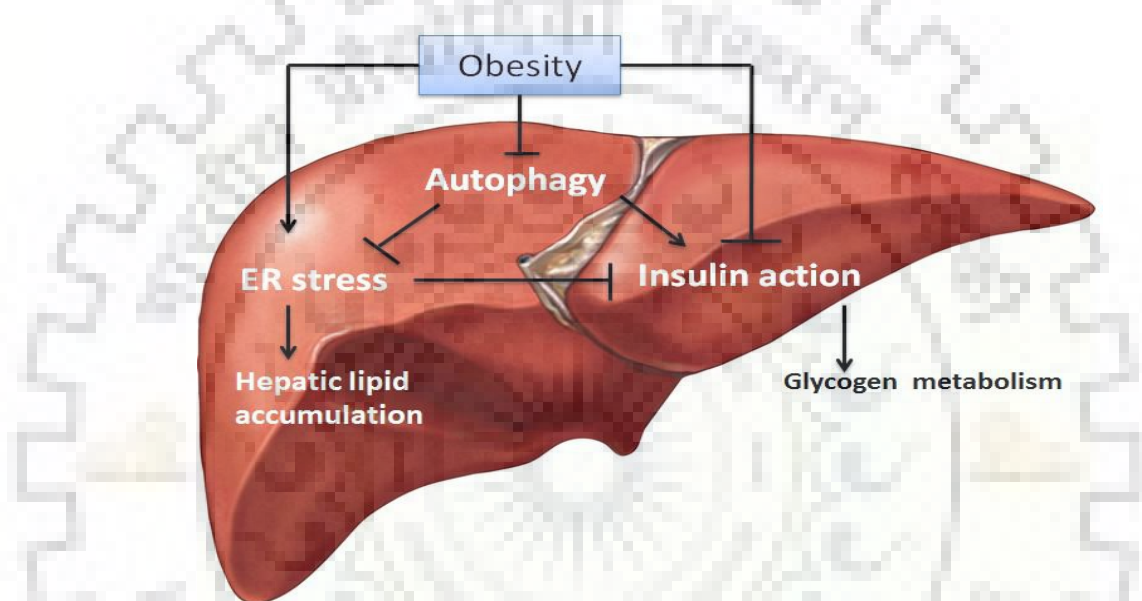


Fig. 2.13. General scheme showing effect of autophagy in liver

2.7.4. Hepatic steatosis and lipophagy

Hepatic autophagy plays a vital role during nutrient deprivation condition in the liver. During the process, the lipid droplets are degraded to form free fatty acids for ATP production. This phenomenon of degradation of lipids is called lipophagy. Hence this process helps in the elimination and excess triglycerides and prevention of steatosis. In an experiment, inhibition of autophagy by genetic knockdown of Atg5 or by pharmacological inhibitors like 3-methyladenine significantly increases the triglycerides in the cultured cells. Retention of excessive triglycerides and cholesterol in the lipid droplets result in the reduction of fatty acid oxidation which in turn inhibits macroautophagy. A recent report proved the direct interaction

of LC3 with lipids droplets before autophagosome formation. As per the study the lysosomes fuse with the autophagosome having lipid droplets. It has also been observed that 16 weeks HFD fed mice have an impairment of autophagy in the liver which occurs due to the decreased mobilization of lipid into autophagic compartments (Singh et al., 2009). The possible mechanism of inhibition of macroautophagy by HFD is due to the alternations of membrane structures by lipid accumulation which in turn result in a decrease in fusion efficiency. The same study also suggests that liver of starved mice have increased lipid droplets, autophagosomes, autophagolysosomes and lysosomes (Singh et al., 2009). Another report states that *Atg7* deficient knockout mice have significant enlargement of liver and accumulation of poly-ubiquitinated proteins (Komatsu et al., 2005). An increase in hepatic triglycerides and cholesterol is also seen in these mice which prove the role of autophagy in the regulation of lipid metabolism. In obesity and fatty liver, autophagy is inhibited in liver cells. Fig. 2.14 gives a brief illustration of involvement of amino acids and/or insulin through Akt/PKB and mTOR signaling pathways. Obesity is directly or indirectly related to the inhibition of hepatic autophagic turnover by insulin resistance and hyperinsulinemia. As per a report, in obese mice having hepatic steatosis, a decrease in LC3-II and increase in p62 is observed, a protein degraded by autophagy (Liu et al., 2009). The same report also states that hyper-insulinemia activates Akt/PKB, which in turn inactivates FoxO1. FoxO1 regulates the expression of *Vps34*, *Atg12* and *Gabarapl1* at the mRNA level. Hence, preventing Akt/PKB will up-regulate these genes promoting autophagy. In contrast to this fact, hepatic autophagy is not affected and up-regulated in type 1 diabetic mice (Liu et al., 2009; Yang et al., 2010). The process is evaluated by the accumulation of LC3-II and decrease in p62 protein. As per a study, the activation of mTOR due to overnutrition and by elevated amino acid concentration can negatively regulate autophagy by inhibiting ULK1 (Codogno and Meijer, 2010). Several emerging reports prove the crosslink between ER-stress, obesity, insulin resistance and T2DM (Harding et al., 2001; Kaneto et al., 2005; Codogno and Meijer, 2010; Bhatia et al., 2014). However, the defective autophagy in the liver in case of obesity could promote insulin resistance and ER stress (Codogno and Meijer, 2010). Since mis/unfolded proteins are eliminated by autophagy, the deterioration of hepatic autophagy could lead to accumulation of these proteins and induction of ER stress. In some studies, it is found that overexpression of *Atg7* in the liver of obese mice has significantly reduced ER stress, enhanced glucose tolerance and sensitivity to insulin. Hence a vicious cycle is maintained between hyperinsulinemia, hepatic autophagy, ER stress and obesity (Fig. 2.13).

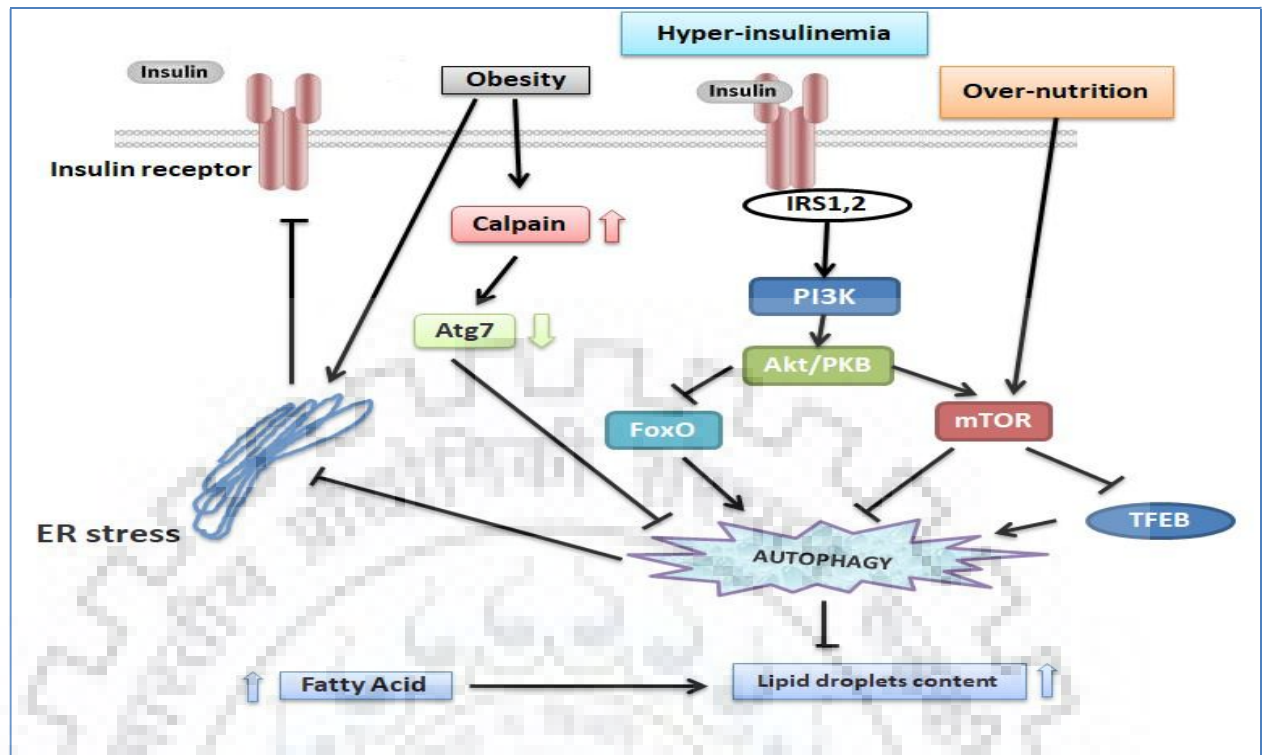


Fig. 2.14. Schematic representation showing crosstalk between obesity, hyperinsulinemia and autophagy

2.7.5. ER stress-induced hepatic insulin resistance

ER stress can be caused by several ways such as dysfunction of calcium regulation, mutational load, nutrient deprivation and oxidative stress (Moon et al., 2014; Panigrahy et al., 2017). Most importantly, the ER stress as the name suggests is not localized to ER only and are spread to interacting organelles and whole cell as well also. At the initial stage of ER stress, prosurvival effects are observed to reduce the misfolded protein and restore cellular homeostasis. However cumulative unresolved ER stress results in a switch to programmed cell death. The pro-survival part of ER stress has some vital functions like- up-regulation of misfolded proteins clearance by ERAD pathway and increasing protein folding capacity. In most of the cases, molecular chaperones such as heat shock proteins, foldases and lectins are overexpressed in response to ER stress in order to enhance protein folding and expanding ER itself. Under normal condition, these molecular chaperones help in proper folding of proteins and later undergo modifications but in stressed condition these help in refolding of the misfolded proteins. As per some recent studies, the molecular chaperones recognize the misfolded proteins through the exposed hydrophobic regions which are usually hidden in their

native states (Schroder and Kaufman, 2005). A series of proteins get activated and initiate compensatory response upon ER stress like ER kinase (PERK), inositol-requiring enzyme-1 α (IRE1 α) and activating transcription factor-6 (ATF6). During ER stress a series of signaling cascades operate and a collection of one of such sets is called Unfolded Protein Response (UPR). Proteins like PERK, IRE1 α and ATF-6 are the key regulator of UPR.

The core defect in T2DM is Insulin Resistance and it is associated with obesity and the metabolic syndrome. The metabolic effects of insulin are exerted on the whole body. It stimulates synthesis of fatty acids and glycogen, induces cell proliferation, causes a reduction in blood glucose and improves microcirculation. Under normal physiological conditions, when insulin binds to its membrane receptor it promotes receptor autophosphorylation. The adaptor molecules insulin receptor substrate 1 and 2 (IRS1 and 2) are phosphorylated by the activated receptor and then a complex cascade of signaling events is initiated.

Insulin resistance is a condition where there is a decrease in insulin action on target tissues, like liver, skeletal muscle and adipocytes. In the liver, insulin resistance causes a decrease in glycogen synthesis and an increase in gluconeogenesis (Hatting et al., 2018). With respect to the adipose tissue, insulin action failure promotes lipolysis and results in the release of high levels of free fatty acids into the circulation. In skeletal muscle, in insulin-resistant state the insulin-stimulated glucose uptake is markedly reduced. Multiple factors determine insulin resistance, such as aging, inflammation, ER stress and mitochondrial dysfunction. Till now, there has been no consensus for a unifying mechanism of insulin resistance. Mechanisms contributing to insulin resistance are complex. It is generally considered that the hepatic insulin resistance is developed mainly by ER stress. The following may be the supporting evidences: (1) ER stress activates stress kinases that impair insulin signaling. During ER stress IRE1 activation stimulates JNK and inhibitor of κ kinase (IKK), both inhibit insulin signaling by phosphorylating IRS1 on serine residues (Hu et al., 2006; Urano et al., 2000). Both gluconeogenesis and lipogenesis are paradoxically triggered, in insulin-resistant conditions. The transcription of critical hepatic enzymes implicated in gluconeogenesis or lipogenesis can be regulated by ER stress-activated transcription factors and hence participate in the abnormal stimulation of these pathways. (3) ER stress promotes fat accumulation in hepatocytes which may disrupt insulin signalling. Hepatic ER stress enhances degradation of apolipoprotein B100 (apoB100) (Ota et al., 2008; Qiu et al., 2009) which impairs very low-density lipoprotein (VLDL) synthesis and export. In addition, the role of ER stress on insulin signaling in adipose cells and muscle cells has been identified. It has been demonstrated that ER stress could

decrease insulin signaling in 3T3-L1 adipocytes (Xu et al., 2010). Insulin receptor expression is down-regulated upon ER stress. It has also been shown that decrease in insulin signaling by the IRE1-JNK pathway in muscle cells (Hwang et al., 2012; Peng et al., 2011) is due to ER stress. It is well established that pivotal factor in causing insulin resistance is ER stress, yet the underlying mechanisms are not fully characterized. Nonetheless, recent studies on the regulation of insulin signaling that describe ER stress as the main factor have been performed only *in vitro*. To confirm that ER stress leads to IR, we need further *in vivo* research. Current studies indicate that defective autophagic response is another factor in the development of insulin resistance. Liver of obese mice is deficient in autophagy and its upregulation will be able to combat insulin resistance (Yang et al., 2010). Zhou et al. indicated that the down-regulation of insulin receptors (Zhou et al., 2009) may be related to autophagy. Conversely, in the presence of insulin resistance autophagy activity is inhibited (Liu et al., 2009). Though studies show that autophagy is associated with insulin resistance, further investigation would be required to establish a direct causal relationship.

2.7.6. Autophagy: a potential link between ER stress and insulin resistance

Down-regulation of insulin receptor induced by ER stress may be an important factor in IR. The insulin receptor is a key molecule involved in cell metabolism and insulin signaling. In insulin-sensitive tissues of db/db mice and high-fat diet treated mice, the ER stress marker C/EBP homologous protein (CHOP) negatively influences the expression levels of insulin receptor (Zhou et al., 2009). In addition, ER stress-induced insulin resistance triggers autophagy in the peripheral insulin target tissues. Being a putative adaptive catabolic process and through its constitutive activity autophagy could generate energy for cells in starvation and also help to restore cellular homeostasis in nutrient-rich conditions. However, the role of autophagy is thought to be two way. ER stress-induced decrease in insulin receptor cellular levels was markedly ameliorated by the autophagy inhibitor 3-methyladenine (3- MA) (Zhou et al., 2009). Other reports at the same time show additional mechanisms involved in autophagy and insulin resistance. These authors have postulated that autophagy is a key modulator of insulin signaling and organelle function. Dysregulated autophagy is a major contributor to abnormal insulin action. In both genetic (ob/ob) and dietary (high-fat diet-induced [HFD]) models of murine obesity, hepatic autophagy is severely depressed, particularly in Atg7 expression levels (Xu et al., 2010). It is verified that Atg7-deficient cells have defective autophagy. Inhibition of Atg7 led to the decreased insulin-stimulated Akt Ser-

473 and insulin receptor β subunit phosphorylation both in the liver of intact lean mice and in murine hepatoma cells (Xu et al., 2010). By observations in both cellular systems and whole animals, the importance of autophagy in insulin signaling is clearly indicated. Nevertheless, the mechanisms of impaired autophagy in obesity are controversial. In obesity, insulin resistance and autophagy cause hyperinsulinemia that is negatively regulated by the activity of insulin-mTOR pathway. With insulin resistance and hyperinsulinemia, the autophagy process and transcript levels of several pivotal autophagy genes such as vps34, atg12, and gabarapl1 genes were decreased in the livers of mice. Autophagy can be inhibited by insulin by suppressing the expression of crucial autophagy genes in a FoxO1-dependent manner directly or indirectly (Liu et al., 2009). Conversely, according to a study, the downregulation of Atg7 and defective autophagy (Yang et al., 2010) is caused due to the increase in calpain 2 rather than the high insulin levels seen in obese mice. Mechanisms involved in the autophagy suppression in case of obesity are still under intensive research. Additionally, as evident by the stimulation of eIF2 α and PERK phosphorylation, loss of autophagy could cause ER stress in the liver tissue of lean mice.

In vitro cell models Inhibition of autophagy added to impaired insulin action and increased ER stress. Conversely, overexpression of Atg7 in liver contributed to improved insulin sensitivity, dampened ER stress, and systemic glucose tolerance (Codogno and Meijer, 2010). In concise, autophagy is must for promoting cell survival by eliminating damaged organelles and misfolded large molecules. Down-regulation of autophagy leads to the accumulation of these molecules and aged organelles which can be the cause of IR and ER stress. A study showed that down-regulated autophagy can cause degeneration of β -cells, by allowing intracellular accumulation of dysfunctional mitochondria (Gonzalez et al., 2011). Nevertheless, it is yet not clear if autophagy plays a protective or harmful role in diabetes. Autophagy could show different defects depending on the types of tissues or cells and environmental context. This relates to insulin action and ER stress in the liver with autophagy and confirms the systemic metabolic impact of hepatic autophagy deficiency *in vivo*. Furthermore, it has been demonstrated that 4-PBA and tauroursodeoxycholic acid (TUDCA), can decrease ER stress, which are two different chemical structures having chemical chaperone activity in common. The increase in ER stress may promote insulin receptor correct folding and membrane targeting, contributing to improved insulin action. In the pathophysiology of diabetes, the observations suggest a relevance of autophagy and ER stress.

2.7.7. Autophagy and β -cell

In obesity, the β -cell acclimatizes to insulin resistance by augmenting the production and secretion of insulin (Leibowitz et al., 2009). The perpetual impetus for the β -cell to secrete copious amounts of insulin for maintaining euglycemia is concomitant with an elevated protein-folding load in the endoplasmic reticulum (ER) which may cause accretion of misfolded proteins, notably proinsulin, ensuing ER stress (Scheuner and Kaufman, 2008; Eizirik et al., 2007). The ER stress, along with the oxidative stress stimulated by excessive reactive oxygen species (ROS) generated from mitochondria, causes β -cell dysfunction (Poitout and Robertson, 2007; Prentki and Nolan, 2006; Gerber and Rutter, 2017); which is the major cause for the affliction of glycaemic control in diabetes over the time. T2D is accompanied by a raised level of hyperglycemia, non-esterified fatty acids (NEFA) and inflammation which escalates cellular stress, as a consequence generating a feed-forward vicious cycle that affects β -cell function, and may induce apoptosis and possibly β -cell dedifferentiation (Talchai et al., 2012; Hameed et al., 2015).

Autophagy may protect the stressed β -cell by eradicating impaired organelles (e.g. endoplasmic reticulum i.e. reticulophagy and mitochondria i.e. mitophagy (Kroemer et al., 2010; Mizushima and Komatsu, 2011) and/or misfolded proteins, particularly proinsulin (Fig. 2.15). This notion is supported by a number of reports and put forward that lysosomal degradation pathways, including autophagy and crinophagy, are imperative for β -cell homeostasis both in physiology as well as in diabetes.

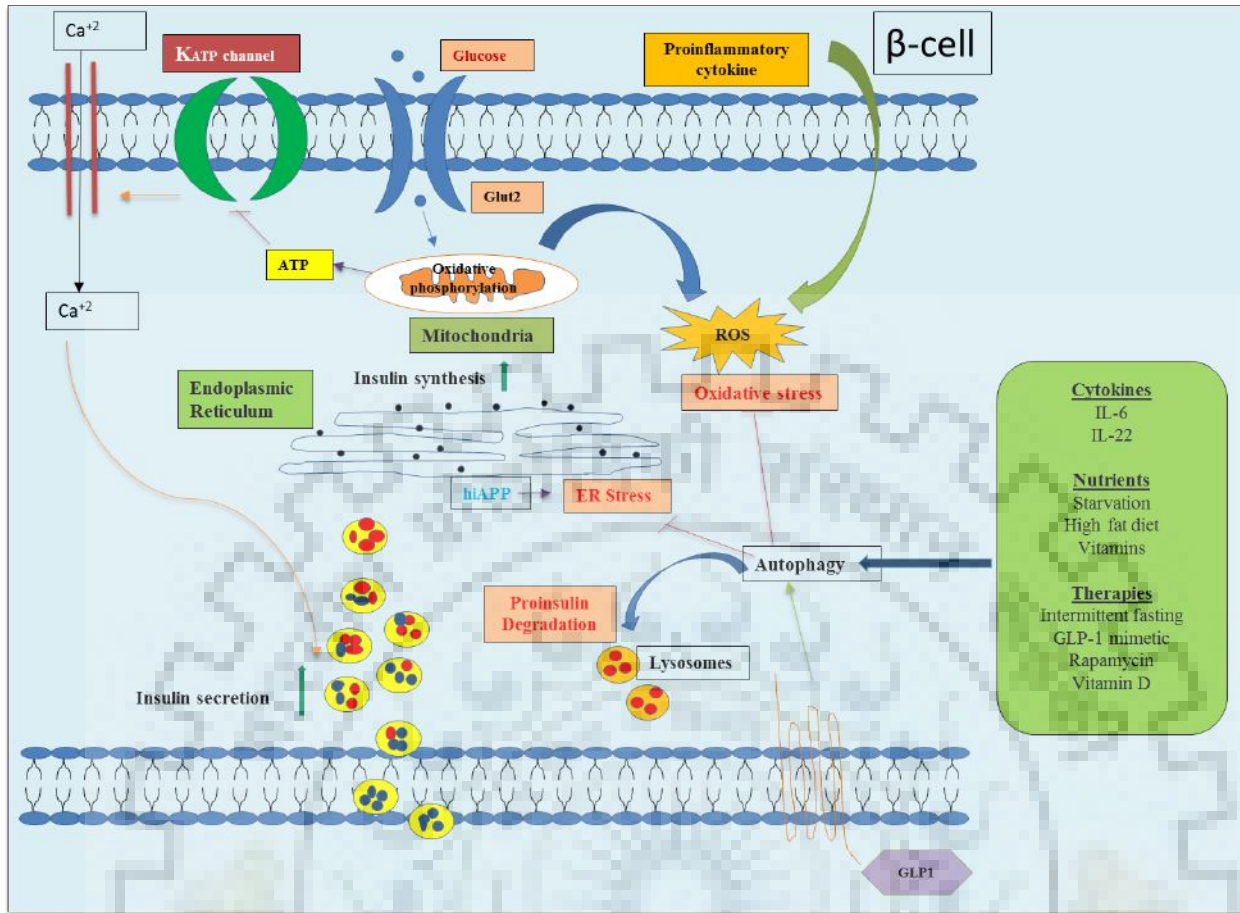


Fig. 2.15. Autophagy in the context of β -cell dysfunction

In β -cell, various key roles are played by autophagy; for instance, aiding in β -cell function (Riahi et al., 2016) and apropos differentiation during development (Ren et al., 2017). Notably, autophagy promotes survival under conditions of β -cell stress that can lead to cell death, including nutrient depletion, ER stress, oxidative stress, mitochondrial damage, and hypoxia (Kroemer et al., 2010; Hayes et al., 2017). Loss of autophagy in the β -cell was pronounced a long time ago in the mice with a beta-cell-specific deficiency for the enzyme ATG7 in autophagosome biogenesis. A reduced insulin secretion and impaired glucose tolerance were observed in *atg7* knockout mice and it was unveiled that the mice were having reduced β -cell mass due to increased apoptosis and decreased proliferation (Jung et al., 2008).

So, induced autophagy is an adaptive response to insulin resistant condition. Although autophagy has gained importance in the recent past, our understanding of the same is still growing and thus pre-emptive interpretation can easily mislead about the role of autophagy in various disease models. Some *in vitro* studies have also reported that the induction of autophagy in palmitic acid (PA)-challenged pancreatic β -cells, isolated rat, and human

pancreatic islets, exerts the protective effect against PA-induced apoptosis (Choi et al., 2009; Martino et al., 2012). Some recent studies asserted that prolonged exposure of β -cell to FFAs leads to increase in autophagosomes due to suppressed autophagic turnover which is clearly evident from increased LC3-II as well as p62 accumulation. Autophagy turnover was drastically impaired in the presence of fatty acids which subsequently lead to pancreatic β -cell death (Masini et al., 2009; Bartolomé et al., 2014; Mir et al., 2015).

On the basis of this pre-notion, rapamycin (a mTOR inhibitor and known activator of autophagy) has been validated to exert the cytoprotective effect on PA-induced β -cell by reducing the blockage of autophagic turnover (Mir et al., 2015). Similarly, other well-known antidiabetic drugs like rosiglitazone and metformin were also found to rescue β -cells from PA-induced apoptosis through modulation of autophagy (Wu et al., 2013; Jiang et al., 2014). Thus, induction of autophagy could be a potential target to combat saturated fatty acid-mediated apoptotic cell death (Stienstra et al., 2014).

Apart from its role in β -cell survival, autophagy is also reported to play an active role in the regulation of insulin homeostasis. Acute inhibition of β -cell autophagy by siRNA-mediated knockdown of atg5/7 led into elevated levels of insulin as well as proinsulin (Riahi et al., 2016). However, reduced insulin secretion from mouse and human islets was observed when the autophagy was stimulated by rapamycin-mediated inhibition of mTORC1 (Blandino-Rosano et al., 2017). The significance of commensurate regulation of autophagy for β -cell survival is further underlined by the observations that both activation and inhibition of autophagy through knockout or hyperactivation of mTORC1, respectively, lead to enhanced β -cell apoptosis and a drop in β -cell mass (Blandino-Rosano et al., 2017; Bartolomé et al., 2014). Cumulatively, all these data indicate that autophagy plays a crucial role in the maintenance of β -cell survival and function through diversified mechanisms.

2.7.7.1. Autophagy in the resolution of β -cell ER stress

A functional ER is critical for stimulus-secretion coupling in the β -cell, allowing the β -cell to secrete insulin in response to an exogenic stimulus. The immense demand of β -cells to produce and secrete insulin in response to environmental variations makes them vulnerable to ER stress. The β -cell must quickly ramp up insulin synthesis in response to upsurges in glucose while sustaining the ability to appropriately convert proinsulin to the insulin. Interruptions to this delicate steadiness can cause β -cell dysfunction. Under these conditions, if normal ER homeostasis is not reinstated, then cells eventually undergo apoptosis which is prompted by the

unfolded protein response. Chronically raised glucose and fatty acids associated with T2D have been found to trigger β -cell ER stress (Elouil et al., 2007; Cnop et al., 2007; Laybutt et al., 2007; Kharroubi et al., 2004; Karaskov et al., 2006), and mutations in components of the unfolded protein response pathway have been linked to the development of diabetes in rodents and humans (Eizirik et al., 2007; Cnop et al., 2012). ER stress has been implicated as one of the mechanisms contributing to the development of human islet amyloid polypeptide (hIAPP) oligomers (Abedini and Schmidt, 2013), probably through defects in the processing of the protein precursor, ProhIAPP, to hIAPP.

IAPP is co-secreted with insulin and plays a crucial role in glycemic regulation. It can form amyloid aggregates that have been associated with β -cell death and the subsequent development of T2D in humans, however, the same is not reported for mice and rats (Saafi et al., 2001; Matveyenko and Butler, 2006; Kahn et al., 1999). Some recent studies have shown that autophagy is important for ameliorating the cytotoxic effects of hIAPP. In β -cells, blocking autophagy augmented the toxicity of hIAPP (Shigihara et al., 2014). Moreover, mice expressing hIAPP in autophagy-deficient β -cells developed diabetes, whereas neither hIAPP nor loss of autophagy alone was sufficient to induce the disease (Kim et al., 2014). This suggests that autophagy plays a vital role in clearing hIAPP oligomers, thus precluding cytotoxicity, β -cell failure/death, and the development of diabetes.

ER stress results from the amassing of misfolded and unfolded proteins can trigger apoptosis if the stress conditions are not resolved. Stimulation of autophagy can degrade the misfolded proteins or dysfunctional regions of the ER, thus restoring structural and functional integrity (Bernales et al., 2006; Ogata et al., 2006, Hamaeher-Brady et al., 2006). Recent reports suggest that ER stress itself stimulates autophagy, perhaps as a feedback mechanism to protect the cell. For instance, Kong et al., 2017 observed that obstructing ER stress blocked autophagy and blocking autophagy increased ER stress. Quan et al., 2012 witnessed that loss of autophagy in the β -cell compromised the unfolded protein response, as a consequence an increased incidence of diabetes. Even though the mechanisms by which autophagy responds to ER stress are not completely understood, some connections are becoming clear. Activation of ER stress leads to the phosphorylation and inactivation of the eukaryotic translation initiation factor eIF2 α , consequently inhibiting ribosome assembly which results in the global down-regulation of protein translation. Apart from this, the expression of some transcription factors and protein chaperones like ATF4 and CHOP is up-regulated. ATF4 and CHOP have been found to regulate the expression of autophagy genes, increasing the transcription of genes

required for autophagosome formation and function (Maurin et al., 2016). Furthermore, Takatani et al., 2016 have found that signaling through eEF2K, which phosphorylates eEF2, thus contributing to the translation block induced by ER stress, also regulates autophagy. These findings provide insight into the potential molecular links between ER stress and the stimulation of autophagy. However, further research is needed to comprehend the mechanisms by which autophagy promotes cell survival under conditions of stress.

2.7.7.2. Extracellular Signals That Regulate β -cell Autophagy

Numerous factors such as dietary components, cytokines, and GLP-1 have been reported to stimulate autophagy in the β -cell. Importantly, although the context is important, all of these factors may contribute to the regulation of β -cell autophagy during the pathogenesis of both T1D and T2D. Starvation and deprivation of amino acids are eminent activators of autophagy in multiple cell types. However, mixed reports are there whether nutrient deprivation induces β -cell autophagy. Autophagy is found to be stimulated by fasting and calorie-restricted diet both *in vitro* and *in vivo* in some reports (Sun et al., 2016; Fujimoto et al., 2009; Ebato et al., 2008; Liu et al., 2017) but not in others (Goginashvili et al., 2015; Ebato et al., 2008). These incongruities in the findings could be due to differences in the length of starvation and in the type of autophagy that is stimulated. Reports witnessing stimulation of autophagy by nutrient deprivation used longer periods of starvation than the reports that did not observe induction of autophagy. However, according to a study by Goginashvili et al., 2015, starvation may actually inhibit autophagy and, instead, stimulate crinophagy, in which insulin granules directly fuse to lysosomes. Therefore, conceivably shorter duration of nutrient deprivation may stimulate β -cell crinophagy, whereas lengthier periods of starvation may be required to trigger classical macroautophagy in the β -cell.

Excess lipids are also known to play a role in autophagy regulation, with varying effects that are context dependent. For instance, autophagy protects against β -cell apoptosis induced solely by fatty acids such as palmitate and cholesterol *in vitro* (Choi et al., 2008; Martino et al., 2012; Wu et al., 2017), whereas excess fatty acids and glucose which generate circumstances of glucolipotoxicity can inhibit β -cell autophagic flux and lead to cell death (Mir et al., 2014; Las et al., 2011; Trudeau et al., 2016). This inhibition of autophagy is probably due to the lysosomal defects under these conditions, as reacidification of lysosomes using photoactivatable nanoparticles was able to bring back the autophagic flux in cells exposed to lipotoxicity (Trudeau et al., 2016). Numerous studies on rats and mice have shown up-

regulated autophagy in the β -cell when the animals were fed high-fat diets (HFDs), and inhibition of β -cell autophagy aggravated the metabolic defects instigated by a combined high-fat and high-glucose diet (Sheng et al., 2017). Collectively, these data propound that chronic, excessive exposure to fatty acids and glucose may block the endogenous adaptive mechanism by which β -cell protect themselves from these sources of stress and toxicity, which then contributes to the development of diabetes.

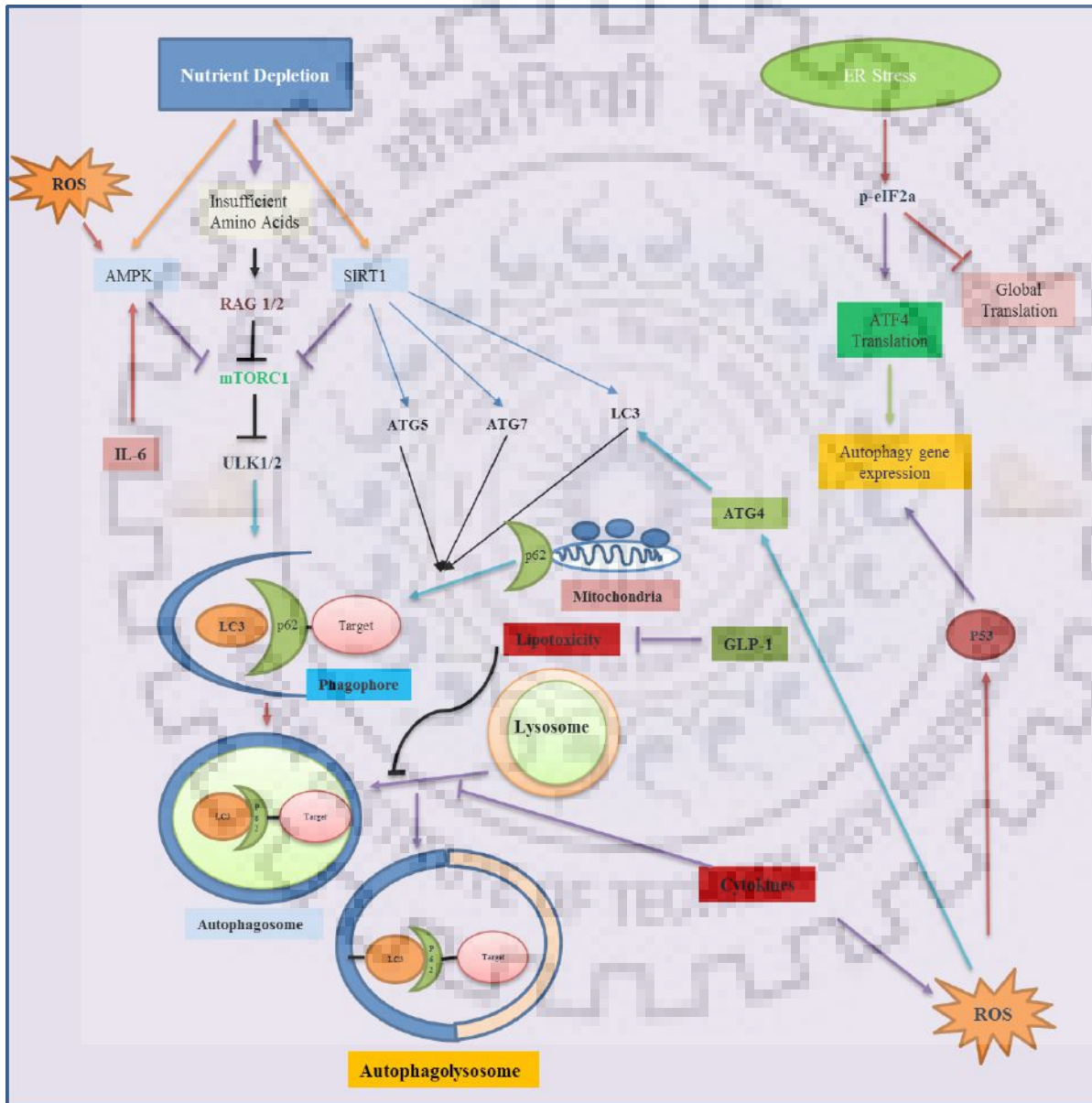


Fig. 2.16. Schematic representation showing regulation of β -cell autophagy

2.7.8. Novel therapeutic approaches to target autophagy in endocrine and metabolic disorders

Nowadays, modulation of autophagy has gained immense importance in the area of metabolism and endocrinology. Many of the known pro-autophagic drugs which were not originally designed or developed to induce autophagy may exert their beneficial effects via autophagy-mediated regulation. The various classes of autophagy modulators affecting different stages of autophagy signaling in metabolic disorders can be categorized as follows:

2.7.8.1. mTORC1 inhibitors and rapalogs

mTORC1 is a master negative regulator of autophagy and its inhibition has been used to initiate autophagy in mammalian cells. Concerning this, the classical mTORC1 inhibitor, rapamycin, has shown promising outcomes in various pre-clinical studies on treating metabolic diseases. For instance, rapamycin treatment was found to reduce diabetic nephropathy (DN) in streptozotocin-treated animals (Lloberas et al., 2006; Sakaguchi et al., 2006; Ding and Choi, 2014). This protection was accompanied with the diminutions in glomerular α -smooth muscle actin expression, renal hypertrophy and mesangial matrix accumulation in streptozotocin-induced diabetes. Apart from this, reduced expression of several pro-proliferative cytokines and monocyte chemoattractant protein-1 was also recorded (Yang et al., 2007). Similar effects were also witnessed with mTORC1 inhibition in DN models using db/db mice (Mori et al., 2009). Unluckily, chronic rapamycin treatment is found to be associated with the insulin resistance and hyperglycemia in both the animals and humans (Di Paolo et al., 2006). The induction of diabetes by rapamycin mimics “starvation diabetes” and may not be pathological. However, due to its potential side effects, the usage of rapamycin for diabetes management is still under investigation and remains controversial. There have been positive results for the use of mTORC1 inhibitors to induce autophagy in NAFLD. In various animal models of NASH and NAFLD, Rapamycin exhibited beneficial effects in reducing hepatic steatosis by increasing autophagy (Farah et al., 2016; Lin et al., 2013; Nakadera et al., 2016). Other mTORC1 inhibitors such as caffeine have also exhibited progressive effects on liver fat clearance via autophagy.

2.7.8.2. AMPK/SIRT1 activators

AMPK is a nutrient-sensing kinase which is activated under energy-depleted conditions and is, in contrast to the mTORC1 pathway, a positive regulator of autophagy. Several

hormones, natural compounds, and drugs that induce AMPK activity have increased islet β -cell survival (Wu et al., 2013; Pichiah et al., 2011; Han et al., 2010) and protected against diabetic complications (Tanaka et al., 2011; Mellor et al., 2011; Dagon et al., 2015; Yerra and Kumar, 2017; Yao et al., 2016). AMPK activators also showed beneficial effects in reducing lipid accumulation in non-adipose tissues by inducing autophagy in animal models of obesity (Kim et al., 2013; Liu et al., 2014; He et al., 2016). Similar to the direct AMPK activators, SIRT1 activators also exhibited beneficial metabolic outcomes by activating AMPK and inducing autophagy (Wang et al., 2014; Colak et al., 2014; Zhang et al., 2016; Li et al., 2016). In this regard, both resveratrol as well as metformin protected against diet-induced NAFLD and tissue injury (Colak et al., 2014; Wang et al., 2014; Li et al., 2015; Song et al., 2015).

2.7.8.3. Other strategies to modulate autophagy in metabolic disorders

Recently, calcium channel blockers were shown to prevent the pathological manifestations of NAFLD and NASH (Park and Lee, 2014; Park et al., 2014). The rationale for their use was the restoration of autophagy that was blocked by induction of hepatic calcium flux during obesity. This increase in intracellular calcium concentration inhibited autophagosome-lysosome fusion and autophagic flux. Interestingly, impairment of autophagosomal-lysosomal dynamics also has been implicated in several lysosomal storage diseases (Lieberman et al., 2012). In this regard, induction of autophagic flux by increasing the activity of TFEB (transcriptional master regulator of autophagy-lysosomal genes) has shown promising beneficial effects (Spampanato et al., 2013). Recently, several small molecule activators of TFEB were discovered that may be potentially effective in the treatment of genetic and metabolic diseases that have impairments in autophagy (Song et al., 2016). Tatbeclin-1 peptide represents a highly specific and targeted pro-autophagy inducer which has potential efficacy in the treatment of autophagic defects in human diseases (Shoji-Kawata et al., 2013).

Since autophagy often is increased in cancer, autophagy inhibitors have been proposed as therapeutic adjuncts. However, in endocrine and metabolic disorders, autophagy usually is impaired either in the endocrine gland or the target tissues. So far, only autophagy inhibitors have been evaluated for cancer treatment in clinical trials; however, further work is needed in order to develop highly specific and less toxic autophagy inducers for clinical use in metabolic diseases (Levine et al., 2015). In endocrine glands such as the pituitary or pancreatic islets, deficiencies in autophagy may lead to decreased polypeptide hormone secretion and their

increased degradation by crinophagy. In target tissues such as fat, heart, muscle and liver, impaired autophagy can lead to abnormal lipolysis or decreased β -oxidation of fatty acids. Additionally, autophagy can protect against glucotoxicity, lipotoxicity, and ROS damage in the cell. Over time, these defects often lead to insulin resistance, inflammation, and secondary damage in target tissues. Thus, understanding autophagy in both endocrine glands and their target tissues may lead to novel therapeutic approaches to increase hormone secretion as well as enhance sensitivity to hormones and tissue viability. For example, it is possible that autophagy induction, either by hormones or pharmacologically, may lead to increased secretion of insulin from islet β -cells or confer protection against lipotoxicity, glucotoxicity, or inflammation to increase their viability (Barlow and Thomas, 2015). Likewise, increasing lipophagy and mitophagy in the liver could lead to decreased hepatosteatosis in NAFLD and lysosomal storage diseases (Yan et al., 2018). Indeed, a number of hormone and drug therapies have shown initial promise for this condition (Farah et al., 2016; Mao et al., 2016; Ward et al., 2016). Thus, harnessing the beneficial powers of autophagy in the endocrine system and targeting them to appropriate tissues to improve hormone secretion, hormone sensitivity, and/or intracellular metabolism will be an exciting challenge that holds great promise for the future.

2.8. Conventional versus herbal medicines

Due to the increased demand for combating diabetes, many synthetic drugs have been developed such as biguanides, sulfonylurea, thiazolidinediones, meglitinide derivatives and α -glucosidase inhibitors but these are not fully effective, expensive and also have many side effects such as weight gain, hypoglycemia, abdominal discomfort, gastrointestinal adverse effects, liver failure and increased risk of congestive heart failure (Marín-Peñalver et al., 2016).

As the knowledge of heterogeneity of this disorder increases, there is a need to search for more efficacious agents with lesser side effects. Although the modern medicines and therapies can mitigate diabetes to some extent, there are several unprecedented complications that have to be taken care may be by a holistic approach through validation of our traditional knowledge of Ayurveda and combining it with the modern scientific approach. The traditional plant-based medicines are safe, effective, economical, non-toxic with no or lesser side effects (Mukherjee et al., 2015). Hence these plant resources are considered to be excellent and

alternative candidates in diabetes management. Thus, as the prevalence of the disease is progressing unabated, there is an urgent requirement of identifying effective natural sources in order to develop new effective therapeutics (Gupta et al., 2016).

Some scientifically validated and popular anti-diabetic plants include *Aegle marmelos*, *Aloe vera*, *Allium cepa*, *Allium sativum*, *Azadirachta indica*, *Eugenia jambolana*, *Ficus religiosa*, *Mangifera indica*, *Momordica charantia*, *Morus alba*, *Ocimum sanctum*, *Opuntia streptacantha*, *Phyllanthus amarus*, *Silibum marianum*, *Trigonella foenumgraecum* (Mukherjee et al., 2013; Prakash et al., 2015; Kar et al., 2015).

The fundamental mode of action of natural plant resources and phytochemicals for their antidiabetic activity can be summarized as follows (Awasthi et al., 2016);

- Protection of pancreatic β -cell mass and function
- Stimulation of insulin secretion and insulin sensitivity
- Promoting glucose uptake and utilization in muscles, adipose tissues
- Lowering glucose absorption in the intestine (α -glucosidase inhibitor)
- Inhibition of gluconeogenesis and glycogenolysis in liver
- Stimulation of glycogenesis
- Reduction of inflammation and oxidative stress

2.8.1. Phytochemicals

Phytochemicals are the natural plant-derived compounds that are produced for their own defense and protection, against various environmental stresses such as bacteria, fungi, insects, pollution, weather change and various diseases (Romeo, 2012). Though phytochemicals are considered as non-essential nutrients as they are not required to sustain life, but recent research has revealed that they can also protect humans against several diseases such as oxidative damage (Lee et al., 2017; Zhang et al., 2015), inflammation (Yenuganti et al., 2014; Vashisht et al., 2018), diabetes (Firdous, 2014), cancer (Parihar et al., 2012; Agarwal et al., 2013; Amin et al., 2014; Shukla et al., 2015; Li et al., 2016; Sirohi et al., 2017), cardiovascular disorders (R Vasanthi et al., 2012), neurodegenerative disorders (Venkatesan et al., 2015; Chakraborty et al., 2015) and aging (Larsson and Sonny, 2009). There are more than thousand known phytochemicals but most studied include polyphenols and carotenoids.

Among polyphenols, flavonoids and isoflavones are well-known subclasses found to be beneficial in combating various health disorders.

In the past few decades, food and nutrition have been recognized as critical factors in the management of diseases and their cure. Since time immemorial, by virtue of traditional knowledge, the indigenous people utilized various herbs and medicinal plants for the treatment of several disorders. Since the new generation of treatment modalities to mitigate dreadful diseases is constrained to use synthetic drugs, which are costly and may sometime end up with unpredictable side effects, major research focus is on identifying novel phytochemicals that can modulate and maintain physiological functions. Also phytochemicals because of their lesser side effects, more reliable pharmacological action and cost-effectiveness are emerging as the new generation's therapeutic strategy to combat various diseases like cancer, diabetes, cardiovascular disease, bone disorders and neurodegeneration.

Phytochemicals are considered as important nutraceuticals employing several aspects of health benefits. Phytochemicals play role as substrates for biochemical reactions, act as cofactors/inhibitors of enzymatic reactions, ligands for surface/intracellular receptors as agonist/antagonist, scavengers of reactive or toxic substances, as enhancers of bioavailability of essential nutrients and selective growth factors for beneficial gastrointestinal microbiota or selective inhibitors of deleterious intestinal bacteria (Dillard et al., 2000).

Classification

The phytochemicals can be classified based upon their chemical structures. The major classifications could be alkaloids, aromatic acids, phenolics, lactones, terpenoids, fatty acids and organosulfur compounds.

2.8.1.1. Phenolics

Phenolic phytochemicals have a phenol ring with different functional groups attached to it. These are the largest category of phytochemicals and are distributed widely throughout the plant kingdom. Based on the functional group side chains, phenolic compounds can be further classified as- phenolic acids, phenolic aldehydes, phenolic glucosides, flavonoids, lignans etc. The structural diversity of these groups of phytochemicals is mainly due to hydroxylation patterns, stereochemistry and different patterns of methoxylation and glycosylation (Koleckar et al., 2008).

2.8.1.1.1. Flavonoids

The term “Flavonoid” is derived from the Greek word *flavus* meaning yellow (Miranda et al., 2001; Procházková et al., 2011). These are ubiquitous secondary metabolites which are also responsible for red, blue and purple pigmentation in plants (Winkel-Shirley, 2001). This clearly indicates that these molecules are linked to pigmentation in plants. In earlier days, flavonoids were thought to be the metabolic waste of plants that are toxic and are therefore be stored away in vacuoles. Some authors also described the same to be an evolutionary remnant having no current functions. However, due to their wide range of biological activities, major research focus has shifted to decipher their medicinal properties and mode of actions in cellular level.

Classification of flavonoids

Flavonoids can be mainly classified based upon their chemical structures. The basic skeleton of almost all flavonoids is same i.e., 2-phenylbenzopyrone. They differ from one another in the pattern of hydroxylation or methylation, degree of unsaturation and type of sugars attached. In general, flavonoids can be classified into following types: (a) flavonols, (b) flavones, (c) flavanols, (d) flavanones, (e) anthocyanidins and (f) isoflavones.

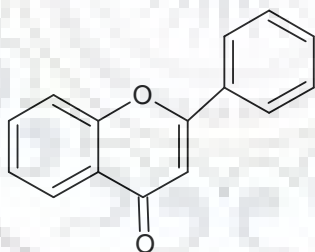


Fig. 2.17. Structure of 2-phenylbenzopyrone

2.8.1.1.1.1. Flavonols

These groups of flavonoids have 3-hydroxyflavone backbone. The different positions of –OH group in the backbone is the only reason for the chemical diversity of this group. As far as flavonols in human diets are concerned, these are mainly found in vegetables, fruits and beverages like tea and wine (Favre et al., 2018; De Beer et al., 2017; Tsanova-Savova et al., 2018). Some of the widely studied flavonols are discussed below.

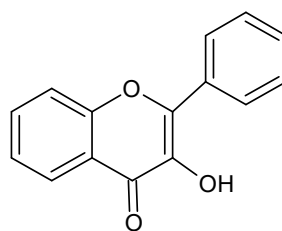


Fig. 2.18. Hydroxyflavone as a basic flavone structure

2.8.1.1.1.1. Quercetin

According to IUPAC system quercetin is known as 2-(3,4-dihydroxyphenyl)-3,5,7-trihydroxy-4H-chromen-4-one. It is the most abundant dietary flavonoid found in fruits, green leafy vegetables, olive oil, red wine and tea. Structurally, quercetin contains 5 hydroxyl groups and the position of the same determines its diversity. Glycosides and ethers are the major derivatives of the compound. However, sulfate and prenyl substituents are also observed but less frequently (Harborne and Williams., 2000; Williams and Grayer, 2004). Normally, quercetin is not found in free form; rather form a complex with phenolic acids, sugars and alcohols. After ingestion, the derivatives of the quercetin are hydrolyzed in the gastrointestinal tract and then absorbed in the body (Scalbert et al., 2000; Walle, 2004). This group of flavonols also exhibit diverse pharmacological effects like antiviral (Falcó et al., 2018; Wong et al., 2017), anti-carcinogenic (Kashyap et al., 2018; Tang et al., 2018) and anti-inflammatory effects (Lesjak et al., 2018; Lee et al., 2018; Lin et al., 2017). Recent evidence prove the efficacy of the compound in diabetes and obesity. It is found to increases plasma insulin level and decrease blood glucose level, decrease oxidative stress and inflammation by inhibiting Ikk- β and TNF α expression in STZ-nicotinamide induced diabetic rats (Roslan et al., 2017). As per another study, quercetin induces a significant decrease in blood glucose level through an increase in GLUT 4 expression and exhibition of antioxidant activity in alloxan-induced type 2 diabetic mice (Alam et al., 2014).

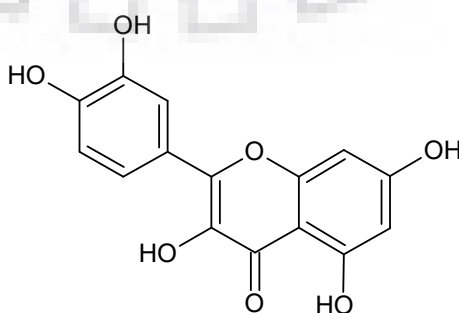


Fig. 2.19. Structure of Quercetin

2.8.1.1.1.2. Rutin

The IUPAC name of Rutin is 2-(3,4-dihydroxyphenyl)-5,7-dihydroxy-3-[α -L-rhamnopyranosyl-(1 \rightarrow 6)- β -D-glucopyranosyloxy]-4*H*-chromen-4-one. It's mainly formed by the combination of glycoside with quercetin and the disaccharide rutinose. It is mainly found in the citrus foods. However, the name rutin originates from the plant *Ruta graveolens* where it is found abundantly. As per some recent reports, rutin has been proved as an effective agent against various ailments but these are still under preliminary clinical research for their potential biological effects. However, the only problem in this compound is its poor bioavailability due to poor absorption, high metabolism, and rapid excretion. In terms of diabetes and obesity, the compound seems to be potent both *in vitro* as well as *in vivo* systems. As per a study, the compound exhibits antihyperglycemic activity, improves oral glucose tolerance and oral sucrose tolerance in alloxan-induced type 2 diabetic rats (Calzada et al., 2017). Rutin also found to restore HFD-induced elevation in ER stress markers in epididymal fat, as well as altered p-JNK, PPAR γ , and DsbA-L protein expression under obese conditions (Chen et al., 2016). As per another report, rutin reduces blood glucose and increases insulin levels and stimulates adipocyte differentiation and adiponectin secretion in 3T3-L1 cells (Naowaboot et al., 2015).

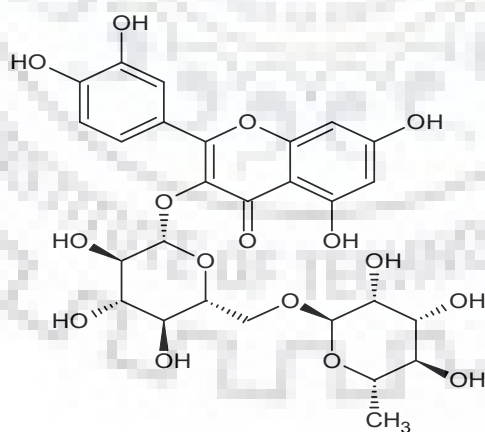


Fig. 2.20. Structure of Rutin

2.8.1.1.1.3. Myricetin

IUPAC name of Myricetin is 3,5,7-Trihydroxy-2-(3,4,5-trihydroxyphenyl)-4-chromenone. Myricetin is found throughout the plant kingdoms but mostly found in the species of the families Myricaceae (Patel et al., 2017; Jones et al., 2010), Polygonaceae (Abd El-kader et al., 2013) and Pinaceae (Saab et al., 2018). Structurally, myricetin (Fig. 2.21) is closely related to kaempferol, quercetin, morin and fisetin. Due to its structural closeness with quercetin, it is also referred as hydroxyquercetin. Myricetin was first isolated from *Myricanagi* Thunb (from family Myricaceae) (Perkin, 1896). These are mainly found in vegetables, berries, nuts, tea (Corell et al., 2018) and mostly in wine (Basli et al., 2012). This compound possess various pharmaceutical activities like- anti-cancer (Sun et al., 2012; Kim et al., 2014,) anti-diabetic (Li et al., 2017; Sobeh et al., 2017), anti-inflammatory (Hou et al., 2018; Tan et al., 2018), anti-oxidant (Mendes et al., 2018) and hepatoprotective (Zakaria et al., 2018) activities. In terms of diabetes and obesity, recent evidence proved the anti-diabetic activity of the compound in both *in vitro* as well as *in vivo* systems. In an experiment in High-fat, high-sucrose (HFHS) diet-induced mice, myricetin alleviates insulin resistance, improves obesity and reduces serum proinflammatory cytokine levels (Choi et al., 2014). Another report proves the inhibitory activity of α -Glucosidase in STZ-induced diabetic rats (Kang et al., 2015). It is also observed that the compound acts as a GLP-1R agonist and exerts glucoregulatory activity in isolated islets and GLP-1R-deficient mice (Li et al., 2017).

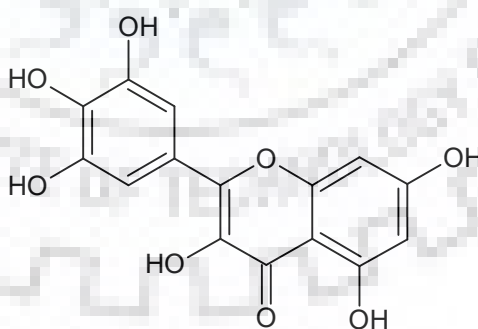


Fig. 2.21. Structure of Myricetin

2.8.1.1.1.4. Kaempferol

IUPAC name of kaempferol is- 3,5,7-Trihydroxy-2-(4-hydroxyphenyl)-4H-chromen-4-one. These are very common in plants and are widely distributed throughout the plant kingdom. As per a review article by Montano et al., 2011, 400 plant species from various families are listed along with types of kaempferol isolated (M Calderon-Montano et al., 2011). Kaempferol is found either in its native form or may be bound to glucose, galactose and rhamnose to form the glycosides. However, as far as dietary kaempferol is concerned, it is abundantly found in tea, broccoli, apples, strawberries and beans (Somerset et al., 2008). Kaempferol exhibits various therapeutic activities and is supposed to be a potent drug against various ailments. The biggest advantage of this phytochemical is its selective cytotoxicity to cancerous cells (Yang et al. 2018; Kim et al., 2013; Mylonis et al., 2010) rather than normal cells (Zhang et al., 2008). Apart from this, kaempferol also has potential therapeutic activity against diabetes (Zang et al., 2014; Lima et al., 2018; Zhang et al., 2011), inflammation (Kong et al., 2013; Rho et al., 2011) and cardiovascular diseases (Vishwakarma et al., 2018). In terms of diabetes and obesity, several pieces of evidence prove the efficacy of the compound. It is also observed that kaempferol also alleviates insulin resistance by inhibiting the phosphorylation of insulin IRS-1, I κ B kinase α , and I κ B kinase β in HFD induced rats (Luo et al., 2015). Kaempferol also ameliorates hyperglycemia, glucose tolerance, and blood insulin levels and islet β -cell mass via increased Glut4 and AMPK expressions in HFD –induced mice (Alkhalidy et al., 2015).

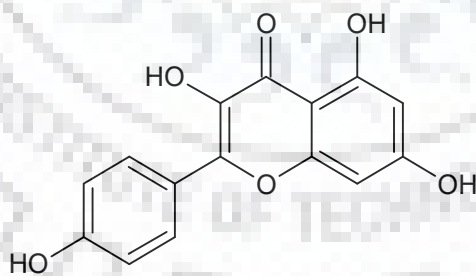


Fig. 2.22. Structure of Kaempferol

2.9. The problem addressed in the present thesis

Keeping in mind all the above mentioned recent strategies and targets, in the present thesis, the major research focus was on identifying natural autophagy modulators which can protect β -cell mass and function as a principal approach in the prevention of obesity-linked T2DM and further understanding the mechanism of action in detail. The initial part of this thesis dealt with a screening of some flavonoids for their anti-obesity, anti-diabetic and autophagy stimulatory activities. In the next phase of the study, the major emphasis was on to determine the underlying mechanism and signaling pathways involved in cross-talk between anti-diabetic and autophagy stimulatory effects of kaempferol, the flavonoid found most potent out of all flavonoids tested in the initial screening. In another part of this study, the role of kaempferol-mediated autophagy was elucidated in the lipid deposition and insulin resistance in lipid-induced hepatocytes.





CHAPTER 3

MATERIALS AND METHODS

Chapter 3. Materials and Methods

3.1. Introduction

This chapter represents the detail *in vitro* and *in vivo* experimental procedures carried throughout the thesis to establish the effect of potent flavonoids against obesity-linked type-2 diabetes. It also deals with several techniques that are used to decipher the underlying molecular pathways of action of these flavonoids.

3.2. Materials

All cell culture reagents including RPMI-1640, DMEM medium, trypsin, fetal bovine serum (FBS), and antibiotic solution (penicillin-streptomycin) were purchased from GIBCO (BRL, Inchinnan, UK). Dimethyl sulphoxide (DMSO), MTT [3-(4,5-dimethylthiazol-2-yl)-2,5-diphenyltetrazolium bromide], cell culture grade palmitic acid (PA) and analytical grade chemicals were purchased from HiMedia (Mumbai, India). LysoTracker red DND-99 was obtained from Life Technologies, USA. Kaempferol, wortmannin, chloroquine, compound C, temsirolimus, metformin mono dansylcadaverine (MDC), Hoechst 33342, Collagenase V, DAPI (4',6-Diamidino-2-Phenylindole) were procured from Sigma-Aldrich (St. Louis, MO, USA). All the reagents for RT-PCR were purchased from NEB (New England Biolabs, USA). BCA Protein Assay Kit was purchased from Pierce (Pierce Biotechnology, USA). All primary antibodies and secondary antibodies were purchased from Santa Cruz (Santa Cruz, CA, USA) while antibody against Caspase-3 was from Cell Signaling Technology (Danvers, MA, USA). ECL detection kit was purchased from Santa Cruz (Santa Cruz, CA, USA). Insulin enzyme immunoassay kit was procured from SPI-Bio (Bertin Pharma, Montigny-le-Bretonneux, France). Accu-chek active glucometer and glucose strips were from Roche Diagnostics (Barcelona, Spain). Rat/human-specific predesigned siRNA for Atg7 and negative control siRNA were purchased from Qiagen (Valencia, CA, USA) while AMPK siRNA was obtained from Ambion (Life Technologies GmbH, Darmstadt, Germany). The plasmid for EGFP-LC3 (Addgene plasmid # 11546) was acquired from Addgene Plasmid Repository (Cambridge, MA, USA) which was donated to the repository by Dr. Karla Kirkegaard (Stanford University, USA). The pcMX-PPAR α and co-regulator plasmid were kind gift from Professor Ronald M. Evans (The Salk Institute for Biological Studies, California, USA) and Professor Michael R.

Stallcup (University of Southern California, Los Angeles, CA, USA). Insulin enzyme immunoassay kit was procured from SPI-Bio (Bertin Pharma, Montigny-le-Bretonneux, France).

3.3. *In vitro* experimental models

3.3.1. Cell lines and cell culture

Rat pancreatic beta cell line RIN-5F; Human liver cancer cell line (HepG2 cells); Murine preadipocyte cell line (3T3-L1 cells); Rat skeletal muscle cell line (L6 cells) were used in this study. All the cell lines were purchased from National Centre for Cell Science (NCCS), Pune, India.

HepG2 cells (from passage number 30-35) were grown in DMEM with 10% fetal bovine serum (heat inactivated) and 1% antibiotic (100 U/ml of penicillin and 100µg/ml streptomycin) mix at 37°C in a humidified atmosphere in a 5% CO₂ incubator. The medium of the cells was changed after every alternate day to avoid nutrient stress.

3T3-L1 cells (from passage number 10-15) were cultured in DMEM supplemented with 10% fetal bovine serum, 2 mM L-glutamine, 0.1 mM nonessential amino acids and 1 mM sodium pyruvate along with 1% antibiotic (100 U/ml of penicillin and 100µg/ml streptomycin). Cells were maintained at 37°C in a humidified atmosphere in a 5% CO₂ incubator.

L6 cells (from passage number 40-45) were grown in DMEM with 10% fetal bovine serum (heat inactivated) and 1% antibiotic (100 U/ml of penicillin and 100µg/ml streptomycin) mix at 37°C in a humidified atmosphere in a 5% CO₂ incubator.

RIN-5F (from passage number 30-38) were grown in RPMI with 10% fetal bovine serum (heat inactivated) and 1% antibiotic (100 U/ml of penicillin and 100µg/ml streptomycin) mix at 37°C in a humidified atmosphere in a 5% CO₂ incubator.

3.4. Isolation and culture of rat pancreatic islets for *ex vivo* studies

The rat pancreatic islets were isolated as described elsewhere with some modifications (Martino et al., 2012). Briefly, the female Sprague-Dawley rats of age 8–10 weeks were sacrificed by cervical dislocation and the pancreas was removed aseptically. The harvested pancreas was then cut into small pieces and washed with Hanks' balanced salt solution (HBSS). Thereafter, the resulting pancreatic pieces were then digested in collagenase V (Sigma–Aldrich, USA) in HBSS for 10 min at 37°C with gentle shaking. The digested samples were then rinsed thrice with cold HBSS. Finally, the islet purification was performed by centrifugation at 800 x g for 15 min at 4°C on Ficoll density gradient centrifugation (density: 1.100, 1.077) (Sigma Chemical Co., St Louis, MO, USA). After being washed with HBSS containing 2% BSA, the islets were cultured in RPMI 1640 supplemented with 10% FBS 1% streptomycin–penicillin and L-glutamine (2 mM) at 37°C in a humidified atmosphere containing 5% CO₂.

3.4.1. Identification of pancreatic islets

The purified islets were tested for their specificity by dithizone (DTZ) staining. For DTZ staining, the culture dishes were incubated at 37°C for 15 min in the DTZ solution. After the incubation period, dishes were rinsed three times with HBSS and subsequently monitored under a microscope to identify clusters of stained crimson red as islets. After examination, the dishes were replenished with culture media. The stain completely disappeared from the cells after 4 h. For treatment, DTZ-stained islets were counted and divided into various groups and were given the respective treatments.

3.5. *In vivo* experimental models

Male laboratory mouse:

Phylum: Chordata
Subphylum: Vertebrata
Class: Mammalia
Order: Rodentia
Family: Muridae
Genus: *Mus*
Species: *musculus*
Strain: C57BL/6

All the animal experiments were performed as per CPCSEA guidelines with prior approval from Institutional Animal Ethics Committee (approval number BT/IAEC/2017/02). Male C57BL/6 mice of age 7 weeks old were procured from CSIR-Institute of Microbial Technology, Chandigarh, India. Female Sprague-Dawley rats of age 8–10 weeks old were procured from National Institute of Pharmaceutical Education and Research, Mohali, India with the approval of Institutional Animal Ethics Committee (MMCP/IAEC/16/05). Animals were housed under standard conditions (temperature $23\pm 2^{\circ}\text{C}$ and 12 h dark-light cycle) in a well-maintained animal house and acclimatized for two weeks prior to start of the experiments. The animals were fed ad libitum with either standard chow-fed or a high-fat diet and allowed free access to water.

3.5.1. Experimental design

After acclimatizing, the mice were divided into different groups mentioned in respective chapters.

3.5.2. Model development

Obesity-linked type 2 diabetes was induced in mice of all the groups; except for group I (Normal control group) by feeding mice with HFD that contained approximately 60% kcal fat, 20% kcal protein and 20% kcal carbohydrate wherein soybean oil and lard were used as the fat source (D12492, Research Diets, New Brunswick, NJ, USA) for 10 weeks. While normal control group was fed with standard chow diet which contained approximately 7.5% kcal fat, 17.5% kcal protein, 75% kcal carbohydrate (RM1, Special Diet Services, Witham, Essex, UK). Weight gain was monitored after every two weeks. After 10 weeks of HFD feeding, obese mice were fasted overnight and intraperitoneally injected with a low dose of STZ [35 mg/kg dissolved in freshly prepared 0.1 M cold citrate buffer (pH 4.5)], while normal control mice from the group I were given the same volume of 0.1 M cold citrate buffer (pH 4.5). After one week, mice with fasting glucose > 240 mg/dl were considered as diabetic and then allowed to stabilize for one more week. The mice from all the groups were continued with respective diet till 16 weeks of the whole experiment.

3.5.3. Experimental treatment

After two weeks of STZ injection (after 12 weeks of HFD), diabetic mice from group III and IV were injected intraperitoneally with metformin (25 mg/kg/day) and rapamycin (2 mg/kg/day) respectively. While group V and VI were injected intraperitoneally with low (10 mg/kg body weight/day) and high dose (25 mg/kg body weight/day) of kaempferol respectively. The mice from the group I and II were injected with sterile 10% ethanol: 40% PEG 400: 50% PBS as vehicle control. All the compounds i.e., metformin, rapamycin and kaempferol were dissolved in same solvent i.e., sterile 10% ethanol: 40% PEG 400: 50% PBS for experimental uniformity within each group. The mice were then allowed to continue to feed on their respective diets until the end of the study (total 16 weeks).

3.5.4. Autophagy flux determination

For autophagic flux determination, mice from Group VII and Group VIII were given an intraperitoneal injection of chloroquine (25 mg/ kg body weight/day) for last 10 days before completion of the experiment.

3.6. Preparation of palmitic acid-containing media

The RPMI media and DMEM media containing 0.5 mM PA was prepared as described elsewhere (Tu et al., 2014). Briefly, 100 mM PA stock solution was prepared in DMSO, which was subsequently diluted to 5 mM in 10% BSA (BSA dissolved in RPMI media/DMEM media). The resultant mixture was further diluted with pre-warmed (37°C) incomplete RPMI media/DMEM media supplemented with 1% streptomycin–penicillin solution to attain 0.5 mM PA concentration in the media. The final concentration of BSA in PA-containing media was 1 %, thus RPMI media/DMEM media supplemented with 1% BSA was used as vehicle control for experiments.

3.7. MTT assay for cell viability

The cytotoxicity as caused by several test compounds was measured according to the protocol reported by Mosmann [1983], which is described below in details. A sub-confluent monolayer of cells was trypsinized and collected in the respective culture media. In brief, 5×10^3

cells/well were seeded in 96 well plates (NEST, Korea). After 24 of attachment and respective treatment period MTT [3-(4, 5-Dimethyl-2-thiazolyl)-2, 5-diphenyltetrazolium bromide] solution in PBS was added at a final concentration of 0.5 mg/ml along with the fresh media and the cells were further incubated in the CO₂ incubator at 37°C for 4 h. Thereafter, the media was aspirated from each well and the formazan product formed was dissolved in 200 µl DMSO. The absorbance was measured at 570 nm using Fluostar Optima Plate Reader (BMG Labtech, Germany). The percentage of cell viability was calculated by the following formula; Percentage Cell Viability = (Mean OD of treated cells / Mean OD of untreated cells) X 100

3.8. Adipocyte differentiation

The pre-adipocyte cell line (3T3-L1 cells) were grown as 100% confluent monolayer in DMEM supplemented with 10% FBS and 1% antibiotic (100 U/ml of penicillin and 100 µg/ml streptomycin). Post-confluency, the DMEM was replaced with adipogenic differentiation inducing media (DMEM containing 1 µg/ml insulin, 0.5 mM IBMX and 1 µM dexamethasone cocktail) for 2 days and then followed by an induction media (DMEM media with 1 µg/ml insulin) for the next 6 days in presence or absence the test compounds for guiding the complete maturation of pre-adipocytes. The media was replenished along with the test compounds in every alternate days.

3.9. Oil Red O staining for lipids

The detection of neutral lipids was observed and quantified with Oil Red O staining. The cells were seeded in 6 well plates (approximately 5 X 10⁵ cells/well). After 24 h, the cells were treated with kaempferol with or without various inhibitors i.e., wortmannin, chloroquine and compound C in presence of 0.5 mM PA. The cells incubated with only PA and without PA were taken as positive and negative controls respectively. After 48 h of incubation, the cells were washed with sterile phosphate buffer saline and fixed with 10% formalin in phosphate buffer saline for 30 min at RT. Subsequently, the cells were washed with phosphate buffer saline and incubated with 60% isopropanol for 10 min then stained with 0.5% freshly prepared Oil Red O solution in 60% isopropanol for 15 min. The cells were then washed thrice with distilled water and imaged under an inverted light microscope (Zeiss, Axiovert 25, Germany).

Meanwhile accumulated lipids were extracted with 100% isopropanol and absorbance was estimated at 510 nm using a plate Reader (Fluostar Optima, BMG Labtech, Germany).

3.10. Measurement of intracellular triglyceride content

Intracellular triglyceride levels were measured to estimate the content of lipoprotein particles. For the estimation of cellular triglyceride content, cells were seeded in 6 well plates at a density of 5×10^5 cells in each well and treated with test compounds with or without various inhibitors for 48 h. On completion of the incubation, the cells were harvested and washed with cold phosphate buffer saline. Further, the cells were homogenized in 1 ml of 5% NP-40 and slowly heated to 80°C in water bath for 5 min and then cooled down to room temperature, the heating and cooling steps were repeated again to solubilize all triglycerides. Thereafter, the samples were centrifuged at 12000 x g for 2 min and supernatant of each sample was diluted 10-fold with distilled water before proceeding with the quantification. The triglyceride level was estimated in each sample using the commercially available kits (Erba, Germany) according to the manufacturer's instructions. The content of protein in each sample was determined by BCA Protein Assay Kit (Pierce Biotechnology, USA). The intracellular triglyceride content was represented as $\mu\text{g}/\text{mg}$ cellular protein.

3.11. Labeling of lipid droplets with BODIPY stain

BODIPY or boron dipyrromethene is a class of strong ultraviolet-absorbing dyes for staining neutral lipids in live or fixed cells. For labeling lipid droplets, cells were seeded onto coverslips at a density of 2.5×10^5 cells/ coverslip and treated with respective treatments. After 48 h of treatment, the cells were washed with phosphate buffer saline and fixed with 4% formaldehyde for 10 min at room temperature. Further, the cells were washed with phosphate buffer saline and incubated with BODIPY 493/503 at a working concentration of 5 $\mu\text{g}/\text{ml}$ in phosphate buffer saline for 20 min at room temperature. After incubation, the cells were washed twice with phosphate buffer saline and counterstained with DAPI. The slides were prepared and the cells were imaged under confocal laser scanning microscope (LSM 780, Carl Zeiss, Germany) at excitation and emission wavelengths of 493 and 503 nm, respectively.

3.12. L6 cell differentiation

The L6 cells were maintained in high glucose DMEM supplemented with 10% heat-inactivated FBS and 1% streptomycin–penicillin solution at 37°C in a humidified atmosphere with 5% CO₂. To differentiate the L6 cells, once they attained 80% confluency, the cells were supplemented with myogenic differentiation media (DMEM supplemented 2% horse serum and 1% penicillin/streptomycin solution) for 7 days.

3.13. Glucose uptake assay

After differentiation of L6 cells, the differentiating media was replaced with DMEM containing 0.2% BSA and the differentiated myotubes were incubated with different concentration of quercetin, rutin, myricetin and kaempferol in presence or absence of 0.5 mM PA for 24 h. The cells were then washed with Krebs-Ringer bicarbonate (KRB) buffer and then placed in KRB buffer containing 0.2% BSA and 20 mM glucose for 1 h incubation. The cells were incubated with or without insulin (100 nM) in the presence of quercetin, rutin, myricetin and kaempferol up to 60 min. Then aliquots of 25 µl were removed from incubation mixture and glucose concentration was determined using GOD-POD glucose estimation kit (ERBA Diagnostics Mannheim GmbH, Germany).

3.14. Bromo-2'-deoxyuridine (BrdU) incorporation assay

The incorporation of thymidine analog BrdU (5-bromo-2'-deoxyuridine) into freshly synthesized DNA and then anti-BrdU antibody labeling, quantitatively measure the cell proliferation. Briefly, 5×10^3 cells/well were seeded in poly-D-lysine coated black/clear bottom 96 well plates and incubated for 24 h, thereafter treated with respective treatments for another 48 h. On completion of incubation, the cells were supplemented with 10 µM BrdU (Himedia, Mumbai, India) for 24 h. At the end of incubation period, the cells were briefly rinsed with PBS and fixed with 4% paraformaldehyde in PBS at 4°C for 30 min. Further, the cells were washed with PBS, followed by permeabilization with 0.2% Triton X-100 for 10 min. The resulting cells were then incubated with 2 N HCl for 20 min at RT to denature the DNA and then neutralize with 0.1 M sodium borate (pH 8.5) for 5 min. After an additional wash with PBS, the cells were incubated with mouse monoclonal FITC conjugated anti-BrdU antibody

(sc-32323 FITC, Santa Cruz Biotechnology, CA, USA) at 1:200 dilutions in PBS at 4°C for overnight. The cells were then gently washed with PBS and counterstained with DAPI and visualized under a fluorescence microscope (Zeiss, Axiovert 25, Germany). The fluorescent intensities for BrdU uptake were measured by Fluostar Optima Plate Reader (BMG Labtech, Germany) at respective excitation and emission wavelengths of 488/520 nm for FITC and 350/461 nm for DAPI (Kiyota et al., 2015).

3.15. Hoechst 33342 staining for monitoring nuclear morphology of apoptotic cells

Hoechst 33342 is a cell permeable dye which stains the nucleus. For nuclear staining, cells were seeded in 12 well plates (5×10^4 cells/well) in complete media with 10% FBS. After 24 h of seeding, the cells were supplemented with media containing 0.5 mM PA and subsequently treated with the test compounds and with or without specific inhibitors. After 48 h of treatment, the cells were stained with Hoechst 33342 (1 μ g/ml in PBS) for 5 min. Thereafter, the cells were visualized and imaged under the Confocal Laser Scanning Microscope (LSM 780, Carl Zeiss, Germany) equipped with 405 nm excitation laser.

3.16. DNA ladder assay

The fragmentation of chromosomal DNA into multiple nucleosomal units of approximately 180 bp length observed as DNA laddering is considered as a hallmark of apoptosis. The pattern of DNA cleavage due to cell cytotoxicity by compounds was assessed by extracting genomic DNA from treated cells and visualizing it on an agarose gel. For this assay, cells were seeded in 6-well plate at a seeding density of 5×10^5 cells/well in media with 10% FBS. After 24 h of seeding, the cells were treated with test compounds in presence or absence of various inhibitors in 0.5 mM PA-containing media. At the end of 48 h of incubation, the cells were harvested and centrifuged at 1000 X g for 5 min. The cells in the resultant pellet were lysed with lysis buffer (10 mM Tris-HCl pH 8.0, 10 mM EDTA and 0.5% Triton X-100) and treated with DNase-free RNase (0.1 mg/ml) for 1 h at 37°C to digest the RNA content. After this, the proteins were digested with Proteinase K (0.2 mg/ml) for 2 h at 50°C. The cellular DNA was extracted with a mixture of phenol, chloroform, and isoamyl alcohol (25:24:1). Thereafter, the DNA was selectively precipitated by adding an equal volume of isopropanol. The samples were then stored overnight at -20°C and then centrifuged at 12,000 rpm for 15 min. The

resultant DNA pellets were air dried and resuspended in 20 μ l Tris-EDTA buffer. The extracted DNA was then quantified using DS-11 spectrophotometer (Denovix, Wilmington, DE, USA) and the equal amount of each sample DNA was electrophoretically separated on a 1.5% agarose gel containing 0.5 μ g/ml ethidium bromide and visualized and photographed under Gel Documentation system (Bio-Rad, USA) (Kotamraju et al., 2000).

3.17. Labeling of autophagic vacuoles and lysosomes with MDC and LysoTracker

MDC is widely used as a probe to label autophagic vacuoles while LysoTracker Red DND-99 is used to specifically tag lysosomes. After 48 h of treatment, the cells were washed with PBS and stained with 0.5 mM MDC in PBS for 15 min at 37°C. On completion of the incubation, the cells were rinsed with PBS and further treated with 50 nM of LysoTracker Red DND-99 in PBS for 15 min at 37°C. The cells were then rinsed with PBS and fixed with 2% glutaraldehyde and further analyzed and imaged under confocal laser scanning microscope (LSM 780, Carl Zeiss, Germany) at 355 nm and 577 nm excitation and 460 nm and 590 nm emission wavelengths for MDC and LysoTracker respectively. Similarly, the isolated rat islet cells after treatment were stained with MDC and LysoTracker stains as mentioned earlier and images were acquired at different depths by using the z-stack option in confocal laser scanning microscope (LSM 780, Carl Zeiss, Germany). The acquired images were then overlaid to generate a composite 3D image of islet clusters.

3.18. Cell transfection and stable cell line establishment

For LC3 puncta assay, an importance assay to monitor the status of autophagy in cells, EGFP-LC3 expressing stable RIN-5F cell line were established. To generate stable EGFP-LC3 expressing cells, 2 μ g EGFP-LC3 plasmid was transfected to 70 - 80% confluent cells using Polyfect transfection reagent (Qiagen, USA) according to the manufacturer's instructions. The transfected cells were screened with 500 μ g/ml G418 (Sigma) until stable cell lines were established.

3.19. LC3 puncta assays

The cells undergoing autophagy can be marked by visualizing fluorescently labeled LC3 puncta. The cells stably expressing EGFP-LC3 were treated with or without test compounds in the presence or absence of chloroquine for 48 h. After incubation, the cells were fixed with 2% formaldehyde and observed under Confocal Laser Scanning Microscope (LSM 780, Carl Zeiss, Germany) for EGFP-LC3 puncta formation. The cells with more than ten EGFP-LC3 punctate dots were considered as positive and were counted.

3.20. Flow cytometer analysis for autophagy quantification

Flow Cytometer Analysis was performed as described elsewhere (Eng et al., 2010). For this assay, the stable RIN-5F cells expressing the EGFP-LC3 plasmid were adapted to monitor autophagy by flow cytometry. Around 5×10^4 cells were seeded in a six-well plate and were treated with the test compound with or without inhibitor in the presence of PA. On completion of the treatment, the cells were harvested by trypsinization and the resultant cells in the suspension were subsequently fixed with 2% glutaraldehyde for 2 min. The excess glutaraldehyde in the fixation step was removed by washing the cells twice with PBS. After glutaraldehyde fixation, the cells were consequently permeabilized by briefly treating them with 0.05% saponin in PBS in order to selectively remove soluble cytoplasmic non-autophagosome associated EGFP-LC3 from the cells. The cells were then washed again with PBS and resuspended in 100 μ l PBS prior to being analyzed by flow cytometer (BD FACSVerser™, BD Biosciences, USA). Around 10,000 cell's fluorescence was acquired for each sample which was further analyzed using suitable software (BD FACSuite™ software BD Biosciences, USA) and the results were represented as histogram between normalized frequency percentages versus EGFP-LC3 fluorescence intensity.

3.21. Transmission electron microscopy analysis

Samples for TEM analysis were prepared according to the standardized protocol developed by “Sophisticated Analytical Instrument Facility” of All India Institute of Medical Sciences, New Delhi, India. For sample preparation, the cells were harvested after treatment. For *in vivo* study, the pancreas and liver tissues were isolated from mice and sliced into 2 mm² sections.

These samples were fixed with 2% paraformaldehyde and 2.5% glutaraldehyde in 0.1 M phosphate buffer (pH 7.4) for 6 h at 4°C and then washed with 0.1 M phosphate buffer. Further, samples were post-fixed with 1% OsO₄ in Sorensen phosphate buffer (0.05 M Sorensen phosphate buffer, 1% OsO₄, and 0.25 M glucose) for 1 h and subsequently washed with distilled water twice. The samples were then double stained with uranyl acetate and lead citrate solution for 12 h. Finally, the samples were analyzed by the TECNAI 200 KV TEM (Fei, Electron Optics) transmission electron microscope at All India Institute of Medical Sciences, New Delhi, India.

3.22. Insulin secretion and content analysis

For measurement of total insulin content, pancreas slices were lysed with acid/ethanol (0.18 N HCl in 70% ethanol) overnight at 4°C and further homogenized. After centrifugation, the lysates were neutralized to pH 7.2 with 0.4 M Tris buffer pH 8.0. Further, the insulin levels in each lysate were measured with insulin enzyme immunoassay kit (SPI-Bio, Bertin Pharma, Montigny-le-Bretonneux, France).

3.23. Bacterial transformation and plasmid preparation

DH5 α strain of *E.coli* was grown at 37°C and 250 rpm in shaker incubator to an OD₆₀₀ of 0.8. Then culture was allowed to chill at 4°C in a pre-chilled falcon tube. These cells were pelleted at 5000 rpm for 10 min at 4°C and re-suspended in 40 ml of pre-chilled 80mM CaCl₂ and 20mM MgCl₂ solution. The cells were then centrifuged and suspended in 2-3 ml of 0.1ml CaCl₂ to obtain the competent cells. Small aliquots of competent cells (150-200 μ L) were added with 5 ng of plasmid DNA, mixed gently and incubated for 30 min at 4°C. Proper negative and positive controls with no plasmid and known plasmids respectively were included to ascertain the transformation procedure. On completion of the incubation period, the cells were given a heat shock at 42°C for 90 sec and immediately transferred to ice. LB broth was mixed with each sample and incubated at 37°C for 45 min. The transformed cells were finally spread plated on antibiotic containing plates corresponding to the antibiotic resistant gene in the plasmid. The culture plates were then incubated overnight at 37°C.

3.24. Plasmid isolation

The transformed bacteria were inoculated into 5 ml of LB broth containing respective antibiotic and placed overnight in a shaker incubator at 37°C and 250 rpm. A small aliquot of 1.5 ml culture was centrifuged at 10,000 rpm for 3 min and the bacterial pellet was suspended in lysis buffer and stepwise methodology was opted for plasmid preparation according to the protocol provided in the instruction manual (ZIPPY™ plasmid miniprep, Zymo Research, USA). Finally, the plasmid DNA was eluted with elution buffer. The quality of the eluted plasmid DNA was confirmed by running the DNA on the agarose gel.

For quantification of DNA, 1 µl of each sample was loaded on to the spectrophotometer (Nanodrop 2000 spectrophotometer, Thermo Scientific, USA). The OD was determined at 260nm and 280nm setting nuclease free as blank. The ratio of the OD260/280 was considered to check the purity of the recovered nucleic acid.

3.25. Transfection of DNA into mammalian cell lines

The day before transfection, cells were seeded in a 12-well plate at a density of 4×10^4 cells/well and incubated overnight at 37°C in a 5% CO₂ incubator. Then the cells were incubated in serum-free DMEM for 6 h before performing transfection. Subsequently, the cells were transiently transfected with 200 ng/well of PPREx3-tk-Luc reporter plasmid and 25 ng pcMX-PPAR α plasmid using Polyfect transfection reagent (Qiagen), according to the protocol provided by the manufacturer. As an internal control for transfection, the β -gal plasmid was also transfected with the luciferase reporter plasmids. Briefly, 15 µl of polyfect reagent (Superfect transfection reagent, Qiagen, USA) was mixed with the DNA solution and pipetted up and down for 5-6 times. The samples were then placed at RT for 5 to 10 min to allow the complex formation. During the incubation, the cell medium was aspirated from the petri plate and the cells were rinsed twice with PBS. To the plate, fresh medium was added and then allowed to stand. After the incubation of the transfection mix, complete growth medium was added to it and gently mixed. The whole transfection mix was then added to the petri plate. The plate was gently whirled for uniform distribution of the complexes and incubated in a 37°C and 5 % CO₂ incubator for next 24 h. The transfected cells were then exposed to various concentrations of kaempferol in the PA-containing medium and incubated for 24 h.

3.26. Luciferase assay

Luciferase assay was done to investigate the promoter activity of a gene at the transcription level (Voleti et al., 2012). For this assay, the transfected cells were lysed with the lysis buffer containing 0.6 M NaCl, 0.1 M EDTA, 0.2 M DTT, 0.1% Triton-X, 0.8 M tricine and 0.2 M MgSO₄. The cell lysates were then analyzed for the relative luciferase activity using luciferin as substrate. The values of luciferase activity for each lysate were normalized to the β-gal activity of the respective lysates. Each experimental condition was repeated thrice. The value of luciferase for each lysate was normalized to the luciferase inductions in response to treated cells and was expressed as fold luciferase activity with respect to vehicle-treated cells.

3.27. siRNA transfections

Species-specific pre-designed siRNA were purchased from Qiagen (Valencia, CA, USA) and Ambion (Life Technologies GmbH, Darmstadt, Germany). Negative control siRNA for the respective genes were procured from Qiagen. Then 50 nM of each siRNA were transfected into cells. For this, Attractene transfection reagent (Qiagen) was used for transfection, according to the protocol mentioned by the manufacturer. Briefly, 5 X 10⁵ cells were seeded in 6 well plates. After 24 h, the cells were transfected with 50 nM of each siRNA in respective wells with the transfection reagent according to manufacturer's protocol and incubated in a CO₂ incubator at 37°C. After 24 h of incubation, the cells were treated with or without 10 μM kaempferol in presence of 0.5 mM PA for another 48 h.

3.28. RNA isolation

The total RNA was extracted from the treated cells with Trizol reagent (Sigma-Aldrich, St. Louis, MO, USA) according to the instructions given by the manufacturer. Briefly, 1 X 10⁴ cells were seeded in a 6-well plate. After the respective drug treatment, the cells were rinsed with 1 ml of 1xPBS (pH 7.4) and the cell pellets were collected by centrifugation at 200g. Subsequently, the cell pellets were homogenized in 1 ml of Trizol reagent and 200 μl chloroform was added to each of the samples. The samples were then agitated vigorously for 15 sec and left for 5 min at room temperature for achieving phase separation. The aqueous and organic phases were separated by a centrifugation of the samples at 12000g for 15 min at 4°C.

The upper aqueous phase containing total RNA was removed carefully and transferred to a fresh tube. The RNA from each sample was precipitated by adding an equal volume of isopropyl alcohol, incubated for 10 min at room temperature followed by a centrifugation at 12000g for 10 min at 4°C. To avoid the residual salt and impurities, the pellets were washed with 75% ethanol twice for 5 min each at 7500g. Finally, the obtained RNA was dissolved in nuclease-free water and stored at -80°C. The extracted total RNA was finally quantified with Nanodrop 2000 spectrophotometer (Thermo Scientific, USA) and a ratio of OD₂₆₀: OD₂₈₀>1.8 was further considered for RT PCR analysis.

3.29. Semi-quantitative reverse transcription polymerase chain reaction (RT PCR)

3.29.1. First strand cDNA synthesis (reverse transcription)

The total RNA quantified with a ratio of OD₂₆₀: OD₂₈₀>1.8 was taken for first strand cDNA synthesis. 2 µg of total RNA of each sample was transcribed to cDNA with the help of RT-PCR kit from New England Biolabs, USA. Approximately 2 µg of RNA was taken in a 0.2ml vial and to this 2 µl of Oligo (dT)₁₈ primer and nuclease-free water were added to make the final volume to 13.7 µl. The vials were incubated at 65°C for 10 min and then immediately shifted in the ice. Then the following reagents were added in the reaction mixture;

4 µl RT buffer (5X)

2 µl dNTP mix (30mM)

0.3 µl M-MuLV reverse transcriptase (50U/ µl)

The solutions were mixed properly and then incubated at 42°C for 1 h. Subsequently, the RNA-cDNA hybrids were denatured at 95°C for 3 min. The samples were then spun down and quickly stored at -40°C for further processing.

3.29.2. PCR amplification

PCR amplification for a 25 µl reaction volume was set with the desired number of cycles by preparing a PCR cocktail consisting of the following components from New England Biolabs, USA ;

12.75 µl sterile water

5 µl 10X PCR buffer

1 μ l 30 mM dNTP mixes
 1 μ l Forward primer (100 ng/ μ l)
 1 μ l Reverse primer (100ng/ μ l)
 0.25 μ l Taq DNA polymerase (3U/ μ l)
 4 μ l cDNA (obtained above)

Once the PCR mixture was ready, PCR was performed in the thermocycler machine (PTC-200 thermal cycler, MJ Research, USA) using the following program;

Steps	Temperature	Time
Step 1 (Denaturation)	94°C	2 min
Step 2 (Denaturation)	94°C	45 sec
Step 3 (Annealing)	**°C	30/45 sec
Step 4 (Extension)	72°C	2 min
Step 5 Go to step 2 for 30-35 cycles		
Step 6 (Final Extension)	72°C	10 min
Step 7 (End)		
Step 8 (Product storage)	4°C	infinite

** annealing temperature varies according to the primer length and base composition. β -actin was used as endogenous control to normalize the gene expressions. The amplified PCR products were stored at -40°C refrigerator and finally were resolved on 1.5% agarose gel. The details of the primer sequences and PCR conditions are presented in Table 3.1. All the primers used were purchased from Eurofins Scientific, USA.

Table 3.1. List of primers used in semi-quantitative RT-PCR

Primers	Sense (5'-3')	Antisense (5'-3')	Annealing temp. (°C)	Product (bp)
<i>β-actin</i> (Human/ Mouse/Rat)	TCACCCACACTGTGC CCCATCTACGA	CAGCGGAACCGCTCA TTGCCAATGG	58	300
<i>p62</i> (<i>Sqstm1</i>) (Rat)	CCTCAGCCCTCTAGG CATCG	GTACAGGGCAGCTTC CTTCA	60	415
<i>Map1lc3b</i> (Rat)	GCCTGTCCTGGATAA GACC	TTGGGAGGCATAGAC CATGT	56	217

<i>Atg7</i> (Rat)	TGTCAGCCTGGCATT GATAA	TCACTCATGTCCCAGA TCTCA	60	183
<i>Atg5</i> (Rat)	ACGTGTGGTTTGGAC GGATT	TTTCAGGGGTGTGCCT TCAT	60	206
<i>Ulk1</i> (Rat)	CATGACCTCCCTTGCA TGTAAC	ACCAGGTGGTGGGTA AGGAAC	60	106
<i>Becn1</i> (Rat)	GTGCTCCTGTGGAAT GGAAT	CCACTTGAGATTCGTC AGCA	56	431
<i>Casp3</i> (Rat)	GAAACCTCCGTGGAT TCAA	AGCCCATTCAGGGTA ATCC	56	124
<i>Bad</i> (Rat)	CAGTGATCTGCTCCA CATT	TCCAGCTAGGATGAT AGGAC	60	340
<i>Bax</i> (Rat)	CCAGGACGCATCCAC CAAGAAGC	TGCCACACGGAAGAA GACCTCTCG	60	136
<i>Bcl2</i> (Rat)	ATCGCTCTGTGGATG ACTGAGTAC	AGAGACAGCCAGGAG AAATCAAAC	60	134
<i>Bcl-xl</i> (Rat)	TCTAACATCCCAGCTT CAT	GCAATCCGACTCACC AATA	58	180
<i>Plin2</i> (Rat)	TCCGCAATGTTACCTC CTTC	AAGGGACCTACCAGC CAGTT	60	145
<i>Plin3</i> (Rat)	GGAAGTGGTGTGCATC AACAG	GGTCACATCCACTGCT CCTG	60	109
<i>ACO1</i> (Human)	CCTCTGGATCTTCACT TGGGC	TGGGTTTCAGGGTCAT ACG	188	58
<i>PPARα</i> (Human)	CTATCATTTGCTGTGG AGATCG	AAGATATCGTCCGGG TGGTT	121	57
<i>HSL</i> (Human)	GTGCAAAGACGGAGG ACCACTCCA	GACGTCTCGGAGTTTC CCCTCAG	298	60
<i>ATGL</i> (Human)	ACCAGCATCCAGTTC AACCT	ATCCCTGCTTGACAT CTCT	97	61

3.29.3. Agarose gel electrophoresis

Agarose gel electrophoresis was done to visualize RNA/DNA. 1.5% the agarose gel was prepared by dissolving 1.5g agarose in 100 ml of 1X TAE buffer [24.2g Tris base, 5.7ml glacial acetic acid, 2ml of 0.5mM EDTA (pH 8.0)]. The mixture was then heated in a microwave oven until the agarose was dissolved completely and the solution was clear. Then 5 μ l EtBr (10mg/ml stock) was added to this solution when it became lukewarm and casted into the gel cast tray fitted with an appropriate comb and further allowed to solidify. The comb was

carefully removed from the solidified gel and then the gel was submerged in the electrophoresis chamber filled with 1X TAE. The DNA samples or isolated plasmid samples were mixed with 6X gel loading dye (10mM TrisCl pH. 7.6, 60 mM EDTA pH 8.0, 0.03% xylene cyanol FF, 0.03% bromophenol blue, 60% glycerol) and carefully loaded in the wells. The samples were electrophoresed at 7-8V/cm for 1 h and visualized under UV visible transilluminator (Gel documentation system, Bio-Rad, USA).

3.30. Western blot analysis

The total proteins from cells and tissue samples were prepared by using RIPA lysis buffer (150 mM NaCl, 50 mM Tris pH 7.6, 0.5% sodium deoxycholate, 0.1% SDS, 1% Triton X-100 and 1X protease inhibitor cocktail). Briefly, 5×10^5 cells were plated on to a 6-well plate and exposed to respective treatments. Then the cells were harvested in RIPA lysis buffer. The tissue samples were chopped in small pieces and were homogenized in RIPA lysis buffer with a precooled mechanical tissue homogenizer. The prepared lysates were then centrifuged at 12,000 rpm for 15 min. The resulting supernatants containing total proteins were quantified by BCA protein estimation kit and 50 μ g of total protein samples were resolved with 8, 10 or 15% polyacrylamide gel (depending on the molecular size of proteins to be analyzed). Subsequently, the immunoblot analysis was performed. Briefly, the resolved proteins were transferred to PVDF membrane in transfer buffer for 1 h at 90 V. Further, the membranes were blocked with 5% skimmed milk in TBST (20 mM Tris-HCl, pH 7.5, 150 mM sodium chloride, 0.05% Tween 20) for 1 h and then washed thrice with TBST for 10 min each, followed by incubation with primary antibodies (1:500 in TBST) for overnight at 4°C. Details of the antibodies used are mentioned in Table 3.2. The membranes were then washed thrice with TBST for 15 min each and incubated with anti-rabbit secondary antibodies (1:10,000 in TBST) conjugated to horseradish peroxidase for 1 h at room temperature. The blots were then developed in dark by using ECL detection kit (Santa Cruz, CA, USA). The developed blots were then subjected to densitometry analysis by Image J 1.45 software (NIH, USA) and normalized with β -actin as internal control.

Table 3.2. List of primary antibodies used in western blotting

Primary antibody	Catalogue Number	Dilutions	Secondary antibody	Dilutions	Chromogen
β actin	sc-130656	1:500	Anti-rabbit	1:10000	ECL
p62	sc-514790	1:500	Anti-mouse	1:10000	ECL
p-AMPK α1/2(Thr172)	sc-33524	1:500	Anti-rabbit	1:10000	ECL
BrdU (FITC conjugated)	sc-32323	1:500	Anti-mouse	1:10000	ECL
APG7	sc-376212	1:500	Anti-mouse	1:10000	ECL
pmTOR	sc-293133	1:500	Anti-mouse	1:10000	ECL
MAP LC3b	sc-271625	1:500	Anti-mouse	1:10000	ECL
SQSTM1 (ADRP/PLIN 2)	sc-32888	1:500	Anti-rabbit	1:10000	ECL
GADD153 (CHOP 10)	sc-575	1:500	Anti-rabbit	1:10000	ECL
PPARγ	sc-7273	1:500	Anti-mouse	1:10000	ECL
Caspase 3	sc-7148	1:500	Anti-rabbit	1:10000	ECL
p-IRS1(Ser307)	CST#2381	1:500	Anti-rabbit	1:10000	ECL
pAkt (Ser473)	sc-7985	1:500	Anti-rabbit	1:10000	ECL
Akt	sc-1619	1:500	Anti-goat	1:10000	ECL
pJNK	sc-6254	1:500	Anti-mouse	1:10000	ECL
Insulin	sc-8033	1:500	Anti-mouse	1:10000	ECL

3.31. Immunofluorescence study

For immunofluorescence study, 1×10^5 cells were seeded on each sterile coverslip and incubated for 24 h, thereafter treated with respective test chemicals for another 48 h. On completion of the incubation, the cells were fixed with 4% formaldehyde for 15 min followed

by three PBS washes for 5 min each. The fixed cells were then permeabilized with 0.1% Triton X-100 for 10 min, thereafter the cells were washed thrice with PBS for 5 min each and then blocked with 2% BSA in PBS for 1 h at room temperature. After blocking, the cells were incubated with primary antibody (1: 200 in PBS) overnight at 4°C. The cells were then washed three times with PBS followed by incubation with the FITC-labeled secondary antibody (1:500 in PBS) for 1 h at room temperature. Further, the cells were washed with PBS and incubated with Hoechst 33342 stain for 5 min to stain the nucleus. Then coverslips were mounted on slides and visualized under the confocal microscope equipped with 488 nm and 405 nm laser under FITC and DAPI filters respectively (LSM 780, Carl Zeiss, Germany).

3.32. Double immunofluorescence and co-localization studies

For studying co-localization of LC3 protein with LDs, the cells were seeded on sterile coverslips at a density of 2.5×10^5 cells/ coverslip and incubated for 24 h, thereafter treated with respective test chemicals for another 48 h. On completion of incubation, the cells were fixed with 4% formaldehyde for 15 min followed by washing with phosphate buffer saline thrice for 5 min each. The fixed cells were then permeabilized with 0.1% Triton X-100 for 10 min, thereafter the cells were washed and blocked with 2% bovine serum albumin for 1 h at room temperature. After blocking, the cells were incubated with primary antibody (1:250) overnight at 4°C followed by incubation with the Texas red-conjugated secondary antibody (1:500) for 1 h at room temperature. Further, the cells were washed and incubated with BODIPY (5 µg/ml in phosphate buffer saline) for 20 min at room temperature. Then, the cells were counterstained with DAPI for 5 min to stain the nucleus.

For double immunofluorescence labeling, after blocking the cells were incubated with primary antibody (1:250) for 2 h at room temperature and subsequently washed and then incubated with fluorescein isothiocyanate (FITC)-conjugated respective secondary antibody for 1 h. Thereafter, the cells were washed and incubated with another primary antibody (1:250) for 1 h at room temperature. The cells were then incubated with Texas red-conjugated appropriate secondary antibody for next 1 h. Then coverslips were mounted on slides and visualized under the confocal microscope equipped with 405 nm, 488 nm and 543 nm lasers (LSM 780, Carl Zeiss, Germany).

3.33. Measurement of lipid profile

To measure the total cholesterol, triglyceride, LDL and NEFA content, the serum was isolated from blood samples of the animals and further analyzed with the help of commercially available kits (Erba, Germany) according to the manufacturer's instructions.

3.34. Estimation of fasting blood glucose (FBG) and glucose tolerance test (GTT)

On completion of 16 weeks of the experiment, the fasting blood glucose of each mouse was recorded with a glucometer (Accu-chek active, Roche Diagnostics, Barcelona, Spain). For intraperitoneal glucose tolerance test (IPGTT), the mice fasted for 6 h and then, each mouse received an intraperitoneal injection of glucose (1 g/kg body weight). Thereafter, the blood glucose of each mice was monitored at 15, 30, 60, 90 and 120 min after glucose injection while baseline blood glucose measurements were estimated just before glucose administration. The results were represented in terms of milligrams per deciliter of blood (mg/dl).

3.35. Insulin tolerance test

For insulin tolerance test, the mice were fasted for 6 h and further administered an intraperitoneal injection of insulin (0.75 U/kg body weight). Blood glucose of each mice was then monitored at 15, 30 and 60 min after insulin injection while blood glucose measurements for 0 min were taken just before insulin administration. The results were represented in terms of milligrams per deciliter of blood (mg/dl).

3.36. Fasting and glucose-stimulated insulin secretion

On completion of treatment, the mice were fasted for 6 h and intraperitoneally injected with glucose (1 g/kg body weight). The blood was withdrawn from the tail vein at 0, 15, 30, 45 and 60 min. Thereafter, plasma was separated and insulin level was checked with insulin enzyme immunoassay kit (SPI-Bio, Bertin Pharma, Montigny-le-Bretonneux, France).

3.37. Pancreatic insulin content analysis

For measurement of total insulin content, pancreas slices were lysed with acid/ethanol (0.18 N HCl in 70% ethanol) overnight at 4°C and further homogenized. After centrifugation, the

lysates were neutralized to pH 7.2 with 0.4 M Tris buffer pH 8.0. Further, the insulin levels in each lysate were measured with insulin enzyme immunoassay kit (SPI-Bio, Bertin Pharma, Montigny-le-Bretonneux, France).

3.38. Histopathological studies

For histopathological studies, the tissues were removed and immediately fixed in 10% neutral buffered PBS. After fixation, the tissues were dehydrated with upgrading from 30 to 70% series of alcohol for 1 h each then incubated in xylene for next 1 h followed by embedding in paraffin wax at 60°C (changed twice). The tissues were then sectioned to 4 µm thickness and fixed on glass slides. The sections were then deparaffinized in xylene followed by hydration in gradations of alcohol (100-70% ethanol) for an incubation of 2 min each. Thereafter, these slides were stained with Harry's hematoxylin for 30 sec, washed with tap water for 1 min and again dehydrated in 70-90% ethanol for 2 min. Then the sections were counterstained with eosin for 2 min followed by dehydration again in 90% and absolute ethanol for 2 min each. These sections were finally cleaned through xylene for 1 min and mounted with DPX as described elsewhere (Ebato et al., 2008).

3.39. Immunohistochemistry

The paraffin-embedded tissues were sectioned at a thickness of 4 µm and mounted on positive-charged slides. The slides were transferred into boiling citrate buffer for 15 min and then incubated with 3 % hydrogen peroxide and blocking serum. The tissue sections were incubated with the primary antibody (1:100 in PBS) overnight at 4°C. The sections were washed with PBS followed by incubation with texas red-conjugated secondary antibody for 2 h at room temperature. The slides were examined and images were taken under a confocal microscope (LSM 780, Carl Zeiss, Germany).

3.40. Statistical analysis

Quantitative data are presented as means \pm standard deviation (SD) of three independent experiments and statistically evaluated by one-way ANOVA followed by Tukey's post hoc test using Graph Pad Prism 6 software (Graph Pad Software, San Diego, CA, USA). For the data analysis, $p < 0.05$ was considered to be statistically significant.







CHAPTER 4

***SCREENING OF VARIOUS FLAVONOIDS FOR
THEIR ANTI-OBESITY AND ANTIDIABETIC
ACTIVITIES: AN IN VITRO AND IN VIVO STUDY***

Chapter 4. Screening of various flavonoids for their anti-obesity and antidiabetic activities: an *in vitro* and *in vivo* study

4.1. Introduction

Obesity is a major risk factor associated with various diseases such as diabetes, cardiovascular disease, hypertension, bone disorders and cancer (Formiguera and Cantón, 2004). Obesity is an ailment in which adipocytes become large by accumulating an enormous amount of lipids. At the cellular level, it is characterized by a surge in number and size of differentiated adipocytes in adipose tissue. The adipocytes are the primary site which stores energy in form of lipids and indirectly responsible for insulin sensitivity (Smith and Kahn, 2016). Adipocytes are formed from pre-adipocytes which are undifferentiated fibroblasts cells. This differentiation process involves a series of steps which progresses in a particular pattern regulated by a wide variety of transcription factors such as peroxisome proliferator-activated receptor (PPAR- γ) and CCAAT/enhancer-binding proteins (C/EBPs) which further regulates various adipocyte-specific genes (Guo et al., 2014).

In obese condition, the elevated level of circulating free fatty acids (FFA) is one of the predisposing factors in the development of insulin resistance and hyperglycemic conditions linked with type 2 diabetes mellitus (T2DM) (Giacca et al., 2010). Skeletal muscle accounts for the major portion of glucose uptake thus skeletal muscle insulin resistance is a primary risk factor for T2DM (DeFronzo and Tripathy, 2009). It is well-known that saturated fatty acids, such as PA, has been implicated in impairment of insulin signaling which, in turn, is associated with the pathogenesis of insulin resistance and compromised glucose disposal in muscle cells (Hirabara et al., 2010). GLUT4 is the most abundant glucose transporter expressed in skeletal muscle which facilitates glucose uptake inside cells and primarily regulated by insulin. A cascade of events comprising of classical insulin signaling PI3K/Akt pathway and GLUT4 translocation to the membrane of muscle cells are involved in insulin-stimulated glucose entry into cells (Ijuin and Takenawa, 2012). Additionally, activation of AMPK has been shown as an alternative mechanism to promote translocation of GLUT4 to the membrane, thus stimulating glucose uptake (O'Neill, 2013). Numerous studies have reported that well-known anti-diabetic drug, metformin, enhances glucose uptake through AMPK activation (Kim et al., 2016; Kristensen et al., 2014).

Autophagy is a lysosomal degradation process involved in cell quality control during adverse conditions like starvation and stress (Mizushima, 2007). The role of autophagy in sustaining pancreatic β -cell mass and function is well established and its failure has been linked to the pathophysiology of type 2 diabetes (Codogno & Meijer, 2010). Recent studies showed that dysfunctional autophagy is involved in the loss of β -cell mass and function hence pathophysiology of obesity-linked diabetes (Masini et al., 2009; Bartolomé et al., 2014; Mir et al., 2015). On the basis of this pre-notion, rapamycin (a mTOR inhibitor and known activator of autophagy) has been reported to exert the cytoprotective effect on PA-induced β -cell by reducing the blockage of autophagic turnover (Mir et al., 2015). Thus, identifying agents that could modulate autophagy in pancreatic β -cells in lipid-excess stressful conditions could be a better target in developing therapies for obesity-linked T2DM.

Flavonoids are the largest group of phytochemicals and are abundantly found in various vegetables, fruits, grains, spices, beverages and medicinal plants (Kozłowska and Szostak-Wegierek, 2014). Numerous investigations have reported a wide range of biological activities of this class of phytochemicals and their role in prevention and cure of various diseases such as obesity, diabetes, cancer, heart diseases and bone disorders (Kumar and Pandey, 2013; Chen et al., 2014). The flavonoids are considered to be excellent and alternative candidates for diseases management as these plant-based phytochemicals are safe, effective, economical, non-toxic with no or lesser side effects. Therefore, flavonoids have recently been gaining importance for developing therapeutics for obesity and diabetes management (Kawser et al., 2016).

In the present study, we have selected four flavonoids namely: quercetin, rutin, myricetin and kaempferol, extensively present in various plant sources, to determine their anti-obesity and antidiabetic activities and underlying mechanism (Kozłowska and Szostak-Wegierek, 2014; Panche et al., 2016). There are some pre-existing reports which showed anti-hyperlipidemic and anti-hyperglycemic effects of these flavonoids (Unnikrishnan et al., 2014; Vinayagam and Xu, 2015); however, their precise mode of action still remains elusive. Additionally, in this study, we have made a comparative analysis of tested flavonoids for their effects on adipogenesis and insulin resistance in adipocyte and muscle cells respectively.

4.2. Brief methodology

4.2.1. Cell culture and treatment

3T3-L1 (undifferentiated fibroblastic cells), L6 (undifferentiated muscle cells) and RIN-5F (Clonal pancreatic β -cells) cell lines were procured from National Centre for Cell Science (NCCS), Pune, India and were cultured according to the protocol mentioned in materials and methods section (chapter 3) of this thesis.

4.2.2. MTT assay for determination of cell viability

The cytotoxicity as caused by several test compounds was measured according to the protocol described in chapter 3.

4.2.3. Adipocyte differentiation assay

The pre-adipocyte cell line (3T3-L1 cells) were grown as 100% confluent monolayer in DMEM supplemented with 10% FBS and 1% antibiotic (100 U/ml of penicillin and 100 μ g/ml streptomycin). Post-confluency, the DMEM was replaced with adipogenic differentiation inducing media (DMEM containing 1 μ g/ml insulin, 0.5 mM IBMX and 1 μ M dexamethasone cocktail) for 2 days and then followed by an induction media (DMEM media with 1 μ g/mL insulin) for the next 6 days in presence or absence the test compounds for guiding the complete maturation of pre-adipocytes. The media was replenished along with the test compounds in every alternate day.

4.2.4. Estimation of intracellular lipid contents

The accumulated neutral lipids in differentiated 3T3-L1 cells were observed and quantified with Oil Red O staining. Further, intracellular triglyceride content was measured according to the protocol mentioned in chapter 3 of this thesis.

4.2.5. Preparation of palmitic acid (PA)-containing media

The media containing 0.5 mM PA was prepared as discussed in chapter 3. Briefly, 100 mM PA stock solution was prepared in DMSO, which was subsequently diluted to 5 mM in 10% BSA. The resultant mixture was further diluted with pre-warmed (37°C) incomplete media supplemented with 1% streptomycin–penicillin solution to attain 0.5 mM PA concentration in the media. The final concentration of BSA in PA-containing media was 1%. Thus, media supplemented with 1% BSA was used as vehicle control for further experiments.

4.2.6. L6 cell culture and differentiation

The L6 cells were maintained in high glucose DMEM supplemented with 10% heat-inactivated FBS and 1% streptomycin–penicillin solution at 37°C in a humidified atmosphere with 5% CO₂. To differentiate the L6 cells, once they attained 80% confluency, the cells were supplemented with myogenic differentiation media (DMEM supplemented 2% horse serum and 1% penicillin/streptomycin solution) for 7 days.

4.2.7. Glucose uptake assay

After differentiation of L6 cells, the differentiating media was replaced with DMEM containing 0.2% BSA and the differentiated myotubes were incubated with different concentration of quercetin, rutin, myricetin and kaempferol in presence or absence of 0.5 mM PA for 24 h. The cells were then washed with Krebs-Ringer bicarbonate (KRB) buffer and then placed in KRB buffer containing 0.2% BSA and 20 mM glucose for 1 h incubation. The cells were incubated with or without insulin (100 nM) in the presence of quercetin, rutin, myricetin and kaempferol up to 60 min. Then aliquots of 25 µl were removed from incubation mixture and glucose concentration was determined using GOD-POD glucose estimation kit (ERBA Diagnostics Mannheim GmbH, Germany).

4.2.8.. Experimental animals

All the animal experiments were performed as per CPCSEA guidelines with prior approval from Institutional Animal Ethics Committee with approval number "BT/IAEC/2017/02". For this, the male C57BL/6 mice of age 7 weeks old were procured from CSIR-Institute of Microbial Technology, Chandigarh, India. They were housed under standard conditions (temperature 23±2°C and 12 h dark-light cycle) in a well-maintained animal house and acclimatized for two weeks prior to start of the experiment. Mice were fed ad libitum with either standard chow-fed or a high-fat diet and allowed free access to water.

4.2.9. Experimental design

After acclimatizing, mice were divided into eight groups (n=6) as follow;

Group I - Standard normal chow-fed mice (Normal Control)

Group II - HFD fed mice + streptozotocin (STZ) (Diabetic control)

Group III - HFD fed + streptozotocin + treated with metformin 25 mg/kg body weight (bw)/day (Positive control)

Group IV -HFD fed + streptozotocin + treated with 25 mg/kg bw/day quercetin

Group V -HFD fed + streptozotocin + treated with 25 mg/kg bw/day rutin

Group VI - HFD fed + streptozotocin + treated with 25 mg/kg bw/day myricetin

Group VII - HFD fed + streptozotocin + treated with 25 mg/kg bw/day kaempferol

4.2.10. Model development

Obesity-linked type 2 diabetes was induced in mice of all the groups [except for group I (Normal control group)] by feeding mice with high-fat diet that contained approximately 60% kcal fat, 20% kcal protein and 20% kcal carbohydrate wherein soybean oil and lard were used as the fat source (D12492, Research Diets, New Brunswick, NJ, USA) for 10 weeks. The normal control group was fed with standard chow diet which contained approximately 7.5% kcal fat, 17.5% kcal protein, 75% kcal carbohydrate (RM1, Special Diet Services, Witham, Essex, UK). Weight gain

was monitored after every two weeks. After 10 weeks of HFD feeding, obese mice were fasted overnight and intraperitoneally injected with a low dose of streptozotocin (35 mg/kg dissolved in freshly prepared 0.1 M cold citrate buffer (pH 4.5), while normal control mice from group I were given the same volume of 0.1 M cold citrate buffer (pH 4.5). After one week, the mice with fasting glucose > 240 mg/dl were considered as diabetic and were then allowed to stabilize for one more week. The mice from all the groups were continued with respective diet till 16 weeks of the whole experiment.

4.2.11. Experimental treatment

After two weeks of STZ injection (after 12 weeks of HFD), diabetic mice from group III, IV, V, VI and VII were injected intraperitoneally with 25 mg/kg/day dose of metformin, quercetin, rutin, myricetin and kaempferol respectively. Mice from the group I and II were injected with sterile solvent mixture of 10% ethanol: 40% PEG 400: 50% PBS as vehicle control. All the compounds were dissolved in the same solvent i.e., sterile 10 % ethanol: 40 % PEG 400: 50 % PBS for experimental uniformity within each group. The mice were allowed to continue to feed on their respective diets until the end of the study (total 16 weeks).

4.2.12. Estimation of blood parameters

On completion of 16 weeks of the experiment, fasting blood glucose of each mouse was recorded with a glucometer (Accu-chek active, Roche Diagnostics, Barcelona, Spain). The other blood parameters such as serum cholesterol, triglycerides, low-density lipoprotein (LDL) and Non-esterified fatty acids (NEFA) levels were quantified by using commercially available kits as discussed in chapter 3 in detail.

4.2.13. Glucose tolerance test (GTT) and insulin tolerance test (ITT)

Glucose and insulin tolerance test were performed according to the protocol mentioned in chapter 3.

4.2.14. Statistical analysis

All the experimental results were represented as the mean \pm standard deviation (SD) of three independent experiments. The comparison between groups was done by one-way/ two-way ANOVA followed by Turkey's post hoc test using Graph Pad Prism 6 software (Graph Pad Software, San Diego, CA, USA). The statistical significance of the experimental results was considered for a p -value < 0.05 .

4.3. Results

4.3.1 Anti-adipogenic activity of flavonoids on 3T3-L1 cells

In order to determine if the selected flavonoids pose any toxicity to 3T3-L1 cells, MTT assay was carried out. The 3T3-L1 cells were treated with (1, 10, 50 μ M concentrations of each flavonoid for 48 h. As shown in Fig. 4.1a, all tested flavonoids except quercetin were found to be non-cytotoxic till 50 μ M concentration. Henceforth, these three doses (1, 10, 50 μ M) were used for further experiments.

To determine the role of flavonoids in adipogenesis, cell differentiation assay was performed in 3T3-L1 cells in presence of selected flavonoids. As shown in Fig. 4.1b, the tested flavonoids were found to be effective in inhibiting the differentiation of pre-adipocytes to mature adipocytes as evidenced by a reduction in the level of Oil Red O staining in response to the test flavonoids albeit with varying efficiency by different flavonoids. Further, lipid quantification study exhibited that all tested flavonoids showed a significant dose-dependent decrease in lipid and triglyceride contents in differentiated 3T3-L1 cells, among them, kaempferol and rutin had the strong inhibitory effects on lipid and triglyceride deposition ($p < 0.05$) (Fig. 4.1c and d).

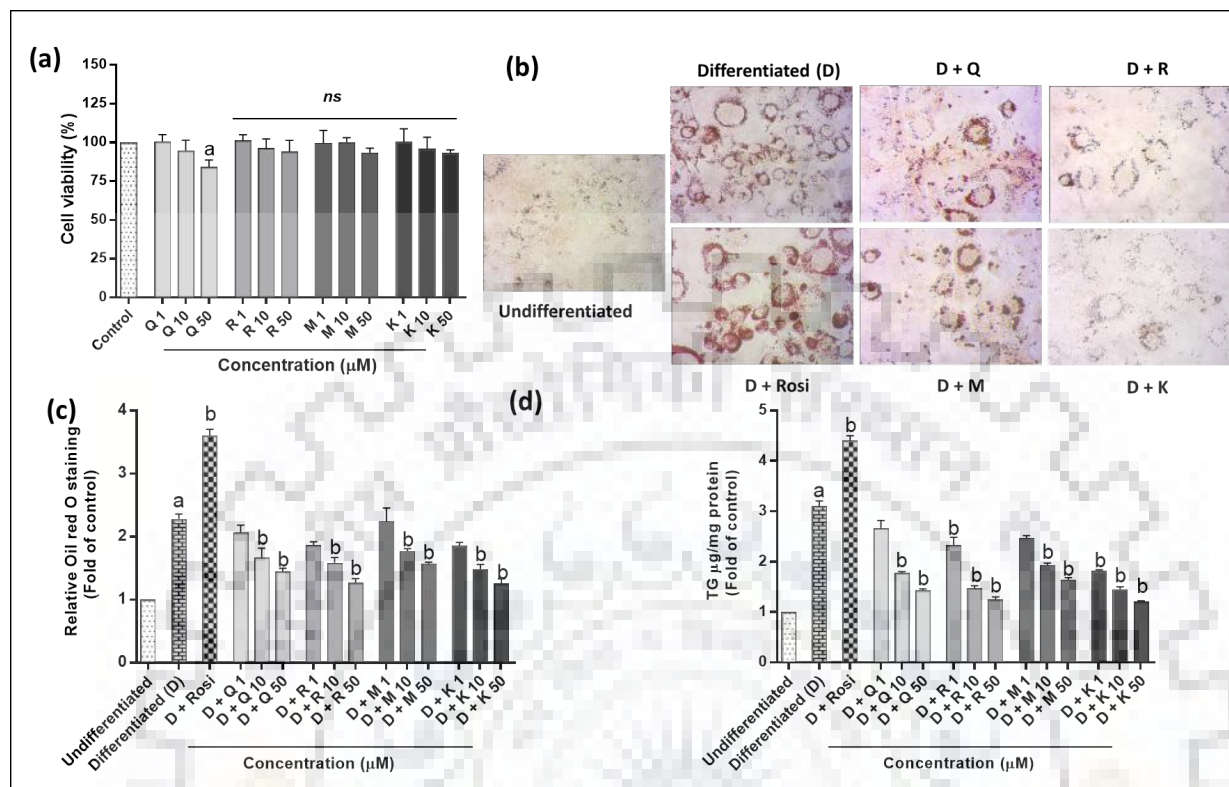


Fig. 4.1. Effects of flavonoids on cell viability and 3T3-L1 pre-adipocyte differentiation. The 3T3-L1 cells were differentiated according to the protocol described in the methods section and treated with varying concentrations of quercetin/ rutin/ myricetin or kaempferol throughout differentiation (Day 0-8) followed by (a) MTT assay after 48 h; (b) Representative images showing Oil Red O staining after 8 days of differentiation. Histogram representing (c) lipid content and (d) intracellular triglyceride content of treated cells. Results are mean \pm SD of three independent experiments. a, $p < 0.05$ versus undifferentiated control group; b, $p < 0.05$ versus differentiated control group. D, differentiated; Rosi, Rosiglitazone; Q, quercetin; R, rutin; M, myricetin; K, kaempferol; ns, non-significant.

4.3.2 Flavonoids alter genes involved in pre-adipocyte differentiation

In order to assess the role of test flavonoids on the anti-adipogenic activity at the genetic level, RT-PCR analysis of selected genes involved in adipocyte differentiation was performed. Adipocyte differentiation is regulated by a transcriptional cascade, the key regulator of which is peroxisome proliferator-activated receptor gamma (PPAR- γ), a member of the nuclear receptor family. PPAR- γ is highly expressed in adipose tissue and plays a major role in regulating genes involved in adipocyte differentiation, among them, *Cebpa* and *Fabp4* are the key factors involved in adipogenesis and serve as markers of adipocyte differentiation process (Guo et al., 2014). The results showed that exposure of 3T3-L1 pre-adipocytes to the flavonoids led to down-regulation of *Pparg*, *Cebpa* and *Fabp4* in a dose-dependent manner (Fig. 4.2a). As expected, rosiglitazone (the positive control of adipogenesis) showed marked up-regulation in adipocyte-specific genes. Among all tested flavonoids, kaempferol and rutin, at 10 μ M concentration, exhibited promising down-regulation of most of the adipocytes specific genes if not all ($p < 0.05$) (Fig 4.2a). Kaempferol inhibited the adipogenic genes by almost 50% at 10 μ M concentration ($p < 0.05$). This data corroborates well with the lipid and triglyceride quantification data. Likewise, immunoblot analysis showed down-regulation of PPAR- γ protein in response to all tested flavonoids, out of which, kaempferol showed maximum down-regulation (~2-fold) at 10 μ M concentration ($p < 0.05$) (Fig. 4.2b). Together, it could be speculated that all tested flavonoids were found to be anti-adipogenic in nature.

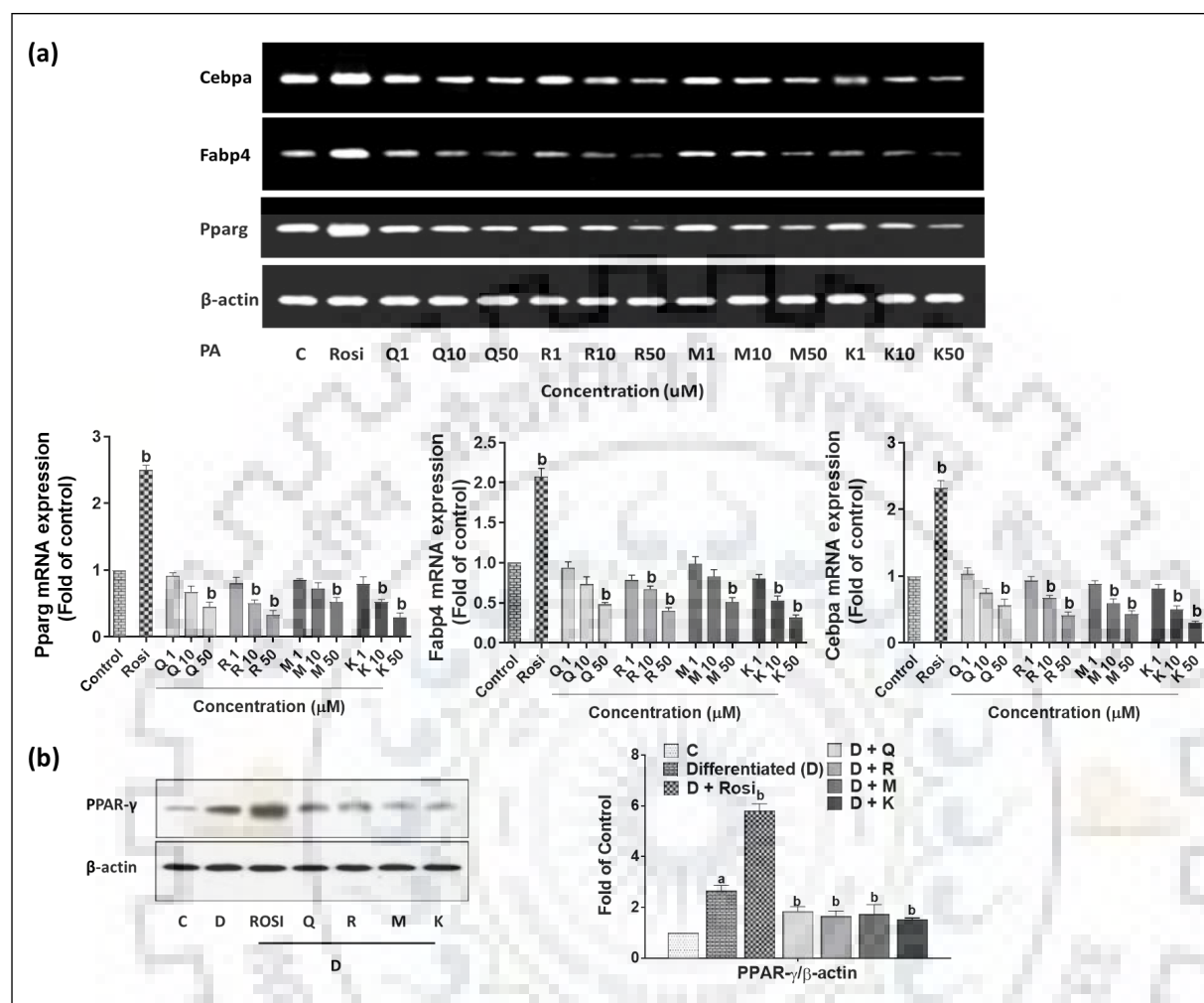


Fig. 4.2. Effects of flavonoids on adipocyte-specific genes in differentiated 3T3-L1 adipocytes. Representative (a) RT-PCR analysis of genes involved in adipogenesis; (b) Immunoblot of PPAR- γ protein in response to 10 μ M concentration of quercetin/ rutin/ myricetin or kaempferol. The histogram below (Fig. 4.2a)/ in the right panel (Fig. 4.2b) represents the mean relative arbitrary pixels intensities of mean \pm S.D. of three independent experiments expressed as fold change with respect to differentiated control group (Fig. 4.2a)/ undifferentiated control group (Fig. 4.2b). a, $p < 0.05$ versus undifferentiated control group; b, $p < 0.05$ versus differentiated control group. D, differentiated; Rosi, Rosiglitazone; Q, quercetin; R, rutin; M, myricetin; K, kaempferol.

4.3.3. Flavonoids instigate glucose uptake in PA-induced L6 muscle cells

In our subsequent study, we attempted to explore the antidiabetic activity of the selected flavonoids. As was discussed in the introduction section, muscle insulin resistance is one of the major pathophysiology involved in obesity-linked type 2 diabetes (DeFronzo and Tripathy, 2009). It has been well reported that PA treatment induces insulin resistance through impaired insulin signaling and thus diminished glucose uptake (Dimopoulos et al., 2006; Powell et al., 2004; Olsen and Hansen, 2002; Li et al., 2015; Wu et al., 2015). Thus, to mimic obesity-linked insulin resistance *in vitro*, differentiated L6 muscle cells were incubated with PA and the effects of flavonoids on glucose uptake were determined. In order to execute this study, firstly, various concentrations of each flavonoid were initially screened for their cytotoxic activity on L6 muscle cells in normal and PA-treated condition. As shown in Fig. 4.3a and b, all tested flavonoids were found to be non-cytotoxic to L6 cells till the maximum dose tested i.e., 50 μM both in presences and absence of PA ($p < 0.05$). Based on this data, three doses i.e., 1, 10, 50 μM were selected for further studies.

As expected, we found that PA treatment prominently decreased insulin-stimulated glucose uptake in L6 myotubes ($p < 0.05$) (Fig. 4.3c). However, flavonoids treatment significantly abrogated PA-inhibited glucose uptake in a dose-dependent manner ($p < 0.05$) (Fig. 4.3c). At 10 μM concentration, quercetin, rutin, myricetin and kaempferol exhibited around 1.35-, 1.28-, 1.24- and 1.38-fold increase in glucose uptake as compared to PA-induced L6 myotubes ($p < 0.05$) (Fig. 4.3c). Among all the test flavonoids quercetin and kaempferol showed the highest activity in instigating glucose uptake.

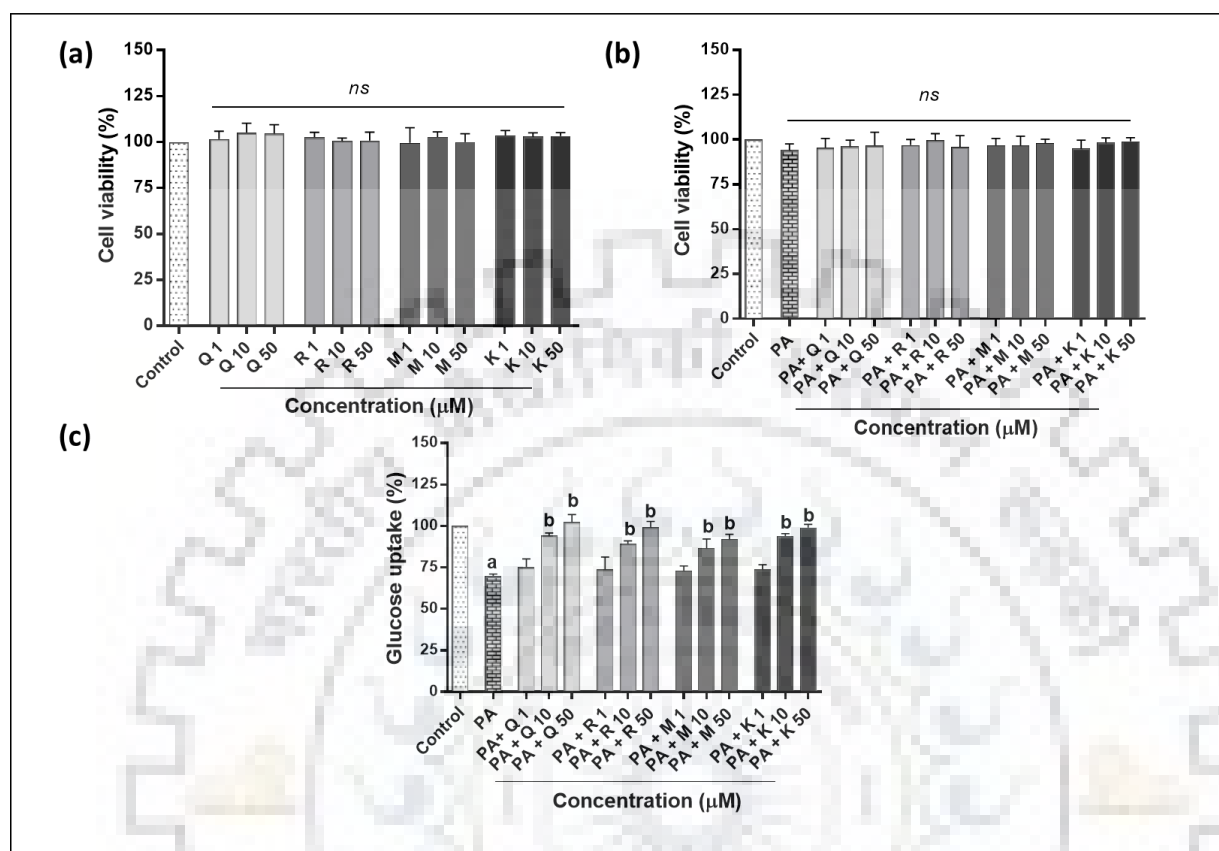


Fig. 4.3. Role of flavonoids on cell viability and insulin-stimulated glucose uptake in differentiated L6 muscle cells. L6 muscle cells were differentiated as per the protocol described in the methods section. The differentiated L6 cells were treated with various concentration (1, 10, 50 μ M) of quercetin/ rutin/ myricetin/ kaempferol for 24 h. Representative histogram showing MTT assay in (a) absence and (b) presence of PA (0.5 mM) along with respective flavonoids for 24 h; (c) Glucose uptake in insulin-stimulated differentiated L6 cells in presence of PA treatment. The differentiated L6 cells were treated with various concentration of quercetin/ rutin/ myricetin/ kaempferol along with 0.5 mM PA for 24 h. Cells were stimulated with 100 nM insulin just before 1 h of completion of the experiment. Results are mean \pm SD of three independent experiments expressed as a percentage of the vehicle-treated control group. a, $p < 0.05$ versus vehicle-treated control group; b, $p < 0.05$ versus only PA-treated group. Ns, non-significant; Q, quercetin; R, rutin; M, myricetin; K, kaempferol; PA, palmitic acid.

4.3.4. Flavonoids stimulate GLUT4 expression and related insulin signaling pathway in PA-induced L6 muscle cells

In our subsequent studies, gene and protein expression analysis of glucose transporter 4 (GLUT4) were performed. GLUT4 is a major glucose transporter present in muscle cells and involved in glucose uptake inside cells under the control of insulin. As shown in Fig. 4.4a, the tested flavonoids, except myricetin, significantly up-regulated *Glut4* gene expression in a dose-dependent manner ($p < 0.05$). Furthermore, to elucidate the specific mechanisms involved in flavonoids-mediated enhanced glucose uptake, we detected key proteins involved in the insulin signaling pathway. As described earlier, PA treatment impaired insulin signaling by phosphorylating IRS-1 at serine residue with a concomitant decrease in Akt phosphorylation which leads to inhibition of GLUT4 translocation and glucose uptake. In our study too, PA treatment significantly increased IRS-1 phosphorylation at ser307 in insulin-stimulated L6 myotubes which were interestingly found to be significantly abrogated in presence of each tested flavonoids at 10 μ M concentration ($p < 0.05$) (Fig. 4.4b). Additionally, GLUT4 protein expression (like mRNA expression as shown earlier) was found to be up-regulated in response to all tested flavonoids where kaempferol exhibited maximum activity at 10 μ M concentration (~2-fold increase) as compared to PA-treated L6 myotubes ($p < 0.05$) (Fig. 4.4b).

In order to determine whether the classical signaling pathway was involved in the flavonoids-mediated increase in glucose uptake, protein expression analysis of p-AKT was performed in presence of PA in insulin-stimulated myotubes. As shown in Fig. 4.4b, only myricetin and rutin exhibited a significant increase in Akt phosphorylation (ser473) at 10 μ M concentration as compared to PA-treated myotubes while kaempferol and quercetin exhibited only a marginal increase in p-Akt expression ($p < 0.05$). It is well established that the AMPK pathway is an alternative route which may be involved in glucose uptake inside muscle cells (Olsen and Hansen, 2002; Wu et al., 2015). Therefore, the p-AMPK (phosphorylation at Thr172) expression was analyzed in response to flavonoids. Kaempferol and quercetin, at 10 μ M concentration, significantly increased p-AMPK expression (~2-fold) as compared to PA-treated insulin-stimulated cells ($p < 0.05$) (Fig.4.4b). Myricetin and rutin showed a marginal increase in p-AMPK expression at 10 μ M concentration (Fig. 4.4b). Together, based on the current data it could be speculated that rutin and myricetin exhibited their increased insulin activity primarily through Akt

stimulation while AMPK signaling was involved in kaempferol and quercetin-mediated increase in glucose uptake in PA-stressed insulin resistant L6 myotubes. However, further detailed studies are needed using *in vitro* and *in vivo* setups to validate this finding.

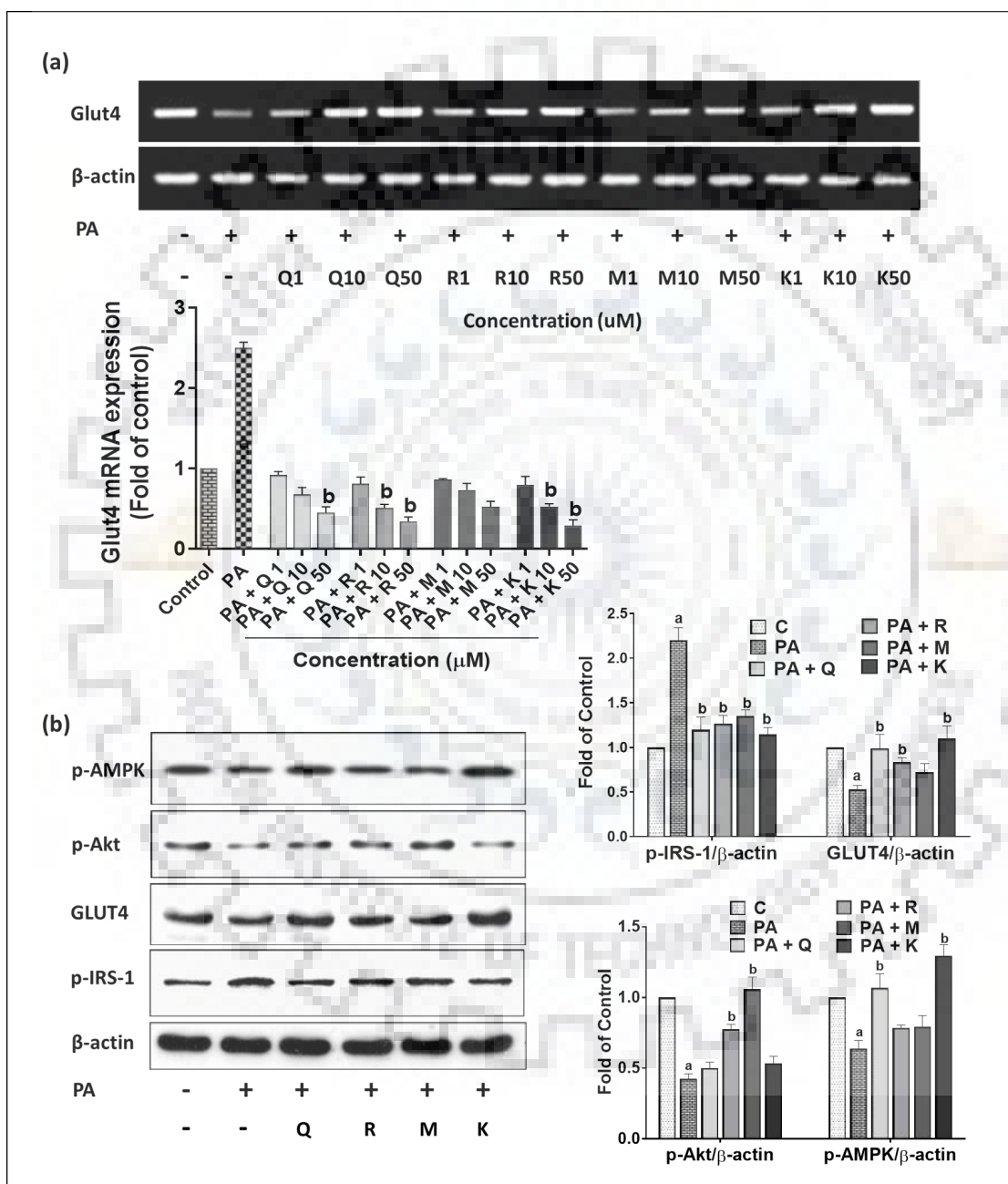


Fig. 4.4. Effects of flavonoids on insulin signaling pathway in PA-induced insulin resistant L6 myotubes. The differentiated L6 cells were treated with various concentrations of quercetin/

rutin/ myricetin/ kaempferol along with 0.5 mM PA for 24 h. The cells were stimulated with 100 nM insulin just before 1 h of completion of the experiment. Representative (a) RT-PCR analysis of *Glut4* gene; (b) Immunoblots of proteins involved in insulin signaling pathway and glucose uptake. The histogram below (Fig. 4.4a)/ in the right panel (Fig. 4.4b) represents the mean relative arbitrary pixels intensities of mean \pm S.D. of three independent experiments expressed as fold change with respect to vehicle-treated control group. a, $p < 0.05$ versus vehicle-treated control group; b, $p < 0.05$ versus only PA-treated group. Ns, non-significant; Q, quercetin; R, rutin; M, myricetin; K, kaempferol; PA, palmitic acid.

4.3.5. Flavonoids improve body weight and lipid profile in HFD-STZ-induced diabetic mice

To investigate the anti-hyperlipidemic and anti-hyperglycemic role of flavonoids, HFD-STZ induced mice were developed and were subjected to 4 weeks of daily treatment of each flavonoid (25 mg/kg bw) in respective groups. As shown in Fig. 4.5a, the HFD-STZ-induced diabetic mice displayed a significant increase in body weight as compared to normal control group ($p < 0.05$). However, among all the test flavonoids, kaempferol-treated diabetic mice showed significantly decreased body weight which was comparable to that of the normal control group ($p < 0.05$) (Fig. 4.5a). Conversely, quercetin, rutin, myricetin and metformin (the positive control drug for diabetes) treated mice demonstrated marginally reduced body weight as compared to HFD-STZ group ($p < 0.05$) (Fig. 4.5a). Furthermore, flavonoids-treated mice showed a significant decrease in serum triglycerides, cholesterol, LDL and NEFA levels as compared to diabetic mice with varying potentiality ($p < 0.05$) (Fig. 4.5b, c, d and e). Out of all, kaempferol exhibited most prominent effects in improving body weight and lipid profiles (almost close to 2-fold reduction) in HFD-STZ diabetic mice ($p < 0.05$).

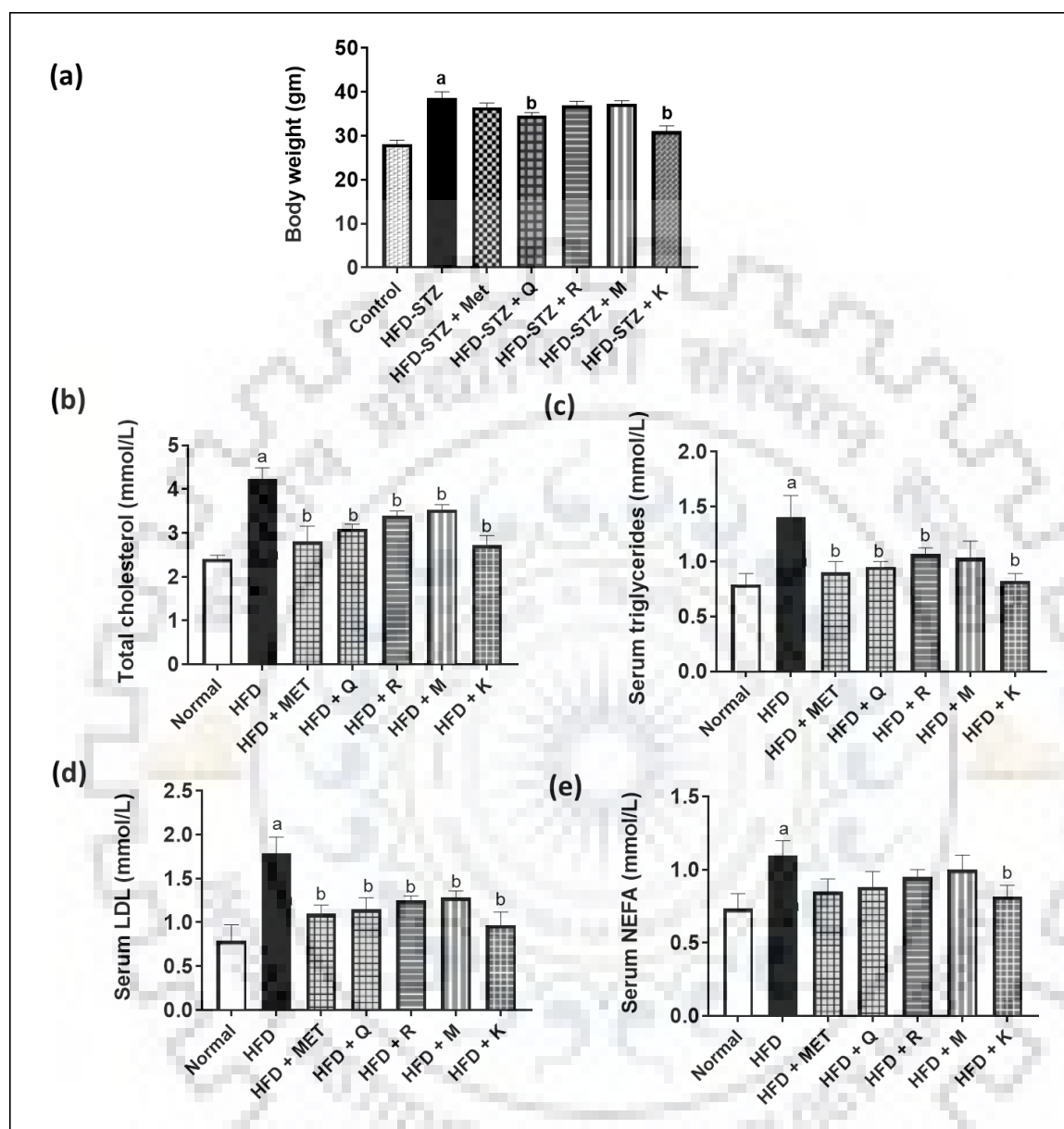


Fig. 4.5. Effects of flavonoids on metabolic profile in diabetic mice. The experimental mice were fed with normal chow diet (control) or with high-fat diet for 10 weeks followed by injection with streptozotocin (35 mg/kg bw) and successive treatments with quercetin/ rutin/ myricetin/ kaempferol (25 mg/kg bw i.p. daily) for 4 weeks. Histogram showing (a) Body weight; (b) Total cholesterol; (c) Triglycerides; (d) LDL and (e) NEFA level in serum of treated mice. Blood glucose concentrations measured (f) during fasting condition; after administration of (g) glucose for glucose tolerance test (GTT) and (h) insulin for insulin tolerance test (ITT) after 16 weeks of the experiment. Data are mean \pm SD of $n = 6$ for each group. a, $p < 0.05$ versus normal control; b,

$p < 0.05$ versus HFD-STZ control. HFD, high-fat diet; STZ, streptozotocin; Met, metformin; Q, quercetin; R, rutin; M, myricetin; K, Kaempferol; LDL, Low-density lipoprotein; NEFA, Non-esterified fatty acids.

4.3.6. Flavonoids improve fasting blood glucose level, glucose tolerance and insulin sensitivity in HFD-STZ-induced diabetic mice

After 16 weeks of the experiment, HFD-STZ control mice had a high baseline fasting blood glucose level of $\sim 272 \pm 17$ mg/dl as compared to normal control group ($\sim 107 \pm 12$ mg/dl) ($p < 0.05$) (Fig. 4.6a). However, this level was reduced down significantly when the mice were treated with quercetin/ rutin/ myricetin/ kaempferol at 25 mg/kg bw respectively albeit with a varying degree of effectiveness ($p < 0.05$) (Fig. 4.6a). As expected, metformin also showed a significant decrease in fasting blood glucose level with respect to HFD mice ($p < 0.05$) (Fig. 4.6a).

Since type T2DM is characterized by impaired glucose intolerance and insulin resistance, the glucose and insulin tolerance test were performed at end of the experiment by injecting glucose and insulin intraperitoneally respectively to evaluate the beneficial metabolic effects of selected flavonoids. As shown in Fig. 4.6b, HFD mice displayed hyperglycemia at 0 min which was exacerbated by glucose load. The augmented glucose level of HFD mice did not decrease significantly even at 120 min, indicating impaired glucose tolerance. However, administration of flavonoids to diabetic mice resulted in significant improvement in glucose tolerance within 60 min of glucose load ($p < 0.05$) (Fig. 4.6a). Further, to check the effect of flavonoids on insulin sensitivity, insulin tolerance test was performed by injecting insulin intraperitoneally. As shown in Fig. 4.6c, all tested flavonoids significantly enhanced insulin sensitivity in diabetic mice as indicated by a decline in glucose level with increasing time ($p < 0.05$). Interestingly, among all tested flavonoids, kaempferol had the most promising effects on improving blood glucose level, glucose tolerance and insulin sensitivity ($p < 0.05$) (Fig. 4.6a, b and c).

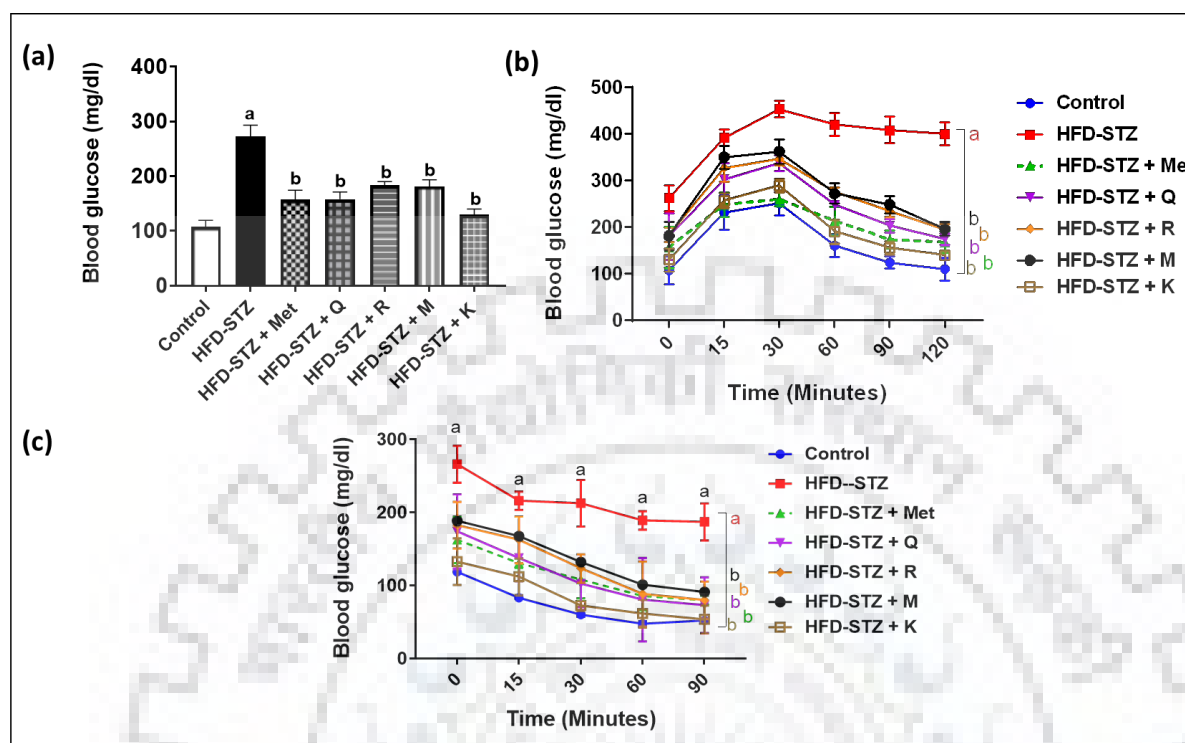


Fig. 4.6. Effects of flavonoids in the improvement of glucose and insulin tolerance in diabetic mice. Mice were fed with normal chow diet (control) or with high-fat diet for 10 weeks followed by injection with streptozotocin (35 mg/kg BW) and successive treatments with quercetin/ rutin/ myricetin/ kaempferol (25 mg/kg bw i.p. daily) for 4 weeks. (a) Histogram showing fasting glucose levels of mice from different treatment groups. Blood glucose concentrations measured after administration of (b) glucose for glucose tolerance test and (c) insulin for insulin tolerance test after 16 weeks of the experiment. Data are mean \pm SD of $n = 6$ for each group. a, $p < 0.05$ versus normal control; b, $p < 0.05$ versus HFD-STZ control. HFD, high-fat diet; STZ, streptozotocin; Met, metformin; Q, quercetin; R, rutin; M, myricetin; K, Kaempferol.

4.3.7. Effects of flavonoids in autophagy induction in RIN-5F clonal pancreatic β -cells

Recent studies showed that dysfunctional autophagy is involved in the loss of β -cell mass and function hence pathophysiology of obesity-linked diabetes (Masini et al., 2009; Bartolomé et al., 2014; Mir et al., 2015). Thus, identifying agents that could restore autophagy in degenerated β -cells are of great importance under the current therapeutic regime. In the next phase of our study, we intended to determine whether these flavonoids could enhance autophagy in PA-stressed RIN-5F clonal pancreatic β -cells. In order to determine the effects of flavonoids on clonal pancreatic β -cells, firstly, various concentrations of each flavonoid were initially screened for their cytotoxic activity on RIN-5F cells in PA-treated condition. All tested doses i.e., 1, 10, 50 μ M of each flavonoid were found to be non-cytotoxic to the cells, rather, kaempferol at 10 and 50 μ M exhibited increased cell viability ($p < 0.05$) (Fig. 4.7a). Hence, to determine regulation of autophagy, 10 μ M concentrations of each flavonoid were selected and MDC-LysoTracker co-staining was performed. MDC selectively stains autophagosomes whereas LysoTracker stains lysosomes and both collectively determine the status of autophagy in cells. The mTOR inhibitor, temsirolimus, was considered as a positive control of autophagy in these set of experiment. As shown in Fig. 4.7b, PA treatment exhibited a marginal increase in MDC stained regions while limited lysoTracker stained regions indicative of impaired autophagy. Surprisingly, all tested flavonoids exhibited an increase in a combined MDC-LysoTracker staining, out of which, kaempferol was found to be most promising autophagy activator as evidenced by increased autophagosomes as well as lysosomes formation (Fig. 4.7b). Based on this data it could be hypothesized that kaempferol-mediated promising antidiabetic effects may be attributed to autophagy stimulatory activity of this phytochemical. Hence this aspect needs further detailed deliberation as was taken up in the remaining part of the thesis.

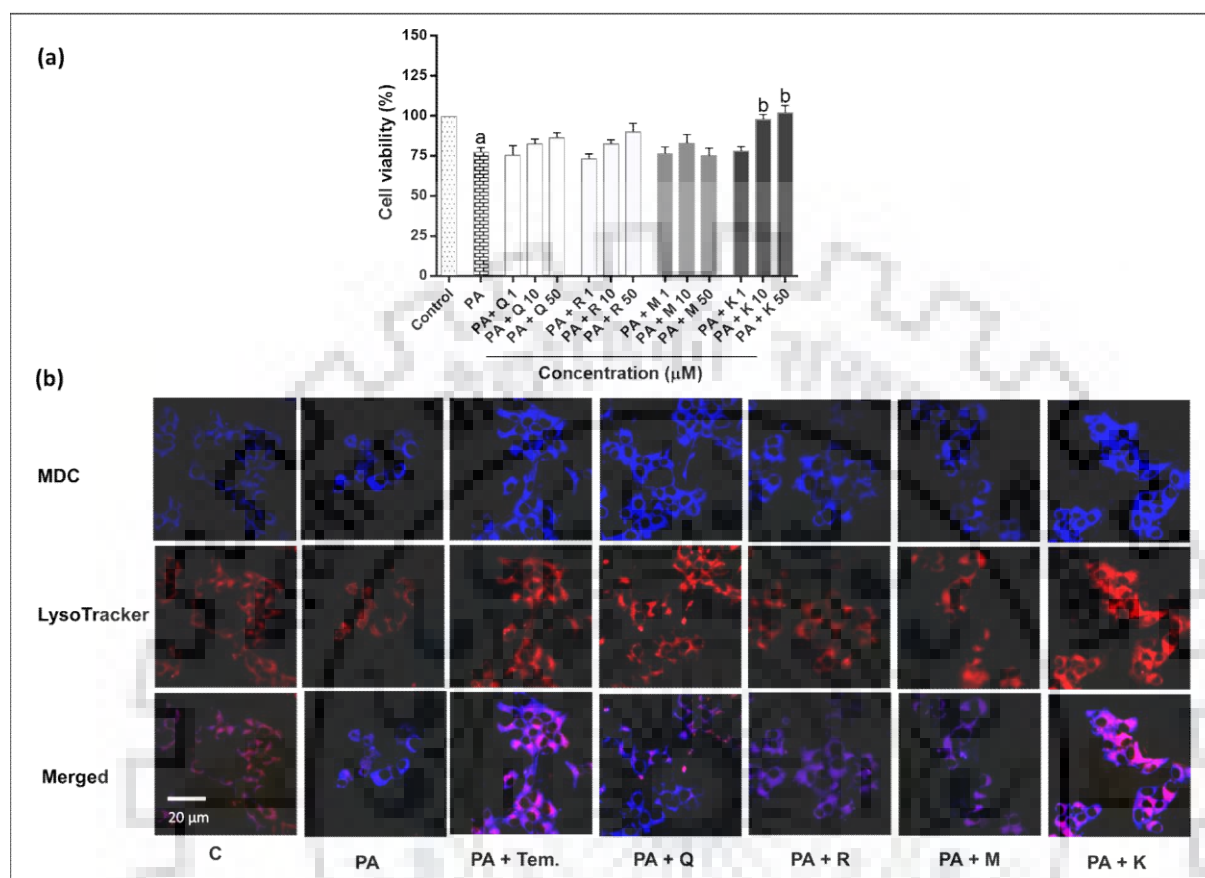


Fig. 4.7. Role of flavonoids in instigating autophagy in PA-induced RIN-5F clonal β -cells. RIN-5F cells were treated with various concentrations of quercetin/ rutin/ myricetin/ kaempferol with 0.5 mM PA for 24 h followed by (a) MTT assay, Results are the mean \pm S.D. of three independent experiments. a, $p < 0.05$ versus vehicle-treated control group; b, $p < 0.05$ versus only PA-treated group. (b) Representative confocal images of MDC-LysoTracker stained cells to selectively stain autophagosomes and lysosomes in response to 10 μ M concentration of quercetin/ rutin/ myricetin/ kaempferol or 200 nM temsirolimus (positive control) in presence of 0.5 mM PA for 24 h. Images are representative of three independent experiments. Ns, non-significant; Q, quercetin; R, rutin; M, myricetin; K, kaempferol; PA, palmitic acid; Tem., temsirolimus.

4.4. Discussion

The prevalence of T2DM is increasing worldwide, the incidence of which correlates in most of the cases with development of obesity (Al-Goblan et al., 2014). Obesity is an ailment in which adipocytes become large by accumulating an enormous amount of lipids. At the cellular level, it is characterized by a surge in number and size of differentiated adipocytes in adipose tissue (Schwartz et al., 2017). In obese condition, the elevated level of circulating FFA is one of the predisposing factors in the development of insulin resistance and hyperglycemic conditions linked with diabetes (Giacca et al., 2010). In this study, we attempted to screen some flavonoids namely: quercetin, rutin, myricetin and kaempferol, which are abundant in various dietary sources, for their anti-obesity and antidiabetic activities. Firstly, we elucidated the role of flavonoids in the inhibition of adipocyte differentiation. To determine the anti-adipogenic activity, the mouse pre-adipocytes 3T3-L1 cells were used as it has been widely used as a cellular model of adipose biology. Our study revealed that all the tested flavonoids were found to be effective in inhibiting the differentiation of pre-adipocytes 3T3-L1 cells to mature adipocytes which were confirmed by Oil Red O staining and lipid quantification assays. The marked decrease in the lipid accumulation was further confirmed by down-regulation of genes involved in adipocyte differentiation (*Pparg*, *Cebpa* and *Fabp4*) as evidenced by transcriptional analysis by RT-PCR. Further, the immunoblot analysis of PPAR- γ expression strengthened the findings. These findings are consistent with the reports which showed that quercetin, rutin, myricetin and kaempferol exhibited anti-hyperlipidemic effects, however, the precise mode of action is still elusive (Roslan et al., 2017; Calzada et al., 2017; Kang et al., 2015; Zhang and Liu, 2011). Besides, to the best of our knowledge, this is the first report which showed the comparative analysis of anti-obesity and anti-diabetic effects of these major dietary flavonoids that are abundant in various plants mainly fruits and vegetables and principally involved in the prevention of a large number of diseases/disorders. This *in vitro* data revealed that among all tested flavonoids, kaempferol and rutin had the strongest inhibitory effects on adipogenesis.

In the next phase of our study, antidiabetic effects of flavonoids were determined by using L6 muscle cells. Insulin resistance in skeletal muscles plays a major role in hyperglycemic conditions associated with type 2 diabetes (DeFronzo and Tripathy, 2009). It is already reported that excess FFAs leads to insulin resistance in muscle cells by impairing insulin signaling

(Kraegen and Cooney, 2008; Martins et al., 2012). In order to mimic obesity-linked insulin resistance *in vitro*, differentiated L6 muscle cells were incubated with PA, a cell-based model that has been widely used to determine the antidiabetic role of compounds (Dimopoulos et al., 2006; Wu et al., 2015; Sinha et al., 2004). The stimulatory effects of flavonoids on glucose uptake along with the determination of expression patterns of GLUT4, a marker for glucose uptake, in insulin-stimulated PA-treated L6 cells were demonstrated. All tested flavonoids were found to be effective in significantly up-regulating insulin-stimulated glucose uptake which was found to be abrogated in PA conditions. PA-treatment also showed impaired insulin signaling as evidenced by increased phosphorylation of ser307 in IRS-1 and decreased p-Akt which was further linked to decreased GLUT4 expression which were significantly improved by the test flavonoids. Our data is in line with the studies which showed that PA treatment impaired insulin-stimulated glucose uptake (Dimopoulos et al., 2006; Powell et al., 2004; Olsen and Hansen, 2002; Li et al., 2015; Wu et al., 2015). However, the PA-mediated impaired glucose uptake was restored by all tested flavonoids, out of which, kaempferol and quercetin showed profound activity. Further, the specific mechanisms involved in glucose uptake stimulatory activity of flavonoids were elucidated. Our study revealed that myricetin and rutin treatment exhibited increased expression of p-Akt and thus restore the classical signaling pathway. Our this observation is in line with the study which showed restoring p-AKT in PA-induced insulin resistant muscle cells led to improved insulin signaling (Li et al., 2015). Conversely, there was no significant difference in p-Akt expression in response to kaempferol and quercetin, although there was an increase in GLUT4 expression which suggested that probably kaempferol and quercetin exerted their effects through a different pathway, which needs further validation. In recent years, studies have shown that AMPK pathway is an alternative pathway of glucose uptake activated in muscle cells (Olsen and Hansen, 2002; Kundu et al., 2014; Wu et al., 2015). In our studies, we found that kaempferol and quercetin showed a significant increase in the expression of AMPK phosphorylation (Thr172) indicative of the role of AMPK in inducing glucose uptake. These are consistent with the report showing that the commonly used antidiabetic drug, metformin, exerted their stimulatory effect on glucose uptake through AMPK activation (Wu et al., 2015). Taken together, it can be speculated that kaempferol and quercetin are the most potent anti-hyperglycemic agents out of all tested flavonoids to be taken up further as therapeutic agents.

In the next phase, in order to validate the earlier obtained *in vitro* data in more physiologically relevant *in vivo* model, HFD-STZ-induced diabetic model was developed. This model has been extensively used in various studies to test anti-obesity and antidiabetic effects of various compounds (Skovsø, 2014). The type 2 diabetes in the induced HFD-STZ mice was characterized by hyperglycemia, glucose intolerance, insulin resistance and decreased insulin secretion. To test anti-obesity and antidiabetic effects of these flavonoids, the developed diabetic mice were treated with these phytochemicals. Our *in vivo* data revealed that all of the flavonoids showed a marked reduction in serum triglyceride, cholesterol and LDL levels of HFD-STZ-induced diabetic mice, however, only kaempferol was found to significantly improve serum profile at the dose tested. Furthermore, all tested flavonoids significantly improved blood glucose level, glucose and insulin tolerance in diabetic mice. Interestingly, among all tested flavonoids, kaempferol had the most promising effects on blood glucose level, glucose tolerance and insulin sensitivity. Collectively, *in vitro* and *in vivo* data demonstrated that out of all tested flavonoids, kaempferol exhibited most promising anti-obesity and antidiabetic effects.

Recent studies showed that dysfunctional autophagy is involved in the loss of β -cell mass and function hence pathophysiology of obesity-linked diabetes (Mir et al., 2015; Masini et al., 2009; Bartolome et al., 2014). Thus, identifying agents that could restore autophagy in degenerated β -cells are of great importance presently. Our MDC-LysoTracker data revealed that PA treatment exhibited a marginal increase in MDC stained regions and limited lysoTracker stained regions indicative of impaired autophagy and this is consistent with a recent study which showed that PA impairs autophagy in pancreatic β -cells (Mir et al., 2015). Surprisingly, all tested flavonoids exhibited an increase in MDC-LysoTracker staining, out of which, kaempferol was found to be most promising autophagy activator as evidenced by maximally increased autophagosomes and lysosomes formation with increased co-localization of both as compared other three tested flavonoids (quercetin, rutin and myricetin). This data is in line with the study which showed that kaempferol treatment increased autophagy and protected neurons in animal models of rotenone-mediated acute toxicity (Filomeni et al., 2012). Therefore, it can be hypothesized that the superior antidiabetic activity of kaempferol may also be due to the restoration of kaempferol-mediated autophagy which in turn may improve the diabetic condition *in vitro* and *in vivo*. The present study thus suggested that among above-selected flavonoids kaempferol had potent anti-obesity, antidiabetic, and autophagy stimulating activities as obtained

from initial screening tests. Therefore, kaempferol was chosen for further detailed and mechanistic studies for next phase of our study to confirm the role of kaempferol-mediated autophagy in the protection of functional β -cell mass and improvement of insulin sensitivity as it is well established that β -cell mass and insulin resistance are the two pathophysiological abnormalities associated with obesity-linked diabetes (Al-Goblan et al., 2014). All these aspects have been discussed in the successive chapters of this thesis to establish the exact cross-talk between kaempferol and autophagic processes. About the involvement of other flavonoids (quercetin, rutin and myricetin) for the cure and management of diabetes and obesity further in detailed studies are warranted where these data would provide a base to take them forward.





CHAPTER 5

UNDERSTANDING THE AUTOPHAGY STIMULATORY AND ANTI-APOPTOTIC EFFECTS OF KAEMPFEROL IN PANCREATIC β -CELLS



CHAPTER 5.1

***ESTABLISHMENT OF RIN-5F EGFP-LC3
EXPRESSING STABLE CELL LINE***

5.1. Establishment of RIN-5F-EGFP-LC3 expressing stable cell line

5.1.1. Introduction

Electron microscopic assessment of autophagic vacuoles is an expensive, tedious and time-consuming process that requires tremendous specialized expertise. Currently, it is being replaced by light microscopic observation and biochemical methods that are more convenient and easily accessible to the researchers (Klionsky et al., 2016; Mizushima et al., 2010). The mammalian autophagy protein, LC3, is a marker of autophagosomes. The LC3 protein is found in two forms i.e. cytosolic LC3-I form and autophagosome membrane localized LC3-II form. After its synthesis, the nascent LC3 is processed at its C-terminus by Atg4, a protease involved in autophagic process, and becomes LC3-I. Further, LC3-I is conjugated to phosphatidylethanolamine, an event also called as lipidation of LC3-I to become LC3-II (LC3-PE) by a ubiquitination-like enzymatic reaction. Lipidated LC3 is subsequently recruited to autophagosomal membranes during the ensuing events of autophagy and leads to the formation of LC3 puncta which serves as a reliable marker to monitor autophagosomes formation (Klionsky et al., 2012). LC3-II is localized both on the outer and inner membranes of the autophagosome (Fig. 5.1.1). The event of lysosomal fusion results in the cleavage of LC3 on the outer membrane by Atg4 whereas lysosomal enzymes degrade LC3 on the inner membrane resulting in very low LC3 content in the autolysosome. Therefore, endogenous LC3 or GFP-LC3/EGFP-LC3 (LC3 protein tagged with a fluorescent protein EGFP at its N terminus) is visualized through indirect immunofluorescence or direct fluorescence microscopy either as a diffuse cytoplasmic pool or as punctate structures representing autophagosomes (Larsen et al., 2010). However, the endogenous protein expression depends on the ability to detect it in the system of interest. When the endogenous amount is below the level of detection, the exogenous constructs are used. Additionally, EGFP-LC3, and probably even endogenous LC3, if overexpressed or co-expressed with other aggregate-prone proteins, can be easily aggregated and is often indistinguishable from true autophagosomes by fluorescence microscopy observation. Additionally, in the case of transient transfection using EGFP-LC3 construct, often high levels of expression results in artificial aggregation for which a great caution needs to be exercised while using the system.

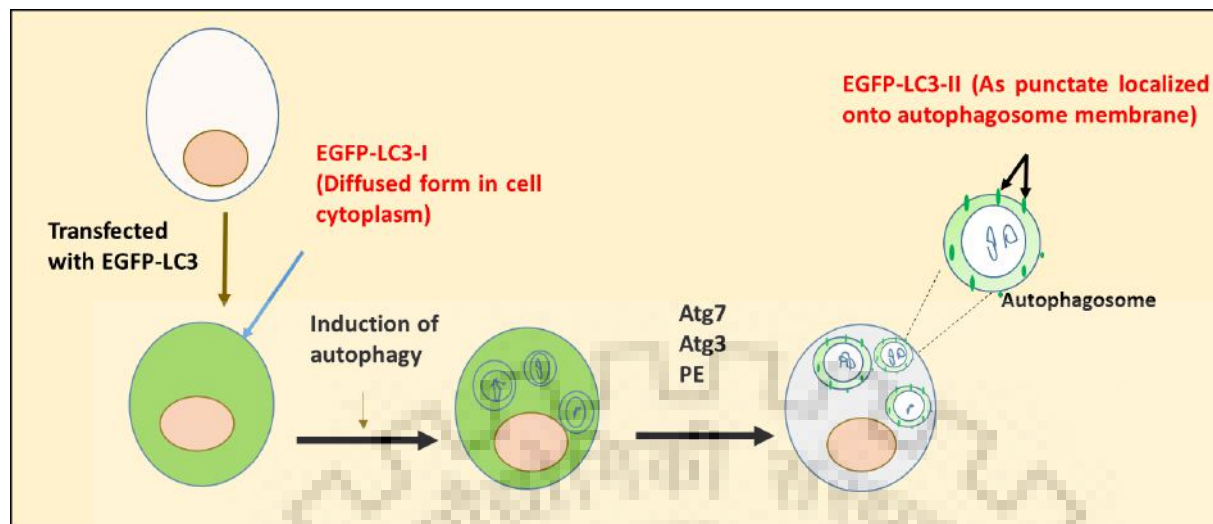


Fig. 5.1.1. Schematic representation showing EGFP-LC3 puncta formation in response to autophagy induction in EGFP-LC3 transfected cells. The cells are transfected with EGFP-LC3 plasmid and stable cell line expressing EGFP-LC3 is developed. EGFP-LC3 positive cells exhibit diffused EGFP fluorescence which after induction of autophagy shows puncta formation due to the localization of LC3-II onto autophagosomes membrane. These punctas can be used as a reliable marker for autophagy induction.

Thus to exclude the possibility of artificial aggregation, use of stable EGFP-LC3 transformants is widely recommended where clones expressing appropriate levels of EGFP-LC3 can be selected. The homogeneous protein expression in the stably-transfected cell lines along with decreased variability of signal intensity and size within a cell population is an additional advantage. Due to the lower protein expression, the stable transformants often have reduced background. It is also advantageous over transient transfection as it eliminates artifacts resulting from recent exposure to transfection reagents. Also, with stable transfection, nearly 95-100% of the population will express tagged LC3, thus, more transformed cells can be evidently analyzed.

The current study thus deals with the establishment of a stable cell line expressing EGFP-LC3 that was used further to access the process of autophagy in the concurrent study.

5.1.2. Methodology

5.1.2.1. Cell line and culture

RIN-5F cells were cultured in RPMI media with 10% fetal bovine serum and 1% antibiotic (100 U/ml of penicillin and 100µg/ml streptomycin) mix at 37°C in a humidified atmosphere in a 5% CO₂ incubator.

5.1.2.2. Bacterial transformation and plasmid preparation

The DH5α strain of E.coli was grown and transformed with EGFP-LC3 plasmid. The detail culture conditions and transformation protocols have been described in Chapter-3 (3.26).

5.1.2.3. Plasmid isolation

The transformed bacteria were subjected to isolation of transformed plasmid (in this case EGFP-LC3). The plasmid for EGFP-LC3 (Addgene plasmid # 11546) was acquired from Addgene Plasmid Repository (Cambridge, MA, USA) which was donated to the repository by Dr. Karla Kirkegaard (Stanford University, USA). The detail procedure has been described in Chapter-3 (section 3.27).

5.1.2.4. Cell transfection and stable cell line establishment

To generate stable EGFP-LC3 expressing cell line, ~ 5X 10⁵ RIN-5F cells were seeded in 60 mm cell culture dish in RPMI media containing 10% FBS. After reaching 70-80% confluency, cells were transfected with 2 µg EGFP-LC3 plasmid using Polyfect transfection reagent (Qiagen, USA) according to the manufacturer's instructions. The transfected cells were screened with 500 µg/ml G418 (Sigma) for around 15 days. When a number of resistant cell clones was observed, the cells were further trypsinized and transferred to new culture flasks for further culture. Subsequently, the subcultured cells were maintained in RPMI media supplemented with 500 µg/ml G418 for next 15 days. Only the fluorescent cells were picked and maintained as stable cell line for EGFP-LC3 and were named as RIN-5F-EGFP-LC3 cells.

5.1.3. Results

We have successfully developed RIN-5F-EGFP-LC3 cell line for detection of LC3 puncta in response to kaempferol with or without inhibitors. After 48 h of transfection, around 60-70% cells were found positive for EGFP-LC3 expression as observed under a fluorescent microscope (Fig. 5.1.2). Further, stably expressing EGFP-LC3 cells were screened in RPMI media supplemented with G418 (500 µg/ml) for the next 15 days and routinely evaluated for the screening of GFP-LC3 clones. The EGFP-LC3 clones were then subcultured and maintained in media containing G418. After 15 days of screening, it was observed that the percentage of EGFP-LC3 positive cells were increased to about 80-85% (Fig. 5.1.2). Interestingly, around 90-95 % of GFP-positive cells were obtained after 30 days which were further subcultured and maintained for longer periods (Fig. 5.1.3). As shown in the data (Fig. 5.1.3), the cells were stably expressing LC3 till passage 10 without any compromise in fluorescent patterns. This level of fluorescent intensity was available till 30 passages (data not shown).

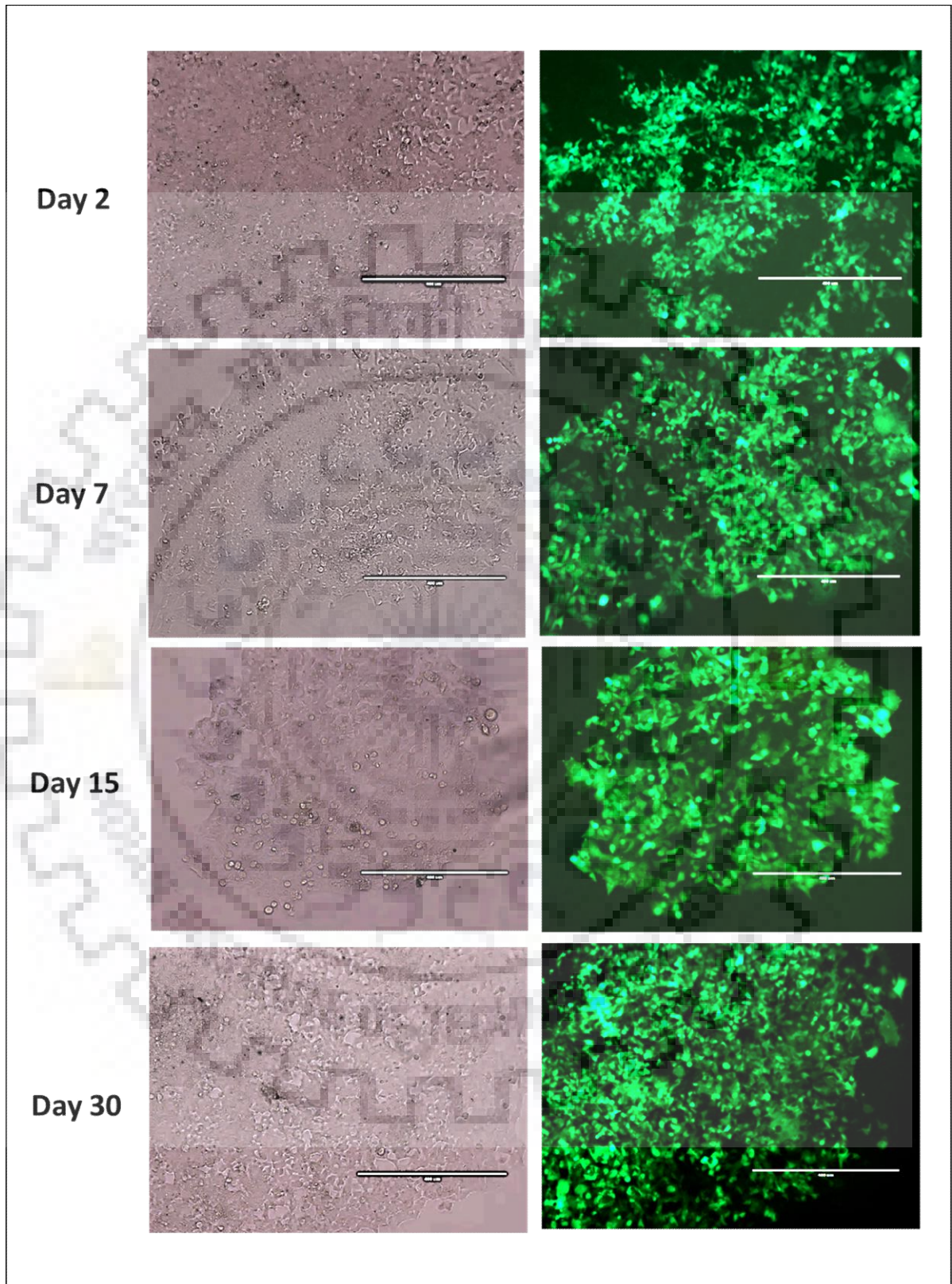


Fig. 5.1.2. Phase contrast and fluorescent microscopic images of EGFP-LC3 transfected RIN-5F cells at different time intervals. Scale bar 400 μ m.

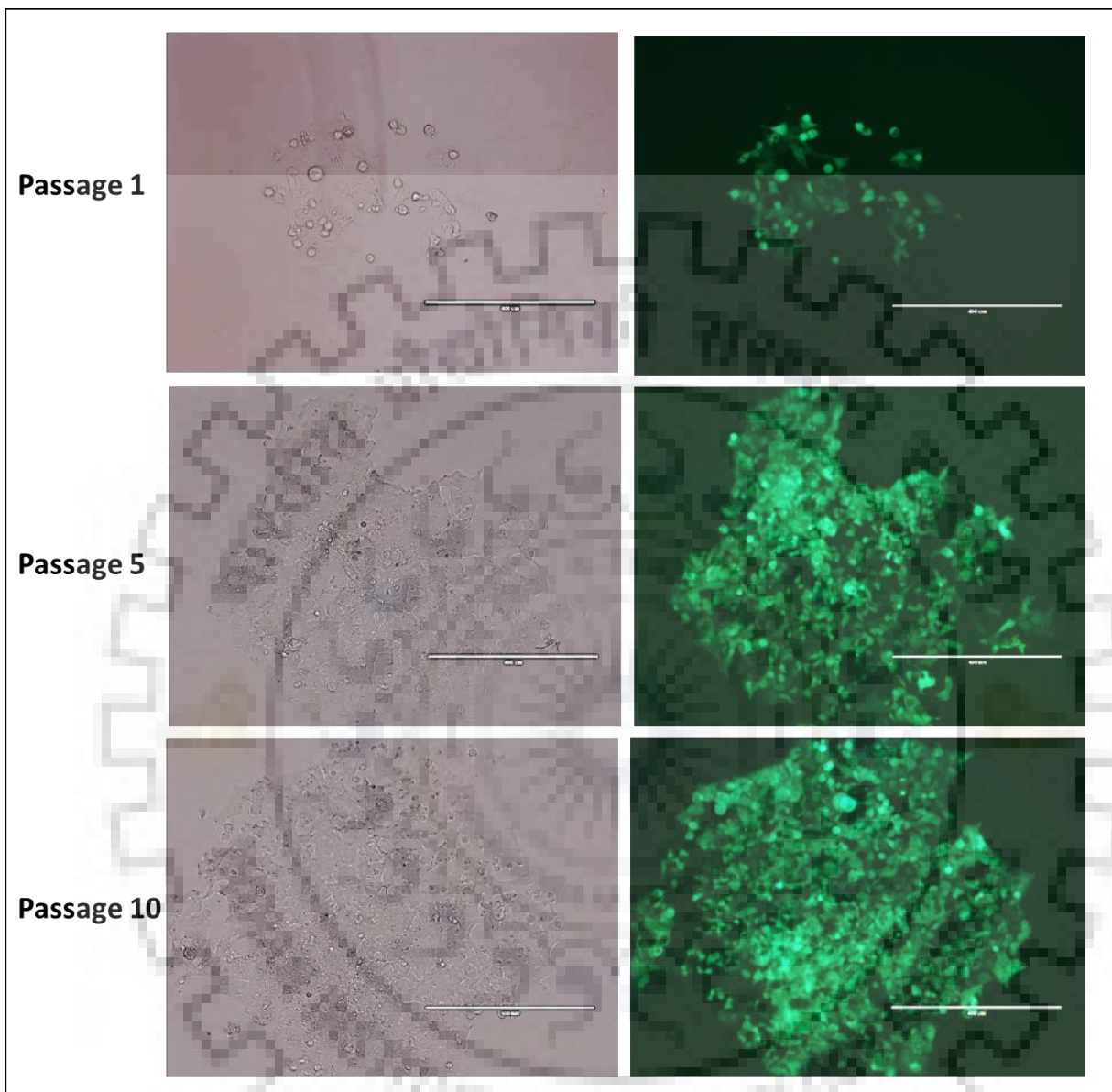


Fig. 5.1.3. Phase contrast and fluorescent microscopic images of RIN-5F-EGFP-LC3 cells stably expressing EGFP-LC3 at different passage numbers in culture. Scale bar 400 µm.

5.1.4. Discussion

The role of autophagy was recently identified as a key regulatory mechanism involved in several disorders including cancer, inflammation, neurodegeneration and obesity-linked type 2 diabetes (Jiang and Mizushima, 2014). Autophagy is an intracellular lysosomal degradative process of defective proteins, macromolecules, damaged organelles and toxic aggregates,

which plays a pivotal role in maintaining cell homeostasis (Mizushima, 2007). Autophagy is a dynamic cellular process; hence, accurate detection methods are essentially required to monitor the process of autophagy (Orhon and Reggiori, 2017). In recent years, LC3 protein has been identified to play a major role in autophagy. There are various methods by which LC3 expression can be monitored such as immunocytochemistry, immunoblotting, LC3 puncta formation assay to name a few (Mizushima et al., 2010). EGFP-LC3 puncta formation method is the reliable and convenient method to monitor autophagic process (Larsen et al., 2010).

Transiently transfected cells pose various limitations such as artificial aggregates which are often indistinguishable by fluorescence microscopy from true autophagosomes, also, may result in artifacts from recent exposure to transfection reagents. This may lead to overestimation of the autophagic process. Therefore, generation of a stable cell line with EGFP-LC3 provides a better option than other methods to have a more accurate estimation of autophagosome formation. With this aim, in this study, we have established the RIN-5F cell lines stably expressing EGFP-LC3. The screened cell lines positively expressed the EGFP-LC3 protein for an extended period of time. These stable cell lines were used in our further study to monitor kaempferol-mediated induction of autophagy.

EGFP-LC3 provides a marker that is relatively easy to use for monitoring autophagy induction based on the appearance of puncta; however, monitoring this chimera does not determine flux unless utilized in conjunction with inhibitors of lysosomal fusion and/or degradation. Thus it is recommended that lysosomal inhibitors such as chloroquine or bafilomycin can be used to inhibit autophagosomal degradation of LC3 for detecting autophagic flux (Mizushima et al., 2010). Moreover, flow cytometry analysis can be used to quantify LC3-puncta in response to various treatments/conditions. In addition, it is recommended that results obtained by EGFP-LC3 fluorescence microscopy be verified by additional assays such as western blot analysis of LC3-II/LC3-I and p62 expression to determine the exact status of autophagy in the cell in study. The stable cell line as developed in this part of the study can be used for screening various chemical entities for their role in autophagy by estimating the levels of LC3-puncta formation.





CHAPTER 5.2

***ROLE OF KAEMPFEROL IN THE MODULATION
OF AUTOPHAGY AND ITS EFFECT ON
CYTOPROTECTION OF PANCREATIC β -CELLS
UNDER LIPID OVERLOAD CONDITION***

Chapter 5.2. Role of kaempferol in the modulation of autophagy and its effect on protection of pancreatic β -cells under lipid overload condition

5.2.1. Introduction

Type II diabetes mellitus (T2DM) is a metabolic disease characterized by elevated blood glucose level and insulin resistance. Among all diabetic conditions, type II diabetes is most prevalent and accounts for nearly 90-95% of patients diagnosed with diabetes worldwide. A common health condition which often accompanies T2DM is obesity and thus draws clear correlation vice-versa (American Diabetes Association, 2011). It is already known that obese conditions render the individual even more susceptible to develop T2DM. The saturated fats derived from fat depots of obese individual increases free fatty acids in circulation which consequently impairs skeletal muscle responsiveness to insulin. The hyperglycemic conditions that subsequently prevails, induces the compensatory increase in insulin synthesis and secretion which breakdown at later time points due to pancreatic β -cell failure (Donath and Halban, 2004; Boden, 2011; Al-Goblan et al., 2014).

A major cause of onset and progression of T2DM is the loss of β -cell mass and function due to elevated levels of free fatty acids (lipotoxicity) and glucose (glucotoxicity) (Butler et al., 2003). *In vitro*, chronic exposure to free fatty acids (FFA) leads to pancreatic β -cell's apoptosis and impaired insulin secretion (Maedler et al., 2001; Lupi et al., 2002; Yuan et al., 2010). Therefore, protection of β -cells against lipid overload can be an effective strategy for counteracting obesity linked T2DM (DeFronzo and Abdul-Ghani, 2011; Song et al., 2015).

Recent studies have elucidated that in the presence of saturated fatty acids and hyperglycemic conditions, β -cells undergo apoptosis due to impairment of autophagic turnover. Exposure of human pancreatic islets and β -cell lines to fatty acids and glucose blocks autophagic flux which leads to apoptotic cell death (Mir et al., 2015). Type II diabetic patients and high-fat diet mice model often exhibit dysregulated autophagic activity which further ascertains the implication of impaired autophagy in the pathophysiology of T2DM (Masini et al., 2009; Codogno and Meijer, 2010).

Autophagy is an intracellular lysosomal degradative process of defective proteins, macromolecules, damaged organelles and toxic aggregates, which plays a pivotal role in maintaining cell homeostasis (Mizushima, 2007). Apart from this, autophagy can also be instigated in response to stress conditions like nutrient deprivation, infection, and diseased state, wherein it plays a cytoprotective role. Autophagy has been broadly classified into 3

major categories (1) Macroautophagy; (2) Chaperone-mediated autophagy and (3) Microautophagy (Moreau et al., 2010). Among these, macroautophagy plays a pivotal role in determining the fate of pancreatic β -cells because of which it invariably remains as extensively studied event so far (Jung and Lee, 2009). During the initial stages of macroautophagy, cytoplasmic substrates are gradually sequestered within cytosolic double-membrane vesicles termed autophagosomes. The autophagosomes subsequently fuse with lysosomes to form autophagolysosomes wherein proteolytic enzymes and acidic constituents of lysosomes breakdown the payload brought in by the autophagosomes (Mizushima, 2007).

These autophagosomes were also witnessed to be prominently augmented in various diabetic and obese rodent models such as high-fat diet mice model, ob/ob mice, db/db mice, Zucker fatty rats (Li et al., 2006; Ebato et al., 2008). However, the increase in autophagosomes can be manifested as an outcome of the increase in autophagic activation or impairment of autophagosomes turnover which has to be ascertained before drawing any conclusion. In one such instance, although enhanced autophagosomes were reported in ob/ob mice it was found to be inconsistent with the simultaneous surge in p62 expression, an adaptor protein which binds to LC3-II and acts as a selective substrate of autophagy (Quan et al., 2012). Such results are an outcome of impairment of autophagosomes turnover. Similarly in another study, β -cells specific Atg7 knockout mice (β -cells specific autophagy-deficient mice) fed with high-fat diet exhibited progressive β -cells degeneration with impaired insulin secretion and compromised glucose tolerance and increased apoptotic cell death (Ebato et al., 2008). Thus, these studies clearly established that in diabetic or insulin resistant condition, autophagosomes accumulation may be enhanced because the formed autophagosomes do not meet the increased demand of its turnover for the destruction of non-functional organelles and dysfunctional proteins in type II diabetes and obese models. So, induced autophagy is an adaptive response against insulin resistant condition. Although autophagy has gained importance in the recent past, our understanding of the same is still growing and thus preemptive interpretation can easily mislead about the role of autophagy in various disease models. Some *in vitro* studies have also reported that the induction of autophagy in palmitic acid (PA)-challenged pancreatic β -cells, isolated rat, and human pancreatic islets, exerts the protective effect against PA-induced apoptosis (Choi et al., 2009; Martino et al., 2012). Some recent studies asserted that prolonged exposure of β -cell to FFAs leads to increase in autophagosomes due to suppressed autophagic turnover which is clearly evident from increased LC3-II as well as p62 accumulation.

Autophagy turnover was drastically impaired in the presence of fatty acids which subsequently lead to pancreatic β -cell death (Masini et al., 2009; Bartolomé et al., 2014; Mir et al., 2015).

On the basis of this pre-notion, rapamycin (an mTOR inhibitor and known activator of autophagy) has been validated to exert the cytoprotective effect on PA-induced β -cell by reducing the blockage of autophagic turnover (Mir et al., 2015). Similarly, other well-known antidiabetic drugs like rosiglitazone and metformin were also found to rescue β -cells from PA-induced apoptosis through modulation of autophagy (Wu et al., 2013; Jiang et al., 2014). Thus, induction of autophagy could be a potential target to combat saturated fatty acid mediated apoptotic cell death (Stienstra et al., 2014). On the basis of the cytoprotective action of autophagy in β -cell rescue, in the present study, we evaluated the potential role of a flavonol i.e., kaempferol, to instigate autophagy in PA-induced clonal pancreatic β -cells (RIN-5F cell line) and isolated primary cultures of rat islets.

Kaempferol (3,5,7,4-tetrahydroxyflavone) is natural flavonol found in various fruits and vegetables such as apples, berries, grapes, beans, broccoli, cabbage, onions, tomatoes, green tea and is also present in medicinal plants which include *Equisetum* spp., *Sophora japonica*, and *Ginkgo biloba* (M Calderon-Montano et al., 2011). A number of pre-existing literature studies have already reported the cardioprotective, anti-osteoporotic, neuroprotective, anti-oxidative, anti-inflammatory and anticancer activities of kaempferol (Lin et al., 2007; Huang et al., 2010; Filomeni et al., 2012; Abo-Salem, 2014; Liao et al. 2016). Recently, the antidiabetic and anti-obesity activity of kaempferol fractions isolated from unripe soybean leaves have been reported in high-fat diet mice model (Zang et al., 2015). Apart from this, kaempferol was also reported to increase insulin secretion and β -cell mass in chronic hyperlipidemia condition and in obese diabetic mice (Zhang and Liu., 2011; Zhang et al., 2013; Alkhalidy et al., 2015). Although kaempferol was found to exert cytoprotective activity on pancreatic β -cells, to the best of our knowledge, the role of autophagy in cytoprotective and anti-apoptotic activity of kaempferol on pancreatic β -cells still remains to be elucidated.

In this study, we investigated the effects of kaempferol on apoptosis and autophagy of clonal pancreatic β -cells and isolated rat primary islets in PA-induced stressed condition. We further illustrated the cross-talk between apoptosis and autophagy in response to kaempferol and thereby established the probable underlying mechanism and signaling pathways involved.

5.2.2. Brief methodology

5.2.2.1. Cell culture and treatment

RIN-5F cells were cultured in RPMI 1640 media supplemented with 10% heat-inactivated FBS and 1% streptomycin–penicillin solution at 37°C in a humidified atmosphere with 5% CO₂. Prior to the cell based assays, media was replaced with RPMI 1640 media containing 1% bovine serum albumin (BSA) and 0.5 mM PA and the cells were then treated with different doses of kaempferol with or without certain inhibitors i.e., wortmannin (inhibitor of initial stage of autophagy) or chloroquine (a lysosomotropic agent and late-stage autophagy inhibitor) or compound C (an AMPK inhibitor). For each experiment, wortmannin (100 nM), chloroquine (10 μ M) and compound C (10 μ M) were added to the respective wells 1 h prior to the kaempferol treatment. The RPMI media containing only 1% BSA was used for normal control cells. The cells treated with PA in combination with 200 nM temsirolimus, the mTOR inhibitor, were considered as a positive control for this study.

5.2.2.2. siRNA transfections

Rat specific predesigned siRNA for Atg7 and AMPK were purchased from Qiagen (Valencia, CA, USA) and Ambion (Life Technologies GmbH, Darmstadt, Germany) respectively. Negative control siRNA for the above genes were procured from Qiagen. Then 50 nM of each siRNA were transfected to RIN-5F cells. For this, Attractene transfection reagent (Qiagen) was used for transfection, according to the protocol mentioned by the manufacturer. Briefly, 5 X 10⁵ RIN-5F cells were seeded in 6 well plates. After 24 h, the cells were transfected with 50 nM of each siRNA in respective wells with the transfection reagent according to manufacturer's protocol and incubated in a CO₂ incubator at 37°C. After 24 h of incubation, the cells were treated with or without 10 μ M kaempferol in presence of 0.5 mM PA for another 48 h.

5.2.2.3. Animals

Female Sprague-Dawley rats of age 8–10 weeks old were procured from National Institute of Pharmaceutical Education and Research, Mohali, India with the approval of Institutional

Animal Ethics Committee (MMCP/IAEC/16/05). They were housed under standard conditions and allowed to acclimatize for two weeks before use. All the animal study experiments were performed according to the guidelines and approval of the Institutional Animal Ethics Committee.

5.2.2.4. Islets isolation and treatment

The rat pancreatic islets were isolated as described elsewhere with some modifications (Martino et al., 2012). Briefly, the rats were sacrificed by cervical dislocation and the pancreas was removed aseptically. The harvested pancreas was then cut into small pieces and washed with Hanks' balanced salt solution (HBSS). Thereafter, the resulting pancreatic pieces were then digested in collagenase V (Sigma–Aldrich, USA) in HBSS for 10 min at 37°C with gentle shaking. The digested samples were then rinsed thrice with cold HBSS. Finally, the islet purification was performed by centrifugation at 800 x g for 15 min at 4°C on Ficoll density gradient centrifugation (density: 1.100, 1.077) (Sigma Chemical Co., St Louis, MO, USA). After being washed with HBSS containing 2% BSA, the islets were cultured in RPMI 1640 supplemented with 10% FBS 1% streptomycin–penicillin and L-glutamine (2 mM) at 37°C in a humidified atmosphere containing 5% CO₂. The purified islets were then tested for their specificity by dithizone (DTZ) staining. For DTZ staining, the culture dishes were incubated at 37°C for 15 min in the DTZ solution. After the incubation period, dishes were rinsed three times with HBSS and subsequently monitored under a microscope to identify clusters of stained crimson red as islets. After examination, the dishes were replenished with culture media. The stain completely disappeared from the cells after 4 h. For treatment, DTZ-stained islets were counted and divided into various groups and were given the respective treatments.

5.2.2.5. Preparation of PA-containing media

The RPMI media containing 0.5 mM PA was prepared as described elsewhere (Tu et al., 2014). Briefly, 100 mM PA stock solution was prepared in DMSO, which was subsequently diluted to 5 mM in 10% BSA (BSA dissolved in RPMI media) The resultant mixture was further diluted with pre-warmed (37°C) incomplete RPMI media supplemented with 1% streptomycin–penicillin solution to attain 0.5 mM PA concentration in the media. The final

concentration of BSA in PA-containing media was 1 %, thus RPMI media supplemented with 1% BSA was used as vehicle control for experiments.

5.2.2.6. 5-Bromo-2'-deoxyuridine (BrdU) incorporation assay

The incorporation of thymidine analog BrdU (5-bromo-2'-deoxyuridine) into freshly synthesized DNA and then anti-BrdU antibody labeling, were used to quantitatively measure the cell proliferation in response to kaempferol. The detailed protocol is mentioned in chapter 3

5.2.2.7. Hoechst 33342 staining for monitoring nuclear morphology of apoptotic cells

Hoechst 33342 is a cell permeable dye which stains the nucleus. For nuclear staining, RIN-5F cells were seeded in 12 well plates (5×10^4 cells/well) in RPMI 1640 media with 10% FBS. After 24 h of seeding, the cells were treated with respective treatments and were stained with Hoechst 33342 (1 μ g/ml in PBS) for 5 min according to the protocol mentioned in chapter 3

5.2.2.8. DNA ladder assay

The DNA ladder assay was performed to detect DNA fragmentation, one of the hallmark feature of apoptotic cells. The assay was performed as discussed in chapter 3.

5.2.2.9. Labeling of autophagic vacuoles and lysosomes with MDC and LysoTracker

MDC is widely used as a probe to label autophagic vacuoles while LysoTracker Red DND-99 is used to specifically tag lysosomes. MDC-LysoTracker staining was performed to monitor kaempferol-mediated autophagy in presence or absence of various inhibitors. The staining protocol is described in chapter 3.

5.2.2.10. Cell transfection and stable cell line establishment

For LC3 puncta assay, an importance assay to monitor the status of autophagy in cells, EGFP-LC3 expressing stable RIN-5F cell line were established. To generate stable EGFP-LC3 expressing RIN-5F cells, 2 μ g EGFP-LC3 plasmid was transfected to 70 - 80% confluent RIN-

5F cells using Polyfect transfection reagent (Qiagen, USA) according to the manufacturer's instructions. The transfected cells were screened with 500 μ g/ml G418 (Sigma) until stable cell lines were established.

5.2.2.11. LC3 puncta assays

The RIN-5F cells stably expressing EGFP-LC3 were treated with or without kaempferol in the presence or absence of chloroquine for 48 h. After incubation, the cells were fixed with 2% formaldehyde and observed under Confocal Laser Scanning Microscope (LSM 780, Carl Zeiss, Germany) for EGFP-LC3 puncta formation. The cells with more than ten EGFP-LC3 punctate dots were considered as positive and were counted.

5.2.2.12. Flow cytometer analysis for autophagy quantification

Flow Cytometer Analysis was performed as described elsewhere (Eng et al., 2010). For this assay, the stable clones of RIN-5F cells expressing EGFP-LC3 were adapted to monitor autophagy by flow cytometry. Around 5×10^4 cells were seeded in a six-well plate and were treated with kaempferol with or without chloroquine in the presence of PA. On completion of the treatment, the cells were harvested by trypsinization and the resultant cells in the suspension were subsequently fixed with 2% glutaraldehyde for 2 min. The excess glutaraldehyde in the fixation step was removed by washing the cells twice with PBS. After glutaraldehyde fixation, the cells were consequently permeabilized by briefly treating them with 0.05% saponin in PBS in order to selectively remove soluble cytoplasmic non-autophagosome associated EGFP-LC3 from the cells. The cells were then washed again with PBS and resuspended in 100 μ l PBS prior to being analyzed by flow cytometer (BD FACSVerser™, BD Biosciences, USA). Around 10,000 cell's fluorescence was acquired for each sample which was further analyzed using suitable software (BD FACSuite™ software BD Biosciences, USA) and the results were represented as histogram between normalized frequency percentages versus EGFP-LC3 fluorescence intensity.

5.2.2.13. Transmission electron microscopy analysis of autophagic vacuoles

TEM analysis of treated RIN-5F cells was performed to visualize autophagic vacuoles in response to various treatments as per the protocol mentioned in chapter 3.

5.2.2.14. Immunofluorescence study

For immunofluorescence study, 1×10^5 cells were seeded on each sterile coverslip and incubated for 24 h, thereafter treated with respective test chemicals for another 48 h. On completion of the incubation, the cells were fixed with 4% formaldehyde for 15 min followed by three PBS wash for 5 min each. The fixed cells were then permeabilized with 0.1% triton – X 100 for 10 min, thereafter the cells were washed thrice with PBS for 5 min each and then blocked with 2% BSA in PBS for 1 h at room temperature. After blocking, the cells were incubated with LC3B antibody (1: 200 in PBS) overnight at 4°C. The cells were then washed three times with PBS followed by incubation with the FITC-labeled anti-rabbit secondary antibody (1:500 in PBS) for 1 h at room temperature. Further, the cells were washed with PBS and incubated with Hoechst 33342 stain for 5 min to stain the nucleus. Then coverslips were mounted on slides and visualized under the confocal microscope equipped with 488 nm and 405 nm laser under FITC and DAPI filters respectively (LSM 780, Carl Zeiss, Germany).

5.2.2.15. Statistical analysis

Quantitative data are presented as means \pm standard deviation (SD) of three independent experiments and statistically evaluated by one-way ANOVA followed by Tukey's post hoc test using Graph Pad Prism 6 software (Graph Pad Software, San Diego, CA, USA). For the data analysis, $p < 0.05$ was considered to be statistically significant.

5.2.3. Results

5.2.3.1. Effect of kaempferol on cell viability and proliferation

The MTT assay is a colorimetric assay for quantifying metabolically active viable cells on the basis of oxidoreductase enzyme's ability to convert the tetrazolium salt to purple colored formazan crystals. Various concentrations of kaempferol were initially tested for cytotoxic activity in RIN-5F cells. The results showed that kaempferol was non-cytotoxic till 75 μM concentration (Fig. 5.2.1a). On the contrary, there was a significant increase in cell viability at 10 and 25 μM concentrations ($p < 0.05$) in response to kaempferol. Further, in order to confirm if the increase in cell viability in response to kaempferol was due to proliferative response, BrdU incorporation was monitored in RIN-5F cells in response to different doses of kaempferol. In contrast to the vehicle control, the percentage of BrdU-incorporated cells was significantly increased in kaempferol-treated RIN-5F cells, which was ~ 1.18 and 1.25-fold over control ($p < 0.05$) (Fig. 5.2.1b). Based on the above data, three concentrations i.e. 1, 10, and 50 μM were selected for our further studies.

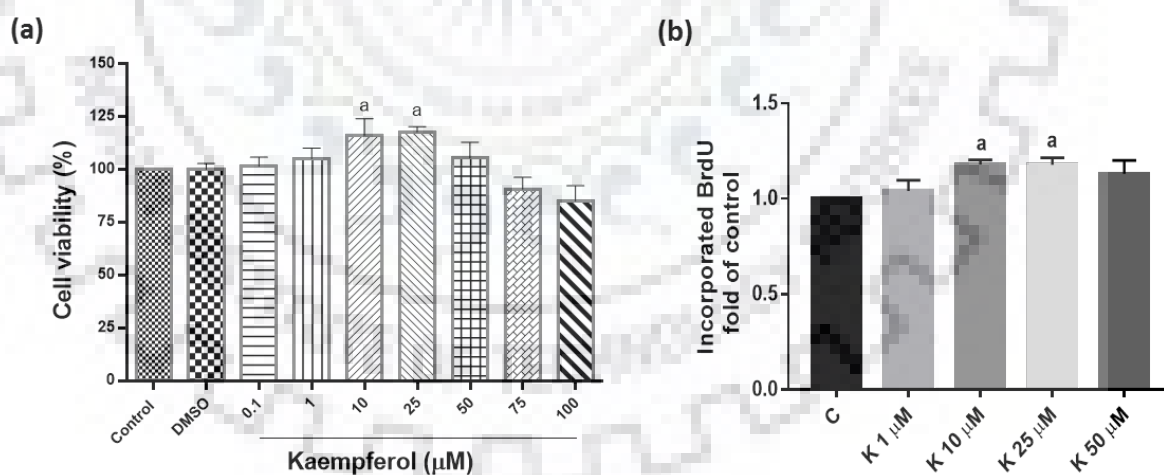


Fig. 5.2.1. Effect of kaempferol on the viability and proliferation of RIN-5F cells. RIN-5F cells were treated with various concentrations of kaempferol for 48 h followed by (a) MTT assay and (b) BrdU incorporation assay. Data are expressed as percentage of viable cells (a) and fold change over control (b) and are represented as the mean \pm SD of three independent experiments. ^a $p < 0.05$ versus vehicle control.

5.2.3.2. Kaempferol attenuates PA-induced lipotoxicity in RIN-5F cells

One of the major causes of β -cell dysfunction in obesity-linked insulin resistance and type II diabetes is lipotoxicity, which in turn, arises due to progressive accumulation of lipids in non-adipose tissues. Among such class of lipids, the PA, in particular, was reported to manifest prominent cytotoxicity in β -cells where, a prominent apoptosis was observed in β -cells that were exposed to 0.5 mM PA for 48 h (Maedler et al., 2001; Yuan et al., 2010). On the basis of such claims, we initially investigated whether kaempferol could rescue RIN-5F cells from PA-induced cell death by MTT assay. It was observed that upon subjecting RIN-5F cells to 0.5 mM PA for 48 h the viability of cells declined drastically by about 32% whereas, co-incubation with kaempferol gradually attenuated PA-mediated cell death in a dose-dependent manner. Kaempferol at a concentration of 10 μ M could rescue almost all the cells (98%) from the cytotoxic effects of PA and consequently narrowed down PA-induced cell death from 32% to 2%. (Fig. 5.2.2a) ($p < 0.05$). Furthermore, in order to verify if the cytoprotective role of kaempferol is mediated by attenuation of apoptosis, we performed Hoechst 33342 staining, DNA fragmentation assay, RT-PCR analysis of apoptotic genes and immunoblot analysis of cleaved caspase-3. The cells undergoing apoptosis exhibits characteristic changes in their nucleus which includes nuclear condensation and DNA fragmentation. In PA-treated cells, the events of nuclear condensation and fragmentation were prominently observed indicating instigation of apoptosis (Fig. 5.2.2b). On the other hand, co-treatment with kaempferol led to inhibition of such instance of nuclear condensation and fragmentation and was observed to be nearly absent at 50 μ M concentration. Apart from this, the protective effect of kaempferol on nuclear fragmentation was confirmed further by DNA ladder assay. In close correlation with Hoechst 33342 staining results, PA-treated cells depicted fragmented and ladder pattern of nuclear DNA which ascertains events of nuclear fragmentation in apoptotic cells (Fig. 5.2.2c). In contrast to that, DNA fragmentation was progressively attenuated with increasing doses of kaempferol. In order to further validate these results, gene expression analysis was performed for some pro-apoptotic and anti-apoptotic marker genes. Temsirolimus (200 nM) (a potent mTOR inhibitor and also reported to rescue β -cells from PA-induced apoptosis) treated cells were adapted as the positive control for apoptotic gene expression analysis. As shown in Fig. 5.2.2d, upon treating the cells with 10 μ M kaempferol *Bax*, *Bad* and *Casp3* (caspase-3) gene expressions were found to be down-regulated by 1.4, 1.2 and 1.7-fold respectively ($p < 0.05$)

whereas a marginal increase in the expression of *Bcl2* was manifested with respect to PA-treated control cells. Thereafter, a cleaved caspase-3 expression, which is a hallmark apoptosis marker, was monitored by immunoblot analysis (Porter and Jänicke, 1999). As shown in Fig. 5.2.2e, the increase in caspase-3 cleavage mediated by PA treatment was markedly inhibited by kaempferol in a dose-dependent manner. The cleaved caspase-3 gradually depreciated by 2.5-fold in the presence of 10 μ M kaempferol ($p < 0.01$). Thus, the results of apoptotic assays corroborate well with each other and clearly suggest the cytoprotective and anti-apoptotic effect of kaempferol against PA-induced apoptosis in RIN-5F cells.

Although the cytoprotective and the anti-apoptotic role of kaempferol was evident in both concentrations (i.e. 10 and 50 μ M) considering the clinical significance of the test material i.e. kaempferol, the lower dosage of kaempferol (i.e. 10 μ M) was used for subsequent studies.

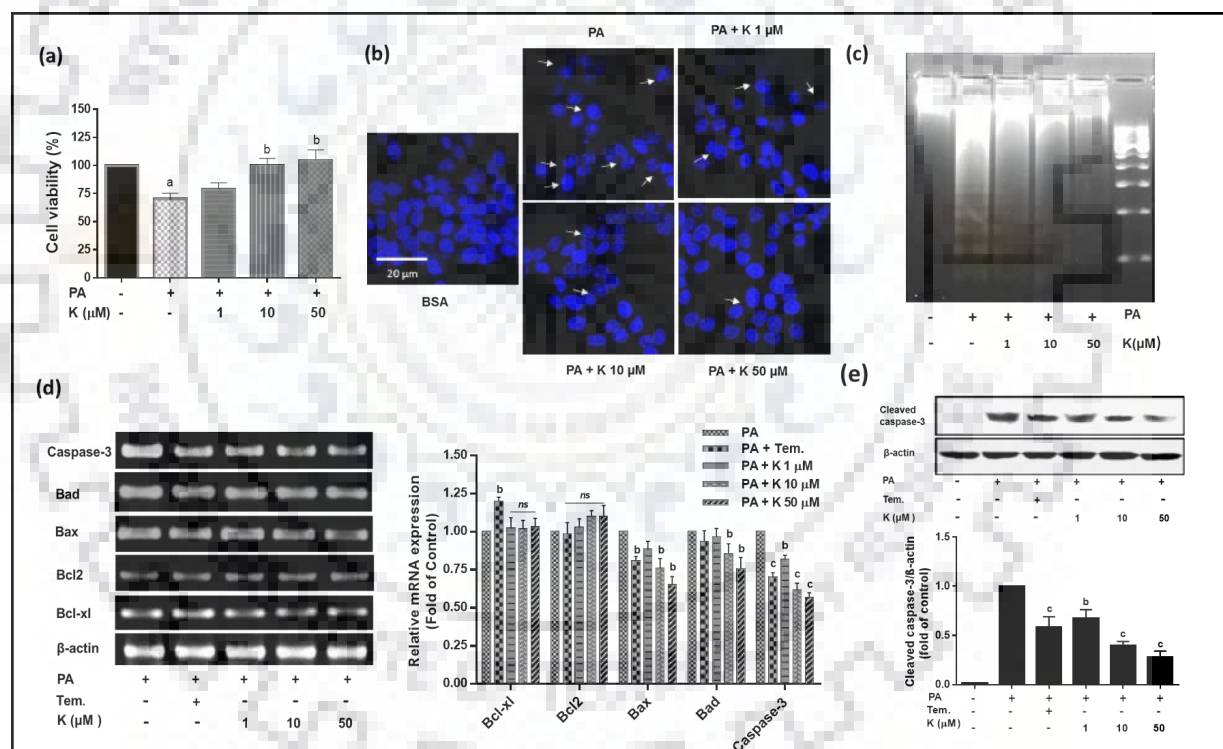


Fig. 5.2.2. Kaempferol attenuates PA-induced lipotoxicity of RIN-5F cells. RIN-5F cells were treated with varying concentrations (1, 10, 50 μ M) of kaempferol or 200 nM of temsirolimus in presence of 0.5 mM PA for 48 h. (a) Cell viability as determined by MTT assay; (b) Nuclear morphological changes as monitored by Hoechst 33342 staining; (c) Apoptotic nucleic acid as detected by DNA ladder formation analysis; (d) Representative RT-PCR for pro-apoptotic and anti-apoptotic marker genes. The histogram in the right panel represents the mean \pm S.D. of arbitrary pixel intensities of PCR products for three individual

experiments expressed as fold change with respect to PA control; (e) Immunoblot analysis for cleaved caspase-3. The histogram in the lower panel represents the mean relative arbitrary pixels intensities as mean \pm S.D. of three independent experiments expressed as fold change with respect to PA control. ^ap < 0.05 versus BSA control; ^bp < 0.05, ^cp < 0.01 versus PA control. PA, palmitic acid; K, kaempferol; Tem, temsirolimus.

5.2.3.3. Kaempferol induces autophagy in PA-stressed RIN-5F cells

Previous studies strongly suggested that autophagy effectively protects pancreatic β -cells against PA-induced apoptosis (Han et al., 2010; Wu et al., 2013; Jiang et al., 2014; Mir et al., 2015). In order to confirm this, in our subsequent studies, we investigated whether the cell survival effect of kaempferol could be due to induction of autophagy in PA-stressed RIN-5F cells. The RIN-5F cells were initially treated with 10 μ M kaempferol in the presence of 0.5 mM PA for 48 h and ensuing events of autophagy were monitored by various assays (Mizushima et al., 2010; Klionsky et al., 2012). The cells treated with PA alone or in combination with temsirolimus were considered as the vehicle and positive controls respectively for autophagy studies. For assessment of autophagosomes and autophagolysosomes formation, RIN-5F cells were subjected to PA treatment alone or in combination with 10 μ M concentration of kaempferol and were subsequently co-stained with MDC and LysoTracker red. MDC accumulate specifically within autophagic vacuoles and makes them distinctly visible under DAPI filter, whereas LysoTracker red specifically stains the lysosomes. The results depicted in Fig. 5.2.3a suggests that, upon treating RIN-5F cells with kaempferol, the concerted increase in MDC and LysoTracker stained features were observed which clearly indicates the surge in a number of autophagosomes and lysosomes respectively. Furthermore, it was also observed that under normal conditions kaempferol by itself induces autophagosomes formation which was further augmented in PA-stressed conditions. PA-treated cells showed a marginal increase in autophagosomes formation but the little presence of fusion of autophagosomes with the lysosomes. While kaempferol (10 μ M) in the presence of PA led to the prominent increase in co-localization of autophagosomes with lysosomes, which suggests the formation of autophagolysosomes. Thus, kaempferol apart from increasing autophagosomes formation also manifests their subsequent fusion with lysosomes so as to degrade the internalized cargo. In order to further confirm the induction of autophagy by kaempferol, the expressions of autophagy-specific genes were monitored by RT-PCR

analysis. Both *Becn1* (beclin) and *Ulk1* are involved in autophagy induction, whereas *Atg5*, *Atg7*, and *Map1lc3b* (*Lc3b*) are the important downstream regulators of autophagosome expansion and maturation. Apart from these another gene which is involved in targeting the cargo to autophagosome for degradation i.e. *p62/Sqstm1* is also included in the study. RT-PCR analysis revealed that when the cells were treated with kaempferol (10 μ M) in the presence of PA, the upstream genes, *Becn1* and *Ulk1*, involved in autophagy induction, were up-regulated by about 1.7 and 1.3-fold respectively as compared to only PA-treated control cells (Fig. 5.2.3b) ($p < 0.05$). Similarly, expressions of *Atg5*, *Atg7*, and *Lc3b* genes were also up-regulated in a concerted manner by about 1.4, 1.9 and 1.4-fold ($p < 0.05$). This trend of enhanced expression of genes was augmented further with increased concentration of kaempferol (50 μ M). However, there was no significant change in the expression of *p62/SQSTM1* at any of the doses tested.



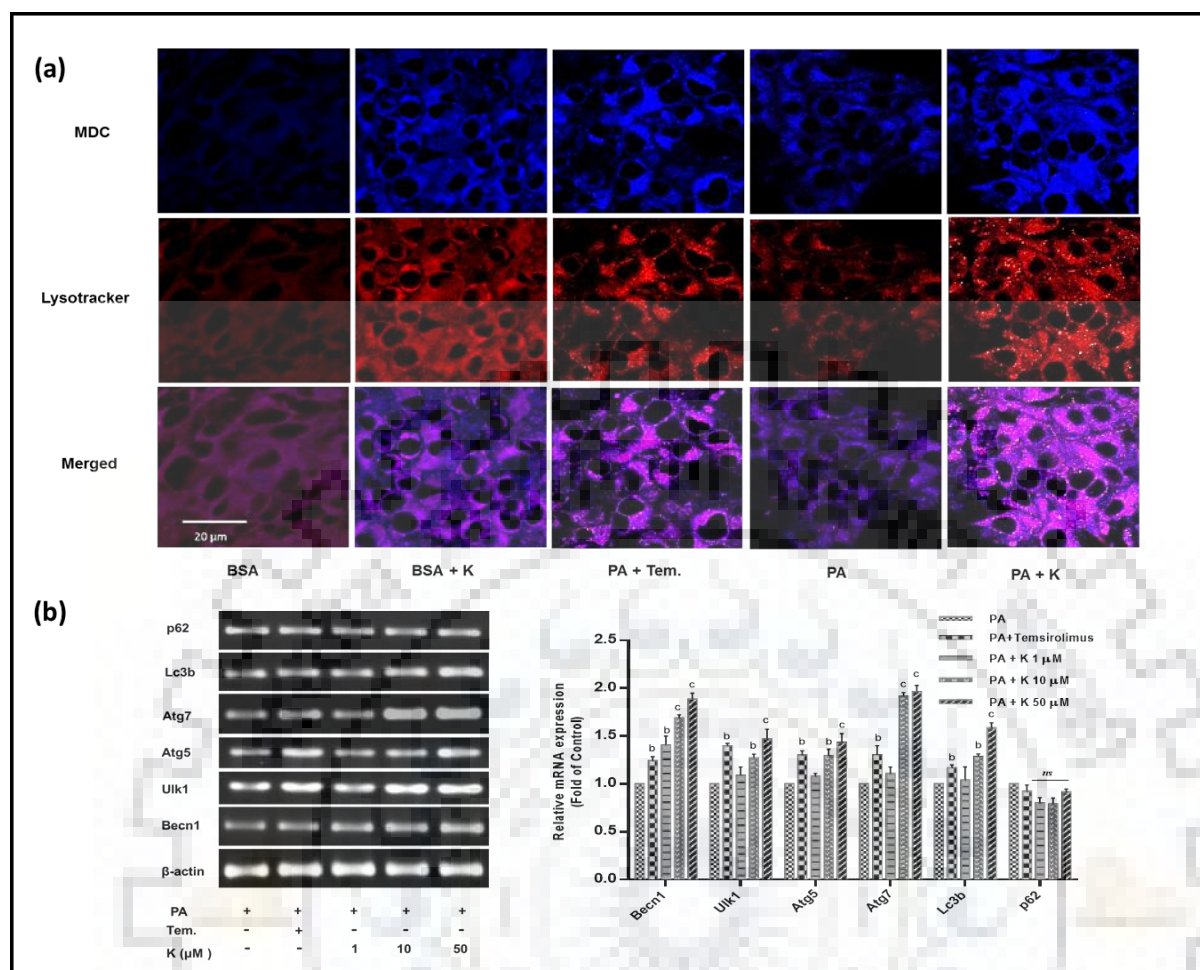


Fig. 5.2.3. Kaempferol induces autophagy in PA-stressed clonal pancreatic β -cells. RIN-5F cells were treated with 10 μ M kaempferol with or without 0.5 mM PA and/or 200 nM temsirolimus (positive control) for 48 h. (a) Representative confocal images to show autophagosomes, lysosomes and autophagolysosomes stained cells using MDC-LysoTracker stain. Images are representative of three independent experiments. (b) Representative RT-PCR analysis showing autophagy-related genes in response to increasing doses of kaempferol. The histogram in the right panel represents the mean \pm S.D. of arbitrary pixel intensities of PCR product bands of three independent experiments expressed as fold change with respect to PA control. ^b $p < 0.05$, ^c $p < 0.01$ versus PA control. PA, palmitic acid; K, kaempferol; Tem, temsirolimus; ns, non-significant.

In order to further ascertain the events of kaempferol-induced autophagy in RIN-5F cells, the formation of EGFP-LC3 puncta, a marker of autophagy, was monitored. The LC3 protein is found in two forms i.e. cytosolic LC3-I form and autophagosome membrane localized LC3-II form. LC3-II is formed by conjugation of LC3-I to phosphatidylethanolamine, an event also called as lipidation of LC3-I which is considered as

the main marker of autophagosome formation induction (Klionsky et al., 2012). Lipidated LC3 is subsequently recruited to autophagosomal membranes during the ensuing events of autophagy and leads to the formation of LC3 puncta which serves as a reliable marker to monitor autophagosomes formation. In order to deduce these events, stably transfected EGFP-LC3-RIN-5F cells were treated with 10 μ M kaempferol in presence or absence of 0.5 mM PA and EGFP-LC3 puncta were visualized under the confocal microscope. The results indicated that temsirolimus (positive control) and kaempferol drastically increased EGFP-LC3 puncta formation in cells whereas untreated vehicle control and PA-treated cells showed diffused cytoplasmic EGFP fluorescence with a few visible puncta (Fig. 5.2.4a). The extensive prominence of EGFP-LC3 puncta in kaempferol-treated cells clearly illustrates that the observed increase in autophagosomes is an outcome of kaempferol treatment.

We further examined the expression of LC3-II protein by immunoblot analysis. As shown in Fig. 5.2.4b and c, co-treatment of kaempferol with PA promoted conversion of LC3-I to LC3-II in dose (Fig. 5.2.4b) and time (Fig. 5.2.4c) dependent manner. The LC3-II protein expression was found to increase by about 3.5-fold when PA-stressed cells were treated with 10 μ M kaempferol for 48 h ($p < 0.01$). Another valuable means of interpreting autophagy was deduced by normalizing LC3-II expression profile with respect to LC3-I, which was found to be ~ 6 -fold for cells treated with 10 μ M kaempferol for 48 h ($p < 0.01$). Although the observed increase in LC3-II accumulation indicates increased autophagosomes, it can also be an outcome of artifact in autophagic turnover. Thus, in order to examine if observed increase in the expression of LC3-II is solely due to increase in autophagic activity and not due to impairment of autophagy turnover we further performed p62 protein expression analysis which acts as the specific substrate of autophagy. The protein p62 directly binds to LC3 and selectively incorporates itself into autophagosomes which are degraded at later stages upon fusion with lysosomes. Thus, the expression level of p62 inversely correlates with the cellular autophagic activity (Mizushima et al., 2010). The immunoblot analysis of p62 protein revealed that the cells treated with kaempferol under PA-stressed condition showed significant decline in p62 protein expression in both doses (Fig. 5.2.4b) and time-dependent (Fig. 5.2.4c) manner causing ~ 2.7 -fold decrease in its expression in response to 10 μ M kaempferol for 48 h (Fig. 5.2.4b and c) ($p < 0.01$). As an outcome of this, it could be inferred that kaempferol could manifest induction of autophagic turnover in dose and time dependent manner.

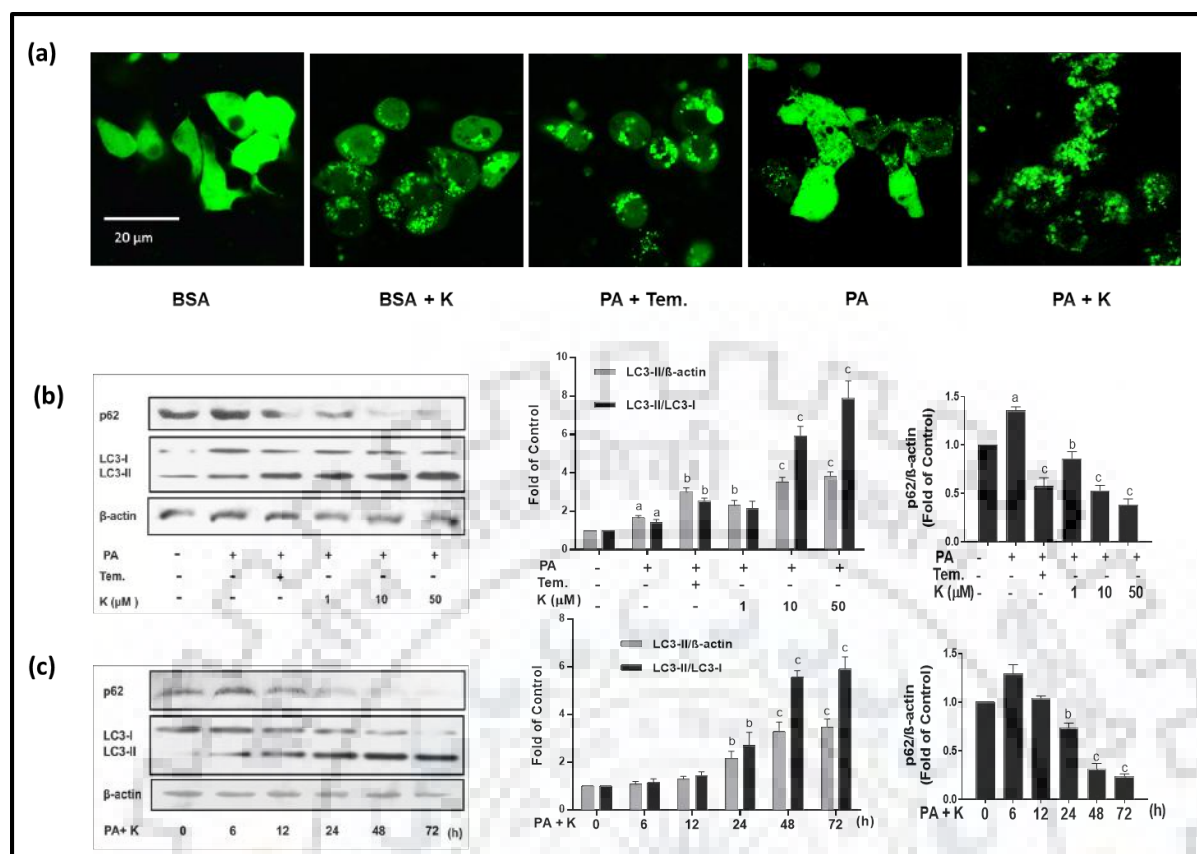


Fig. 5.2.4. Kaempferol induces autophagy by altering the expression of genes involved in autophagic process in RIN-5F cells. (a) Representative confocal images depicting EGFP-LC3 puncta formation in response to various treatments. Images are representative of three independent experiments. Representative immunoblot analysis for the expression of LC3 and p62 with (b) increasing doses and (c) time duration of kaempferol treatment. The histogram in the right panel of each figure represents the mean relative arbitrary pixel intensities in terms of fold over control [BSA for dose-dependent studies and 0 h (PA + K) for time-dependent studies]. Results are the mean \pm S.D. of three independent experiments. ^a $p < 0.05$ versus vehicle (BSA) control; ^b $p < 0.05$, ^c $p < 0.01$ versus PA control/ (PA + K) treatment for 0 hours. PA, palmitic acid; K, kaempferol; Tem, temsirolimus.

5.2.3.4. Autophagy inhibitors impair kaempferol-induced autophagic activity

Further, in order to draw a clear correlation between kaempferol and autophagy induction, autophagy inhibitors i.e., wortmannin and chloroquine, were included in the ensuing studies. Wortmannin effectively suppresses autophagosomes formation via inhibition of class III PI3K and thereby inhibiting autophagy in the initial stages itself, whereas chloroquine prevents autophagosome–lysosome fusion by inhibiting lysosomes acidification and thus inactivating

later stage of autophagy. Since chloroquine inhibits autophagolysosomes formation, the event of autophagosomes degradation is halted which further leads to progressive accumulation of autophagosomes within the cell. Thus, chloroquine mediated accumulation of autophagosomes helped us to deduce whether the observed increase in autophagosomes accumulation arises solely due to induction of autophagy itself or is merely an artifact in autophagic turnover. In order to assess this, RIN-5F cells were pre-treated for 1 h with wortmannin (100 nM) or chloroquine (10 μ M). It was observed that wortmannin treatment significantly inhibited kaempferol-induced autophagosomes formation which is clearly evident from the decline in MDC stained regions (Fig. 5.2.5). On the other hand, when the cells pre-treated with chloroquine were treated with kaempferol the prominent increase in MDC stained features was observed which is due to inhibition of lysosomal degradation of autophagosomes by chloroquine. Thus, chloroquine treatment further confirmed that observed increase in autophagosomes accumulation in the presence of kaempferol is solely due to increase in autophagic flux itself and not due to impairment of autophagosomes turnover (Fig. 5.2.5).

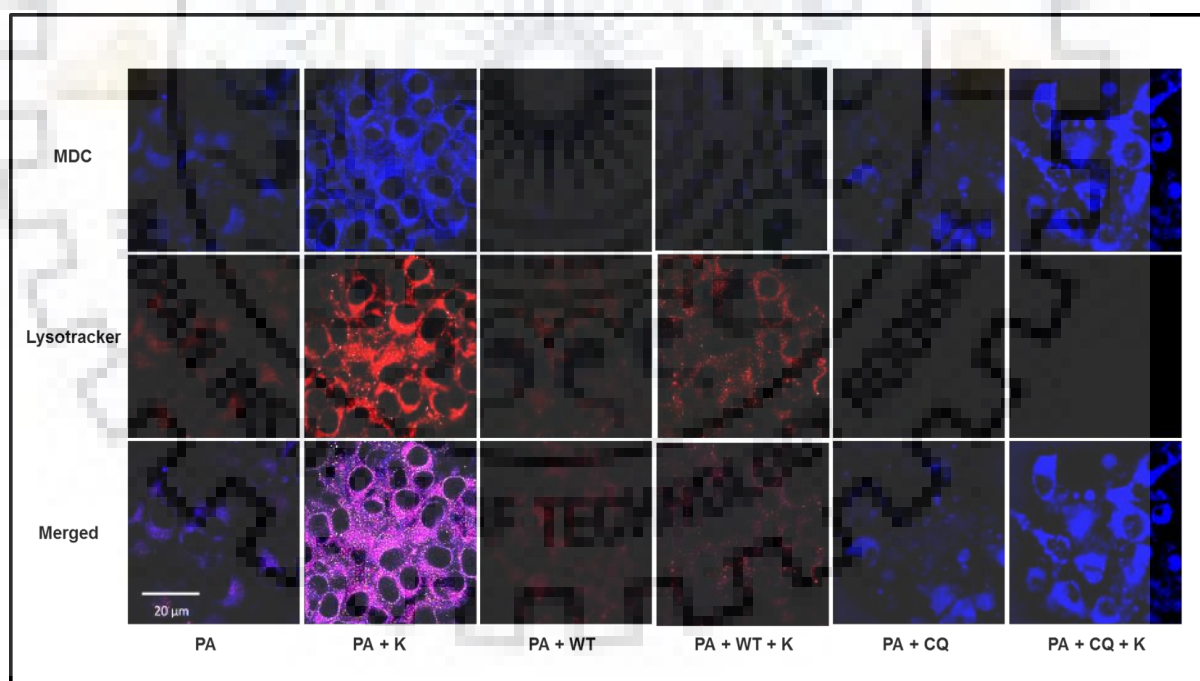


Fig. 5.2.5. Autophagy inhibitors impair kaempferol-induced autophagy. Representative confocal images of three independent experiments showing autophagosomes, lysosomes and autophagolysosomes stained by MDC-LysoTracker stain. RIN-5F cells were treated with 10 μ M Kaempferol with or without wortmannin (100 nM) or chloroquine (10 μ M) in presence of

PA (0.5 mM) followed by MDC-Lysotracker staining. PA, palmitic acid; K, kaempferol; WT, wortmannin; CQ, chloroquine.

Likewise, under transmission electron microscopy the cells co-treated with kaempferol and PA showed abundant late phase autophagosomes (autophagolysosomes) characterized by the unilamellar or degraded membrane of vesicles with degraded organelles and cytoplasm sequestered within them and fewer double-membraned autophagosomes (Fig. 5.2.6). In contrast to this, the cells treated with only PA exhibited a limited number of autophagosomes as well as autophagolysosomes. Inhibition of autophagosomes degradation by chloroquine led to significant increase in accumulation of autophagic vacuoles in cells co-treated with kaempferol as compared to cells treated with kaempferol alone in presence of PA. These results were in accordance with MDC-LysoTracker staining data.

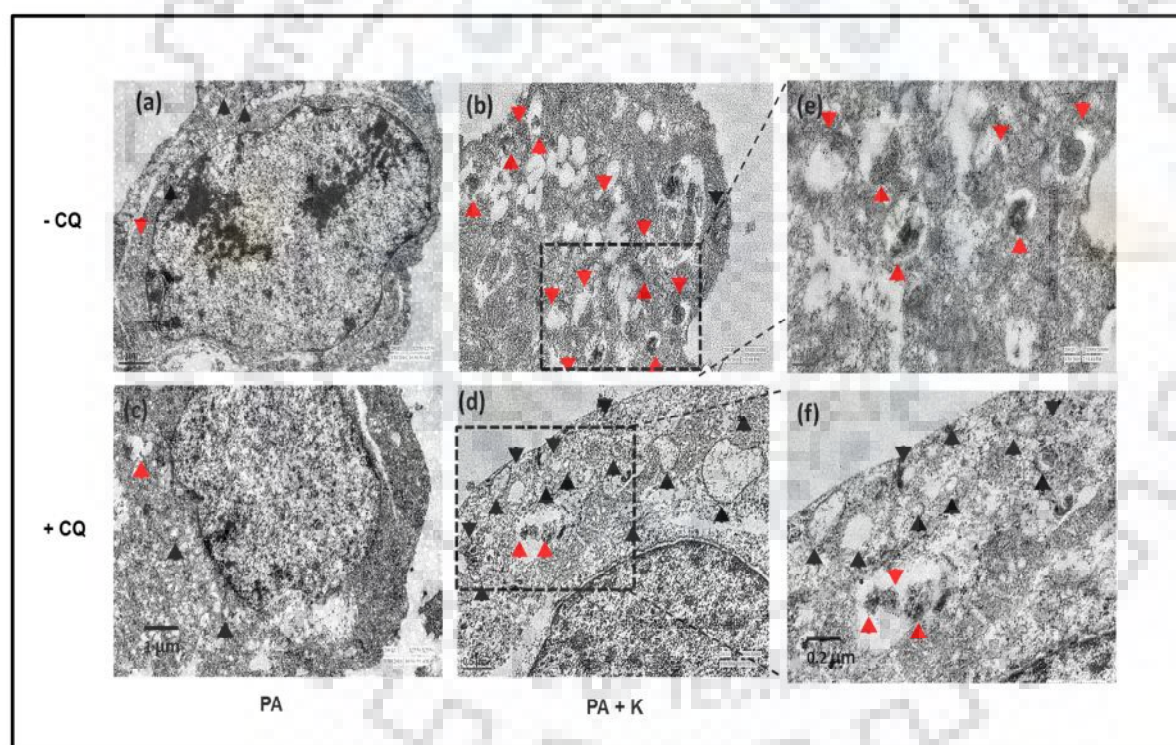


Fig. 5.2.6. Autophagy inhibitors alter cellular architectures in kaempferol-induced autophagy. Representative TEM images showing ultrastructure of RIN-5F cells incubated with kaempferol (10 μ M) with or without chloroquine (10 μ M) in presence of PA (0.5 mM). The red and black arrowheads indicate the unilamellar and multilamellar autophagic vacuoles respectively. Representative images are of two independent experiments. The scale bars in Fig. (a), (b), (c) & (d) represents 1 μ m whereas, Fig (e) and (f) are the magnified TEM images of

portions of (b) and (d) respectively (dotted lines), where the scale bar is 0.2 μ m. PA, palmitic acid; K, kaempferol; CQ, chloroquine.

In order to further ascertain this claim, the hallmark event of autophagy i.e. LC3-II puncta formation was also assessed after treating the cells with kaempferol with or without chloroquine. In the presence of chloroquine, a marked increase in EGFP-LC3 puncta was attained, in cells treated with kaempferol (Fig. 5.2.7a). Such an observation is affirmative of the fact that, the observed increase in autophagy is manifested by kaempferol itself and is not an outcome of impaired autophagosomes degradation.

The role of kaempferol in augmenting autophagy in RIN-5F cells was further confirmed by quantifying cellular levels of autophagosomes associated EGFP-LC3-II by flow cytometric analysis. Prior to this, the free cytoplasmic EGFP-LC3-I proteins were selectively permeabilized out of the cells by brief saponin treatment. The remnant intracellular fluorescence that remains after saponin treatment can be solely ascribed to the lipidated form of LC3-II protein sequestered into the autophagosomal membranes. Thus, the remnant cell-associated fluorescence indirectly represents the extent of autophagosomes formation. Based on this EGFP-LC3-II associated cell fluorescence intensity was quantified by the flow cytometer in order to deduce the extent of autophagy induction under different conditions. Thus, the cells undergoing autophagy were associated with higher fluorescence due to increased presence of autophagosomes-associated EGFP-LC3-II and were easily distinguishable from lower fluorescence of control cells with relatively less EGFP-LC3-II. As shown in Fig. 5.2.7b, PA-treated RIN-5F cells were associated with minimal EGFP-LC3-II fluorescence thus were prominently distributed around the region of lower fluorescence intensity in the histogram. In contrast to this, RIN-5F cells under PA-induced stress conditions shifted towards higher fluorescence region when co-treated with kaempferol. The observed shift in cell population towards higher intensity upon kaempferol treatment certainly arises due to progressive sequestration of EGFP-LC3-II into the autophagosome bilayer membrane during the course of autophagy. When kaempferol-treated cells were subsequently treated with lysosome inhibitor i.e. chloroquine, the EGFP-LC3-II associated cell fluorescence was observed to increase further due to progressive accumulation of autophagosomes, indicative of increased autophagic turnover by kaempferol treatment. Further, immunoblot analysis (Fig. 5.2.7c) showed that wortmannin blocked the kaempferol-induced conversion of LC3-I to LC3-II as a result of which no significant increase in protein levels with respect to PA alone treated

cells was observed. Whereas, when chloroquine was added in kaempferol-treated cells under the PA-stressed conditions, LC3-II protein expression increased from 3.5 to 7-fold and 6 to 9-fold when normalized with respect to β -actin and LC3-I expressions respectively ($p < 0.05$). The increase in LC3-II protein accumulation in chloroquine and kaempferol co-treated group could be attributed to inhibition of LC3-II degradation in the lysosomes. While protein expression analysis of p62 revealed that, autophagy inhibitors averted p62 degradation induced by kaempferol (Fig. 5.2.7c) ($p < 0.05$). Further, for genetic inhibition of autophagy, Atg7 siRNA was used for knocking down Atg7, an essential protein which has a dual function in autophagosomal biogenesis. Firstly, it conjugates Atg5 to Atg12, which is a necessary step for formation of a functional autophagosome. Secondly, Atg7 converts immature cytosolic LC3-I into mature autophagosomal membrane-bound form i.e., LC3-II by adding a phosphatidylethanolamine group. Thus Atg7 is necessary for autophagic function, genetic deletion of which causes an evident loss of autophagy (Ebato et al., 2008; Martino et al., 2012). As shown in Fig. 5.2.7d, Atg7 knockdown significantly inhibited the kaempferol-induced conversion of LC3-I to LC3-II. Atg7 inhibition also averted the kaempferol-induced p62 degradation. Taken together, these data strongly suggested that kaempferol not only augments autophagy induction but also induces the increase in autophagosomes turnover, which is partially impaired by PA.

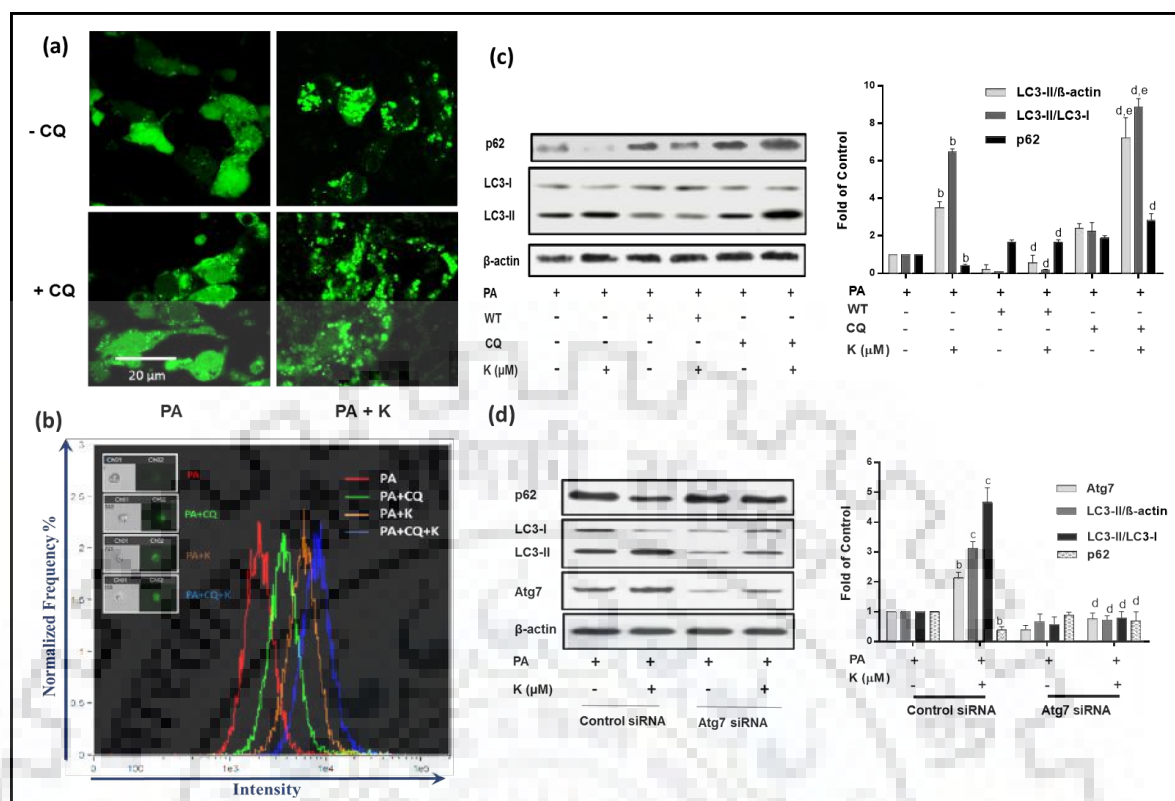


Fig. 5.2.7. Autophagy inhibitors impair kaempferol-induced autophagy by altering autophagy-linked gene expressions. (a) Representative confocal images of EGFP-LC3 puncta formation in response to various treatments. (b) Representative histogram showing normalized frequency percentage versus EGFP-LC3 fluorescence intensity as depicted by flow cytometry analysis of RIN-5F cells stably expressing EGFP-LC3. Representative data is of three independent experiments. (c) and (d) Representative immunoblot analysis of autophagy marker proteins in response to various treatments. The histogram in the right panel represents the mean relative arbitrary pixels intensities in terms of the fold of PA-treated control group. Results are the mean \pm S.D. of three independent experiments. ^b $p < 0.05$ versus PA control; ^c $p < 0.01$ versus PA control; ^d $p < 0.05$ versus (PA + K) group; ^e $p < 0.05$ versus (PA + CQ) group. PA, palmitic acid; K, kaempferol; WT, wortmannin; CQ, chloroquine.

The EGFP-LC3 puncta formation as illustrated in earlier sections was correlated further with LC3 immunostaining results. As shown in Fig. 5.2.8, the cells treated with kaempferol showed increased level of LC3-II which appeared as dots due to their localization in autophagosomes membrane, while in case of control cells (BSA or PA-treated) they were diffused. In the presence of autophagosomes inhibitor, wortmannin, the increase in expression of LC3-II mediated by kaempferol was abolished. As expected, in the case of chloroquine

treatment progressive accumulation of LC3-II was attained in kaempferol-treated RIN-5F cells. This data further corroborated well with kaempferol mediated autophagy induction.

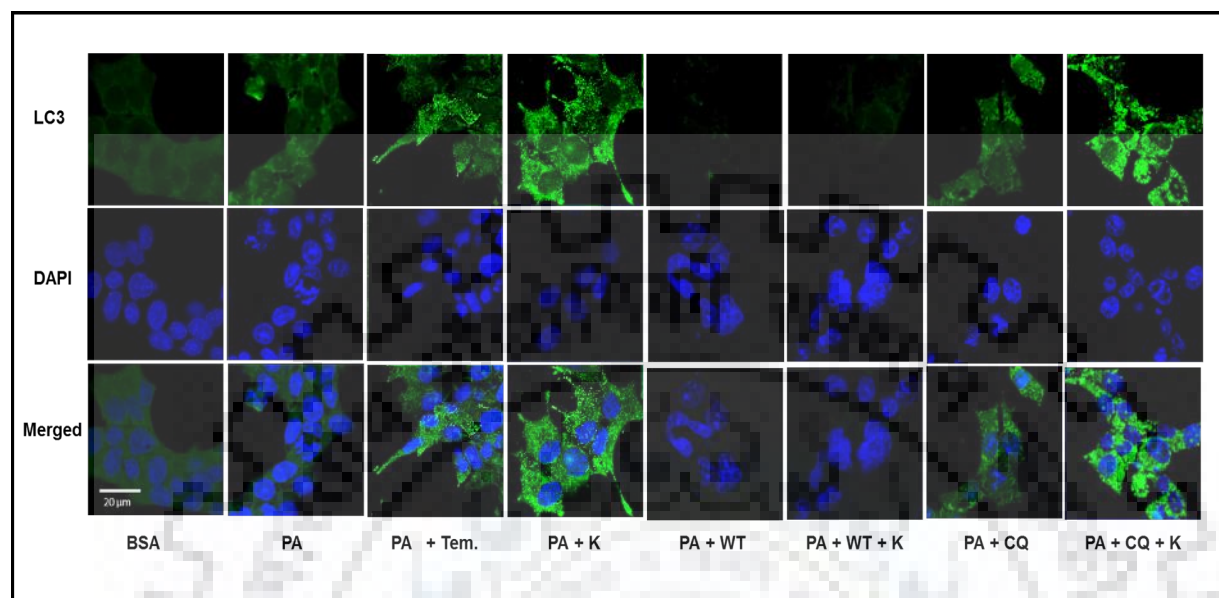


Fig. 5.2.8. Effects of autophagy inhibitors on the expression LC3 protein. Representative immunofluorescence analysis for the expression of LC3 in RIN-5F cells in presence of various treatments and imaged under a confocal microscope. Upper panel indicates immunostaining with LC3 antibody, middle panel represents counterstaining with Hoechst 33342 and the lowermost panel is merged image of previous two. Representative images are of three independent experiments. PA, palmitic acid; K, kaempferol; WT, wortmannin; CQ, chloroquine; Tem, temsirolimus.

5.2.3.5. Kaempferol instigates autophagy through AMPK/mTOR pathway

It is already established that mTOR signaling pathway is the main regulatory pathway of autophagy (Kim et al., 2011). In order to further elucidate the underlying mechanism driving kaempferol mediated autophagy induction, regulation of mTOR expression was checked. As shown in Fig. 5.2.9a and b, mTOR phosphorylation was drastically suppressed upon kaempferol treatment in a time- and dose-dependent manner respectively. Apart from this, in order to verify the upstream regulator of mTOR inhibition, phosphorylation of AMPK was analyzed. It has been reported earlier that inhibition of p-mTOR through AMPK activation instigates autophagy (Han et al., 2010). As shown in Fig. 5.2.9a and b, phosphorylation of AMPK also gradually increased upon kaempferol treatment in PA-stressed RIN-5F cells in a

time- and dose-dependent manner. Kaempferol (10 μ M) treatment in the presence of 0.5 mM PA for 48 h increased AMPK phosphorylation by about 2.8-fold, while concomitant \sim 3.4-fold decline in mTOR phosphorylation ($p < 0.01$). Based on this data it could be speculated that kaempferol activates AMPK/mTOR signaling which subsequently instigates autophagy.

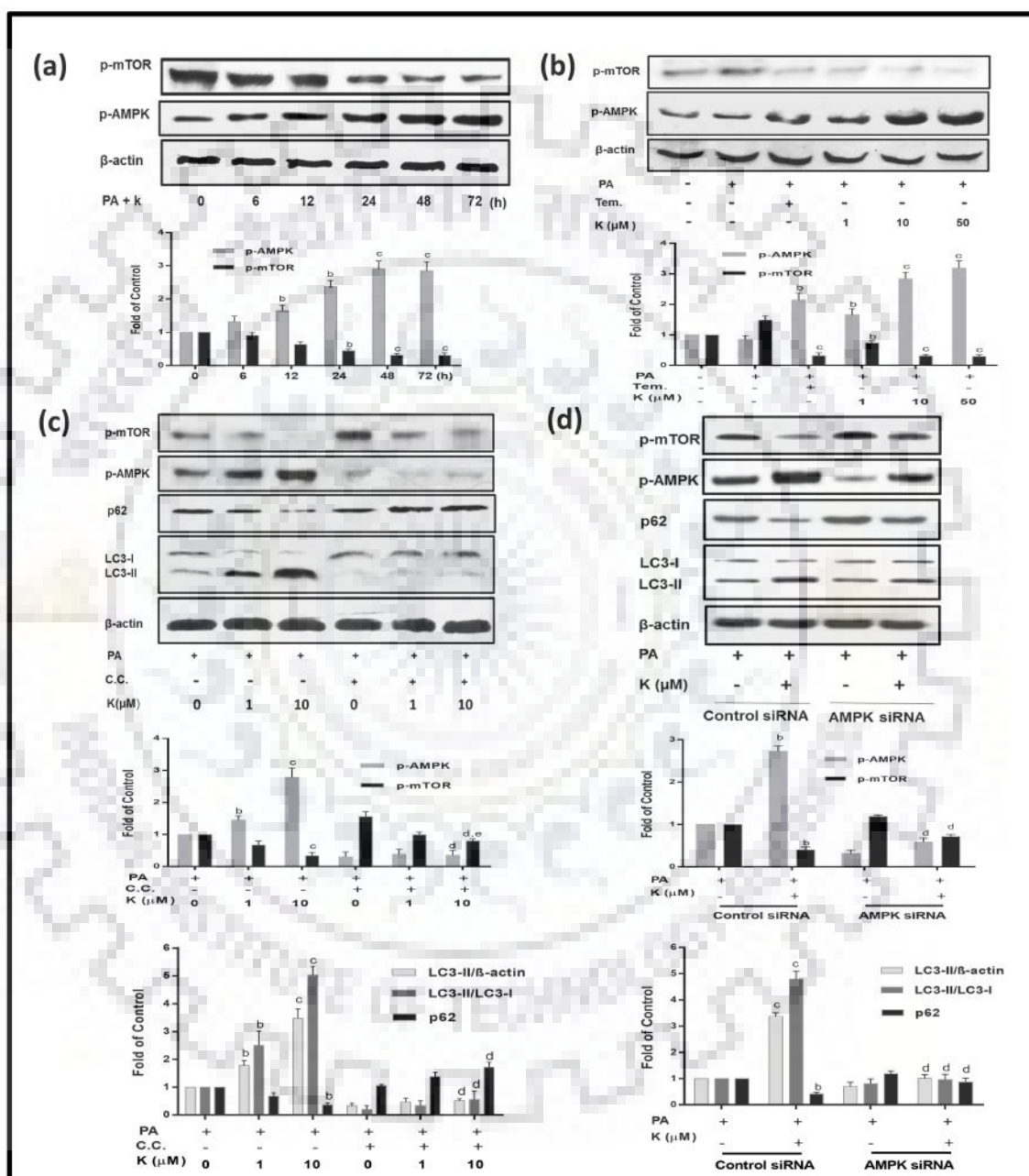


Fig. 5.2.9. Kaempferol-induced regulation of autophagy through AMPK/mTOR pathway. Representative immunoblot analysis of the phosphorylation of AMPK and mTOR in RIN-5F cells in response to kaempferol treatment for varying (a) time period; (b) dosages; (c) dosages in presence of AMPK inhibitor i.e. compound C (10 μ M); and (d) at 10 μ M dose in

presence of AMPK siRNA. RIN-5F cells were transfected with AMPK siRNA for 24 h and then treated with or without kaempferol (10 μ M) for 48 h in presence of PA. The histogram below each figure represents the mean relative arbitrary pixels intensities in terms of fold over control in respective figures. Results are the mean \pm S.D. of three independent experiments. For Fig (a) ^bp < 0.05, ^cp < 0.01 versus 0 h (PA + K) treated control group whereas for Fig (b) ^bp < 0.05, ^cp < 0.01 versus PA control and for Fig (c) ^bp < 0.05, ^cp < 0.01 versus PA control group; ^dp < 0.05 versus (PA + K 10 μ M); ^ep < 0.05 versus (PA + C.C.). PA, Palmitic acid; K, Kaempferol; C.C., compound C; Tem, temsirolimus.

In order to confirm the specific involvement of activated AMPK in autophagy induction by kaempferol, chemical and genetic AMPK inhibitors were also included in further studies. As shown in Fig. 5.2.9c and d, kaempferol-induced up-regulation of AMPK phosphorylation were significantly down-regulated in presence of compound C and AMPK siRNA indicative of the specific involvement of AMPK pathway. With the decrease in the level of AMPK, there was subsequent inhibition of LC3-II and progressive accumulation p62 proteins within cells thus confirming a gross decline in the process of autophagy in the cells in response to AMPK inhibition which could not be rescued by kaempferol. The results depicted in fig. 5.2.9c and d clearly indicate down-regulation of AMPK phosphorylation with simultaneous up-regulation of mTOR phosphorylation in kaempferol-treated cells in the presence of compound C or AMPK siRNA (p < 0.05). This further confirms kaempferol mediated AMPK activation is involved in the inhibition of mTOR. Interestingly, the results also indicated dose-dependent down-regulation of mTOR phosphorylation to some extent even when AMPK was inhibited (Fig. 5.2.9c), which could be attributed to the fact that kaempferol might be downregulating the phosphorylation of mTOR in both direct and indirect (by activating AMPK) manner which ultimately leads to induction of autophagy. However, this aspect needs further validation and exploration which is a limitation of this study.

In close correlation with this observation, as shown in Fig. 5.2.10a, the kaempferol-induced autophagosomes formation in PA-stressed RIN-5F cells (lane 2) was completely abolished in presence of compound C as depicted by the complete disappearance of fluorescence in MDC as well LysoTracker co-staining (lane 3). This could only be marginally recovered by kaempferol (lane 4). A similar pattern of the abolition of EGFP-LC3 puncta formation was observed in presence of compound C in PA-induced stressed cells (Fig. 5.2.10b). LC3 immunofluorescence staining also showed a similar pattern of its inhibition in presence of compound C (Fig. 5.2.10c), thus confirming that compound C inhibited

kaempferol-induced autophagosomes formation and thereby averted LC3 accumulation. In summary, all these data corroborated well with each other to arrive at the common fact that kaempferol instigates autophagy by means of AMPK/mTOR pathway.

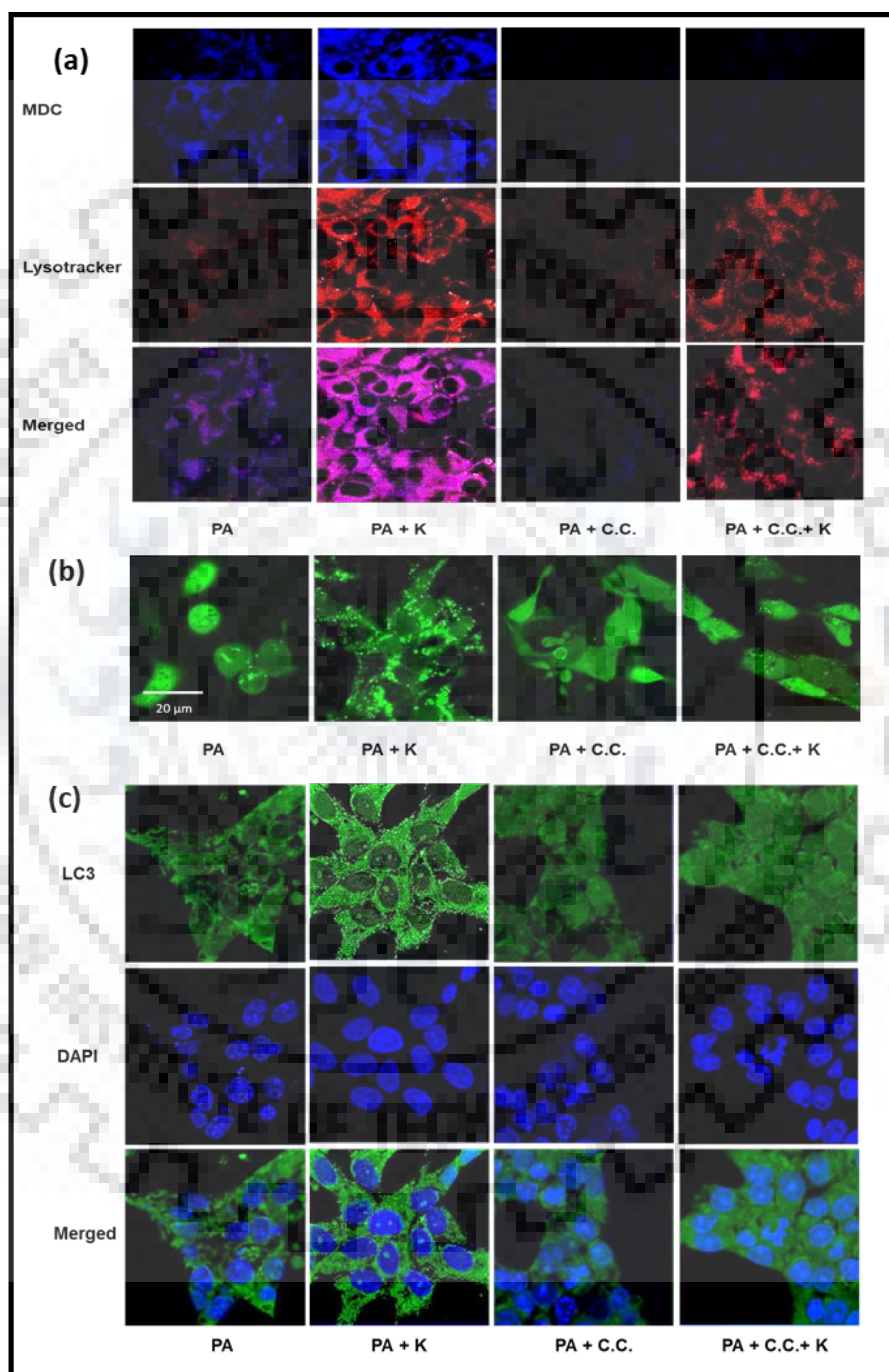


Fig. 5.2.10. Effect of AMPK inhibitor on autophagolysosomes formation in RIN-5F cells. Representative confocal images depicting (a) Autophagosomes, lysosomes and autophagolysosomes stained by MDC-LysoTracker stain; (b) EGFP-LC3 puncta formation

and (c) Immunofluorescence analysis for the expression of LC3 in RIN-5F cells treated with kaempferol (10 μ M) with or without compound C (10 μ M) in presence of PA. Representative images are of three independent experiments. PA, Palmitic acid; K, Kaempferol; C.C., compound C.

5.2.3.6. Inhibition of autophagy impairs the cytoprotective role of kaempferol

To determine whether autophagy is involved in the cytoprotective role of kaempferol in PA-stressed RIN-5F cells, autophagy inhibitors (wortmannin and chloroquine) and AMPK inhibitor (Compound C) were used. Inhibition of kaempferol mediated autophagy by wortmannin, chloroquine, and compound C prominently revoked cell survival effect of kaempferol and caused much greater extent of cell death which accounts for the observed decline in cell viability in MTT assay. Co-treatment of cells with wortmannin and kaempferol reduced the cell viability from 98% to 63% (Fig. 5.2.11a) whereas, inhibitors like chloroquine and compound C reduced cell viability to 50% and 62% respectively (Fig. 5.2.11b and c) ($p < 0.05$). Moreover, BrdU incorporation study demonstrated that PA reduced the RIN-5F cell proliferation as well. RIN-5F cells treated with 0.5 mM PA for 48 h showed \sim 2-fold reduction in BrdU incorporation over BSA control while co-treatment of kaempferol with PA increased incorporation of BrdU \sim 1.4-fold of the PA-treated control group ($p < 0.05$) (Fig. 5.2.11d). This data confirms the fact that PA exerts an antiproliferative effect on RIN-5F cells which is rescued by kaempferol to a great extent, if not completely. Further, co-treatment of kaempferol with inhibitors of autophagy and AMPK led to reduced BrdU incorporation as induced by kaempferol. Furthermore, Hoechst 33342 staining also revealed the presence of numerous condensed nuclei (indicative of apoptosis) in the inhibitor and kaempferol co-treated cells as compared to only kaempferol-treated cells (Fig. 5.2.11e). These observations were also in close agreement with the DNA fragmentation assay results which showed that in the presence of those inhibitors there was enhanced DNA ladder formation which was marginally rescued by kaempferol (Fig. 5.2.12a).

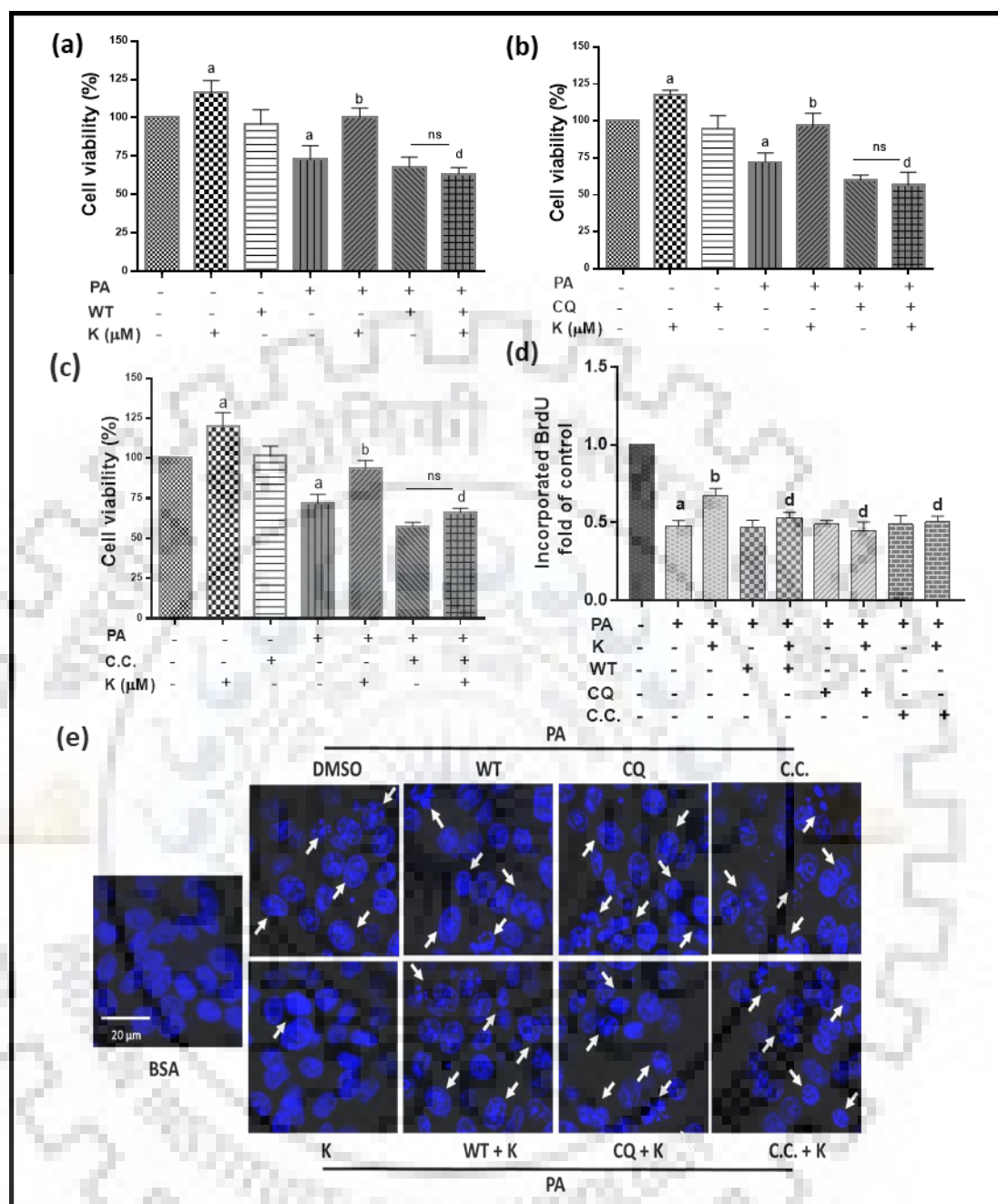


Fig. 5.2.11. Inhibition of autophagy impairs the cytoprotective role of kaempferol. RIN-5F cells were incubated with kaempferol (10 μ M) with or without wortmannin (100 nM) or chloroquine (10 μ M) or compound C (10 μ M) in presence of PA (0.5 mM) for 48 h. The histograms in (a), (b) and (c) represent percentage cell viability in response to various treatments and expressed as percent of cell viability over control (BSA) as depicted by MTT assay. (d) The histogram shows quantification of incorporated BrdU represented as fold change in fluorescent intensity of control in response to various treatments. (e) Representative confocal images of nuclear staining of treated cells showing condensed and fragmented nucleus (arrows). Results are the mean \pm S.D. of three independent experiments. ^a $p < 0.05$

versus BSA control; ^bp < 0.05 versus PA control; ^dp < 0.05 versus (PA + K 10 μ M). PA, palmitic acid; K, kaempferol; WT, wortmannin; CQ, chloroquine; C.C., Compound C.

Subsequently, western blot analysis revealed that inhibition of kaempferol-induced autophagy and AMPK increased the cleavage of caspase-3 and hence cellular apoptosis. Co-treatment of kaempferol with wortmannin, chloroquine, and compound C increased the expression of cleaved caspase-3 by 3-, 5- (Fig. 5.2.12b) and 3.2-fold (Fig. 5.2.12c) ($p < 0.05$) respectively, as compared to kaempferol treatment. Similarly, genetic inhibition of autophagy and AMPK by Atg7 and AMPK siRNA respectively also showed increased cleaved caspase-3 expressions which were significantly rescued by kaempferol (fig. 5.2.12d and 5.2.12e) ($p < 0.05$). Taken together, these data strongly suggested that inhibition of autophagy-impaired the cytoprotective effect of kaempferol in PA-induced RIN-5F cells. Interestingly, autophagy inhibition also enhanced the cell death induced by PA treatment. The results acquired for compound C and AMPK siRNA indicated that AMPK inhibition may reverse the cytoprotective effect of kaempferol in PA-induced RIN-5F cells.

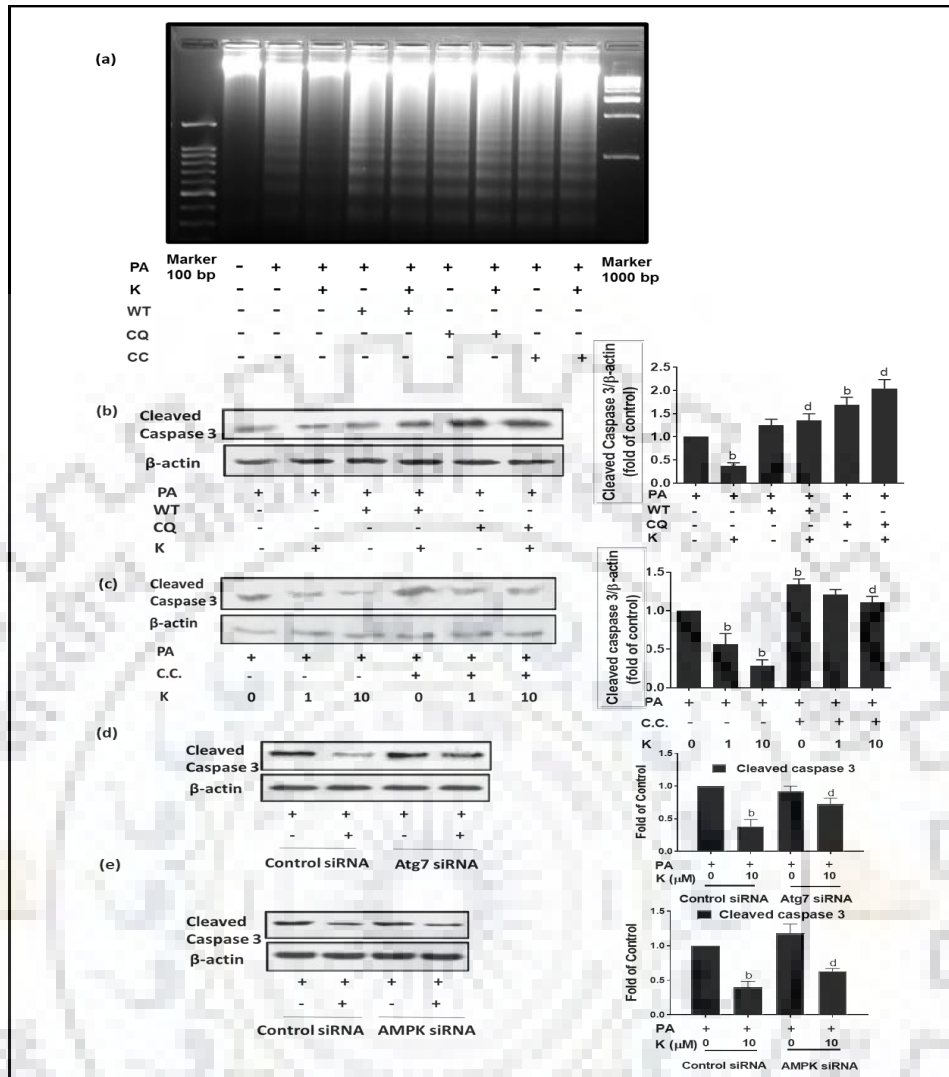


Fig. 5.2.12. AMPK/mTOR mediated autophagy is involved in kaempferol-mediated cytoprotective role on PA-stressed RIN-5F cells. (a) Representative gel image showing the DNA ladder formation in response to various treatments. Representative immunoblot showing the expression of cleaved caspase-3 in response to (b) wortmannin and chloroquine, (c) compound C, (d) Atg7 siRNA and (e) AMPK siRNA. The histograms in the right panel of each immunoblot represent the mean relative arbitrary pixels intensities in terms of the fold of only PA control. Results are the mean \pm S.D. of three independent experiments. ^ap < 0.05 versus BSA control; ^bp < 0.05 versus PA control; ^dp < 0.05 versus (PA + K 10 μ M). PA, palmitic acid; K, kaempferol; WT, wortmannin; CQ, chloroquine; C.C., Compound C.

5.2.3.7. Effects of kaempferol on isolated rat pancreatic islets under PA-induced condition

Even though RIN-5F cells (an insulin secreting rat insulinoma cell line) has been widely used as a pancreatic β -cell model, primary culture of isolated murine pancreatic islets always provided a more physiologically relevant model. Hence in the next phase of the study, we reconfirmed some of our studies using the primary culture of rat pancreatic islets.

In order to confirm the induction of autophagy in isolated rat pancreatic islets in response to kaempferol in PA-stressed condition, MDC-LysoTracker staining was performed. As shown in Fig. 5.2.13a kaempferol-treated pancreatic islets showed enhanced co-localization of MDC and LysoTracker stained regions as compared to only PA-treated islets, which indicates that kaempferol-induced the formation of autophagosomes as well autophagolysosomes in PA-stressed islets. Further, inhibition of autophagy by means of inhibitors like wortmannin, chloroquine, and compound C showed the similar pattern as was with RIN-5F cells. These inhibitors abolished the kaempferol-induced autophagy induction which further confirms the induction of autophagy in response to kaempferol in PA-challenged islets.

We further analyzed the LC3 and p62 expression through immunoblot analysis. As shown in Fig. 5.2.13b, co-treatment of kaempferol and PA, stimulated the higher conversion of LC3-I to LC3-II. The LC3-II protein was increased by about 2.3-fold in PA-challenged islets when treated with 10 μ M kaempferol for 48 h ($p < 0.05$). The increased LC3 accumulation indicates the enhanced autophagosomes formation. Moreover, a significant decrease in the expression of p62 in kaempferol-treated group confirmed that the increased expression of LC3-II was due to increase in autophagy induction rather than an artifact in autophagic turnover (Fig. 5.2.13b). Induction of autophagy was further confirmed by inhibition of autophagy by means of autophagy inhibitors. Wortmannin treatment inhibited the kaempferol-induced increase in LC3 expression and led to significant accumulation of p62 while chloroquine treatment showed a significant increase in LC3-II and p62 which could be due to inhibition of their degradation in the lysosomes. Thus it further confirmed that kaempferol augments autophagy induction not only in RIN-5F cells but also in isolated pancreatic islets.

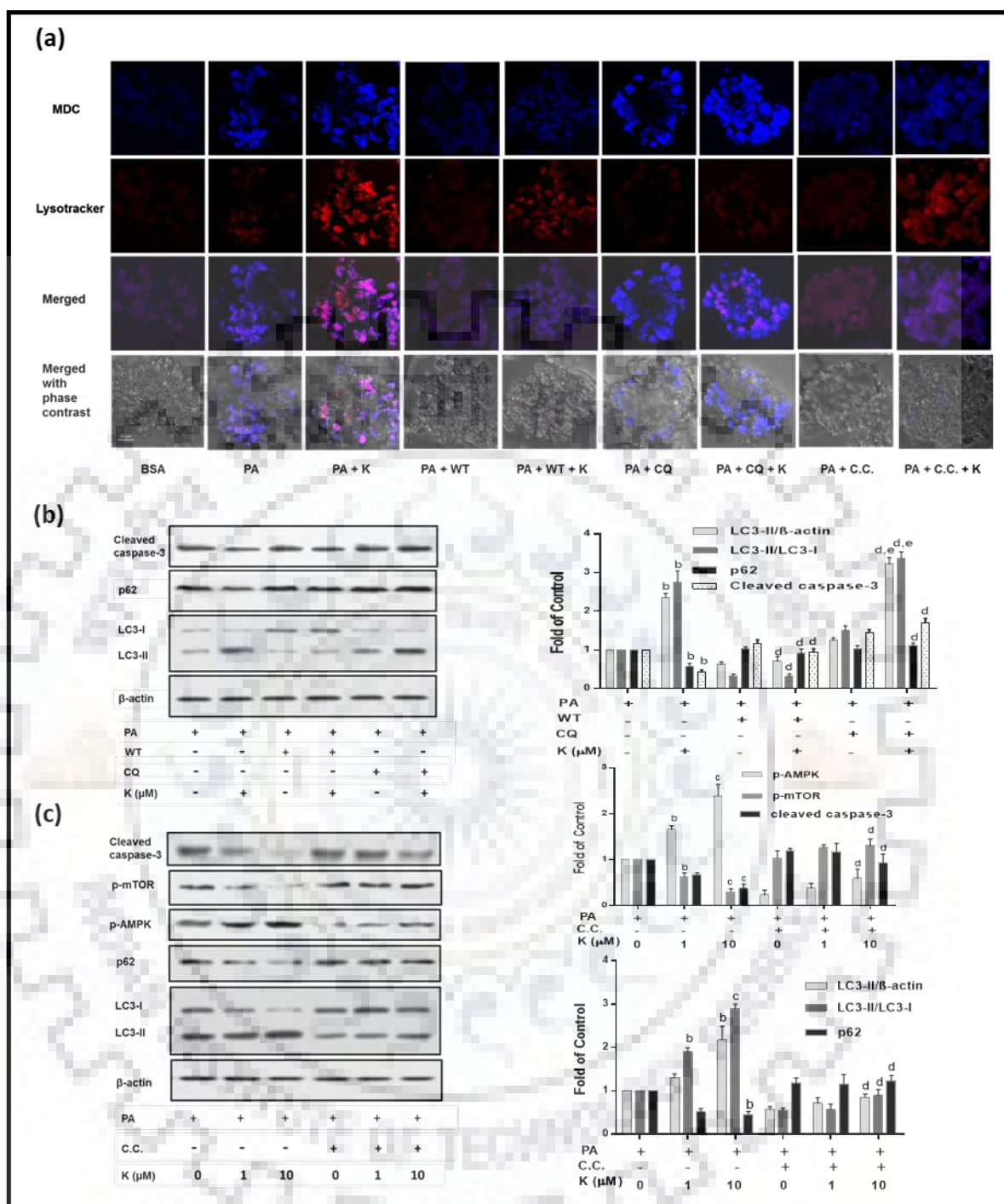


Fig. 5.2.13. Kaempferol exerts cytoprotective role on rat pancreatic islets through AMPK/mTOR-mediated autophagy induction. The islets cells were incubated with kaempferol (10 μ M) with or without wortmannin (100 nM) or chloroquine (10 μ M) or compound C (10 μ M) in presence of PA (0.5 mM) for 48 h. **(a)** Representative confocal images to show autophagosomes, lysosomes and autophagolysosomes stained islet cells using MDC-LysoTracker stain. Representative images are of three independent experiments. Representative immunoblot analysis of various proteins in response to inhibitors of **(b)** autophagy and **(c)** AMPK. The histogram in the right panel of each figure represents the mean

relative arbitrary pixels intensities in terms of the fold of PA control. Results are the mean \pm S.D. of three independent experiments. ^b $p < 0.05$ versus PA control; ^c $p < 0.01$ versus PA control; ^d $p < 0.05$ versus (PA + K 10 μ M); ^e $p < 0.05$ versus (PA + CQ). PA, palmitic acid; K, kaempferol; WT, wortmannin; CQ, chloroquine; C.C., Compound C.

Furthermore, to confirm the involvement of AMPK-mTOR pathway in kaempferol-induced autophagy the expression of p-AMPK and p-mTOR was analyzed. As shown in Fig. 5.2.13c, kaempferol was found to activate p-AMPK expression in PA-induced islets while there was a significant decrease in expression of p-mTOR, the downstream regulator of p-AMPK ($p < 0.05$). Furthermore, islet cells co-treated with kaempferol and compound C showed a significant reduction in LC3-II expression and increased accumulation of p62 ($p < 0.05$) (Fig. 5.2.13c). These results are in close agreement with the RIN-5F cell's data and further, confirm that kaempferol instigates autophagy by means of AMPK/mTOR pathway. Further, as shown in Fig 5.2.13b and c, kaempferol treatment decreased the cleaved caspase-3 expressions indicative of the anti-apoptotic effect of kaempferol while co-treatment of kaempferol with autophagy and AMPK inhibitors augmented the cleaved caspase-3 expressions hence causing apoptosis of pancreatic islet cells.

5.2.4. Discussion

One of the major causes of obesity linked T2DM is the deterioration of β -cell mass and function due to lipotoxicity (Butler et al., 2003). Identifying agents or mechanisms that could protect β -cells against chronic FFA overload induced damage has become a matter of concern in clinical therapies for obesity-linked T2DM (DeFronzo and Abdul-Ghani, 2011; Song et al., 2015). Naturally occurring plant derived compounds, particularly flavonoids, are promising candidates because of their cost-effectiveness, abundance in nature and very limited side effects than those interrelated with pharmaceutical agents currently under clinical use (Pandey and Rizvi, 2009).

One such natural flavonoid with profound therapeutic potential is kaempferol. It is abundantly found in various medicinal plants, fruits, and vegetables including green teas, berries, grapes, apples, citrus fruits, onions etc. Kaempferol is already known for its anti-oxidative, anti-inflammatory, anticancer and antimicrobial activities (M Calderon-Montano et al., 2011; Abo-Salem, 2014; Liao et al., 2016). Recently, the antidiabetic and anti-obesity activity of kaempferol fractions isolated from unripe soybean leaves has been reported in high-

fat diet mice model (Zang et al., 2015). Apart from this, kaempferol was also reported to increase insulin secretion and β -cell mass in obese diabetic mice (Alkhalidy et al., 2015). Although kaempferol was found to rescue β -cell mass in obese diabetic mice model but little is known about the underlying mechanism by which kaempferol exerts its cytoprotective activity. To the best of our knowledge, this is the first ever report providing evidence that kaempferol may rescue clonal pancreatic β -cells (RIN-5F cells) and isolated rat pancreatic islets from PA-induced apoptosis by inducing AMPK/mTOR-mediated autophagy. Here, we have demonstrated that kaempferol could alleviate PA-induced death in RIN-5F cells and primary islets. Our results indicate that RIN-5F cells incubated with PA showed condensed and fragmented nuclear DNA and increased caspase activity while co-treatment with kaempferol significantly abolished such changes thus acting as a cytoprotective agent.

Although flavonoids including kaempferol have been known to demonstrate potential health benefits, their poor bioavailability poses a limitation in various therapeutic applications. Initially, while deciding the concentrations to be used in this study a wide range of kaempferol concentrations (1 – 50 μ M) was adapted and finally, 10 μ M concentrations was found to be optimum for most of the effects as shown here. However, 10 μ M concentration may be of physiologically relevance since it has been reported that in case of rodents and humans the attainable plasma concentrations of flavonoids through dietary supplementation are within the range of several micromolar i.e., below 20 μ M for kaempferol (Gates et al., 2007; Zhang et al., 2013). Hence, it is interesting to speculate that the favorable effects of kaempferol on primary islets or RIN-5F cells *in vitro* may also be achieved in the relevant environment *in vivo*. However, further, in detailed studies are needed to elucidate the exact cross talks between dose and health beneficial effects using *in vitro* and *in vivo* animal models and analysis of their bioavailability where the current and already reported data can provide the base.

Increasing evidence suggested that activating autophagy is an effective mean to inhibit apoptosis in various stress and diseased state (Moreau et al., 2010). The role of autophagy in sustaining pancreatic β -cell mass and function is well established from the very fact that its dysregulation has been associated with insulin resistance, obesity and type II diabetes (Codogno and Meijer, 2010). Autophagy is a lysosome-dependent process for the turnover of dysfunctional or damaged intracellular organelles and molecules in response to several stress conditions which includes endoplasmic reticulum (ER) stress and oxidative stress. Such events of turnover further enable cells to maintain its homeostasis and protect them against stress

(Mizushima, 2007). Chronic exposure of β -cells to high levels of saturated fatty acids leads to induction of β -cell apoptosis due to oxidative ER stress and accumulation of ubiquitinated proteins within cells (Biden et al., 2014; Mir et al., 2015). Therefore, removal of these accumulated components by means of autophagy is beneficial to rescue the cell from stress. Earlier it was reported that PA overload itself induces autophagy in pancreatic β -cell as evident by autophagosomes accumulation and increased LC3 expression in these cells. In that study, activated autophagy has been proposed as a cell survival response to lipid overload (Choi et al., 2009). In contrast to those studies, another report revealed inhibition of autophagy during maturation phase of autophagy in human type 2 diabetic pancreatic β -cells (Masini et al., 2009). Likewise, recent reports supported these findings and showed that PA-induced increased accumulation of autophagosomes and LC3-II (an early phase autophagy marker) are due to decreased autophagic turnover. Thus impaired autophagy, as confirmed by marked accumulation of LC3 binding protein i.e., p62 (an autophagy substrate), likely to get cleared during the late phase of autophagy. Inhibition of autophagy turnover can be either due to hyperactivation of mTORC1 or defect in autophagosomes maturation and lysosomal fusion events (Bartolomé et al., 2014; Mir et al., 2015). Our results were also consistent with those findings, indicating PA-induced suppression of autophagic turnover in β -cells. Our results showed that there was a marginal increase in autophagosomes formation and limited fusion of autophagosomes with lysosomes (autophagolysosomes formation) in RIN-5F cells and rat islets treated with PA. This was accompanied by increased expressions of LC3-II and LC3 binding p62 proteins. Hence, together it can be assumed that PA leads to suppression of autophagic turnover in β -cells. Defective autophagy is responsible for suppression of β -cell mass and its function (Quan et al., 2012). Mice models with β -cell specific autophagy deficiency (β -cell specific Atg7 knockout mice) exhibited impaired glucose tolerance, suppressed insulin secretion and increased β -cell degeneration (Ebato et al., 2008). In contrast, activation of autophagy by metformin (AMPK activator) and rapamycin (mTOR inhibitor) protected β -cells against PA-induced β -cell death (Jiang et al., 2014; Mir et al., 2015). Thus activating autophagy can be used as a protective mechanism against PA-induced stress. In the present study, we have shown that kaempferol induces autophagy in PA-induced RIN-5F cells and primary rat islets. Our results revealed that kaempferol promoted the formation of autophagosomes as well autophagolysosomes accompanied by increased LC3 and decreased p62 expression. Based on these results it could be conceived that kaempferol alleviates PA-

induced impaired autophagy. Further, inhibition of kaempferol mediated autophagy using autophagy inhibitors abolished the cytoprotective role of kaempferol. This further strengthened our hypothesis that kaempferol mediated autophagy exerts cytoprotective effects on PA-induced β -cells. Our results were consistent with a recent report which showed that treatment with kaempferol increases neuronal survival via enhancement of autophagy in animal models of rotenone-mediated acute toxicity (Filomeni et al., 2012).

In subsequent studies, molecular mechanisms involved in the kaempferol-mediated induction of autophagy were analyzed. The pre-existing literature strongly suggests that AMPK is the positive regulator of autophagy and acts by down-regulating phosphorylation of mTOR. mTOR is a major negative regulator of autophagy that inhibits autophagy by phosphorylating ULK1 and preventing AMPK-ULK1 interactions, thus concomitantly attenuating autophagy (Han et al., 2010; Kim et al., 2011). Naturally, the inhibition of mTOR leads to the induction of autophagy in a cell. Moreover, well known antidiabetic drugs like rosiglitazone and metformin were also found to stimulate autophagy through induction of AMPK/mTOR pathway in PA stressed condition (Wu et al., 2013; Jiang et al., 2014). Likewise, it was also reported that rapamycin, the mTOR inhibitor, induced autophagy by decreasing p-mTOR expression (Mir et al., 2015). With this as the basis, we further investigated the role of AMPK-mediated signaling pathway in kaempferol-induced autophagy in PA-stressed RIN-5F cells and primary rat islets. Our results showed that kaempferol activated the AMPK/mTOR pathway, as evidenced by the increased p-AMPK and decreased p-mTOR expressions. These results are consistent with the earlier studies which showed that kaempferol activated autophagy through AMPK/mTOR pathway in Hela cells and thus exerting cytoprotection against apoptosis (Filomeni et al., 2010). Moreover, AMPK inhibitor (compound C) abolished kaempferol-induced autophagy and subsequently increased β -cell cytotoxicity.

In summary, all the results delineated in the present study corroborate well with each other to arrive at the conclusion that, kaempferol exerts cytoprotective actions by inducing autophagy via AMPK/mTOR signaling pathway in PA-stressed RIN-5F cells and rat pancreatic islets. To the best of our knowledge, this study provides new insights into our understanding of kaempferol's therapeutic potential and suggests that it could be a promising candidate either singly or in combination with other drugs/ chemicals for the prevention of obesity linked type II diabetes. Based on these data further detailed studies are warranted using

in vitro cell and *in vivo* animal based models to establish the exact cross-talks among various pathways in causing autophagy by this phytochemical.





CHAPTER 6

ROLE OF KÄEMPFEROL-MEDIATED AUTOPHAGY IN ALLEVIATION OF PALMITIC ACID-INDUCED LIPID STORES, ENDOPLASMIC RETICULUM STRESS AND PANCREATIC β -CELL DYSFUNCTION

Chapter 6. Role of kaempferol-mediated autophagy in alleviation of palmitic acid-induced lipid stores, endoplasmic reticulum stress and pancreatic β -cell dysfunction

6.1. Introduction

Type 2 diabetes mellitus (T2DM), a common subtype of diabetes, is characterized by a progressive decline in β -cell function and chronic insulin resistance. One of the major predisposing factors for the development of T2DM is obesity, in part due to elevated circulating free fatty acids (FFAs) and later ectopic fat deposition in nonadipose tissues (Giacca et al., 2011). Chronic lipid accumulation in pancreatic islet cells plays a vital role in β -cell dysfunction characterized by impaired glucose-stimulated insulin secretion (GSIS) and increased levels of apoptosis, being recognized as lipotoxicity (Assimakopoulos-Jeannet, 2004; Lim et al., 2011; Singh et al., 2017). Increased lipid deposition in pancreatic islets with subsequent apoptosis and β -cell dysfunction has been reported in animal models of T2DM such as Zucker diabetic fatty rats (Lee et al., 1994). Shimabukuro et al. have reported that treatment with thiazolidinediones lower islet fat deposition and preserves β -cell function in diabetic animal models (Shimabukuro et al., 1998). Therefore, protection of β -cells against lipid overload can be an effective strategy for counteracting obesity linked T2DM (DeFronzo and Abdul-Ghani, 2011; Song et al., 2015).

Lipids are stored in the cells as triglycerides within organelles called lipid droplets (LDs) enveloped by a monolayer of phospholipids. In addition to lipids, various proteins localize on the surface of LDs which play a significant role in lipid metabolism. The perilipins (PLINs) constitute the major LD proteins which comprise of five members, PLIN1 to PLIN5 (Bickel et al., 2009; Shao et al., 2013). Of these, perilipin 2/adipophilin (PLIN2/ADFP/ADRP) is highly expressed in pancreatic β -cells and plays an important role in intracellular lipid metabolism and serves as a marker of lipid deposition (Faleck et al., 2010; Shao et al., 2013). Recently, it was found that high-fat diet or FFAs exposure could prominently increase intracellular lipid deposition and up-regulate the PLIN2 expression level in murine and human islets (Faleck et al., 2010; Chen et al., 2017). Further, the inhibition of PLIN2 via antisense oligonucleotide was shown to reverse the FFAs-induced increase in intracellular lipid deposition exhibiting the role of PLIN2 in lipid accumulation (Faleck et

al., 2010). Similarly, Chen et al. have shown that PLIN2 is involved in triggering ER stress as well as lipid accumulation in diabetic Akita mice islets that led to the loss of β -cell mass and function (Chen et al., 2017).

ER stress is one of the major features of pathological conditions associated with obesity and diabetes. Prolonged exposure of fatty acids is well known to induce ER stress in β -cells contributing to β -cell lipotoxicity (Biden et al., 2014; Han and Kaufman, 2016). In obese and T2DM patients, the higher demand for insulin production along with increased levels of FFAs, lead to chronic ER stress in β -cells (Sharma et al., 2014). The palmitate-treated murine islets exhibited activated ER stress as well as unfolded protein response pathways (Biden et al., 2014). The unfolded protein response is an adaptive response to ER stress that first attempts to alleviate ER stress by reducing ER protein load and improving folding capacity and clearance of misfolded proteins but shifts toward apoptosis in prolonged and severe ER stress (Rashid et al., 2015). The transcription factor C/EBP homologous protein (CHOP) is a downstream component of ER stress pathways and a key mediator of cell death in response to ER stress found to be increased in PA- and high glucose-treated pancreatic β -cells (Oyadomari and Mori, 2004).. Moreover, previous studies showed that the targeted disruption or deletion of this gene delayed the onset of diabetes in Akita mice (Oyadomari et al., 2002). Likewise, the CHOP deficiency restored the β -cell mass in murine models of type 2 diabetes emphasizing that ER stress is at a middle stage in the pathophysiology of diabetes along with other factors (Song et al., 2008).

Autophagy is a lysosomal degradation pathway of dysfunctional macromolecules and organelles which protects cells from stressed conditions and acts as an adaptive pro-survival response (Klionsky et al., 2016). This process comprises of several consecutive steps: sequestration, transport to the lysosome, degradation, and utilization of degradation products (Mizushima, 2007). Recently, intracellular LDs have been also distinguished as the substrate for autophagy. Autophagy mobilizes lipids from LDs for maintenance of lipid homeostasis thus averting intracellular lipid overload. This unique cellular process is known as lipophagy (Singh et al., 2009; Dong and Czaja, 2011). In lipophagy, the LDs, triglycerides and cholesterol are engulfed by autophagosomes and delivered to lysosomes targeted for degradation by acid hydrolases. Lipophagy regulates cellular energy homeostasis by generating FFAs through the breakdown of triglycerides and further enhances the rate of mitochondrial β -oxidation. Impaired lipophagy exhibited increased cellular triglyceride content and LDs

number in response to a lipid challenge in cultured hepatocytes confirming the role of autophagy in lipid metabolism (Singh et al. 2009). Loss of autophagy has been found to be associated with lipid metabolic disorders such as fatty liver and obesity (Singh and Cuervo, 2012). In later studies, lipophagy was evident in various cell types including neurons, fibroblasts and stellate cells (Liu and Czaja, 2013). Furthermore, when autophagy is impaired, the architecture and function of β -cells could not be maintained (Fujitani et al., 2009). Autophagy was found to be inhibited by palmitic acid in pancreatic β -cell lines and primary β -cells that led to the loss of β -cell mass and function (Mir et al., 2015). Similarly, in another study, β -cell specific Atg7 knockout mice (β -cells specific autophagy-deficient mice) fed with high-fat diet exhibited progressive β -cells degeneration with impaired insulin secretion, compromised glucose tolerance and increased apoptotic cell death (Ebato et al., 2008). It was reported earlier that activated autophagy could reduce ER stress and thus β -cell apoptosis but its impairment may lead to the chronic stage of ER stress, thus eliciting the expression of the stress-CHOP protein (Bachar-Wikstrom et al., 2013; Mir et al., 2015). Similarly, autophagy stimulation in response to rapamycin decreased ER stress (Mir et al., 2015). Thus on one side activated autophagy could reduce lipid-induced ER stress while on another side, autophagy has been shown to degrade lipid droplets (Dong and Czaja, 2011). Thus it can be hypothesized that stimulation of autophagy could inhibit PA-induced lipid deposition in β -cells which may further lead to the reduction of ER stress and inhibition of loss of β -cells mass and function. Although, it is evident that autophagy is essential for maintenance of β -cell mass and function in lipid overload conditions, to the best of our knowledge the exact cross-talk between autophagy and lipid metabolism in pancreatic β -cells in a hyper-lipidic condition has rarely been reported. Therefore, further studies on the cellular mechanisms by which lipophagy regulate lipid metabolism in pancreatic β -cells with special emphasis on the role of phytochemicals will certainly discover new insights making this pathway a potential therapeutic target in obesity-linked T2DM.

Kaempferol, a natural flavonol, is well known for its anti-oxidative and anti-inflammatory effects. It is found abundantly in various fruits and vegetables such as berries grapes, apples, green tea, broccoli, cabbage, kale, beans and tomato (M Calderon-Montano et al., 2011). Kaempferol has also been reported for its role as an osteogenic, neuroprotective and anticancer agent (Kashyap et al., 2017). Recently, the antidiabetic and anti-obesity effects of

kaempferol have been reported in high-fat diet mice model (Zang et al., 2015). Likewise, kaempferol was also reported to increase insulin secretion and β -cell mass in chronic hyperlipidemic condition and in obese diabetic mice (Zang et al., 2015; Varshney et al., 2017). We have previously reported that kaempferol protects β -cells from PA-induced apoptosis through induction of autophagy (Varshney et al., 2017). As discussed earlier, ER stress generated due to the accumulation of lipid in β -cells is the major cause of cell death in lipid overload conditions. Based on this information in this study we evaluated the inhibitory effects of kaempferol-induced autophagy on PA-induced ER stress and lipid deposition.

6.2. Brief methodology

6.2.2. Cell culture and treatment

The RIN-5F cell line was maintained in RPMI 1640 media supplemented with 10% heat-inactivated fetal bovine serum and 1% streptomycin–penicillin solution under an atmosphere of 5% CO₂ and 95% humidified air at 37°C. Prior to the cell-based assays, basal media was replaced with RPMI 1640 media supplemented with 1% bovine serum albumin and 0.5 mM PA and the cells were further treated with various concentrations of kaempferol in presence or absence of certain inhibitors i.e., wortmannin (inhibitor of initial stage of autophagy that blocks formation of autophagosomes) or chloroquine (a lysosomotropic agent and late-stage autophagy inhibitor that blocks fusion of autophagosomes with lysosomes) or compound C (an AMPK inhibitor). For each experiment, wortmannin (100 nM), chloroquine (10 μ M) and compound C (10 μ M) were added to the respective wells 1 h prior to the kaempferol treatment (unless stated). The normal control cells were treated with only RPMI media containing 1% bovine serum albumin.

6.2.3. siRNA transfections

The oligonucleotide small interfering RNA (siRNA) specifically targeting rat Atg7 and AMPK were used in the study. Cell were transfected according to protocol described in chapter 3. After 24 h of incubation, the cells were treated with or without 10 μ M kaempferol in

presence of 0.5 mM PA for another 48 h.

6.2.4. Animals

Female Sprague-Dawley rats of age 8–10 weeks old were procured from National Institute of Pharmaceutical Education and Research, Mohali, India with the approval of Institutional Animal Ethics Committee (MMCP/IAEC/16/05) of M. M. College of Pharmacy, Maharishi Markandeshwar University, Mullana-Ambala, India. They were housed under standard conditions and allowed to acclimatize for two weeks before the experiment. All the animal-related experiments were performed according to the guidelines and approval of the Institutional Animal Ethics Committee.

6.2.5. Islets isolation and treatment

The rat pancreatic islets were isolated as described in chapter 3 of this thesis. The purified islets were then screened for their specificity by dithizone staining. For treatment, dithizone-stained islets were counted and divided into various groups for respective treatments.

6.2.6. Preparation of palmitic acid-containing media

The RPMI media containing 0.5 mM PA was prepared as discussed in chapter 3 of this thesis.

6.2.7. Labeling of lipid droplets with BODIPY stain

For this assay, the RIN-5F cells were seeded onto coverslips at a density of 2.5×10^5 cells/coverslip and treated with respective treatments. After 48 h of treatment, the cells were washed with phosphate buffer saline and fixed with 4% formaldehyde for 10 min at room temperature. Further, the cells were washed with phosphate buffer saline and incubated with BODIPY 493/503 at working concentration of 5 μ g/ml in phosphate buffer saline for 20 min at room temperature. After incubation, the cells were washed twice with phosphate buffer saline and counterstained with DAPI. The slides were prepared and the cells were imaged under confocal

laser scanning microscope (LSM 780, Carl Zeiss, Germany) at excitation and emission wavelengths of 493 and 503 nm, respectively.

6.2.8. Double immunofluorescence and co-localization studies

For studying co-localization of LC3 protein with LDs, the cells were seeded on sterile coverslips at a density of 2.5×10^5 cells/ coverslip and incubated for 24 h, thereafter treated with respective test chemicals for another 48 h. On completion of incubation, the cells were fixed with 4% formaldehyde for 15 min followed by washing with phosphate buffer saline thrice for 5 min each. The fixed cells were then permeabilized with 0.1% Triton X-100 for 10 min, thereafter the cells were washed and blocked with 2% bovine serum albumin for 1 h at room temperature. After blocking, the cells were incubated with primary antibody (1:250) overnight at 4°C followed by incubation with the Texas red-conjugated secondary antibody (1:500) for 1 h at room temperature. Further, the cells were washed and incubated with BODIPY (5 μ g/ml in phosphate buffer saline) for 20 min at room temperature. Then, the cells were counterstained with DAPI for 5 min to stain the nucleus.

For double immunofluorescence labeling, after blocking the cells were incubated with primary antibody against LC3 (1:250) for 2 h at room temperature and subsequently washed and then incubated with fluorescein isothiocyanate (FITC)-conjugated respective secondary antibody for 1 h. Thereafter, the cells were washed and incubated with the PLIN2 antibody (1:250) for 1 h at room temperature. The cells were then incubated with Texas red-conjugated appropriate secondary antibody for next 1 h. Then coverslips were mounted on slides and visualized under the confocal microscope equipped with 405 nm, 488 nm and 543 nm lasers (LSM 780, Carl Zeiss, Germany).

6.2.9. Insulin secretion and content analysis

The RIN-5F cells (2×10^5 cells/ well) or rat isolated primary islets (15 islets/ well) were seeded into 12-well plate and incubated for 24 h in 5% CO₂ atmosphere. Then the cells/ islets were treated with various test chemicals for 48 h. Thereafter, the cells were washed and pre-incubated with glucose-free Krebs buffer containing 0.25% BSA for 1 h prior to incubation with Krebs buffer containing 2.8 mM (Basal) or 16.7 mM glucose (High glucose) for next 1 h.

On completion of treatment, the level of released insulin by the cells/ islets were measured by rat insulin enzyme immunoassay kit (SPI-Bio, Bertin Pharma, France) according to manufacturer's protocol and estimated at 410 nm using a plate reader (Fluostar Optima, BMG Labtech, Germany). For measurement of total insulin content, after completion of the incubations, the cells and islets were lysed with acid/ethanol (0.18 N HCl in 70% ethanol) overnight at 4°C and then homogenized. After centrifugation, the lysates were neutralized to pH 7.2 with 0.4 M Tris buffer pH 8.0. Further, insulin levels in all the samples were measured as stated above and normalized with whole cellular protein content.

6.2.10. Statistical analysis

Quantitative data are presented as means \pm standard deviation (SD) of three independent experiments and statistically evaluated by one-way ANOVA followed by Tukey's post hoc test using Graph Pad Prism 6 software (Graph Pad Software, San Diego, CA, USA). For the data analysis, $p < 0.05$ was considered to be statistically significant.

6.3. Results

6.3.1. Kaempferol inhibits intracellular lipid accumulation in RIN-5F cells

As discussed earlier, chronic exposure of PA exhibits lipid accumulation in β -cells that lead to the loss of β -cell mass and function. Thus to determine the effect of kaempferol on PA-induced lipid accumulation, the intracellular lipid was analyzed by Oil Red O staining and quantified at 510 nm using a plate reader (Fluostar Optima, BMG Labtech, Germany). As shown in Fig. 6.1a, PA-treated RIN-5F cells showed significantly increased lipid accumulation which was significantly reduced in presence of kaempferol (PA + K). Further, quantification of stored lipid exhibited that kaempferol treatment reduced lipid content by about 1.75-fold as compared to PA alone treated group ($p < 0.05$) (Fig. 6.1b). Since triglycerides are the major component of the LDs, thus its content in treated cells was also evaluated. As shown in Fig. 6.1c, the intracellular triglyceride content was also remarkably increased in PA-treated cells and found to be around ~ 3 fold of normal control cells. However, the cells co-treated with PA and kaempferol exhibited decreased TG content which was reduced down by about 2-fold as

compared to PA-treated group ($p < 0.05$). Similarly, BODIPY staining data showed that kaempferol-treated group exhibited fewer LDs than the PA-treated group, indicative of kaempferol-induced reduction of LDs (Fig. 6.1d). Together, it can be inferred that kaempferol could alleviate PA-induced lipid accumulation in RIN-5F cells. The major reason of selecting this dose of kaempferol (10 μ M) is that it showed optimum response with kaempferol as compared to other doses as observed in the study reported in chapter 1, at the same time it is also a physiologically relevant dose.

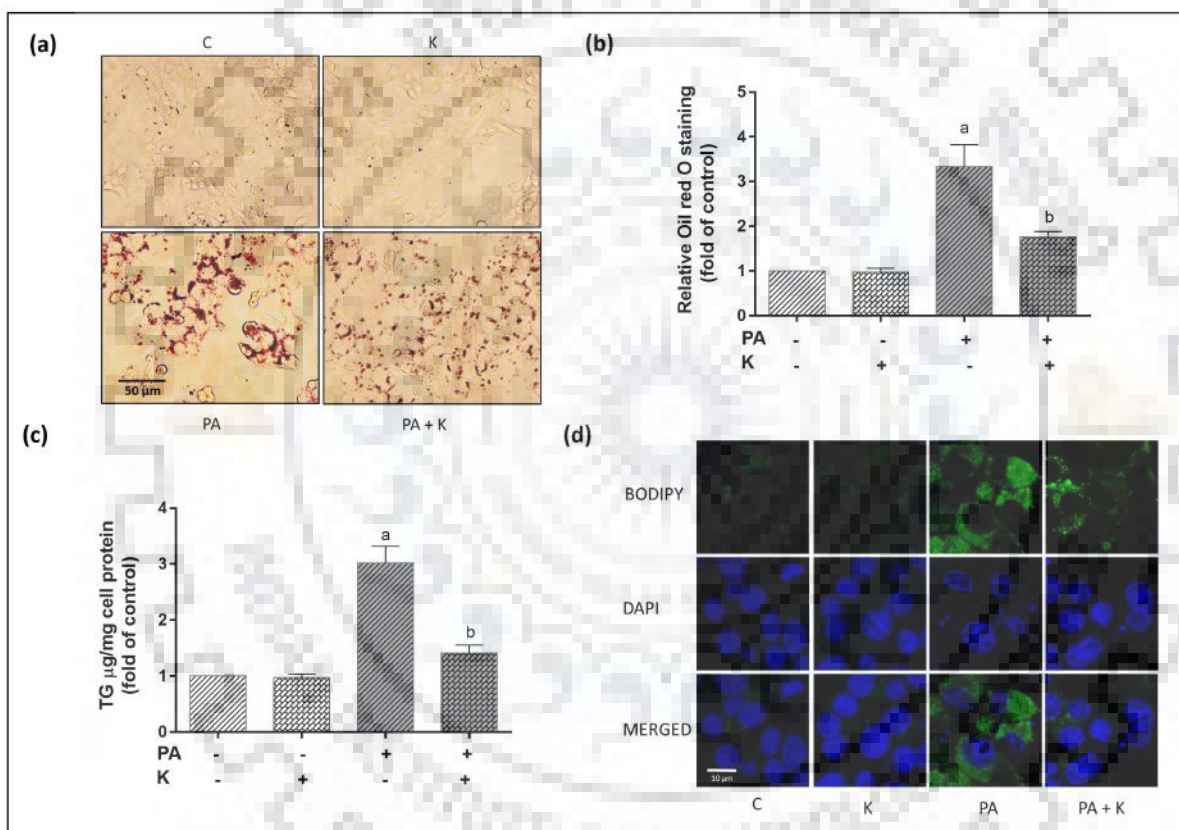


Fig. 6.1. Kaempferol alleviates PA-induced clonal pancreatic β -cells lipid stores. RIN-5F cells were treated with kaempferol (10 μ M) in presence or absence of PA (0.5 mM) for 48 h. (a) Microscopic images of Oil Red O stained cells; Histogram representing (b) lipid content; (c) triglyceride content within treated cells. Results are the mean \pm S.D. of three independent experiments; (d) Representative confocal images showing BODIPY- and DAPI-stained cells. a and b indicates statistically significant at $p < 0.05$ with respect to vehicle- and PA-treated control groups respectively. C, control; PA, palmitic acid; K, kaempferol.

Further, to validate the findings mRNA expression analysis of *Plin2* and *Plin3*, the genes involved in the expression of the respective LD coat proteins and are associated with pancreatic β -cells lipid accumulation, was performed by RT-PCR. In PA-treated cells, *Plin2* and *Plin3* mRNA expressions were found to be increased by around 3- and 2.5-fold respectively as compared to normal control cells while kaempferol treatment exhibited reduced *Plin2* and *Plin3* mRNA expressions in a dose-dependent manner ($p < 0.05$) (Fig. 6.2a). At 10 μM concentration, kaempferol treatment reduced PA-induced *Plin2* mRNA expressions from \sim 3- to 2.4-fold whereas there was only marginal reduction in *Plin3* expression ($p < 0.05$) (Fig. 6.2a).

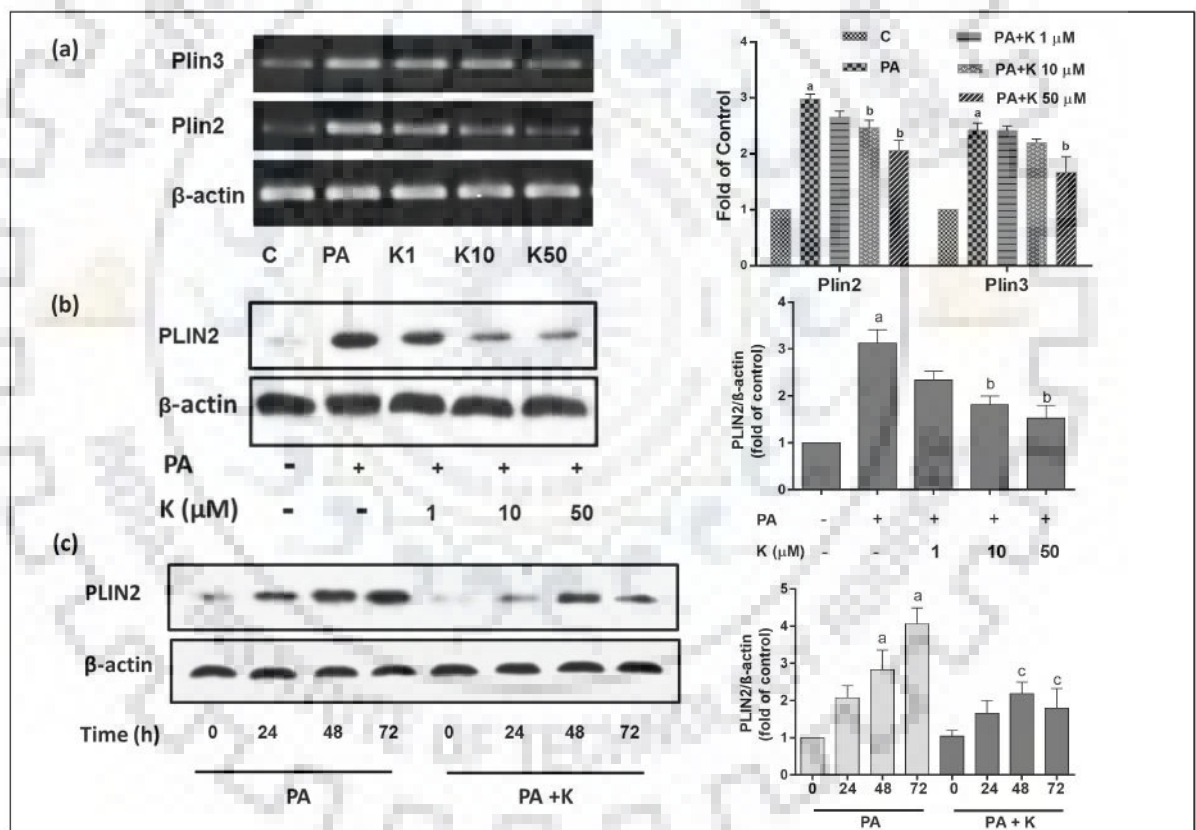


Fig. 6.2. Kaempferol alters expression of genes involved in lipid metabolism. Representative (a) RT-PCR analysis of lipid droplets marker genes and (b) immunoblot of PLIN2 with increasing dose and (c) time durations. The histogram in the right panel represents the mean relative arbitrary pixel intensities of mean \pm S.D. of three independent experiments expressed as fold change with respect to the vehicle-treated control group. For Fig (a and b) a, $p < 0.05$ versus vehicle-treated control group; b, $p < 0.05$ versus PA-treated control group

whereas for Fig (c) a, $p < 0.05$ versus PA (0 h) treated control group; c, $p < 0.05$ versus PA-treated group of respective time duration. C, control; PA, palmitic acid; K, kaempferol.

Thereafter, PLIN2 protein expression was monitored by immunoblot analysis. As shown in Fig. 6.2b and c, the increase in PA-mediated PLIN2 expression was markedly inhibited by kaempferol in a dose- and time-dependent manner respectively. The PLIN2 protein expression was found to be down-regulated by ~ 2 -fold when PA-challenged cells were co-treated with 10 μM kaempferol for 48 h with respect to only PA-treated group ($p < 0.05$) (Fig. 6.2b and c). Thus, together it can be clearly speculated that kaempferol inhibits PA-induced lipid accumulation in RIN-5F cells.

6.3.2. Kaempferol-induced autophagy facilitates a decrease in PA-induced lipid stores

In our previous study, we have shown that kaempferol protects pancreatic β -cells from PA-induced apoptosis through induction of autophagy (Varshney et al., 2017). In the present study, we intended to determine whether the autophagy is involved in kaempferol-mediated attenuation of lipid accumulation in RIN-5F cells. To analyze the role of autophagy in kaempferol's lipid inhibitory activity, various inhibitors were included in the study i.e., (i) wortmannin for inhibition of autophagosomes formation; (ii) chloroquine for inhibition of lysosomal action; and (iii) Atg7 siRNA for knockdown of Atg7 which is an important protein involved in the formation of matured autophagosomes. As shown in Fig. 6.3a and b, inhibition of autophagy by wortmannin and chloroquine prominently abolished the kaempferol-mediated inhibition of lipid accumulation and led to increased accumulation of lipids in PA-challenged RIN-5F cells as determined by Oil Red O staining ($p < 0.05$). Similarly, kaempferol-induced inhibition of triglyceride content in PA-stressed cells was also shown to be reverted in presence of autophagy inhibitors. Co-treatment of PA-induced cells with wortmannin and chloroquine along with kaempferol showed a significant increase in triglyceride content by about ~ 3 - and 3.2-fold respectively as compared to only kaempferol-treated cells ($p < 0.05$) (Fig. 6.3c).

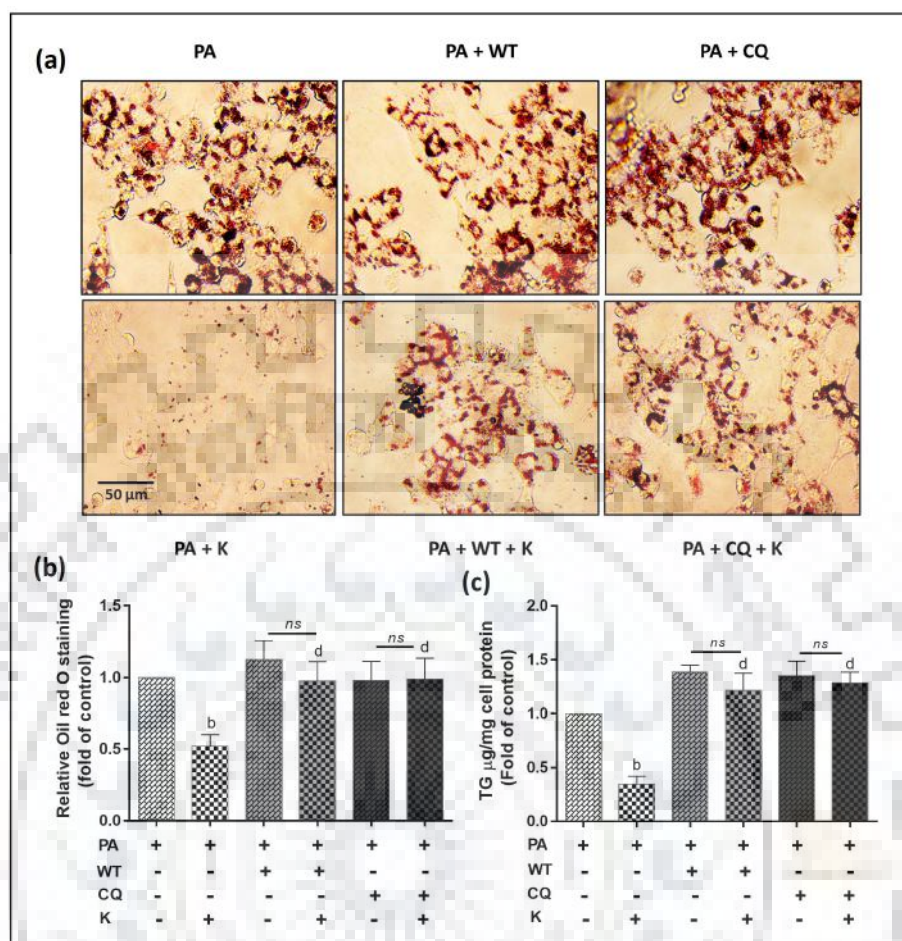


Fig. 6.3. Kaempferol-induced autophagy facilitates decrease in PA-induced lipid stores. RIN-5F cells were incubated with kaempferol (10 μ M) with or without wortmannin (100 nM) or chloroquine (10 μ M) in presence of PA (0.5 mM) for 48 h. (a) Microscopic images of Oil Red O stained cells; Histogram representing (b) lipid content; (c) triglyceride content of treated cells. Results are the mean \pm S.D. of three independent experiments. b, $p < 0.05$ versus PA control; d, $p < 0.05$ versus (PA + K) group. PA, palmitic acid; K, kaempferol; WT, wortmannin; CQ, chloroquine; ns, non-significant.

Further, BODIPY staining also confirmed that autophagy inhibition led to more accumulation of lipids. As shown in Fig. 6.4a, the cells co-treated with kaempferol and wortmannin/chloroquine exhibited more LDs (stained by BODIPY) as compared to kaempferol-treated cells in presence of PA. To exclude the possibility that kaempferol may inhibit the formation of LDs, kaempferol was added to the cells at two different time periods i.e., (i) simultaneous incubation of cells with PA and kaempferol and (ii) pre-incubated with PA followed by kaempferol treatment. As shown in Fig. 6.4b, the numbers of LDs were almost

identical in both the cases of co- or post-treatment of kaempferol with respect to PA treatment. This suggests that the effect of kaempferol on LDs reduction is mainly reliant on degradation but not inhibition of formation.

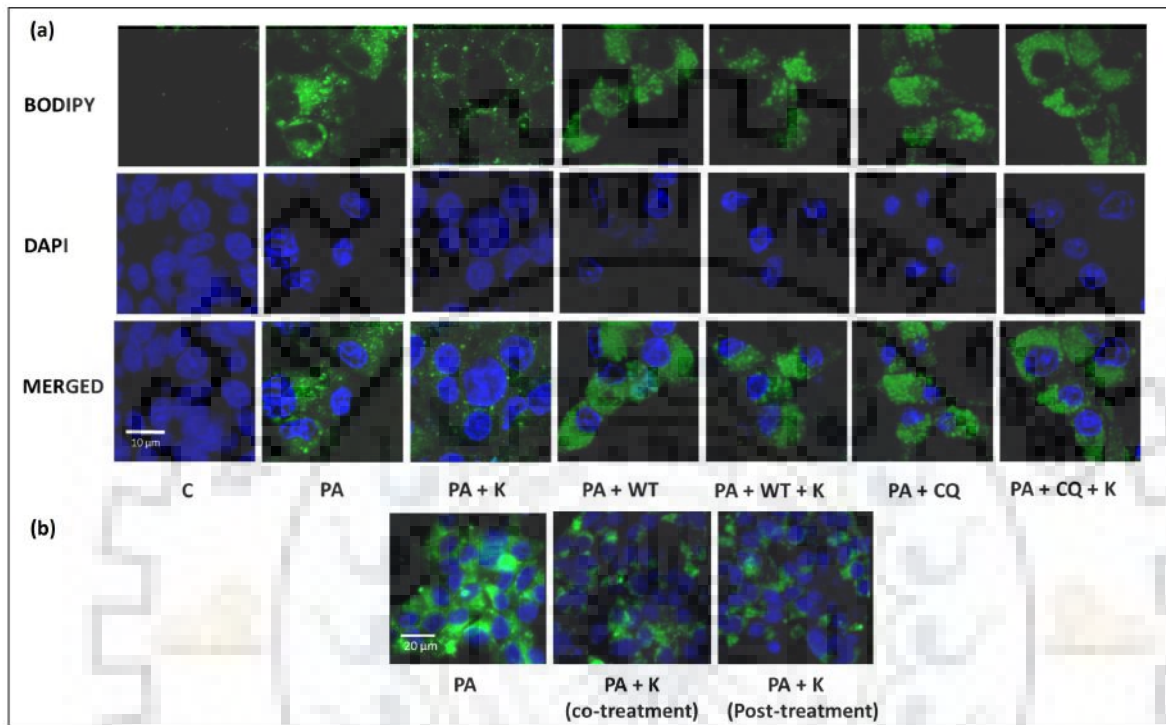


Fig. 6.4. Autophagy inhibition abolishes kaempferol-reduced lipid droplets accumulation. Representative confocal images showing lipid droplets as stained by BODIPY stain and counterstaining with DAPI after RIN-5F cells were incubated with (a) kaempferol (10 μ M) with or without wortmannin (100 nM) or chloroquine (10 μ M) in presence of PA (0.5 mM) for 48 h; (b) kaempferol in two different conditions i.e., co-treatment with PA and kaempferol for 48 h or pre-incubated with PA for 12 h followed by kaempferol treatment for next 36 h. C, control; PA, palmitic acid; K, kaempferol; WT, wortmannin; CQ, chloroquine.

Moreover, to determine whether LDs are associated with lipophagy, the co-localization studies of autophagosomes, lysosomes and LDs were performed. As shown in Fig. 6.5, kaempferol treatment exhibited increased autophagosomes and lysosomes as indicated by MDC and LysoTracker staining respectively while a limited number of LDs. PA-treated cells displayed BODIPY-stained LDs found to be co-localized with few autophagosomes but with limited lysosomes as indicated by some degree of white-stained regions while kaempferol treatment exhibited more co-localization of LDs with autophagosomes as well as lysosomes

(increased white stained regions). Further, inhibition of kaempferol-induced autophagy by means of wortmannin showed very few white stained regions indicating limited co-localization of LDs with autophagosomes and lysosomes. While chloroquine treatment displayed enhanced co-localization of LDs with autophagosomes with respect to PA group as well as PA and kaempferol co-treated group which could be due to inhibition of lysosomal degradation of LDs sequestered autophagosomes (Fig. 6.5). Collectively, it can be inferred that kaempferol-induced increase in autophagosomes and lysosomes are involved in lipid degradation in PA-challenged RIN-5F cells.

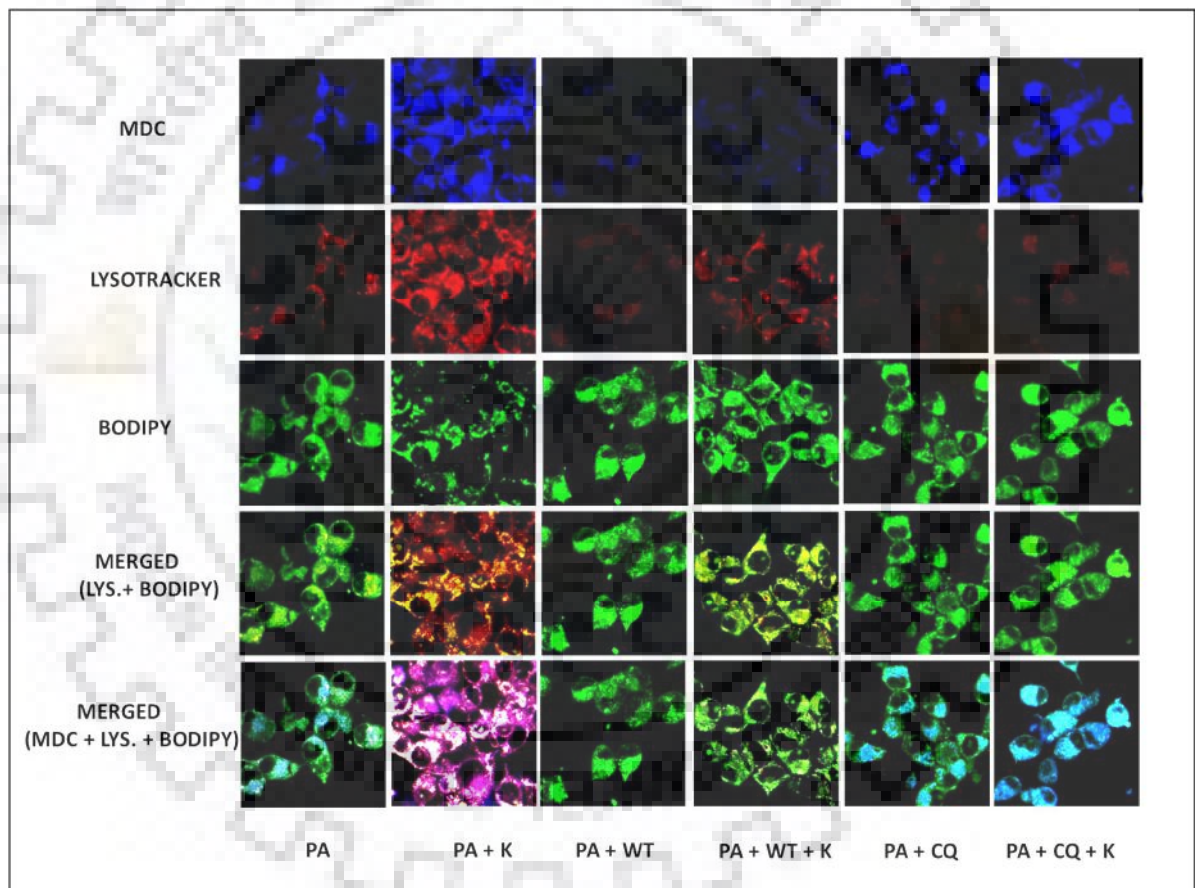


Fig. 6.5. Kaempferol treatment exhibits co-localization of lipid droplets to autophagolysosomes. Representative confocal images showing co-localization of BODIPY stained lipid droplets to autophagosomes as well as lysosomes stained by MDC and LysoTracker respectively. PA, palmitic acid; K, kaempferol; WT, wortmannin; CQ, chloroquine.

Further, immunoblot analysis of PLIN2, the LD coat protein, revealed that inhibition of autophagy increased the PLIN2 expression and hence lipid accumulation in the kaempferol-treated cells. Co-treatment of kaempferol with wortmannin and chloroquine increased the expression of PLIN2 by ~ 1.9 - and 2.1 -fold respectively as compared to kaempferol treatment ($p < 0.05$) (Fig. 6.6a). As usual, the expression of other autophagy markers like LC3, p62 and Atg7 showed similar patterns as expected in the autophagic process (reported earlier) thus further confirming the involvement of autophagy in the lipid sequestration process in RIN 5F cells (Fig. 6.6a). Similarly, inhibition of autophagy by Atg7 siRNA also significantly increased PLIN-2 expressions in kaempferol treated PA-challenged cells ($p < 0.05$) (Fig. 6.6b).

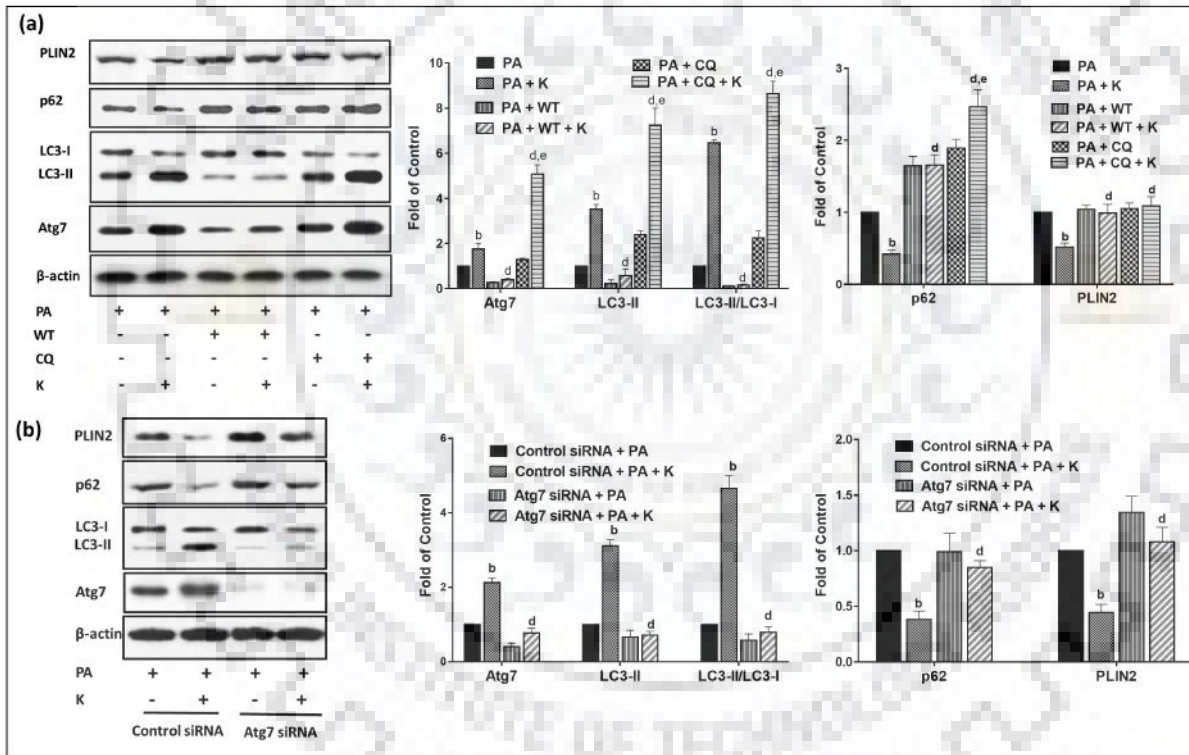


Fig. 6.6. Autophagy inhibitors impair kaempferol-induced reduction of lipid deposition by altering autophagy-linked gene expressions. Representative immunoblots of various proteins in response to (a) wortmannin and chloroquine and (b) Atg7 siRNA. The histogram in the right panel represents the mean relative arbitrary pixels intensities in terms of the fold of PA-treated control group for respective genes. Results are the mean \pm S.D. of three independent experiments. b, $p < 0.05$ versus PA control; d, $p < 0.05$ versus (PA + K); e, $p < 0.05$ versus (PA + CQ). PA, palmitic acid; K, kaempferol; WT, wortmannin; CQ, chloroquine.

Additionally, the co-localization study of LC3, the main marker of autophagosomes with LDs/ PLIN2 (the maker of LDs) by double immunofluorescence study further strengthened the findings. As shown in Fig. 6.7 and 6.8, the cells treated with PA exhibited a limited number of co-localization of LC3 with LDs (Fig. 6.7, column 1) or PLIN2 (Fig. 6.8, column 1) as evidenced by limited yellow dots while cells co-treated with PA and kaempferol showed increased number of co-localization of LC3 with LDs (Fig. 6.7, column 2) or PLIN2 (Fig. 6.8, column 2) as indicated by more yellow dots. This data demonstrated a direct association of LDs/PLIN2 with LC3 in kaempferol-treated RIN-5F cells. Further, inhibition of autophagosomes by means of Atg7 siRNA inhibited the kaempferol-mediated increase in co-localization of LC3 and LDs/PLIN2 (Fig. 6.7, column 8)/ (Fig. 6.8, column 8). Atg7-mediated inhibition led to decrease in LC3 expression while the increase in more LDs in kaempferol-treated RIN-5F cells which confirms the involvement of autophagosomes in lipid degradation. While in presence of chloroquine, kaempferol treatment exhibited an increased number of co-localization as compared to cells treated with kaempferol alone (Fig. 6.7, column 4)/ (Fig. 6.8 column 4). Such an observation is affirmative of the fact that increase in autophagosomes, as well as LDs, are due to inhibition of their degradation by lysosomes. Thus, together it can be clearly inferred that kaempferol-induced lipophagy is involved in LDs degradation in PA-induced RIN-5F cells.

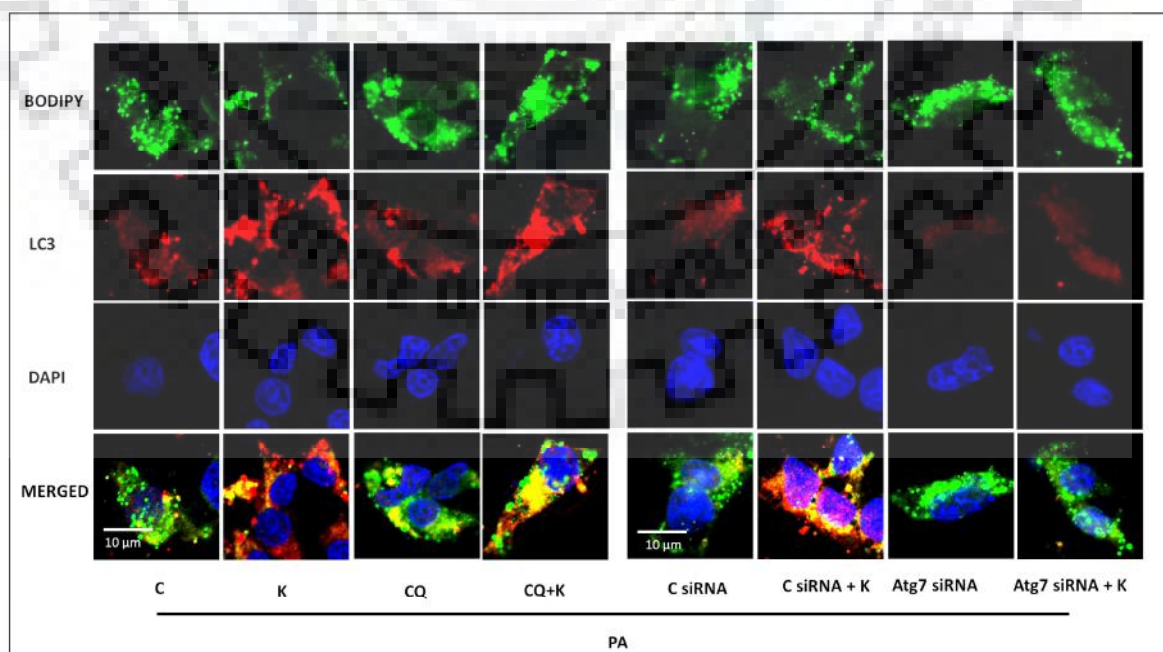


Fig. 6.7. Autophagy inhibitors attenuate kaempferol-induced sequestration of lipid droplets into autophagosomes. Representative confocal images showing co-localization of

immunostained LC3 protein with BODIPY-stained lipid droplets after RIN-5F cells were treated with kaempferol (10 μ M) with or without various inhibitors in presence of PA (0.5 mM) for 48 h. PA, palmitic acid; K, kaempferol; C, control; CQ, chloroquine.

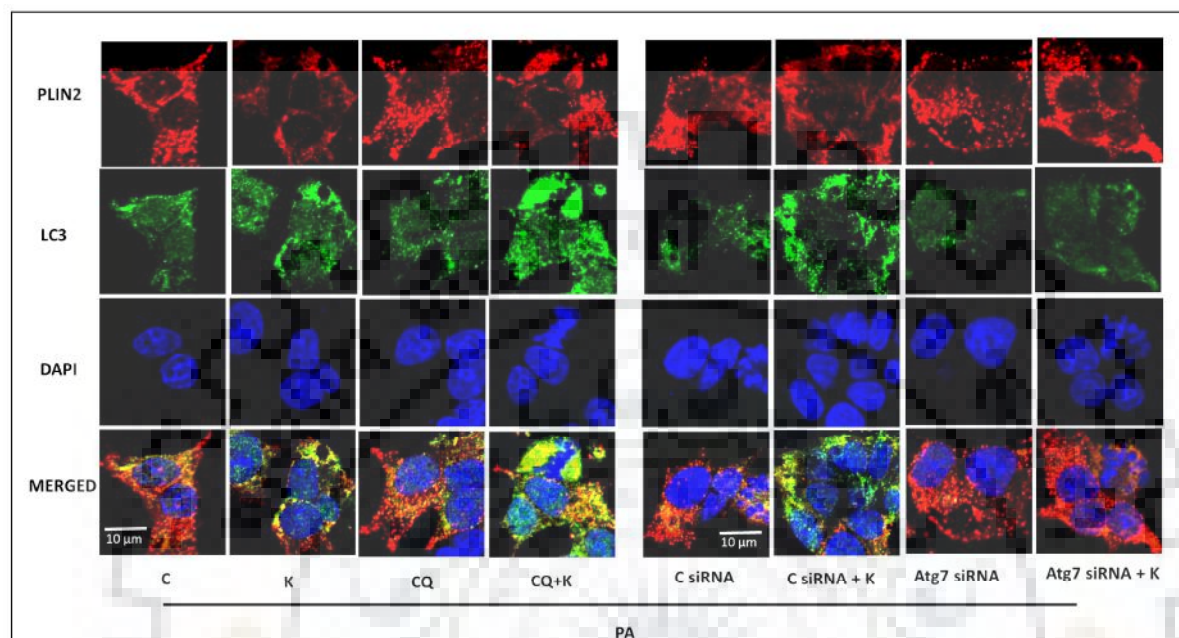


Fig. 6.8. Inhibition of autophagy impairs interaction of LC3 protein with PLIN2 protein. Representative confocal images showing co-localization of LC3 protein with PLIN2 protein as visualized by double immunofluorescence labeling. PA, palmitic acid; K, kaempferol; C, control; CQ, chloroquine.

6.3.3. AMPK/mTOR pathway signaling mediates kaempferol-mediated lipophagy

In our previous study, we showed that AMPK/mTOR pathway is involved in kaempferol-induced autophagy (Varshney et al., 2017). Thus we intended to determine whether AMPK/mTOR signaling is involved in kaempferol-mediated lipid degradation as well. In order to confirm the specific involvement of AMPK signaling in lipophagy induction, intracellular lipid deposition was analyzed in presence of AMPK inhibitors namely compound C and AMPK siRNA. As shown in Fig. 6.9a, b and c, the compound C treatment abolished the kaempferol-induced decrease in lipid stores (Fig. 6.9a and b) and led to increase in triglyceride content (Fig. 6.9c). The cells co-treated with kaempferol and compound C showed about 2- and 3.5-fold increase in lipid (Fig. 6.9b) and triglyceride (Fig. 6.9c) content respectively as

compared to kaempferol-treated cells in presence of PA ($p < 0.05$). Further, compound C and kaempferol co-treated cells exhibited more BODIPY stained regions with respect to kaempferol-treated cells (Fig. 6.9d), indicative of AMPK dependent actions.

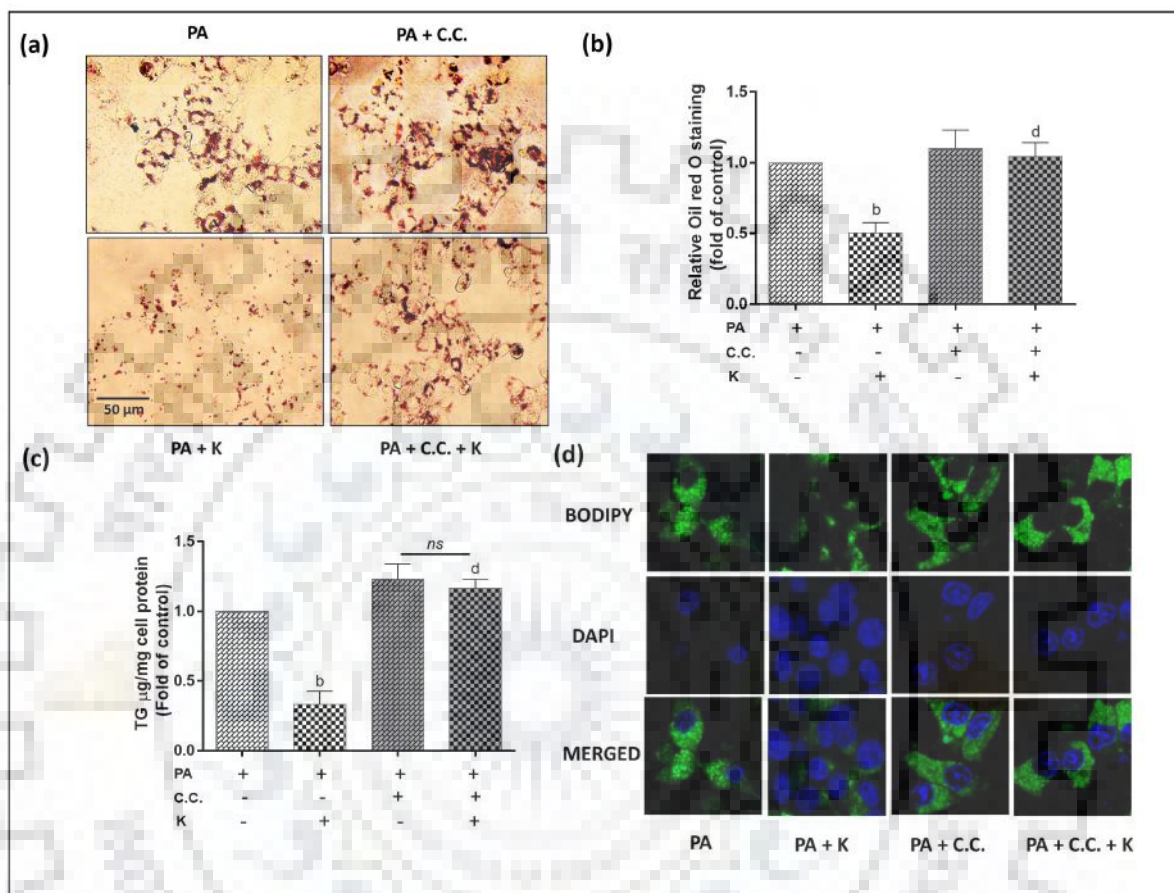


Fig. 6.9. AMPK/mTOR signaling is involved in kaempferol-induced reduction of lipid stores. The RIN-5F cells were incubated with kaempferol (10 μ M) with or without compound C (10 μ M) in presence of PA (0.5 mM) for 48 h. (a) Representative microscopic images of Oil Red O stained cells. Histograms represent quantification of (b) lipid and (c) triglyceride content within cells. Results are the mean \pm S.D. of three independent experiments. (d) Representative confocal images showing BODIPY- and DAPI-stained cells. b, $p < 0.05$ versus PA control; d, $p < 0.05$ versus (PA + K). PA, palmitic acid; K, kaempferol; C.C., compound C.

In the next phase, the immunoblot analysis of cells treated with kaempferol in presence of compound C (Fig. 6.10a) or AMPK siRNA (Fig. 6.10b) showed an increased level of PLIN2 protein as compared to cells treated with kaempferol alone ($p < 0.05$). Interestingly, as expected, inhibition of AMPK by compound C or siRNA also abolished the kaempferol-induced

conversion of LC3-I to LC3-II and led to increased p62 accumulation within cells with concomitant increase in the level of mTOR, indicative of inhibition of autophagy (Fig. 6.10a and b).

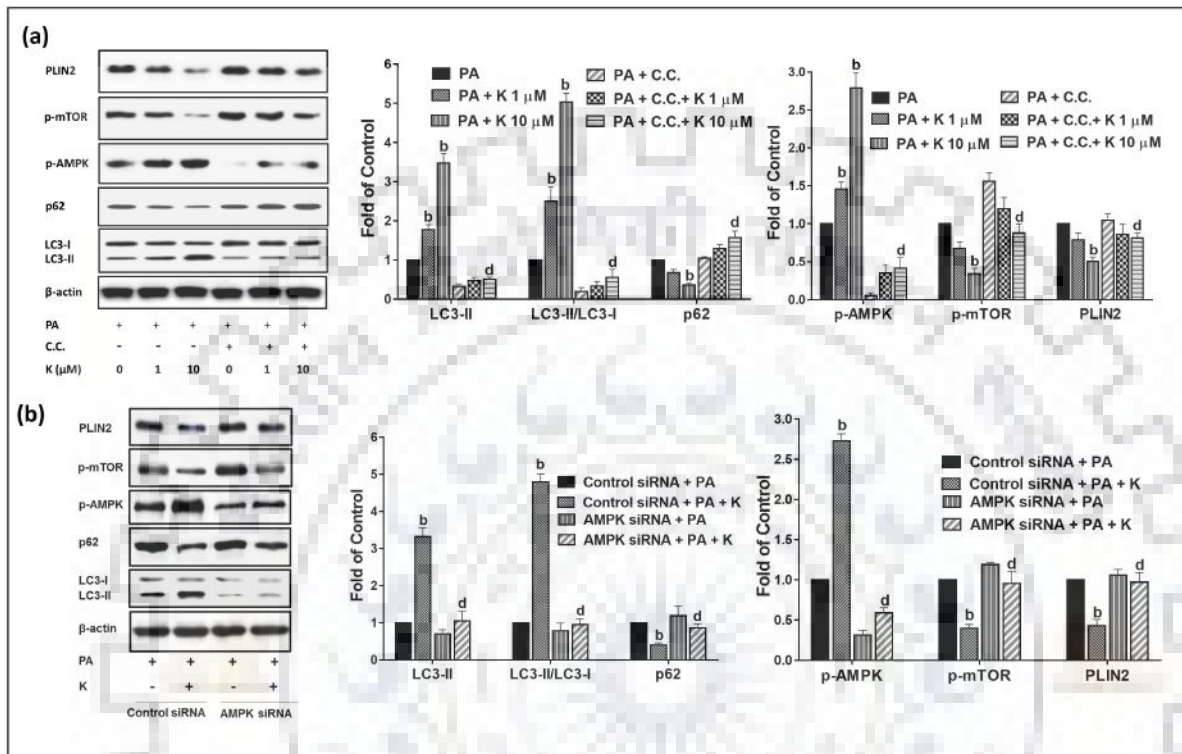


Fig. 6.10. AMPK inhibitors abolish kaempferol-mediated lipophagy. Representative immunoblots of various proteins in presence of (a) compound C (10 μ M) and (b) AMPK siRNA. The histogram in the right panel of each figure represents the mean relative arbitrary pixels intensities in terms of fold over control (PA) in respective figures. Results are the mean \pm S.D. of three independent experiments. b, $p < 0.05$ versus PA control; d, $p < 0.05$ versus (PA + K 10 μ M). PA, palmitic acid; K, kaempferol; C.C., compound C.

Moreover, LC3 and LDs/PLIN2 co-localization studies in presence of AMPK inhibitor strengthened the fact that AMPK/mTOR signaling is involved in kaempferol-induced lipophagy as indicated by decreased number of co-localization of LC3 with LDs (Fig. 6.11a, column 4) or PLIN2 (Fig. 6.11b, column 4) in cells treated with kaempferol respectively in presence of AMPK siRNA. This could be attributed to the fact that the treatment with AMPK siRNA inhibited the kaempferol-mediated autophagosomes formation which in turn led to inhibition of lipid degradation and further deposition of lipids in RIN-5F cells.

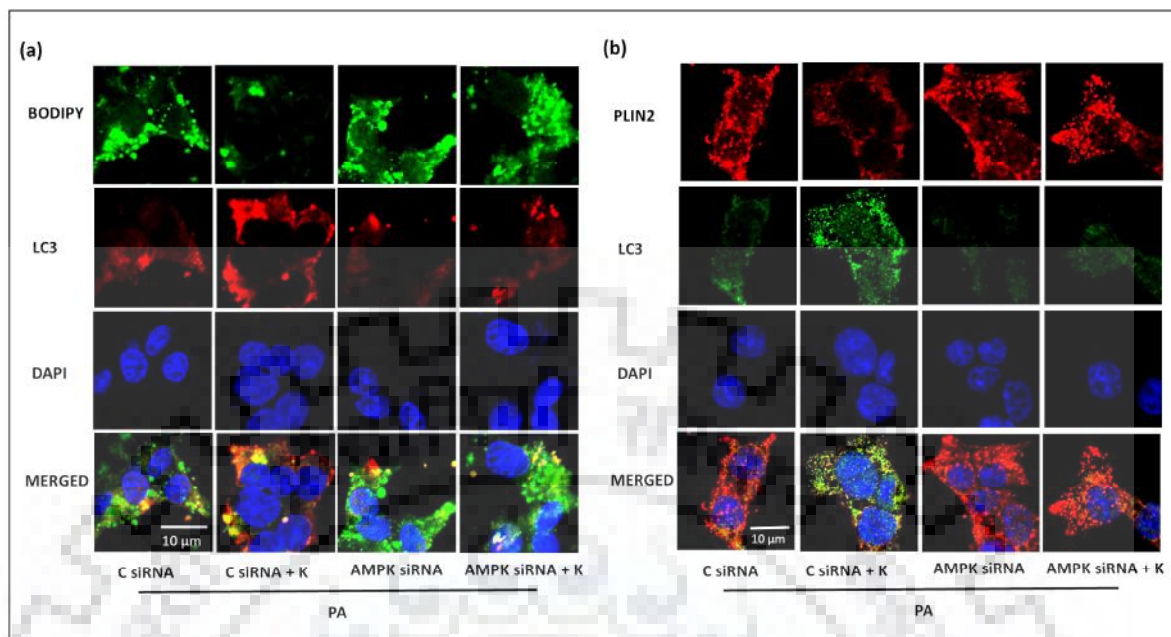


Fig. 6.11. Inhibition of AMPK prevents sequestration of lipid droplets into autophagosomes. Representative confocal images showing immunostained co-localization of (a) LC3 protein with BODIPY-stained lipid droplets and (b) LC3 and PLIN2, as detected by double immunofluorescence staining. PA, palmitic acid; K, kaempferol; C, control.

6.3.4. Kaempferol-induced autophagy abolishes PA-induced ER stress in RIN-F cells

In order to determine whether kaempferol-induced autophagy can relieve the PA-induced ER stress the immunoblot analysis of CHOP, the main ER stress marker involved in ER-induced apoptosis, was performed. As shown in Fig. 6.12a and b, kaempferol treatment down-regulated the CHOP expression in a dose- (Fig. 6.12a) and time- (Fig. 6.12b) dependent manner. At 48 h, kaempferol treatment (10 μ M) exhibited \sim 2.5-fold decrease in CHOP expression as compared to respective PA-treated group. Further, to confirm the role of autophagy in kaempferol-induced attenuation of ER stress, the autophagy inhibitors i.e., wortmannin, chloroquine and Atg7 siRNA were included in the following study. As shown in Fig. 6.12c and d, inhibition of kaempferol-induced autophagy increased the CHOP protein expression. Co-treatment of kaempferol with wortmannin and chloroquine increased expression of CHOP by about 2.6- and 3.5-fold ($p < 0.05$) respectively (Fig. 6.12c) with respect to only kaempferol-treated cells. Similarly, genetic inhibition of autophagy by means of Atg7 siRNA also averted the kaempferol-inhibited CHOP expression by \sim 3.2 fold ($p < 0.05$) (Fig. 6.12d). Thereafter, to

determine whether AMPK signaling is involved in the kaempferol-mediated abolition of ER stress, the immunoblot analysis of CHOP was performed in presence of compound C and AMPK siRNA. The results exhibited that AMPK phosphorylation was involved in kaempferol-mediated inhibition of PA-induced ER stress in RIN-5F cells as indicated by increased CHOP expression in kaempferol and compound C/AMPK siRNA co-treated group which could be only marginally rescued by kaempferol treatment ($p < 0.05$) (Fig. 6.12e and f).

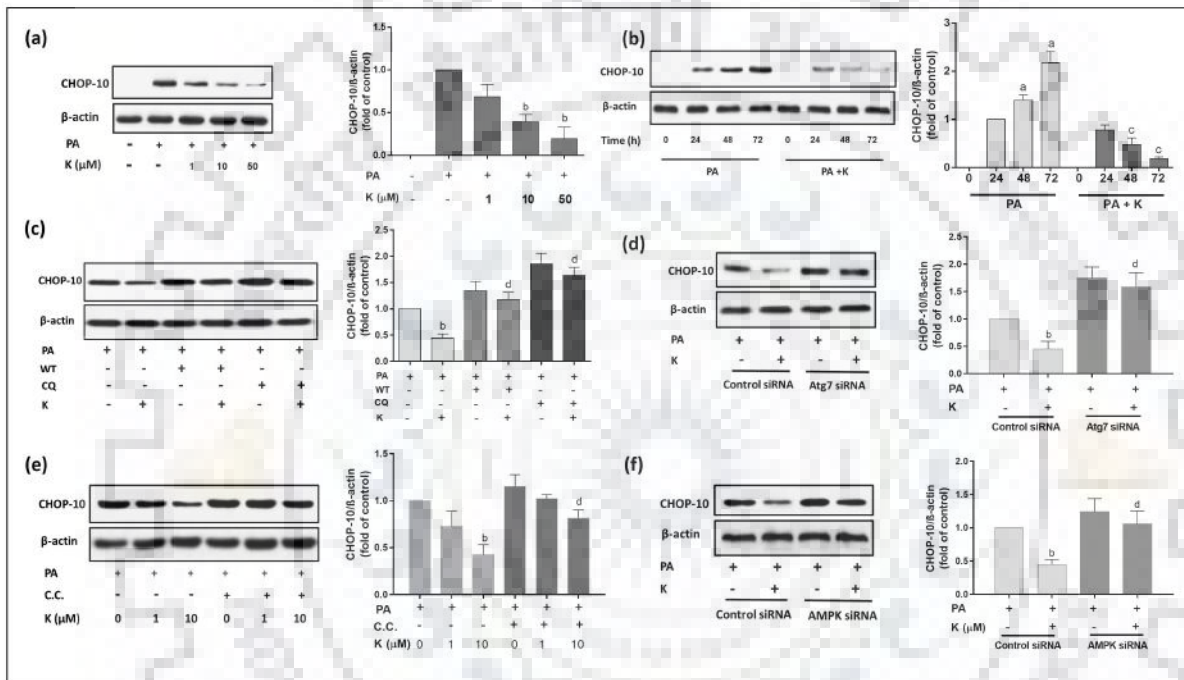


Fig. 6.12. Kaempferol-induced autophagy abolishes PA-induced ER stress in RIN-5F cells. Representative immunoblot showing expression of CHOP protein in response to kaempferol treatment with (a) increasing doses; (b) varying time; (c) chemical inhibitors of autophagy; (d) Atg7 siRNA; (e) chemical inhibitor of AMPK and (f) AMPK siRNA. In all the figures except “a” and “e”, kaempferol was used at a concentration of 10 μ M. The histogram in the right panel of each figure represents the mean relative arbitrary pixels intensities in terms of fold over control in respective figures. Results are the mean \pm S.D. of three independent experiments. a, $p < 0.05$ versus PA-treated control group for 0 h; b, $p < 0.05$ versus PA control group; c, $p < 0.05$ versus PA-treated group of respective time duration; d, $p < 0.05$ versus (PA + K 10 μ M). PA, palmitic acid; K, kaempferol; WT, wortmannin; CQ, chloroquine; C.C., compound C.

6.3.5. Kaempferol-induced autophagy restores the PA-induced β -cells dysfunction

In our subsequent study, we evaluated whether the kaempferol-induced inhibition of lipid deposition and ER stress in PA-challenged β -cells are also associated with improved β -cell function. Chronic exposure of RIN-5F cells to PA for 48 h reduced the glucose (16.7 mM) stimulated insulin secretion by ~ 2.5 fold with respect to vehicle-treated cells ($p < 0.05$) (Fig. 6.13a). Further, the addition of kaempferol significantly stimulated the insulin secretion in both normal and PA-treated RIN-5F cells and exhibited about 1.3 and 2.7-fold increase as compared to normal and PA-treated group respectively ($p < 0.05$). While insulin secretion at basal glucose level (2.8 mM) was only marginally increased in kaempferol-treated normal as well as PA-challenged RIN-5F cells (Fig. 6.13a). Moreover, autophagy and AMPK inhibitors significantly ($p < 0.05$) abolished the kaempferol-induced improved glucose-stimulated insulin secretion in presence of 16.7 mM glucose. Kaempferol-induced insulin secretion was found to be inhibited by about 2.1-, 3- and 2.5-fold in presence of wortmannin, chloroquine and compound C respectively as compared to only kaempferol-treated PA stressed cells ($p < 0.05$) (Fig. 6.13b). Likewise, the enhanced level of intracellular insulin content was also found to be inhibited by about 2-fold in presence of PA in RIN-5F cells ($p < 0.05$) (Fig. 6.13c). Like PA other autophagy inhibitors also significantly abolished the intracellular insulin levels ($p < 0.05$) (Fig. 6.13d). The decreased insulin content in presence of inhibitors is affirmative of the role of AMPK-mediated autophagy in kaempferol-stimulated restoration of β -cell function.

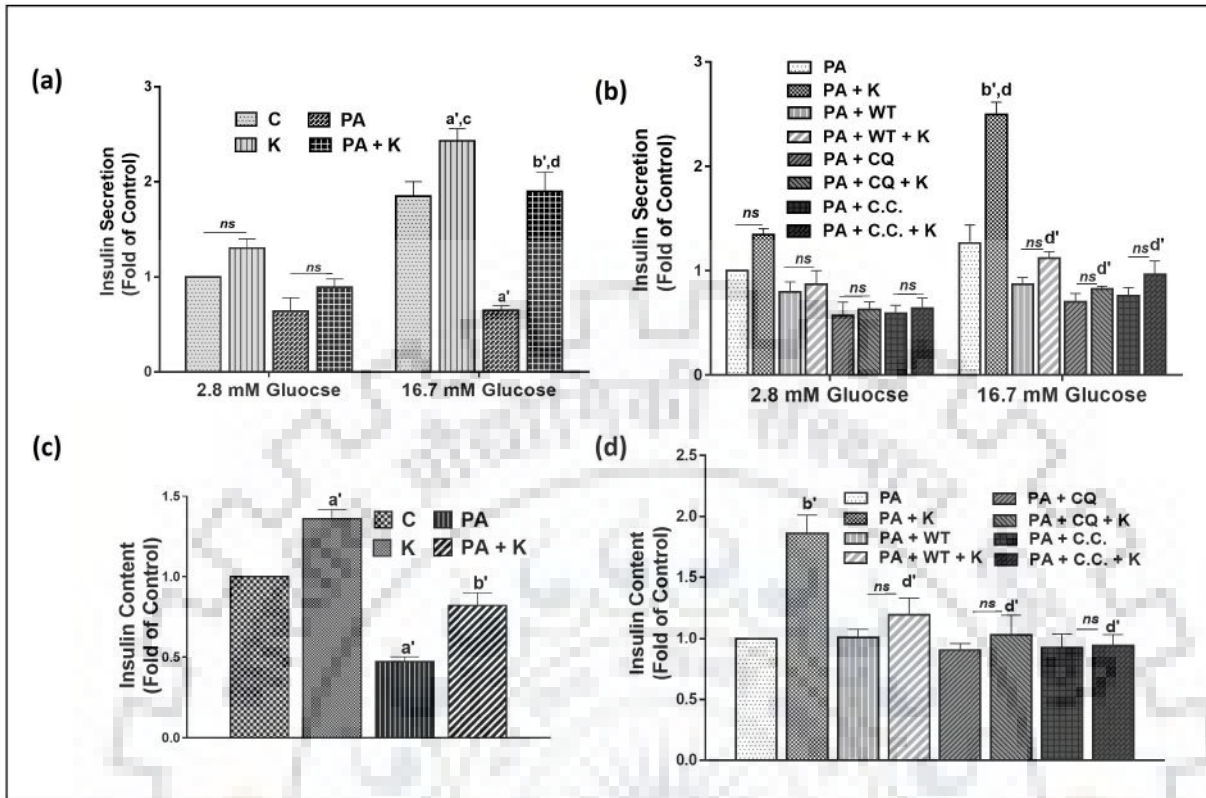


Fig. 6.13. Kaempferol-induced autophagy restores the insulin-secreting function of PA-stressed RIN 5F cells. The RIN-5F cells were treated with 10 μ M kaempferol with or without wortmannin (100 nM) or chloroquine (10 μ M) or compound C (10 μ M) in presence or absence of PA (0.5 mM) for 48 h followed by incubation with glucose for 1 h. The histograms in (a) and (b) represents the level of secreted insulin in response to various treatments in presence of 2.8 or 16.7 mM glucose; while (c) and (d) represents intracellular insulin contents in presence of 16.7 mM glucose. Results are the mean \pm S.D. of two independent experiments performed in duplicates. c and d represent $p < 0.05$ with respect to K and (PA+K)-treated groups respectively in presence of 2.8 mM glucose. a', b' and d' represents $p < 0.05$ with respect to vehicle, PA and (PA + K)-treated groups respectively in presence of 16.7 mM glucose. PA, palmitic acid; K, kaempferol; WT, wortmannin; CQ, chloroquine; C.C., compound C, ns, non-significant.

6.3.6. Kaempferol-induced autophagy abolishes PA-induced increased lipid stores, ER stress and β -cell dysfunction in primary islets

In our next phase of the study, we validated our findings using more physiologically relevant model, the isolated rat islets. To confirm the role of kaempferol-mediated lipophagy in degradation of PA-induced lipid stores in pancreatic β -cells, the autophagosomes-LDs-lysosomes co-localization study was performed. As shown in Fig. 6.14a, kaempferol-treated islets exhibited decreased BODIPY-stained lipid droplets with respect to PA-treated islets. Moreover, kaempferol-treated islets exhibited more co-localization of LDs with autophagosomes as well as lysosomes as indicated by increased white-stained regions while PA-treated islets displayed a limited number of co-localization of LDs with autophagolysosomes. Further, autophagy and AMPK inhibitors abolished the kaempferol-induced co-localization of LDs with autophagosomes and lysosomes. These inhibitors inhibited kaempferol-mediated induction of autophagy thus exhibited increased lipid stores. Additionally, immunoblot analysis demonstrated the increased LC3-II expression with a concomitant decrease in p62 expression in kaempferol-treated islets indicative of increased autophagy ($p < 0.05$) (Fig. 6.14b). Furthermore, kaempferol treatment also showed decreased PLIN2 and CHOP-10 expression which could be due to kaempferol-mediated inhibition of lipid deposition and ER stress ($p < 0.05$) (Fig. 6.14b). Likewise, inhibition of autophagy using autophagy inhibitors abolished kaempferol-mediated inhibition of PLIN2 and CHOP expression which confirms the involvement of autophagy ($p < 0.05$) (Fig. 6.14b). Further, to confirm the involvement of AMPK signaling in kaempferol-mediated effects, immunoblot analysis of PLIN2 and CHOP-10 was performed in presence of compound C, the AMPK inhibitor. As shown in Fig. 6.14c, kaempferol-treated islets exhibited a dose-dependent increase in p-AMPK expression with concomitantly decrease in p-mTOR expression ($p < 0.05$). Moreover, islet cells co-treated with kaempferol and compound C exhibited a significant up-regulation of PLIN2 and CHOP-10 expressions ($p < 0.05$) (Fig. 6.14c).

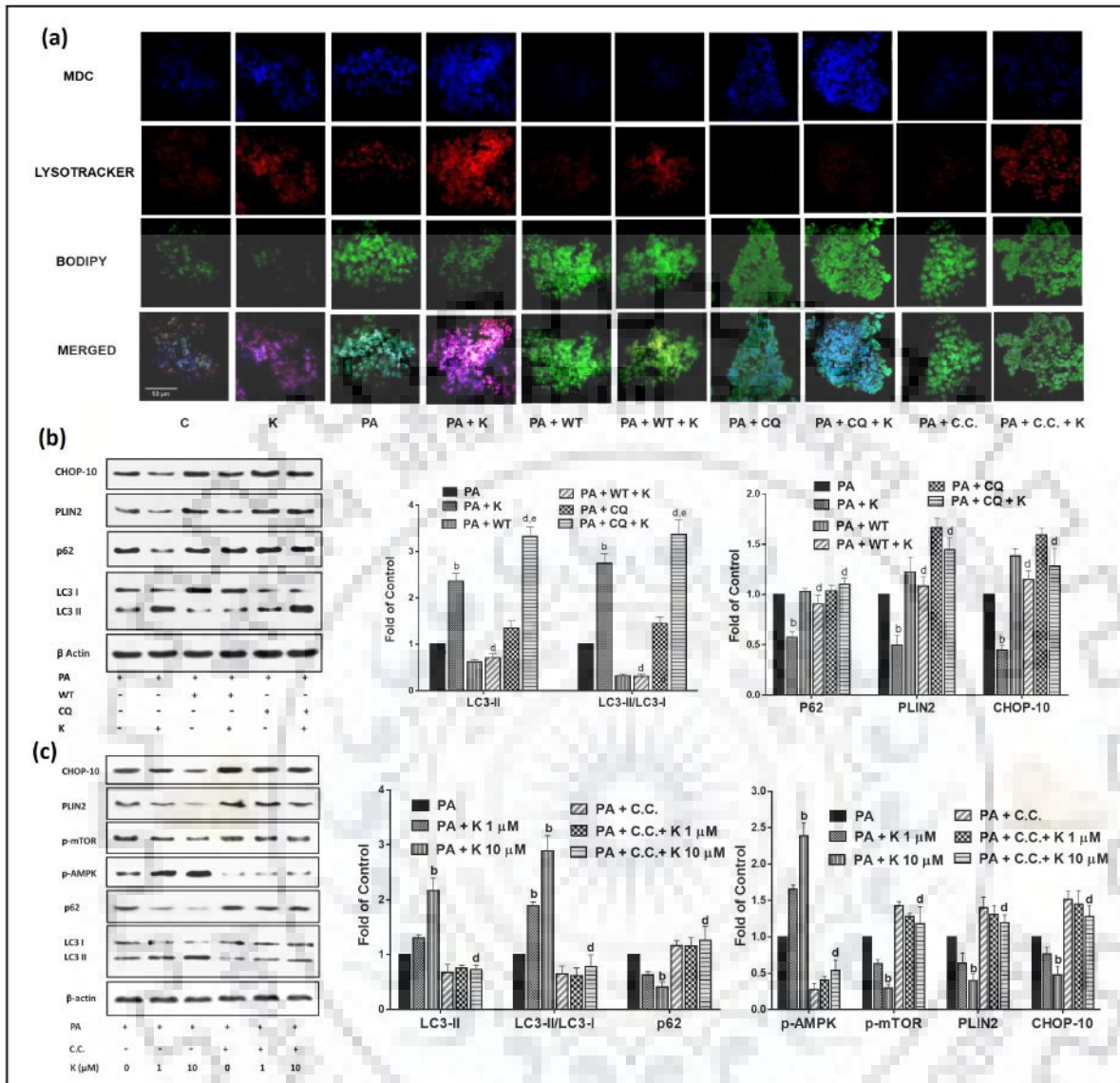


Fig. 6.14. AMPK/mTOR-mediated lipophagy is involved in kaempferol-facilitated decrease in lipid stores in rat primary islets cells. Isolated primary rat islets cells were incubated with kaempferol (10 μ M) with or without wortmannin (100 nM) or chloroquine (10 μ M) or compound C (10 μ M) in presence of PA (0.5 mM) for 48 h. (a) Representative confocal images showing co-localization of BODIPY stained lipid droplets to autophagosomes as well as lysosomes stained by MDC and LysoTracker respectively. Representative immunoblots of various proteins in presence of (b) wortmannin and chloroquine; (c) compound C. The histogram in the right panel of each figure represents the mean relative arbitrary pixels intensities in terms of fold over control in respective figures. Results are the mean \pm S.D. of three independent experiments. b, $p < 0.05$ versus PA control; d, $p < 0.05$ versus (PA + K 10 μ M); e, $p < 0.05$ versus (PA + CQ). PA, palmitic acid; K, kaempferol; WT, wortmannin; CQ, chloroquine; C.C., compound C.

To extend our findings, insulin and LC3 double immunostaining were performed in isolated rat islets. As shown in Fig. 6.15a, PA-treated islets exhibited decreased expression of insulin as compared to untreated control islets. While the addition of kaempferol led to increased expression of insulin with concomitant increase in LC3 expression. Further, autophagy and AMPK inhibition by means of inhibitors showed decreased insulin expression confirmative of involvement of AMPK-mediated autophagy in kaempferol-induced insulin expression. Additionally, kaempferol-treated rat islets also exhibited increased glucose-stimulated insulin secretion and insulin content in PA overload condition which was further found to be inhibited in presence of autophagy and AMPK inhibitors ($p < 0.05$) (Fig. 6.15b, c, d and e). Chronic exposure of isolated rat islets to PA for 48 h reduced glucose-stimulated insulin secretion and intracellular insulin content by about 2.8- and 2.2-fold with respect to untreated islets while addition of kaempferol led to its increased release and insulin content by about 3.1- and 2-fold respectively ($p < 0.05$) (Fig. 6.15b and d). Further, kaempferol-induced glucose-stimulated insulin secretion and intracellular insulin content were found to be inhibited in presence of wortmannin, chloroquine and compound C as compared to only kaempferol-treated islets in presence of PA ($p < 0.05$) (Fig. 6.15c and e). Together, these results are in close agreement with the RIN-5F cell's data and collectively confirmed that AMPK/mTOR signaling-mediated lipophagy is involved in a kaempferol-facilitated decrease in lipid stores and ER stress and restores β -cell function in PA-challenged pancreatic clonal β -cells and primary islets.

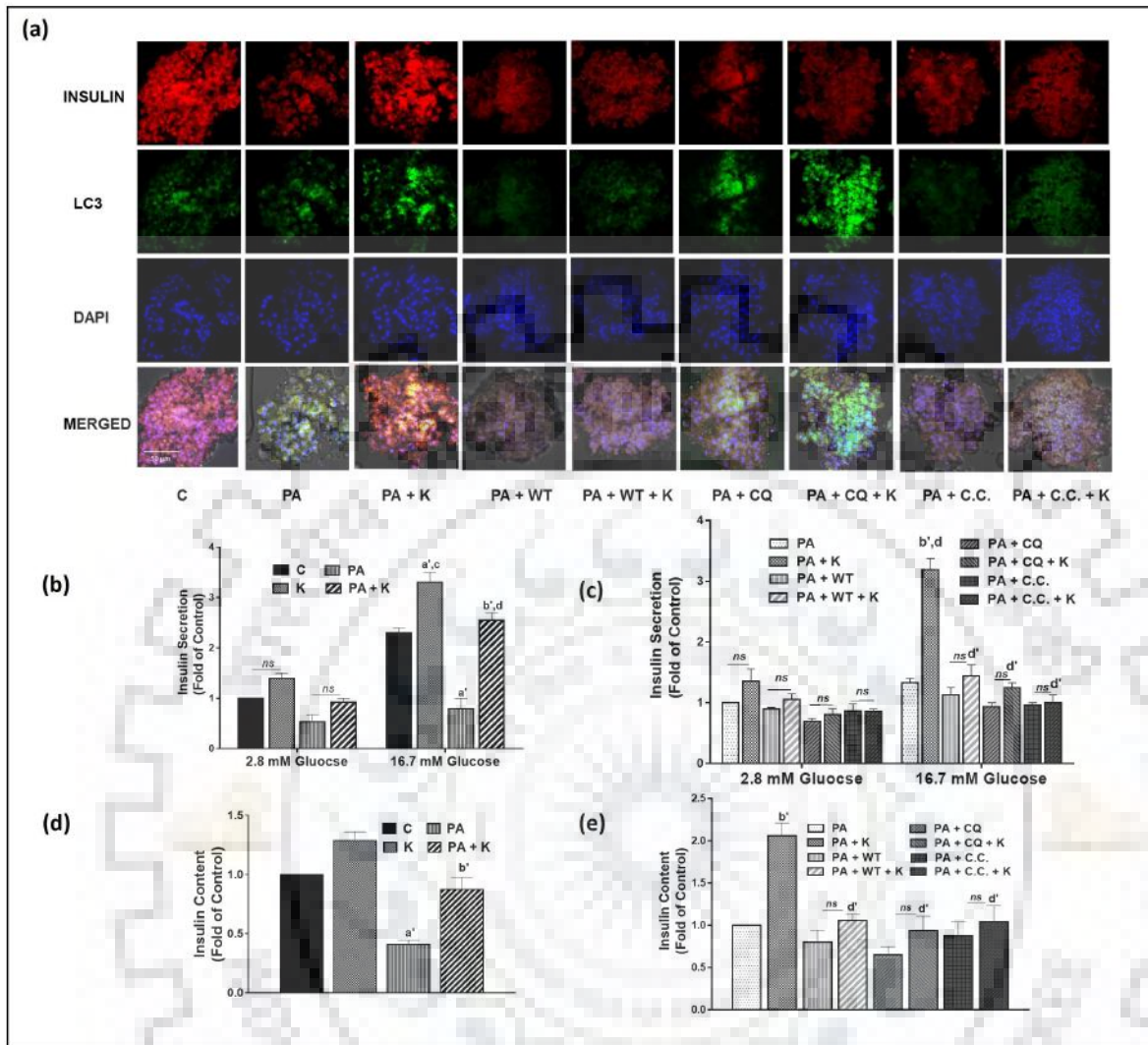


Fig. 6.15. Autophagy and AMPK inhibitors abolish the kaempferol-mediated restoration of insulin content in isolated rat pancreatic β -cells. The isolated rat primary islets were treated with kaempferol (10 μ M) with or without various inhibitors in presence or absence of PA (0.5 mM) for 48 h followed by glucose incubation for 1 h. (a) Representative confocal images showing immunostained co-localization of insulin and LC3 as detected by double immunofluorescence staining. The histograms at (b) and (c) represent the level of secreted insulin for various treatments in presence of 2.8 or 16.7 mM glucose; while (d) and (e) represents intracellular insulin contents for various treatments in presence of 16.7 mM glucose. Results are the mean \pm S.D. of two independent experiments performed in duplicates. c and d represent $p < 0.05$ with respect to K and (PA+K)-treated groups respectively in presence of 2.8 mM glucose. a', b' and d' represents $p < 0.05$ with respect to vehicle, PA and (PA + K)-treated groups respectively in presence of 16.7 mM glucose. PA, palmitic acid; K, kaempferol; WT, wortmannin; CQ, chloroquine; C.C., compound C, ns, non-significant.

6.4. Discussion

Kaempferol, a natural flavonoid, known for its various anti-oxidative and anti-inflammatory properties, is found abundantly in various plants including green teas, berries, grapes, apples, citrus fruits, onions etc. (M Calderon-Montano et al., 2011). Recently, kaempferol was reported to increase insulin secretion and β -cell mass in obese diabetic mice but its role in lipid metabolism under chronic FFA overload conditions and the underlying mechanism is poorly studied (Zang et al., 2015). Here, we have identified a novel mechanism of lipid mobilization in pancreatic β -cells mediated by kaempferol-induced autophagy.

The role of autophagy in sustaining pancreatic β -cell mass and function is well established from the very fact that its deregulation has been associated with insulin resistance, obesity and type II diabetes (Codogno and Meijer, 2010). Chronic exposure of lipids (high-fat diet-fed animals) or acute exposure to high concentration of lipids (such as oleate or palmitate) may change the lipid composition of autophagosomal and lysosomal membranes that could modify their fusogenic abilities, and thus contribute to impaired autophagosomes clearance (Koga et al., 2010). Similarly, recent reports supported these findings and showed that FFAs impair autophagy by inhibiting autophagic turnover in β -cells (Mir et al., 2015). (Singh et al., 2009). Thus FFA-induced lipid accumulation in β -cells may be due to inhibition of autophagy by chronic exposure to FFAs, since autophagy has been known to play an important role in lipid degradation in various cell types including adipocytes and hepatocytes and its (autophagy) inhibition leads to accumulation of lipids and triglycerides (Singh et al., 2009). Although the beneficial role of autophagy in the regulation of β -cell mass and function is well known its role in β -cell lipid metabolism is rarely established.

In our recent study, we have reported that kaempferol protects pancreatic β -cells from PA-induced apoptosis through activation of autophagy (Varshney et al., 2017). It is already reported that lipid deposition in β -cells is one of the major causes of loss of β -cell mass and function (Assimacopoulos-Jeannet, 2004; Lim et al., 2011; Singh et al., 2017). Therefore, in this study, we intended to determine whether kaempferol-induced autophagy can also inhibit PA-induced lipid deposition which in turn may be linked to the cytoprotective effect of kaempferol in PA-induced β -cells. To the best of our knowledge, this is the first ever report showing the anti-lipotoxic effect of kaempferol in the elimination of stored lipid droplets in clonal pancreatic β -cells (RIN-5F cells) and primary islets under PA overload conditions through AMPK/mTOR-mediated lipophagy.

Here, we have demonstrated that kaempferol could alleviate PA-induced lipid deposition in RIN-5F cells. Our results indicated that RIN-5F cells incubated with PA showed increased LDs, triglyceride content and PLIN-2 expression while the PA-induced accumulation of LDs and triglyceride was markedly reduced by kaempferol treatment. The cells co-treated with kaempferol and PA showed significant down-regulation of PLIN2 as evident by RT-PCR and immunoblot analysis. PLIN2 is major lipid droplet coat protein in pancreatic β -cells and is reported to be overexpressed in β -cells during conditions of lipid deposition (Faleck et al., 2010; Chen et al., 2017). PLIN2 accumulation increases lipid and triglyceride stores in pancreatic β -cells thus impairing its mass and function, while genetic ablation of PLIN2 was shown to lower triglyceride content and ER stress and thus partially restoring β -cells mass and function (Chen et al., 2017). Our results are in line with these studies showing that PLIN2 down-regulation led to decreased triglyceride stores in β -cells.

Subsequently, to confirm the link between kaempferol-induced autophagy and decreased lipid content, autophagy inhibitors were included in the study. Autophagy inhibitors namely, wortmannin and chloroquine abolished the kaempferol-mediated reduction in LDs and triglyceride content and led to increased lipid stores in PA-challenged β -cells. Moreover, autophagy inhibitors inhibited kaempferol-induced down-regulation of PLIN-2 expression. This data demonstrates that autophagy may be involved in the kaempferol-mediated reduction of lipid stores. Further, co-localization studies allowed us to infer that kaempferol-treated group exhibited an increased number of LDs co-localized with autophagosomes as well as lysosomes as compared to PA alone treated cells. In addition, co-localization of lipid droplets with autophagosomes was significantly increased in the kaempferol-treated cells when lysosomal degradation was blocked by chloroquine treatment. The reason for the lesser number of LDs and fewer co-localization with autophagosomes/ LC3 in presence of kaempferol without chloroquine could be due to rapid degradation of LDs. Moreover, increased kaempferol-mediated association of LC3 and PLIN2 indicated that the LDs directly fuse to autophagosomes which further fuse to lysosomes for their degradation. Our data were consistent with the recent report which showed that Epigallocatechin gallate-mediated lipophagy inhibited the palmitate-induced accumulation of LDs in endothelial cells (Chen et al., 2017). Thus the data revealed that kaempferol-mediated lipophagy is involved in degradation of PA-induced LDs in β -cells.

In our subsequent studies, underlying mechanism involved in kaempferol-induced lipophagy was elucidated. AMPK is known to be a key regulator of cellular lipid metabolism and is a nutrient sensor which sustains cellular energy homeostasis (Hardie et al., 2012). It is well known that AMPK activation regulates lipid metabolism while its inhibition is linked to diabetes and obesity in lipid overload conditions (Hardie, 2004; Zhang et al., 2009). On the other hand, the pre-existing literature strongly suggests that AMPK is the positive regulator of autophagy and acts by down-regulating phosphorylation of mTOR (Han et al., 2010; Kim et al., 2011; Yao et al., 2016). Recently, we found that AMPK/mTOR pathway is involved in kaempferol-induced autophagy (Varshney et al., 2017). With this as the basis, we further investigated the role of AMPK/mTOR-mediated signaling pathway in kaempferol-stimulated lipid degradation. Our results showed that AMPK inhibitors (compound C and AMPK siRNA) abolished kaempferol-induced autophagy and subsequently increased lipid and triglyceride stores in PA-challenged β -cells. Likewise, AMPK inhibitors also inhibited the kaempferol-induced LDs-autophagosomes-lysosomes co-localization. So, together it can be inferred that AMPK signaling is involved in kaempferol-mediated lipophagy.

It is well known that ER stress is one of the main features of obesity and diabetes associated pathological conditions. Chronic exposure of β -cells to saturated FFAs leads to induction of β -cell apoptosis due to oxidative ER stress and accumulation of ubiquitinated proteins within cells (Mir et al., 2015). The transcription factor CHOP is a downstream component of ER stress pathways and a key mediator of cell death in response to ER stress found to be augmented in PA- and high glucose-treated β -cells (Oyadomari and Mori, 2004). Additionally, the previous study showed that in murine models of type 2 diabetes, the CHOP deletion restored the β -cell mass (Song et al., 2008). In some other studies, it was shown that activated autophagy could reduce ER stress and thus β -cell apoptosis but its impairment may lead to the chronic stage of ER stress, thus eliciting the expression of stress-CHOP protein expression (Bachar-Wikstrom et al., 2013; Mir et al., 2015). Our results were also consistent with those findings, indicating that PA-induced suppression of autophagic turnover in β -cells leads to increased CHOP expression whereas treatment with kaempferol exhibited down-regulation of CHOP protein. Further, autophagy and AMPK inhibitors abolished the kaempferol-mediated down-regulation of CHOP protein. Based on these results it could be inferred that kaempferol alleviates ER-stress induced CHOP-mediated death pathway in PA-challenged β -cells. Thus, kaempferol-stimulated autophagy could reduce lipid-activated

ER stress and simultaneously autophagy has been shown to degrade lipid droplets (Dong and Czaja, 2011). Therefore, it can be inferred that stimulation of kaempferol-mediated autophagy could inhibit PA-induced lipid deposition as well as ER stress in β -cells which may further lead to cytoprotection of these cells. Moreover, the cytoprotected RIN-5F cells and rat primary islets were also found to be functional in nature as indicated by increased glucose-stimulated insulin secretion and intracellular insulin content. It is to be noted that insulin-secreting capacity of β -cells is always considered to be a prominent marker of healthy cells. Based on these facts it could be asserted that our findings are in close agreement with the previous study which showed that PA inhibited glucose stimulated insulin secretion while stimulation of autophagy by means of rapamycin, a positive regulator of autophagy, restored the PA-inhibited insulin secretion in INS1 cells (Las et al., 2011).

In summary, all the results delineated in the present study corroborate well with each other to arrive at the conclusion that kaempferol restores PA-induced loss of β -cell mass and function through AMPK/mTOR-mediated autophagy. In this study, we reported that kaempferol-mediated autophagy abolished the PA-induced ER stress and lipid accumulation which seems to be one of the possible mechanisms by which kaempferol attenuates PA-induced cellular lipotoxicity of β -cells which in turn lead to restoration of β -cell function. To the best of our knowledge, this study uncovers a novel phytochemical based therapeutic strategy to restore pancreatic β -cell mass and function in obesity-linked type 2 diabetic condition. Thus, this study suggests that kaempferol could be a promising candidate as nutraceutical either singly or in combination with other drugs/ chemicals for the prevention of obesity-linked type II diabetes. Though flavonoids have been known for their various health beneficial effects, their poor bioavailability poses a limitation in therapeutic applications. However, the dose of kaempferol (10 μ M) which is found to be significant in exerting its positive effect on pancreatic β -cells in our study, may be of physiological relevance since it has been reported that attainable plasma concentrations of flavonoids through diet are within several micromolar ranges (Gates et al., 2007 and Zhang et al., 2013). However, further comprehensive *in vivo* and clinical studies are needed to establish the exact cross-talks among various pathways in causing autophagy and its related effects by kaempferol to establish nutraceutical potential of this phytochemical where our data would provide a base for such studies. That would indeed help in the management of obesity-linked type-2 diabetes using this phytochemical.



CHAPTER 7

***ROLE OF KAEMPFEROL IN RESTORATION OF
AUTOPHAGY AND FUNCTIONAL PANCREATIC
 β -CELL MASS IN A MURINE MODEL OF TYPE 2
DIABETES***

Chapter 7. Role of kaempferol in restoration of autophagy and functional pancreatic β -cell mass in a murine model of type 2 diabetes

7.1. Introduction

The prevalence of type 2 diabetes mellitus (T2DM) is increasing worldwide, the incidence of which correlates in most of the cases with development of obesity. In obese condition, the elevated level of circulating free fatty acids (FFAs) is one of the predisposing factors in the development of insulin resistance and hyperglycemia in the early phase of diabetes (Giacca et al., 2010). The initial response to increased insulin resistance in peripheral tissues is the compensatory increase in β -cell mass and insulin secretion by pancreatic β -cells. However, with the progression of diabetes, dysfunction and loss of β -cells occur in response to increased metabolic load which further leads to complications associated with T2DM (Assimacopoulos-Jeannet, 2004; Boden, 2011). Accumulating evidence suggests that the loss of β -cells in T2DM is closely related to increased apoptosis of β -cells, secondary to increased glucotoxicity and lipotoxicity (Maedler et al., 2001; Lupi et al., 2002; Yuan et al., 2010). Chronic lipid accumulation, endoplasmic reticulum (ER) stress and impaired autophagy could be the key pathways involved in the loss of β -cell mass and function (Assimacopoulos-Jeannet, 2004; Biden et al., 2014; Masini et al., 2009).

Chronic lipid accumulation with subsequent loss of β -cell mass and function has been reported in islets of T2DM animal models and human subjects (Lee et al., 1994; Tushuizen et al., 2007). PLIN2 is a lipid coat protein which helps in lipid deposition and has been reported to be up-regulated in human and murine islets in chronic lipid overload conditions (Shao et al., 2013; Faleck et al., 2010; Chen et al., 2017). Recently, it has been reported that increased expression of PLIN2 is involved in triggering ER stress and apoptosis in islets of diabetic Akita mice which further links to β -cell death and dysfunction.

ER stress is one of the key mediators involved in the middle stage of the pathophysiology of diabetes (Ozcan & Tabas, 2012). In obese and insulin resistant conditions, the increased demand for insulin production along with higher levels of FFAs, lead to chronic ER stress in β -cells (Sharma & Alonso, 2014). The transcription factor C/EBP homologous protein (CHOP) is a

downstream component of ER stress pathways and a key mediator of cell death in response to ER stress found to be increased in high glucose and palmitic acid-treated pancreatic β -cells. However, CHOP deficiency has been found to restore β -cell mass and function in type 2 diabetic murine models (Song et al., 2008).

Macroautophagy (hereafter mentioned as autophagy) is a cellular quality control process. It involves engulfment and lysosomal degradation of damaged organelles, fat droplets, nonfunctional proteins and other macromolecules which serve as an alternative energy source during adverse conditions like starvation and stress (Mizushima, 2007; He & Klionsky, 2009; Jung & Lee, 2009). Several pathophysiological conditions including T2DM have been linked to impaired autophagy (Singh & Cuervo, 2011). Recently, it is reported that autophagy is important in islet homeostasis and compensatory increase of β -cell mass in response to high-fat diet (HFD). The autophagy-deficient β -cell specific Atg7 knockout mice fed with HFD showed progressive degeneration of β -cells with impaired insulin secretion and compromised glucose tolerance (Ebato et al., 2008). Moreover, HFD-induced mice model and type 2 diabetic patients often show aberrant autophagic activity that further confirms the effect of deregulated autophagic process in the progression of the pathophysiology of T2DM (Masini et al., 2009; Codogno & Meijer, 2010). Thus, induction of autophagy could be a potential target to combat FFA-mediated apoptotic cell death and progression of T2DM (Stienstra et al., 2014).

Kaempferol (3,5,7,4-tetrahydroxyflavone), a natural flavonol found in several fruits and vegetables such as berries, grapes, apples, cabbage, beans, onion, garlic, tomatoes, green tea (M Calderon-Montano et al., 2011) holds a great promise as a phytotherapeutic agent. It has been explored extensively for its physiological beneficial role as anti-oxidative, cardioprotective, neuroprotective, anti-inflammatory, anti-osteoporotic and anticancer agent (Liao et al. 2016; Lin et al. 2007; Abo-Salem, 2014; Filomeni et al., 2012; Huang et al., 2010). Recently, some studies have reported the antidiabetic and antiobesity activity of kaempferol (Zang et al., 2015; Alkhalidy et al., 2015). However, the underlying mechanisms regarding such activities remain poorly understood. In our recent *in vitro* and *ex vivo* studies, we demonstrated that kaempferol activates autophagy and preserves β -cell mass and function in clonal pancreatic β -cells and isolated islets

under chronic lipid overloaded condition (Varshney et al., 2017). In continuation to that study, we found that kaempferol-induced autophagy alleviates lipid deposition and ER stress generated during lipid overload condition in β -cells which was supposed to be etiological factors that usually predispose the pancreatic β -cells to undergo apoptosis (Varshney et al., 2018). Based on these studies, further comprehensive *in vivo* and clinical studies are warranted to establish the exact cross-talks among kaempferol's effect on β -cell mass and function and the various pathways involved establishing nutraceutical potential of this phytochemical. Therefore, in this present study, we intended to validate our findings in more promising diabetic model, the HFD and STZ-induced type 2 diabetic mice, an alternative animal model of type 2 diabetes, simulating human syndrome which has been extensively used to test antidiabetic effects of various drugs/compounds (Skovsø, 2014). These animals are raised on an HFD to induce insulin resistance and glucose intolerance and further exposed to low dose of streptozotocin which results in compromised β -cell mass and function (Skovsø, 2014). In the present study, we evaluated the role of kaempferol on autophagy in pancreatic β -cells of HFD-STZ induced diabetic mice. Our data showed that kaempferol preserves the function and mass of pancreatic β -cells of the diabetic mice involving autophagy.

7.2. Brief methodology

7.2.1. Experimental animals

All the animal experiments were performed as per CPCSEA guidelines with prior approval from Institutional Animal Ethics Committee (approval number: BT/IAEC/2017/02). Male C57BL/6 mice of age 7 weeks old were procured from CSIR-Institute of Microbial Technology, Chandigarh, India. They were housed under standard conditions (temperature $23\pm 2^{\circ}\text{C}$ and 12 h dark-light cycle) in a well-maintained animal house and acclimatized for two weeks prior to start of the experiments. The mice were fed ad libitum with either standard chow-fed or a HFD and allowed to free access to water.

7.2.2. Experimental design

After acclimatizing, the mice were divided into eight groups (n = 6) as follow:

Group I – Standard normal chow-fed (Normal control)

Group II – HFD fed + streptozotocin (Diabetic control)

Group III – HFD fed + streptozotocin + metformin (25 mg/kg body weight (bw)/day) (Positive control)

Group IV – HFD fed + streptozotocin + rapamycin (0.2 mg/kg bw/day) (Positive control for autophagy)

Group V – HFD fed + streptozotocin + kaempferol (10 mg/kg bw/day) (Low dose)

Group VI – HFD fed + streptozotocin + kaempferol (25 mg/kg bw/day) (High dose)

Group VII – HFD fed + streptozotocin + chloroquine (25 mg/kg bw/day) (Autophagy-impaired diabetic control)

Group VIII – HFD fed + streptozotocin + kaempferol (25 mg/kg bw/day) + chloroquine (25 mg/kg bw /day) (Autophagy-impaired treatment)

7.2.3. Model development

Obesity-linked type 2 diabetes was induced in mice of all the groups; except for group I (Normal control group) by feeding mice with HFD that contained approximately 60% kcal fat, 20% kcal protein and 20% kcal carbohydrate wherein soybean oil and lard were used as the fat source (D12492, Research Diets, New Brunswick, NJ, USA) for 10 weeks. While normal control group was fed with standard chow diet which contained approximately 7.5% kcal fat, 17.5% kcal protein, 75% kcal carbohydrate (RM1, Special Diet Services, Witham, Essex, UK). The weight gain was monitored after every two weeks. After 10 weeks of HFD feeding, obese mice were fasted overnight and intraperitoneally injected with a low dose of STZ [35 mg/kg dissolved in freshly prepared 0.1 M cold citrate buffer (pH 4.5)], while normal control mice from the group I

received the same volume of 0.1 M cold citrate buffer (pH 4.5). After one week, the mice with fasting glucose > 240 mg/dl were considered as diabetic and were then allowed to stabilize for one more week. The mice from all the groups were continued with respective diet till 16 weeks of the whole experiment.

7.2.4. Experimental treatment

After two weeks of STZ injection (after 12 weeks of HFD), diabetic mice from group III and IV were injected intraperitoneally with metformin (25 mg/kg bw/day) and rapamycin (0.2 mg/kg bw/day) respectively. While group V and VI were injected intraperitoneally with low (10 mg/kg bw/day) and high dose (25 mg/kg bw/day) of kaempferol respectively. The mice from the group I and II were injected with sterile 10% ethanol: 40% PEG 400: 50% PBS as vehicle control. All the compounds i.e., metformin, rapamycin and kaempferol were dissolved in same solvent i.e., sterile 10% ethanol: 40% PEG 400: 50% PBS for experimental uniformity within each group. The mice were then allowed to continue to feed on their respective diets until the end of the study (total 16 weeks).

7.2.5. Autophagy flux determination

For autophagic flux determination, mice from Group VII and Group VIII were given an intraperitoneal injection of chloroquine (25 mg/kg bw/day) for last 10 days before completion of the experiment.

7.2.6. Estimation of blood parameters

On completion of 16 weeks of the experiment, fasting blood glucose of each mouse was recorded with a glucometer (Accu-chek active, Roche Diagnostics, Barcelona, Spain). The other blood

parameters such as serum cholesterol, triglycerides, LDL and NEFA levels were quantified by using commercially available kits as discussed in chapter 3 in detail.

7.2.7. Glucose tolerance test (GTT) and insulin tolerance test (ITT)

Glucose and insulin tolerance test were performed according to the protocol mentioned in chapter 3.

7.2.8. Fasting and glucose-stimulated insulin secretion

On completion of treatment, the mice were fasted for 6 h and then intraperitoneally injected with glucose (1 g/kg bw). The blood was withdrawn from the tail vein at 0, 15, 30, 45 and 60 min. Thereafter, the plasma was separated and insulin level was checked with insulin enzyme immunoassay kit as per the manufacturer' instructions (SPI-Bio, Bertin Pharma, Montigny-le-Bretonneux, France).

7.2.9. Pancreatic insulin content analysis

For measurement of total insulin content, pancreas slices were lysed with acid/ethanol (0.18 N HCl in 70% ethanol) overnight at 4°C and further homogenized. After centrifugation, the lysates were neutralized to pH 7.2 with 0.4 M Tris buffer pH 8.0. Further, the insulin levels in each lysate were measured with insulin enzyme immunoassay kit (SPI-Bio, Bertin Pharma, Montigny-le-Bretonneux, France).

7.2.10. Immunoblot analysis

The islets were isolated with collagenase method as described in chapter 3. The lysates were prepared by harvesting the islets in RIPA lysis buffer (150 mM NaCl, 50 mM Tris pH 7.6, 0.5%

sodium deoxycholate, 0.1% SDS, 1% Triton X-100 and 1X protease inhibitor cocktail). The total proteins were quantified by BCA method and immunoblot analysis was performed protocol described in chapter 3. The developed blots were then subjected to densitometric analysis by Image J 1.45 software (NIH, USA) and normalized with β -actin as internal control.

7.2.11. Histopathological studies

For histopathological studies, pancreas tissues were removed and immediately fixed in 10% neutral buffered PBS. After fixation, the tissues were dehydrated with upgrading from 30 to 70% series of alcohol for 1 h each then incubated in xylene for next 1 h followed by embedding in paraffin wax. The tissues were then sectioned to 4 μ m thickness and stained with hematoxylin and eosin as described elsewhere (Ebato et al., 2008).

7.2.12. Immunohistochemistry

The paraffin-embedded pancreatic tissues were sectioned at a thickness of 4 μ m and mounted on positive-charged slides. The slides were transferred into boiling citrate buffer for 15 min and then incubated with 3% hydrogen peroxide and blocking serum. The tissue sections were then incubated with the primary anti-insulin antibody (1:100 in PBS) overnight at 4°C. The sections were washed with PBS followed by incubation with texas red-conjugated secondary antibody for 2 h at room temperature. The slides were then examined and images were taken under a confocal microscope (LSM 780, Carl Zeiss, Germany).

7.2.13. Statistical analysis

Quantitative data are presented as means \pm standard deviation (SD) of three independent experiments and statistically evaluated by one-way/ two-way ANOVA followed by Tukey's post hoc test using Graph Pad Prism 6 software (Graph Pad Software, San Diego, CA, USA). A p-value < 0.05 was considered to be statistically significant for data analysis.

7.3. Results

7.3.1. Kaempferol improves body weight and lipid profile in HFD-STZ-induced diabetic mice

To investigate the systemic effects of kaempferol, mice were subjected to 4 weeks of daily kaempferol treatment at 10 or 25 mg/kg bw doses after 12 weeks of HFD-STZ treatment. As shown in Fig. 7.1a and b, after 16 weeks of treatment, the HFD-STZ mice (the diabetic group) exhibited a significant increase in body weight ($\sim 38.5 \pm 2.7$ gm) as compared to normal control group ($\sim 28.1 \pm 1.6$) ($p < 0.05$). While kaempferol (25 mg/kg bw) treated diabetic mice showed significantly decreased body weight ($\sim 31 \pm 2.1$) which was comparable to that of the normal control group ($p < 0.05$) (Fig. 7.1a and b). Moreover, metformin- (the positive control drug for diabetes) and rapamycin- (the positive control of autophagy) treated mice displayed marginally reduced body weight as compared to HFD-STZ group ($p < 0.05$) (Fig. 7.1a and b).

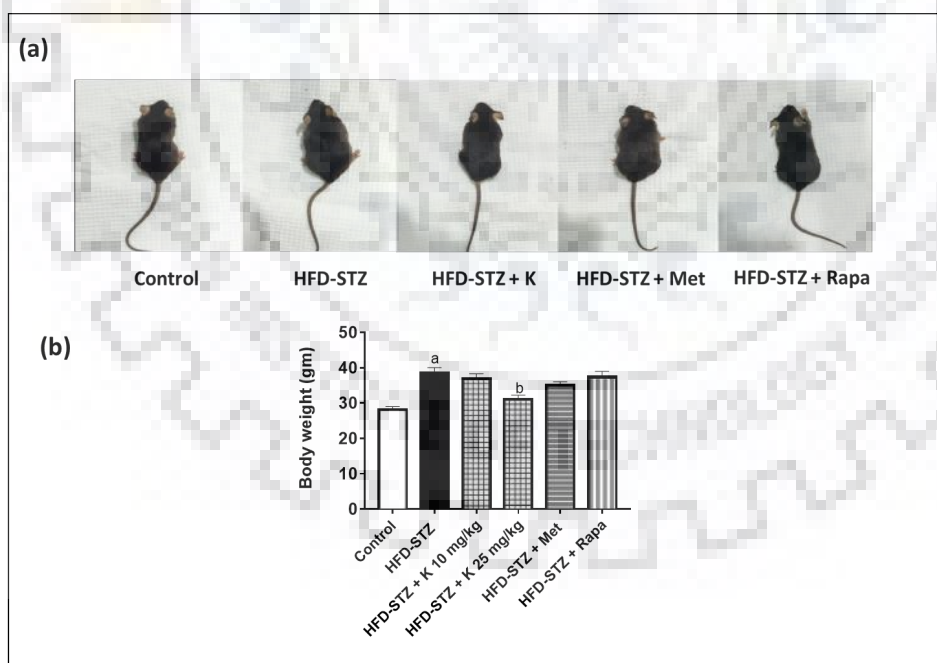


Fig. 7.1. Kaempferol decreases the body weight of HFD-STZ induced diabetic mice. (a) Representative images of mice fed with normal chow diet (control) or with high-fat diet for 10

weeks followed by injection with streptozotocin (35 mg/kg bw) and successive treatments for 4 weeks; (b) Body weight measurements of mice of respective groups. Data are mean \pm SD of $n = 6$ for each group. a, $p < 0.05$ versus normal control; b, $p < 0.05$ versus HFD-STZ control. HFD, high-fat diet; STZ, streptozotocin; K, Kaempferol; Met, metformin; Rapa, rapamycin.

7.3.2. Kaempferol improves fasting glucose level, glucose tolerance and insulin sensitivity

After 16 weeks of the experiment, HFD-STZ control mice had a high baseline fasting blood glucose level ($\sim 272 \pm 17$ mg/dl) as compared to normal control group ($\sim 107 \pm 12$ mg/dl) ($p < 0.05$) (Fig. 7.2a). However, this level was reduced down to $\sim 168 \pm 21$ and $\sim 130 \pm 16$ mg/dl when the mice were treated with kaempferol at 10 and 25 mg/kg bw respectively. As expected, metformin and rapamycin also exhibited a significant decrease in fasting blood glucose level with respect to HFD-STZ mice ($p < 0.05$).

As discussed earlier, impaired glucose tolerance and insulin resistance are the key characteristics of T2DM. Therefore, glucose tolerance was evaluated at the end of the experiment by administering glucose overload to the mice. As shown in Fig. 7.2b, HFD-STZ mice exhibited hyperglycemia at 0 min which was further exacerbated by glucose load. The increased glucose level of HFD mice did not reduce significantly even at 120 min, indicating impaired glucose tolerance. Administration of kaempferol to HFD mice resulted in significant and dose-dependent improvement in glucose tolerance which was almost comparable to normal animals ($p < 0.05$) (Fig. 7.2b). Further, to check the effect of kaempferol on insulin sensitivity, insulin tolerance test (ITT) was performed by injecting insulin intraperitoneally. As shown in Fig. 7.2c, kaempferol treatment significantly improved insulin sensitivity at both the doses tested with better effect at 25 mg/kg bw dose in diabetic mice as indicated by a decrease in glucose level with increasing time ($p < 0.05$). Together, it can be concluded that kaempferol-treated mice exhibited significant improvements in glucose tolerance and insulin sensitivity at both the doses with respect to HFD-STZ-induced diabetic mice.

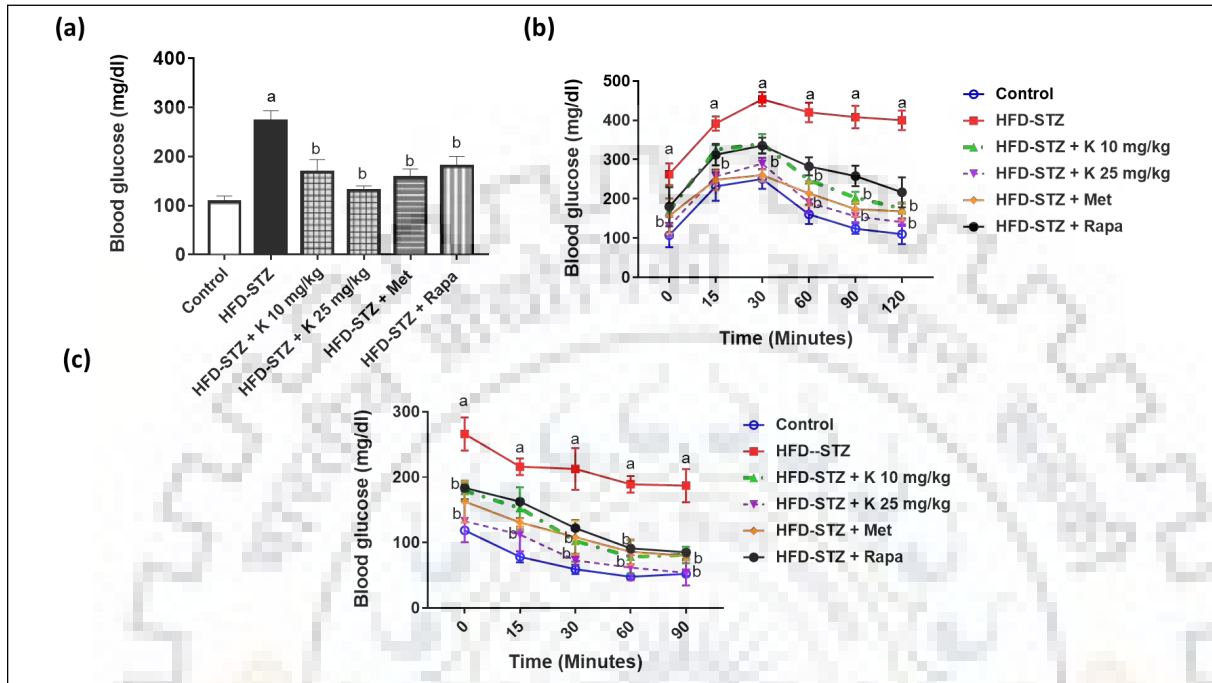


Fig. 7.2. Kaempferol improves glucose and insulin tolerance in diabetic mice. (a) Histogram showing fasting glucose levels of mice from different treatment groups. Blood glucose concentrations measured after administration of (b) glucose for glucose tolerance test (GTT) and (c) insulin for insulin tolerance test (ITT) after 16 weeks of the experiment. Data are mean \pm SD of $n = 6$ for each group. a, $p < 0.05$ versus normal control; b, $p < 0.05$ versus HFD-STZ control. HFD, high-fat diet; STZ, streptozotocin; K, Kaempferol; Met, metformin; Rapa, rapamycin.

7.3.3. Kaempferol improves pancreatic insulin content and insulin secretion

In subsequent studies, we investigated whether kaempferol-induced fasting glucose level, glucose tolerance and insulin sensitivity were accompanied by increased insulin content and secretion. As demonstrated in Fig. 7.3a and b, HFD-STZ induced diabetic mice had significantly reduced levels of plasma insulin level (Fig. 7.3a) and pancreatic insulin content (Fig. 7.3b) as compared to normal mice in both the cases. As expected, kaempferol treatment improved plasma and pancreatic insulin contents in HFD-STZ mice at both the doses albeit it was significantly high at a higher dose ($p < 0.05$) (Fig. 7.3a and b). Metformin and rapamycin treatment also exhibited a

marginal increase in plasma and pancreatic insulin contents. Further, to evaluate the normal β -cell function the glucose-stimulated insulin secretion (GSIS) was evaluated. GSIS is a hallmark assay for testing functionality of β -cells which plays a major role in lowering postprandial glucose levels and thereby maintaining glucose homeostasis. As displayed in Fig. 7.3c, kaempferol significantly enhanced GSIS at both the doses tested by us ($p < 0.05$). Kaempferol-treated (25 mg/kg bw) HFD-STZ mice resulted in about 2-fold increase in plasma insulin concentration at 15 min after glucose administration as compared to HFD-STZ control mice ($p < 0.05$). A similar pattern of improvement was observed with both metformin and rapamycin albeit to a lesser extent than that of a higher dose of kaempferol. Collectively, these findings suggest that kaempferol-induced GSIS is likely to have a positive impact on maintaining glucose homeostasis in a glucose overloaded condition. Thus based on these data it could be inferred that kaempferol not only improves glucose intolerance and insulin resistance but also restores β -cell functions.

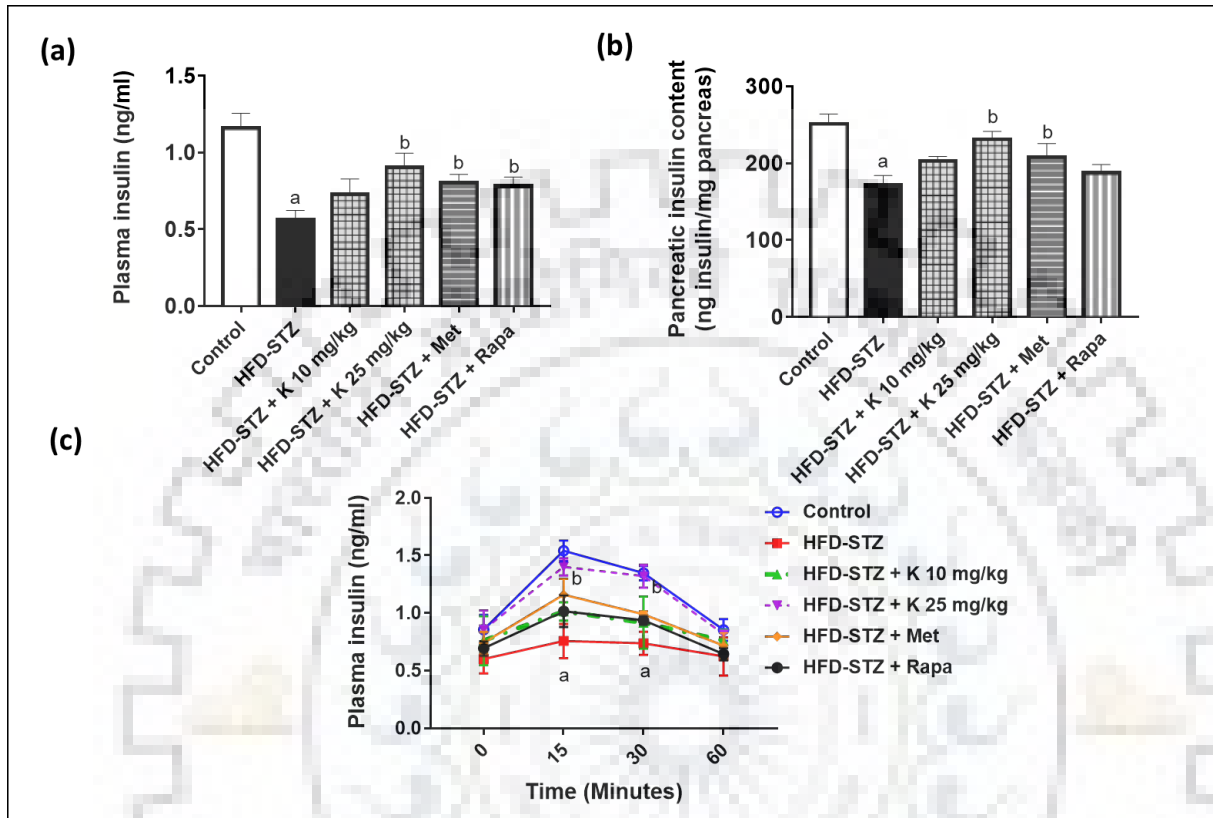


Fig. 7.3. Kaempferol enhances insulin secretion and content in pancreatic islet cells. Histogram showing (a) plasma insulin; (b) pancreatic insulin content; (c) plasma insulin measured during intraperitoneal glucose tolerance test of mice treated with various chemicals as mentioned. Data are mean \pm SD of $n = 6$ for each group. a, $p < 0.05$ versus normal control; b, $p < 0.05$ versus HFD-STZ control. HFD, high-fat diet; STZ, streptozotocin; K, Kaempferol; Met, metformin; Rapa, rapamycin.

7.3.4. Kaempferol induces autophagy in HFD-STZ-induced diabetic mice

In our recent study, we have reported that kaempferol protects clonal pancreatic β -cells (RIN-5F cells) and isolated islets against palmitic acid-induced apoptosis, lipid accumulation and ER stress through modulation of autophagy (Varshney et al., 2017; Varshney et al., 2018). Thus, in the present study, we sought to determine the *in vivo* efficacy of kaempferol in the modulation of autophagy and its related effects. To determine if kaempferol induces autophagy in pancreatic β -

cells of HFD-STZ-induced diabetic mice, initially, the expressions of autophagy-linked genes were analyzed. It has already been reported that both LC3 and Atg7 plays critical roles in autophagosomes formation and maturation and hence are considered as a reliable marker for autophagosomes formation. Apart from these, another protein which is involved in targeting the cargo to autophagosomes is p62 which degrades during autophagic flux. As shown in Fig. 7.4a, HFD-STZ mice exhibited increased expression of LC3-II protein (~ 1.82 fold) in isolated islets preparation which was further increased in kaempferol-treated HFD-STZ mice by about 2.29 and 2.67-fold at 10 and 25 mg/kg bw doses respectively ($p < 0.05$). As expected, rapamycin (an autophagy inducer) treatment exhibited increased expression of LC3-II. Moreover, the expression of Atg7 protein was also upregulated in a similar manner ($p < 0.05$) though there was a marginal increase in islets of HFD-STZ control mice (Fig. 7.4a). Although the observed increase in LC3-II indicates increased autophagosomes, it can also be an outcome of artifact in autophagic turnover which may lead to accumulation of autophagosomes. Thus, in order to confirm that the increase in LC3-II expression is solely due to increase in autophagic activity and not due to impairment of autophagy turnover, we further checked the expression of p62 protein which acts as the specific substrate of autophagy and is degraded during autophagosomal degradation. As shown in Fig. 7.4a, there was a significantly high level of accumulation of p62 (~ 2.4-fold) in HFD-STZ mice islets as compared to normal control mice indicative of the impairment of autophagosomes degradation ($p < 0.05$). Interestingly, kaempferol treatment showed a dose-dependent decrease in p62 expression with respect to HFD-STZ mice ($p < 0.05$) (Fig. 7.4a). Based on this data it could be inferred that kaempferol could manifest induction of autophagy in β -cells of HFD-STZ mice.

It is already established that mTOR signaling pathway is the main regulatory pathway of autophagy (Kim et al., 2011). In our previous study, we have also reported that AMPK/mTOR pathway is involved in the induction of kaempferol mediated autophagy (Varshney et al., 2017). Thus in order to validate these findings in diabetic mice model, immunoblot analysis of p-AMPK and p-mTOR was performed in the current set of experiments. As shown in Fig. 7.4b, kaempferol treatment dose-dependently up-regulated the AMPK phosphorylation in pancreatic islets of diabetic mice with a concomitant decrease in p-mTOR expression ($p < 0.05$). In comparison to

HFD-STZ group, kaempferol at 25 mg/kg bw dose increased AMPK phosphorylation by about 2.9-fold with simultaneous reduction of mTOR phosphorylation by about 2.3-fold ($p < 0.05$) (Fig. 7.4b). Based on this data it could be speculated that kaempferol affects AMPK/mTOR signaling pathway which subsequently instigates autophagy.

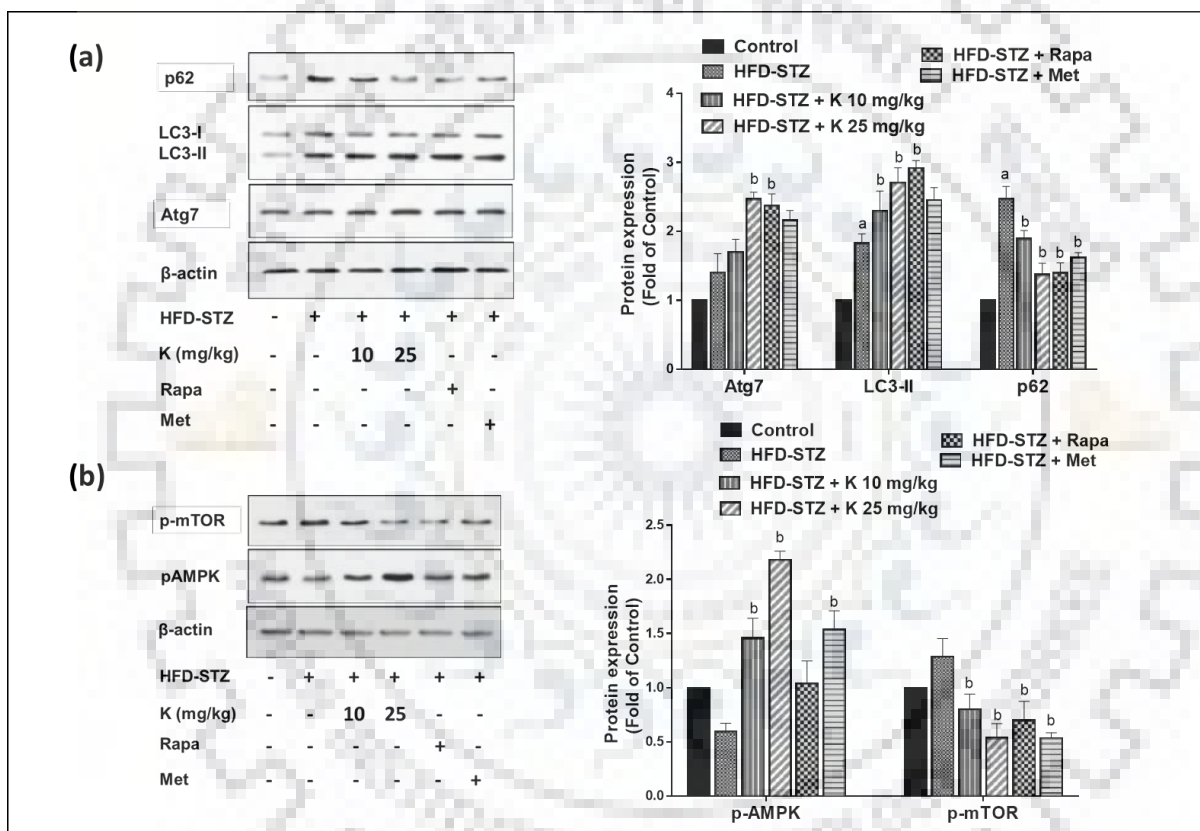


Fig. 7.4. Kaempferol induces autophagy and inhibits apoptosis in pancreatic islet cells. Representative immunoblot analysis of (a) autophagy-, lipid droplets, ER stress- and apoptosis-related proteins and (b) p-AMPK and p-mTOR, in isolated islets from respective mice groups. The histogram in right panel represents the mean relative arbitrary pixels intensities in terms of the fold of normal control mice group for respective proteins. Data are mean \pm SD of $n = 6$ for each group. a, $p < 0.05$ versus normal control; b, $p < 0.05$ versus HFD-STZ control. HFD, high-fat diet; STZ, streptozotocin; K, Kaempferol; Met, metformin; Rapa, rapamycin.

7.3.5. Chloroquine treatment impairs kaempferol-induced autophagic flux

In order to analyze the correlation between kaempferol-mediated autophagy and its related effects, in the next phase, the autophagy inhibitor chloroquine was included in the study. Chloroquine is a lysosomotropic agent which inhibits fusion of autophagosomes with lysosomes and leads to inhibition of autophagic flux and increased accumulation of autophagosomes. Thus, to study autophagic flux, HFD-STZ control and kaempferol treated mice groups were injected with chloroquine for last ten days of the experiment followed by collection of pancreatic islets from the animals. As shown in 7.5a, chloroquine treatment exhibited a non-significant but marginal increase in LC3-II, Atg7 and p62 expression ($p < 0.05$) (Fig. 7.5a) which further confirms that in diabetic condition autophagosomes formation occur but those autophagosomes do not further degrade which leads to inhibition of autophagy flux. At the same time, chloroquine treatment displayed significant accumulation of LC3-II, Atg7 and p62 proteins in islets of kaempferol-treated HFD-STZ mice ($p < 0.05$) as marked by their enhanced expressions (Fig. 7.5a). This accumulation further ascertains that kaempferol stimulates autophagy in HFD-STZ-induced diabetic mice.

Likewise, TEM analysis revealed that pancreatic β -cells in HFD-STZ mice showed a few numbers of double or multilamellar autophagosomes and a limited number of unilamellar or degraded membraned autophagolysosomes which was associated with limited lysosomes (Fig. 7.5b). Moreover, no significant increase in the number of autophagic vacuoles was observed in β -cells of chloroquine-treated HFD-STZ mice which confirmed that the increased autophagosomes in β -cells of HFD-STZ were solely due to impairment of autophagic flux and not due to increased autophagy. Besides, a high number of degenerating β -cells were found in HFD-STZ and chloroquine-treated HFD-STZ mice on the basis of the observation that they contained condensed nuclear chromatin (a characteristic feature of the apoptotic cell), distorted mitochondria and limited insulin granules (Fig. 7.5b). In kaempferol treated mice, TEM examination demonstrated that β -cells had increased autophagolysosomes with degraded organelles and cytoplasm sequestered within them and fewer double-membrane autophagosomes. These cells also exhibited

an increased number of lysosomes. Inhibition of autophagosomes degradation by chloroquine led to significant increase in accumulation of autophagic vacuoles in β -cells of kaempferol treated HFD-STZ mice as compared to only kaempferol-treated HFD-STZ mice (Fig. 7.5b). These cells exhibited non-condensed nuclear chromatin, healthy mitochondria and increased number of insulin granules. These protective effects of kaempferol were abrogated by chloroquine treatment. Taken together, these data strongly suggested that kaempferol not only augments autophagy induction but also induces the increase in autophagosomes turnover, which is partially impaired in HFD-STZ mice. These results were in accordance with immunoblot data. Moreover, TEM analysis also revealed the protective effect of kaempferol induced autophagy on degenerating β -cells of HFD-STZ diabetic mice.



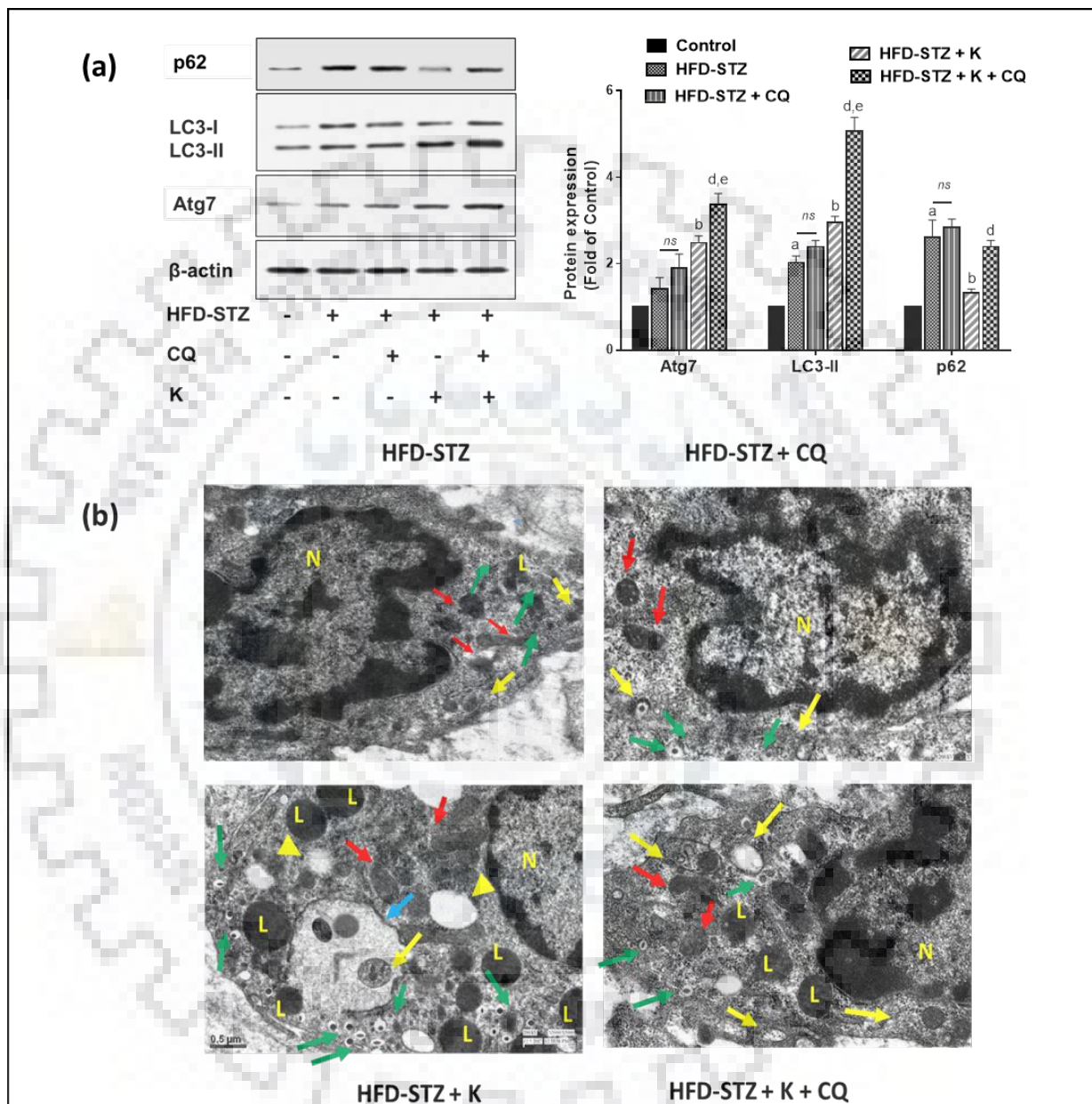


Fig. 7.5. Chloroquine treatment inhibited kaempferol-induced autophagic flux. (a) Representative immunoblot analysis of autophagy marker proteins in the respective groups. The histogram in right panel represents the mean relative arbitrary pixels intensities in terms of the fold of normal control mice group for respective proteins. Data are mean \pm SD of $n = 6$ for each group.

a, $p < 0.05$ versus normal control; b, $p < 0.05$ versus HFD-STZ control; d, $p < 0.05$ versus HFD-STZ + K; e, $p < 0.05$ versus HFD-STZ + CQ. (b) Representative transmission electron microscopy images of pancreatic β -cells after various treatments; the yellow arrow and arrowheads indicate autophagosomes and lysosomes respectively. Whereas, red and green arrows indicate mitochondria and insulin granules respectively. The fusion of autophagosome with lysosome in β -cells of kaempferol treated HFD-STZ are marked with blue arrows. N and L indicate nucleus and lysosome respectively. The scale bar in each image represents 0.5 μm . HFD, high-fat diet; STZ, streptozotocin; K, Kaempferol; CQ, chloroquine; ns, non-significant.

7.3.6. Kaempferol-induced autophagy alleviates ER stress and apoptosis of β -cells and preserves β -cell mass

In our subsequent studies, we validated whether kaempferol could help in reduction of lipid deposition in β -cells. Recently, it has been established that PLIN2, the lipid droplet coat protein, is involved in lipid deposition and triggering ER stress in diabetic Akita mice islets that led to the loss of β -cell mass and function (Chen et al., 2017). Similarly, in our recent study, we reported that kaempferol inhibited PLIN2 expression which in turn reduced lipid accumulation and ER stress in clonal pancreatic β -cells (RIN-5F cells) and isolated islets (Varshney et al., 2018). Thus, to validate our recent findings *in vivo*, immunoblot analysis of PLIN2 was performed. As compared to normal control mice islets, the PLIN2 expression was significantly increased (~ 2.4 -fold) in islets of HFD-STZ mice which was further down-regulated by kaempferol treatment in a dose-specific manner. At 25 mg/kg bw dose, kaempferol exhibited ~ 1.65 -fold decrease in PLIN2 expression with respect to HFD-STZ control ($p < 0.05$) (Fig. 7.6a). As expected, rapamycin treatment also down-regulated PLIN2 expression in HFD-STZ mice. In order to determine whether kaempferol treatment can relieve the PA-induced ER stress the immunoblot analysis of CHOP, the main ER stress marker involved in ER-induced apoptosis was performed. As shown in Fig. 7.6a, the islets of HFD-STZ group showed increased CHOP expression while kaempferol treatment down-regulated the CHOP expression in a dose-specific manner. Kaempferol treatment (25 mg/kg bw) showed ~ 3.5 -fold decrease in CHOP expression as compared to HFD-STZ control group ($p < 0.05$) (Fig. 7.6a). Thus it can be inferred that kaempferol treatment inhibited ER stress

in HFD-STZ mice. Further, to determine whether kaempferol-mediated alleviated ER stress was also linked to reduced apoptosis of β -cells, protein expression analysis of cleaved caspase-3, a hallmark apoptosis marker, was performed (Porter & Jeanicke, 1999). As shown in Fig. 7.6a, the increase in cleaved caspase-3 mediated by HFD-STZ was markedly reduced by kaempferol treatment at both the doses. The cleaved caspase-3 expression was reduced by ~ 3.1 fold in islets of kaempferol (25 mg/kg bw) treated mice ($p < 0.05$). Thus, these results clearly suggest that kaempferol alleviates lipid deposition and ER-stress induced death pathway in HFD-STZ mice thus protecting β -cells from apoptosis.

Furthermore, as shown in Fig. 7.6b, inhibition of autophagy by means of chloroquine averted the kaempferol-inhibited PLIN2, CHOP and cleaved caspase 3 expressions which indicate the involvement of autophagy in a kaempferol-mediated reduction in lipid deposition, ER stress and apoptosis ($p < 0.05$).

In our subsequent studies, we intended to determine whether kaempferol induced alleviation of ER stress and the antiapoptotic property was also associated with increased β -cell mass and for this the morphometric and immunohistochemical analysis was performed. As shown in Fig. 7.6c, in HFD-STZ and chloroquine-treated HFD-STZ group, islets showed a significant reduction in size which was associated with multiple cyst-like structures inside, exhibiting a decreased number of cells. Whereas, in the kaempferol-treated group, the islets size was significantly improved with a reduced number of cysts like structures and increased cell number. Kaempferol-mediated this effect was abolished in islets of chloroquine and kaempferol co-treated mice, indicative of the role of induced autophagy in the protection of islets morphology. Further, insulin immunolabeling in islets confirmed that kaempferol-induced islet mass was actually associated with increased β -cell mass as observed by an increased number of insulin-stained β -cells (Fig. 7.6d). On the contrary, chloroquine treatment abolished the kaempferol-mediated improvement of the islet morphology and β -cell number. Collectively, it could be inferred that kaempferol-mediated autophagy improves β -cell mass in HFD-STZ induced diabetic mice.

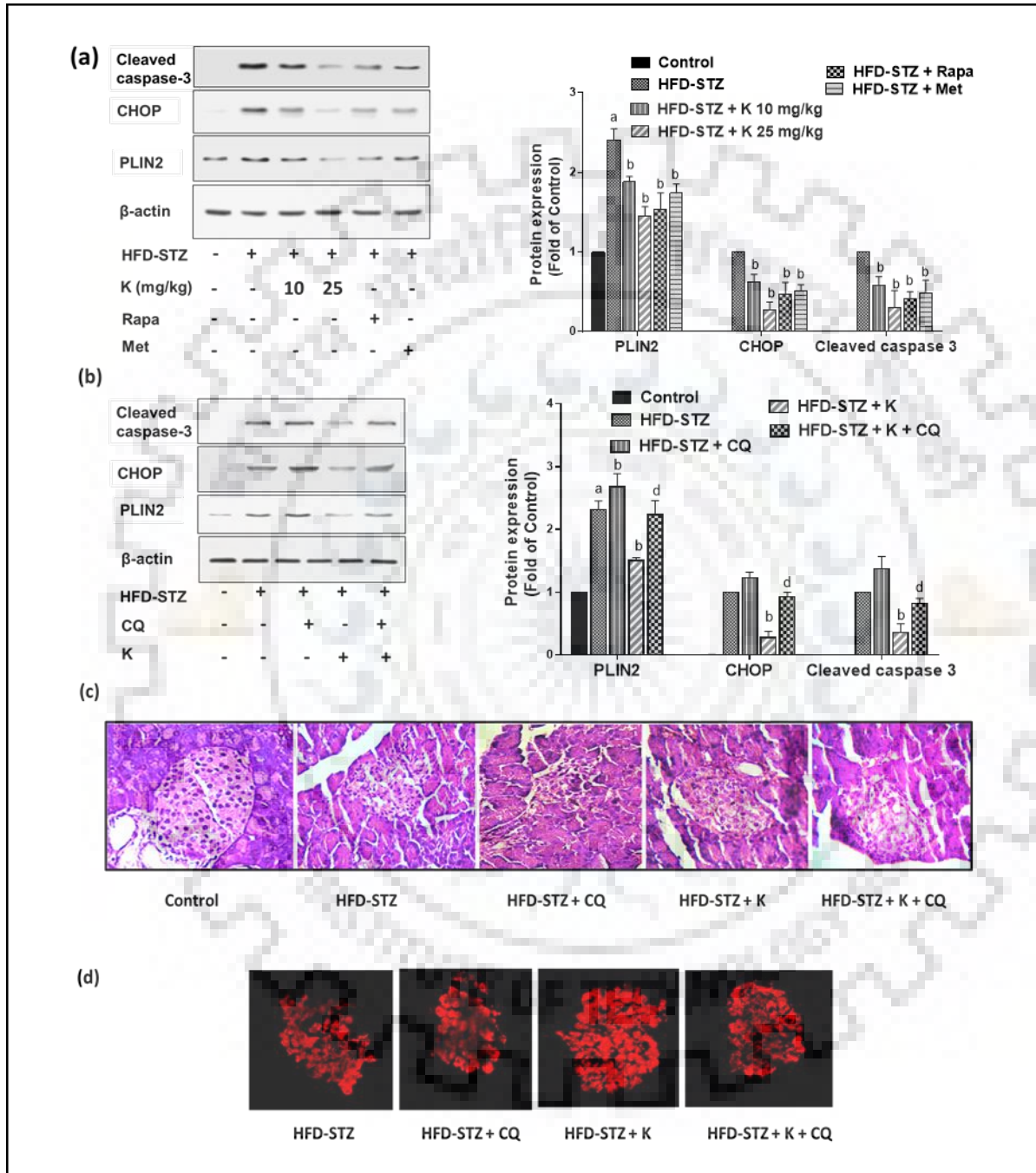


Fig. 7.6. Inhibition of autophagy abolished the kaempferol-mediated protection of pancreatic β -cells. Representative immunoblot analysis for lipid droplets, ER stress and apoptosis marker proteins in (a) absence and (b) presence of chloroquine, over and above the respective treatments

as mentioned in materials and methods. The histogram in right panel represents the mean relative arbitrary pixels intensities in terms of the fold of normal control mice group for respective proteins except for CHOP and cleaved caspase where it was with respect to HFD-STZ mice group. Data are mean \pm SD of $n = 6$ for each group. a, $p < 0.05$ versus normal control; b, $p < 0.05$ versus HFD-STZ control; d, $p < 0.05$ versus HFD-STZ + K. (c) Representative histological images of hematoxylin and eosin stained pancreases of respective groups (original magnification, $\times 400$); (d) Representative immunofluorescence images of pancreatic islets from mice of various treatment groups for presence of insulin. HFD, high-fat diet; STZ, streptozotocin; K, Kaempferol; CQ, chloroquine.

7.3.7. Kaempferol-induced autophagy improved insulin content and secretion

In our subsequent study, we evaluated if kaempferol-mediated autophagy was also involved in the improvement of pancreatic insulin content and glucose-stimulated secretion by estimating the levels of insulin in serum and pancreatic islets of treated animals. As shown in Fig. 7.7, chloroquine treatment significantly abrogated kaempferol mediated improvement in insulin content (Fig. 7.7b) and secretion in fasting (Fig. 7.7a) and glucose fed (Fig. 7.7c) conditions ($p < 0.05$).

Further, to determine the involvement of autophagy in the kaempferol-mediated improvement of glucose tolerance and insulin sensitivity, we investigated the physiological effects of kaempferol-induced autophagy in presence of chloroquine. Inhibition of autophagy by chloroquine exhibited a marginal increase in body weight in kaempferol-treated HFD-STZ mice (Fig. 7.8a). Also, the chloroquine and kaempferol co-treated HFD-STZ mice had significantly higher fasting blood glucose levels (Fig. 7.8b) and impaired glucose tolerance (Fig. 7.8c) as compared to only kaempferol-treated HFD-STZ mice ($p < 0.05$) (Fig. 7.8b and c). Autophagy-impaired kaempferol-treated mice also showed a significant increase in insulin resistance ($p < 0.05$) (Fig. 7.8d). Thus, together it could be inferred that kaempferol-mediated autophagy is involved in enhanced glucose tolerance and insulin sensitivity in HFD-STZ mice.

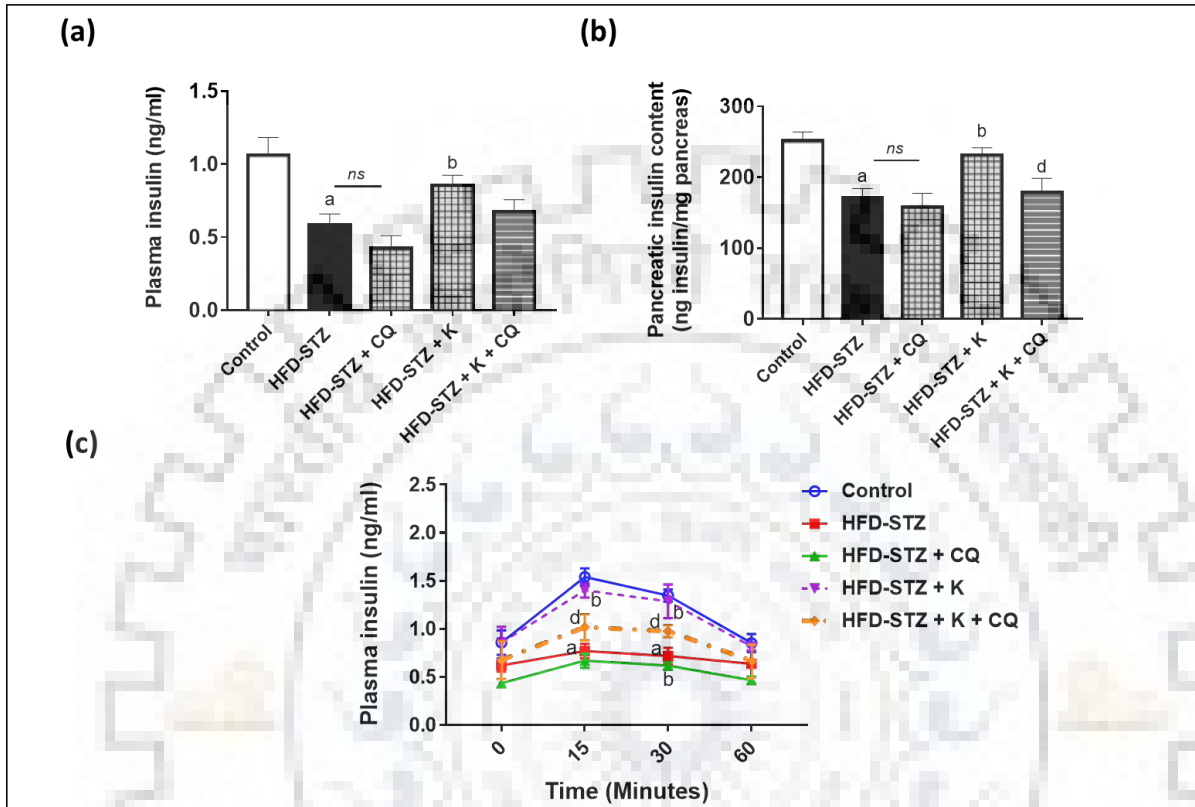


Fig. 7.7. Inhibition of autophagy by chloroquine abolished kaempferol-mediated insulin functions. Histogram showing the level of insulin in the (a) plasma of fasting mice; (b) pancreatic tissues of treated mice; (c) plasma of glucose administered mice measured during intraperitoneal glucose tolerance test after treated with various chemicals as mentioned. Data are mean \pm SD of $n = 6$ for each group. a, $p < 0.05$ versus normal control; b, $p < 0.05$ versus HFD-STZ control; d, $p < 0.05$ versus HFD-STZ + K. HFD, high-fat diet; STZ, streptozotocin; K, Kaempferol; CQ, chloroquine; ns, non-significant.

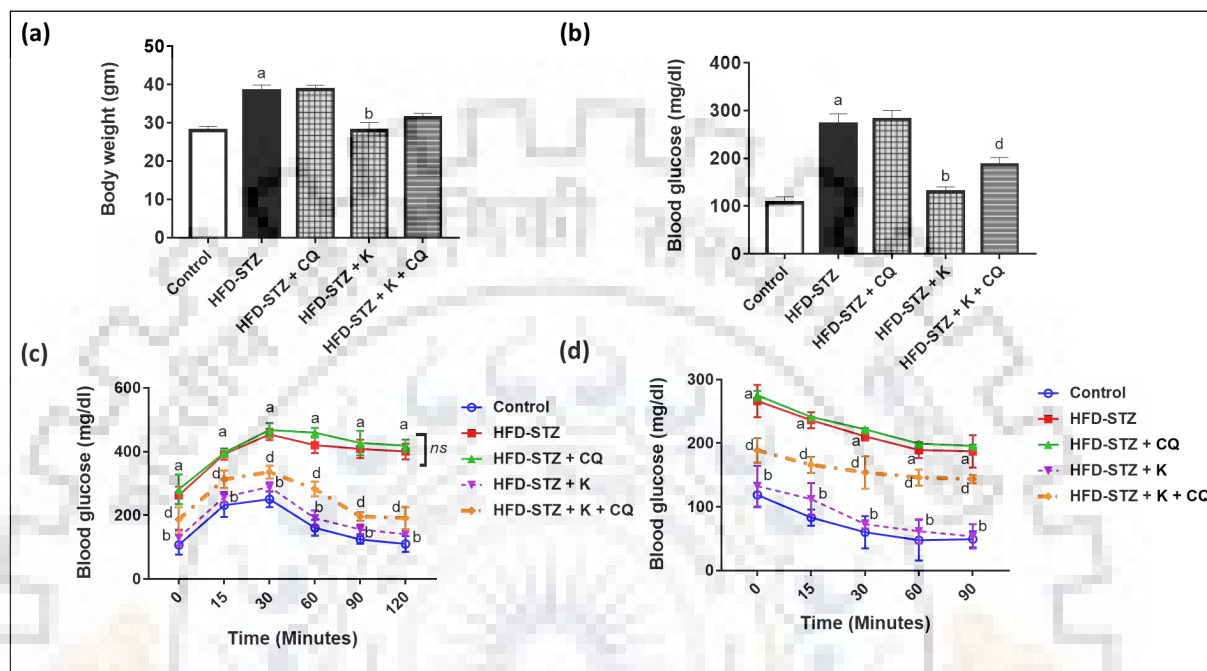


Fig. 7.8. Inhibition of autophagy abrogated kaempferol-mediated enhanced glucose and insulin tolerance. Histogram showing (a) body weights and (b) fasting blood glucose levels of mice treated with respective treatments; Blood glucose concentrations measured during (c) intraperitoneal glucose tolerance test and (d) intraperitoneal insulin tolerance test from mice of various groups. Data are mean \pm SD of $n = 6$ for each group. a, $p < 0.05$ versus normal control; b, $p < 0.05$ versus HFD-STZ control; d, $p < 0.05$ versus HFD-STZ + K. HFD, high-fat diet; STZ, streptozotocin; K, Kaempferol; CQ, chloroquine.

7.4. Discussion

The two pathophysiologic abnormalities of obesity-linked T2DM are insulin resistance and β -cell failure. Lipid and glucose overload are the major risk factors predisposing individuals to T2DM. At the organelle level, dysfunction or stress of ER and mitochondria is a major etiological component in diabetes development. Recently, it is well established that autophagy dysfunction due to lipid overload can lead to ER and mitochondrial dysfunction in β -cells that in turn may lead

to loss of β -cell mass and function. Autophagy is a lysosomal degradation process involved in cell quality control during adverse conditions like starvation and stress (Mizushima, 2007). The role of autophagy in sustaining pancreatic β -cell mass and function is well established and its failure has been linked to the pathophysiology of type 2 diabetes (Codogno & Meijer, 2010). Thus, identifying agents that could modulate autophagy in pancreatic β -cells in lipid-excess stressful conditions could be a better target in developing therapies for obesity-linked T2DM.

Currently, an active area of diabetes research focuses on identifying naturally occurring phytochemicals that can be modulated or developed into diabetes therapies due to their intriguing role in treating various diseases. One such phytochemical found extensively in various plants is kaempferol. Kaempferol has been known for its anti-oxidant and protective effects in various diseases. In our recent *in vitro* and *ex vivo* studies, to the best of our knowledge, we were the first group to report that kaempferol activates autophagy and thus preserves β -cell mass and function in clonal pancreatic β -cells and isolated islets under lipid overloaded condition (Varshney et al., 2017). In our subsequent studies, we found that kaempferol-induced autophagy alleviates palmitic acid-induced lipid deposition and ER stress that usually predispose the pancreatic β -cells to undergo apoptosis (Varshney et al., 2018). Thus, in the present study, we sought to determine the *in vivo* efficacy of kaempferol in the modulation of autophagy and its related effects. To the best of our knowledge, this is the first ever report providing evidence that kaempferol protects β -cell mass and function through AMPK-mTOR mediated autophagy in HFD-STZ induced type 2 diabetic mice.

In the present study, we have successively developed HFD-STZ induced type 2 diabetic mice characterized by hyperglycemia, glucose intolerance, insulin resistance and decreased insulin secretion. This model has been extensively used in various studies to test antidiabetic effects of various compounds (Skovsø, 2014). To test antidiabetic and its related effect of kaempferol the developed diabetic mice were treated with this phytochemical. Kaempferol treatment resulted in significant improvement in glycemic control and metabolic profile. The improved glucose homeostasis was found to be associated with increased insulin sensitivity. Our results are in

accordance with a recent study which demonstrated that kaempferol improves hyperglycemia and insulin sensitivity in middle aged-old obese mice (Alkhalidy et al., 2015)

In our subsequent study, we attempted to elucidate the level of autophagy in pancreatic β -cells of HFD-STZ control and kaempferol-treated mice. Numerous studies have shown that β -cells of HFD-fed animals exhibited increased autophagy which is an adaptive endogenous mechanism that protects themselves from HFD-mediated stress (Ebato et al., 2008; Sun et al., 2016). On the other hand, chronic exposure of HFD led to impaired autophagy which exacerbated metabolic stress and contributes to the development of diabetes (Liu et al., 2017; Sheng et al., 2017). In spite of long known implication of autophagy in diabetes, it is still poorly understood whether this adaptive increased autophagy response is defective in diabetes. Thus, detailed studies are warranted to decipher the level of autophagy in β -cells of HFD induced obese or diabetic mice. In this study, we found that the β -cells of HFD-STZ induced diabetic mice exhibited compromised autophagy. These cells displayed a marginal increase in autophagosomes accompanied by limited fusion of autophagosomes with lysosomes. Also, LC3-II and p62 expression were elevated in islets of HFD-STZ diabetic mice compared to those of normal control mice which suggests impaired autophagy. This data is in line with the studies which exhibited impaired autophagy in diabetic mice and T2DM patients reported earlier (Masini et al., 2009; Codogno & Meijer, 2010). Conversely, kaempferol treatment exhibited significantly enhanced autophagy in pancreatic islets as evidenced by the up-regulated level of Atg7 and LC3-II with a concomitant decrease in p62 expression which corroborated well with TEM analysis showing increased autophagic vacuoles and lysosomes. Together, it is evident that kaempferol-mediated increase in autophagosomes and LC3-II expression was not due to impairment of autophagosomes degradation but solely due to increased autophagy flux. Apart from this, kaempferol was found to up/down-regulate AMPK/mTOR phosphorylation respectively. It is well established that AMPK and mTOR are the positive and negative regulators of autophagy respectively and activation of AMPK-mediated autophagy pathway protects β -cells from apoptosis (Han et al., 2010). Our data are consistent with the report which showed that kaempferol exhibited increased autophagy in the rotenone-induced neuronal model (Filomeni et al., 2010).

Additionally, kaempferol treated mice islets exhibited decreased PLIN2 expression which was found to be elevated in diabetic mice. PLIN2 is major lipid droplet coat protein which is reported to be overexpressed in β -cells during conditions of lipid deposition (Faleck et al., 2010; Chen et al., 2017). Genetic ablation of PLIN2 was shown to lower triglyceride content and ER stress and thus partially restoring β -cells (Chen et al., 2017). Further, to confirm the role of kaempferol in the alleviation of ER stress, CHOP expression was analyzed. CHOP is a downstream component of ER stress pathways and a key mediator of cell death in response to ER stress that has been demonstrated to be increased in PA-treated β -cells and murine models of type 2 diabetes, the deletion of which restored the β -cell mass (Oyadomari & Mori, 2004). In our study, CHOP was found to be up-regulated in islets of HFD-STZ induced diabetic mice while kaempferol treatment significantly down-regulated CHOP and cleaved caspase 3 indicative of a reduction in ER stress-mediated apoptosis. Our data are consistent with the report by Chen et al. which demonstrated that PLIN2 downregulation alleviates ER stress which further links to the protection of β -cell mass and function (Chen et al., 2017).

Further, chloroquine-treated mice groups were evaluated to establish a link between kaempferol-induced autophagy and its positive effects on metabolic parameters and β -cell protection. As discussed earlier, chloroquine blocks fusion of autophagosomes with the lysosomes thus inhibiting autophagic flux. Inhibition of autophagy attenuated kaempferol-induced down-regulation of PLIN-2, CHOP and cleaved caspase 3 which was further linked to degenerated β -cell mass as evidenced by hematoxylin-eosin stain and decreased the number of insulin-stained β -cells. These data are consistent with studies which demonstrated that stimulation of autophagy improves ER-stress-induced diabetes and protects functional β -cell mass (Bachar-Wikstrom et al., 2013; Sheng et al., 2017). Moreover, chloroquine treatment abrogated the kaempferol-mediated improvement in hyperglycemia and glucose tolerance which is associated with decreased insulin sensitivity and insulin secretion. Our present data is in line with a recent finding which showed that dipeptidyl peptidase-4 inhibitor, MK-626, restores insulin secretion through enhancing autophagy in HFD-induced mice (Liu et al., 2016).

In summary, all results delineated in the present study corroborate well with each other to arrive at the conclusion that, kaempferol induced autophagy is involved in the protection of β -cell mass and function which in part ameliorates diabetes in HFD-STZ induced diabetic mice. To the best of our knowledge, this study provides new insights into our understanding of kaempferol's therapeutic potential and suggests that it could be a promising candidate either singly or in combination with other drugs/ chemicals for the prevention of obesity-linked type 2 diabetes. However, based on these data further comprehensive studies are warranted involving transgenic mouse models and human subjects to establish the exact cross-talks among various pathways in causing autophagy and its associated effects by kaempferol. This sort of study would help in establishing the nutraceutical potential of this phytochemical where our data would provide a base.





CHAPTER 8

***ROLE OF KAEMPFEROL-INDUCED
AUTOPHAGY IN AMELIORATION OF HEPATIC
LIPID ACCUMULATION AND INSULIN
RESISTANCE: AN IN VITRO AND IN VIVO
STUDY***

Chapter 8. Role of kaempferol-induced autophagy in amelioration of hepatic lipid accumulation and insulin resistance: an *in vitro* and *in vivo* study

8.1 Introduction

The non-alcoholic fatty liver disease is a most common form of the chronic liver disease, which is linked to obesity and diabetes (El-Kader and El-Den Ashmawy, 2015). The incidence of this ailment is increasing in parallel with the increase in obesity. In mammalian system, the liver plays a central role in modulation of fatty acid metabolism. The export of lipid in the form of triglycerides (TGs), deposited in lipid droplets (LDs) within the hepatocytes, depends on the synthesis as well as the availability of TGs (Zechner et al., 2012; Alves-Bezerra and Cohen, 2017). Decreased turnover of hepatic lipid droplets can lead to the development of non-alcoholic fatty liver disease (NAFLD) (Greenberg et al., 2011). Excessive accumulation of these TGs leads to oxidative and ER stress which in turn triggers hepatic insulin resistance (Farese Jr et al., 2012).

Insulin resistance is the major pathological conditions related to obesity-linked NAFLD and diabetes. Several studies revealed the positive correlation between HFD-induced insulin resistance and its lipogenic effect, which leads to the fact that ectopic lipid accumulation can interrupt insulin signaling pathway (Samuel and Shulman, 2012). Importantly, ER stress recently emerged as another mechanism underlying insulin resistance (Samuel et al., 2004; Fu et al., 2012). Major regulators of unfolded protein response (UPR) pathways like protein kinase RNA-like endoplasmic reticulum kinase (PERK) and inositol-requiring enzyme 1 (IRE1) can activate c-Jun N-terminal kinase (JNK)/inhibitory-B kinase (IKK), that are involved in the inhibition of insulin signal transduction by phosphorylating insulin receptor substrate 1 (IRS1) at serine sites (Urano et al., 2000; Aguirre et al., 2002; Liang et al., 2006).

A number of recent reports indicate that the impairment of autophagy is associated with obesity-linked ER stress, insulin resistance and diabetes (Codogno and Meijer, 2010; Yang et al., 2010; Toshima et al., 2018). In addition, some reports also claim the close association of ER stress and autophagy, a self-degradative process to remove damaged organelles and protein aggregates in

order to balance the sources of energy inside the cells (Yorimitsu et al., 2006; Wang et al., 2015). Apart from ER-associated proteasomal degradation, autophagy is supposed to be an alternative machinery to degrade lipids in hepatic cells (Qiu et al., 2011; Yamada and Singh, 2012; Gracia-Sancho and Guixé-Muntet, 2018).

Autophagy is a well-orchestrated physiological phenomenon with a vital function in balancing sources of energy and maintaining cellular homeostasis (Singh and Cuervo, 2011). It also plays a housekeeping role in removing the misfolded proteins, eliminating damaged organelles and recycling the cytosolic components during nutritional stress (Glick et al., 2010). Recently, lipids are also reported as the target of macroautophagy which is known as lipophagy (Dong and Czaja, 2011; Schulze et al., 2017). Lipophagy plays an important role in the selective removal of LDs which helps in balancing the intracellular lipid storage, cellular level of free fatty acids and eventually the energy homeostasis (Singh et al., 2009; Singh and Cuervo, 2012). In liver, the impairment of autophagy can lead to steatosis which in turn results in liver injury as well as steatohepatitis (Czaja, 2010; Gonzalez-Rodriguez et al., 2014). Animals fed with an HFD have shown reduced hepatic autophagy (Yang et al., 2010; Wang et al., 2015). A number of evidences suggests that autophagy plays an indispensable role in regulating lipid metabolism in the liver (Singh et al., 2009; Gonzalez-Rodriguez et al., 2014). It is evident that *in vivo* and *in vitro* inhibition of autophagy results into the intracellular accumulation of fat whereas enhancement of autophagy ameliorates the condition of hepatic steatosis which further suggests that strategic inhibition of autophagy may be adapted for treating fatty liver disease (Hsiao et al., 2017; Wang et al., 2015; Yang et al., 2010; Zhang et al., 2017). Hence, autophagy is now regarded as one of the emerging targets for abnormalities in lipid metabolism as well as accumulation.

Kaempferol (3,5,7,4-tetrahydroxyflavone), a natural flavonoid, has been known for its anti-oxidant and protective effects in various diseases. It is found in various dietary resources such as apples, cabbage, beans, berries, grapes, garlic, tomatoes, green tea and onion (M Calderon-Montano et al., 2011). Recently, our group has reported that kaempferol preserved pancreatic β -cell mass and function under lipid overloaded condition (Varshney et al., 2017; Varshney et al., 2018). It is well established that the two pathophysiological abnormalities which links obesity to

type 2 diabetes mellitus (T2DM) are insulin resistance and β -cell failure. Thus, in this study, we intended to determine the effects of kaempferol in the alleviation of insulin resistance and impaired insulin signal transduction. The current study investigates the potential role of autophagy in kaempferol-mediated amelioration of lipid accumulation and insulin resistance in palmitic acid (PA)-challenged HepG2 cells *in vitro* and in the liver of HFD-STZ induced diabetic mice *in vivo*.

8.2. Materials and methods

8.2.1. Cell culture and treatment

HepG2 cell line, a human hepatoma-derived cell line was cultured in DMEM with 10% heat-inactivated fetal bovine serum and 1% penicillin-streptomycin solution under a humidified atmosphere with 5% CO₂ maintained at 37°C. Before initiating the cell-based assays, the basal media was replaced with complete DMEM supplemented with 1% bovine serum albumin and 0.5 mM PA. The cells were then treated with different concentrations of kaempferol in presence or absence of chloroquine (10 μ M). One hour prior to addition of kaempferol the cells were treated with chloroquine. The cells treated with only DMEM containing 1% bovine serum albumin were considered as normal control group.

8.2.2. siRNA transfections

Specific siRNAs targeting human Atg7 and AMPK along with a negative control siRNA were used in the experiments. Briefly, the HepG2 cells were seeded in 6 well plates at a density of 5 X 10⁵ cells/well. The cells were transiently transfected with 50 nM of each siRNA in respective wells using the transfection reagent (Qiagen, Valencia, USA) according to the manufacturer's instructions and incubated for 24 h in a 5% CO₂ incubator at 37°C. Further, the transfected cells were treated with or without 10 μ M kaempferol in presence of 0.5 mM PA and incubated in a CO₂ incubator at 37°C at this condition for another 24 h.

8.2.3. Luciferase reporter assay

HepG2 cells were seeded in a 12-well plate at a density of 4×10^4 cells/well and incubated overnight at 37°C in a 5% CO₂ incubator. Then the cells were incubated in serum-free DMEM for 6 h before performing transfection. Subsequently, the cells were transiently transfected with 200 ng/well PPREx3-tk-Luc reporter plasmid and 25 ng pcMX-PPAR α plasmid using Polyfect transfection reagent (Qiagen), according to the protocol provided by the manufacturer. As an internal control for transfection, β -gal plasmid was also transfected with the luciferase reporter plasmid. The transfected cells were then exposed to various concentrations of kaempferol and vehicle in the charcoal-stripped medium and incubated for 24 h. After the treatment period was accomplished, the cells were lysed with lysis buffer (0.6 M NaCl, 0.2 M MgSO₄, 0.1 M EDTA, 0.08 M Tricine, 0.1 % Triton X-100, 0.2 M DTT) and the luminescence was estimated using luciferin as substrate. The experiment was repeated in triplicates with all the experimental treatment conditions. The observed luciferase values for each lysate were normalized to β -galactosidase activity of respective lysate and expressed as fold luciferase activity with respect to the vehicle-treated cells.

8.2.4. Preparation of PA-containing media

The DMEM media with 0.5 mM PA was prepared as discussed earlier in chapter 3 of this thesis. DMEM containing 1% bovine serum albumin was used as vehicle control all throughout the experiments (until and unless mentioned) as the final concentration of serum was 1% in PA-containing DMEM.

8.2.5. Oil Red O staining for lipids

The lipid accumulations in the HepG2 cells were verified with Oil Red O staining. The assay was performed according to the protocol described in chapter 3.

8.2.6. Labeling of autophagic vacuoles and lysosomes with mono dansylcadaverine (MDC) and LysoTracker stains

MDC is widely used as a probe to label autophagic vacuoles whereas LysoTracker Red DND-99 is used for labeling lysosomes specifically. The MDC-LysoTracker staining was performed as per protocol mentioned in chapter 3. The cells were analyzed and imaged under confocal laser scanning microscope (LSM 780, Carl Zeiss, Germany) at 355 nm and 577 nm excitation and 460 nm and 590 nm emission wavelengths for MDC and LysoTracker respectively.

8.2.7. Experimental animals

All the experimental procedures conducted on laboratory mice were conducted in accordance with the approved guidelines of Committee for the Purpose of Control and Supervision of Experiments on Animals (CPCSEA), India, with prior approval from Institutional Animal Ethics Committee (Approval number: BT/IAEC/2017/02). For the experiment, 7 weeks old male C57BL/6 mice were procured from CSIR-Institute of Microbial Technology, Chandigarh, India and housed in a well-maintained animal house under standard conditions (12 h dark-light cycle and temperature $23\pm 2^{\circ}\text{C}$). The mice were acclimatized under this ideal condition for two weeks prior to the start of experiment and they were provided *ad libitum* access to either normal chow diet or a HFD and water till the completion of the experiment.

8.2.8. Experimental design

After acclimatizing, mice were divided into eight groups (n=6) as follow;

Group I -Standard normal chow-fed mice (Normal Control)

Group II – HFD fed mice + STZ (Diabetic control)

Group III – HFD fed + STZ + metformin (25 mg/kg body weight (bw)/day) (Positive control)

Group IV – HFD fed + STZ + rapamycin (0.2 mg/kg bw /day) (Positive control for autophagy)

Group V – HFD fed + STZ+ kaempferol (10 mg/kg bw /day) (low dose)

Group VI - HFD fed + STZ + kaempferol (25 mg/kg bw /day) (High dose)

Group VII – HFD fed + STZ (Diabetic control) + chloroquine (25 mg/kg bw /day) (Autophagy-impaired diabetic control)

Group VIII – HFD fed + STZ+ kaempferol (25 mg/kg bw/day) + chloroquine (25 mg/kg bw/day) (Autophagy-impaired treatment group)

8.2.9. Model development

Diet-induced obesity-linked type 2 diabetes mice model was developed in all the groups; except for group I (Normal control group). The normal control group was fed with standard chow diet containing approximately 17.5% kcal protein, 75% kcal carbohydrate and 7.5% kcal fat (RM1, Special Diet Services, Witham, Essex, UK) whereas the obesity-induced mice were fed with high-fat diet containing approximately 20% kcal protein, 20% kcal carbohydrate and 60% kcal fat (D12492, Research Diets, New Brunswick, NJ, USA) in which lard and soybean oil were primarily used as the fat source for 10 weeks. The mice were monitored for the change in their weight every two weeks. After completion of 10 weeks of high-fat diet induction, the obese mice were kept under fasting condition for overnight and were intraperitoneally injected with an optimum dose of STZ(35 mg/kg dissolved in freshly prepared 0.1 M cold citrate buffer (pH 4.5). The normal control mice group were injected with equal volume of 0.1 M cold citrate buffer (pH 4.5). After one week, the mice were monitored for fasting blood glucose and the animals having glucose level > 240 mg/dl were considered as diabetic and were kept in this condition for one more week for stabilization. All the mice groups were fed on their respective diet formulations until the completion of the experiment (for a total period of 16 weeks).

8.2.10. Experimental treatment

After 12 weeks of HFD and simultaneous two weeks of STZ induction during this period, the diabetic mice from group III and IV were injected intraperitoneally with metformin (25 mg/kg bw/day) and rapamycin (0.2 mg/kg bw/day) respectively. The group V and VI were

intraperitoneally injected with low dose (10 mg/kg bw/day) and high dose (25 mg/kg bw/day) of kaempferol respectively. The control group mice i.e., from the group I and II were administered with a solvent of sterile 10% ethanol: 40% PEG 400: 50% PBS as vehicle. To maintain homogeneity of treatment conditions, all the compounds were dissolved in the same solvent containing sterile 10% ethanol: 40% PEG 400: 50% PBS. The mice were fed with their respective diet until the completion of the study (for a total period of 16 weeks).

8.2.11. Autophagy flux determination

Mice from group VII and VIII were intraperitoneally injected with chloroquine (25 mg/kg bw/day) for the last 10 days before the completion of the experiment allowing determination of flux as a more precise measure of autophagic activity.

8.2.12. Transmission electron microscopy (TEM) analysis

The liver samples isolated from the mice were chopped uniformly and sliced into 2 mm² sections. The samples were further prepared as per protocol mentioned in chapter 3.

8.2.13. Measurement of lipid profile

To measure the total cholesterol, triglyceride, LDL and NEFA content, the serum was isolated from blood samples of the animals and further analyzed with the help of commercially available kits (Erba, Germany) according to the manufacturer's instructions.

8.2.14. Statistical analysis

All the experimental results were represented as the mean \pm standard deviation (SD) of three independent experiments. The comparison between groups were evaluated by one-way/ two-way ANOVA followed by Turkey's post hoc test using Graph Pad Prism 6 software (Graph Pad

Software, San Diego, CA, USA). The statistical significance of the experimental results was considered for a p-value < 0.05.

8.3. Results

8.3.1. Kaempferol inhibits lipid accumulation in PA-induced HepG2 cells

Firstly, to determine the effect of kaempferol on lipid deposition in PA-induced HepG2 cells, the intracellular lipid content was determined by oil red o staining. As shown in Fig. 8.1a and b, PA-treated cells exhibited a significant increase in lipid deposition which was significantly reduced in response to kaempferol treatment in a dose-dependent manner ($p < 0.05$). Since TGs are the main components during lipid deposition, we next analyzed the TGs accumulation into each treatment group. Interestingly, kaempferol treatment led to a reduction in triglycerides accumulation in a dose-dependent manner ($p < 0.05$) (Fig. 8.1c). As displayed in Fig. 8.1b and c, kaempferol at 10 μM dose exhibited around 1.84- and 2.1-fold decrease in lipid and TG accumulation with respect to PA-treated HepG2 cells ($p < 0.05$). Additionally, mRNA expression analysis of *PLIN2*, a gene which expresses PLIN2 protein (a lipid droplet coat protein involved in hepatic lipid accumulation), was performed by RT-PCR analysis. PA-treated cells exhibited ~ 3.2 -fold increase in *PLIN2* gene expression as compared to normal cells, which however, was significantly down-regulated by kaempferol in a dose-dependent manner ($p < 0.05$) (Fig. 8.1d). Kaempferol at 10 μM dose showed ~ 1.4 -fold decrease in *PLIN2* expression with respect to PA-treated HepG2 cells ($p < 0.05$) (Fig. 8.1d). Moreover, immunoblot analysis exhibited that kaempferol treatment led to significant down-regulation of PLIN2 protein in a dose- (Fig. 8.1e) and time (Fig. 8.1f)-dependent manner ($p < 0.05$). As shown in Fig. 8.1e, PA-induced PLIN2 expression was markedly inhibited ~ 2.3 -fold by kaempferol at 10 μM concentration ($p < 0.05$). Similarly, kaempferol inhibited the PA-induced time dependent upregulation of PLIN2 till 48 h (Fig. 8.1f) ($p < 0.05$). Thus, together it can be clearly inferred that kaempferol treatment inhibited PA-induced lipid accumulation in HepG2 cells. In our subsequent studies, 10 μM dose of kaempferol was chosen as this is the lowermost

dose at which kaempferol showed a significant reduction in lipid accumulation and this concentration is also physiologically relevant.

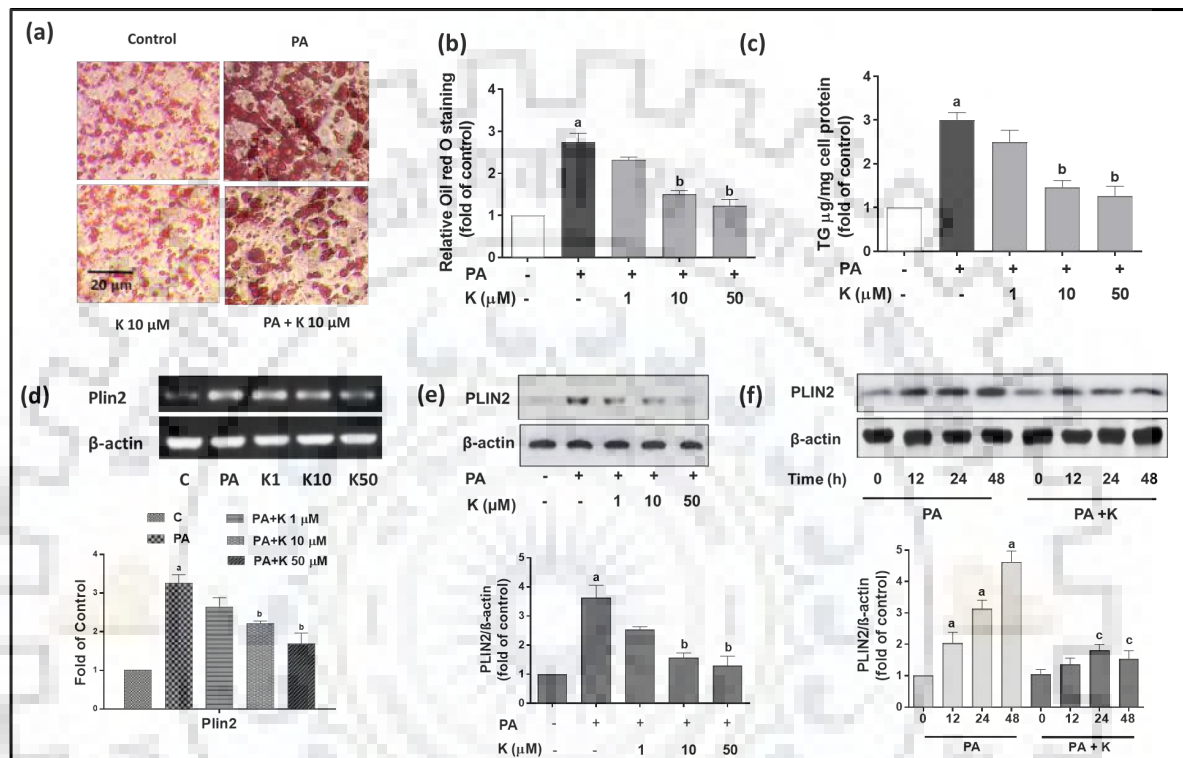


Fig. 8.1. Kaempferol treatment inhibits PA-induced lipid accumulation in HepG2 cells. HepG2 cells were treated with various concentrations of kaempferol in presence of 0.5 mM PA for 24 h. (a) Microscopic images of Oil Red O stained-HepG2 cells; Histograms showing (b) lipid content; (c) triglycerides content of treated cells; Representative (d) RT PCR analysis of PLIN2 gene; (e) immunoblot analysis of PLIN2 with increasing dose and (f) time durations. The histogram below each figure denotes the mean relative arbitrary pixels intensities expressed as fold change with respect to vehicle-treated control cells. The results are mean \pm S.D. of three independent experiments. a, b and c indicates $p < 0.05$ versus vehicle-treated control group, PA-treated control group and PA-treated group of respective time durations respectively. C, control; PA, palmitic acid; K, kaempferol.

8.3.2. Kaempferol up-regulates PPAR- α expression and increases cytosolic lipolysis in PA-induced HepG2 cells

Peroxisome proliferator-activated receptor alpha (PPAR- α) is a key transcriptional regulator of hepatic lipid metabolism and its activation is known to reduce hepatic intracellular lipid content. To determine the role of kaempferol on lipid metabolism, the expression level of PPAR- α and its responsive genes were analyzed in PA-induced HepG2 cells. Firstly, we investigated whether kaempferol activated PPAR- α in cell-based transactivation system using luciferase as reporter system. As shown in Fig. 8.2a, kaempferol transactivated PPAR- α in a dose-dependent manner in presence of PA whereas PA treatment alone did not show any such response. Kaempferol at 10 μ M concentration significantly activated \sim 2.2-fold PPAR- α activity with respect to PA treatment ($p < 0.05$) (Fig. 8.2a). Moreover, mRNA (Fig. 8.2b) and protein (Fig. 8.2c) expression levels of PPAR- α were up-regulated significantly in kaempferol-treated PA-challenged HepG2 cells in a dose dependent manner ($p < 0.05$). Likewise, mRNA expressions of genes involved in cytosolic lipolysis pathway i.e., adipose triglyceride lipase (*ATGL*) and hormone-sensitive lipase (*HSL*) were also increased significantly in response to kaempferol treatment ($p < 0.05$) (Fig. 8.2b). Besides, genes which mediates β -oxidation of fatty acids i.e., carnitine palmitoyltransferase I (*CPT-1A*) and acyl-CoA oxidase (*ACOX1*) were also significantly up-regulated in kaempferol-treated cells ($p < 0.05$) (Fig. 8.2b). This data suggests that cytosolic lipolysis and β -oxidation were involved in kaempferol-mediated hypolipidemic effects.

Recently, an alternative pathway for lipid degradation has been identified known as lipophagy (lipo-macro-autophagy). In the lipophagy process, the hepatic degradation of lipid droplets are caused by lysosomal acid lipases (LAL) in lysosomes, which mobilizes large amounts of lipid rapidly. Thus to elucidate whether kaempferol exerts its lipolytic effect through lipophagy the mRNA expression analysis of *LAL* was performed. Interestingly, the *LAL* expression was found to be up-regulated by about \sim 4-folds in kaempferol (10 μ M)-treated cells suggesting the role of lysosomes in kaempferol-mediated degradation of lipids ($p < 0.05$) (Fig. 8.2b).

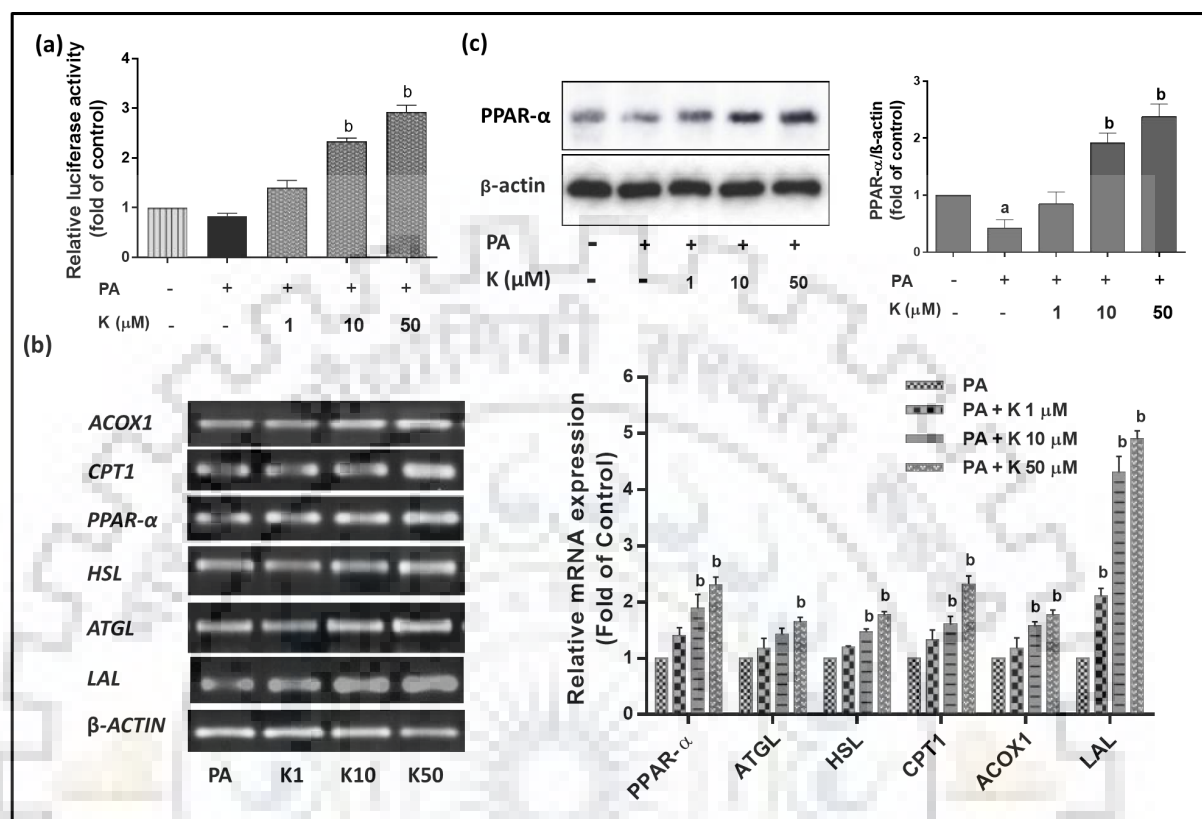


Fig. 8.2. Kaempferol alters expression of genes involved in cytosolic lipolysis and β -oxidation. Representative (a) histogram showing relative PPAR- α luciferase activity expressed as fold of vehicle-treated control; (b) RT-PCR analysis of genes involved in cytosolic lipolysis and β -oxidation and (c) immunoblot analysis of PPAR- α protein. The histogram in the right panel represents the mean relative arbitrary pixels intensities of mean \pm S.D. of three independent experiments expressed as fold change with respect to the vehicle-treated control group or only PA treated control group (for b). a, $p < 0.05$ versus vehicle-treated control group; b, $p < 0.05$ versus the PA-treated control group. C, control; PA, palmitic acid; K, kaempferol.

8.3.3. Kaempferol enhances autophagy in PA-induced HepG2 cells

As discussed earlier, autophagy is one of major mechanisms which is involved in hepatic lipid catabolism and found to be impaired during lipid overload conditions which in turn lead to lipid accumulation inside the cells. In order to determine if autophagy was induced by kaempferol in

PA-induced HepG2 cells, MDC-LysoTracker co-staining was performed. As shown in Fig. 8.3a, in normal condition, kaempferol treatment exhibited an increased number of autophagosomes and lysosomes as evidenced by a concerted increase in MDC and LysoTracker staining respectively. Whereas, PA-treated cells displayed few numbers of autophagosomes co-localized with a limited number of lysosomes which in presence of kaempferol led to a prominent increase in co-localization of autophagosomes with the lysosomes, thus, forming autophagolysosomes. Collectively, this data suggests that kaempferol induces autophagolysosomes formation in normal as well as PA-treated condition, however, the increase in autophagolysosomes formation was more prominent in PA-challenged condition (Fig. 8.3a). In order to reconfirm this further, protein expression analysis of LC3 and p62, the major proteins involved in autophagy process, were analyzed. LC3-II is a major protein involved in autophagosomes formation and serves as a reliable marker of autophagy induction. The immunoblot analysis revealed the dose (Fig. 8.3b)- and time (Fig. 8.3c)-dependent increase in LC3-II/LC3-I protein expression in response to kaempferol treatment which was found to be decreased in PA-treated cells ($p < 0.05$). At 10 μM concentration, kaempferol showed ~ 2.8 -fold up-regulation in LC3-II/LC3-I expression as compared PA-treated control cells for 24h ($p < 0.05$) (Fig. 8.3c). Though, the concerted increase in LC3-II protein exhibited an increased number of autophagosomes, however, it can be due to inhibition of autophagosomes turnover. Thus, in order to elucidate whether the increase in LC3-II expression was solely due to the increased number of autophagosomes, protein expression analysis of p62 was performed. The p62 is the specific autophagy substrate which directly binds to LC3 and degrades at later stages upon fusion with lysosomes. As shown in Fig. 8.3b and c, kaempferol treatment showed the significant decline in p62 expression in dose- and time-dependent manner which was found to be up-regulated in PA-treated control cells. PA treatment increased p62 expression by ~ 3.3 -fold which was then decreased to ~ 1.67 -fold in response to kaempferol at 10 μM concentration ($p < 0.05$) (Fig. 8.3b). In this experiment temsirolimus was used as positive control (Fig. 8.3b) which is a potent autophagy inducer. Interestingly our data showed that kaempferol showed almost similar effect as that of temsirolimus at 10 μM concentration.

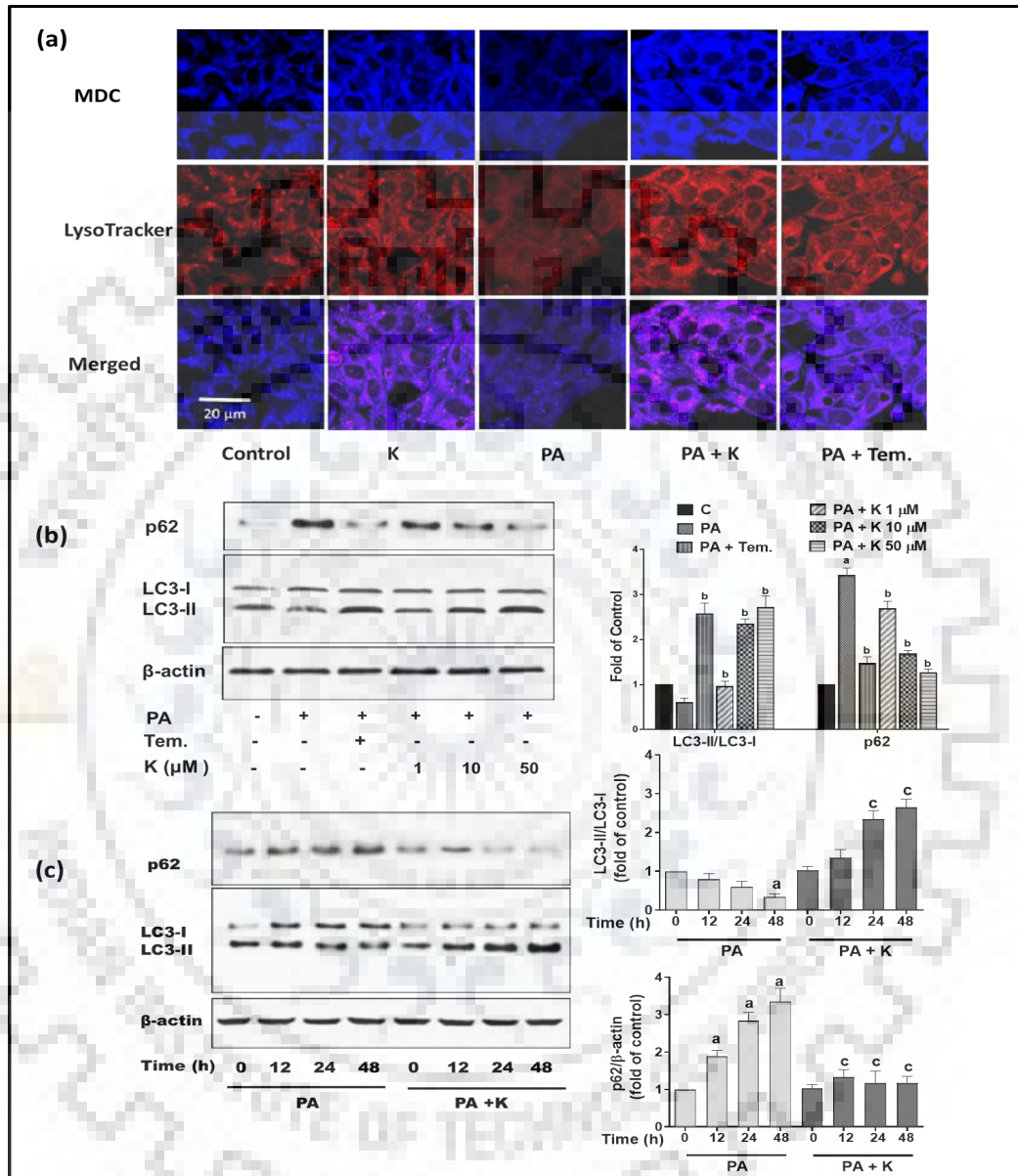


Fig. 8.3. Kaempferol induces autophagy in PA-challenged HepG2 cells. HepG2 cells were treated with kaempferol (10 μM) with or without 0.5 mM PA and/or 200 nM temsirolimus (positive control) for 24 h. (a) Representative confocal images of MDC-LysoTracker stained cells to selectively stain autophagosomes and lysosomes. Images are representative of three independent experiments. Representative immunoblot analysis for the expression of LC3 and p62

with (b) increasing doses and (c) time duration of kaempferol treatment. The histogram in the right panel of each figure represents the mean relative arbitrary pixels intensities in terms of fold over vehicle-treated control (for dose-dependent studies) and PA (0h) for time-dependent studies. Results are the mean \pm S.D. of three independent experiments. a, $p < 0.05$ versus vehicle-treated control, whereas, a, $p < 0.05$ versus PA (0h) group for Fig. 8.3c; b, $p < 0.05$ versus PA-treated control; c, $p < 0.05$ versus PA control of respective time duration. PA, palmitic acid; K, kaempferol; Tem, temsirolimus.

In the subsequent studies, autophagy inhibitor chloroquine was used to detect autophagic flux. Chloroquine is a lysosomotropic agent which inhibits fusion of autophagosomes with lysosomes thus inhibiting autophagic flux. EGFP-LC3 puncta formation, a marker of autophagy, was monitored to ascertain kaempferol-induced autophagy in PA-induced HepG2 cells. The LC3 protein is found in two forms i.e., cytosolic LC3-I form and membrane-bound LC3-II form. LC3-II is formed by lipidation of LC3-I and subsequently recruited onto autophagosomal membranes and leading to the formation of LC3 puncta (as indicated by large number of dotted spots in cells) which serves as a reliable marker to monitor autophagosomes formation. To monitor EGFP-LC3 puncta formation, stably transfected EGFP-LC3-HepG2 cells were treated with kaempferol with or without chloroquine. As shown in Fig. 8.4a, kaempferol treatment exhibited a prominent increase in EGFP-LC3 puncta which was further increased in presence of chloroquine. On the contrary, PA treatment showed limited puncta with diffused cytoplasmic EGFP fluorescence which could only marginally increased further in response to chloroquine treatment (Fig. 8.4a). Such an observation is affirmative of the fact that observed increase in autophagosomes is due to kaempferol-mediated induction of autophagy itself not due to impairment of autophagic turnover. Moreover, immunoblot analysis revealed that chloroquine treatment increased expression of autophagic marker proteins (LC3-II/LC3-I, Atg7 and p62) in kaempferol treated cells (as compared on PA + kaempferol treated group) which could be attributed to inhibition of lysosomal degradation of autophagosomes ($p < 0.05$) (Fig. 8.4b). Together, this data confirmed that kaempferol treatment not only enhances autophagy induction but also augments autophagic flux.

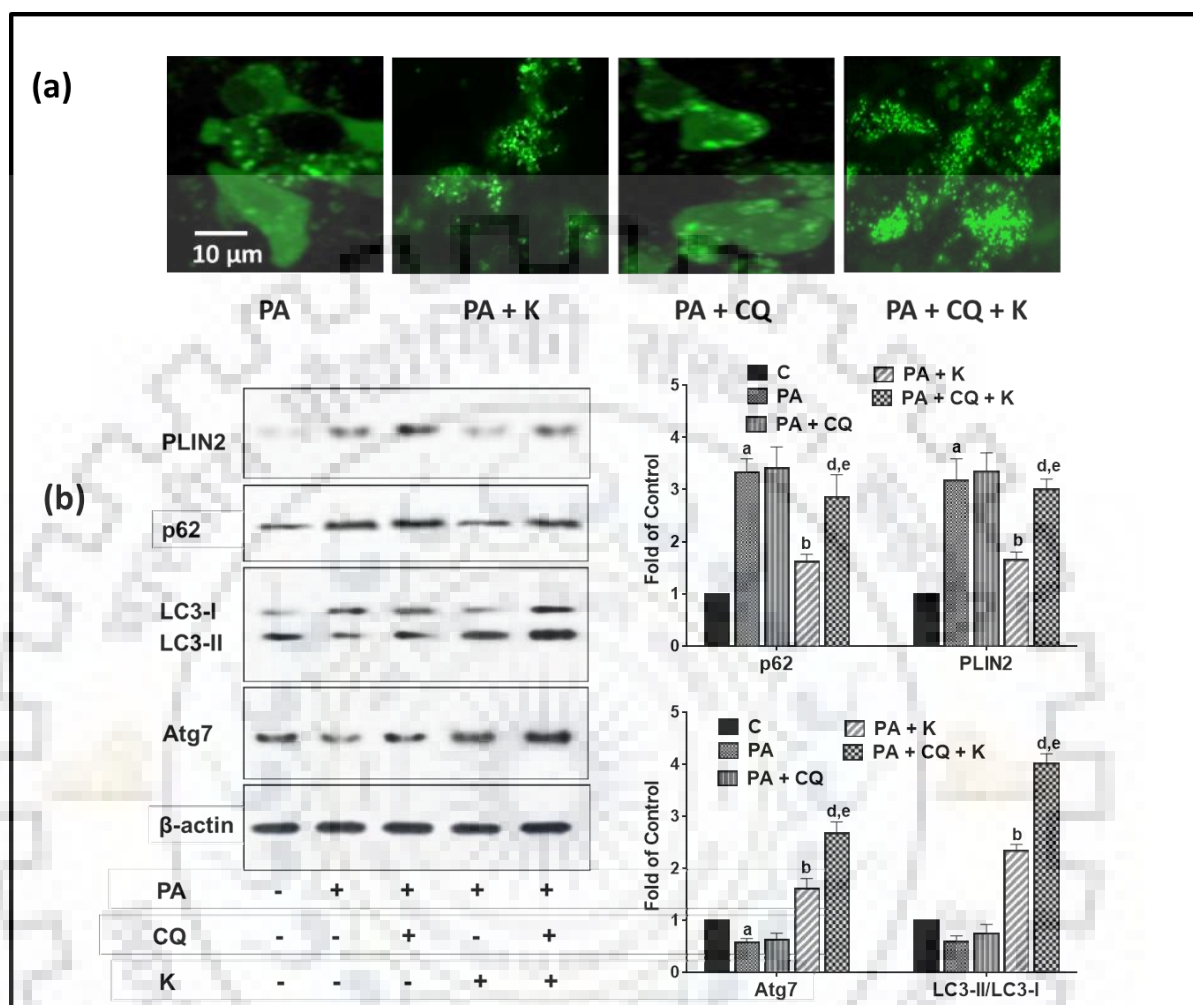


Fig. 8.4. Chloroquine treatment impairs kaempferol-mediated autophagic flux. HepG2 cells were treated with kaempferol (10 μM) with or without 10 μM chloroquine in presence of 0.5 mM PA for 24 h. Representative (a) confocal images of EGFP-LC3 puncta formation in response to various treatments and (b) immunoblot analysis of autophagy marker proteins in response to various treatments. The histogram in the right panel of “b” represents the mean relative arbitrary pixels intensities in terms of the fold of vehicle-treated control group. Results are the mean ± S.D. of three independent experiments. a, p<0.05 versus vehicle-treated control; b, p<0.05 versus PA control; d, p<0.05 versus (PA + K) group; e, p<0.05 versus (PA + CQ) group. PA, palmitic acid; K, kaempferol; CQ, chloroquine.

8.3.4. AMPK signaling is involved in kaempferol-mediated autophagy induction

It is well established that hyper-nutrition conditions during obesity can inhibit AMPK and subsequently activate mTORC1 which may further be linked to impaired autophagy and increased anabolic metabolism in the liver. Thus, we further elucidated whether kaempferol may activate AMPK/mTOR pathway which in turn activates autophagy. The treatment of HepG2 cells with kaempferol resulted in a dose-dependent increase in AMPK phosphorylation with a simultaneous decrease in mTOR phosphorylation (Fig. 8.5a and b). Kaempferol (10 μ M) treatment increased AMPK phosphorylation by \sim 2.9-fold with concomitant \sim 2.1-fold decline in mTOR phosphorylation with respect to PA treatment for 24h ($p < 0.05$) (Fig. 8.5a). A similar pattern of time dependent expression was observed for AMPK and mTOR in response to 10 μ M of kaempferol (Fig. 8.5b). Based on this data, it could be speculated that kaempferol differentially effects AMPK/mTOR signaling which may instigate autophagy.

In order to confirm the specific involvement of kaempferol-activated AMPK in autophagy induction, AMPK siRNA was included in further studies. As shown in Fig. 8.5c, kaempferol-induced up-regulation of AMPK phosphorylation were significantly down-regulated in presence of AMPK siRNA ($p < 0.05$). With the decrease in the level of AMPK, there was subsequent inhibition of LC3-II with progressive accumulation of p62 proteins thus confirming a gross decline in the process of autophagy in the cells which could not be rescued by kaempferol ($p < 0.05$) (Fig. 8.5c). The results depicted in Fig. 8.5c clearly indicate that with the down-regulation of AMPK phosphorylation there is simultaneous up-regulation of mTOR phosphorylation in kaempferol-treated cells in the presence of AMPK siRNA ($p < 0.05$). This further confirms kaempferol-mediated AMPK activation is involved in the inhibition of mTOR and thus autophagy induction.

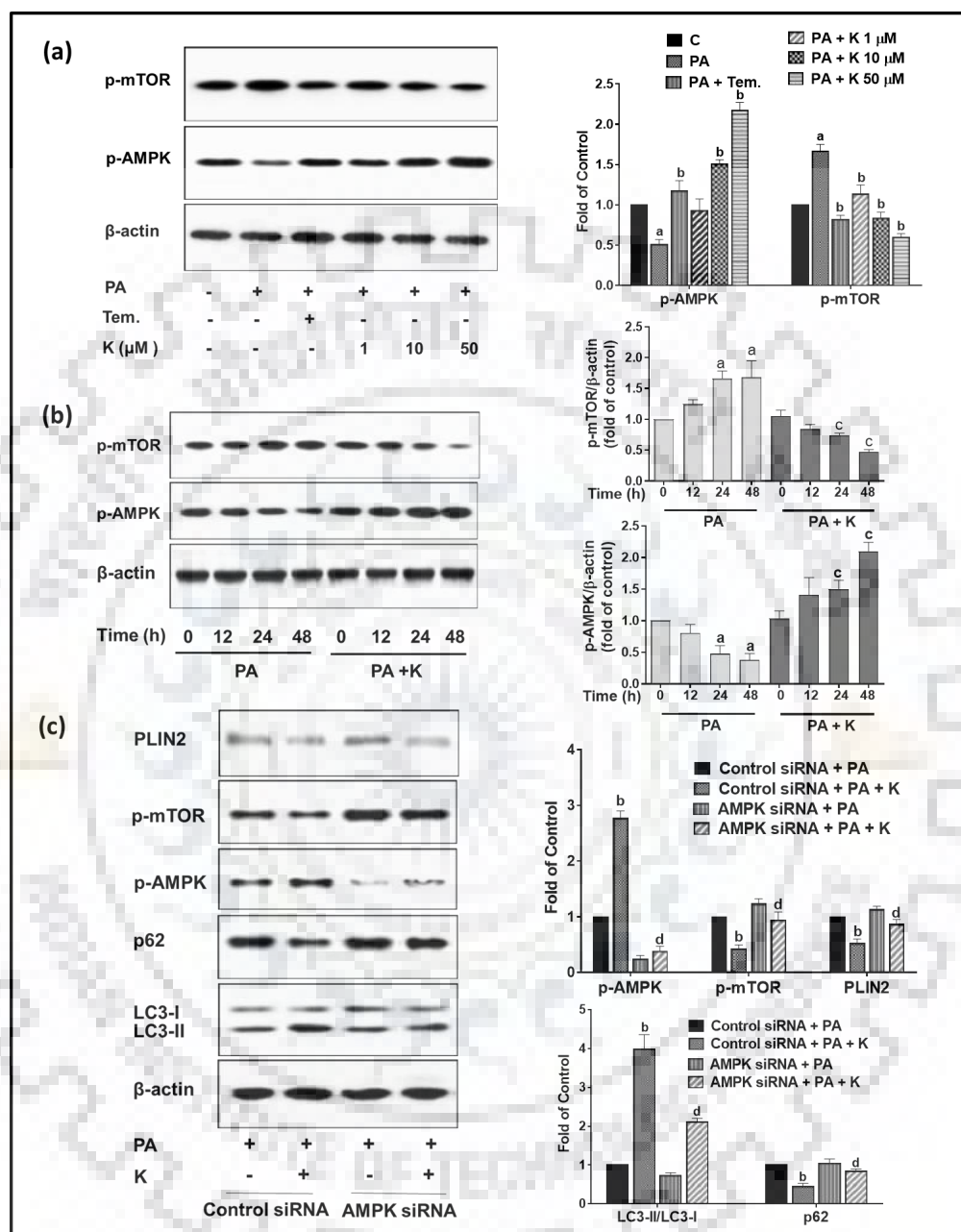


Fig. 8.5. Kaempferol instigates autophagy through AMPK/mTOR pathway. Representative immunoblot analysis of the phosphorylation of AMPK and mTOR in HepG2 cells in response to kaempferol treatment for varying (a) dosages; (b) time period and (c) at 10 μ M dose in presence of AMPK siRNA. The histogram in the right panel of each figure represents the mean relative arbitrary pixels intensities in terms of fold over control in respective figures. Results are the mean

± S.D. of three independent experiments. a, $p < 0.05$ versus vehicle-treated control group and PA (0h) for Fig. 8.5a and Fig. 8.5b respectively; b, $p < 0.05$ versus PA-treated control group; c, $p < 0.05$ versus PA-treated group of respective time duration; d, $p < 0.05$ versus (PA + K) group. PA, Palmitic acid; K, Kaempferol; Tem, temsirolimus.

8.3.5. Inhibition of autophagy blocks kaempferol-induced reduction of lipid accumulation

To draw a clear correlation between lipid inhibitory and autophagy inducing effects of kaempferol, in our subsequent studies, autophagy and AMPK inhibitors were included. For this Atg7 siRNA was used for knocking down the expression of this protein which is an essential protein involved in autophagosomes formation and maturation. As shown in Fig. 8.5c and Fig. 8.6a, inhibition of autophagy by AMPK and Atg7 siRNAs led to inhibition of the kaempferol-mediated increase in LC3-II and Atg7 expressions ($p < 0.05$). Additionally, inhibition of autophagy exhibited a significant increase in p62 expression which could only partially be rescued in kaempferol-treated HepG2 cells ($p < 0.05$) (Fig. 8.5c and 8.6a). Further, immunoblot analysis of PLIN2, the lipid droplet coat protein, revealed that inhibition of autophagy increased its expression even in the kaempferol-treated cells ($p < 0.05$) (Fig. 8.5c and Fig. 8.6a). Co-treatment of kaempferol with AMPK and Atg7 siRNA increased the expression of PLIN2 by ~ 1.5- and -1.3-fold respectively as compared to kaempferol treatment ($p < 0.05$) (Fig. 8.5c and Fig. 8.6a) indicating its role in regulation of lipid droplets..

Additionally, chloroquine (an autophagy inhibitor), Atg7 and AMPK siRNAs prominently abolished the kaempferol-mediated inhibition of lipid accumulation and led to increased accumulation of lipids in PA-challenged HepG2 cells as determined by Oil Red O staining ($p < 0.05$) (Fig. 8.6b, c and d). As shown in Fig Fig. 8.6b, PA-induced lipid accumulation was prominently inhibited by kaempferol (PA + K). However, this activity was significantly abolished either by autophagy inhibitor (chloroquine) or when the autophagy inducers were inhibited (AMPK and Atg7) by siRNA. Kaempferol could only partially rescue this situation. As shown in Fig. 8.6c and d, estimation of stained lipid droplets showed that the inhibitory activities raised the level of lipid droplets by about 2-fold as compared to only kaempferol treatment (PA + K) ($p < 0.05$). Similarly, kaempferol-induced inhibition of triglyceride content in PA-stressed cells was

also shown to be reverted in presence of autophagy inhibitors. Co-treatment of PA-induced cells with Atg7 and AMPK siRNAs along with kaempferol showed a significant increase in triglyceride content as compared to only kaempferol-treated cells ($p < 0.05$) (Fig. 8.6e and f). Thus, together it can be clearly inferred that kaempferol-induced AMPK/mTOR-mediated autophagy is involved in the inhibition of lipid accumulation in PA-induced HepG2 cells.

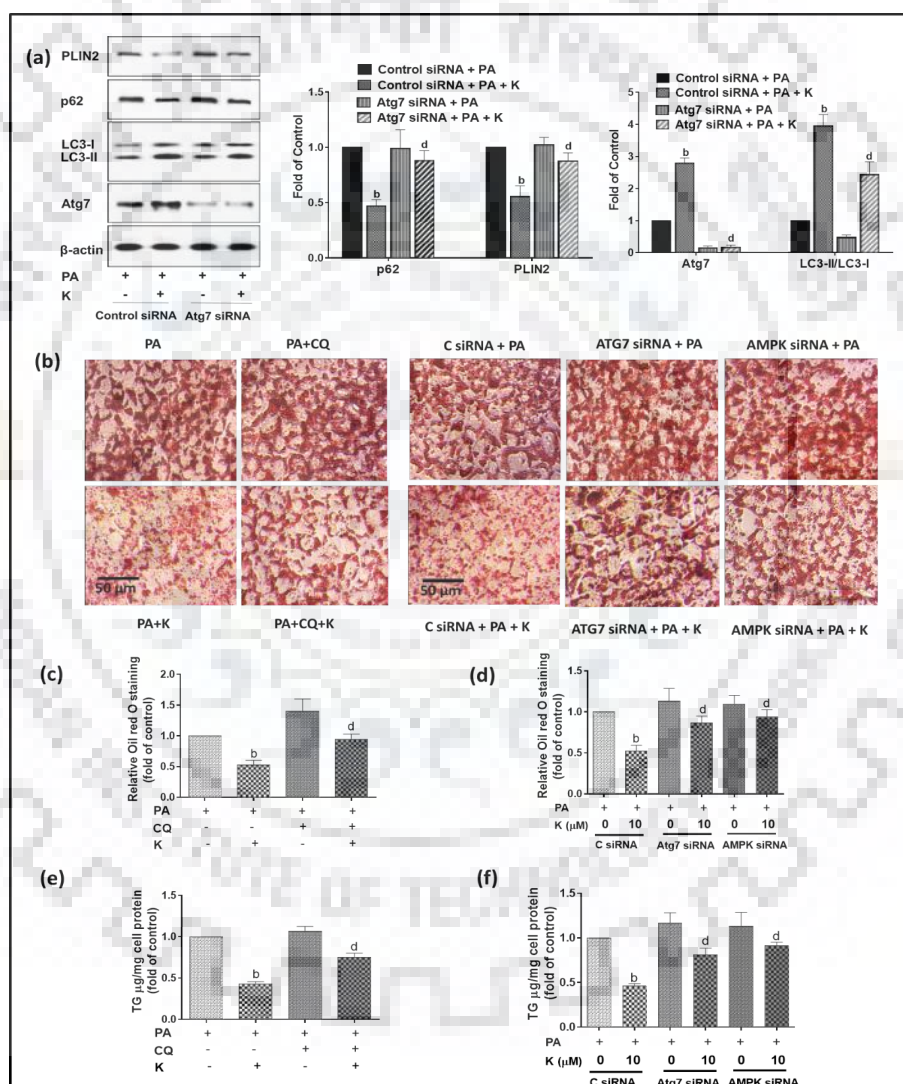


Fig. 8.6. Kaempferol-induced autophagy facilitates a decrease in PA-induced lipid stores. HepG2 cells were incubated with kaempferol (10 μ M) with various inhibitors in presence of PA (0.5 mM) for 24 h. (a) Representative immunoblots of various proteins in response to Atg7

siRNA. The histogram in the right panel represents the mean relative arbitrary pixels intensities of mean \pm S.D. of three independent experiments expressed as fold change with respect to the PA-treated group. (b) Microscopic images of Oil Red O stained cells with or without various inhibitors; Histogram representing (c) and (d) lipid content; (e) and (f) triglyceride content of treated cells. Results are the mean \pm S.D. of three independent experiments. b, $p < 0.05$ versus PA control; d, $p < 0.05$ versus (control siRNA + PA + K) group, whereas, d, $p < 0.05$ versus (PA + K) for fig 6c and 6e. PA, palmitic acid; K, kaempferol; CQ, chloroquine.

8.3.6. Kaempferol improves lipid profile and insulin resistance in HFD-STZ induced diabetic mice

To investigate the systemic effects of kaempferol, mice were subjected to 4 weeks of daily kaempferol treatment at 10 mg/kg body weight (bw) or 25 mg/kg bw doses after 12 weeks of HFD-STZ treatment. The kaempferol treated diabetic mice exhibited a significant decrease in weight, however, there was no difference in food intake between different groups (data not shown). The HFD-STZ diabetic mice exhibited the marked increase in total cholesterol, triglycerides (TG), low-density lipoprotein (LDL) and non-esterified fatty acids (NEFA) levels which were significantly reversed by kaempferol administration at 25 mg/kg bw dose ($p < 0.05$) (Fig. 8.7a, b, c and d).

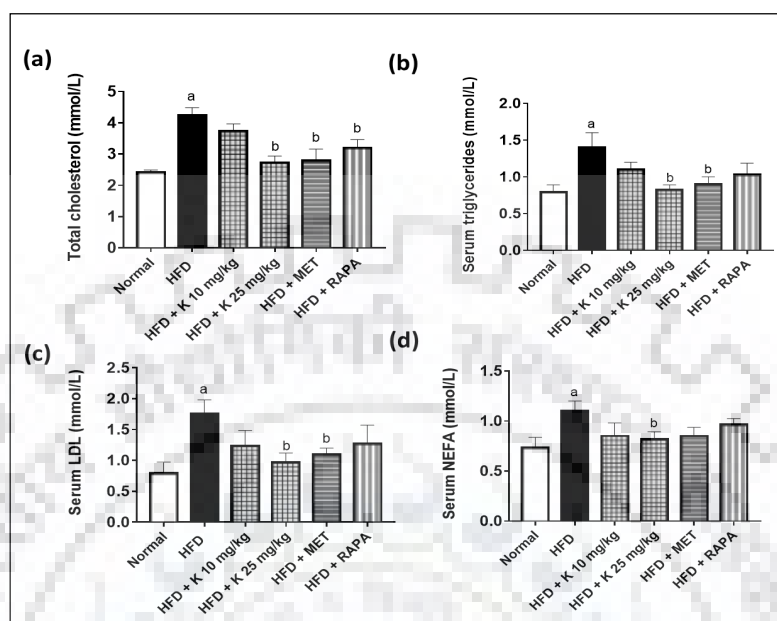


Fig. 8.7. Kaempferol improves metabolic profile in diabetic mice. Mice were fed with normal chow diet (control) or with high-fat diet for 10 weeks followed by injection with streptozotocin (35 mg/kg BW) and successive treatments for 4 weeks. Histogram showing (a) Total cholesterol (b) Triglycerides (c) LDL (d) NEFA level in serum of treated mice. Data are mean \pm SD of $n = 6$ for each group. a, $p < 0.05$ versus normal control; b, $p < 0.05$ versus HFD-STZ control. HFD, high-fat diet; STZ, streptozotocin; K, Kaempferol; Met, metformin; Rapa, rapamycin; LDL, Low-density lipoprotein; NEFA, Non-esterified fatty acids.

8.3.7. Kaempferol induces autophagy in the liver of HFD-STZ mice

To determine whether kaempferol induces autophagy in the liver of HFD-STZ mice, the immunoblot analysis of autophagy-linked genes were evaluated in liver tissue of kaempferol-administered mice. As shown in Fig. 8.8a, the level of LC3-II and Atg7 were dramatically reduced, with subsequent and significant increase in the level of p62 in vehicle-treated HFD-STZ mice as compared to normal control mice indicative of decreased autophagy ($p < 0.05$). However, on treating the HFD-STZ mice with kaempferol, the expressions of Atg7 and LC3-II were significantly increased with concomitant decline in p62 expression thus indicating a direct involvement of kaempferol in the autophagic process in liver. Further, to study the impact of

autophagic flux, HFD-STZ control and kaempferol-treated mice groups were injected with chloroquine for last ten days to inhibit autophagic flux. As shown in Fig. 8.8a, there was no significant difference in the level of LC3-II, Atg7 and p62 proteins among livers of HFD-STZ control mice and HFD-STZ mice treated with chloroquine. However, chloroquine treatment displayed significant accumulation of LC3-II, Atg7 and p62 proteins in livers of kaempferol-treated HFD-STZ mice ($p < 0.05$) (Fig. 8.8a). This accumulation further ascertains that kaempferol stimulates autophagy in HFD-STZ-induced diabetic mice.

Further, immunoblot analysis of pAMPK and p-mTOR was performed to reconfirm the finding in HepG2 cells for the involvement of this pathway *in vivo* in kaempferol-treated HFD fed diabetic mice. As shown in Fig. 8.8b, kaempferol treatment dose-dependently up-regulated the AMPK phosphorylation in livers of diabetic mice with a concomitant decrease in p-mTOR expression ($p < 0.05$). In comparison to HFD-STZ group, kaempferol at 25 mg/kg BW dose increased AMPK phosphorylation by about 3.1-fold with simultaneous reduction of mTOR phosphorylation by ~ 1.9 -fold ($p < 0.05$) (Fig. 8.8b). The effect of kaempferol in inducing this autophagic process was comparable to rapamycin and metformin, two potent drugs known to induce autophagy (Fig. 8.8b). This *in vivo* data is in line with the HepG2 data and thus collectively it could be speculated that kaempferol affects AMPK/mTOR signaling pathway which subsequently instigates autophagy.

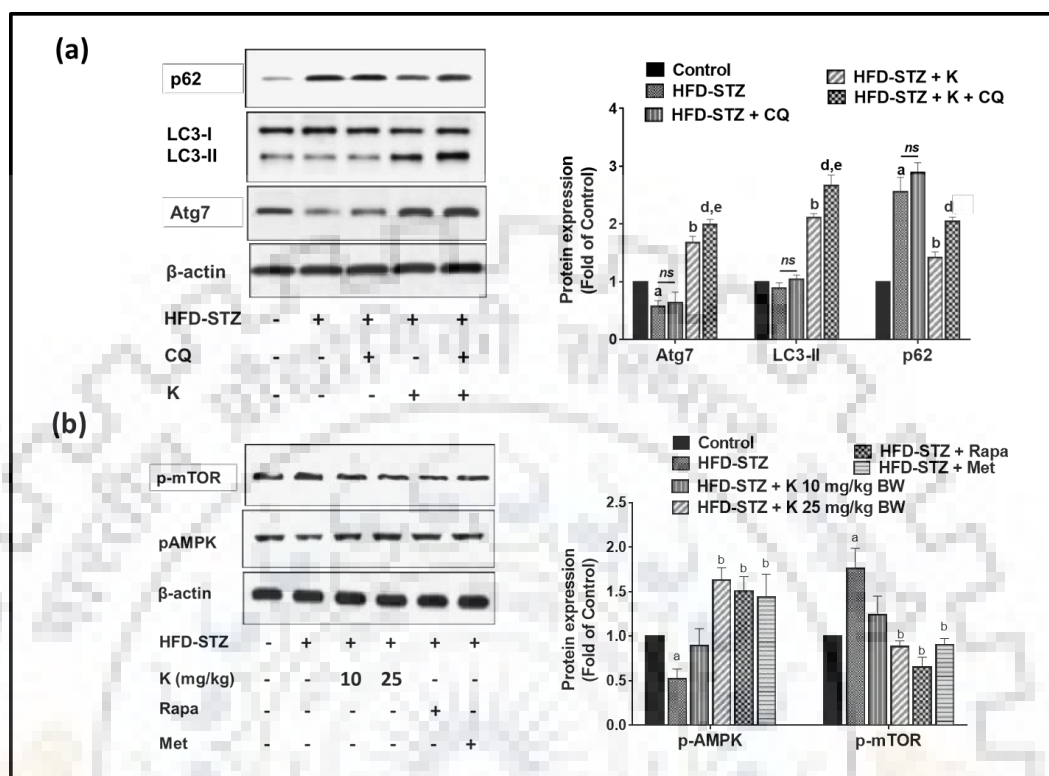


Fig. 8.8. Kaempferol induces autophagy in livers of HFD-STZ diabetic mice. Representative immunoblots of (a) autophagy-related proteins and (b) p-AMPK and p-mTOR, in livers of respective mice groups. The histogram in right panel represents the mean relative arbitrary pixels intensities in terms of the fold of normal control micegroup for respective proteins. Data are mean \pm SD of $n = 6$ for each group. a, $p < 0.05$ versus normal control; b, $p < 0.05$ versus HFD-STZ control; d, $p < 0.05$ versus HFD-STZ + K. HFD, high-fat diet; STZ, streptozotocin; K, Kaempferol; Met, metformin; Rapa, rapamycin; CQ, chloroquine; ns, non-significant.

8.3.8. Kaempferol-induced autophagy is involved in inhibition of lipid accumulation in the liver of HFD-STZ mice

We further evaluated whether kaempferol could improve liver weight and TG content which was found to be increased in HFD-STZ diabetic mice. As shown in Fig. 8.9a and b, kaempferol administration abolished the HFD-mediated increase in liver weight and TG content and

rescued it back close to normalcy ($p < 0.05$). Further, inhibition of autophagic flux by means of chloroquine partially abolished kaempferol-induced reduction in liver weight and TG content which suggests the involvement of kaempferol-mediated autophagy (Fig. 8.9a and b). Since, obesity-linked diabetes also involves damaging effects in the function of liver, we next wanted to assess if kaempferol could rescue the liver from this process by inducing autophagy. As shown in Fig. 8.9, kaempferol-treated mice showed improved liver function as serum alanine aminotransferase (ALT) (Fig. 8.9c) and aspartate aminotransferase (AST) (Fig. 8.9d) levels were significantly decreased by 2 and 1.5-fold respectively with respect to HFD-STZ mice ($p < 0.05$). Interestingly, kaempferol could only partially improve the liver function when autophagy was blocked by chloroquine treatment ($p < 0.05$) (Fig. 8.9c and d). On analyzing the histopathology of the liver sections with hematoxylin and eosin (H&E) staining in various groups of treated animals, it was found that the livers from HFD-STZ mice showed ballooned hepatocytes with accumulation of fat inside cells as observed in liver sections (Fig. 8.9e). However, kaempferol treatment showed limited accumulation of fat which was comparable to livers of normal control mice. The livers of mice co-administered with kaempferol and chloroquine exhibited increased fat accumulation as compared to livers of kaempferol treated HFD-STZ mice indicative of the involvement of autophagy in kaempferol-mediated inhibition of lipid accumulation (Fig. 8.9e). Further, immunoblot analysis showed that as compared to normal control mice, PLIN2 expression was significantly increased (~2.4-fold) in livers of HFD-STZ mice which was down-regulated almost to normalcy by kaempferol treatment ($p < 0.05$) (Fig. 8.9f). At 25 mg/kg bw dose, kaempferol exhibited ~1.7-fold decrease in PLIN2 expression with respect to HFD-STZ control, which however, was abrogated in presence of chloroquine treatment ($p < 0.05$) (Fig. 8.9f).

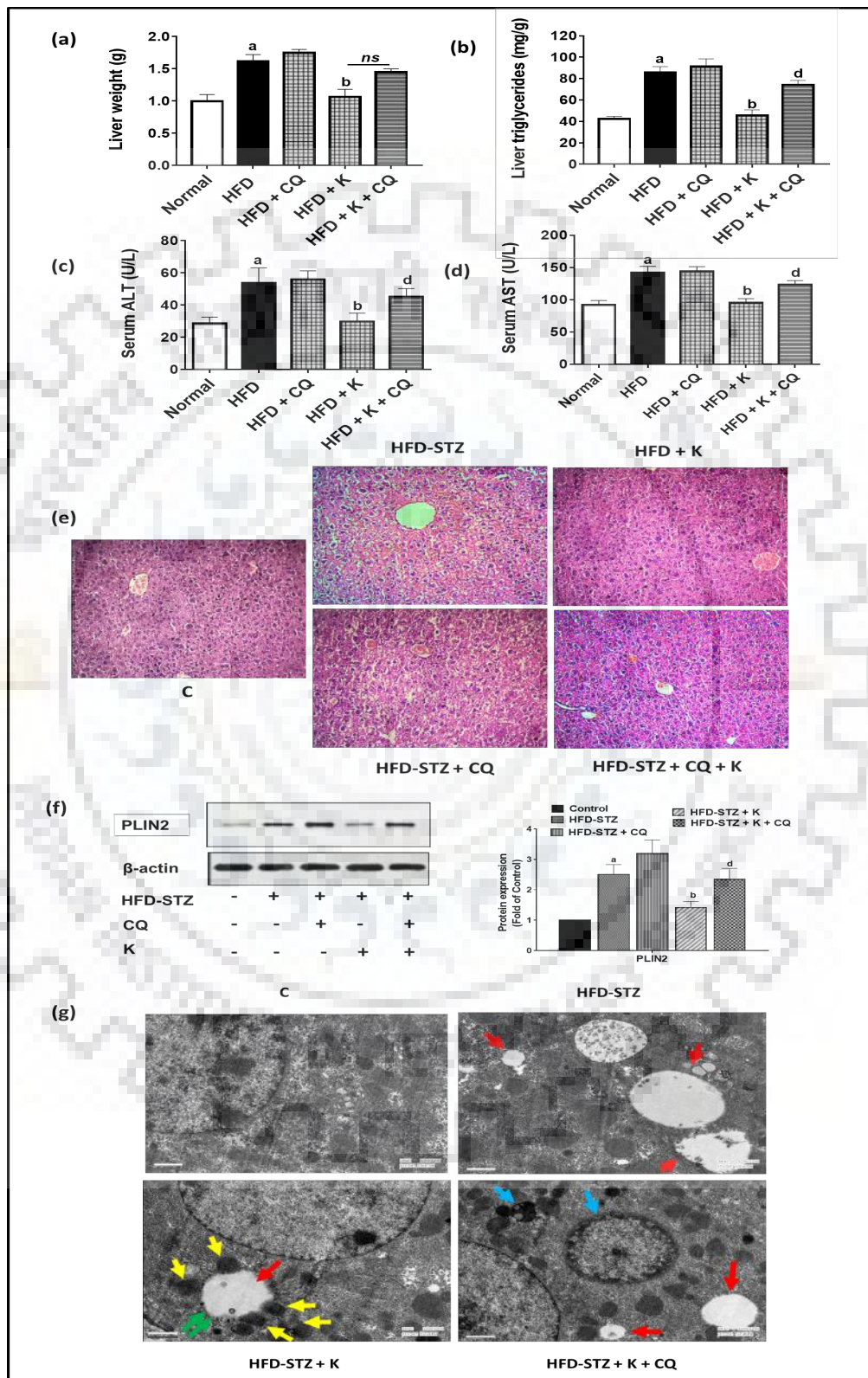


Fig. 8.9. Kaempferol-mediated autophagy induces inhibition of lipid stores in livers of HFD-STZ diabetic mice. Histogram showing (a) liver weight; (b) liver triglycerides; (c) serum ALT and (d) serum AST level of mice treated with various chemicals as mentioned. (e) Representative histological images of hematoxylin and eosin stained livers of respective groups (original magnification, $\times 400$); (f) Representative immunoblots of PLIN2 in the respective groups. The histogram in right panel represents the mean relative arbitrary pixels intensities in terms of the fold of normal control mice group. Data are mean \pm SD of $n = 6$ for each group. a, $p < 0.05$ versus normal control; b, $p < 0.05$ versus HFD-STZ control; d, $p < 0.05$ versus HFD-STZ + K. (g) Representative transmission electron microscopy images of pancreatic β -cells after various treatments; the red, blue and yellow arrows indicate lipid droplets, autophagosomes and lysosomes respectively. Whereas, fusion of autophagosome with the lysosomes (autophagolysosomes) in livers of kaempferol-treated HFD-STZ are marked with a paired-green arrows. The scale bar in each image represents 1 μm . HFD, high-fat diet; STZ, streptozotocin; K, Kaempferol; CQ, chloroquine.

Likewise, TEM analysis revealed that hepatic cells in HFD-STZ mice showed a limited number of autophagic vacuoles and lysosomes with increased lipid droplets (Fig. 8.9g). In kaempferol treated mice, the hepatic cells exhibited an increased number of autophagic vacuoles fused with numerous lysosomes with a limited number of lipid droplets. Inhibition of autophagosomes degradation by chloroquine led to significant increase in accumulation of autophagic vacuoles and lipid droplets in hepatic cells of kaempferol-treated HFD-STZ mice as compared to only kaempferol-treated HFD-STZ mice (Fig. 8.9g). Collectively, these data strongly suggested that kaempferol not only augments autophagy induction but also induces the increase in autophagosomes turnover, which is inhibited in HFD-STZ mice. Besides, TEM analysis also revealed the lipid inhibitory effect of kaempferol-induced autophagy in hepatic cells of HFD-STZ diabetic mice.

8.3.9. Kaempferol-induced autophagy rescues HFD induced ER-stress and insulin signaling

In the next phase of study prior to determining the ER stress and insulin signaling pathways in the lipid overload condition we performed glucose tolerance and insulin sensitivity tests. Our data showed that inhibition of autophagy by chloroquine significantly impaired both kaempferol-mediated improved glucose tolerance and insulin sensitivity as compared to kaempferol-treated HFD-STZ animals (Shown in chapter 7). As discussed earlier, free fatty acid -induced ER-stress mediated-pathway has been reported to activate JNK which has been reported to impair insulin signal transduction by phosphorylating IRS-1 at serine sites. Thus, in order to determine whether kaempferol treatment can relieve the PA-induced ER stress the immunoblot analysis of CHOP, the main ER stress marker found to be elevated in HFD fed conditions, was performed. As shown in Fig. 8.10c, the livers of HFD-STZ group showed increased CHOP expression while kaempferol treatment significantly down-regulated its expression ($p < 0.05$). Chloroquine treatment further abrogated the kaempferol-mediated decrease in CHOP expression indicative of the involvement of autophagy in the alleviation of ER stress ($p < 0.05$) (Fig. 8.10c). As expected, phosphorylation of JNK and IRS-1 were significantly increased in liver of HFD-STZ mice ($p < 0.05$) (Fig. 8.10c). This was further linked to inhibition of insulin-stimulated phosphorylated Akt ($p < 0.05$) (Fig. 8.10d). Whereas, treatment with kaempferol significantly abolished the HFD-mediated increase in JNK and IRS-1 phosphorylation ($p < 0.05$) (Fig. 8.10c). As a result, insulin-stimulated phosphorylation of Akt was restored in response to kaempferol ($p < 0.05$) (Fig. 8.10d). Kaempferol at 25 mg/kg bw dose exhibited ~ 1.5 and ~ 1.35 -fold decrease in p-JNK and p-IRS-1 respectively with a concomitant increase in pAKT (~ 2.2 -fold) with respect to HFD-STZ control mice ($p < 0.05$) (Fig. 8.10c and d). However, chloroquine administration significantly abolished kaempferol-mediated effects on insulin signal transduction pathway, thus, indicating kaempferol-mediated restoration of autophagy is involved in its effect on insulin signal transduction pathway.

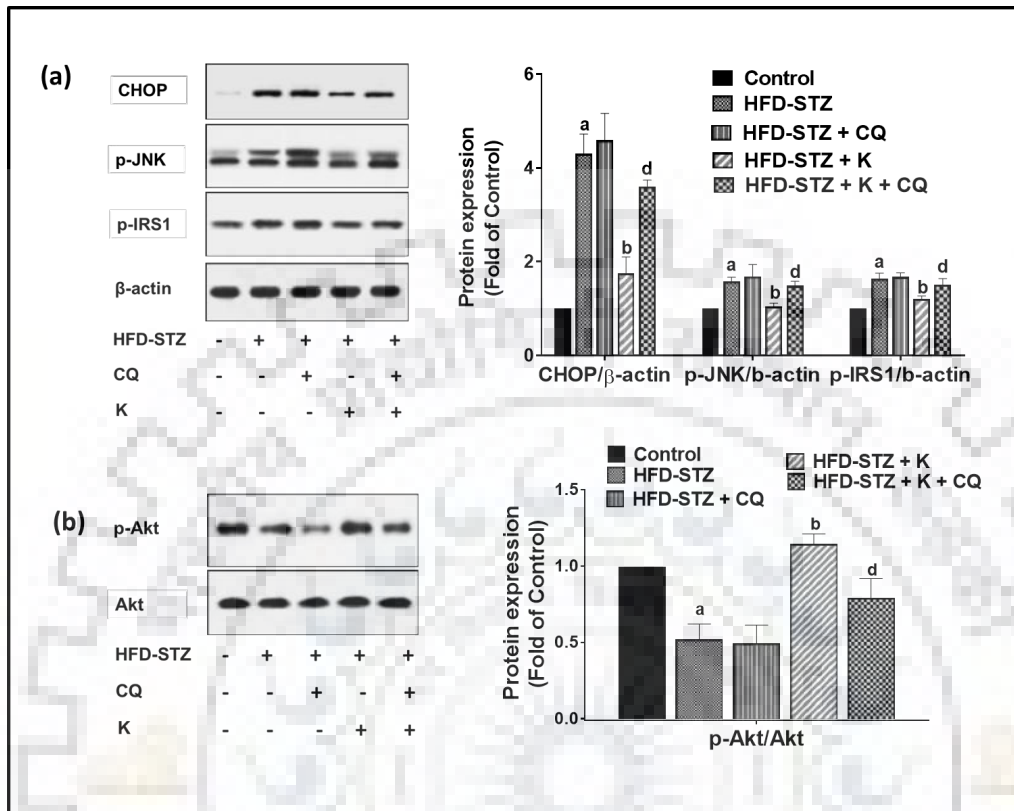


Fig. 8.10. Kaempferol-mediated autophagy improves insulin sensitivity and insulin signal transduction in livers of HFD-STZ diabetic mice. Representative immunoblots of (a) proteins involved in HFD-mediated insulin resistance and insulin signal transduction and (b) insulin-stimulated Akt and p-Akt proteins. The histogram in right panel represents the mean relative arbitrary pixels intensities in terms of the fold of normal control mice group. Data are mean \pm SD of $n = 6$ for each group. a, $p < 0.05$ versus normal control; b, $p < 0.05$ versus HFD-STZ control; d, $p < 0.05$ versus HFD-STZ + K. HFD, high-fat diet; STZ, streptozotocin; K, Kaempferol; CQ, chloroquine.

8.4. Discussion

The two pathophysiologic abnormalities which link obesity to T2DM, are β -cell failure and insulin resistance (Al-Goblan et al., 2014). Kaempferol, a natural flavonoid, has been known for its anti-oxidant and protective effects in various diseases (M Calderon-Montano et al., 2011). Recently, our group has reported that kaempferol preserved pancreatic β -cell mass and function under lipid overloaded condition (Varshney et al., 2017; Varshney et al., 2018). In the present study, we intended to determine the role of kaempferol in hepatic insulin resistance and its underlying mechanism. To the best of our knowledge, this is the first study to evaluate the role of autophagy in kaempferol-mediated effects on hepatic lipid metabolism and insulin signal transduction in PA-challenged HepG2 cells and livers of HFD-STZ induced diabetic mice. Several key findings have emerged from this study. First, we found that chronic lipid condition significantly increased lipid accumulation in HepG2 cells and livers of HFD-STZ mice whereas kaempferol treatment led to inhibition of lipid deposition. Second, kaempferol treatment induces AMPK-mTOR mediated autophagy in both HepG2 cells and livers of HFD-STZ mice which were found to be linked to its lipid inhibitory effect. Third, kaempferol-mediated restoration of autophagy alleviates ER stress-induced hepatic insulin resistance and improves insulin signal transduction.

Autophagy is a lysosomal degradation process involved in cell quality control during adverse conditions like starvation and stress (Mizushima, 2007). Emerging evidence suggests that the progression of NAFLD is concomitant with dysfunctional hepatic autophagic activity in the HFD-fed mice (Mao et al., 2016). In our study, firstly we showed that kaempferol inhibited PA-induced lipid accumulation in HepG2 cells as evidenced by decreased lipid droplets and TGs content. The RT-PCR and immunoblot analysis exhibited significant downregulation of PLIN2 protein, the lipid droplet coat protein found to be involved in lipid droplets accumulation under lipid overload conditions. Our results are in line with the recent report which showed that PLIN2 deficiency enhances TG catabolism and protects mice against ER stress-induced hepatosteatosis (Tsai et al., 2017).

Subsequently, to elucidate the underlying mechanism, we investigated the kaempferol-mediated transcriptional regulation of genes involved in lipolysis and β -oxidation. Kaempferol treatment

enhanced PPAR- α expression, the key regulator involved in the stimulation of hepatic β -oxidation of fatty acids (Pawlak et al., 2015). The genes involved in lipolysis (ATGL and HSL) and β -oxidation (ACOX1 and CPT1) were also found to be up-regulated in response to kaempferol treatment which further suggested the lipid inhibitory role of kaempferol in PA-induced hepatic cells that might be arbitrated by the elevated lipolysis and β -oxidation.

Recent studies have demonstrated that in addition to cytosolic lipolysis, autophagy is an alternative and important mechanism involved in bulk degradation of lipids in hepatocytes and mobilizes a large number of lipids rapidly (Dong and Czaja., 2011; Schulze et al., 2017). Numerous studies have reported that in lipid overload conditions such as in HFD fed condition autophagy is impaired in hepatocytes due to significant down-regulation of Atg7 and related proteins involved in the autophagic process which in turn leads to hepatosteatosis (Hsiao et al., 2017; Yang et al., 2010). Conversely, hepatic overexpression of Atg7 has been shown to improve fatty liver and insulin resistance in HFD-mice (Yang et al., 2010). Consistent with these reports, our study also demonstrated that hepatic autophagy was impaired in PA-challenged HepG2 cells and livers of HFD-STZ diabetic mice. Interestingly, kaempferol treatment significantly attenuated the dampened autophagy in both PA-treated HepG2 cells and livers of HFD-STZ mice.

In subsequent studies, the probable mechanism involved in the kaempferol-mediated induction of autophagy was determined. Numerous reports suggest that AMPK, which is recognized as a major sensor of energy and regulates cellular energy homeostasis, plays an important role in the activation of autophagy (Hardie, 2011). AMPK activates autophagy by downregulating mTOR phosphorylation, the major negative regulator of autophagy (Akers et al., 2012). Recent studies strongly suggest that hyper-nutrition conditions during obesity can inhibit AMPK and subsequently activate mTORC1 which may further be linked to impaired autophagy and increased anabolic metabolism in the liver (Namkoong et al., 2018). Concurrent with previous reports, our results also demonstrated the reduced AMPK activity and enhanced expression of p-mTOR in the livers of HFD-STZ treated mice as compared with the non-diabetic control mice. Whereas, kaempferol treatment significantly upregulated p-AMPK and downregulated p-mTOR expression. Moreover, AMPK siRNA further abolished kaempferol induced autophagy in PA-challenged HepG2 cells and livers of HFD-STZ mice which indicates the involvement of

AMPK/mTOR pathway in kaempferol mediated autophagy induction. Our data is consistent with the previous finding which showed that kaempferol activated autophagy through AMPK/mTOR pathway in hepatocellular carcinoma cells (Han et al., 2017).

Further, to determine the specific involvement of autophagy in kaempferol-mediated lipid mobilization, we used pharmacological (chloroquine) and genetic (Atg7 siRNA) inhibitors of autophagy which abolished the kaempferol-mediated lipid inhibitory effect. These results were further corroborated well with the TEM analysis showing a fusion of lipid droplets with autophagosomes and lysosomes, indicating the lysosomal degradation of lipid droplets. Collectively, these results suggested that kaempferol-mediated inhibition of hepatic lipid accumulation is mainly by induction of autophagy. Our results are in line with the report which showed that autophagy induction through rapamycin, a well-known autophagy activator, improves hepatosteatosis and insulin sensitivity in HFD mice (Lin et al., 2013).

Currently, studies have shown that autophagy dysfunction due to lipid overload can lead to ER and oxidative stress that in turn may lead to hepatic insulin resistance which plays a central role in the pathogenesis of T2DM (Kim et al., 2015). Thus, in our next phase of the study, we intended to determine whether kaempferol-mediated induction of autophagy could restore hepatic insulin sensitivity under lipid overload condition. Interestingly, kaempferol reversed ER stress-mediated induction of CHOP and p-JNK expression in livers of HFD-STZ mice. It is well established that hepatic TG accumulation leads to activation of ER stress which may further activate JNK pathway (Kim et al., 2015). Furthermore, activation of JNK phosphorylates its downstream target, IRS-1 at serine sites and may lead to deactivation of Akt and inhibition of insulin transduction (Urano et al., 2000; Aguirre et al., 2002). Kaempferol treatment significantly abolished the HFD-mediated increase in IRS-1 phosphorylation; as a result, insulin-stimulated phosphorylation of Akt was restored. This observation is consistent with the recent report which showed that restoration of autophagy by means of rapamycin or resveratrol reversed hepatic ER stress and impaired insulin transduction in high-fructose-fed mice (Wang et al., 2015).

In summary, all results delineated in the present study corroborate well with each other to arrive at the conclusion that, kaempferol-induced AMPK-mTOR mediated autophagy is involved in alleviation of hepatic lipid accumulation and impaired insulin signal transduction in PA-induced

HepG2 cells and livers of HFD-STZ induced diabetic mice which, in part, ameliorates insulin resistance and hyperglycemia. To the best of our knowledge, this study provides new insights into kaempferol's therapeutic potential and suggests that it could be a promising candidate for the prevention of obesity-linked type 2 diabetes and its impact in the functioning of liver. However, based on these data further detailed investigations are warranted to explore the intriguing mechanisms involved in the kaempferol-mediated autophagy in the restoration of hepatic insulin sensitivity and its plausible metabolic impacts where our data would provide a base for such studies. These comprehensive data would help in the establishment of a base for the therapeutic potential of a phytochemical like kaempferol.





CHAPTER 9

SUMMARY

Chapter 9. Summary

Diabetes mellitus is an unbeaten health challenge for humankind. Worldwide, the prevalence of diabetes is still rising and requires an appropriate strategy to reduce morbidity and mortality arising from this disorder. Although the current medicines and therapies can mitigate diabetes to some extent, there are several unprecedented complications. The major one of them is that these therapies do not significantly improve β -cell mass and function simultaneously, thus become less effective over time as a result of progressive stress on β -cells. Therefore, the protection and recovery of β -cell mass and function should be the prime target for treatment and prevention of T2DM (Chen et al., 2017). Currently, no antidiabetic drug has been proven clinically effective for the prevention of β -cell atrophy although thiazolidinediones (TZDs) and glucagon-like peptide-1 (GLP-1) analogues have testified being effective in animals (Gastaldelli et al., 2007; Tourrel et al., 2002). Recent studies showed that dysfunctional autophagy is involved in the loss of β -cell mass and function, hence, demonstrating pathophysiology of obesity-linked diabetes. Therefore, identifying agents that could restore autophagy in degenerated β -cells could be a better target under the current therapeutic regime. Considering the importance of above mentioned recent strategies and targets, the major focus of this work was to search for novel autophagy modulators which can protect β -cell mass and function as a principal approach in the prevention of obesity-linked type 2 diabetes with an additional impacts on liver functions and further understanding their mechanism of action in detail. This chapter is devoted to summarizing the major findings of the current thesis. Here we provide an overview of the entire thesis and message delivered, in terms of autophagy stimulatory and antidiabetic activities of flavonoids tested and their various targets and different modes of actions during the course of the study.

Currently, an active area of diabetes research focuses on identifying naturally occurring flavonoids, a group of phytochemicals that can be modulated or developed into diabetic therapeutics due to their intriguing role in treating various diseases (Chang et al., 2013). Also, these phytochemicals because of their lesser side effects, more reliable in pharmacological actions and cost-effectiveness, are considered to be excellent alternative candidates in diabetes

management. In this study, firstly, we attempted to screen some flavonoids namely: quercetin, rutin, myricetin and kaempferol, which are abundant in various dietary sources, for their anti-obesity and antidiabetic activities.

Obesity is a major risk factor associated with T2DM (Formiguera and Cantón, 2004). Obesity is an ailment in which adipocytes enlarge by accumulating an enormous amount of lipids. At cellular level, it is characterized by a surge in number and size of differentiated adipocytes in adipose tissues. Adipocytes are the primary site which stores energy in the form of lipids and indirectly responsible for insulin sensitivity (Smith and Kahn, 2016). Firstly, we elucidated the role of flavonoids in the inhibition of adipocyte differentiation. To determine the anti-adipogenic activity, the mouse pre-adipocytes 3T3-L1 cells were used as it has been widely accepted as a cellular model of adipose biology. Our study revealed that all the tested flavonoids were found to be effective in inhibiting the differentiation of pre-adipocytes 3T3-L1 cells to mature adipocytes which were confirmed by Oil Red O staining and lipid quantification assays with concomitant down-regulation of genes involved in adipocyte differentiation (*Pparg*, *Fabp4* and *Cebpa*). This *in vitro* data revealed that among all tested flavonoids, kaempferol and rutin had the strongest inhibitory effects on adipogenesis.

In the next phase of this study, antidiabetic effects of flavonoids were determined by using L6 muscle cells. Insulin resistance in skeletal muscles plays a major role in hyperglycemic conditions associated with type 2 diabetes (DeFronzo and Tripathy, 2009). It is already reported that excess FFAs lead to insulin resistance in muscle cells by impairing insulin signaling (Kraegen and Cooney, 2008; Martins et al., 2012). In order to mimic obesity-linked insulin resistance *in vitro*, differentiated L6 muscle cells were incubated with PA, a cell-based model that has been widely used to determine the antidiabetic role of compounds (Dimopoulos et al., 2006; Wu et al., 2015; Sinha et al., 2004). Our data showed that all tested flavonoids were found to be effective in significantly up-regulating insulin-stimulated glucose uptake which was found to be abrogated in PA-treated conditions. PA-treatment also showed impaired insulin signaling as evidenced by increased phosphorylation of ser307 in IRS-1 and decreased p-Akt which was further linked to decreased GLUT4 expression and all these were significantly improved by the test flavonoids. Our data is in line with the studies which showed that PA treatment impaired insulin-stimulated

glucose uptake (Dimopoulos et al., 2006; Powell et al., 2004; Olsen and Hansen, 2002; Li et al., 2015; Wu et al., 2015). However, the PA-mediated impaired glucose uptake was restored by all tested flavonoids, out of which, kaempferol and quercetin showed profound activity. Further, the specific mechanisms involved in glucose uptake stimulatory activity of flavonoids were elucidated. Our study revealed that myricetin and rutin treatment exhibited increased expression of p-Akt and thus restores the classical signaling pathway. Our this observation is in line with the study which showed that restoring p-AKT in PA-induced insulin resistant muscle cells led to improved insulin signaling (Li et al., 2015). Conversely, it was found that kaempferol and quercetin showed a significant increase in the expression of AMPK phosphorylation (Thr172) indicative of the role of AMPK in inducing glucose uptake. This data is in agreement with the report that showed the commonly used antidiabetic drug, metformin, exerted their stimulatory effect on glucose uptake through AMPK activation (Wu et al., 2015). Taken together, we found that kaempferol and quercetin are the most potent anti-hyperglycemic agents out of all tested flavonoids to be taken up further as therapeutic agents.

In the subsequent study, in order to validate the earlier obtained *in vitro* data in more physiologically relevant *in vivo* model, HFD-STZ-induced diabetic model was developed. This model has been extensively used in various studies to test anti-obesity and antidiabetic effects of various compounds (Skovsø, 2014). These animals are raised on an HFD to induce insulin resistance and glucose intolerance and further exposed to low dose of STZ which results in compromised β -cell mass and function (Skovsø, 2014). The type 2 diabetes in the induced HFD-STZ mice was characterized by hyperglycemia, glucose intolerance, insulin resistance and decreased insulin secretion. To test anti-obesity and antidiabetic effects of these flavonoids, the developed diabetic mice were treated with these phytochemicals. Our *in vivo* data revealed that all of the flavonoids showed a marked reduction in serum triglyceride, cholesterol and LDL levels of HFD-STZ-induced diabetic mice, however, only kaempferol was found to significantly improve serum NEFA profile at the dose tested. Furthermore, all tested flavonoids significantly improved blood glucose level, glucose and insulin tolerance in diabetic mice. Interestingly, among all tested flavonoids, kaempferol had the most promising effects on blood glucose level, glucose tolerance and insulin sensitivity. Collectively, *in vitro* and *in vivo* data demonstrated that out of all tested

flavonoids, kaempferol exhibited the most promising anti-obesity and antidiabetic effects (Fig. 9.1).

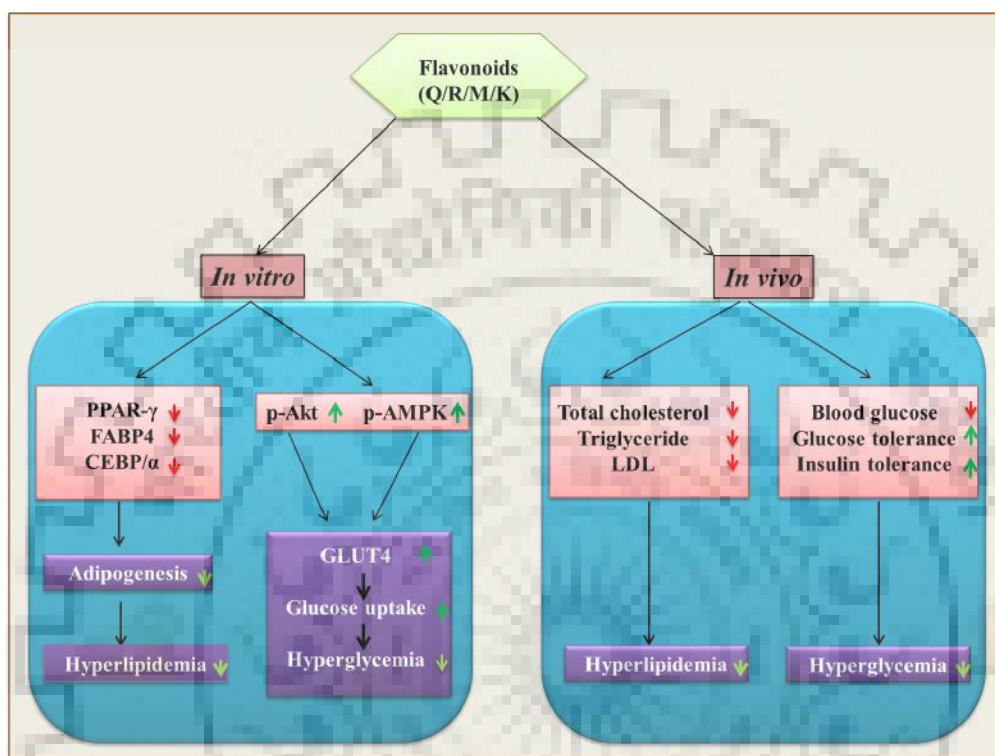


Fig. 9.1. Schematic representation showing the anti-obesity and antidiabetic activities of various flavonoids. Q, quercetin; R, rutin; M, myricetin; K, kaempferol.

Recent studies showed that dysfunctional autophagy is involved in the loss of β -cell mass and function hence pathophysiology of obesity-linked diabetes (Mir et al., 2015; Masini et al., 2009; Bartolome et al., 2004). Autophagy is a lysosomal degradation pathway of dysfunctional macromolecules and organelles which protects the cells from stressed conditions and acts as an adaptive pro-survival response. Thus, identifying agents that could restore autophagy in degenerated β -cells are of great importance presently. Our MDC-LysoTracker data revealed that PA treatment exhibited a marginal increase in MDC stained regions and limited lysoTracker stained regions indicative of impaired autophagy and this is consistent with a recent study which showed that PA impairs autophagy in pancreatic β -cells (Mir et al., 2015). Surprisingly,

kaempferol was found to be the most promising autophagy activator as evidenced by maximally increased autophagosomes and lysosomes formation with increased co-localization of both as compared other three tested flavonoids (quercetin, rutin and myricetin). This data is in line with the study which showed that kaempferol treatment increased autophagy and protected neurons in animal models of rotenone-mediated acute toxicity (Filomeni et al., 2012). Therefore, it can be hypothesized that the superior antidiabetic activity of kaempferol may also be due to the restoration of autophagy which in turn may improve the diabetic condition *in vitro* and *in vivo*. The present study thus suggested that among above-selected flavonoids kaempferol had potent anti-obesity, antidiabetic, and autophagy stimulating activities as obtained from initial screening tests. Therefore, kaempferol was chosen for further detailed and mechanistic studies for next phase of our study to confirm the role of kaempferol-mediated autophagy in the protection of functional β -cell mass and improvement of insulin sensitivity as it is well established that β -cell mass and insulin resistance are the two pathophysiological abnormalities associated with obesity-linked diabetes (Al-Goblan et al., 2014).

Autophagy is a dynamic and complicated process thus needs to be validated with two or more specific assays to rule out experimental artifacts. Though in initial screening it was found that kaempferol stimulates autophagy in PA-induced RIN-5F cells, we further validated kaempferol-mediated induction of autophagy with more specific methods such as EGFP-LC3 puncta assay, LC3-II/LC3-I and p62 expression analysis in presence or absence of autophagic flux inhibitor (chloroquine) and TEM analysis. Even at lower concentration (10 μ M), Kaempferol exhibited prominent autophagy stimulatory activity in PA-stressed RIN-5F cells and rat primary islets which was comparable to temsirolimus (an autophagy activator). Moreover, we found that kaempferol-mediated restoration of autophagy was involved in the protection of β -cells from PA-induced apoptosis as validated through pharmacological (wortmannin and chloroquine) and genetic (Atg7 siRNA) inhibitors of autophagy the presence of which blocked kaempferol-induced positive impacts (Fig. 9.2).

In subsequent studies, molecular mechanisms involved in the kaempferol-mediated induction of autophagy were analyzed. The pre-existing literature strongly suggests that AMPK is the positive regulator of autophagy and acts by down-regulating phosphorylation of mTOR. This

mTOR is a major negative regulator of autophagy that inhibits it by phosphorylating ULK1 and preventing AMPK-ULK1 interactions, thus concomitantly attenuating autophagy (Han et al., 2010; Kim et al., 2011). With this as the basis, we further investigated the role of an AMPK-mediated signaling pathway in kaempferol-induced autophagy in PA-stressed RIN-5F cells and primary rat islets. Our results showed that kaempferol activated the AMPK/mTOR pathway, as evidenced by the increased p-AMPK and decreased p-mTOR expressions. These results are consistent with the earlier studies which showed that kaempferol activated autophagy through the AMPK/mTOR pathway in Hela cells and thus exerting cytoprotection against apoptosis (Filomeni et al., 2010). Moreover, AMPK inhibitors (compound C and AMPK siRNA) abolished kaempferol-induced autophagy and subsequently increased β -cell cytotoxicity. Taken together, all the results delineated in the present study corroborate well with each other to arrive at the conclusion that, kaempferol exerts cytoprotective actions by inducing autophagy via AMPK/mTOR signaling pathway in PA-stressed RIN-5F cells and rat pancreatic islets (Fig. 9.2).

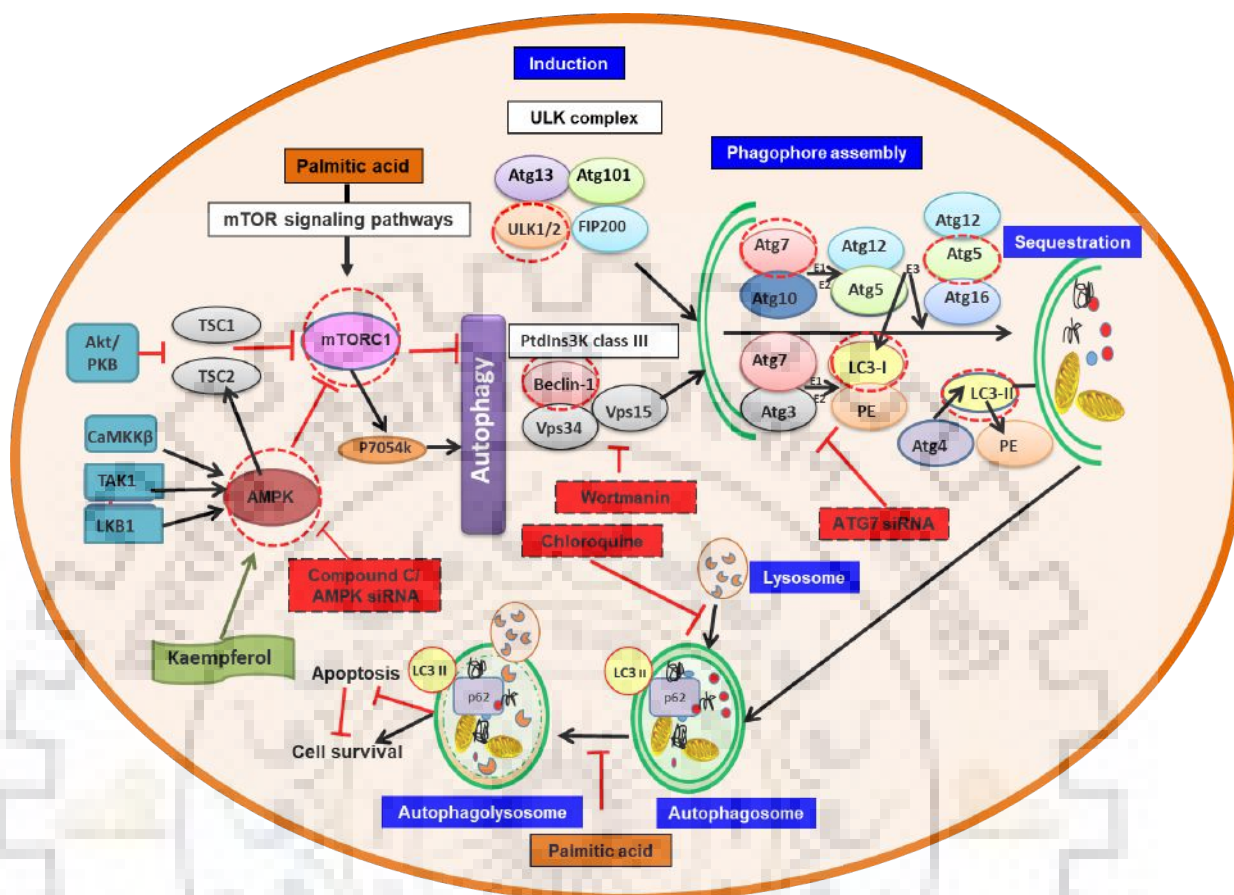


Fig. 9.2. Schematic representation showing mechanism underlying the kaempferol-mediated protection of β -cell mass involving autophagy. The genes/ proteins highlighted by the dotted red circles are the targets which were monitored and found to be involved in the kaempferol-mediated induction of autophagy.

In the next phase of our study, the molecular mechanism involved in cross-talk between kaempferol-mediated autophagy and its anti-apoptotic effect in PA-stressed β -cells were determined. Endoplasmic reticulum (ER) stress generated due to the accumulation of lipid in β -cells is one of the major features of pathological conditions involved in cell death under lipid overload conditions. Interestingly, autophagy has been reported to be involved in the alleviation of lipid-induced ER stress thus protecting β -cell from apoptosis. Additionally, autophagy has also been reported to degrade lipid droplets in hepatocytes, however, its role in lipid metabolism of β -

cell is rarely reported. Based on this information in this phase of study, the inhibitory effects of kaempferol-induced autophagy on PA-induced lipid deposition and ER stress were evaluated. Our studies showed that kaempferol-induced AMPK/mTOR-mediated autophagy abolished PA-induced ER stress and lipid accumulation which seems to be one of the possible mechanisms involved in the kaempferol-mediated restoration of β -cell mass. Moreover, the cytoprotected RIN-5F cells and rat primary islets were also found to be functional in nature as indicated by increased glucose-stimulated insulin secretion and intracellular insulin content. It is to be noted that the insulin-secreting capacity of β -cells is always considered to be a prominent marker of healthy cells. Based on these facts it could be asserted that our findings are in close agreement with the previous study which showed that PA inhibited glucose stimulated insulin secretion while stimulation of autophagy by means of rapamycin, a positive regulator of autophagy, restored the insulin secretion in INS1 cells (Las et al., 2011). To the best of our knowledge, this study uncovers a novel phytochemical based therapeutic strategy to restore pancreatic β -cell mass and function in obesity-linked type 2 diabetic condition (Fig. 9.3).

Based on these studies, Furthermore, we intended to validate our findings in more promising diabetic model, the HFD and STZ-induced type 2 diabetic mice. Our results exhibited that kaempferol treatment resulted in significant improvement in glycemic control and metabolic profiles in HFD-STZ-induced diabetic mice. The improved glucose homeostasis was found to be associated with increased insulin sensitivity. Further, it was evident that kaempferol-induced autophagy was involved in the alleviation of lipid deposition and ER stress which led to protection β -cell mass and function. Thus, our *in vivo* data was in accordance with our earlier *in vitro* findings. To the best of our knowledge, this is the first ever report providing evidence that kaempferol protects β -cell mass and function through AMPK-mTOR mediated autophagy which in part ameliorates diabetes in HFD-STZ induced type 2 diabetic mice (Fig. 9.3). Our data is in line with the recent finding which showed that the intermittent fasting, a clinically sustainable therapeutic strategy, stimulates autophagic flux to protect functional β -cell mass and ameliorate obesity-induced diabetes.

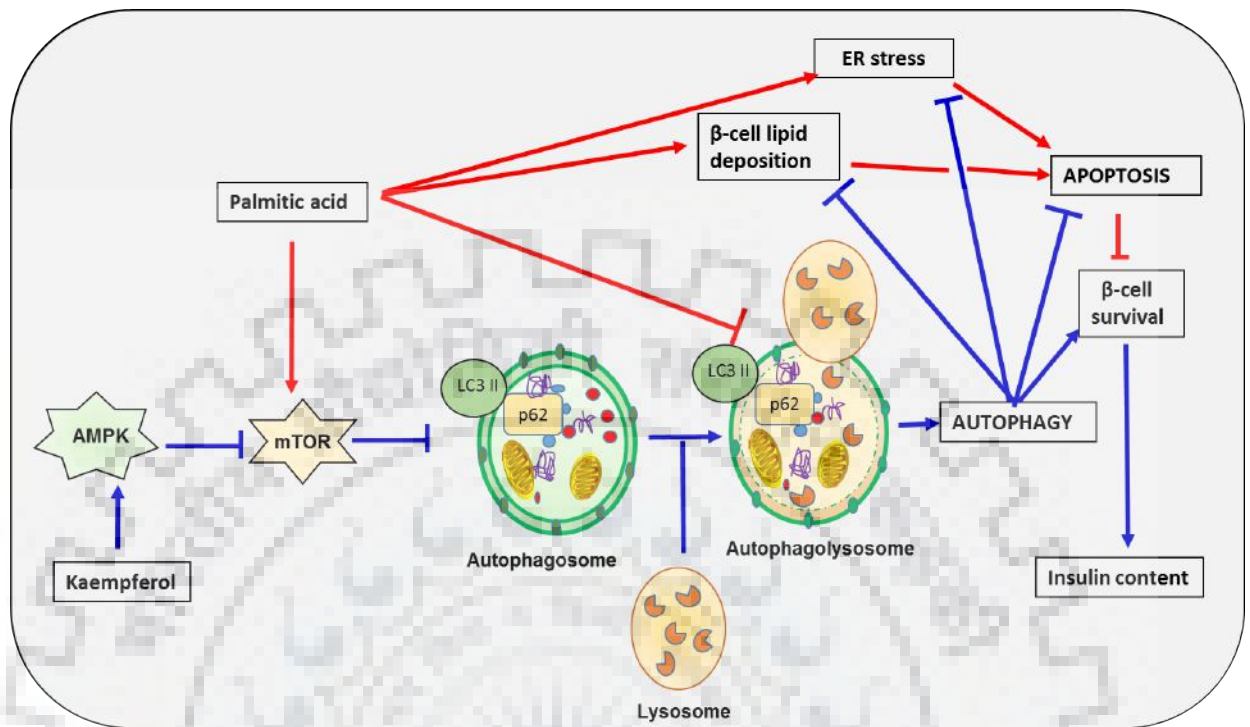


Fig. 9.3 Proposed mechanism of kaempferol-mediated autophagy in PA-challenged pancreatic β -cells and in islets of HFD-STZ diabetic mice. Palmitic acid (PA) impairs autophagy and induces lipid accumulation and endoplasmic reticulum (ER) stress in β -cells which in turn leads to loss of β -cell mass and function. Treatment with kaempferol inhibits PA/HFD-induced lipid deposition and ER stress thus preventing apoptosis of β -cells by activating AMPK and inhibiting mTOR thus involving autophagy.

The two pathophysiologic abnormalities which link obesity to T2DM, are β -cell failure and insulin resistance. Hence, in next phase of our study, we evaluated the effects of kaempferol on hepatic insulin resistance and insulin signal transduction *in vitro* and *in vivo* in PA-challenged HepG2 cells and livers of HFD-STZ-induced diabetic mice respectively. Dysfunctional autophagy and ER stress due to increased ectopic lipid accumulation in hepatocytes are the pathological manifestation involved in lipid-induced impairment of insulin signaling and thus insulin resistance. Therefore, lipid inhibitory effects of kaempferol were determined in *in vitro* and *in vivo* models. Our results showed that kaempferol exerted its lipid inhibitory effects in hepatocytes through induction of autophagy and β -oxidation mechanism under lipid overload conditions. Further, kaempferol-mediated autophagy protected the liver function in HFD fed mice in two ways, firstly it significantly inhibited the phosphorylation of JNK (Thr183/Tyr185) and IRS-1 (Ser307) which was an off shoot of ER stress and secondly restoration of insulin-stimulated phosphorylation of Akt (Ser473). Our results are in accordance with an earlier report which showed that autophagy induction through rapamycin, a prominent autophagy activator, improves hepatosteatosis and insulin sensitivity in HFD mice (Lin et al., 2013). Together, this study revealed that kaempferol-induced AMPK-mTOR-mediated autophagy is involved in the alleviation of hepatic lipid accumulation and impaired insulin signal transduction in PA-induced HepG2 cells and livers of HFD-STZ-induced diabetic mice which, in part, ameliorates insulin resistance and hyperglycemia (Fig. 9.4).

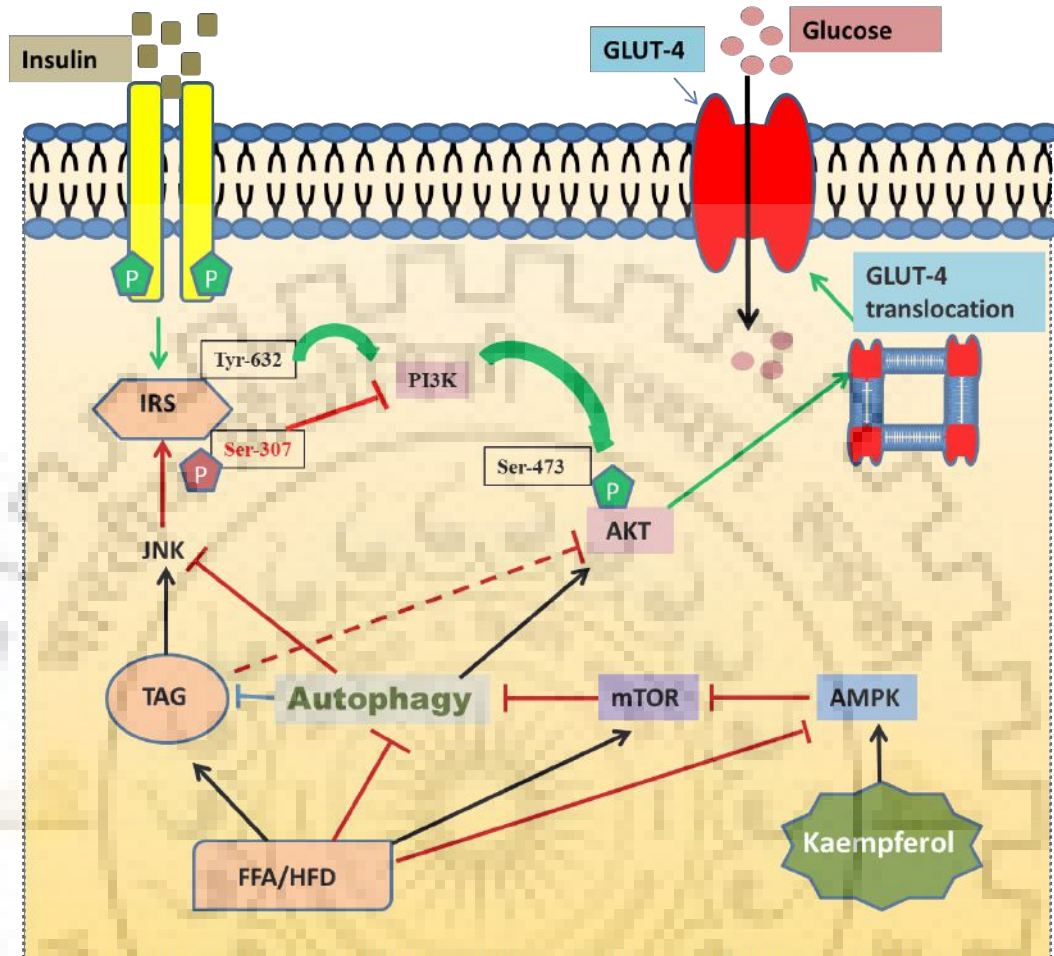


Fig. 9.4. The proposed mechanism of kaempferol-mediated effects in hepatic cells. In normal condition, insulin binds to the insulin receptor (IR) and induces glucose uptake by activation of a cascade of signaling pathways. Activated IR promotes phosphorylation of insulin receptor substrate 1/2 (IRS1/2) at tyrosine residues and thus activates phosphoinositide-3-kinase (PI3K) which in turn induces and phosphorylates Akt resulting the translocation of GLUT4 to the plasma membrane from intracellular vesicles and inducing efficient glucose uptake. On the other hand, TAG accumulation activates a major serine/threonine kinases, such as JNK. JNK-mediated increase in the serine phosphorylation on IRS inhibits its tyrosine phosphorylation which in turn blocks insulin signaling pathway. However, kaempferol activates AMPK that inhibits mTOR phosphorylation, the major negative regulator of autophagy. Activation of autophagy impairs TAG accumulation and ultimately promotes insulin signal transduction by inhibiting JNK pathway that eventually blocks the serine phosphorylation of IRS-1. Kaempferol thus increases insulin-stimulated Akt phosphorylation and promotes insulin signaling transduction. TAG, triacylglycerol

Collectively, all results delineated in the present study corroborate well with each other to arrive at the conclusion that, kaempferol induced autophagy is involved in the protection of functional β -cell mass and hepatic insulin sensitivity thus ameliorating diabetes (obesity-linked) as was evidenced by *in vitro* cell based analyses as well as in HFD-STZ induced diabetic mice models *in vivo*. To the best of our knowledge, this study provides new insights into our understanding of kaempferol's therapeutic potential and suggests that it could be a promising candidate either singly or in combination with other drugs/ chemicals for the prevention of obesity-linked type 2 diabetes. However, based on these data further comprehensive studies are warranted involving transgenic mouse models and human subjects to establish the exact cross-talks among various pathways in causing autophagy and its associated effects by kaempferol. This sort of study would help in establishing the nutraceutical potential of this phytochemical where our data would provide a base.



CHAPTER 10

BIBLIOGRAPHY



CHAPTER 10

BIBLIOGRAPHY

Chapter 10. Bibliography

1. Abd El-kader, A.M., El-Readi, M.Z., Ahmed, A.S., Nafady, A.M., Wink, M. and Ibraheim, Z.Z., 2013. Polyphenols from aerial parts of *Polygonum bellardii* and their biological activities. *Pharmaceutical biology*, 51(8), pp.1026-1034.
2. Abdul-Ghani, M. and DeFronzo, R.A., 2017. Is it time to change the type 2 diabetes treatment paradigm? Yes! GLP-1 RAs should replace metformin in the type 2 diabetes algorithm. *Diabetes Care*, 40(8), pp. 1121-1127.
3. Abedini, A. and Schmidt, A.M., 2013. Mechanisms of islet amyloidosis toxicity in type 2 diabetes. *FEBS letters*, 587(8), pp.1119-1127.
4. Abo-Salem, O.M., 2014. Kaempferol attenuates the development of diabetic neuropathic pain in mice: Possible anti-inflammatory and anti-oxidant mechanisms. *Macedonian Journal of Medical Sciences*, 7(3), pp.424-430.
5. Agarwal, P., Srivastava, R., Srivastava, A.K., Ali, S. and Datta, M., 2013. miR-135a targets IRS2 and regulates insulin signaling and glucose uptake in the diabetic gastrocnemius skeletal muscle. *Biochimica et Biophysica Acta (BBA)-Molecular Basis of Disease*, 1832(8), pp. 1294-1303.
6. Agarwal, S., Amin, K.S., Jagadeesh, S., Baishay, G., Rao, P.G., Barua, N.C., Bhattacharya, S. and Banerjee, P.P., 2013. Mahanine restores RASSF1A expression by down-regulating DNMT1 and DNMT3B in prostate cancer cells. *Molecular cancer*, 12(1), p.99.
7. Aguirre, V., Werner, E.D., Giraud, J., Lee, Y.H., Shoelson, S.E. and White, M.F., 2002. Phosphorylation of Ser307 in insulin receptor substrate-1 blocks interactions with the insulin receptor and inhibits insulin action. *Journal of Biological Chemistry*, 277(2), pp.1531-1537.
8. Ahn, J.S., Ann, E.J., Kim, M.Y., Yoon, J.H., Lee, H.J., Jo, E.H., Lee, K., Lee, J.S. and Park, H.S., 2016. Autophagy negatively regulates tumor cell proliferation through phosphorylation dependent degradation of the Notch1 intracellular domain. *Oncotarget*, 7(48), pp. 79047–79063.
9. Akinci, E., Banga, A., Greder, L.V., Dutton, J.R. and Slack, J.M., 2012. Reprogramming of pancreatic exocrine cells towards a beta (β) cell character using Pdx1, Ngn3 and MafA. *Biochemical Journal*, 442(3), pp.539-550.

10. Alam, M.M., Meerza, D. and Naseem, I., 2014. Protective effect of quercetin on hyperglycemia, oxidative stress and DNA damage in alloxan induced type 2 diabetic mice. *Life sciences*, 109(1), pp.8-14.
11. Alers, S., Löffler, A.S., Wesselborg, S. and Stork, B., 2012. Role of AMPK-mTOR-Ulk1/2 in the regulation of autophagy: cross talk, shortcuts, and feedbacks. *Molecular and cellular biology*, 32(1), pp.2-11.
12. Al-Goblan, A.S., Al-Alfi, M.A. and Khan, M.Z., 2014. Mechanism linking diabetes mellitus and obesity. *Diabetes, metabolic syndrome and obesity: targets and therapy*, 7, pp. 587–591.
13. Alkhalidy, H., Moore, W., Zhang, Y., McMillan, R., Wang, A., Ali, M., Suh, K.S., Zhen, W., Cheng, Z., Jia, Z. and Hulver, M., 2015. Small molecule kaempferol promotes insulin sensitivity and preserved pancreatic β -cell mass in middle-aged obese diabetic mice. *Journal of diabetes research*, 2015.
14. Alves-Bezerra, M. and Cohen, D.E., 2011. Triglyceride metabolism in the liver. *Comprehensive Physiology*, 8(1), pp.1-22.
15. Aly, H., Rohatgi, N., Marshall, C.A., Grossenheider, T.C., Miyoshi, H., Stappenbeck, T.S., Matkovich, S.J. and McDaniel, M.L., 2013. A novel strategy to increase the proliferative potential of adult human β -cells while maintaining their differentiated phenotype. *PLoS One*, 8(6), p.e66131.
16. American Diabetes Association, 2009. Standards of medical care in diabetes—2009. *Diabetes care*, 32(Suppl 1), p.S13.
17. American Diabetes Association, 2011. Diagnosis and classification of diabetes mellitus, 2011. *Diabetes Care* 34, s62–s69.
18. American Diabetes Association, 2014. Diagnosis and classification of diabetes mellitus. *Diabetes care*, 37(Supplement 1), pp.S81-S90.
19. American Diabetes Association, 2015. 2. Classification and diagnosis of diabetes. *Diabetes care*, 38(Supplement 1), pp.S8-S16.
20. American Diabetes Association, 2015. 6 Glycemic targets. *Diabetes Care*. 38(Supplement 1), pp. S33-S40.
21. American Diabetes Association, 2017. 7. Obesity management for the treatment of type 2 diabetes. *Diabetes Care*, 40(Supplement 1), pp. S57-S63.

22. American Diabetes Association, 2018. 2. Classification and diagnosis of diabetes: standards of medical care in diabetes—2018. *Diabetes Care*, 41(Supplement 1), pp. S13-S27.
23. American Diabetes Association, 2018. 5. Prevention or delay of Type 2 diabetes: Standards of medical care in diabetes. *Diabetes Care*, 41(Supplement 1), pp. S51-S54.
24. American Diabetes Association, 2018. 8. Pharmacologic approaches to glycemic treatment: Standards of medical care in diabetes. *Diabetes Care*, 41(Supplement 1), pp. S73-S85.
25. Amin, K.S., Jagadeesh, S., Baishya, G., Rao, P.G., Barua, N.C., Bhattacharya, S. and Banerjee, P.P., 2014. A naturally derived small molecule disrupts ligand-dependent and ligand-independent androgen receptor signaling in human prostate cancer cells. *Molecular cancer therapeutics*, 13(2), pp.341-352.
26. Asmat, U., Abad, K. and Ismail, K., 2016. Diabetes mellitus and oxidative stress—a concise review. *Saudi Pharmaceutical Journal*, 24(5), pp.547-553.
27. Assimacopoulos-Jeannet, F., 2004. Fat storage in pancreas and in insulin-sensitive tissues in pathogenesis of type 2 diabetes. *International Journal of Obesity*, 28(S4), p.S53.
28. Aune, D., Norat, T., Leitzmann, M., Tonstad, S. and Vatten, L.J., 2015. Physical activity and the risk of type 2 diabetes: a systematic review and dose–response meta-analysis. *BMJ*, 350, pp. 529-542.
29. Awasthi, A., Parween, N., Singh, V.K., Anwar, A., Prasad, B. and Kumar, J., 2016. Diabetes: Symptoms, Cause and Potential Natural Therapeutic Methods. *Advances in Diabetes and Metabolism*, 4(1), pp.10-23.
30. Bachar-Wikstrom, E., Wikstrom, J.D., Ariav, Y., Tirosh, B., Kaiser, N., Cerasi, E. and Leibowitz, G., 2013. Stimulation of autophagy improves endoplasmic reticulum stress–induced diabetes. *Diabetes*, 62(4), pp.1227-1237.
31. Barlow, A.D. and Thomas, D.C., 2015. Autophagy in diabetes: β -cell dysfunction, insulin resistance, and complications. *DNA and cell biology*, 34(4), pp.252-260.
32. Bartolomé, A., Kimura-Koyanagi, M., Asahara, S.I., Guillén, C., Inoue, H., Teruyama, K., Shimizu, S., S., Kanno, A., García-Aguilar, A., Koike, M., Uchiyama, Y., Benito, M., Noda, T., Kido, Y., 2014. Pancreatic β -cell failure mediated by mTORC1 hyperactivity and autophagic impairment. *Diabetes*, 63, pp.2996–3008.

33. Basli, A., Soulet, S., Chaher, N., Mérillon, J.M., Chibane, M., Monti, J.P. and Richard, T., 2012. Wine polyphenols: potential agents in neuroprotection. *Oxidative medicine and cellular longevity*, 2012.
34. Baynes, H.W., 2015. Classification, pathophysiology, diagnosis and management of diabetes mellitus. *Journal of diabetes and metabolism*, 6(5), pp.1-9.
35. Bernales, S., McDonald, K.L. and Walter, P., 2006. Autophagy counterbalances endoplasmic reticulum expansion during the unfolded protein response. *PLoS biology*, 4(12), p. e423.
36. Bhatia, H., Verma, G. and Datta, M., 2014. miR-107 orchestrates ER stress induction and lipid accumulation by post-transcriptional regulation of fatty acid synthase in hepatocytes. *Biochimica et Biophysica Acta (BBA)-Gene Regulatory Mechanisms*, 1839(4), pp. 334-343.
37. Bhonde, R.R., Sheshadri, P., Sharma, S. and Kumar, A., 2014. Making surrogate β -cells from mesenchymal stromal cells: perspectives and future endeavors. *The international journal of biochemistry & cell biology*, 46, pp.90-102.
38. Bickel, P.E., Tansey, J.T. and Welte, M.A., 2009. PAT proteins, an ancient family of lipid droplet proteins that regulate cellular lipid stores. *Biochimica et Biophysica Acta (BBA)-Molecular and Cell Biology of Lipids*, 1791(6), pp.419-440.
39. Biden, T.J., Boslem, E., Chu, K.Y., Sue, N., 2014. Lipotoxic endoplasmic reticulum stress, β cell failure, and type 2 diabetes mellitus. *Trends Endocrinol. Metab.* 25, 389–398. doi:10.1016/j.tem.2014.02.003
40. Bjerg, L., Hulman, A., Charles, M., Jørgensen, M.E. and Witte, D.R., 2018. Clustering of microvascular complications in Type 1 diabetes mellitus. *Journal of diabetes and its complications*, 32(4), pp.393-399.
41. Black, C., Donnelly, P., McIntyre, L., Royle, P.L., Shepherd, J.P. and Thomas, S., 2007. Meglitinide analogues for type 2 diabetes mellitus. *The Cochrane database of systematic reviews*, (2), pp.cd004654-cd004654.
42. Blandino-Rosano, M., Barbaresso, R., Jimenez-Palomares, M., Bozadjieva, N., Werneck-de-Castro, J.P., Hatanaka, M., Mirmira, R.G., Sonenberg, N., Liu, M., Rüegg, M.A. and Hall, M.N., 2017. Loss of mTORC1 signalling impairs β -cell homeostasis and insulin processing. *Nature communications*, 8, p. 16014.
43. Boden, G., 2011. 45Obesity, insulin resistance and free fatty acids. *Current opinion in endocrinology, diabetes, and obesity*, 18(2), p.139.

44. Boles, A., Kandimalla, R. and Reddy, P.H., 2017. Dynamics of diabetes and obesity: epidemiological perspective. *Biochimica et Biophysica Acta (BBA)-Molecular Basis of Disease*, 1863(5), pp. 1026-1036.
45. Boucher, J., Kleinridders, A. and Kahn, C.R., 2014. Insulin receptor signaling in normal and insulin-resistant states. *Cold Spring Harbor perspectives in biology*, 6(1), p.a009191.
46. Brøns, C. and Grunnet, L.G., 2017. Mechanisms in endocrinology: Skeletal muscle lipotoxicity in insulin resistance and type 2 diabetes: a causal mechanism or an innocent bystander?. *European Journal of Endocrinology*, 176(2), pp. 67-78.
47. Brown-Clay, J.D., Shenoy, D.N., Timofeeva, O., Kallakury, B.V., Nandi, A.K. and Banerjee, P.P., 2015. PBK/TOPK enhances aggressive phenotype in prostate cancer via β -catenin-TCF/LEF-mediated matrix metalloproteinases production and invasion. *Oncotarget*, 6(17), pp.15594-609.
48. Brownlee, M., Aiello, L.P., Cooper, M.E., Vinik, A.I., Plutzky, J. and Boulton, A.J., 2017. Complications of diabetes mellitus. In *Williams Textbook of Endocrinology (Thirteenth Edition)* pp. 1484-1581.
49. Butler, A.E., Janson, J., Bonner-Weir, S., Ritzel, R., Rizza, R.A. and Butler, P.C., 2003. β -cell deficit and increased β -cell apoptosis in humans with type 2 diabetes. *Diabetes*, 52(1), pp.102-110.
50. Calo, N., Ramadori, P., Sobolewski, C., Romero, Y., Maeder, C., Fournier, M., Rantakari, P., Zhang, F.P., Poutanen, M., Dufour, J.F. and Humar, B., 2016. Stress-activated miR-21/miR-21* in hepatocytes promotes lipid and glucose metabolic disorders associated with high-fat diet consumption. *Gut*, 65(11), pp. 1871-1881.
51. Calzada, F., Solares-Pascasio, J.I., Ordoñez-Razo, R.M., Velazquez, C., Barbosa, E., García-Hernández, N., Mendez-Luna, D. and Correa-Basurto, J., 2017. Antihyperglycemic activity of the leaves from *Annona cherimola* miller and rutin on alloxan-induced diabetic rats. *Pharmacognosy research*, 9(1), p.1-6
52. Cantley, J. and Ashcroft, F.M., 2015. Q&A: insulin secretion and type 2 diabetes: why do β -cells fail? *BMC biology*, 13(1), p.33.
53. Cecconi, F. and Levine, B., 2008. The role of autophagy in mammalian development: cell makeover rather than cell death. *Developmental cell*, 15(3), pp.344-357.
54. Chakraborty, J., Rajamma, U., Jana, N.R. and Mohanakumar, K.P., 2015. Quercetin improves the activity of the ubiquitin-proteasomal system in 150Q mutated huntingtin

- expressing cells but exerts detrimental effects on neuronal survivability. *Journal of Neuroscience Research*, 93(10), pp. 1581-1591.
55. Chala, T.S. and Ali, G.Y. 2016. Recent advance in diabetes therapy: pancreatic beta cell regeneration approaches. *Diabetes*, 6(6), pp. 108–118.
56. Chandel, S., Tiwari, R.K. and Dixit, M., 2017. Endothelial dysfunction in diabetes. In *Mechanisms of Vascular Defects in Diabetes Mellitus*, 17, pp. 109-128.
57. Chang, C.L., Lin, Y., Bartolome, A.P., Chen, Y.C., Chiu, S.C. and Yang, W.C., 2013. Herbal therapies for type 2 diabetes mellitus: chemistry, biology, and potential application of selected plants and compounds. *Evidence-Based Complementary and Alternative Medicine*, 2013.
58. Chatterjee, S., Khunti, K. and Davies, M.J., 2017. Type 2 diabetes. *The Lancet*, 389(10085), pp. 2239-2251.
59. Chaudhury, A., Duvoor, C., Dendi, R., Sena, V., Kraleti, S., Chada, A., Ravilla, R., Marco, A., Shekhawat, N.S., Montales, M.T. and Kuriakose, K., 2017. Clinical review of antidiabetic drugs: Implications for type 2 diabetes mellitus management. *Frontiers in Endocrinology*, 8, p. 6.
60. Chen, C., Cohrs, C.M., Stertmann, J., Bozsak, R. and Speier, S., 2017. Human beta cell mass and function in diabetes: Recent advances in knowledge and technologies to understand disease pathogenesis. *Molecular metabolism*, 6(9), pp.943-957.
61. Chen, E., Tsai, T.H., Li, L., Saha, P., Chan, L. and Chang, B.H.J., 2017. PLIN2 is a key regulator of the unfolded protein response and endoplasmic reticulum stress resolution in pancreatic β cells. *Scientific reports*, 7, p.40855.
62. Chen, N., Lei, T., Xin, L., Zhou, L., Cheng, J., Qin, L., Han, S. and Wan, Z., 2016. Depot-specific effects of treadmill running and rutin on white adipose tissue function in diet-induced obese mice. *Journal of physiology and biochemistry*, 72(3), pp.453-467.
63. Choi, H.N., Kang, M.J., Lee, S.J. and Kim, J.I., 2014. Ameliorative effect of myricetin on insulin resistance in mice fed a high-fat, high-sucrose diet. *Nutrition research and practice*, 8(5), pp.544-549.
64. Choi, S.E., Lee, S.M., Lee, Y.J., Li, L.J., Lee, S.J., Lee, J.H., Kim, Y., Jun, H.S., Lee, K.W. and Kang, Y., 2008. Protective role of autophagy in palmitate-induced INS-1 β -cell death. *Endocrinology*, 150(1), pp. 126-134.
65. Cnop, M., Foufelle, F. and Velloso, L.A., 2012. Endoplasmic reticulum stress, obesity and diabetes. *Trends in molecular medicine*, 18(1), pp. 59-68.

66. Cnop, M., Ladriere, L., Hekerman, P., Ortis, F., Cardozo, A.K., Dogusan, Z., Flamez, D., Boyce, M., Yuan, J. and Eizirik, D.L., 2007. Selective inhibition of eukaryotic translation initiation factor 2 α dephosphorylation potentiates fatty acid-induced endoplasmic reticulum stress and causes pancreatic β -cell dysfunction and apoptosis. *Journal of Biological Chemistry*, 282(6), pp. 3989-3997.
67. Codogno, P. and Meijer, A.J., 2010. Autophagy: a potential link between obesity and insulin resistance. *Cell metabolism*, 11(6), pp.449-451.
68. Coelho, M., Oliveira, T., and Fernandes, R., 2013. Biochemistry of adipose tissue: an endocrine organ. *Archives of Medical Science : AMS*, 9(2), 191–200.
69. Coelho, O.G.L., da Silva, B.P., Rocha, D.M.U.P., Lopes, L.L. and Alfenas, R.D.C.G., 2017. Polyunsaturated fatty acids and type 2 diabetes: impact on the glycemic control mechanism. *Critical Reviews in Food Science and Nutrition*, 57(17), pp. 3614-3619.
70. Colak, Y., Yesil, A., Mutlu, H.H., Caklili, O.T., Ulasoglu, C., Senates, E., Takir, M., Kostek, O., Yilmaz, Y., Yilmaz Enc, F. and Tasan, G., 2014. A potential treatment of non-alcoholic fatty liver disease with SIRT1 activators. *Journal of Gastrointestinal and Liver Diseases*, 23(3), pp.311-319.
71. Corell, L., Armenta, S., Esteve-Turrillas, F.A. and de la Guardia, M., 2018. Flavonoid determination in onion, chili and leek by hard cap espresso extraction and liquid chromatography with diode array detection. *Microchemical Journal*, 140, pp.74-79.
72. Czaja, M.J., 2010. Autophagy in health and disease. 2. Regulation of lipid metabolism and storage by autophagy: pathophysiological implications. *American Journal of Physiology-Cell Physiology*, 298(5), pp.C973-C978.
73. Czech, M.P., 2017. Insulin action and resistance in obesity and type 2 diabetes. *Nature Medicine*, 23(7), pp. 804-814.
74. Dabelea, D., Stafford, J.M., Mayer-Davis, E.J., D'Agostino, R., Dolan, L., Imperatore, G., Linder, B., Lawrence, J.M., Marcovina, S.M., Mottl, A.K. and Black, M.H., 2017. Association of type 1 diabetes vs type 2 diabetes diagnosed during childhood and adolescence with complications during teenage years and young adulthood. *Jama*, 317(8), pp.825-835.
75. Dagon, Y., Mantzoros, C. and Kim, Y.B., 2015. Exercising insulin sensitivity: AMPK turns on autophagy!. *Metabolism-Clinical and Experimental*, 64(6), pp. 655-657.

76. Dang, L.T.T., Phan, N.K. and Truong, K.D., 2017. Mesenchymal stem cells for diabetes mellitus treatment: new advances. *Biomedical Research and Therapy*, 4(1), pp. 1062-1081.
77. De Beer, D., Joubert, E., Gelderblom, W.C.A. and Manley, M., 2017. Phenolic compounds: a review of their possible role as in vivo antioxidants of wine. *South African Journal of Enology and Viticulture*, 23(2), pp.48-61.
78. Deepthi, B., Sowjanya, K., Lidiya, B., Bhargavi, R.S. and Babu, P.S., 2017. A modern review of diabetes mellitus: an annihilatory metabolic disorder. *Journal of In Silico & In Vitro Pharmacology*, 3(1), p.14.
79. DeFronzo, R.A. and Abdul-Ghani, M.A., 2011. Preservation of β -cell function: the key to diabetes prevention. *The Journal of Clinical Endocrinology & Metabolism*, 96(8), pp.2354-2366.
80. DeFronzo, R.A. and Tripathy, D., 2009. Skeletal muscle insulin resistance is the primary defect in type 2 diabetes. *Diabetes Care*, 32(suppl 2), pp.S157-S163.
81. DeFronzo, R.A., Ferrannini, E., Groop, L., Henry, R.R., Herman, W.H., Holst, J.J., Hu, F.B., Kahn, C.R., Raz, I., Shulman, G.I. and Simonson, D.C., 2015. Type 2 diabetes mellitus. *Nature Reviews Disease Primers*, 1, p. 15019.
82. Deng, S., Vatamaniuk, M., Huang, X., Doliba, N., Lian, M.M., Frank, A., Velidedeoglu, E., Desai, N.M., Koeberlein, B., Wolf, B. and Barker, C.F., 2004. Structural and functional abnormalities in the islets isolated from type 2 diabetic subjects. *Diabetes*, 53(3), pp.624-632.
83. Di Bartolomeo, S., Corazzari, M., Nazio, F., Oliverio, S., Lisi, G., Antonioli, M., Pagliarini, V., Matteoni, S., Fuoco, C., Giunta, L. and D'Amelio, M., 2010. The dynamic interaction of AMBRA1 with the dynein motor complex regulates mammalian autophagy. *The Journal of cell biology*, 191(1), pp.155-168.
84. Di Paolo, S., Teutonico, A., Leogrande, D., Capobianco, C. and Schena, P.F., 2006. Chronic inhibition of mammalian target of rapamycin signaling downregulates insulin receptor substrates 1 and 2 and AKT activation: a crossroad between cancer and diabetes?. *Journal of the American Society of Nephrology*, 17(8), pp. 2236-2244.
85. Dietz, W.H., 2004. Overweight in childhood and adolescence. *New England Journal of Medicine*, 350(9), pp.855-857.
86. Dillard, C.J. and German, J.B., 2000. Phytochemicals: nutraceuticals and human health. *Journal of the Science of Food and Agriculture*, 80(12), pp.1744-1756.

87. Dimopoulos, N., Watson, M., Sakamoto, K. and Hundal, H.S., 2006. Differential effects of palmitate and palmitoleate on insulin action and glucose utilization in rat L6 skeletal muscle cells. *Biochemical Journal*, 399(3), pp.473-481.
88. Ding, Y. and Choi, M.E., 2014. Autophagy in diabetic nephropathy. *Journal of Endocrinology*, 224(1), pp. R15-30.
89. Domínguez-Bendala, J., Inverardi, L. and Ricordi, C., 2012. Regeneration of pancreatic beta-cell mass for the treatment of diabetes. *Expert opinion on biological therapy*, 12(6), pp.731-741.
90. Donath, M.Y. and Halban, P.A., 2004. Decreased beta-cell mass in diabetes: significance, mechanisms and therapeutic implications. *Diabetologia*, 47(3), pp.581-589.
91. Dong, H. and Czaja, M.J., 2011. Regulation of lipid droplets by autophagy. *Trends in Endocrinology & Metabolism*, 22(6), pp.234-240.
92. Eaton, S.B. and Eaton, S.B., 2017. Physical inactivity, obesity, and type 2 diabetes: An evolutionary perspective. *Research Quarterly for Exercise and Sport*, 88(1), pp. 1-8.
93. Ebato, C., Uchida, T., Arakawa, M., Komatsu, M., Ueno, T., Komiya, K., Azuma, K., Hirose, T., Tanaka, K., Kominami, E. and Kawamori, R., 2008. Autophagy is important in islet homeostasis and compensatory increase of beta cell mass in response to high-fat diet. *Cell metabolism*, 8(4), pp.325-332.
94. Eizirik, D.L., Cardozo, A.K. and Cnop, M., 2007. The role for endoplasmic reticulum stress in diabetes mellitus. *Endocrine reviews*, 29(1), pp.42-61.
95. El-Kader, S.M.A. and El-Den Ashmawy, E.M.S., 2015. Non-alcoholic fatty liver disease: The diagnosis and management. *World journal of hepatology*, 7(6), pp.846-858.
96. Elouil, H., Bensellam, M., Guiot, Y., Vander Mierde, D., Pascal, S.M.A., Schuit, F.C. and Jonas, J.C., 2007. Acute nutrient regulation of the unfolded protein response and integrated stress response in cultured rat pancreatic islets. *Diabetologia*, 50(7), pp.1442-1452.
97. Emanuel, A.L., Nieuwenhoff, M.D., Klaassen, E.S., Verma, A., Kramer, M.H., Strijers, R., Vrancken, A.F., Eringa, E., Groeneveld, G.J. and Serné, E.H., 2017. Relationships between type 2 diabetes, neuropathy, and microvascular dysfunction: Evidence from patients with cryptogenic axonal polyneuropathy. *Diabetes Care*, 40(4), pp. 583-590.

98. Eng, K.E., Panas, M.D., Hedestam, G.B.K. and McInerney, G.M., 2010. A novel quantitative flow cytometry-based assay for autophagy. *Autophagy*, 6(5), pp.634-641.
99. Falcó, I., Randazzo, W., Gómez-Mascaraque, L.G., Aznar, R., López-Rubio, A. and Sánchez, G., 2018. Fostering the antiviral activity of green tea extract for sanitizing purposes through controlled storage conditions. *Food Control*, 84, pp.485-492.
100. Faleck, D.M., Ali, K., Roat, R., Graham, M.J., Crooke, R.M., Battisti, R., Garcia, E., Ahima, R.S. and Imai, Y., 2010. Adipose differentiation-related protein regulates lipids and insulin in pancreatic islets. *American Journal of Physiology-Endocrinology and Metabolism*, 299(2), pp.E249-E257.
101. Farah, B.L., Landau, D.J., Sinha, R.A., Brooks, E.D., Wu, Y., Fung, S.Y.S., Tanaka, T., Hirayama, M., Bay, B.H., Koeberl, D.D. and Yen, P.M., 2016. Induction of autophagy improves hepatic lipid metabolism in glucose-6-phosphatase deficiency. *Journal of hepatology*, 64(2), pp.370-379.
102. Farese Jr, R.V., Zechner, R., Newgard, C.B. and Walther, T.C., 2012. The problem of establishing relationships between hepatic steatosis and hepatic insulin resistance. *Cell metabolism*, 15(5), pp.570-573.
103. Favre, G., González-Neves, G., Piccardo, D., Gómez-Alonso, S., Pérez-Navarro, J. and Hermosín-Gutiérrez, I., 2018. New acylated flavonols identified in *Vitis vinifera* grapes and wines. *Food Research International*. 112, pp. 98-107.
104. Ferrannini, E., Gastaldelli, A., Miyazaki, Y., Matsuda, M., Mari, A. and DeFronzo, R.A., 2005. β -Cell function in subjects spanning the range from normal glucose tolerance to overt diabetes: a new analysis. *The Journal of Clinical Endocrinology & Metabolism*, 90(1), pp.493-500.
105. Fiaschi-Taesch, N.M., Salim, F., Kleinberger, J., Troxell, R., Cozar-Castellano, I., Selk, K., Cherok, E., Takane, K.K., Scott, D.K. and Stewart, A.F., 2010. Induction of human β -cell proliferation and engraftment using a single G1/S regulatory molecule, cdk6. *Diabetes*, 59(8), pp.1926-1936.
106. Filomeni, G., Desideri, E., Cardaci, S., Graziani, I., Piccirillo, S., Rotilio, G. and Ciriolo, M.R., 2010. Carcinoma cells activate AMP-activated protein kinase-dependent autophagy as survival response to kaempferol-mediated energetic impairment. *Autophagy*, 6(2), pp.202-216.
107. Filomeni, G., Graziani, I., De Zio, D., Dini, L., Centonze, D., Rotilio, G. and Ciriolo, M.R., 2012. Neuroprotection of kaempferol by autophagy in models of rotenone-

- mediated acute toxicity: possible implications for Parkinson's disease. *Neurobiology of aging*, 33(4), pp.767-785.
108. Firdous, S.M., 2014. Phytochemicals for treatment of diabetes. *EXCLI journal*, 13, p.451.
109. Flamment, M., Hajduch, E., Ferré, P. and Foufelle, F., 2012. New insights into ER stress-induced insulin resistance. *Trends in Endocrinology & Metabolism*, 23(8), pp. 381-390.
110. Fomina-Yadlin, D., Kubicek, S., Walpita, D., Dančik, V., Hecksher-Sørensen, J., Bittker, J.A., Sharifnia, T., Shamji, A., Clemons, P.A., Wagner, B.K. and Schreiber, S.L., 2010. Small-molecule inducers of insulin expression in pancreatic α -cells. *Proceedings of the National Academy of Sciences*, 107(34), pp.15099-15104.
111. Formiguera, X. and Cantón, A., 2004. Obesity: epidemiology and clinical aspects. *Best practice & research Clinical Gastroenterology*, 18(6), pp.1125-1146.
112. Fu, S., Watkins, S.M. and Hotamisligil, G.S., 2012. The role of endoplasmic reticulum in hepatic lipid homeostasis and stress signaling. *Cell metabolism*, 15(5), pp.623-634.
113. Fu, Z., R Gilbert, E. and Liu, D., 2013. Regulation of insulin synthesis and secretion and pancreatic Beta-cell dysfunction in diabetes. *Current diabetes reviews*, 9(1), pp.25-53.
114. Fujimoto, K., Hanson, P.T., Tran, H., Ford, E.L., Han, Z., Johnson, J.D., Schmidt, R.E., Green, K.G., Wice, B.M. and Polonsky, K.S., 2009. Autophagy regulates pancreatic beta cell death in response to Pdx1 deficiency and nutrient deprivation. *Journal of Biological Chemistry*, 284(40), pp. 27664-27673.
115. Fujita, N., Itoh, T., Omori, H., Fukuda, M., Noda, T. and Yoshimori, T., 2008. The Atg16L complex specifies the site of LC3 lipidation for membrane biogenesis in autophagy. *Molecular biology of the cell*, 19(5), pp.2092-2100.
116. Fujitani, Y., Kawamori, R. and Watada, H., 2009. The role of autophagy in pancreatic β -cell and diabetes. *Autophagy*, 5(2), pp.280-282.
117. Gang, T.B., Hanley, G.A. and Agrawal, A., 2015. C-reactive protein protects mice against pneumococcal infection via both phosphocholine-dependent and phosphocholine-independent mechanisms. *Infection and immunity*, 83(5), pp.1845-1852.

118. Gastaldelli, A., Ferrannini, E., Miyazaki, Y., Matsuda, M. and DeFronzo, R.A., 2004. Beta-cell dysfunction and glucose intolerance: results from the San Antonio metabolism (SAM) study. *Diabetologia*, 47(1), pp.31-39.
119. Gastaldelli, A., Ferrannini, E., Miyazaki, Y., Matsuda, M., Mari, A. and DeFronzo, R.A., 2007. Thiazolidinediones improve β -cell function in type 2 diabetic patients. *American Journal of Physiology-Endocrinology and Metabolism*, 292(3), pp.E871-E883.
120. Gastaldelli, A., Gaggini, M. and DeFronzo, R.A., 2017. Role of adipose tissue insulin resistance in the natural history of type 2 diabetes: results from the San Antonio Metabolism Study. *Diabetes*, 66(4), pp. 815-822.
121. Gates, M.A., Tworoger, S.S., Hecht, J.L., De Vivo, I., Rosner, B. and Hankinson, S.E., 2007. A prospective study of dietary flavonoid intake and incidence of epithelial ovarian cancer. *International journal of cancer*, 121(10), pp.2225-2232.
122. Geng, J. and Klionsky, D.J., 2008. The Atg8 and Atg12 ubiquitin-like conjugation systems in macroautophagy. *EMBO reports*, 9(9), pp.859-864.
123. Gerber, P.A. and Rutter, G.A., 2017. The role of oxidative stress and hypoxia in pancreatic beta-cell dysfunction in diabetes mellitus. *Antioxidants & Redox Signaling*, 26(10), pp. 501-518.
124. Giacca, A., Xiao, C., Oprescu, A.I., Carpentier, A.C. and Lewis, G.F., 2010. Lipid-induced pancreatic β -cell dysfunction: focus on in vivo studies. *American Journal of Physiology-Endocrinology And Metabolism*, 300(2), pp.E255-E262.
125. Gianani, R., 2011. Beta cell regeneration in human pancreas. *Seminars in immunopathology*, 33(1), pp. 23-27.
126. Glick, D., Barth, S. and Macleod, K.F., 2010. Autophagy: cellular and molecular mechanisms. *The Journal of pathology*, 221(1), pp.3-12.
127. Goginashvili, A., Zhang, Z., Erbs, E., Spiegelhalter, C., Kessler, P., Mihlan, M., Pasquier, A., Krupina, K., Schieber, N., Cinque, L. and Morvan, J., 2015. Insulin secretory granules control autophagy in pancreatic β cells. *Science*, 347(6224), pp.878-882.
128. Gonzalez, C.D., Lee, M.S., Marchetti, P., Pietropaolo, M., Towns, R., Vaccaro, M.I., Watada, H. and Wiley, J.W., 2011. The emerging role of autophagy in the pathophysiology of diabetes mellitus. *Autophagy*, 7(1), pp.2-11.

129. Gonzalez-Rodriguez, A., Mayoral, R., Agra, N., Valdecantos, M.P., Pardo, V., Miquilena-Colina, M.E., Vargas-Castrillón, J., Iacono, O.L., Corazzari, M., Fimia, G.M. and Piacentini, M., 2014. Impaired autophagic flux is associated with increased endoplasmic reticulum stress during the development of NAFLD. *Cell death & disease*, 5(4), p.e1179.
130. Goossens, G.H., 2008. The role of adipose tissue dysfunction in the pathogenesis of obesity-related insulin resistance. *Physiology & behavior*, 94(2), pp.206-218.
131. Gracia-Sancho, J. and Guixé-Muntet, S., 2018. The many-faced role of autophagy in liver diseases. *Journal of Hepatology*, 68(3), pp.593-594.
132. Greenberg, A.S., Coleman, R.A., Kraemer, F.B., McManaman, J.L., Obin, M.S., Puri, V., Yan, Q.W., Miyoshi, H. and Mashek, D.G., 2011. The role of lipid droplets in metabolic disease in rodents and humans. *The Journal of clinical investigation*, 121(6), pp.2102-2110.
133. Grulich-Henn, J. and Klose, D., 2017. Understanding childhood diabetes mellitus: new pathophysiological aspects. *Journal of inherited metabolic disease*, pp.1-9.
134. Grumati, P., Coletto, L., Schiavinato, A., Castagnaro, S., Bertaggia, E., Sandri, M. and Bonaldo, P., 2011. Physical exercise stimulates autophagy in normal skeletal muscles but is detrimental for collagen VI-deficient muscles. *Autophagy*, 7(12), pp.1415-1423.
135. Guilherme, A., Virbasius, J.V., Puri, V. and Czech, M.P., 2008. Adipocyte dysfunctions linking obesity to insulin resistance and type 2 diabetes. *Nature reviews Molecular cell biology*, 9(5), pp.367-377.
136. Guiot, Y., Sempoux, C., Moulin, P. and Rahier, J., 2001. No decrease of the (beta)-cell mass in type 2 diabetic patients. *Diabetes*, 50, p.S188.
137. Guo, L., Li, X. and Tang, Q.Q., 2014. Transcriptional regulation of adipocyte differentiation: a central role for CCAAT/enhancer-binding protein (C/EBP) β . *Journal of biological chemistry*, 290(2), pp. 755–761.
138. Gupta, P., Bala, M., Gupta, S., Dua, A., Dabur, R., Injeti, E. and Mittal, A., 2016. Efficacy and risk profile of anti-diabetic therapies: Conventional vs traditional drugs—A mechanistic revisit to understand their mode of action. *Pharmacological research*, 113, pp.636-674.
139. Hamaeher-Brady, A., Brady, N.R. and Gottlieb, R.A., 2006. Endoplasmic reticulum stress triggers autophagy. *Journal of Biological Chemistry*, 281(40), pp.29776-29787.

140. Hameed, I., Masoodi, S.R., Mir, S.A., Nabi, M., Ghazanfar, K. and Ganai, B.A., 2015. Type 2 diabetes mellitus: from a metabolic disorder to an inflammatory condition. *World Journal of Diabetes*, 6(4), pp. 598-612.
141. Han, B., Yu, Y.Q., Yang, Q.L., Shen, C.Y. and Wang, X.J., 2017. Kaempferol induces autophagic cell death of hepatocellular carcinoma cells via activating AMPK signaling. *Oncotarget*, 8(49), pp.86227- 86239.
142. Han, D., Yang, B., Olson, L.K., Greenstein, A., Baek, S.H., Claycombe, K.J., Goudreau, J.L., Yu, S.W. and Kim, E.K., 2010. Activation of autophagy through modulation of 5'-AMP-activated protein kinase protects pancreatic β -cells from high glucose. *Biochemical Journal*, 425(3), pp.541-551.
143. Han, J. and Kaufman, R.J., 2016. The role of ER stress in lipid metabolism and lipotoxicity. *Journal of lipid research*, pp.jlr-R067595.
144. Hanada, T., Noda, N.N., Satomi, Y., Ichimura, Y., Fujioka, Y., Takao, T., Inagaki, F. and Ohsumi, Y., 2007. The Atg12-Atg5 conjugate has a novel E3-like activity for protein lipidation in autophagy. *Journal of Biological Chemistry*, 282(52), pp.37298-37302.
145. Hara, T., Takamura, A., Kishi, C., Iemura, S.I., Natsume, T., Guan, J.L. and Mizushima, N., 2008. FIP200, a ULK-interacting protein, is required for autophagosome formation in mammalian cells. *The Journal of cell biology*, 181(3), pp.497-510.
146. Harborne, J.B. and Williams, C.A., 2000. Advances in flavonoid research since 1992. *Phytochemistry*, 55(6), pp.481-504.
147. Hardie, D.G., 2004. AMP-activated protein kinase: a master switch in glucose and lipid metabolism. *Reviews in Endocrine and Metabolic Disorders*, 5(2), pp.119-125.
148. Hardie, D.G., 2011. AMP-activated protein kinase—an energy sensor that regulates all aspects of cell function. *Genes & development*, 25(18), pp.1895-1908.
149. Hardie, D.G., Ross, F.A. and Hawley, S.A., 2012. AMPK: a nutrient and energy sensor that maintains energy homeostasis. *Nature reviews Molecular cell biology*, 13(4), p.251.
150. Harding, H.P., Zeng, H., Zhang, Y., Jungries, R., Chung, P., Plesken, H., Sabatini, D.D. and Ron, D., 2001. Diabetes mellitus and exocrine pancreatic dysfunction in *perk*^{-/-} mice reveals a role for translational control in secretory cell survival. *Molecular cell*, 7(6), pp.1153-1163.

151. Hashemian, S.J., Kouhnavard, M. and Nasli-Esfahani, E., 2015. Mesenchymal stem cells: rising concerns over their application in treatment of type one diabetes mellitus. *Journal of diabetes research*, 2015.
152. Hatting, M., Tavares, C.D., Sharabi, K., Rines, A.K. and Puigserver, P., 2018. Insulin regulation of gluconeogenesis. *Annals of the New York Academy of Sciences*, 1411(1), pp. 21-35.
153. Hayes, H.L., Peterson, B.S., Haldeman, J.M., Newgard, C.B., Hohmeier, H.E. and Stephens, S.B., 2017. Delayed apoptosis allows islet β -cells to implement an autophagic mechanism to promote cell survival. *PloS one*, 12(2), p.e0172567.
154. He, C. and Klionsky, D.J., 2009. Regulation mechanisms and signaling pathways of autophagy. *Annual review of genetics*, 43, pp. 67-93.
155. He, C., Bassik, M.C., Moresi, V., Sun, K., Wei, Y., Zou, Z., An, Z., Loh, J., Fisher, J., Sun, Q. and Korsmeyer, S., 2012. Exercise-induced BCL2-regulated autophagy is required for muscle glucose homeostasis. *Nature*, 481(7382), pp.511-515.
156. He, C., Sumpter, Jr, R. and Levine, B., 2012. Exercise induces autophagy in peripheral tissues and in the brain. *Autophagy*, 8(10), pp.1548-1551.
157. He, C., Wei, Y., Sun, K., Li, B., Dong, X., Zou, Z., Liu, Y., Kinch, L.N., Khan, S., Sinha, S. and Xavier, R.J., 2013. Beclin 2 functions in autophagy, degradation of G protein-coupled receptors, and metabolism. *Cell*, 154(5), pp.1085-1099.
158. He, H., Dang, Y., Dai, F., Guo, Z., Wu, J., She, X., Pei, Y., Chen, Y., Ling, W., Wu, C. and Zhao, S., 2003. Post-translational modifications of three members of the human MAP1LC3 family and detection of a novel type of modification for MAP1LC3B. *Journal of Biological Chemistry*, 278(31), pp.29278-29287.
159. He, Q., Sha, S., Sun, L., Zhang, J. and Dong, M., 2016. GLP-1 analogue improves hepatic lipid accumulation by inducing autophagy via AMPK/mTOR pathway. *Biochemical and biophysical research communications*, 476(4), pp.196-203.
160. Hirabara, S.M., Curi, R. and Maechler, P., 2010. Saturated fatty acid-induced insulin resistance is associated with mitochondrial dysfunction in skeletal muscle cells. *Journal of cellular physiology*, 222(1), pp.187-194.
161. Holst, J.J., Vilsbøll, T. and Deacon, C.F., 2009. The incretin system and its role in type 2 diabetes mellitus. *Molecular and cellular endocrinology*, 297(1-2), pp.127-136.
162. Hosokawa, N., Hara, T., Kaizuka, T., Kishi, C., Takamura, A., Miura, Y., Iemura, S.I., Natsume, T., Takehana, K., Yamada, N. and Guan, J.L., 2009. Nutrient-dependent

- mTORC1 association with the ULK1–Atg13–FIP200 complex required for autophagy. *Molecular biology of the cell*, 20(7), pp.1981-1991.
163. Hou, W., Hu, S., Su, Z., Wang, Q., Meng, G., Guo, T., Zhang, J. and Gao, P., 2018. Myricetin Attenuates LPS-induced Inflammation in RAW 264.7 Macrophages and Mouse Models. bioRxiv, p.299420.
164. Hsiao, P.J., Chiou, H.Y.C., Jiang, H.J., Lee, M.Y., Hsieh, T.J. and Kuo, K.K., 2017. Pioglitazone Enhances Cytosolic Lipolysis, β -oxidation and Autophagy to Ameliorate Hepatic Steatosis. *Scientific reports*, 7(1), p.9030.
165. Hu, F.B., Van Dam, R.M. and Liu, S., 2001. Diet and risk of type II diabetes: the role of types of fat and carbohydrate. *Diabetologia*, 44(7), pp.805-817.
166. Hu, P., Han, Z., Couvillon, A.D., Kaufman, R.J. and Exton, J.H., 2006. Autocrine tumor necrosis factor alpha links endoplasmic reticulum stress to the membrane death receptor pathway through IRE1 α -mediated NF- κ B activation and down-regulation of TRAF2 expression. *Molecular and cellular biology*, 26(8), pp.3071-3084.
167. Huang, J. and Klionsky, D.J., 2007. Autophagy and human disease. *Cell cycle*, 6(15), pp.1837-1849.
168. Huang, W.W., Chiu, Y.J., Fan, M.J., Lu, H.F., Yeh, H.F., Li, K.H., Chen, P.Y., Chung, J.G. and Yang, J.S., 2010. Kaempferol induced apoptosis via endoplasmic reticulum stress and mitochondria-dependent pathway in human osteosarcoma U-2 OS cells. *Molecular nutrition & food research*, 54(11), pp.1585-1595.
169. Hwang, S.L., Li, X., Lee, J.Y. and Chang, H.W., 2012. Improved insulin sensitivity by rapamycin is associated with reduction of mTOR and S6K1 activities in L6 myotubes. *Biochemical and biophysical research communications*, 418(2), pp.402-407.
170. Ijuin, T. and Takenawa, T., 2012. Regulation of insulin signaling and glucose transporter 4 (GLUT4) exocytosis by phosphatidylinositol 3, 4, 5-trisphosphate (PIP3) phosphatase, skeletal muscle, and kidney enriched inositol polyphosphate phosphatase (SKIP). *Journal of Biological Chemistry*, 287(10), pp.6991-6999
171. Imamura, F., Micha, R., Wu, J.H., de Oliveira Otto, M.C., Otite, F.O., Abioye, A.I. and Mozaffarian, D., 2016. Effects of saturated fat, polyunsaturated fat, monounsaturated fat, and carbohydrate on glucose-insulin homeostasis: a systematic review and meta-analysis of randomised controlled feeding trials. *PLoS medicine*, 13(7), p.e1002087.
172. Inaishi, J., Saisho, Y., Sato, S., Kou, K., Murakami, R., Watanabe, Y., Kitago, M., Kitagawa, Y., Yamada, T. and Itoh, H., 2016. Effects of obesity and diabetes on α -and

- β -cell mass in surgically resected human pancreas. *The Journal of Clinical Endocrinology & Metabolism*, 101(7), pp.2874-2882.
173. Internal clinical guidelines team. 2015. Type 2 diabetes in adults: Management. London: *National Institute for Health and Care Excellence*, p.28.
174. Itakura, E. and Mizushima, N., 2010. Characterization of autophagosome formation site by a hierarchical analysis of mammalian Atg proteins. *Autophagy*, 6(6), pp.764-776.
175. Itakura, E., Kishi, C., Inoue, K. and Mizushima, N., 2008. Beclin 1 forms two distinct phosphatidylinositol 3-kinase complexes with mammalian Atg14 and UVRAG. *Molecular biology of the cell*, 19(12), pp.5360-5372.
176. Jäger, S., Bucci, C., Tanida, I., Ueno, T., Kominami, E., Saftig, P. and Eskelinen, E.L., 2004. Role for Rab7 in maturation of late autophagic vacuoles. *Journal of cell science*, 117(20), pp.4837-4848.
177. Jain, P., Vig, S., Datta, M., Jindel, D., Mathur, A.K., Mathur, S.K. and Sharma, A., 2013. Systems biology approach reveals genome to phenome correlation in type 2 diabetes. *PloS one*, 8(1), p. e53522.
178. Jana, N.R., 2010. Role of the ubiquitin–proteasome system and autophagy in polyglutamine neurodegenerative diseases. *Future Neurology*, 5(1), pp. 105-112.
179. Jensen, C.C., Cnop, M., Hull, R.L., Fujimoto, W.Y., Kahn, S.E. and American Diabetes Association GENNID Study Group, 2002. β -Cell function is a major contributor to oral glucose tolerance in high-risk relatives of four ethnic groups in the US. *Diabetes*, 51(7), pp.2170-2178.
180. Jiang, P. and Mizushima, N., 2014. Autophagy and human diseases. *Cell research*, 24(1), pp.69-79.
181. Jiang, Y., Huang, W., Wang, J., Xu, Z., He, J., Lin, X., Zhou, Z. and Zhang, J., 2014. Metformin plays a dual role in MIN6 pancreatic β cell function through AMPK-dependent autophagy. *International journal of biological sciences*, 10(3), p.268-277.
182. Jin, J., Wang, Y. and Deng, Z., 2017. Increased risk of diabetes in inflammatory orthopedics diseases. *AME Medical Journal*, 2(6).
183. Jones, J.R., Lebar, M.D., Jinwal, U.K., Abisambra, J.F., Koren III, J., Blair, L., O’Leary, J.C., Davey, Z., Trotter, J., Johnson, A.G. and Weeber, E., 2010. The diarylheptanoid (+)-a R, 11 S-myricanol and two flavones from bayberry (*Myrica cerifera*) destabilize the microtubule-associated protein Tau. *Journal of natural products*, 74(1), pp.38-44.

184. Jung, C.H., Jun, C.B., Ro, S.H., Kim, Y.M., Otto, N.M., Cao, J., Kundu, M. and Kim, D.H., 2009. ULK-Atg13-FIP200 complexes mediate mTOR signaling to the autophagy machinery. *Molecular biology of the cell*, 20(7), pp.1992-2003.
185. Jung, H.S. and Lee, M.S., 2009. Macroautophagy in homeostasis of pancreatic β -cell. *Autophagy*, 5(2), pp.241-243.
186. Jung, H.S., Chung, K.W., Kim, J.W., Kim, J., Komatsu, M., Tanaka, K., Nguyen, Y.H., Kang, T.M., Yoon, K.H., Kim, J.W. and Jeong, Y.T., 2008. Loss of autophagy diminishes pancreatic β cell mass and function with resultant hyperglycemia. *Cell metabolism*, 8(4), pp.318-324.
187. Kabadi, U.M., 2017. Major pathophysiology in prediabetes and type 2 diabetes: decreased insulin in lean and insulin resistance in obese. *Journal of the Endocrine Society*, 1(6), pp.742-750.
188. Kabeya, Y., Mizushima, N., Ueno, T., Yamamoto, A., Kirisako, T., Noda, T., Kominami, E., Ohsumi, Y. and Yoshimori, T., 2000. LC3, a mammalian homologue of yeast Apg8p, is localized in autophagosome membranes after processing. *The EMBO journal*, 19(21), pp.5720-5728.
189. Kahn, S.E., Andrikopoulos, S. and Verchere, C.B., 1999. Islet amyloid: a long-recognized but underappreciated pathological feature of type 2 diabetes. *Diabetes*, 48(2), pp.241-253.
190. Kalra, S., Aamir, A.H., Raza, A., Das, A.K., Azad Khan, A.K., Shrestha, D., Qureshi, M.F., Md, F., Pathan, M.F., Jawad, F. and Bhattarai, J., 2015. Place of sulfonylureas in the management of type 2 diabetes mellitus in South Asia: A consensus statement. *Indian J Endocrinol Metab*, 19(5), pp.577-596.
191. Kaneto, H., Matsuoka, T.A., Nakatani, Y., Kawamori, D., Miyatsuka, T., Matsuhisa, M. and Yamasaki, Y., 2005. Oxidative stress, ER stress, and the JNK pathway in type 2 diabetes. *Journal of molecular medicine*, 83(6), pp.429-439.
192. Kang, S.J., Park, J.H.Y., Choi, H.N. and Kim, J.I., 2015. α -glucosidase inhibitory activities of myricetin in animal models of diabetes mellitus. *Food science and biotechnology*, 24(5), pp.1897-1900.
193. Kar, A., Mukherjee, P.K., Saha, S., Bahadur, S., Ahmmed, S.K. and Pandit, S., 2015. Possible herb-drug interaction of *Morus alba* L.-a potential anti-diabetic plant from Indian traditional medicine. *Indian Journal of Traditional Knowledge*, 14(4), pp. 626-631.

194. Karaskov, E., Scott, C., Zhang, L., Teodoro, T., Ravazzola, M. and Volchuk, A., 2006. Chronic palmitate but not oleate exposure induces endoplasmic reticulum stress, which may contribute to INS-1 pancreatic β -cell apoptosis. *Endocrinology*, *147*(7), pp.3398-3407.
195. Kartha, G.K., Moshal, K.S., Sen, U., Joshua, I.G., Tyagi, N., Steed, M.M. and Tyagi, S.C., 2008. Renal mitochondrial damage and protein modification in type-2 diabetes. *Acta Diabetologica*, *45*(2), pp. 75-81.
196. Kashyap, D., Sharma, A., Tuli, H.S., Sak, K., Punia, S. and Mukherjee, T.K., 2017. Kaempferol—A dietary anticancer molecule with multiple mechanisms of action: Recent trends and advancements. *Journal of functional foods*, *30*, pp.203-219.
197. Kashyap, D., Tuli, H.S., Garg, V.K., Bhatnagar, S. and Sharma, A.K., 2018. Ursolic acid and quercetin: Promising anticancer phytochemicals with antimetastatic and antiangiogenic potential. *Tumor and Microenvironment*, *1*(1), pp.9-15.
198. Katsarou, A., Gudbjörnsdóttir, S., Rawshani, A., Dabelea, D., Bonifacio, E., Anderson, B.J., Jacobsen, L.M., Schatz, D.A. and Lernmark, Å., 2017. Type 1 diabetes mellitus. *Nature reviews Disease primers*, *3*, p.17016.
199. Kaushik, S. and Cuervo, A.M., 2012. Chaperone-mediated autophagy: a unique way to enter the lysosome world. *Trends in cell biology*, *22*(8), pp.407-417.
200. Kawser Hossain, M., Abdal Dayem, A., Han, J., Yin, Y., Kim, K., Kumar Saha, S., Yang, G.M., Choi, H.Y. and Cho, S.G., 2016. Molecular mechanisms of the anti-obesity and anti-diabetic properties of flavonoids. *International journal of molecular sciences*, *17*(4), p.569
201. Khan, A.A., Rahmani, A.H. and Aldebasi, Y.H., 2017. Diabetic Retinopathy: Recent Updates on Different Biomarkers and Some Therapeutic Agents. *Current diabetes reviews*, *13*, pp.1-11.
202. Kharroubi, I., Ladrière, L., Cardozo, A.K., Dogusan, Z., Cnop, M. and Eizirik, D.L., 2004. Free fatty acids and cytokines induce pancreatic β -cell apoptosis by different mechanisms: role of nuclear factor- κ B and endoplasmic reticulum stress. *Endocrinology*, *145*(11), pp.5087-5096.
203. Kihara, A., Kabeya, Y., Ohsumi, Y. and Yoshimori, T., 2001. Beclin-phosphatidylinositol 3-kinase complex functions at the trans-Golgi network. *EMBO reports*, *2*(4), pp.330-335.

204. Kim, H.S. and Lee, M.K., 2016. β -Cell regeneration through the transdifferentiation of pancreatic cells: Pancreatic progenitor cells in the pancreas. *Journal of diabetes investigation*, 7(3), pp.286-296.
205. Kim, H.S., Montana, V., Jang, H.J., Parpura, V. and Kim, J.A., 2013. Epigallocatechin-gallate (EGCG) stimulates autophagy in vascular endothelial cells: a potential role for reducing lipid accumulation. *Journal of Biological Chemistry*, 288(31), pp. 22693-22705.
206. Kim, J., Cheon, H., Jeong, Y.T., Quan, W., Kim, K.H., Cho, J.M., Lim, Y.M., Oh, S.H., Jin, S.M., Kim, J.H. and Lee, M.K., 2014. Amyloidogenic peptide oligomer accumulation in autophagy-deficient β cells induces diabetes. *The Journal of clinical investigation*, 124(8), pp.3311-3324.
207. Kim, J., Kundu, M., Viollet, B., & Guan, K.-L. (2011). AMPK and mTOR regulate autophagy through direct phosphorylation of Ulk1. *Nature Cell Biology*, 13(2), 132–141.
208. Kim, J., Yang, G., Kim, Y., Kim, J. and Ha, J., 2016. AMPK activators: mechanisms of action and physiological activities. *Experimental & molecular medicine*, 48(4), p.e224.
209. Kim, M.E., Ha, T.K., Yoon, J.H. and Lee, J.S., 2014. Myricetin induces cell death of human colon cancer cells via BAX/BCL2-dependent pathway. *Anticancer research*, 34(2), pp.701-706.
210. Kim, O.K., Jun, W. and Lee, J., 2015. Mechanism of ER stress and inflammation for hepatic insulin resistance in obesity. *Annals of Nutrition and Metabolism*, 67(4), pp.218-227.
211. Kim, S.H. and Choi, K.C., 2013. Anti-cancer effect and underlying mechanism (s) of kaempferol, a phytoestrogen, on the regulation of apoptosis in diverse cancer cell models. *Toxicological research*, 29(4), pp.229-234.
212. Kirisako, T., Ichimura, Y., Okada, H., Kabeya, Y., Mizushima, N., Yoshimori, T., Ohsumi, M., Takao, T., Noda, T. and Ohsumi, Y., 2000. The reversible modification regulates the membrane-binding state of Apg8/Aut7 essential for autophagy and the cytoplasm to vacuole targeting pathway. *The Journal of cell biology*, 151(2), pp.263-276.
213. Kirkin, V., Lamark, T., Sou, Y.S., Bjørkøy, G., Nunn, J.L., Bruun, J.A., Shvets, E., McEwan, D.G., Clausen, T.H., Wild, P. and Bilusic, I., 2009. A role for NBR1 in

- autophagosomal degradation of ubiquitinated substrates. *Molecular cell*, 33(4), pp.505-516.
214. Klionsky DJ, Abdelmohsen K, Abe A, Abedin MJ, Abeliovich H, Acevedo Arozena A, Adachi H, Adams CM, Adams PD. 2016. Guidelines for the use and interpretation of assays for monitoring autophagy (3rd edition). *Autophagy*, 12(1), pp. 1-222.
215. Klionsky, D.J., Abdalla, F.C., Abeliovich, H., Abraham, R.T., Acevedo-Arozena, A., Adeli, K., Agholme, L., Agnello, M., Agostinis, P., Aguirre-Ghiso, J.A. and Ahn, H.J., 2012. Guidelines for the use and interpretation of assays for monitoring autophagy. *Autophagy*, 8(4), pp.445-544.
216. Knip, M., 2017. Diabetes: Loss of β -cell mass—an acute event before T1DM presentation? *Nature Reviews Endocrinology*, 13(5), pp. 253-254.
217. Koga, H., Kaushik, S. and Cuervo, A.M., 2010. Altered lipid content inhibits autophagic vesicular fusion. *The FASEB Journal*, 24(8), pp.3052-3065.
218. Kolečkar, V., Kubikova, K., Rehakova, Z., Kuca, K., Jun, D., Jahodar, L. and Opletal, L., 2008. Condensed and hydrolysable tannins as antioxidants influencing the health. *Mini reviews in medicinal chemistry*, 8(5), pp.436-447.
219. Komatsu, M., Waguri, S., Ueno, T., Iwata, J., Murata, S., Tanida, I., Ezaki, J., Mizushima, N., Ohsumi, Y., Uchiyama, Y. and Kominami, E., 2005. Impairment of starvation-induced and constitutive autophagy in Atg7-deficient mice. *Journal of Cell Biology*, 169(3), pp.425-434.
220. Kong, F.J., Wu, J.H., Sun, S.Y. and Zhou, J.Q., 2017. The endoplasmic reticulum stress/autophagy pathway is involved in cholesterol-induced pancreatic β -cell injury. *Scientific reports*, 7, p.44746.
221. Kong, L., Luo, C., Li, X., Zhou, Y. and He, H., 2013. The anti-inflammatory effect of kaempferol on early atherosclerosis in high cholesterol fed rabbits. *Lipids in health and disease*, 12(1), p.115.
222. Kozłowska, A. and Szostak-Wegierek, D., 2014. Flavonoids-food sources and health benefits. *RocznikiPaństwowegoZakładuHigieny*, 65(2), pp. 79-85
223. Kraegen, E.W. and Cooney, G.J., 2008. Free fatty acids and skeletal muscle insulin resistance. *Current opinion in lipidology*, 19(3), pp.235-241.
224. Kristensen, J.M., Trebak, J.T., Schjerling, P., Goodyear, L. and Wojtaszewski, J.F., 2014. Two weeks of metformin treatment induces AMPK-dependent enhancement of

- insulin-stimulated glucose uptake in mouse soleus muscle. *American Journal of Physiology-Endocrinology and Metabolism*, 306(10), pp.E1099-E1109
225. Kroemer, G., Mariño, G. and Levine, B., 2010. Autophagy and the integrated stress response. *Molecular cell*, 40(2), pp.280-293.
226. Kumar, S. and Pandey, A.K., 2013. Chemistry and biological activities of flavonoids: an overview. *The Scientific World Journal*, 2013.; Chen, Z., Zheng, S., Li, L. and Jiang, H., 2014. Metabolism of flavonoids in human: a comprehensive review. *Current drug metabolism*, 15(1), pp.48-61.
227. Kundu, M. and Thompson, C.B., 2008. Autophagy: basic principles and relevance to disease. *Annual Review of Pathology: Mechanisms of Disease.*, 3, pp.427-455.
228. Kundu, S., Pushpakumar, S., Khundmiri, S.J. and Sen, U., 2014. Hydrogen sulfide mitigates hyperglycemic remodeling via liver kinase B1-adenosine monophosphate-activated protein kinase signaling. *Biochimica et Biophysica Acta (BBA)-Molecular Cell Research*, 1843(12), pp. 2816-2826.
229. Larsen, K.B., Lamark, T., Øvervatn, A., Harneshaug, I., Johansen, T. and Bjørkøy, G., 2010. A reporter cell system to monitor autophagy based on p62/SQSTM1. *Autophagy*, 6(6), pp.784-793.
230. Larsson, S., 2009. Phytochemicals: aging and health. *Annals of Botany*, 104(7), pp.ix-x.
231. Las, G., Sereda, S., Wikstrom, J.D., Twig, G. and Shirihai, O.S., 2011. Fatty acids suppress autophagic turnover in β -cells. *Journal of Biological Chemistry*, 286(49), pp. 42534-42544.
232. Lastra, G., Syed, S., Kurukulasuriya, L.R., Manrique, C. and Sowers, J.R., 2014. Type 2 diabetes mellitus and hypertension: an update. *Endocrinology and Metabolism Clinics*, 43(1), pp.103-122.
233. Laybutt, D.R., Preston, A.M., Åkerfeldt, M.C., Kench, J.G., Busch, A.K., Biankin, A.V. and Biden, T.J., 2007. Endoplasmic reticulum stress contributes to beta cell apoptosis in type 2 diabetes. *Diabetologia*, 50(4), pp.752-763.
234. Lee, H.N., Shin, S.A., Choo, G.S., Kim, H.J., Park, Y.S., Kim, B.S., Kim, S.K., Cho, S.D., Nam, J.S., Choi, C.S. and Che, J.H., 2018. Anti inflammatory effect of quercetin and galangin in LPS stimulated RAW264. 7 macrophages and DNCB induced atopic dermatitis animal models. *International journal of molecular medicine*, 41(2), pp.888-898.

235. Lee, M.T., Lin, W.C., Yu, B. and Lee, T.T., 2017. Antioxidant capacity of phytochemicals and their potential effects on oxidative status in animals—A review. *Asian-Australasian journal of animal sciences*, 30(3), pp.299-308.
236. Lee, Y., Hirose, H., Ohneda, M., Johnson, J.H., McGarry, J.D. and Unger, R.H., 1994. Beta-cell lipotoxicity in the pathogenesis of non-insulin-dependent diabetes mellitus of obese rats: impairment in adipocyte-beta-cell relationships. *Proceedings of the National Academy of Sciences*, 91(23), pp.10878-10882.
237. Leibowitz, G., Kaiser, N. and Cerasi, E., 2009. Balancing needs and means: the dilemma of the β -cell in the modern world. *Diabetes, Obesity and Metabolism*, 11, pp.1-9.
238. Leitner, D.R., Frühbeck, G., Yumuk, V., Schindler, K., Micic, D., Woodward, E. and Toplak, H., 2017. Obesity and type 2 diabetes: Two diseases with a need for combined treatment strategies-EASO can lead the way. *Obesity Facts*, 10(5), pp. 483-492.
239. Lesjak, M., Beara, I., Simin, N., Pintać, D., Majkić, T., Bekvalac, K., Orčić, D. and Mimica-Dukić, N., 2018. Antioxidant and anti-inflammatory activities of quercetin and its derivatives. *Journal of Functional Foods*, 40, pp.68-75.
240. Levine, B., Packer, M. and Codogno, P., 2015. Development of autophagy inducers in clinical medicine. *The Journal of clinical investigation*, 125(1), pp.14-24.
241. Li, H.B., Yang, Y.R.Y., Mo, Z.J., Ding, Y. and Jiang, W.J., 2015. Silibinin improves palmitate-induced insulin resistance in C2C12 myotubes by attenuating IRS-1/PI3K/Akt pathway inhibition. *Brazilian Journal of Medical and Biological Research*, 48(5), pp.440-446.
242. Li, W., Guo, Y., Zhang, C., Wu, R., Yang, A.Y., Gaspar, J. and Kong, A.N.T., 2016. Dietary phytochemicals and cancer chemoprevention: A perspective on oxidative stress, inflammation, and epigenetics. *Chemical research in toxicology*, 29(12), pp.2071-2095.
243. Li, W., Li, X., Wang, B., Chen, Y., Xiao, A., Zeng, D., Ou, D., Yan, S., Li, W. and Zheng, Q., 2016. ZLN005 protects cardiomyocytes against high glucose-induced cytotoxicity by promoting SIRT1 expression and autophagy. *Experimental cell research*, 345(1), pp.25-36.
244. Li, X., Zhang, L., Meshinchi, S., Dias-Leme, C., Raffin, D., Johnson, J.D., Treutelaar, M.K. and Burant, C.F., 2006. Islet microvasculature in islet hyperplasia and failure in a model of type 2 diabetes. *Diabetes*, 55(11), pp.2965-2973.

245. Li, Y., Zheng, X., Yi, X., Liu, C., Kong, D., Zhang, J. and Gong, M., 2017. Myricetin: a potent approach for the treatment of type 2 diabetes as a natural class B GPCR agonist. *The FASEB Journal*, 31(6), pp.2603-2611.
246. Li, Z., Xu, J., Zheng, P., Xing, L., Shen, H., Yang, L., Zhang, L. and Ji, G., 2015. Hawthorn leaf flavonoids alleviate nonalcoholic fatty liver disease by enhancing the adiponectin/AMPK pathway. *International journal of clinical and experimental medicine*, 8(10), p.17295.
247. Liang, C., Feng, P., Ku, B., Dotan, I., Canaani, D., Oh, B.H. and Jung, J.U., 2006. Autophagic and tumour suppressor activity of a novel Beclin1-binding protein UVRAG. *Nature cell biology*, 8(7), pp.688-698.
248. Liang, S.H., Zhang, W., Mcgrath, B.C., Zhang, P. and Cavener, D.R., 2006. PERK (eIF2 α kinase) is required to activate the stress-activated MAPKs and induce the expression of immediate-early genes upon disruption of ER calcium homoeostasis. *Biochemical Journal*, 393(1), pp.201-209.
249. Liang, X.H., Jackson, S., Seaman, M., Brown, K., Kempkes, B., Hibshoosh, H. and Levine, B., 1999. Induction of autophagy and inhibition of tumorigenesis by beclin 1. *Nature*, 402(6762), p.672-676.
250. Liao, W., Chen, L., Ma, X., Jiao, R., Li, X. and Wang, Y., 2016. Protective effects of kaempferol against reactive oxygen species-induced hemolysis and its antiproliferative activity on human cancer cells. *European journal of medicinal chemistry*, 114, pp.24-32.
251. Lieberman, A.P., Puertollano, R., Raben, N., Slaugenhaupt, S., Walkley, S.U. and Ballabio, A., 2012. Autophagy in lysosomal storage disorders. *Autophagy*, 8(5), pp.719-730.
252. Lim E.L., Hollingsworth K.G., Aribisala B.S., Chen M.J., Mathers J.C., Taylor R. 2011. Reversal of type 2 diabetes: normalisation of beta cell function in association with decreased pancreas and liver triacylglycerol. *Diabetologia*, 54(10), pp. 2506-14.
253. Lima, R.D.C.L., Kato, L., Kongstad, K.T. and Staerk, D., 2018. Brazilian insulin plant as a bifunctional food: Dual high-resolution PTP1B and α -glucosidase inhibition profiling combined with HPLC-HRMS-SPE-NMR for identification of antidiabetic compounds in *Myrcia rubella* Cambess. *Journal of Functional Foods*, 45, pp.444-451.
254. Lin, C.W., Zhang, H., Li, M., Xiong, X., Chen, X., Chen, X., Dong, X.C. and Yin, X.M., 2013. Pharmacological promotion of autophagy alleviates steatosis and injury in

- alcoholic and non-alcoholic fatty liver conditions in mice. *Journal of hepatology*, 58(5), pp.993-999.
255. Lin, D.P. and Dass, C.R., 2018. Weak bones in diabetes mellitus—an update on pharmaceutical treatment options. *Journal of Pharmacy and Pharmacology*, 70(1), pp.1-17.
256. Lin, J., Rexrode, K.M., Hu, F., Albert, C.M., Chae, C.U., Rimm, E.B., Stampfer, M.J. and Manson, J.E., 2007. Dietary intakes of flavonols and flavones and coronary heart disease in US women. *American journal of epidemiology*, 165(11), pp.1305-1313.
257. Lin, X., Lin, C.H., Zhao, T., Zuo, D., Ye, Z., Liu, L. and Lin, M.T., 2017. Quercetin protects against heat stroke-induced myocardial injury in male rats: Antioxidative and antiinflammatory mechanisms. *Chemico-biological interactions*, 265, pp.47-54.
258. Lindmo, K. and Stenmark, H., 2006. Regulation of membrane traffic by phosphoinositide 3-kinases. *Journal of cell science*, 119(4), pp.605-614.
259. Liston, A., Todd, J.A. and Lagou, V., 2017. Beta-cell fragility as a common underlying risk factor in type 1 and type 2 diabetes. *Trends in Molecular Medicine*, 23(2), pp. 181-194.
260. Liu, H., Javaheri, A., Godar, R.J., Murphy, J., Ma, X., Rohatgi, N., Mahadevan, J., Hyrc, K., Saftig, P., Marshall, C. and McDaniel, M.L., 2017. Intermittent fasting preserves beta-cell mass in obesity-induced diabetes via the autophagy-lysosome pathway. *Autophagy*, 13(11), pp.1952-1968.
261. Liu, H.Y., Han, J., Cao, S.Y., Hong, T., Zhuo, D., Shi, J., Liu, Z. and Cao, W., 2009. Hepatic Autophagy is suppressed in the presence of insulin resistance and hyperinsulinemia inhibition of FoxO1-dependent expression of key autophagy genes by insulin. *Journal of Biological Chemistry*, 284(45), pp.31484-31492.
262. Liu, K. and Czaja, M.J., 2013. Regulation of lipid stores and metabolism by lipophagy. *Cell death and differentiation*, 20(1), pp.3-11.
263. Liu, L., Liu, J. and Yu, X., 2016. Dipeptidyl peptidase-4 inhibitor MK-626 restores insulin secretion through enhancing autophagy in high fat diet-induced mice. *Biochemical and biophysical research communications*, 470(3), pp.516-520.
264. Liu, Y., Palanivel, R., Rai, E., Park, M., Gabor, T.V., Scheid, M.P., Xu, A. and Sweeney, G., 2014. Adiponectin stimulates autophagy and reduces oxidative stress to enhance insulin sensitivity during high fat diet feeding in mice. *Diabetes*, 64(1), pp. 36-48.

265. Lloberas, N., Cruzado, J.M., Franquesa, M., Herrero-Fresneda, I., Torras, J., Alperovich, G., Rama, I., Vidal, A. and Grinyó, J.M., 2006. Mammalian target of rapamycin pathway blockade slows progression of diabetic kidney disease in rats. *Journal of the American Society of Nephrology*, 17(5), pp. 1395-1404.
266. Lotfy, M., Adeghate, J., Kalasz, H., Singh, J. and Adeghate, E., 2017. Chronic complications of diabetes mellitus: A mini review. *Current diabetes reviews*, 13(1), pp.3-10.
267. Lovshin, J.A., 2017. Glucagon-like peptide-1 receptor agonists: a class update for treating type 2 diabetes. *Canadian Journal of Diabetes*, 41(5), pp. 524-535.
268. Lumelsky, N., Blondel, O., Laeng, P., Velasco, I., Ravin, R. and McKay, R., 2001. Differentiation of embryonic stem cells to insulin-secreting structures similar to pancreatic islets. *Science*, 292(5520), pp.1389-1394.
269. Luo, C., Yang, H., Tang, C., Yao, G., Kong, L., He, H. and Zhou, Y., 2015. Kaempferol alleviates insulin resistance via hepatic IKK/NF- κ B signal in type 2 diabetic rats. *International immunopharmacology*, 28(1), pp.744-750.
270. Lupi, R., Dotta, F., Marselli, L., Del Guerra, S., Masini, M., Santangelo, C., Patané, G., Boggi, U., Piro, S., Anello, M. and Bergamini, E., 2002. Prolonged exposure to free fatty acids has cytostatic and pro-apoptotic effects on human pancreatic islets: evidence that β -cell death is caspase mediated, partially dependent on ceramide pathway, and Bcl-2 regulated. *Diabetes*, 51(5), pp.1437-1442.
271. M Calderon-Montano, J., Burgos-Morón, E., Pérez-Guerrero, C. and López-Lázaro, M., 2011. A review on the dietary flavonoid kaempferol. *Mini reviews in medicinal chemistry*, 11(4), pp.298-344.
272. Maedler, K., Spinas, G.A., Dyntar, D., Moritz, W., Kaiser, N. and Donath, M.Y., 2001. Distinct effects of saturated and monounsaturated fatty acids on β -cell turnover and function. *Diabetes*, 50(1), pp.69-76.
273. Maehr, R., Chen, S., Snitow, M., Ludwig, T., Yagasaki, L., Goland, R., Leibel, R.L. and Melton, D.A., 2009. Generation of pluripotent stem cells from patients with type 1 diabetes. *Proceedings of the National Academy of Sciences*, 106(37), pp.15768-15773.
274. Maiuri, M.C., Le Toumelin, G., Criollo, A., Rain, J.C., Gautier, F., Juin, P., Tasdemir, E., Pierron, G., Troulinaki, K., Tavernarakis, N. and Hickman, J.A., 2007. Functional and physical interaction between Bcl-XL and a BH3-like domain in Beclin-1. The *EMBO journal*, 26(10), pp.2527-2539.

275. Mao, Y., Yu, F., Wang, J., Guo, C. and Fan, X., 2016. Autophagy: a new target for nonalcoholic fatty liver disease therapy. *Hepatic medicine: evidence and research*, 8, pp.27-37.
276. Marchetti, P., Bugliani, M., Lupi, R., Marselli, L., Masini, M., Boggi, U., Filipponi, F., Weir, G.C., Eizirik, D.L. and Cnop, M., 2007. The endoplasmic reticulum in pancreatic beta cells of type 2 diabetes patients. *Diabetologia*, 50(12), pp.2486-2494.
277. Marchetti, P., Del Guerra, S., Marselli, L., Lupi, R., Masini, M., Pollera, M., Bugliani, M., Boggi, U., Vistoli, F., Mosca, F. and Del Prato, S., 2004. Pancreatic islets from type 2 diabetic patients have functional defects and increased apoptosis that are ameliorated by metformin. *The Journal of Clinical Endocrinology & Metabolism*, 89(11), pp.5535-5541.
278. Maria Elizabeth, M.P., Clara, O.C. and Del Carmen, M., 2017. Pancreatic β -Cells and type 2 diabetes development. *Current Diabetes Reviews*, 13(2), pp. 108-121.
279. Marín-Peñalver, J.J., Martín-Timón, I., Sevillano-Collantes, C. and del Cañizo-Gómez, F.J., 2016. Update on the treatment of type 2 diabetes mellitus. *World Journal of Diabetes*, 7(17), pp. 354-395.
280. Márquez-Aguirre, A.L., Canales-Aguirre, A.A., Padilla-Camberos, E., Esquivel-Solis, H. and Díaz-Martínez, N.E., 2015. Development of the endocrine pancreas and novel strategies for β -cell mass restoration and diabetes therapy. *Brazilian Journal of Medical and Biological Research*, 48(9), pp.765-776.
281. Marrif, H.I. and Al-Sunousi, S.I., 2016. Pancreatic β cell mass death. *Frontiers in pharmacology*, 7, p.83.
282. Martino, L., Masini, M., Novelli, M., Befly, P., Bugliani, M., Marselli, L., Masiello, P., Marchetti, P. and De Tata, V., 2012. Palmitate activates autophagy in INS-1E β -cells and in isolated rat and human pancreatic islets. *PloS one*, 7(5), p.e36188.
283. Martins, A.R., Nachbar, R.T., Gorjao, R., Vinolo, M.A., Festuccia, W.T., Lambertucci, R.H., Cury-Boaventura, M.F., Silveira, L.R., Curi, R. and Hirabara, S.M., 2012. Mechanisms underlying skeletal muscle insulin resistance induced by fatty acids: importance of the mitochondrial function. *Lipids in health and disease*, 11(1), p.30.
284. Masini, M., Bugliani, M., Lupi, R., Del Guerra, S., Boggi, U., Filipponi, F., Marselli, L., Masiello, P. and Marchetti, P., 2009. Autophagy in human type 2 diabetes pancreatic beta cells. *Diabetologia*, 52(6), pp.1083-1086.

285. Matsunaga, K., Morita, E., Saitoh, T., Akira, S., Ktistakis, N.T., Izumi, T., Noda, T. and Yoshimori, T., 2010. Autophagy requires endoplasmic reticulum targeting of the PI3-kinase complex via Atg14L. *The Journal of cell biology*, 190(4), pp.511-521.
286. Matveyenko, A.V. and Butler, P.C., 2006. β -cell deficit due to increased apoptosis in the human islet amyloid polypeptide transgenic (HIP) rat recapitulates the metabolic defects present in type 2 diabetes. *Diabetes*, 55(7), pp. 2106-2114.
287. Maurin, A.C., B'Chir, W., Reinhardt, V., Parry, L., Carraro, V., Mesclon, F., Mordier, S., Jousse, C., Bruhat, A., Averous, J. and Fafournoux, P., 2016. The GCN2 kinase is required for activating autophagy in response to indispensable amino acid deficiencies. In *7. Proteasomes & Autophagy Workshop*, p.320.
288. Mayer, J.P., Zhang, F. and DiMarchi, R.D., 2007. Insulin structure and function. *Peptide Science: Original Research on Biomolecules*, 88(5), pp.687-713.
289. McCracken, E., Monaghan, M. and Sreenivasan, S., 2018. Pathophysiology of the metabolic syndrome. *Clinics in dermatology*, 36(1), pp.14-20.
290. McNaughton, D., 2013. 'Diabesity' down under: overweight and obesity as cultural signifiers for type 2 diabetes mellitus. *Critical Public Health*, 23(3), pp.274-288.
291. Meier, J.J., 2008. Beta cell mass in *diabetes*: a realistic therapeutic target?. *Diabetologia*, 51(5), pp.703-713.
292. Mellor, K.M., Reichelt, M.E. and Delbridge, L.M., 2011. Autophagy anomalies in the diabetic myocardium. *Autophagy*, 7(10), pp.1263-1267.
293. Mendes, R.A., Almeida, S.K., Soares, I.N., Barboza, C.A., Freitas, R.G., Brown, A. and de Souza, G.L., 2018. A computational investigation on the antioxidant potential of myricetin 3, 4'-di-O- α -L-rhamnopyranoside. *Journal of molecular modeling*, 24(6), p.133.
294. Menezes Zanoveli, J., de Moraes, H., Caroline da Silva Dias, I., Karoline Schreiber, A., Pasquini de Souza, C. and Maria da Cunha, J., 2016. Depression associated with diabetes: from pathophysiology to treatment. *Current diabetes reviews*, 12(3), pp.165-178.
295. Mir, S.U.R., George, N.M., Zahoor, L., Harms, R., Guinn, Z., Sarvetnick, N.E., 2015. Inhibition of autophagic turnover in β -cells by fatty acids and glucose leads to apoptotic cell death. *Journal of Biological Chemistry*, 290(10), pp.6071-6085.
296. Miranda, C.L., Maier, C.S. and Stevens, J.F., 2001. Flavonoids. *John Wiley & Sons Ltd.: Chichester, 2012*.

297. Mitri, J., Dawson-Hughes, B., Hu, F.B. and Pittas, A.G., 2011. Effects of vitamin D and calcium supplementation on pancreatic β cell function, insulin sensitivity, and glycemia in adults at high risk of diabetes: the Calcium and Vitamin D for Diabetes Mellitus (CaDDM) randomized controlled trial—. *The American journal of clinical nutrition*, 94(2), pp.486-494.
298. Mizushima, N. and Komatsu, M., 2011. Autophagy: renovation of cells and tissues. *Cell*, 147(4), pp.728-741.
299. Mizushima, N., 2007. Autophagy: process and function. *Genes & development*, 21(22), pp.2861-2873.
300. Mizushima, N., Kuma, A., Kobayashi, Y., Yamamoto, A., Matsubae, M., Takao, T., Natsume, T., Ohsumi, Y. and Yoshimori, T., 2003. Mouse Apg16L, a novel WD-repeat protein, targets to the autophagic isolation membrane with the Apg12-Apg5 conjugate. *Journal of cell science*, 116(9), pp.1679-1688.
301. Mizushima, N., Yamamoto, A., Matsui, M., Yoshimori, T. and Ohsumi, Y., 2004. In vivo analysis of autophagy in response to nutrient starvation using transgenic mice expressing a fluorescent autophagosome marker. *Molecular biology of the cell*, 15(3), pp.1101-1111.
302. Mizushima, N., Yoshimori, T. and Levine, B., 2010. Methods in mammalian autophagy research. *Cell*, 140(3), pp.313-326.
303. Modi, H., Jacovetti, C., Tarussio, D., Metref, S., Madsen, O.D., Zhang, F.P., Rantakari, P., Poutanen, M., Nef, S., Gorman, T. and Regazzi, R., 2015. Autocrine action of IGF2 regulates adult β -cell mass and function. *Diabetes*, 64(12), pp. 4148-4157.
304. Mokdad, A.H., Ford, E.S., Bowman, B.A., Dietz, W.H., Vinicor, F., Bales, V.S. and Marks, J.S., 2003. Prevalence of obesity, diabetes, and obesity-related health risk factors, 2001. *Jama*, 289(1), pp.76-79.
305. Moon, J., Koh, S.S., Malilas, W., Cho, I.R., Kaewpiboon, C., Kaowinn, S., Lee, K., Jhun, B.H., Choi, Y.W. and Chung, Y.H., 2014. Acetylshikonin induces apoptosis of hepatitis B virus X protein-expressing human hepatocellular carcinoma cells via endoplasmic reticulum stress. *European journal of pharmacology*, 735, pp.132-140.
306. Moreau, K., Luo, S. and Rubinsztein, D.C., 2010. Cytoprotective roles for autophagy. *Current opinion in cell biology*, 22(2), pp.206-211.
307. Mori, H., Inoki, K., Masutani, K., Wakabayashi, Y., Komai, K., Nakagawa, R., Guan, K.L. and Yoshimura, A., 2009. The mTOR pathway is highly activated in diabetic

- nephropathy and rapamycin has a strong therapeutic potential. *Biochemical and biophysical research communications*, 384(4), pp.471-475.
308. Mounier, C. and Posner, B.I., 2006. Transcriptional regulation by insulin: from the receptor to the gene. *Canadian journal of physiology and pharmacology*, 84(7), pp.713-724.
309. Mukherjee, K., Biswas, R., Chaudhary, S.K. and Mukherjee, P.K., 2015. Botanicals as medicinal food and their effects against obesity. In *Evidence-Based Validation of Herbal Medicine*, pp. 373-403.
310. Mukherjee, P.K., Nema, N.K., Pandit, S. and Mukherjee, K., 2013. Indian medicinal plants with hypoglycemic potential. In *Bioactive Food as Dietary Interventions for Diabetes* pp. 235-264.
311. Murea, M., Ma, L. and Freedman, B.I., 2012. Genetic and environmental factors associated with type 2 diabetes and diabetic vascular complications. *The review of diabetic studies: RDS*, 9(1), pp.6-22.
312. Mylonis, I., Lakka, A., Tsakalof, A. and Simos, G., 2010. The dietary flavonoid kaempferol effectively inhibits HIF-1 activity and hepatoma cancer cell viability under hypoxic conditions. *Biochemical and biophysical research communications*, 398(1), pp.74-78.
313. Nakadera, E., Yamashina, S., Izumi, K., Inami, Y., Sato, T., Fukushima, H., Kon, K., Ikejima, K., Ueno, T. and Watanabe, S., 2016. Inhibition of mTOR improves the impairment of acidification in autophagic vesicles caused by hepatic steatosis. *Biochemical and biophysical research communications*, 469(4), pp.1104-1110.
314. Nakai, A., Yamaguchi, O., Takeda, T., Higuchi, Y., Hikoso, S., Taniike, M., Omiya, S., Mizote, I., Matsumura, Y., Asahi, M. and Nishida, K., 2007. The role of autophagy in cardiomyocytes in the basal state and in response to hemodynamic stress. *Nature medicine*, 13(5), pp.619-624.
315. Nakatogawa, H., Suzuki, K., Kamada, Y. and Ohsumi, Y., 2009. Dynamics and diversity in autophagy mechanisms: lessons from yeast. *Nature reviews Molecular cell biology*, 10(7), pp.458-467.
316. Namkoong, S., Cho, C.S., Semple, I. and Lee, J.H., 2018. Autophagy Dysregulation and Obesity-Associated Pathologies. *Molecules and cells*, 41(1), pp.3-10.

317. National Institute for Clinical Excellence, 2014. Obesity: identification, assessment and management of overweight and obesity in children, young people and adults. *Partial update of CG43. London: Department of Health.*
318. NCD Risk Factor Collaboration, 2016. Worldwide trends in diabetes since 1980: a pooled analysis of 751 population-based studies with 4• 4 million participants. *The Lancet*, 387(10027), pp.1513-1530.
319. Nuttall, F.Q., 2015. Body mass index: obesity, BMI, and health: a critical review. *Nutrition today*, 50(3), pp.117-128.
320. O'Neill, H. M., 2013. AMPK and Exercise: Glucose Uptake and Insulin Sensitivity. *Diabetes & Metabolism Journal*, 37(1), 1–21An, H. and He, L., 2016. Current understanding of metformin effect on the control of hyperglycemia in diabetes. *Journal of Endocrinology*, 228(3), pp.R97-R106.
321. Ogata, M., Hino, S.I., Saito, A., Morikawa, K., Kondo, S., Kanemoto, S., Murakami, T., Taniguchi, M., Tanii, I., Yoshinaga, K. and Shiosaka, S., 2006. Autophagy is activated for cell survival after endoplasmic reticulum stress. *Molecular and cellular biology*, 26(24), pp.9220-9231.
322. Ogurtsova, K., da Rocha Fernandes, J.D., Huang, Y., Linnenkamp, U., Guariguata, L., Cho, N.H., Cavan, D., Shaw, J.E. and Makaroff, L.E., 2017. IDF Diabetes Atlas: Global estimates for the prevalence of diabetes for 2015 and 2040. *Diabetes research and clinical practice*, 128, pp.40-50.
323. Ohlsson, C., Hammarstedt, A., Vandenput, L., Saarinen, N., Ryberg, H., Windahl, S.H., Farman, H.H., Jansson, J.O., Movérare-Skrtic, S., Smith, U., Zhang, F.P., Poutanen, M., Hedjazifar, S., and Sjögren, K., 2017. Increased adipose tissue aromatase activity improves insulin sensitivity and reduces adipose tissue inflammation in male mice. *American Journal of Physiology-Endocrinology and Metabolism*, 313(4), pp. 450-462.
324. Olsen, G.S. and Hansen, B.F., 2002. AMP kinase activation ameliorates insulin resistance induced by free fatty acids in rat skeletal muscle. *American Journal of Physiology-Endocrinology and Metabolism*, 283(5), pp.E965-E970.
325. Orhon, I. and Reggiori, F., 2017. Assays to monitor autophagy progression in cell cultures. *Cells*, 6(3), p.20.
326. Osipovich, A.B. and Magnuson, M.A., 2018. Alpha to beta cell reprogramming: Stepping toward a new treatment for diabetes. *Cell Stem Cell*, 22(1), pp. 12-13.

327. Ota, T., Gayet, C. and Ginsberg, H.N., 2008. Inhibition of apolipoprotein B100 secretion by lipid-induced hepatic endoplasmic reticulum stress in rodents. *The Journal of clinical investigation*, 118(1), pp.316-332.
328. Oyadomari, S. and Mori, M., 2004. Roles of CHOP/GADD153 in endoplasmic reticulum stress. *Cell death and differentiation*, 11(4), pp.381-389.
329. Oyadomari, S., Koizumi, A., Takeda, K., Gotoh, T., Akira, S., Araki, E. and Mori, M., 2002. Targeted disruption of the Chop gene delays endoplasmic reticulum stress-mediated diabetes. *The Journal of clinical investigation*, 109(4), pp.525-532.
330. Ozcan, L. and Tabas, I., 2012. Role of endoplasmic reticulum stress in metabolic disease and other disorders. *Annual review of medicine*, 63, pp.317-328.
331. Panche, A.N., Diwan, A.D. and Chandra, S.R., 2016. Flavonoids: an overview. *Journal of nutritional science*, 5, e47.
332. Pandey, K.B. and Rizvi, S.I., 2009. Plant polyphenols as dietary antioxidants in human health and disease. *Oxidative medicine and cellular longevity*, 2(5), pp.270-278.
333. Panigrahy, S.K., Bhatt, R. and Kumar, A., 2017. Reactive oxygen species: sources, consequences and targeted therapy in type 2 diabetes. *Journal of Drug Targeting*, 25(2), pp. 93-101
334. Pankiv, S., Clausen, T.H., Lamark, T., Brech, A., Bruun, J.A., Outzen, H., Øvervatn, A., Bjørkøy, G. and Johansen, T., 2007. p62/SQSTM1 binds directly to Atg8/LC3 to facilitate degradation of ubiquitinated protein aggregates by autophagy. *Journal of biological chemistry*, 282(33), pp.24131-24145.
335. Parihar, S., Gupta, A., Chaturvedi, A.K., Agarwal, J., Luqman, S., Changkija, B., Manohar, M., Chanda, D., Chanotiya, C.S., Shanker, K. and Dwivedi, A., 2012. Gallic acid based steroidal phenstatin analogues for selective targeting of breast cancer cells through inhibiting tubulin polymerization. *Steroids*, 77(8-9), pp. 878-886.
336. Park, H.W. and Lee, J.H., 2014. Calcium channel blockers as potential therapeutics for obesity-associated autophagy defects and fatty liver pathologies. *Autophagy*, 10(12), pp.2385-2386.
337. Park, H.W., Park, H., Semple, I.A., Jang, I., Ro, S.H., Kim, M., Cazares, V.A., Stuenkel, E.L., Kim, J.J., Kim, J.S. and Lee, J.H., 2014. Pharmacological correction of obesity-induced autophagy arrest using calcium channel blockers. *Nature communications*, 5, p.4834.

338. Patel, V.G., Patel, K.G., Patel, K.V. and Gandhi, T.R., 2017. Development of Standardisation parameters and Isolation of Phytomarker Myricetin from stem bark of *Myrica esculenta* Buch. Ham. Ex d. Don. *Journal of Pharmacognosy and Phytochemistry*, 6(2), pp.29-34.
339. Pattingre, S., Tassa, A., Qu, X., Garuti, R., Liang, X.H., Mizushima, N., Packer, M., Schneider, M.D. and Levine, B., 2005. Bcl-2 antiapoptotic proteins inhibit Beclin 1-dependent autophagy. *Cell*, 122(6), pp.927-939.
340. Pawlak, M., Lefebvre, P. and Staels, B., 2015. Molecular mechanism of PPAR α action and its impact on lipid metabolism, inflammation and fibrosis in non-alcoholic fatty liver disease. *Journal of hepatology*, 62(3), pp.720-733.
341. Peng, G., Li, L., Liu, Y., Pu, J., Zhang, S., Yu, J., Zhao, J. and Liu, P., 2011. Oleate blocks palmitate-induced abnormal lipid distribution, endoplasmic reticulum expansion and stress, and insulin resistance in skeletal muscle. *Endocrinology*, 152(6), pp.2206-2218.
342. Perkin, A.G. and Hummel, J.J., 1896. LXXVI.—The colouring principle contained in the bark of *Myrica nagi*. Part I. *Journal of the Chemical Society, Transactions*, 69, pp.1287-1294.
343. Perry, R. J., Samuel, V. T., Petersen, K. F., & Shulman, G. I., 2014. The role of hepatic lipids in hepatic insulin resistance and type 2 diabetes. *Nature*, 510(7503), pp. 84–91.
344. Pichiah, P.T., Suriyakalaa, U., Kamalakkannan, S., Kokilavani, P., Kalaiselvi, S., SankarGanesh, D., Gowri, J., Archunan, G., Cha, Y.S. and Achiraman, S., 2011. Spermidine may decrease ER stress in pancreatic beta cells and may reduce apoptosis via activating AMPK dependent autophagy pathway. *Medical hypotheses*, 77(4), pp.677-679.
345. Piero, M.N., Nzaro, G.M. and Njagi, J.M., 2015. Diabetes mellitus? a devastating metabolic disorder. *Asian journal of biomedical and pharmaceutical sciences*, 4(40).pp. 1-7.
346. Pittas, A.G., Sun, Q., Manson, J.E., Dawson-Hughes, B. and Hu, F.B., 2010. Plasma 25-hydroxyvitamin D concentration and risk of incident type 2 diabetes in women. *Diabetes care*, 33(9), pp.2021-2023.
347. Poitout, V. and Robertson, R.P., 2007. Glucolipotoxicity: fuel excess and β -cell dysfunction. *Endocrine reviews*, 29(3), pp.351-366.

348. Porter, A.G. and Jänicke, R.U., 1999. Emerging roles of caspase-3 in apoptosis. *Cell death and differentiation*, 6(2), pp.99-104.
349. Powell, D.J., Turban, S., Alexander, G.R.A.Y., Hajdуч, E. and Hundal, H.S., 2004. Intracellular ceramide synthesis and protein kinase C ζ activation play an essential role in palmitate-induced insulin resistance in rat L6 skeletal muscle cells. *Biochemical Journal*, 382(2), pp.619-629.
350. Prakash, O., Kumar, R., Srivastava, R., Tripathi, P. and Mishra, S., 2015. Ajeet. Plants explored with Anti-diabetic properties: A review. *American Journal of Pharmacological Sciences*, 3(3), pp.55-66.
351. Prentki, M. and Nolan, C.J., 2006. Islet β cell failure in type 2 diabetes. *The Journal of clinical investigation*, 116(7), pp.1802-1812.
352. Procházková, D., Boušová, I. and Wilhelmová, N., 2011. Antioxidant and prooxidant properties of flavonoids. *Fitoterapia*, 82(4), pp.513-523.
353. Qaid, M.M. and Abdelrahman, M.M., 2016. Role of insulin and other related hormones in energy metabolism—A review. *Cogent Food & Agriculture*, 2(1), p.1267691.
354. Qiu, W., Su, Q., Rutledge, A.C., Zhang, J. and Adeli, K., 2009. Glucosamine-induced endoplasmic reticulum stress attenuates apolipoprotein B100 synthesis via PERK signaling. *Journal of lipid research*, 50(9), pp.1814-1823.
355. Qiu, W., Zhang, J., Dekker, M.J., Wang, H., Huang, J., Brumell, J.H. and Adeli, K., 2011. Hepatic autophagy mediates endoplasmic reticulum stress-induced degradation of misfolded apolipoprotein B. *Hepatology*, 53(5), pp.1515-1525.
356. Quan, W., Hur, K.Y., Lim, Y., Oh, S.H., Lee, J.C., Kim, K.H., Kim, G.H., Kim, S.W., Kim, H.L., Lee, M.K. and Kim, K.W., 2012. Autophagy deficiency in beta cells leads to compromised unfolded protein response and progression from obesity to diabetes in mice. *Diabetologia*, 55(2), pp.392-403.
357. Quaranta, P., Antonini, S., Spiga, S., Mazzanti, B., Curcio, M., Mulas, G., Diana, M., Marzola, P., Mosca, F. and Longoni, B., 2014. Co-transplantation of endothelial progenitor cells and pancreatic islets to induce long-lasting normoglycemia in streptozotocin-treated diabetic rats. *PloS one*, 9(4), p.e94783.
358. R Vasanthi, H., ShriShriMal, N. and K Das, D., 2012. Phytochemicals from plants to combat cardiovascular disease. *Current medicinal chemistry*, 19(14), pp.2242-2251.

359. Raccach, D., 2017. Basal insulin treatment intensification in patients with type 2 diabetes mellitus: A comprehensive systematic review of current options. *Diabetes & Metabolism*, 43(2), pp. 110-124.
360. Rahier, J., Guiot, Y., Goebbels, R.M., Sempoux, C. and Henquin, J.C., 2008. Pancreatic β -cell mass in European subjects with type 2 diabetes. *Diabetes, Obesity and Metabolism*, 10, pp.32-42.
361. Rai, A., Singh, P.K., Singh, V., Kumar, V., Mishra, R., Thakur, A.K., Mahadevan, A., Shankar, S.K., Jana, N.R. and Ganesh, S., 2018. Glycogen synthase protects neurons from cytotoxicity of mutant huntingtin by enhancing the autophagy flux. *Cell Death & Disease*, 9(2), p.201.
362. Rashid, H.O., Yadav, R.K., Kim, H.R. and Chae, H.J., 2015. ER stress: autophagy induction, inhibition and selection. *Autophagy*, 11(11), pp.1956-1977.
363. Ren, L., Yang, H., Cui, Y., Xu, S., Sun, F., Tian, N., Hua, J. and Peng, S., 2017. Autophagy is essential for the differentiation of porcine PSCs into insulin-producing cells. *Biochemical and biophysical research communications*, 488(3), pp.471-476.
364. Retnakaran, R. and Shah, B.R., 2017. Role of type 2 diabetes in determining retinal, renal, and cardiovascular outcomes in women with previous gestational diabetes mellitus. *Diabetes Care*, 40(1), pp.101-108.
365. Reynolds, C. A. and Macian, F., 2018. Chaperone mediated autophagy and T cell function. *The Journal of Immunology*, 200(1), (Supplement 1).
366. Rho, H.S., Ghimeray, A.K., Yoo, D.S., Ahn, S.M., Kwon, S.S., Lee, K.H., Cho, D.H. and Cho, J.Y., 2011. Kaempferol and kaempferol rhamnosides with depigmenting and anti-inflammatory properties. *Molecules*, 16(4), pp.3338-3344.
367. Riahi, Y., Wikstrom, J.D., Bachar-Wikstrom, E., Polin, N., Zucker, H., Lee, M.S., Quan, W., Haataja, L., Liu, M., Arvan, P. and Cerasi, E., 2016. Autophagy is a major regulator of beta cell insulin homeostasis. *Diabetologia*, 59(7), pp.1480-1491.
368. Rieusset, J., 2017. Role of endoplasmic reticulum-mitochondria communication in type 2 diabetes. In *Organelle Contact Sites* (pp. 171-186). Springer, Singapore.
369. Rocchi, A. and He, C., 2015. Emerging roles of autophagy in metabolism and metabolic disorders. *Frontiers in biology*, 10(2), pp.154-164.
370. Röder, P.V., Wu, B., Liu, Y. and Han, W., 2016. Pancreatic regulation of glucose homeostasis. *Experimental & molecular medicine*, 48(3), p.e219.

371. Romeo, J.T. ed., 2012. Phytochemicals in human health protection, nutrition, and plant defense, *Springer Science & Business Media*, 33.
372. Rosenfeldt, M.T. and Ryan, K.M., 2011. The multiple roles of autophagy in cancer. *Carcinogenesis*, 32(7), pp.955-963.
373. Roslan, J., Giribabu, N., Karim, K. and Salleh, N., 2017. Quercetin ameliorates oxidative stress, inflammation and apoptosis in the heart of streptozotocin-nicotinamide-induced adult male diabetic rats. *Biomedicine & Pharmacotherapy*, 86, pp.570-582.
374. Saab, A.M., Gambari, R., Sacchetti, G., Guerrini, A., Lampronti, I., Tacchini, M., El Samrani, A., Medawar, S., Makhlof, H., Tannoury, M. and Abboud, J., 2018. Phytochemical and pharmacological properties of essential oils from Cedrus species. *Natural product research*, 32(12), pp.1415-1427.
375. Saad, B., Zaid, H., Shanak, S. and Kadan, S., 2017. Introduction to diabetes and obesity. In *Anti-diabetes and Anti-obesity Medicinal Plants and Phytochemicals* (pp. 3-19). Springer, Cham.
376. Saafi, E.L., Konarkowska, B., Zhang, S., Kistler, J. and Cooper, G.J., 2001. Ultrastructural evidence that apoptosis is the mechanism by which human amylin evokes death in RINm5F pancreatic islet β -cells. *Cell biology international*, 25(4), pp.339-350.
377. Sakaguchi, M., Isono, M., Isshiki, K., Sugimoto, T., Koya, D. and Kashiwagi, A., 2006. Inhibition of mTOR signaling with rapamycin attenuates renal hypertrophy in the early diabetic mice. *Biochemical and biophysical research communications*, 340(1), pp.296-301.
378. Sakuraba, H., Mizukami, H., Yagihashi, N., Wada, R., Hanyu, C. and Yagihashi, S., 2002. Reduced beta-cell mass and expression of oxidative stress-related DNA damage in the islet of Japanese Type II diabetic patients. *Diabetologia*, 45(1), pp.85-96.
379. Saltiel, A.R. and Kahn, C.R., 2001. Insulin signalling and the regulation of glucose and lipid metabolism. *Nature*, 414(6865), p.799.
380. Saltiel, A.R. and Olefsky, J.M., 2017. Inflammatory mechanisms linking obesity and metabolic disease. *The Journal of Clinical Investigation*, 127(1), pp. 1-4.
381. Samuel, V.T. and Shulman, G.I., 2012. Mechanisms for insulin resistance: common threads and missing links. *Cell*, 148(5), pp.852-871

382. Samuel, V.T., Liu, Z.X., Qu, X., Elder, B.D., Bilz, S., Befroy, D., Romanelli, A.J. and Shulman, G.I., 2004. Mechanism of hepatic insulin resistance in non-alcoholic fatty liver disease. *Journal of Biological Chemistry*, 279(31), pp.32345-32353
383. Sayin, N., Kara, N. and Pekel, G., 2015. Ocular complications of diabetes mellitus. *World journal of diabetes*, 6(1), pp.92-108.
384. Scalbert, A. and Williamson, G., 2000. Dietary intake and bioavailability of polyphenols. *The Journal of nutrition*, 130(8), pp.2073S-2085S.
385. Scheen, A.J., 2016. Investigational insulin secretagogues for type 2 diabetes. *Expert opinion on investigational drugs*, 25(4), pp.405-422.
386. Scheuner, D. and Kaufman, R.J., 2008. The unfolded protein response: a pathway that links insulin demand with β -cell failure and diabetes. *Endocrine reviews*, 29(3), pp.317-333.
387. Schröder, M. and Kaufman, R.J., 2005. The mammalian unfolded protein response. *Annu. Rev. Biochem.*, 74, pp.739-789.
388. Schulze, R.J., Drižytė, K., Casey, C.A. and McNiven, M.A., 2017. Hepatic lipophagy: new insights into autophagic catabolism of lipid droplets in the liver. *Hepatology communications*, 1(5), pp.359-369.
389. Schwartz, M.W., Seeley, R.J., Zeltser, L.M., Drewnowski, A., Ravussin, E., Redman, L.M. and Leibel, R.L., 2017. Obesity pathogenesis: an Endocrine Society scientific statement. *Endocrine reviews*, 38(4), pp.267-296.
390. Schwartz, S.S., Epstein, S., Corkey, B.E., Grant, S.F., Gavin III, J.R., Aguilar, R.B. and Herman, M.E., 2017. A unified pathophysiological construct of diabetes and its complications. *Trends in Endocrinology & Metabolism*, 28(9), pp. 645-655.
391. Schwartz, S.S., Epstein, S., Corkey, B.E., Grant, S.F., Gavin, J.R. and Aguilar, R.B., 2016. The time is right for a new classification system for diabetes: rationale and implications of the β -cell-centric classification schema. *Diabetes Care*, 39(2), pp.179-186.
392. Sen, U. and Tyagi, S.C., 2010. Homocysteine and hypertension in diabetes: does PPAR γ have a regulatory role? *PPAR Research*, 2010.
393. Sena, C.M., Bento, C.F., Pereira, P., Marques, F. and Seiça, R., 2013. Diabetes mellitus: new challenges and innovative therapies. In *New Strategies to Advance Pre/Diabetes Care: Integrative Approach by PPPM*, 3, pp. 29-87.

394. Shaer, A., Azarpira, N., Vahdati, A., Karimi, M.H. and Shariati, M., 2015. Differentiation of human-induced pluripotent stem cells into insulin-producing clusters. Experimental and clinical transplantation: *official journal of the Middle East Society for Organ Transplantation*, 13(1), pp.68-75.
395. Shah, A.D., Langenberg, C., Rapsomaniki, E., Denaxas, S., Pujades-Rodriguez, M., Gale, C.P., Deanfield, J., Smeeth, L., Timmis, A. and Hemingway, H., 2015. Type 2 diabetes and incidence of cardiovascular diseases: a cohort study in 1•9 million people. *The lancet Diabetes & endocrinology*, 3(2), pp.105-113.
396. Shah, P., Vella, A., Basu, A., Basu, R., Adkins, A., Schwenk, W.F., Johnson, C.M., Nair, K.S., Jensen, M.D. and Rizza, R.A., 2003. Elevated free fatty acids impair glucose metabolism in women: decreased stimulation of muscle glucose uptake and suppression of splanchnic glucose production during combined hyperinsulinemia and hyperglycemia. *Diabetes*, 52(1), pp.38-42.
397. Shao, S., Yang, Y., Yuan, G., Zhang, M. and Yu, X., 2013. Signaling molecules involved in lipid-induced pancreatic beta-cell dysfunction. *DNA and cell biology*, 32(2), pp.41-49.
398. Sharma, R.B. and Alonso, L.C., 2014. Lipotoxicity in the pancreatic beta cell: not just survival and function, but proliferation as well?. *Current diabetes reports*, 14(6), p.492.
399. Shen, W., Taylor, B., Jin, Q., Nguyen-Tran, V., Meeusen, S., Zhang, Y.Q., Kamireddy, A., Swafford, A., Powers, A.F., Walker, J. and Lamb, J., 2015. Inhibition of DYRK1A and GSK3B induces human β -cell proliferation. *Nature communications*, 6, p.8372.
400. Sheng, Q., Xiao, X., Prasad, K., Chen, C., Ming, Y., Fusco, J., Gangopadhyay, N.N., Ricks, D. and Gittes, G.K., 2017. Autophagy protects pancreatic beta cell mass and function in the setting of a high-fat and high-glucose diet. *Scientific reports*, 7(1), p.16348.
401. Shigihara, N., Fukunaka, A., Hara, A., Komiya, K., Honda, A., Uchida, T., Abe, H., Toyofuku, Y., Tamaki, M., Ogihara, T. and Miyatsuka, T., 2014. Human IAPP-induced pancreatic β cell toxicity and its regulation by autophagy. *The Journal of clinical investigation*, 124(8), pp.3634-3644.
402. Shimabukuro, M., Zhou, Y.T., Lee, Y. and Unger, R.H., 1998. Troglitazone lowers islet fat and restores beta cell function of Zucker diabetic fatty rats. *Journal of Biological Chemistry*, 273(6), pp.3547-3550.

403. Shoji-Kawata, S., Sumpter, R., Leveno, M., Campbell, G.R., Zou, Z., Kinch, L., Wilkins, A.D., Sun, Q., Pallauf, K., MacDuff, D. and Huerta, C., 2013. Identification of a candidate therapeutic autophagy-inducing peptide. *Nature*, 494(7436), p.201.
404. Shrama, I. and Singh, D., 2015. Direct action of natural and synthetic PPAR γ ligands on buffalo granulosa cell proliferation and steroidogenesis. *Buffalo Bulletin*, 34(4), pp. 401-415.
405. Shukla, V., Chandra, V., Sankhwar, P., Popli, P., Kaushal, J.B., Sirohi, V.K. and Dwivedi, A., 2015. Phytoestrogen genistein inhibits EGFR/PI3K/NF-kB activation and induces apoptosis in human endometrial hyperplasia cells. *RSC Advances*, 5(69), pp. 56075-56085.
406. Siddle, K., 2011. Signalling by insulin and IGF receptors: supporting acts and new players. *Journal of molecular endocrinology*, 47(1), pp.R1-R10.
407. Siegel, L.C., Sesso, H.D., Bowman, T.S., Lee, I.M., Manson, J.E. and Gaziano, J.M., 2009. Physical activity, body mass index, and diabetes risk in men: a prospective study. *The American journal of medicine*, 122(12), pp.1115-1121.
408. Singh, R. and Cuervo, A.M., 2011. Autophagy in the cellular energetic balance. *Cell metabolism*, 13(5), pp.495-504.
409. Singh, R. and Cuervo, A.M., 2012. Lipophagy: connecting autophagy and lipid metabolism. *International journal of cell biology*, 2012.
410. Singh, R., Kaushik, S., Wang, Y., Xiang, Y., Novak, I., Komatsu, M., Tanaka, K., Cuervo, A.M. and Czaja, M.J., 2009. Autophagy regulates lipid metabolism. *Nature*, 458(7242), p.1131-1135.
411. Sinha, S., Perdomo, G., Brown, N.F. and O'Doherty, R.M., 2004. Fatty acid-induced insulin resistance in L6 myotubes is prevented by inhibition of activation and nuclear translocation of NF κ B. *Journal of Biological Chemistry*. 279, pp.41294-41301.
412. Sirohi, V.K., Popli, P., Sankhwar, P., Kaushal, J.B., Gupta, K., Manohar, M. and Dwivedi, A., 2017. Curcumin exhibits anti-tumor effect and attenuates cellular migration via Slit-2 mediated down-regulation of SDF-1 and CXCR4 in endometrial adenocarcinoma cells. *The Journal of Nutritional Biochemistry*, 44, pp. 60-70.
413. Skovsø, S., 2014. Modeling type 2 diabetes in rats using high fat diet and streptozotocin. *Journal of diabetes investigation*, 5(4), pp.349-358.

414. Smith, U. and Kahn, B.B., 2016. Adipose tissue regulates insulin sensitivity: role of adipogenesis, de novo lipogenesis and novel lipids. *Journal of internal medicine*, 280(5), pp.465-475.
415. Snel, M., Jonker, J.T., Schoones, J., Lamb, H., De Roos, A., Pijl, H., Smit, J.W.A., Meinders, A.E. and Jazet, I.M., 2012. Ectopic fat and insulin resistance: pathophysiology and effect of diet and lifestyle interventions. *International journal of endocrinology*, 2012.
416. Sobeh, M., Mahmoud, M.F., Abdelfattah, M.A., El-Beshbishy, H.A., El-Shazly, A.M. and Wink, M., 2017. Albizia harveyi: Phytochemical profiling, antioxidant, antidiabetic and hepatoprotective activities of the bark extract. *Medicinal Chemistry Research*, 26(12), pp.3091-3105.
417. Somers, S.M. and Johannot, L., 2008. Dietary flavonoid sources in Australian adults. *Nutrition and cancer*, 60(4), pp.442-449.
418. Song, B., Scheuner, D., Ron, D., Pennathur, S. and Kaufman, R.J., 2008. Chop deletion reduces oxidative stress, improves β cell function, and promotes cell survival in multiple mouse models of diabetes. *The Journal of clinical investigation*, 118(10), pp.3378-3389.
419. Song, I., Muller, C., Louw, J. and Bouwens, L., 2015. Regulating the beta cell mass as a strategy for type-2 diabetes treatment. *Current drug targets*, 16(5), pp.516-524.
420. Song, I., Patel, O., Himpe, E., Muller, C.J. and Bouwens, L., 2015. Beta cell mass restoration in alloxan-diabetic mice treated with EGF and gastrin. *PloS one*, 10(10), p.e0140148.
421. Song, J.X., Sun, Y.R., Peluso, I., Zeng, Y., Yu, X., Lu, J.H., Xu, Z., Wang, M.Z., Liu, L.F., Huang, Y.Y. and Chen, L.L., 2016. A novel curcumin analog binds to and activates TFEB in vitro and in vivo independent of MTOR inhibition. *Autophagy*, 12(8), pp.1372-1389.
422. Song, Y.M., Lee, Y.H., Kim, J.W., Ham, D.S., Kang, E.S., Cha, B.S., Lee, H.C. and Lee, B.W., 2015. Metformin alleviates hepatosteatosis by restoring SIRT1-mediated autophagy induction via an AMP-activated protein kinase-independent pathway. *Autophagy*, 11(1), pp.46-59.
423. Spampanato, C., Feeney, E., Li, L., Cardone, M., Lim, J.A., Annunziata, F., Zare, H., Polishchuk, R., Puertollano, R., Parenti, G. and Ballabio, A., 2013. Transcription factor

- EB (TFEB) is a new therapeutic target for Pompe disease. *EMBO molecular medicine*, 5(5), pp.691-706.
424. Stienstra, R., Haim, Y., Riahi, Y., Netea, M., Rudich, A. and Leibowitz, G., 2014. Autophagy in adipose tissue and the beta cell: implications for obesity and diabetes. *Diabetologia*, 57(8), pp.1505-1516.
425. Sun, F., Zheng, X.Y., Ye, J., Wu, T.T., Wang, J.L. and Chen, W., 2012. Potential anticancer activity of myricetin in human T24 bladder cancer cells both in vitro and in vivo. *Nutrition and cancer*, 64(4), pp.599-606.
426. Sun, Q., Nie, S., Wang, L., Yang, F., Meng, Z., Xiao, H., Xiang, B., Li, X., Fu, X. and Wang, S., 2016. Factors that affect pancreatic islet cell autophagy in adult rats: Evaluation of a calorie-restricted diet and a high-fat diet. *PloS one*, 11(3), p.e0151104.
427. Szpigel, A., Hainault, I., Carlier, A., Venteclef, N., Batto, A.F., Hajduch, E., Bernard, C., Ktorza, A., Gautier, J.F., Ferré, P. and Bourron, O., 2018. Lipid environment induces ER stress, TXNIP expression and inflammation in immune cells of individuals with type 2 diabetes. *Diabetologia*, 61(2), pp. 399-412.
428. Takatani, T., Shirakawa, J., Roe, M.W., Leech, C.A., Maier, B.F., Mirmira, R.G. and Kulkarni, R.N., 2016. IRS1 deficiency protects β -cells against ER stress-induced apoptosis by modulating sXBP-1 stability and protein translation. *Scientific reports*, 6, p.28177.
429. Talchai, C., Xuan, S., Lin, H.V., Sussel, L. and Accili, D., 2012. Pancreatic β cell dedifferentiation as a mechanism of diabetic β cell failure. *Cell*, 150(6), pp.1223-1234.
430. Tan, J.Y., Chen, X.Q., Kang, B.J., Qin, Z.X., Chen, J.H., Hu, R.D. and Wu, L.C., 2018. Myricetin protects against lipopolysaccharide-induced disseminated intravascular coagulation by anti-inflammatory and anticoagulation effect. *Asian Pacific Journal of Tropical Medicine*, 11(3), pp.255-259.
431. Tanaka, Y., Guhde, G., Suter, A., Eskelinen, E.L., Hartmann, D., Lüllmann-Rauch, R., Janssen, P.M., Blanz, J., Von Figura, K. and Saftig, P., 2000. Accumulation of autophagic vacuoles and cardiomyopathy in LAMP-2-deficient mice. *Nature*, 406(6798), p.902.
432. Tanaka, Y., Kume, S., Kitada, M., Kanasaki, K., Uzu, T., Maegawa, H. and Koya, D., 2011. Autophagy as a therapeutic target in diabetic nephropathy. *Experimental diabetes research*, 2012.

433. Tang, S.M., Deng, X., Li, Q., Ge, X. and Miao, L., 2018. Sa1467-Anticancer Effects of Quercetin on Cholangiocarcinoma. *Gastroenterology*, 154(6), pp.S-1122.
434. Tanida, I., Minematsu-Ikeguchi, N., Ueno, T. and Kominami, E., 2005. Lysosomal turnover, but not a cellular level, of endogenous LC3 is a marker for autophagy. *Autophagy*, 1(2), pp.84-91.
435. Thirumalai, A., Singh, S.K., Hammond Jr, D.J., Gang, T.B., Ngwa, D.N., Pathak, A. and Agrawal, A., 2017. Purification of recombinant C-reactive protein mutants. *Journal of immunological methods*, 443, pp.26-32.
436. Titchenell, P.M., Lazar, M.A. and Birnbaum, M.J., 2017. Unraveling the regulation of hepatic metabolism by insulin. *Trends in Endocrinology & Metabolism*, 28(7), pp. 497-505.
437. Tooze, S.A. and Yoshimori, T., 2010. The origin of the autophagosomal membrane. *Nature cell biology*, 12(9), pp.831-835.
438. Toshima, T., Shirabe, K., Matsumoto, Y., Itoh, S., Harimoto, N., Ikegami, T., Yoshizumi, T. and Maehara, Y., 2018. Role of Autophagy in Liver Regeneration. In *Autophagy: Cancer, Other Pathologies, Inflammation, Immunity, Infection, and Aging*, 12, pp. 451-461.
439. Tourrel, C., Bailbe, D., Lacorne, M., Meile, M.J., Kergoat, M. and Portha, B., 2002. Persistent improvement of type 2 diabetes in the Goto-Kakizaki rat model by expansion of the β -cell mass during the prediabetic period with glucagon-like peptide-1 or exendin-4. *Diabetes*, 51(5), pp.1443-1452.
440. Tran, K.L., Park, Y.I., Pandya, S., Muliyl, N.J., Jensen, B.D., Huynh, K. and Nguyen, Q.T., 2017. Overview of glucagon-like peptide-1 receptor agonists for the treatment of patients with type 2 diabetes. *American Health & Drug Benefits*, 10(4), pp. 178-188.
441. Tremblay, F. and Marette, A., 2001. Amino acid and insulin signaling via the mTOR/p70 S6 kinase pathway A negative feedback mechanism leading to insulin resistance in skeletal muscle cells. *Journal of Biological Chemistry*, 276(41), pp.38052-38060.
442. Tremblay, F., Krebs, M., Dombrowski, L., Brehm, A., Bernroider, E., Roth, E., Nowotny, P., Waldhäusl, W., Marette, A. and Roden, M., 2005. Overactivation of S6 kinase 1 as a cause of human insulin resistance during increased amino acid availability. *Diabetes*, 54(9), pp.2674-2684.

443. Trikkalinou, A., Papazafiropoulou, A.K. and Melidonis, A., 2017. Type 2 diabetes and quality of life. *World journal of diabetes*, 8(4), pp.120-129.
444. Trudeau, K.M., Colby, A.H., Zeng, J., Las, G., Feng, J.H., Grinstaff, M.W. and Shirihai, O.S., 2016. Lysosome acidification by photoactivated nanoparticles restores autophagy under lipotoxicity. *Journal of Cell Biology*, 214(1), pp.25-34.
445. Tsai, T.H., Chen, E., Li, L., Saha, P., Lee, H.J., Huang, L.S., Shelness, G.S., Chan, L. and Chang, B.H.J., 2017. The constitutive lipid droplet protein PLIN2 regulates autophagy in liver. *Autophagy*, 13(7), pp.1130-1144.
446. Tsanova-Savova, S., Ribarova, F. and Petkov, V., 2018. Quercetin content and ratios to total flavonols and total flavonoids in Bulgarian fruits and vegetables. *Bulgarian Chemical Communications*, 50(1), pp.69-73.
447. Tu, Q.Q., Zheng, R.Y., Li, J., Hu, L., Chang, Y.X., Li, L., Li, M.H., Wang, R.Y., Huang, D.D., Wu, M.C., Hu, H.P., Chen, L., Wang, H.Y., 2014. Palmitic acid induces autophagy in hepatocytes via JNK2 activation. *Acta Pharmacol Sin.* 35, 504-512.doi: 10.1038/aps.2013.170
448. Tushuizen, M.E., Bunck, M.C., Pouwels, P.J., Bontemps, S., Van Waesberghe, J.H.T., Schindhelm, R.K., Mari, A., Heine, R.J. and Diamant, M., 2007. Pancreatic fat content and β -cell function in men with and without type 2 diabetes. *Diabetes care*, 30(11), pp.2916-2921.
449. Tyagi, N., Vacek, J.C., Givvimani, S., Sen, U. and Tyagi, S.C., 2010. Cardiac specific deletion of N-methyl-d-aspartate receptor 1 ameliorates mtMMP-9 mediated autophagy/mitophagy in hyperhomocysteinemia. *Journal of Receptors and Signal Transduction*, 30(2), pp. 78-87.
450. Um, S.H., Frigerio, F., Watanabe, M., Picard, F., Joaquin, M., Sticker, M., Fumagalli, S., Allegrini, P.R., Kozma, S.C., Auwerx, J. and Thomas, G., 2004. Absence of S6K1 protects against age-and diet-induced obesity while enhancing insulin sensitivity. *Nature*, 431(7005), pp.200-205.
451. Unnikrishnan, M.K., Veerapur, V., Nayak, Y., Mudgal, P.P. and Mathew, G., 2014. Antidiabetic, antihyperlipidemic and antioxidant effects of the flavonoids. In *Polyphenols in human health and disease*, 1, pp. 143-161.
452. Urano, F., Wang, X., Bertolotti, A., Zhang, Y., Chung, P., Harding, H.P. and Ron, D., 2000. Coupling of stress in the ER to activation of JNK protein kinases by transmembrane protein kinase IRE1. *Science*, 287(5453), pp.664-666.

453. Vanhaesebroeck, B., Leever, S.J., Ahmadi, K., Timms, J., Katso, R., Driscoll, P.C., Woscholski, R., Parker, P.J. and Waterfield, M.D., 2001. Synthesis and function of 3-phosphorylated inositol lipids. *Annual review of biochemistry*, 70(1), pp.535-602.
454. Varshney, R., Gupta, S. and Roy, P., 2017. Cytoprotective effect of kaempferol against palmitic acid-induced pancreatic β -cell death through modulation of autophagy via AMPK/mTOR signaling pathway. *Molecular and cellular endocrinology*, 448, pp.1-20.
455. Varshney, R., Varshney, R., Mishra, R., Gupta, S., Sircar, D. and Roy, P., 2018. Kaempferol alleviates palmitic acid-induced lipid stores, endoplasmic reticulum stress and pancreatic β -cell dysfunction through AMPK/mTOR-mediated lipophagy. *The Journal of nutritional biochemistry*, 57, pp.212-227.
456. Vashisht, M., Rani, P., Kumar Onteru, S. and Singh, D., 2018. Curcumin primed exosomes reverses LPS-induced pro-inflammatory gene expression in buffalo granulosa cells. *Journal of Cellular Biochemistry*, 119(2), pp. 1488-1500.
457. Velásquez-Rodríguez, C.M., Velásquez-Villa, M., Gómez-Ocampo, L. and Bermúdez-Cardona, J., 2014. Abdominal obesity and low physical activity are associated with insulin resistance in overweight adolescents: a cross-sectional study. *BMC pediatrics*, 14(1), p.258.
458. Venkatesan, R., Ji, E. and Kim, S.Y., 2015. Phytochemicals that regulate neurodegenerative disease by targeting neurotrophins: a comprehensive review. *BioMed Research International*, 2015.
459. Verma, S. and Hussain, M.E., 2017. Obesity and diabetes: an update. *Diabetes & Metabolic Syndrome: Clinical Research & Reviews*, 11(1), pp. 73-79.
460. Vetere, A., Choudhary, A., Burns, S.M. and Wagner, B.K., 2014. Targeting the pancreatic β -cell to treat diabetes. *Nature reviews Drug discovery*, 13(4), pp.278-289.
461. Vinayagam, R. and Xu, B., 2015. Antidiabetic properties of dietary flavonoids: a cellular mechanism review. *Nutrition & Metabolism*, 12(1), p.60.
462. Vishwakarma, A., Singh, T.U., Rungsung, S., Kumar, T., Kandasamy, A., Parida, S., Lingaraju, M.C., Kumar, A., Kumar, A. and Kumar, D., 2018. Effect of Kaempferol Pretreatment on Myocardial Injury in Rats. *Cardiovascular toxicology*, 18, pp.312-328.
463. Voleti, B., Hammond Jr, D.J., Thirumalai, A. and Agrawal, A., 2012. Oct-1 acts as a transcriptional repressor on the C-reactive protein promoter. *Molecular immunology*, 52(3-4), pp.242-248.

464. Walle, T., 2004. Absorption and metabolism of flavonoids. *Free Radical Biology and Medicine*, 36(7), pp.829-837.
465. Wang, B., Yang, Q., Sun, Y.Y., Xing, Y.F., Wang, Y.B., Lu, X.T., Bai, W.W., Liu, X.Q. and Zhao, Y.X., 2014. Resveratrol-enhanced autophagic flux ameliorates myocardial oxidative stress injury in diabetic mice. *Journal of cellular and molecular medicine*, 18(8), pp.1599-1611.
466. Wang, H., Sun, R.Q., Zeng, X.Y., Zhou, X., Li, S., Jo, E., Molero, J.C. and Ye, J.M., 2015. Restoration of autophagy alleviates hepatic ER stress and impaired insulin signalling transduction in high fructose-fed male mice. *Endocrinology*, 156(1), pp.169-181.
467. Wang, P., Fiaschi-Taesch, N.M., Vasavada, R.C., Scott, D.K., García-Ocaña, A. and Stewart, A.F., 2015. Diabetes mellitus—advances and challenges in human β -cell proliferation. *Nature Reviews Endocrinology*, 11(4), pp.201-212.
468. Wang, Q.J., Ding, Y., Kohtz, S., Mizushima, N., Cristea, I.M., Rout, M.P., Chait, B.T., Zhong, Y., Heintz, N. and Yue, Z., 2006. Induction of autophagy in axonal dystrophy and degeneration. *Journal of Neuroscience*, 26(31), pp.8057-8068.
469. Ward, C., Martinez-Lopez, N., Otten, E.G., Carroll, B., Maetzel, D., Singh, R., Sarkar, S. and Korolchuk, V.I., 2016. Autophagy, lipophagy and lysosomal lipid storage disorders. *Biochimica et Biophysica Acta (BBA)-Molecular and Cell Biology of Lipids*, 1861(4), pp.269-284.
470. Wei, R. and Hong, T., 2016. Lineage reprogramming: a promising road for pancreatic β cell regeneration. *Trends in Endocrinology & Metabolism*, 27(3), pp.163-176.
471. Wilcox, G., 2005. Insulin and insulin resistance. *Clinical Biochemist Reviews*, 26(2), p.19.
472. Williams, C.A. and Grayer, R.J., 2004. Anthocyanins and other flavonoids. *Natural product reports*, 21(4), pp.539-573.
473. Winkel-Shirley, B., 2001. Flavonoid biosynthesis. A colorful model for genetics, biochemistry, cell biology, and biotechnology. *Plant physiology*, 126(2), pp.485-493.
474. Wong, G., He, S., Siragam, V., Bi, Y., Mbikay, M., Chretien, M. and Qiu, X., 2017. Antiviral activity of quercetin-3- β -OD-glucoside against Zika virus infection. *Virologica Sinica*, 32(6), pp.545-547.
475. Woodmansey, C., McGovern, A.P., McCullough, K.A., Whyte, M.B., Munro, N.M., Correa, A.C., Gatenby, P.A., Jones, S.A. and de Lusignan, S., 2017. Incidence,

- demographics, and clinical characteristics of diabetes of the exocrine pancreas (type 3c): a retrospective cohort study. *Diabetes care*, 40(11), pp.1486-1493.
476. World Health Organization, 2016. Global report on diabetes: World Health Organization.
477. Wu, J., Kong, F., Pan, Q., Du, Y., Ye, J., Zheng, F., Li, H. and Zhou, J., 2017. Autophagy protects against cholesterol-induced apoptosis in pancreatic β -cells. *Biochemical and biophysical research communications*, 482(4), pp.678-685.
478. Wu, J., Wu, J.J., Yang, L.J., Wei, L.X. and Zou, D.J., 2013. Rosiglitazone protects against palmitate-induced pancreatic beta-cell death by activation of autophagy via 5'-AMP-activated protein kinase modulation. *Endocrine*, 44(1), pp.87-98.
479. Wu, W., Tang, S., Shi, J., Yin, W., Cao, S., Bu, R., Zhu, D. and Bi, Y., 2015. Metformin attenuates palmitic acid-induced insulin resistance in L6 cells through the AMP-activated protein kinase/sterol regulatory element-binding protein-1c pathway. *International journal of molecular medicine*, 35(6), pp.1734-1740.
480. Wu, Y., Ding, Y., Tanaka, Y. and Zhang, W., 2014. Risk factors contributing to type 2 diabetes and recent advances in the treatment and prevention. *International journal of medical sciences*, 11(11), pp.1185-1200.
481. Xin, Y., Yu, L., Chen, Z., Zheng, L., Fu, Q., Jiang, J., Zhang, P., Gong, R. and Zhao, S., 2001. Cloning, expression patterns, and chromosome localization of three human and two mouse homologues of GABA A receptor-associated protein. *Genomics*, 74(3), pp.408-413.
482. Xu, L., Spinas, G.A. and Niessen, M., 2010. ER stress in adipocytes inhibits insulin signaling, represses lipolysis, and alters the secretion of adipokines without inhibiting glucose transport. *Hormone and Metabolic Research*, 42(9), p.643.
483. Yamada, E. and Singh, R., 2012. Mapping autophagy on to your metabolic radar. *Diabetes*, 61(2), pp.272-280.
484. Yan, H., Gao, Y.Q., Zhang, Y., Wang, H., Liu, G.S. and Lei, J.Y., 2018. Chlorogenic acid alleviates autophagy and insulin resistance by suppressing JNK pathway in a rat model of nonalcoholic fatty liver disease. *Journal of biosciences*, 43(2), pp.287-294.
485. Yang, J., Xiao, P., Sun, J. and Guo, L., 2018. Anticancer effects of kaempferol in A375 human malignant melanoma cells are mediated via induction of apoptosis, cell cycle arrest, inhibition of cell migration and downregulation of m-TOR/PI3K/AKT pathway.

- Journal of BU ON.: official journal of the Balkan Union of Oncology*, 23(1), pp.218-223.
486. Yang, L., Li, P., Fu, S., Calay, E.S. and Hotamisligil, G.S., 2010. Defective hepatic autophagy in obesity promotes ER stress and causes insulin resistance. *Cell metabolism*, 11(6), pp.467-478.
487. Yang, Y., Wang, J., Qin, L., Shou, Z., Zhao, J., Wang, H., Chen, Y. and Chen, J., 2007. Rapamycin prevents early steps of the development of diabetic nephropathy in rats. *American journal of nephrology*, 27(5), pp.495-502.
488. Yao, F., Zhang, M. and Chen, L., 2016. 5'-Monophosphate-activated protein kinase (AMPK) improves autophagic activity in diabetes and diabetic complications. *Acta pharmaceutica sinica B*, 6(1), pp.20-25.
489. Ye, J., 2013. Mechanisms of insulin resistance in obesity. *Frontiers of medicine*, 7(1), pp.14-24.
490. Yenuganti, V.R., Ravinder, R. and Singh, D., 2014. Conjugated linoleic acids attenuate LPS induced pro-inflammatory gene expression by inhibiting the NF κ B translocation through PPAR γ in buffalo granulosa cells. *American Journal of Reproductive Immunology*, 72(3), pp. 296-304.
491. Yerra, V.G. and Kumar, A., 2017. Adenosine monophosphate-activated protein kinase abates hyperglycaemia-induced neuronal injury in experimental models of diabetic neuropathy: effects on mitochondrial biogenesis, autophagy and neuroinflammation. *Molecular neurobiology*, 54(3), pp.2301-2312.
492. Yoon, J.H., Mo, J.S., Ann, E.J., Ahn, J.S., Jo, E.H., Lee, H.J., Hong, S.H., Kim, M.Y., Kim, E.G., Lee, K. and Park, H.S., 2016. NOTCH1 intracellular domain negatively regulates PAK1 signaling pathway through direct interaction. *Biochimica et Biophysica Acta (BBA)-Molecular Cell Research*, 1863(2), pp.179-188.
493. Yoon, J.W. and Jun, H.S., 2005. Autoimmune destruction of pancreatic β cells. *American journal of therapeutics*, 12(6), pp.580-591.
494. Yorimitsu, T., Nair, U., Yang, Z. and Klionsky, D.J., 2006. Endoplasmic reticulum stress triggers autophagy. *Journal of Biological Chemistry*, 281(40), pp.30299-30304.
495. Yuan, H., Zhang, X., Huang, X., Lu, Y., Tang, W., Man, Y., Wang, S., Xi, J. and Li, J., 2010. NADPH oxidase 2-derived reactive oxygen species mediate FFAs-induced dysfunction and apoptosis of β -cells via JNK, p38 MAPK and p53 pathways. *PloS one*, 5(12), p.e15726.

496. Zakaria, Z.A., Mahmood, N.D., Mamat, S.S., Nasir, N. and Omar, M.H., 2018. Endogenous Antioxidant and LOX-Mediated Systems Contribute to the Hepatoprotective Activity of Aqueous Partition of Methanol Extract of *Muntingia calabura* L. Leaves against Paracetamol Intoxication. *Frontiers in Pharmacology*, 8, p.982.
497. Zang, Y., Sato, H. and Igarashi, K., 2011. Anti-diabetic effects of a kaempferol glycoside-rich fraction from unripe soybean (Edamame, *Glycine max* L. Merrill. 'Jindai') leaves on KK-Ay mice. *Bioscience, biotechnology, and biochemistry*, 75(9), pp.1677-1684.
498. Zang, Y., Zhang, L., Igarashi, K. and Yu, C., 2015. The anti-obesity and anti-diabetic effects of kaempferol glycosides from unripe soybean leaves in high-fat-diet mice. *Food & function*, 6(3), pp.834-841..
499. Zechner, R., Zimmermann, R., Eichmann, T.O., Kohlwein, S.D., Haemmerle, G., Lass, A. and Madeo, F., 2012. FAT SIGNALS-lipases and lipolysis in lipid metabolism and signaling. *Cell metabolism*, 15(3), pp.279-291.
500. Zhang, B.B., Zhou, G. and Li, C., 2009. AMPK: an emerging drug target for diabetes and the metabolic syndrome. *Cell metabolism*, 9(5), pp.407-416.
501. Zhang, J., Cheng, Y., Gu, J., Wang, S., Zhou, S., Wang, Y., Tan, Y., Feng, W., Fu, Y., Mellen, N. and Cheng, R., 2016. Fenofibrate increases cardiac autophagy via FGF21/SIRT1 and prevents fibrosis and inflammation in the hearts of Type 1 diabetic mice. *Clinical science*, 130(8), pp. 625-641.
502. Zhang, Y. and Liu, D., 2011. Flavonol kaempferol improves chronic hyperglycemia-impaired pancreatic beta-cell viability and insulin secretory function. *European journal of pharmacology*, 670(1), pp.325-332.
503. Zhang, Y., Chen, A.Y., Li, M., Chen, C. and Yao, Q., 2008. Ginkgo biloba extract kaempferol inhibits cell proliferation and induces apoptosis in pancreatic cancer cells. *Journal of Surgical Research*, 148(1), pp.17-23.
504. Zhang, Y., Zhen, W., Maechler, P. and Liu, D., 2013. Small molecule kaempferol modulates PDX-1 protein expression and subsequently promotes pancreatic β -cell survival and function via CREB. *Journal of Nutritional Biochemistr.* 24(4), pp. 638-646.

505. Zhang, Y.J., Gan, R.Y., Li, S., Zhou, Y., Li, A.N., Xu, D.P. and Li, H.B., 2015. Antioxidant phytochemicals for the prevention and treatment of chronic diseases. *Molecules*, 20(12), pp.21138-21156.
506. Zhang, Z., Zhao, S., Yao, Z., Wang, L., Shao, J., Chen, A., Zhang, F. and Zheng, S., 2017. Autophagy regulates turnover of lipid droplets via ROS-dependent Rab25 activation in hepatic stellate cell. *Redox biology*, 11, pp.322-334.
507. Zhao, D. and Liu, H., 2013. Adipose tissue dysfunction and the pathogenesis of metabolic syndrome. *World Journal of Hypertension*, 3(3), pp.18-26.
508. Zheng, Y., Ley, S.H. and Hu, F.B., 2018. Global aetiology and epidemiology of type 2 diabetes mellitus and its complications. *Nature Reviews Endocrinology*, 14(2), pp.88-98.
509. Zhou, L., Zhang, J., Fang, Q., Liu, M., Liu, X., Jia, W., Dong, L.Q. and Liu, F., 2009. Autophagy-mediated insulin receptor down-regulation contributes to endoplasmic reticulum stress-induced insulin resistance. *Molecular pharmacology*, 76(3), pp.596-603.
510. Zhou, Y., Park, S.Y., Su, J., Bailey, K., Ottosson-Laakso, E., Shcherbina, L., Oskolkov, N., Zhang, E., Thevenin, T., Fadista, J. and Bennet, H., 2014. TCF7L2 is a master regulator of insulin production and processing. *Human molecular genetics*, 23(24), pp.6419-6431.
511. Zhu, F.F., Zhang, P.B., Zhang, D.H., Sui, X., Yin, M., Xiang, T.T., Shi, Y., Ding, M.X. and Deng, H., 2011. Generation of pancreatic insulin-producing cells from rhesus monkey induced pluripotent stem cells. *Diabetologia*, 54(9), p.2325.